ENERGY SYSTEMS RESEARCH UNIT
AEROSPACE AND MECHANICAL ENGINEERING DEPARTMENT
FACULTY OF APPLIED SCIENCES
UNIVERSITY OF LIÈGE

EVIDENCE-BASED MODEL CALIBRATION FOR EFFICIENT BUILDING ENERGY SERVICES

A Thesis

Submitted to the Faculty of Applied Sciences

of the

University of Liège

by

Stéphane BERTAGNOLIO

In Partial Fulfillment of the Requirements for the Degree

Of

Doctor of Applied Sciences

Liège, June 2012

A mes parents

“ Simplicity is the Ultimate Sophistication ”

Leonardo da Vinci (1452 – 1519)

Acknowledgments

I would like to thank Prof. Jean Lebrun for his trust, his encouragements and the opportunity he offered me to integrate the Thermodynamics Laboratory and to start a PhD.

I am grateful to Philippe André and Vincent Lemort who supervised my work while leaving me the necessary freedom. I hope that this thesis is worthy of the trust they have placed in me.

I would like to thank all the people I had the opportunity to work with in Katholieke Universiteit van Leuven. Special thanks go to Prof. Lieve Helsen and her colleagues from the Division of Applied Mechanics and Energy Conversion. I also had the chance to work with Prof. Dirk Saelens and the team of the Division of Building Physics. A special thank goes to Wout Parys with whom it was a real pleasure to work with. Bedankt mijn vriend!

I also wish to thank my colleagues from "Centre Energétique Procédés" of "Ecole des Mines de Paris". Thank you to Prof. Dominique Marchio and Prof. Jérôme Adnot for welcoming me in their team. I wish to thank them and their colleagues for their hospitality, their criticisms and for the helping me to see the broader picture in several occasions. Special thanks go to Pascal Stabat for the time he devoted to me. Special thanks go also to all the people I met in Fondation Biermans Lapôtre de Paris.

Special thanks go to Prof. Michel Bernier, Michaël Kummert and their colleagues from "Ecole Polytechnique de Montréal" where I had a very pleasant stay and have enjoyed working very much.

This work could not have been completed without support and help of my colleagues from the Thermodynamics Laboratory of the University of Liège. Special thanks go to Jules and Cleide Hannay and Bernard Georges for sharing their time and experience. I would also like to thank Sylvain, Samuel, François, Jean-François, Sébastien, Roberto, Arnaud, Kévin, Clément and Ludovic for their friendship and their unconditional support. I am also grateful to all the administrative and technical staff of the Department for the team spirit and the nice working atmosphere they contribute to.

I would also like to thank Virginie for her support and sacrifices during the first years of this work.

I thank Adrien (best roommate ever), Az-Eddine, Pierre and all my friends for their friendship and for supporting me in so many ways during the good and the hard times.

Finally, very special words of thanks go to my parents, Gabriel and Michèle, and to my family for their love and for having supported me in all my projects.

ABSTRACT

Energy services play a growing role in the control of energy consumption and the improvement of energy efficiency in non-residential buildings. Most of the energy use analyses involved in the energy efficiency service process require on-field measurements and energy use analysis. Today, while detailed on-field measurements and energy counting stay generally expensive and time-consuming, energy simulations are increasingly cheaper due to the continuous improvement of computer speed.

This work consists in the development of a simulation-based approach dedicated to whole-building energy use analysis for use in the frame of an energy efficiency service process. Focus is given to the development of a new simplified dynamic hourly building energy simulation tool adapted to energy use analysis of existing buildings, its calibration by means of available energy use data and to the integration of the calibration process into the Energy Service Process. The proposed evidence-based calibration methodology is deeply related to on-field inspection and data collection issues and is developed to fit with the audit/inspection process. After calibration, the model can be used to support the other steps of the Energy Services Process, such as ECOs selection and evaluation and continuous performance verification.

The new systematic calibration methodology gives priority to the physical identification of the model's parameters (i.e. to the direct measurement) and relies on the notion of hierarchy among the source of information (as a function of their reliability) used to identify the value of the parameters.

The improved Morris' sensitivity analysis method is used for "factor fixing" (i.e. distinction between non-influential model's parameters) and "parameters screening" (i.e. classification of influential parameters by order of importance) in order to orient the data collection work and guide the parameters adjustment process. At the end of the calibration process, the Latin Hypercube Monte Carlo sampling is used to quantify the uncertainty on the final outputs of the calibrated model.

The developed simulation tool and the associated calibration method are applied to a synthetic case ("Virtual Calibration Test Bed") and to real case study building located in Brussels, Belgium.

Both applications (real and synthetic cases) allow highlighting the complexity and the limits of calibration as it is used today. Calibration remains a highly underdetermined problem and a compromise has to be found between data collection and modeling efforts and model's requirements in order to proceed to efficient energy use analysis. At the end of these applications, it is believed that partially manual methods remain more efficient and the best quality assurance when proceeding to calibration of a building energy simulation model.

The use of an evidence-based method ensures sticking to reality and avoids bad representation and hazardous adjustment of the parameters. Moreover, it is shown that the intensive use of a sensitivity analysis method is of a great help to orient data collection and parameters adjustment processes. Defining confidence/uncertainty ranges for each parameter, in addition to a "best-guess" value, also allowed quantifying the uncertainty on the final outputs of the model and helped the user in evaluating the quality of the calibrated model.

THESIS CONTENT

Chapter 1 General Introduction

1.1. The energy efficiency process and the use of whole-building energy simulation
1.2. Calibration of building energy simulation models
1.3. Objectives of the thesis
1.4. References

Chapter 2 Definition and Development of a Simplified Building Energy Simulation Model

2.1. Existing building energy simulation models
2.2. Modeling requirements for the targeted work
2.3. Inputs, outputs and parameters
2.4. Modeling approach
2.5. Building model
2.6. Secondary HVAC system model
2.7. Primary HVAC system model
2.8. Moist air properties
2.9. Automated pre-sizing
2.10. Implementation
2.11. Summary
2.12. References

Chapter 3 Simulation-Based Whole-Building Energy Performance Analysis Methodology

3.1. Previous work and existing calibration methodologies
3.2. Data gathering
3.3. BES model outputs
3.4. Simulation-based energy use analysis methodology
3.5. Summary
3.6. References

Chapter 4 Integrating Sensitivity and Uncertainty Issues within the Calibration Process

4.1. Introduction
4.2. Sensitivity and uncertainty analysis in building

simulation
4.3. Selection of a sensitivity analysis method
4.4. Application of the Morris method
4.5. Sensitivity and uncertainty issues in the calibration process
4.6. Conclusion
4.7. References

Chapter 5 Assessment of the Calibration Method Using a Virtual Test Bed

5.1. Introduction
5.2. Virtual Calibration Test Bed (VCTB)
5.3. Synthetic data
5.4. Application of the calibration methodology
5.5. Conclusion
5.6. References
5.7. Appendix

Chapter 6 Application to a Building Case Study

6.1. Introduction
6.2. Building description
6.3. HVAC&R system description
6.4. Building use and occupancy
6.5. Energy billing data
6.6. Monitoring campaign: Equipment and data collection
6.7. Available weather data
6.8. Calibration process
6.9. Conclusion
6.10. References
6.11. Appendix

Chapter 7 General Conclusion and Perspectives

CHAPTER 1 GENERAL INTRODUCTION

CHAPTER 1: GENERAL INTRODUCTION 2
1. THE ENERGY EFFICIENCY PROCESS AND THE USE OF WHOLE-BUILDING ENERGY SIMULATION 2
1.1. Context 2
1.2. Energy Audit and Inspection 4
1.2.1. Previous works and Existing Audit Procedures 4
1.2.2. Four-Steps Energy Audit Procedure for the European Market 6
1.3. Energy Performance Measurement and Verification 10
1.4. Continuous and Lifetime/On-going Commissioning 12
2. CALIBRATION OF BUILDING ENERGY SIMULATION MODELS 13
2.1. Definition 13
2.2. Benefits and Limitations of Calibrated Building Energy Simulation Models 14
3. OBJECTIVES OF THE THESIS 17
4. REFERENCES 19

CHAPTER 1: GENERAL INTRODUCTION

1. THE ENERGY EFFICIENCY PROCESS AND THE USE OF WHOLE-BUILDING ENERGY SIMULATION

1.1. CONTEXT

Environmental concerns and the recent increase of energy costs open the door to innovative techniques to reduce energy consumptions. Buildings represent about 40% of the European energy consumption (Perez-Lombard, 2008). Non-residential (tertiary) buildings are part of the main energy consumers and approximately represent 9% of the primary energy consumption in Europe (Directorate-General for Energy and Transport, 2007). The improvement of their energy performance is a major challenge of the 21th century. To this end the European Commission approved the European Directive on Energy Performance of Buildings (EPBD, 2002) on 16 December 2002.

The main objective of the Directive is to promote the improvement of the energy performance of buildings within the EU through cost-effective measures. There are **four main aspects to the EPBD**, taking place at all stages of the building life cycle; from design to renovation through operation and maintenance:

- **Establishment of a calculation methodology**: Member States must implement a methodology for the calculation of the energy performance of buildings, taking account of all factors that influence energy use;
- **Minimum energy performance requirements**: there must be regulations that set minimum energy performance requirements for new buildings and for large existing buildings when they are refurbished;
- **Energy performance certificate**: there must be an energy performance certificate made available whenever buildings are constructed, sold or rented out;
- **Inspections of boilers and air-conditioning**: there must be regulations to require inspections of boilers and heating systems (or an alternative system of providing advice as discussed below), and inspection of air conditioning systems.

Among the different “energy users” in a building, heating and air conditioning systems are culpable of about 25 to 30 % of total energy and consumption (Adnot et al., 2007) and represent an important field for energy savings. In this field, a crucial problem is related to the renovation of the installations: in the coming years, an important part of the stock of heating and air conditioning systems will become obsolete and be renovated. Out of the 2200 Mm² of air conditioned tertiary building area in use in Europe (Figure 1), 800 Mm² date more than 15 years and will need urgent renovation in a near future (Adnot et al., 2007). In this part of the building stock, potential energy savings are estimated between 30% (Directorate-General for Energy and Transport, 2007) and 50% (Adnot et al., 2003).

Optimization of the operation of mechanical and lighting systems is also a crucial issue. Roth et al. (2005) estimate that faults in operation of such systems can account for between 2% and 11% of the total energy consumption of commercial buildings.

In 2011, a global benchmarking project (call the “iServ” project; Knight, 2011) was launched in Europe in order to allow direct and accurate assessment of the energy performance of HVAC systems equipping non-residential buildings in Europe. The collected data will help in accurately quantifying the energy saving potential in Europe.

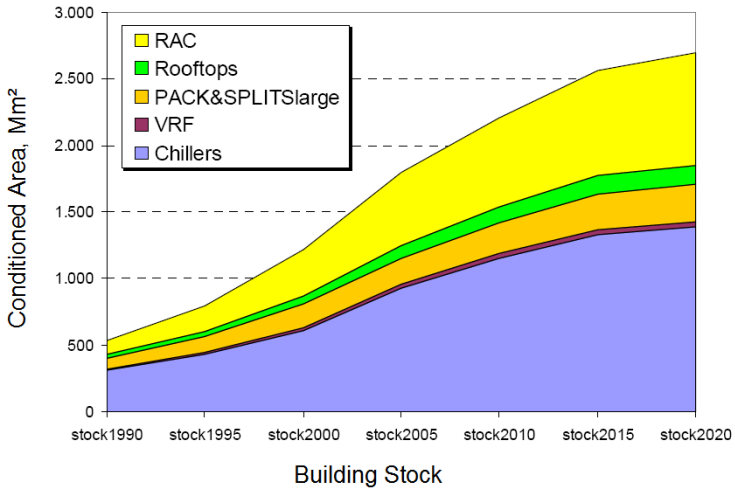

Figure 1: European Conditioned Area (source : EECCAC)

In addition to building energy inspection and renovation, energy management is developing due to the incentive created by the implementation of the EPBD, the taxation frameworks on energy performance and the development of energy services.

Energy services play a growing role in the control of energy consumption and the improvement of energy efficiency in both public and private sectors. In 2006, the European Commission approved the Directive 2006/32/EC promoting the development of a market for energy services in the member states in order to improve the energy efficiency in the building sector and support the energy demand management

EN15900 describes Energy Efficiency Services (EES) as a process based on collected energy use data, designed to achieve an energy efficiency improvement and including a series of steps such as:

1) Energy audit or inspection (as imposed by the EPBD),
2) Measurement and verification of implemented Energy efficiency improvement action(s)
3) Periodic verification of the energy performance of the building and continuous operation optimization.

Energy efficiency improvement actions can include maintenance, building and/or system partial/total renovation, continuous system operation diagnosis and optimization (commissioning) and implementation of an energy management system (as prescribed by EN16001).

Most of the energy use analyses involved in the energy efficiency service process require on-field measurements and energy use analysis. Today, while detailed on-field measurements and energy counting stay generally expensive and time-consuming, energy simulations are increasingly cheaper due to the continuous improvement of computer speed.

Since the 1960s, building energy simulation was more and more investigated to help in improving energy performance of buildings and HVAC&R systems. Initially, building energy simulation (BES) models were mainly used for design purposes (Lebrun and Liebecq, 1988). More recently, the area of application of BES models was extended to further (post-construction) stages of the building life cycle, such as building operation optimization, technical and economical evaluation of Energy Conservation Opportunities (ECOs), commissioning and functional performance testing (Visier and Jandon, 2004), fault detection and diagnosis (Jagpal, 2006), building energy management (Lebrun and Wang, 1993), building performance monitoring (Bertagnolio and Lebrun, 2008) and energy audit

(Auditac, 2007; Harmonac, 2008, Krarti, 2000, Bertagnolio et al., 2010). At the same time, graphical user interfaces were developed to facilitate use of such complex tools (Spitler, 2006).

The main tasks concerned by energy services offers are detailed below. At each level, a specific attention is paid to the possible use of whole-building energy simulation models.

1.2. ENERGY AUDIT AND INSPECTION

As mentioned above, the EPBD directive establishes mandatory inspections of air-conditioning systems to promote improvements in the HVAC installations of existing buildings:

> *Article 9- Inspection of air-conditioning systems*
>
> *With regard to reducing energy consumption and limiting carbon dioxide emissions, Member States shall lay down the necessary measures to establish a regular inspection of air conditioning systems of an effective rated output of more than 12 kW. This inspection shall include an assessment of the air-conditioning efficiency and the sizing compared to the cooling requirements of the building. Appropriate advice shall be provided to the users on possible improvement or replacement of the air-conditioning system and on alternative solutions.*

The inspection (or audit) of HVAC systems is not only a mandatory action as prescribed by the EPBD Article 9 but also a major step of the renovation process. Audit is required to identify the most efficient and cost-effective Energy Conservation Opportunities (ECOs). Energy conservation opportunities can consist in more efficient use or of partial or global replacement of the existing installation.

After the publication of the EPBD Directive, it appears that only a very small number of pre-audit (inspection) and audit methods for air conditioning systems were available, up to date and well adapted to the European building stock. Furthermore, there was very little practical experience of the type of inspections required by the EPBD.

In 2005, Intelligent Energy Europe Programme (IEE) launched the AUDITAC project ("Field Benchmarking and Market Development for Audit Methods in Air Conditioning"), focused on air conditioning systems. Its aim is to provide practical support to all those who are in a position to improve the energy-efficiency of the European A/C market.

The main objectives of the project were:

- To accelerate the adoption of AC inspection as described in the EPB Directive;
- To generate a sufficient number and variety of field demonstrations and benchmarks of inspection and audits;
- To promote best practice examples and procedures in such audits and consequent retrofits;
- To put in place a real outcome into high quality audits, namely investment-grade audits and actual works on the existing A/C facilities in the European Union.

In 2007, IEE launched the HARMONAC project to test and complement the inspection methodologies and inspection tools developed in the frame of the AUDITAC project.

1.2.1. Previous works and Existing Audit Procedures

In the frame of the IEA-ECBCS Annex 11 project, Boysen et al. (1987) proposed a basic definition of the audit process and develop a first package of tools and procedures to help the auditor. Four audit stages have been identified:

1. Building rating for energy audit: identification of the most “interesting” buildings of the building stock;
2. Disaggregation of energy consumption: analysis of measured energy consumption to identify the main energy consumers;
3. ECOs identification and evaluation: identification of the most efficient energy conservation opportunities;
4. Post implementation performance analysis.

The basic ideas of the audit process were already developed in the frame of the Annex 11. The aim of the first step was to identify the buildings which have a good potential for energy conservation. The analysis and the disaggregation of very global measured energy consumptions to understand the behaviour of the studied building was already considered as an important step of the audit process and is still a critical issue. However, only basic analysis methods (such as thermal signatures...) have been studied in the frame of this research project. Building energy simulation models are only briefly addressed and the issue of the application of simulation tools to existing buildings is not mentioned. A list of ECOs, including envelope and system improvements, has also been prepared. Of course, some of the identified ECOs are still valid (building envelope, ductwork and pipework improvement…) but an actualized list is required (cooling system, control...).

ASHRAE (2004) also provides audit procedures. Twenty-five forms are provided to help auditors in reporting basic information in a uniform and efficient way. Once again, four levels of analysis are outlined, starting from preliminary historic energy use and costs analysis (level 0) and going to detailed analysis of capital-intensive modifications focusing on potential costly ECOs (level 3) through walk through analysis in order to identify low-cost improvements (level 1) and more detailed energy survey and analysis including breakdown of the energy use (level 2). Unfortunately, the different steps of this audit procedure are not detailed and no precise description of the tools to use is given. Even if, the simulation issue is not mentioned in this reference, some useful forms to report existing conditions (for baseline model development) are provided.

In his book, Krarti (2000) distinguishes four types of energy audits:

- Walk-trough Audit consisting in a short visit of the building to identify simple and unexpensive improvements that can provide immediate energy savings;
- Utility Cost Analysis consisting in the analysis of the operating costs of the studied installation. This analysis is based on the energy consumption records and aimed to identify the patterns of energy use, weather influences and potential for energy saving;
- Standard Energy Audit providing a comprehensive analysis of the studied installation and predicting the benefits related to the selected energy conservation measures/opportunities by means of simple (hand) calculations;
- Detailed Energy Audit involving advanced on-site measurements and sophisticated computer based simulation tools to evaluate precisely the selected energy retrofits.

Krarti (2000) focuses on the detailed audit and outlines a general procedure and rules of good practice usable for most buildings. This detailed audit procedure involves:

- Building and utility data analysis intended to evaluate the characteristics of the building and the patterns of energy use. This step involves collecting utility data, understanding utility rate structure and performing utility energy use analysis (for benchmarking purposes),
- Walk-through survey intended to determine the existing operating conditions, identify the potential energy conservation opportunities and determine if any further auditing work is needed;

- Baseline for building energy use (BEU) in order to develop a baseline simulation model representing the existing conditions and the actual behavior of the building;
- Evaluation of energy conservation opportunities (ECOs) by means of the baseline model developed during the previous step and determination of a list of cost-effective energy conservation opportunities achieving energetic and economic goals.

In this detailed audit procedure, the main issues of the audit process were covered and detailed. The analysis of energy consumption records appears again as an important step of the audit process. Comparing to the definition proposed in the Annex 11 project (Boysen et al., 1987) and by ASHRAE (2004), the definition of Krarti is more advanced and recent and integrates the development and the use of modern calculation tools.

When looking to the existing audit methodologies developed by Boysen et al. (1987), ASHRAE (2004), Krarti (2000) and to the prescriptions provided in EN15900:2010, it appears that the main issues of an audit process are:

- The analysis of building and utility data, including study of the installed equipment and analysis of energy bills;
- The survey of the real operating conditions;
- The understanding of the building behaviour and of the interactions with weather, occupancy and operating schedules;
- The estimation of energy saving potential;
- The selection and the evaluation of energy conservation opportunities
- The identification of customer concerns and needs.

1.2.2. Four-Steps Energy Audit Procedure for the European Market

All the issues mentioned above have been implemented in a four-step based audit process, very similar to the one proposed by ASHRAE (2004) and Krarti (2000), which was developed in the frame of the AUDITAC project to fit to the current European market:

- **Benchmarking** is made to decide if it is necessary to launch a real audit procedure basing on energy bills and basic calculations;
- **Pre-audit**, **Walk-trough Audit** or **Inspection** consists in determining the existence of faults or possible improvements and orienting the future detailed audit. This inspection is based on visual verifications, study of installed equipment and operating data and detailed analysis of recorded energy consumption;
- **Detailed Audit**, based on the results of the pre-audit, is the quantitative evaluation of ECOs selected to correct the defects or improve the existing installation;
- **Investment Grade Audit** concerns the detailed technical and economical engineering study necessary to justify the investment related to the transformations.

The definition of the audit process developed in the frame of the HARMONAC project has been chosen as reference and the same nomenclature is used in the following parts of this work.

1.2.2.1. Benchmarking

The impossibility of describing all possible situations that might be encountered during an audit means that it is necessary to find a way of describing what constitutes good, average and bad energy performance across a range of situations. The aim of benchmarking is to answer this question. Benchmarking mainly consists in comparing the measured consumption with reference consumption of other similar buildings or generated by simulation tools to identify excessive or unacceptable

running costs. As mentioned before, benchmarking is also necessary to identify buildings presenting interesting energy saving potential.

An important issue in benchmarking is the use of performance indexes to characterize the building. These indexes can be:

- Comfort indexes, comparing the actual comfort conditions to the comfort requirements;
- Energy indexes, consisting in energy demands divided by heated/conditioned area, allowing comparison with reference values of the indexes coming from regulation or similar buildings;
- Energy demands, directly compared to "reference" energy demands generated by means of simulation tools.

In the frame of this work, priority is given to the energy viewpoint even if comfort requirements are not neglected. Indeed, the observed energy consumption has always to be analyzed with respect to the real (and consequently also observed) achievement of the requirements.

Establishing benchmarked performance of buildings is not an easy task and can be made in several ways. In the frame of the AUDITAC project (2007), a Customer Advising Tool and a case studies data base have been developed, based on simulations and on the analysis of case studies. This tool allows assessing quickly some improvements of the building envelope, but also, to associate the studied building to similar buildings, included in the AUDITAC's case studies data base ("AUDIBAC"). A first benchmarking can be made by comparing the observed performance and defaults to those identified during the audit of the selected case study (Alexandre et al., 2006). This approach is similar to empirical benchmarking, proposing comparison between actual building performance and statistical data based on the actual building stock.

Regulation can also be considered as reference for benchmarking and standards can be used as reference for comparison. However, this comparison allows only situating the studied installation in the field of regulation and standards but does not allow assessing the performance of the studied facility.

To ensure comparability between the studied building and the reference data, a normalization of the data has to be made (Bannister and Hinge, 2006). This normalization would allow to eliminate differences in climate, building size and hours of operation from the comparison and to differentiate energy-related issues. So, the performance of a building can be described in terms of energy per m^2 index, corrected to a standard climate and operating hours.

For the size, normalizing to net surface area is well suited to office buildings. To eliminate climate dependence, degree days are usually used to correct the actual consumption of the building. While heating degree days seem to be sufficient to normalize the heating demand of the buildings, simple dry-bulb cooling degree days are not efficient and do not provide good results. Indeed, dry-bulb cooling degree days are inappropriate and cooling demands are more strongly correlated to wet-bulb temperatures. However, such data are not usually available and normalization base on wet-bulb degree days is not always possible.

While (sometimes arbitrary) normalization is required to allow comparison between data recorded on the studied installation and reference values deduced from case studies or statistics; the use of simulation models allow to assess directly the studied installation, without any normalization needed. Indeed, applying a simulation-based benchmarking tool allows an individual normalization and allows avoiding size and climate normalization.

So, rather than looking for very global weather indexes, it seems rational to use a simulation model and run it over a few thousands of hours corresponding to one typical year. The current capabilities of

computers and simulation tools make this approach very efficient and allow considering the climate as it is, without any simplification. Such analysis is based on a code-compliant simulation of the installation under study and has been applied to office buildings (Bertagnolio and Lebrun, 2008). More recently, a similar approach has already been proposed by Haberl et al. (2009) for residential buildings.

1.2.2.2. Inspection and Audit

The primary analysis of measured energy consumption requires disaggregation. This process consists in dividing the measured energy demand into major components. The main purposes of disaggregation are (Boysen et al., 1987):

- To identify the major energy consumers, conservation potentials and promising areas of retrofit;
- To help to make cross-checking energy calculations by using calculation procedures and models.

The level of detail of disaggregation can range from a simple to a rather complex breakdown. Inevitably, the finer the level of detail, the more work is involved but this increased work often leads to a more accurate and detailed picture of the building energy use.

Boysen et al. (1987) proposed to distinguish non-weather, weather and time/occupancy dependent components (Figure 2). Non-weather dependent components include energy consumers remaining constant all over the year (as circulation pumps or Domestic Hot Water production). Weather dependent components deal with energy uses that are influenced by outdoor conditions (as heating or cooling). Time and occupancy dependent components are characterized by short term variations (as switching light).

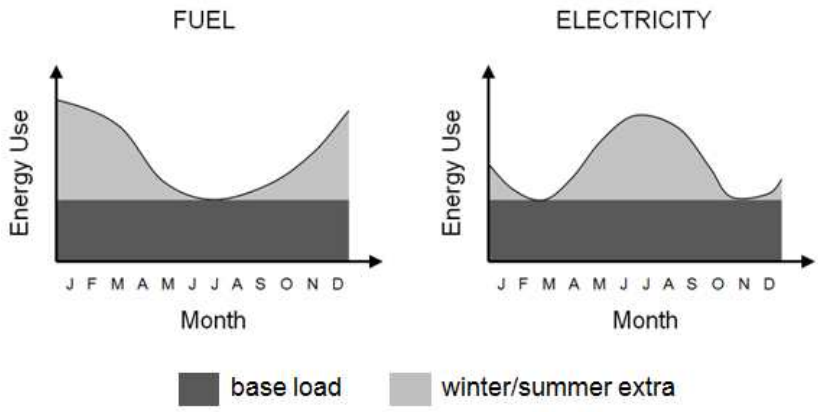

Figure 2: Example of monthly billing data

Utility bills are generally the main source of information about the actual energy performance of the building. Usually, fuel consumption is easily obtained from monthly gas/oil bills even if some attention has to be given to the billing periods which not always correspond to calendar. Based on these data, monthly heating demands of the building can be estimated and the thermal signature of the building can be calculated (Figure 3). This allows identifying the base load (corresponding to DHW production, energy wasting due to standby operation …) and the weather dependent load (corresponding to heating and humidification).

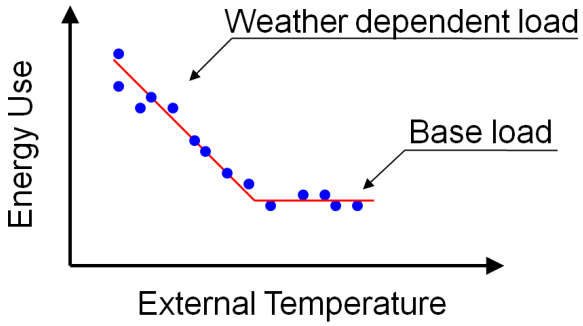

Figure 3: Energy signature

Analysis of electricity bills is more difficult because of the important number of components hidden behind the very global measured monthly consumption. A first step in the analysis would be to estimate separately some components of the total energy use. The energy consumed by lights and electrical appliances (computers...), can be identified by prediction, consisting in making some assumptions and using information about operation profiles and installed capacities.

The remaining electricity consumers should be more directly related to the HVAC system of the building (fans and pumps) and to cooling demand (chillers).

If the cooling demand identification succeeds, a cooling energy signature can be built, as for heating consumption. A correlation can be made based on dry or wet bulb outdoor temperatures. If a better regression is obtained with wet bulb data, the cooling demand signature can be seen as an indication that a significant part of the cooling demand can be attributed to dehumidification. However, considering that, in most of the European countries, HVAC chillers corresponds to 5 to 10% of the total electricity consumption (AUDITAC, 2007), no significant correlation can be expected between the global electricity consumption and the outdoor climate. Moreover, even if the chiller consumption can be identified or measured, it cannot be correlated with a unique climatic variable because cooling demand is generally strongly influenced by internal generated loads and building dynamics.

The auditor must note that the analysis of air conditioning performances using global energy bills will be accurate only if the share of air conditioning energy consumption in the bill is significant. If energy consumption for cooling is totally hidden behind the other energy uses, accurate estimation will be impossible without sub-metering or simulation (AUDITAC, 2007).

Frequently, global monthly consumptions are insufficient to allow an accurate understanding of the building's behaviour. Even if some very rough results can be expected from the analysis of monthly fuel consumption, global electricity consumption records analysis does not allow distinguishing the energy consumption related to AC from the consumption related to other electricity consumers.

While the analysis of the energy bills does not allow accurately identifying the different energy consumers present in the facility, the consumption records (among other information) can be used to to check the adjustment of the parameters of whole-building and system simulation models. Then, the adjusted baseline model can be used to perform various analysis of the building energy use and help in the disaggregation of the global energy consumption of the facility (quantification of specific heating and cooling needs, per HVAC component and/or building zone; electricity consumption disaggregation…). Usually, the developed model is then used to evaluate selected ECO's. The application of building simulation models has been developed several times in the literature (Adam et al., 2006; Hutton et al., 2006; Bertagnolio et al., 2010).

1.2.2.3. Evaluation of ECO's

The evaluation of selected Energy Conservation Opportunities consists in calculating the energy saving related to the studied improvement. It is difficult to estimate these energy savings only by quick hand calculations and more complete calculations, similar to design calculations, are often required in order to assess the performance of the system after modification. Generally, the evaluation of the ECO's has also to be made in terms of comfort, side effects and interactions with other components of the facility.

An easy way to evaluate the chosen ECO's is to implement them on an adjusted simulation model and to compute the comfort variables (temperature, humidity and air quality) and the theoretical energy saving made during a typical meteorological year.

In practice, it is believed that a "well-calibrated" model, able to represent the pre-retrofit situation, is also able to represent the post-retrofit situation. So, ECOs are usually evaluated by arbitrarily modifying the input-file of the model, in order to represent the effects of the retrofit action (Carriere et al., 1999; Pan et al., 2007). This method, among others, is prescribed by the main performance measurement and verification protocols but only rare information is available about its validity.

Since the evaluation of ECO's often consists in the preliminary stage of retrofit process, risk assessment is a critical issue. Such risk analysis is especially necessary for Energy Service Companies (ESCOs) in order to manage risk in retrofit investments (Heo, 2011). Quantifying underperforming risk is particularly important in the case of large-scale/high-cost retrofits requires uncertainty quantification. As it is often considered at the design stage (de Wit, 2002; Hopfe and Hensen, 2011), the study of uncertainty on the simulation outputs is also very important when computing energy savings.

1.3. ENERGY PERFORMANCE MEASUREMENT AND VERIFICATION

The verification of energy performance improvements consists in the assessment of the new (improved) situation by comparing pre and post modification energy consumptions. This comparison requires the evaluation of the amount of energy which would have been consumed if there had no modification (the "adjusted-baseline energy") and the amount of energy which is/should be used after the implementation of the Energy Conservation Opportunity (the "post retrofit energy use", Figure 4).

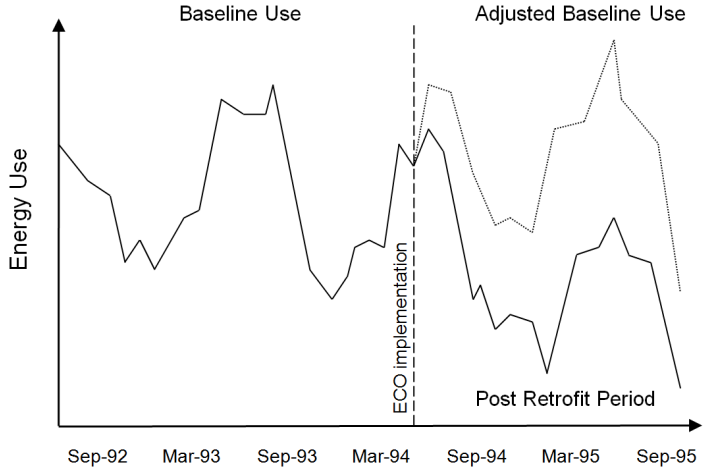

Figure 4: Determining savings (adapted from ASHRAE, 2002)

Three major guidelines provide guidance for energy performance measurement and verification (M&V):

- The International Performance Measurement and Verification Protocol (IPVMP; EVO, 2007)
- The ASHRAE Guideline 14-2002 on Measurement of Energy and Demand Savings (ASHRAE, 2002)
- The M&V Guidelines for Measurement and Verification for Federal Energy Projects (FEMP; US DOE, 2008)

M&V protocols are generally used by energy performance contractors, facility managers and designers. The M&V process consists of using measurements to reliably evaluate savings generated within a given facility by an energy management program.

Good M&V practice is defined in the IPMVP (EVO, 2007) as:

- Accurate: accurate and rigorous estimation of the M&V costs and savings,
- Complete: all the effects of the implemented program have to be evaluated,
- Conservative: savings should be under-estimated by the calculation,
- Relevant: the estimation of the savings should be based on the measurement of the performance parameters of concern,
- Transparent: all M&V activities should be clearly and fully disclosed.

The main M&V standards (EVO, 2007; ASHRAE, 2002 and USDOE, 2008) mention four options for quantification of savings. They differ in their ways of measuring the actual energy use and demand quantities to be used in savings determination. The three protocols consider the use of calibrated BES models as a possible mean to evaluate savings achieved by energy conservation opportunities and provide information about modeling requirements and accuracy criteria (depending on the type and frequency of the data used to perform calibration) but no guidance to perform calibration. Generally, the four M&V options that are considered are:

- A and B: Retrofit isolation/ All or Key parameter approaches – savings are determined by field measurement of the key or all the performance parameter(s) which define the energy use of the ECO's affected system(s) (e.g. lighting, chiller, boiler…) by means of specific meters. ECO-affected systems (or sub-systems) are then isolated from the rest of the facility.
- C: Whole facility approach – Savings are determined by measuring energy use at the whole facility or sub-facility level (e.g. use of monthly utility bills)
- D: Calibrated simulation approach – savings are determined through simulation of the energy use of the whole facility, or of a sub-facility. A model of the pre-retrofit conditions is constructed and checked against actual measured energy use and used to predict energy use of the pre- and post-retrofit conditions.

The four methods have the following common requirements:

- The selection and the study of relevant independent variables influencing the performance of the energy-using system under study (e.g. weather, occupancy…)
- The selection of the baseline period to represent the energy behavior of the installation in pre-retrofit conditions
- The documentation of the baseline conditions in terms of occupancy patterns, operating schedules, setpoints and performance…
- The definition of the evaluation/reporting (post-retrofit) period in order to encompass all operating modes of the retrofitted system, span the full range of the relevant independent variables and provide a satisfying level on accuracy
- The selection of the measurement equipments if used
- The collection of on-site weather data

- The normalization of the calculated savings to a selected common set of conditions to allow comparison between pre- and post-retrofit performance
- The calculation of savings uncertainty.

As stated in IPMVP (EVO, 2007), the calibrated simulation approach (option D) is particularly useful when specific on-field measurements to quantify a given ECO are too difficult or costly and when reporting-period energy data are unavailable or obscured by factors and influences that are difficult to quantify or characterize (such as building occupancy, operation...).

M&V protocols generally advice to use measurements-based approaches in priority. However, considering that on-field measurements are generally expensive and time-consuming, the whole-building simulation approach appears, once again, as an attractive solution, especially if a calibrated model is under construction (or has already been constructed) to support energy performance analysis during another step of the energy service process (such as inspection/audit).

Nevertheless, the advantages of measurements-based methods should not be neglected and a well-balanced approach, combining simulations and measurements, should be set up. So, in order to stick to the reality and (cross-) check the validity of the approach, it seems useful to combine the simulation-based approach with at least partial and/or short-terms on-field measurements. These issues will be discussed in details in the second part of this thesis.

1.4. CONTINUOUS AND LIFETIME/ON-GOING COMMISSIONING

As pointed by Reddy (2006), in addition to identification, selection and evaluation of ECOs and related savings, calibrated whole-building simulation models are also commonly used:

- To help building's owners in understanding patterns in thermal energy and electricity use of their building;
- To disaggregate the electricity consumption of a building by identifying the fraction of the whole electricity use dedicated to plug loads, lighting, fans, pumps, humidification…

Lifetime commissioning or ongoing commissioning consist in continuous performance verification in order to maintain, improve and optimize the performance of building systems during building operation and occupancy (Legris, Milesi Ferretti and Choinière, 2010).

Various methods and procedures are generally used during commissioning processes: manual commissioning methods (checklists...), functional performance testing methods, BEMS-based (Building Energy Management System) commissioning methods and simulation-based methods (Lin and Claridge, 2009).

Achard et al. (1999) propose an on-going verification method based on the use of adjusted energy signatures. Predictive or adjusted signatures are used to assess the energy use of the building and highlight possible degradations of the energy performance of the building. Despite of the simplicity of such models, implementations are quite rare. Indeed, as mentioned above, usually available billing data (monthly utility bills) do generally not allow accurate-enough adjustment of such models.

Among others, global simulation can be used in real time to "emulate" building energy management systems (Lebrun and Wang, 1993). Claridge (2004) mention the following applications of whole-building simulation models as part of the on-going commissioning process:

- Use of as-built (design) simulation for on-going commissioning of an operated building. Significant deviations between measured and predicted performance can be considered as clues to identify problems in the building.

- Develop and run calibrated simulation models (after new or retro-commissioning) and compare predicted consumptions with measured consumptions at some interval (monthly to annually) in order to alarm when building performance decreases.
- Embed (preferably) calibrated model in the BEMS to run on-line simulation and allow direct comparison between predicted and actual energy performance

More detailed and specific models of HVAC components may also help a lot in the commissioning process, among others for functional performance testing (Visier and Jandon, 2004). These detailed models may also be used to support daily system management, among others for fault detection and diagnosis (Jagpal, 2006).

Calibrated models, either embedded or not, appear as the most rational and useful use of whole-building energy simulation in the commissioning process. Results generated by means of non-calibrated models are more difficult to analyze and sometimes not meaningful. Moreover, considering the time (and the related costs) needed to construct such a model and the opportunity to integrate all the influences and variables that have to be considered in the commissioning process into one unique approach, the use of a calibrated model appears as a rational decision. However, a distinction has still to be done between "global" (whole-building) approaches, as prescribed by Claridge (2004), and specific/detailed approaches relying on functional performance testing or fault detection. Indeed, simulation models used in these two types of applications are generally different (in terms of level of details) and require different types/levels of adjustment because of the very different objectives of the two approaches and the difference between available measurement data (i.e. global billing data vs local hourly or sub-hourly performance monitoring).

2. CALIBRATION OF BUILDING ENERGY SIMULATION MODELS

2.1. DEFINITION

As explained above, early developments of simulation tools were mostly oriented towards supporting system design, i.e. mainly the selection and sizing of HVAC components. More recently, with the development of modern simulation tools, it appeared that whole-building simulation may help at all the levels of an energy efficiency service process, from inspection audit to last retrofit and on-going commissioning actions. Indeed, today, the simulation bottleneck is no longer the computer, but the understanding of the user. Simulation models have therefore to be designed according to what is expected from the simulation and to the information actually available, in such a way to make easier this understanding.

Because of the difficulties to face in practice (limited time, bad knowledge of the simulation package…), lots of users of building simulation models are inclined to short-cut the process when using whole-building simulation models and limit the use of BES models to comparison of design or retrofit scenarios. Recent developments and uses of simulation tools showed that accurate models of existing buildings can be developed (Waltz, 2000). Moreover, even if comparative simulations are often useful to evaluate ECOs, they are not valuable if the baseline model is grossly inaccurate (i.e. badly calibrated).

Ahmad and Culp (2006) have developed a blind time-limited test protocol to evaluate the range of discrepancies encountered when using uncalibrated simulations. Two time limits were arbitrary defined to simulate the building in the realm of usability by industry. Level 1 modeling was mainly based on available design data while Level 2 modeling included as-built and operating information obtain from the maintenance personal. Simulated and recorded energy use data for four buildings were then compared. Discrepancies of +/- 30% were observed when comparing recorded and simulated total

energy uses of the buildings. For individual components such as chilled water or hot water consumptions, discrepancies exceeded +/- 90%. The authors also pointed out the importance of operation and occupancy when trying to calibrate a BES model. If the simulations do not adequately represent the real operation of the considered building, improving the level of detail in the representation of the envelope, schedules and mechanical equipment may not improve the prediction capabilities of the simulation.

So, using BES models to help in understanding the thermal behavior of an existing situation requires the BES model to be able to closely represent the actual behavior of the building under study. So, except for benchmarking purposes, adjustment of the model parameters is generally needed when applying a simulation tool to a real case whatever the level of analysis is (inspection/audit, evaluation of ECO's or continuous performance analysis).

The fitting of a BES model to an existing situation involves using as-built information, survey observations and short and/or long term monitoring data to iteratively adjust the parameters of the BES model. Of course, basic data as building envelope characteristics or the type of HVAC system are easily identified but lots of parameters, such as, among others, actual ventilation flow rate and actual use of lighting and appliances, have to be properly adjusted. This definition of the calibration process leads to numerous questions:

- What are the initial objectives of the calibration? What is the calibrated BES model intended for? What are the benefits and the limitations of the calibrated model?
- Which level of details is required for the model? Which type of BES model should be used?
- How should we proceed to adjust the parameters of the model? On which parameters should we focus?
- Which type of data should we gather from the building and which difficulties do we have to face? What are the time-step and the accuracy of the measurements?
- Which level of accuracy do we need to reach? How can we define "accuracy" of the calibration? How much are we confident in the quality of the calibration and what are the abilities of the calibrated model? Does it match with the pre-defined objective (control optimization, ECOs evaluation...)?
- To what extent can we trust the calibrated model? Are the results valuable and how to define/quantify uncertainty on the results?

Of course, each use of a calibrated model involves specific requirements in terms of modeling capabilities, data gathering, parameters adjustment process, level of accuracy depending on what the final calibrated model is intended for. As an example, Liu and Claridge (1998) present an example of use of a calibrated simplified HVAC system model for optimization purposes. This use of calibrated model involved development of a tailored HVAC system model of the component under study, able to simulate the actual control strategy and make efficient use of specific available monitoring data (e.g. hot and chilled water demands at the system component level) to proceed to calibration. The developed calibrated model was then used for fault detection purposes and to develop optimized HVAC control strategies.

2.2. BENEFITS AND LIMITATIONS OF CALIBRATED BUILDING ENERGY SIMULATION MODELS

The use of calibrated building energy simulation models has numerous limitations and benefits. ASHRAE (2002) provides useful remarks about when calibration should be used in priority for ECOs evaluation:

- Pre or post-retrofit whole-building metered data are not available (making evaluation of ECOs impossible) or are available but savings from individual retrofits are desired;
- Savings cannot be estimated using measurements only;
- It is impossible to isolate the effects of the retrofit and interactions should be taken into account;

When performing energy inspection/audit, calibrated models have shown their usefulness to help in identifying important influences and disaggregating whole building energy use (Bertagnolio et al., 2010).

Assuming that a computerized building model is constructed in a good way (i.e. by addressing all the questions mentioned above, one by one), a considerable number of benefits can also be expected from the use of building simulation (Waltz, 2000):

- Confirm the user's knowledge of the building: Constructing the model constrains the modeler to review all the characteristics of the installation (types of equipment, installed power/capacity, performance, operating profiles…)
- Identifies ECOs: Frequently, the calibration is made difficult by undiscovered over-consumptions due to some equipments operating out of control. These elements generally correspond to elementary and very cost-efficient energy conservation opportunities. The calibration of the model and the need to represent the whole-building energy use force the modeler to identify such problems.
- Documents the baseline conditions: A well documented calibrated model is generally a complete and detailed statement of the actual conditions. Raftery et al. (2011) applied this principle and provided a very detailed calibrated model of the installation as well as a complete documentation describing all the steps and intermediate runs of the calibration process.

However, the use of calibrated simulation models has also an important number of limitations.

A first limitation relies in the use of a model itself. Whatever the intended use of the calibrated model, the method employed to build it and the achieved level of accuracy, building energy simulation models remain an abstraction of a certain reality and have numerous limitations. Building energy modeling of course leads to neglect some physical effects influencing the building energy use. Even if a detailed work has been carried out in order to select the main influences and validate the model through comparison with other "reference" models or empirical results, the validation results cannot be considered as an absolute proof of the reliability of the model. In practice, it is often erroneously believed that detailed model (able to simulate numerous physical influences) have better capabilities than simple ones. In fact, when calibrating a model to a real case, multiplying the number of effects/influences makes the adjustment process more complex and increases the risk to lead to high uncertainty (Purdy and Beausoleil-Morrison, 2001) because:

- The number of parameters to adjust is highly increased,
- Lots of parameters will be set to default values without the insurance that they are not influential in the considered case,
- The understanding of the software package by the user is decreased.

So, a compromise will have to be found between model accuracy, reliability, flexibility and simplicity when selecting/developing the BES model.

A second limitation relies on the availability of the data used to check the validation and the achieved level of accuracy. The most common application of calibrated BES models is the evaluation

and the comparison of ECOs (Kaplan et al., 1990, Chen et al., 2006, Pan et al., 2007, Cho and Haberl, 2008a and 2009, Katipumala and Claridge, 1993). Of course, evaluating ECOs requires the model to be sufficiently detailed to simulate the change related to a given ECO (e.g. sufficient representation of the envelope when evaluating the renovation and the insulation of a wall) and sufficiently sensitive to the influences related to the considered ECOs (e.g. sensitivity to climate when evaluating envelope improvement). Supposing the model sufficiently (but not too much) detailed, annual and monthly consumption data are generally used and considered as sufficient to check the validity of the calibration.

In 1994, Reddy et al. shown some comparisons between recorded and predicted energy performance in pre-retrofit and post-retrofit situations. By comparing predicted and recorded energy use during the post-retrofit period, the authors demonstrated that their carefully calibrated model was reliable enough to predict the retrofit savings. They concluded that the most critical step in accurately determining retrofit savings was the development of a complete and accurate pre-retrofit simulation model (i.e. the construction of a calibrated model).

Kaplan et al. (1990) have shown that, even if the calibration seemed to be successful, the finely calibrated model was not necessarily able to ensure an accurate analysis of ECOs because of lack of data on the pre-retrofit situation and use of an “imaginary” baseline building. The authors conclude that, when having to evaluate ECOs after their implementation, it is better to monitor the building before the implementation of the ECOs or with the ECOs turned off to evaluate accurately the related energy savings.

Westphal and Lamberts (2005) confirm that even if a first rough calibration can lead to a good estimation of annual and monthly energy needs, there is often no guarantee that the end-use composition (lighting, HVAC…) is near the reality. In this case, the retrofit study can result in wrong conclusions.

This highlights the “**identifiability problem**”, i.e. the inability to identify a unique solution set for all the parameters since the problem is largely under-determined (large amount of parameters to calibrate vs limited amount of data points). So, it is mandatory to first reduce the order of the model by fixing the less influential parameters to selected “best-guess values” and then calibrate the remaining parameters (Reddy and Maor, 2006). This process is commonly designated as “Factor Fixing”.

Considering these observations, it also seems obvious that calibrated simulation models cannot be considered as the panacea and have to be combined with measurements-based techniques in order to allow a global understanding of the energy use of the facility and check the validity of the calibrated model. Indeed, checking the validity of a calibrated by means of utility billing data is generally not sufficient and cross-checking by means of additional measurements is needed (Reddy and Maor, 2006).

The third limitation is related to the accuracy of the available data. It is necessary to put the question of the accuracy of the model and the data into perspective. As prescribed by Waltz (2000), it is not realistic to try to provide a 1% answer to a 10-15% question. Indeed, knowing that numerous influences have not been considered during the modelling or the calibration process and that available measured data are characterized by a given uncertainty (e.g. due to measurement errors and approximate knowledge of the billing periods), it is generally useless to try calibrating a simulation model with an accuracy better than 5%.

A fourth limitation is linked to the building modeler him/herself. Kreider and Haberl (1994) have shown that, for a determined amount of available data about a given installation, whatever the employed modeling technique, very high and very poor quality simulation results can be obtained

depending of the modeler. This study highlighted the very important influence of the modeler's skills which is one of the main reservations with the widespread use of calibrated models (Reddy and Maor, 2006). This last reservation implies that calibration is more an art than a science/technique and that the results are analyst-specific.

In addition to the limitations mentioned above, ASHRAE (2002) recommends to avoid the calibration approach when:

- ECOs could be analyzed without building simulation;
- The building cannot be simulated (presence of large atriums, underground buildings, complex shading configurations…);
- The HVAC system cannot be simulated (certain control options cannot be represented…);
- The retrofit cannot be simulated;
- Project resources and financial issues are insufficient to support development and use of calibrated simulation.

3. OBJECTIVES OF THE THESIS

Considering the limitations mentioned above, it appears as crucial to develop robust simulation models adapted to the final objective (e.g. energy services activities including: inspection/audit, evaluation of ECO and on-going energy performance diagnosis), as well as systematic and impartial calibration methodologies minimizing the impact of the user's experience, supporting data collection and exploiting all the available information. Such methodology and tool should be able to support the energy efficiency service process while taking advantage of the benefits brought by the use of energy simulation models.

The objective of the present work is the development of a simulation-based approach dedicated to whole-building energy use analysis for use in the frame of an energy efficiency service process. Focus will be given to the development and the calibration of a simulation tool dedicated to the steps of the energy efficiency process requiring energy performance diagnosis of the existing situation, i.e.:

- Energy end use breakdown and analysis at inspection and audit stages;
- ECOs evaluation and post-retrofit performance M&V;
- Whole-building level on-going/continuous commissioning.

A special attention will be paid to the integration of the calibration process into the early stages of the Energy Service Process and to energy end-use analysis. The proposed calibration methodology is deeply related to on-field inspection and data collection issues and is developed to fit with the audit/inspection process.

After calibration, the model should be able to support the other steps of the Energy Services Process, such as ECOs selection and evaluation and continuous performance verification. These issues will not be studied in details within the present work and focus will mainly be given to the construction of the calibrated model.

Other stages such as benchmarking and HVAC component operation optimization and fault-detection will not be studied neither since they do not require particular adjustment of the model's parameters (benchmarking) or require the use of detailed and specific (tailored) simulation models and measurement data (functional performance testing, fault detection...).

Modeling, methodology, data gathering, accuracy and uncertainty issues for the present application of calibrated models are addressed hereunder. Modeling and methodological issues are discussed in the

first chapters. Applications of the developed model and calibration method are presented in the two last chapters.

Chapter 2 starts with a presentation and a comparison of existing software packages and modeling practices. Then a new simplified building energy simulation model for use in the frame of the energy efficiency service process and specifically dedicated to existing buildings energy use analysis (and so, to calibration too) is described. The level of details of the proposed model is established as a function of the needs and the objective of its use (i.e. whole-building level energy performance analysis). This model is composed a series of validated sub-models of building and HVAC system components. In order to check its implementation, the validation of the building zone energy simulation model is briefly presented.

Chapter 3 includes a review of the main calibration issues. Existing calibration methods presented in the literature are compared and criticized in order to address the following questions:

- How should we proceed to adjust the parameters of the model? On which parameters should we focus?
- Which type of data should we gather from the building and which difficulties do we have to face? What are the time-step and the accuracy of the measurements?
- Which level of accuracy do we need to reach? How can we define “accuracy” of the calibration? How much are we confident in the quality of the calibration and what are the abilities of the calibrated model? Does it match with the pre-defined objective ?
- To what extent can we trust the calibrated model? Are the results valuable and how to define/quantify uncertainty on the results?

Data collection and analysis, sensitivity and uncertainty issues are also discussed. Finally, a new evidence-based calibration method, to be used with the previously presented BES model and including sensitivity and uncertainty issues, is presented.

Chapter 4 concerns the integration of sensitivity and uncertainty issues (discussed in Chapter 3) within the calibration process. Most common sensitivity analysis techniques are presented and compared. The “Elementary Effects” method is then selected and applied to two typical base case buildings defined according to available statistical data in order to be representative of the actual building stock in Belgium. The results of this preliminary sensitivity analysis are discussed and put into perspective with the developed evidence-based calibration methodology. The LHMC (Latin Hypercube Monte Carlo) sampling method is also described and selected to run post-calibration uncertainty analyses.

A first application of the developed calibration process and building energy simulation model is presented in Chapter 5. A virtual calibration test-bench consisting in a very detailed model of a typical building (also called a “building emulator”) implemented in Trnsys (Klein et al., 2007) is used to assess the proposed calibration methodology and discuss measurement and accuracy issues.

The sixth chapter presents the application of the proposed calibration methodology to an existing building located in Brussels (Belgium). The whole evidence-based method is applied step-by-step and intermediate and final results are discussed. Retrofitting and continuous-commissioning issues will only be mentioned but will not be developed since no post-retrofit/ post-implementation data are available.

General conclusions about the present work and perspectives for future research are drawn in the last chapter.

4. REFERENCES

Achard, G., Eveno, P., Blanc, E., Souyri, B. 1999 Caractérisation thermique des bâtiments tertiaires occupés à l'aide de leur signature énergétique. IVème colloque Interuniversitaire Franco-Québécois, Montréal, Québec, CA.

Adam, C., André, P., Hannay, C., Hannay, J., Lebrun, J., Lemort, V., Teodorese, I.V. 2006. A contribution to the audit of air-conditioning system: modelling, simulation and benchmarking. Proceedings of the 7th System Simulation in Buildings conference, SSB 2006, Liège, Belgium.

Adnot, J. et al. 2003. Energy Efficiency and Certification of Central Air Conditioners (EECCAC) final report. Directorate General Transportation-Energy of the Commission of the European Union.

Adnot, J. et al. 2007. Field benchmarking and Market development for Audit methods in Air Conditioning (AUDITAC) final report.

Ahmad, M., Culp, C.H. 2006. Uncalibrated Building Energy Simulation Modeling Results. HVAC&R Research, vol. 12, Nr. 4, pp. 1141-1155.

Alexandre, J.L., Knight, I., André, P., Hannay, C., Lebrun, J. 2006. About the audit of air conditioning systems: Customer advising with the help of case studies and benchmarks, modelling and simulation. Proceedings of the Improving Energy Efficiency in Commercial Buildings conference, IEECB 2006, Frankfurt, Germany.

ASHRAE. 2002. ASHRAE Guideline: Measurement of energy and demand savings. ASHRAE Guideline 14-2002.

ASHRAE. 2004. Procedures for Commercial Building Energy Audit. American Society of Heating, Refrigerating and Air-Conditioning Engineers, Inc.

Bannister, P., Hinge, A. 2006. Empirical Benchmarking of Building Performance. Proceedings of the Improving Energy Efficiency in Commercial Buildings conference, IEECB 2006, Frankfurt, Germany.

Bertagnolio, S., Lebrun, J. 2008. Simulation of a building and its HVAC system: Application to benchmarking. Building Simulation: An International Journal. Vol 1. pp 234-250. DOI 10.1007/s12273-008-8219-4

Bertagnolio, S., Andre, P., Lemort, V. 2010. Simulation of a building and its HVAC system: Application to audit. Building Simulation: An International Journal. Vol 3. pp 139-152. DOI 10.1007/s12273-010-0204-z

Bleil de Souza, C., Knight, I., Marsh, A., Dunn, G. 2006. Modelling Buildings for Energy Use: a Study of the Effects of Using Multiple Simulation Tools and Varying Levels of Input Detail. Proceedings of the Improving Energy Efficiency in Commercial Buildings conference, IEECB 2006, Frankfurt, Germany.

Boysen, A. 1987. Source book for energy auditors. International Energy Agency – Energy Conservation in Buildings and Community Systems Programme Annex 11 "Energy Auditing" final report. www.ecbcs.org

Carriere, M., Schoenau, G.J., Besant, R.W. 1999. Investigation of some large building energy conservation opportunities using the DOE-2 model. Energy Conversion and Management, 40, 861-872.

Chen, C., Pan, Y., Huang, Z., Wu, G. 2006. Energy consumption analysis and energy conservation evaluation of a commercial building in Shanghai. Proceedings of the 6th International Conference on Enhanced Building Operation, Shenzhen, China.

Cho, S., Haberl, J. 2008a. Development of a simulation toolkit for the selection of high-performance systems for office buildings in hot and humid climates. Proceedings of the third National Conference of IBPSA-USA, Berkeley, California.

Cho, S., Haberl, J.S. 2009. Development of a high-performance office building simulation model for a hot and humid climate. Proceedings of the 11th IBPSA Conference, Glasgow, UK.

Claridge, D.E. 2002. Using whole building simulation models in commissioning. IEA-ECBCS Annex 40 working paper. Available at http://www.commissioning-hvac.org/files/doc/A40-D2-M4-US-TAMU-02.pdf

Claridge. D.E. 2004. Using Simulation Models for Building Commissioning. Proceedings of the ICEBO Conference, Paris, France.

De Wit, S. 2001. Uncertainty in predictions of thermal comfort in buildings. PhD Thesis, Delft University of Technology.

Directorate-General for Energy and Transport. 2007. 2020 Vision: Saving our energy. Available at http://ec.europa.eu/energy/action_plan_energy_efficiency/doc/2007_eeap_en.pdf

Directive 2002/91/EC of the European Parliament and of the Council of the European Union of 16 December 2002 on the Energy Performance of Buildings (EPBD). Official Journal of the European Communities, 4 January 2003.

Directive 2006/32/EC of the European Parliament and of the Council of the European Union of 5 April 2006 on energy end-use efficiency and energy services. Official Journal of the European Communities, 27 April 2006.

Efficiency Valuation Organization. 2007. International Performance Measurement and Verification Protocol (IPMVP). Concepts and Options for Determining Energy and Water Savings – Volume 1.

EN 15900:2010. Energy efficiency services – Definitions and requirements.

EN 16001:2009. Energy management systems – Requirements with guidance for use.

Haberl, J., Culp, C., Yazdani, B. Development of a web-based, code-compliant 2001 IECC Residential simulation for texas. Proceedings of Building Simulation 2009, Glasgow, UK.

Heo, Y. 2011. Bayesian calibration of building energy models for energy retrofit decision-making under uncertainty. PhD Thesis, Georgia Institute of Technology.

Hopfe, C., Hensen, J.L.M. 2011. Uncertainty analysis in building performance simulation for design support. Energy and Buildings, 43: 2798-2805.

Hutton, A., Good, J., Frisque, A., Furlong, J. 2006. Energy modeling of office building for energy audit and retrofit. Proceedings of the 7th System Simulation in Buildings conference, SSB 2006, Liège, Belgium.

Jagpal R (2006). International Energy Agency – Energy Conservation in Buildings and Community Systems Annex 34 : Computer Aided Evaluation of HVAC System Performance. Synthesis Report. www.ecbcs.org

Katipumala, S., Claridge, D.E. 1993. Use of simplified system models to measure retrofit energy savings. Journal of Solar Energy Engineering, vol. 115, pp. 57-68.

Kaplan, M.B., McFerran, J., Jansen, J., Pratt, R. 1990. Reconciliation of a DOE2.1c model with monitored end-use data for a small office building. ASHRAE Transactions. 11 (1):981-993.

Klein, S.A., 2007. TRNSYS 16 Program Manual. Solar Energy Laboratory, University of Wisconsin, Madison, USA

Knight, I. 2011. iServ project: Inspection of HVAC systems through continuous monitoring and benchmarking. http://www.iservcmb.info/

Kreider, J., Haberl, J. 1994. Predicting Hourly Building Energy Usage: The Great Energy Predictor Shootout: Overview and Discussion of Results, ASHRAE Transactions-Research, Vol. 100, Pt. 2, pp. 1104 - 1118 (June).

Lebrun J, Liebecq G (1988). International Energy Agency – Energy Conservation in Buildings and Community Systems Annex 10: Building HVAC System Simulation. Synthesis Report. www.ecbcs.org

Lebrun J, Wang S (1993). International Energy Agency – Energy Conservation in Buildings and Community Systems Annex 17: Building Energy Management Systems – Evaluation and Emulation Techniques. Synthesis Report. www.ecbcs.org

Legris, C., Milesi Ferretti, N. and Choinière, D., 2010. International Energy Agency – Energy Conservation in Buildings and Community Systems Annex 47: Cost effective commissioning of existing and low energy buildings. Report 1: Commissioning overview. www.ecbcs.org

Lin, G. And Claridge, D.E. 2009. Retrospective Testing of An Automated Building Commissioning Analysis Tool (ABCAT). Proceedings of the 3rd International Conference on Energy Sustainability ASME, San Francisco, USA.

Liu, M., Claridge, D.E. 1998. Use of calibrated HVAC system models to optimize system operation. Journal of Solar Energy Engineering. 120:131-138

Pan, Y., Huang, Z., Wu, G. 2007. Calibrated building energy simulation and its application in a high-rise commercial building in Shanghai. Energy and Buildings, 39, 651-657.

Perez-Lombard, L., Ortiz, J., Pout, C. 2008. A review on buildings energy consumption information. Energy and Buildings 40, 394-398.

Purdy, J., Beausoleil-Morrison, I. 2001. The significant factors in modeling residential buildings. Proceedings of the seventh International IBPSA conference, Rio de Janeiro, Brazil.

Raftery, P. Keane, M., Costa, A. 2009. Calibration of a detailed simulation model to energy monitoring system data: a methodology and case study. Proceedings of the 11th IBPSA Conference, Glasgow, UK.

Reddy, S.N., Hunn, B.D., Hood, D.B. 1994. Determination of retrofit savings using a calibrated building energy similation model. Proceedings of the Ninth Symposium on Improving Building Systems in Hot and Humid Climates, Arlington, TX.

Reddy, T.A. 2006. Literature review on calibration of building energy simulation programs: uses, problems, procedures, uncertainty and tools. ASHRAE Transactions, 112(1): 226-240.

Reddy, T.A., Maor, I. 2006. Procedures for reconciling computer-calculated results with measured energy data. ASHRAE Research Project 1051-RP. Atlanta: American Society of Heating, Refrigerating and Air-Conditioning Engineers, Inc.

Roth, K.W., Westphalen, D., Feng, M.Y., Llana, P., Quartararo, L. 2005. Energy impact of commercial building controls and performance diagnostics: market characterization, energy impact of building faults and energy savings potential. Report prepared for U.S. Departement of Energy. TIAX LCC, Cambridge, MA.

US DOE. 2008. M&V Guidelines: Measurements and Verification for Federal Energy Projects, version 3.0

Visier, J.C., Jandon, M. 2004. International Energy Agency – Energy Conservation in Buildings and Community Systems Annex 40: Commissioning of Building HVAC Systems for Improved Energy Performances. Synthesis Report. www.ecbcs.org

Westphal, F.S., Lamberts, R. 2005. Building Simulation Calibration using Sensitivity Analysis. Proceedings of the 9th IBPSA Building Simulation Conference, Montréal, Canada.

CHAPTER 2 DEFINITION AND DEVELOPMENT OF A SIMPLIFIED BUILDING ENERGY SIMULATION MODEL

« Pluralitas non est ponenda sine necessitate »

Guillaume d'Ockham (1285 – 1347)

CHAPTER 2: DEFINITION AND DEVELOPMENT OF A SIMPLIFIED BUILDING ENERGY SIMULATION MODEL 2
1. EXISTING BUILDING ENERGY SIMULATION MODELS 2
1.1. Inverse and Forward Modeling 2
1.2. Static/Dynamic and Single/Multi-Zone Modeling 3
1.3. Simulation Approaches 4
1.4. Simplification of BES Models 4
2. MODELING REQUIREMENTS FOR THE TARGETED WORK 5
3. INPUTS, OUTPUTS AND PARAMETERS 6
4. MODELLING APPROACH 7
5. BUILDING MODEL 9
5.1. Solar radiations and long-wave exchanges 9
5.2. sensible gains 14
5.3. Ventilation and infiltration 16
5.4. Zone thermal model 17
5.5. Zone humidity model 23
5.6. Sensible Building Zone Model validation 23
6. SECONDARY HVAC SYSTEM MODEL 24
6.1. Air handling unit model 25
6.2. Terminal unit model 34
7. PRIMARY HVAC SYSTEM MODEL 36
7.1. Distribution system model 36
7.2. Heating plant model 37
7.3. Cooling plant model 39
8. MOIST AIR PROPERTIES 47
9. AUTOMATED PRE-SIZING 47
10. IMPLEMENTATION 48
11. SUMMARY 48
12. REFERENCES 48

CHAPTER 2: DEFINITION AND DEVELOPMENT OF A SIMPLIFIED BUILDING ENERGY SIMULATION MODEL

1. EXISTING BUILDING ENERGY SIMULATION MODELS

An important issue when starting an energy analysis is the selection of the BES model to use (Krarti, 2000). Depending of the type (residential, school, health...), the size and the complexity of the building to study, the model will have to account for various conditions and attention must be paid to the level of details required to perform the desired analysis. Indeed, since calibration is highly under-determined (large amount of parameters to adjust and limited amount of available data), a first way to limit the complexity of the calibration problem is to carefully select the building model that will be used. As shown below, different criteria can be considered in order to classify BES models.

1.1. INVERSE AND FORWARD MODELING

Basically, inverse and forward modeling techniques should be differentiated:

- Inverse models (Figure 1) are generated basing only on measured data and generally rely on regression analysis (Fels, 1986, Kissock, 2002, Reddy et al., 1999) to deduce representative building parameters (BLC - building load coefficient, building time constant...). Reddy et al. (1999) propose an inverse model parameter identification scheme to estimate building and ventilation parameters from non-intrusive monitoring of heating and cooling energy use. It appears that the identification process is accurate when daily data over an entire year are used to perform calibration of this model. In the frame of the ASHRAE RP-1050 research project and in relation with the ASHRAE Guideline 14-2002, Kissock et al (2002) developed an inverse linear calculation toolkit for the purpose of measuring energy savings. The toolkit includes the algorithms necessary to find the best-fit for three, four and five-parameters change-point models and to evaluate the uncertainty of model predictions.

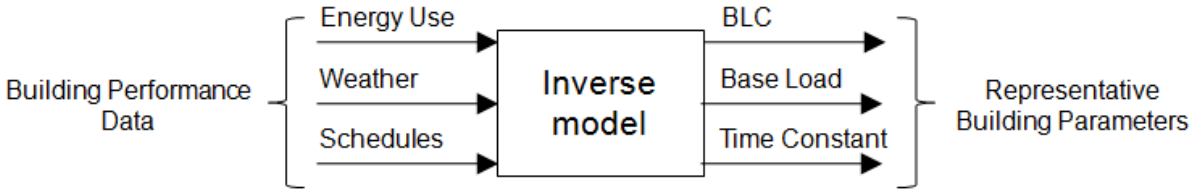

Figure 1: Inverse modeling (Adapted from Krarti, 2000)

- Forward modeling (Figure 2) involves using physical models able to predict the future of a system described by some parameters (geometry, location, nominal performances...). The calibration of such models implies an iterative tuning process of the parameters of the model to match recorded data. The most famous forward building energy simulation platforms are DOE-2 (LBL, 1980), Trnsys (Klein, 2007) and EnergyPlus (US-DOE, 2009).

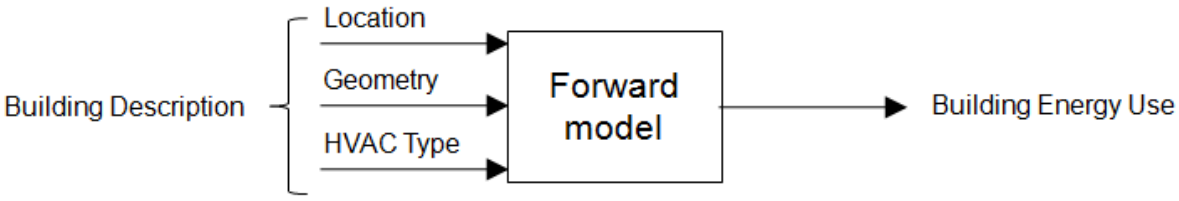

Figure 2: Forward modeling (adapted from Krarti, 2000)

Even if inverse models are generally more simple than forward ones, their flexibility is limited by the representative building parameters used to formulate the model and the accuracy of the recorded data used to calibrate the model. For example, it is not possible to evaluate the impact of replacing an existing chiller by a more efficient one if no parameter of the inverse model deals with chiller performances. On the contrary, forward models are more flexible and rely on physical representations which can be adapted to various situations. Moreover, these models can be continuously updated to take additional influences into account (e.g. developing/implementing a more detailed chiller model to take into account the improvement of part load performance due to the replacement of the chiller). For ECO evaluation purposes, as well as for other applications, forward models are generally preferred to inverse models even if their calibration is often a more complex problem.

1.2. STATIC/DYNAMIC AND SINGLE/MULTI-ZONE MODELING

Secondly, one generally distinguishes static and dynamic BES models, respectively, not able or able to take into account the thermal inertia of the building structure when computing energy balances. Thirdly, single zone and multi zone models can also be compared. The first ones can only simulate the building as a unique zone and cannot consider heat, air and humidity transfers between the different zones of the buildings. Multi zone models can simulate simultaneously a small or large number of zones and allow representing the heat, air and humidity transfers between zones and the simultaneous heating and cooling demands occurring in the building.

Considering only forward models and basing on these two last criteria, Lydberg (1987) have compared BES tools from an auditor's point of view and provide the following comments:

- Static single-zone models, involving a very limited number of parameters and simplified calculations as degree-days calculations, are generally not sufficient for audit of air-conditioned buildings;
- Static multi-zone models are generally appropriate for the evaluation of ECM's related to the building envelope but not adapted to the evaluation of ECM's related to intermittent heating/cooling. These models work with a time step from one day up to one month and give only average values;
- Dynamic single-zone models work with a time step of one hour or less and consider the building interior as uniform. These models can generally predict peak values with an acceptable accuracy and can be used to evaluate ECM's related to air conditioning system. However, multi-zone systems cannot be represented and single-zone hypothesis can lead to bad estimates of the annual heating and cooling loads because of possible compensation;
- Dynamic multi-zone models are the most detailed models and allow very accurate calculation of indoor conditions and heating/cooling demands. Originally, these models were developed for design purposes and they require a detailed description of the building and the coupled system and more efforts to be calibrated to the studied installation (due to the larger number of parameters);

Despite of the supplemental effort needed to calibrate them, dynamic multi-zone models are generally preferred since they are more flexible and can fit to most of the situations that can be encountered in practice. In such models, the HVAC system part is generally represented by static components models since the considered time step is usually equal to one hour which is larger than the time constant of most of the HVAC components. Unfortunately, most of the commercial software packages available on the market have been developed for design purposes and are generally not adapted for (quick and easy) calibration. Indeed, at the design stage, very detailed models (involving numerous parameters) are generally preferred to allow accurate description of the future building/system.

Specific HVAC system models, ranging from simple static to very detailed dynamic models of HVAC components are also used for specific purposes, as HVAC system design, commissioning, fault detection or operation optimization (Katipumala and Claridge, 1993).

1.3. SIMULATION APPROACHES

Reddy and Maor (2006) have also compared the most common "simulation approaches" and distinguish five types of building energy simulation tools:

- Spreadsheet programs ;
- Simplified system simulation method ;
- Fixed schematic hourly simulation programs;
- Modular variable time step simulation programs;
- Specialized simulation programs.

Spreadsheet programs (1) and steady state simplified methods (2) have shown their limits in predicting the energy use of modern buildings. Specialized programs (5) are mostly dedicated to the simulation of particular phenomena (such as contaminants movement, air stratification…). Quasi-steady state fixed schematic hourly simulation (3) programs are generally based on the LSPE (loads - secondary system - primary system - economics) sequential approach. Flexible modular simulation programs (4) are based on more realistic models and take all the interactions (building/system/control) into account.

For energy performance analysis purposes (energy use breakdown and ECMs evaluation), the simple LSPE approach seems sufficient. Studying interactions between control and HVAC components performances and capacities (by means of a modular approach or a specialized simulation program) is needed when optimizing building operation and performing fault detection. However, this requires a more accurate and detailed description of the building, its system and the control laws which generally cannot be expected when proceeding to the energy performance diagnosis of an existing building.

1.4. SIMPLIFICATION OF BES MODELS

Simplification of BES models can also occur at other levels than the number of physical influences taken into account by the model or the calculation approach. Generally, simplified models differ from the detailed ones only in the definition of the building (zone typing, types of walls…) and the HVAC system (HVAC components consolidation/aggregation…) but perform also dynamic building simulations and steady-state system simulations and can provide useful and accurate results. Moreover, it has been highlighted that variances in simulation results among different users are generally larger than those resulting from the use of different (detailed or not) calculation methods (Lydberg, 1987; Liu et al., 2004).

On the building side, Cho and Haberl (2008b) have demonstrated that the use of a simplified box-shaped geometry causes only a very small deviation on the energy consumption results. As-built and

simplified geometry models should be compared in different situations but we can fairly assume that, for common buildings, the use of a box-shaped geometry does not introduce important errors.

Some simplifications are also possible on the HVAC system model side. Liu et al. (2004) propose five rules that should be followed for AHU consolidation (or aggregation):

- The consolidated AHUs should be of the same type (dual-duct, single-duct, VAV, CAV…)
- The consolidated AHUs should serve similar zones (interior zones and/or external zones but no mixing…)
- The AHUs should have similar minimum outside air intake ratios and the same outside air control
- The zones served by the AHUs must have similar occupancies, similar peak loads and similar load profiles
- The consolidated AHU air flow is equal to the sum of each individual AHU's airflow

By following these rules, AHU consolidation can be applied without important loss of accuracy.

These simplifications are often welcome for practitioners since, most of the time, the large amount of input data restricts the simulation programs to researchers. Applying these simplifications in the frame of a calibration process seems to be a rational decision regarding the level of under-determination of the problem. As pointed by Westphal et al. (2005), the development of more friendly tools, customized to user needs, would allow the dissemination of simulation techniques into engineering offices.

2. MODELING REQUIREMENTS FOR THE TARGETED WORK

Regarding modeling requirements, ASHRAE (2002) mentions that only hourly simulation programs can be used for M&V. The simulation tool has to be able to explicitly:

- Simulate thermal mass effects
- Integrate occupancy and operating schedules (for week days and weekends)
- Integrate individual setpoints for different thermal zones and HVAC components
- Use actual hourly weather data (8760 values per year)
- Integrate user-definable performance data for HVAC components

For energy use analysis purposes, the simulation tool must handle with realism:

- building (static and dynamic) response,
- weather loads and internal and occupancy loads and profiles,
- comfort requirements and control/operation strategies (air quality, air temperature and humidity),
- full air conditioning process and characteristics of all HVAC system components (terminal units, Air Handling Units, air and water distribution, heat and cold production units)

These minimal requirements exclude inverse models since they do not allow taking into account physical influences and characteristics of the building/system. Moreover, simulation tools based on average weather data should be avoided since they do not allow using actual weather data, as requested when proceeding to calibration. Taking these facts into account, it seems rational to use a dynamic hourly simulation program allowing integrating all the aspects mentionned before.

However, even if actual control loops cannot be represented in such programs, LSPE-based models seem sufficient for the aimed work (energy use analysis, evaluation of ECMs and on-going global performance control). Of course, increasing the complexity of the model in that way will lead to a more complex calibration work. Fortunately, simplifications such as HVAC component consolidation

can still be envisaged as soon as they do not prevent the identification of important energy consumers, the evaluation of a critical ECM or too important approximation of the actual energy behavior of the system under study.

Most of the existing software packages fulfilling these requirements have been originally developed for design purposes (Trnsys, EnergyPlus,…).and require an important number of parameters to calibrate.

Reddy (2011) recommends the development and the use of building energy simulation models dedicated to application to existing buildings and to calibration. Since a compromise has to be found between model accuracy, reliability, flexibility and simplicity and that no available simulation models answer these questions, it has been decided to develop a new simplified building energy simulation model (Figure 3).

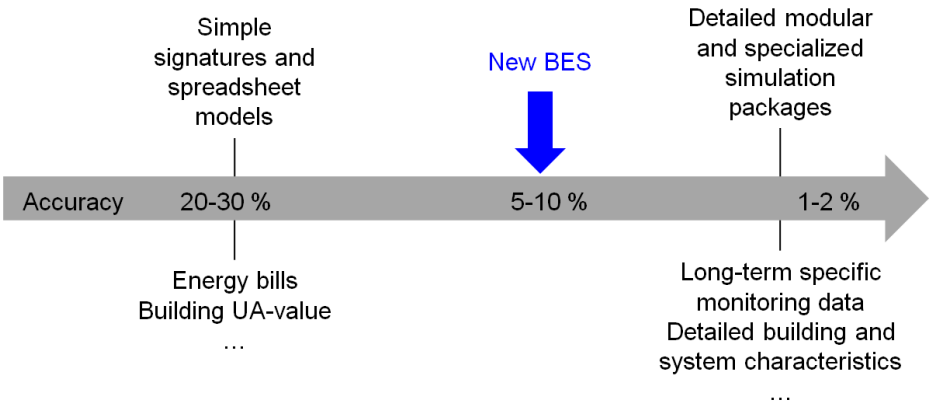

Figure 3: New Building Energy Simulation Model

A quasi-steady state hourly simulation program based on the LSPE sequential approach has been developed in the frame of this work in order to allow easier calibration. This new simplified building energy simulation model is described below.

Simplified but validated modeling methods for building envelope and HVAC components have been used during the development of this tool. At each step of the development process, special attention has been paid to:

- using of simple, robust and validated models for building components as well as systems,
- avoiding the implementation of unnecessary details which could lead to important uncertainty (Purdy and Beausoleil-Morrison, 2001),
- relying on relevant, physically meaningful and identifiable parameters allowing robust and efficient calibration work (regarding the data commonly available to conduct calibration).

The ventilation, heating, cooling and latent needs computed at the zone level are summed and converted into system loads and then, into final energy consumptions. Capacity limits are taken into account to simulate the interactions between the building and the secondary HVAC system but controllers are supposed to be perfect (no inefficiency of the control). This approach allows minimizing the number of iterations needed to simulate the performance of the building and its system and is generally considered as sufficiently accurate when computing global energy use of a building.

3. INPUTS, OUTPUTS AND PARAMETERS

The outputs, inputs and parameters are selected according to the specific needs of the user (i.e. the auditor/inspector). As in Trnsys for instance (Klein et al., 2007), the parameters are here defined as

selected inputs which are not supposed to vary during the simulation. All the inputs/outputs/parameters have been classified regarding the 6 influence factors identified in the IEA-ECBCS Annex 53 project:

1. Climate,
2. Building envelope,
3. Building services and energy systems,
4. Building operation and maintenance,
5. Occupants' activities and behavior,
6. Indoor environmental quality provided.

The main outputs of the tool presented here are:

- Hygro-thermal comfort achievements: temperature, humidity, predicted percentage of dissatisfied (PPD), and predicted mean vote (PMV) on a zone basis;
- Global power and energy consumptions : Fuel/Gas and Electricity consumptions;
- HVAC components specific loads and consumptions
- Performance of the mechanical equipments: instantaneous or seasonal values of COP, efficiencies...

As shown hereunder, the sub-models composing the global building energy simulation model have been selected and developed in order to be characterized by a limited amount of physical and easily measurable/identifiable inputs and parameters (nominal COP and 3 performance points for chillers, nominal efficiency and burner type and age for boilers, specific power for fans…).

Default and rule of thumb values are provided for most of the parameters asked to the user. As shown below, these values have been derived from the analysis of manufacturer data. The other parameters of the model (such as HVAC system components capacities) are automatically computed through a pre-sizing calculation.

The main inputs are:

- Weather data : hourly values of temperature, humidity, global and diffuse radiations;
- Occupancy, lighting and appliances loads and schedules
- Comfort requirements and schedules: air renewal rate, temperature and humidity set points

The main parameters are:

- Dimensions, orientation and general characteristics of the building walls (e.g. "heavy", "medium" or "light" thermal mass and walls U values). Each zone can be surrounded by n walls, each one having a given orientation and including a window or not.
- Type of HVAC systems and components present in the installation: multi-zone or single-zone system, CAV or VAV air handling unit(s), fan coil units, induction units, radiant cooling/heating systems, air or water cooled chillers, direct or indirect contact cooling towers..
- Nominal performance of HVAC components: specific fan and pump powers, nominal efficiencies and effectiveness'
- Sizing factors of the main HVAC components

4. MODELLING APPROACH

The quasi-steady state hourly simulation program developed in this work is based on the LSPE (loads - secondary system - primary system - economics) sequential approach (Reddy and Maor, 2006). The heating, cooling and latent loads computed by the building zone model are summed and converted into system loads and then, into final energy consumptions (Figure 4). Capacity limitations are also taken

into account and may cause bad respect of the setpoints. This approach allows minimizing the number of iterations needed to simulate the performance of the building and its system.

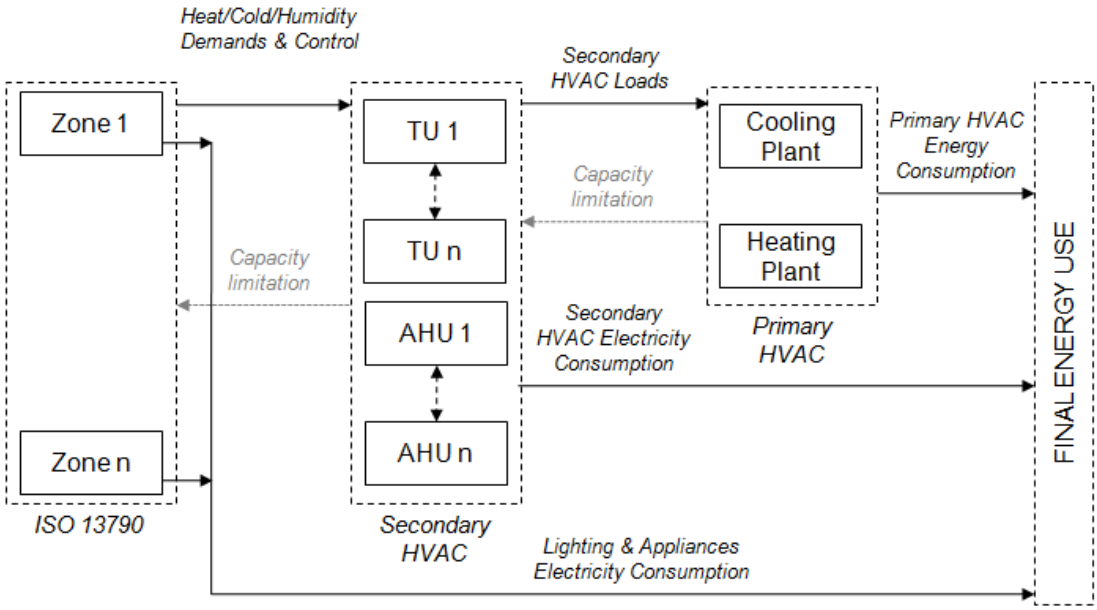

Figure 4: Global building-HVAC model block diagram

The dynamic building zone sensible and latent models are used to simulate the behavior of the building and to compute the heating, cooling, humidification and dehumidification needs in order to maintain the indoor temperature and humidity set points for each zone (Figure 5).

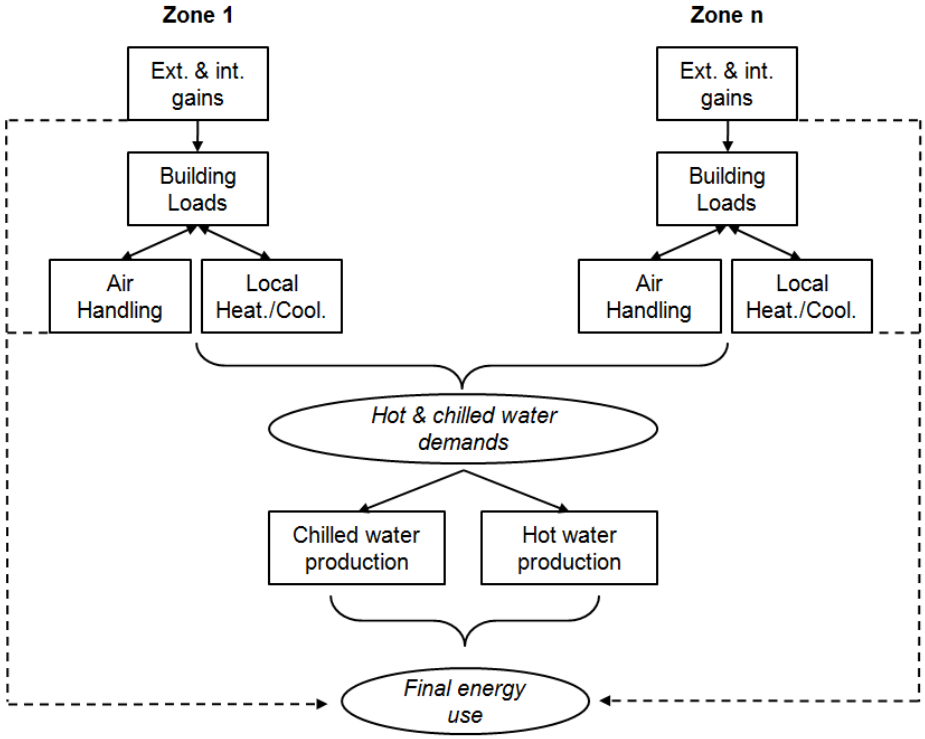

Figure 5: Multi-zone modeling scheme

Each zone of the building can be equipped with heating and/or cooling terminal units. In case of single-zone ventilation system, the ventilation air flow is provided by a unique AHU supplying the building zones. Multi-zone ventilation system includes n Air Handling Units, each serving a zone.

The Terminal Unit (TU) and Air Handling Unit (AHU) models convert heating, cooling, humidification and dehumidification demands into corresponding hot water, cold water and electricity consumptions. Hot and cold water consumptions are converted into final energy consumption by the primary HVAC system model, simulating the performances of the heat and cold production and distribution systems. Lighting, appliances and HVAC energy consumptions are summed to compute the final energy use of the building. Most of these sub-models are simplified and/or semi-empirical models available in standards (normative models) or in the literature.

It is interesting to note that Heo (2011) used a similar approach (use of simple normative models) to develop a simple simulation, easy to calibrate and to use to evaluation energy conservation opportunities. The author showed that simple normative models such as the ISO 13790 coupled to simple HVAC components models are sufficient to support evaluation of ECMs and quantify associated risks by means of uncertainty analysis.

While the simulation model developed by Heo (2011) remains quite limited in its applicability (single-zone model applicable to naturally ventilated buildings), the present simulation tool will allow modelling multi-zone buildings equipped with complete HVAC systems.

5. BUILDING MODEL

5.1. SOLAR RADIATIONS AND LONG-WAVE EXCHANGES

The incident solar radiation on a surface is the sum of the direct radiation, the part of the global radiation reflected on the ground and the sky diffuse radiation reaching the surface (in W/m² of vertical surface). Horizontal global and diffuse radiations are expressed in W/m² of horizontal surface and provided as inputs of the model.

For a given wall (so, for given orientation and slope), the direct solar incident to the wall is computed as function of time following the method described by Duffie and Beckman (1980).

$$I_{dir,h} = I_{glob,h} - I_{diff,h}$$

$$I_{dir,n} = f(t, I_{dir,h}; \theta_z)$$

$$I_{dir,w} = f(t, I_{dir,n}; \theta)$$

Where

$I_{dir,h}$ is the horizontal direct radiation (in W/m²)

$I_{glob,h}$ is the horizontal global radiation (in W/m²)

$I_{diff,h}$ is the horizontal diffuse radiation (in W/m²)

$I_{dir,n}$ is the normal diffuse radiation (in W/m²)

$I_{dir,w}$ is the direct radiation incident to the considered wall (in W/m²)

t is the time (in hours)

θ_z is the zenith angle (in radians)

θ is the solar incidence angle of direct radiation for the corresponding orientation/slope (in radians)

The hemispheric solar radiation (sum of diffuse and reflected radiations) incident to the wall is given by the following equations:

$$I_{diff,w} = \frac{1}{2} * (1 + \cos(\beta)) * I_{diff,h}$$

$$I_{ref,w} = \frac{1}{2} * albedo * (1 - \cos(\beta)) * I_{glob,h}$$

$$I_{hemis,w} = I_{diff,w} + I_{ref,w}$$

Where

β is the slope of the considered wall (in radians)

$albedo$ is the average albedo of the surrounding ground surface,

$I_{diff,h}$ is the diffused radiation incident to the considered wall (in W/m²)

$I_{ref,w}$ is the reflected radiation incident to the considered wall (in W/m²)

The average ground albedo is defined as function of the type of ground surrounding the building. Thevenard and Haddad (2006) provide some typical values for albedo for different types of ground covering (Table 1).

Table 1: Ground albedo average values from literature

Ground cover	Ground albedo
Coniferous forest	0.07
Bituminous and gravel roof	0.13
Dry bare ground	0.2
Weathered concrete	0.22
Green grass	0.26
Dry grassland	0.2-0.3
Desert sand	0.4
Light building surfaces	0.6
Snow	0.75 to 0.95

Shading masks are taken into account by specifying the angular height of the obstruction for each orientation as proposed in the Th-C-E-Ex method (CSTB, 2008).

$$I_{dir,w}{}^{*} = f_{dir,mask,w} * I_{dir,w}$$

$$I_{diff,w}{}^{*} = f_{diff,mask,w} * I_{diff,w}$$

$$I_{hemis,w}{}^{*} = I_{diff,w}{}^{*} + I_{ref,w}$$

Where

$f_{dir,mask,w}$ is the correction factor for direct radiation computed as a function of the obstruction angle,

$f_{diff,mask,w}$ is the correction factor for diffuse radiation computed as a function of the obstruction angle,

The impact of outdoor solar shadings is taken into account by correcting the Solar Heat Gain Coefficient of the window by means of the Indoor solar Attenuation Coefficient (IAC) which corresponds to the fraction of the initial SHGC when the shading device is totally closed, as defined by ASHRAE (2009). For the sake of simplicity, the value of the IAC (and so, the impact of the shading) is supposed to be independent of the solar radiation incidence angle).

$$SHGC_{no\ shading,0} = SGHC_0$$

$$SHGC_{shading,0} = IAC * SGHC_0$$

Where

$SGHC_0$ is the glazing "normal" solar heat gain coefficient (incidence angle = 0°),

IAC is shading device Indoor solar Attenuation Coefficient,

Indoor shadings influence only the radiation-convective split of the incident solar gains. Example values of IAC and convective-radiation split factor are given in ASHRAE (2009).

The solar heat gain coefficient (SHGC) of the glazed surfaces is not supposed to be constant but is computed at each time step, as function of the direct radiation incidence angle for each considered orientation. The following simplified equation is used to represent the incidence angle dependency of SHGC (Laustsen, 2002).

$$SHGC_{dir} = SHGC_0 * (1 - \left[tan\left(\frac{\theta}{2}\right)\right]^p)$$

Where

$SHGC_0$ is the normal solar heat gain coefficient (incidence angle = 0°)

$SHGC_{dir}$ is the solar heat gain coefficient for the considered surface (orientation and slope),

θ is the solar incidence angle of direct radiation for the corresponding orientation/slope (in radians)

p is representing the incidence angle dependency,

The incidence angle dependency can be adjusted to fit to SHGC curves provided in the literature. The SHGC(θ) curve is shown in Figure 6 for a double clear gazing with air layer. The normal SHGC is 0.7. The value of the incidence angle dependency parameter (p) has been identified to fit to the values provided by the software package WINDOWS 5.2a (LBNL, 2010).

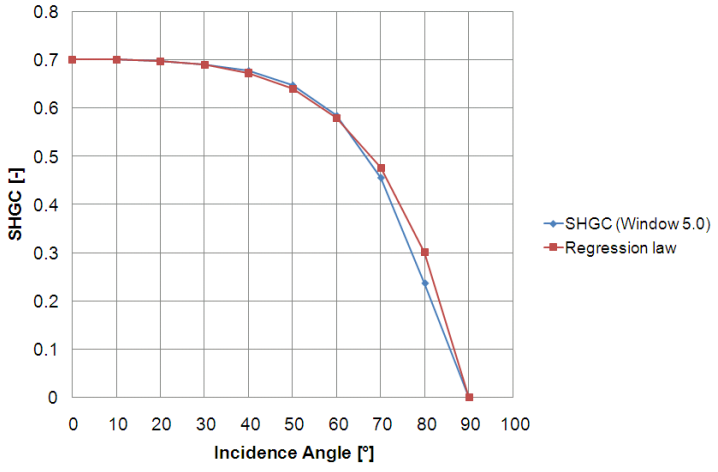

Figure 6: SHGC incidence angle dependency (for $SHGC_0$=0.7 and p=3.2)

A second value of the SHGC is computed for hemispherical (diffuse and reflected) radiation. The hemispherical SHGC (f) is generally between 81 and 94% of the normal SHGC (depending on the type of glazing). A value of 86% is generally used for common glazing systems (Lauststen, 2002).

$$SHGC_{hemis} = f_{hemis} * SHGC_0$$

Where

f_{hemis} is the correction factor for hemispherical SHGC

Values of incidence angle dependency factor and hemispherical-to-normal SHGC ratio have been computed for different types for glazing systems and are given in Table 2.

Table 2: Glazing model parameters for common configurations

ID[1]	Glazing type		Normal SHGC	Incidence angle dependency (p)	Hemispherical-to-normal SHGC ratio (f)
1b	Single glazing (CLR)		0.81	3.99	0.9
5b	Double glazing (6mm) with 12.7 mm air space	CLR CLR	0.7	3.2	0.86
5d		BRZ CLR	0.49	2.77	0.84
5f		GRN CLR	0.49	2.77	0.84
5h		GRY CLR	0.47	2.69	0.83
5j		BLUGRN CLR	0.39	2.82	0.85
21b	Low-e double glazing (6mm) with 12.7 mm air space (LE CLR)		0.6	3.10	0.88
40b	Low-e triple glazing (6mm) with 6.4 mm air space (LE CLR LE)		0.36	2.51	0.83

Finally, for a given value of the shading device operating factor, one obtains:

$$SHGC_{dir}{}^{*} = SHGC_{dir,no\ shading} * \left(1 - f_{shading}\right) + SHGC_{dir,shading} * f_{shading}$$

$$SHGC_{hemis}{}^{*} = SHGC_{hemis,no\ shading} * \left(1 - f_{shading}\right) + SHGC_{hemis,shading} * f_{shading}$$

$$\dot{Q}_{sol,wd} = A_{gl,w} * (SHGC_{dir}{}^{*} * I_{dir,w}{}^{*} + SHGC_{hemis}{}^{*} * I_{hemis,w}{}^{*})$$

Where

$f_{shading}$ is the shading device operating factor,

$A_{gl,w}$ is the glazing area (in m²)

$\dot{Q}_{sol,wd}$ is the solar gain heat transfer rate transmitted through windows (in W)

In the case of automated shading devices, the shading operating factor can be determined as a direct function of the solar radiation. The simulation of the manual solar shading system requires to compute daylighting in the zones. A simplified method (CSTB, 2008) has been implemented. This method defines a shading operation factor calculated as a function of the outdoor daylighting intensity. The daylighting intensity is estimated for each orientation on a basis of 100 lux per W of total solar radiation. Two curves are available to calculate the shading operation factor (Figure 7). The curve proposed by Alessandrini et al. (2006) is based on surveys realized in French office buildings.

[1] ID refers to fenestration assemblies given in ASHRAE (2009). CLR=clear; BRZ=bronze; GRN=green; GRY=gray; BLUGRN=blue-green.

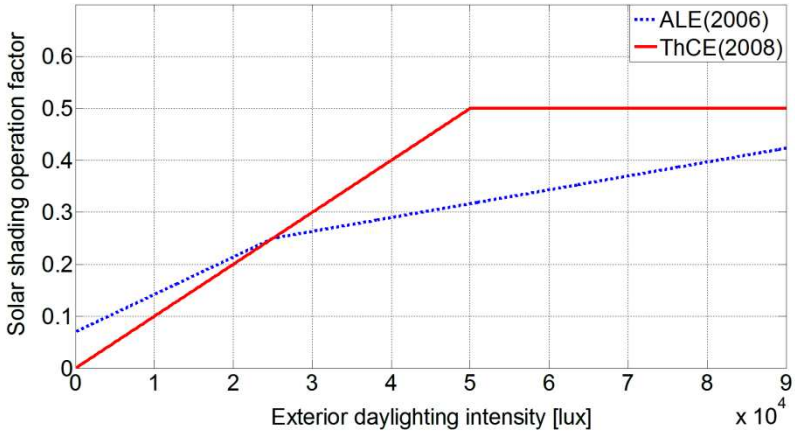

Figure 7: Solar shading operation factor as a function of exterior natural daylighting intensity

A similar set of equations is used to compute the incident solar radiation reaching opaque surfaces. On contrary of the solar heat gain coefficient (SHGC) of the glazed surfaces, the solar absorbance of opaque surfaces is supposed to be constant.

A correction heat flow (Bliss, 1961) varying from 45 to 100 W/m², is also used to take into account that the sky temperature is below the outdoor air temperature. The calculation of this correction, as function of the location and weather conditions is explained by Masy (2008).

$$\dot{Q}_{sky} = \epsilon_{ir} * A * \frac{1}{2} * I_{ir,h}$$

Where

ε_{ir} is the wall surface emissivity

A is the wall area (in m²)

$I_{ir,h}$ is the correction heat flow varying from 45 to 100 W per m² of horizontal surface (in W/m²)

$\dot{Q}_{sky}$ is the long-wave heat rate between the wall and the sky (in W)

Corrected outdoor ("sol-air") temperatures for (vertical and horizontal) light and heavy opaque walls are computed according to ISO13790 (2007) and prEN15255 (2006):

$$t_{out}{}^{*} = t_{out} + R_{s,e} * \left(\dot{Q}_{sol,w} - \dot{Q}_{sky,w}\right)$$

Where

$t_{out}{}^{*}$ is the "sol-air" outdoor air temperature for the considered opaque wall (in °C)

t_{out} is the outdoor air temperature (in °C)

$R_{s,e}$ is the outdoor combined (radiation and convective) resistance for the considered opaque wall (in K/W)

$\dot{Q}_{sol,w}$ is the solar gain heat transfer rate absorbed by the wall (in W)

For windows, only long-wave heat rate is considered to compute the corrected outdoor temperature. Transmitted solar gains are computed as explained above and distributed (radiative-convective distribution) within the indoor ambiance, as explained hereunder.

5.2. *SENSIBLE GAINS*

Sensible gains include four contributions:

- Solar gains transmitted through windows
- Sensible heat gains generated by lighting fixtures and electrical appliances (plug loads)
- Sensible heat gains generated by occupants (as function of the metabolic rate)
- Sensible heat generated or absorbed by heating or cooling terminal units.

As mentioned before, the solar gains entering through windows are split into convective and radiation gains using a repartition factor determined as function of the presence of internal solar shadings or not. Without interior solar shadings, the convective part is limited and represents about 10% of the entering heat flow (EN15255). With interior shadings, the convective part can reach 100% of the solar heat gain (ASHRAE, 2009).

$$\dot{Q}_{c,sol,wd} = f_{c,sol} * \dot{Q}_{sol,wd}$$

$$\dot{Q}_{r,sol,wd} = (1 - f_{c,sol}) * \dot{Q}_{sol,wd}$$

Where

$\dot{Q}_{sol,wd}$ is the solar heat gain transmitted through windows (in W)

$\dot{Q}_{c,sol,wd}$ is the convective part of the solar heat gain (in W)

$\dot{Q}_{r,sol,wd}$ is the radiation part of the solar heat gain (in W)

$f_{c,sol}$ is the convective-radiation repartition factor for solar heat gains

Internal sensible heat gains and heating/cooling flows are also split into radiation and convective heat flows depending on the type of lighting fixtures, appliances, heating and cooling systems and the way they are used (e.g. high or low air speed).

$$\dot{Q}_{c,ihg} = f_{c,occ} * \dot{Q}_{occ} + f_{c,appl} * \dot{Q}_{appl} + f_{c,light} * \dot{Q}_{light}$$

$$\dot{Q}_{r,ihg} = (1 - f_{c,occ}) * \dot{Q}_{occ} + \left(1 - f_{c,appl}\right) * \dot{Q}_{appl} + (1 - f_{c,light}) * \dot{Q}_{light}$$

$$\dot{Q}_{c,heating} = f_{c,htu} * \dot{Q}_{heating}$$

$$\dot{Q}_{r,heating} = (1 - f_{c,htu}) * \dot{Q}_{heating}$$

$$\dot{Q}_{c,cooling} = f_{c,ctu} * \dot{Q}_{cooling}$$

$$\dot{Q}_{r,cooling} = (1 - f_{c,ctu}) * \dot{Q}_{cooling}$$

Where

$\dot{Q}$ is the heat gain (negative for cooling, in W)

$\dot{Q}_c$ is the convective part of the heat gain (in W)

$\dot{Q}_r$ is the radiation part of the heat gain (in W)

f_c is the convective-radiation repartition factor for the considered heat gain

Sensible and latent heat gains due to occupancy are computed based on values proposed in ASHRAE (2009) and ISO7730 (2005). The total metabolic rate is computed as a function of the "Dubois" area (surface area of skin given as function of the weight and height of the individual) and the activity of the occupant defined in "met" (1 met = 58.1 W/m²).

For a man with a weight of 70 kg, a height of 1.73 m and a light activity (1.2 met), this gives an area of 1.8285 m² and a total metabolic rate of approximately 127 W. The latent part of this heat rate can be obtained by using the regression shown in Figure 8 .This regression is based on data provided in ASHRAE (2009) for various types of activities and normal percentage of men, women and children for each application. For the considered types of activities, the mechanical efficiency of the work provided by the occupant is neglected.

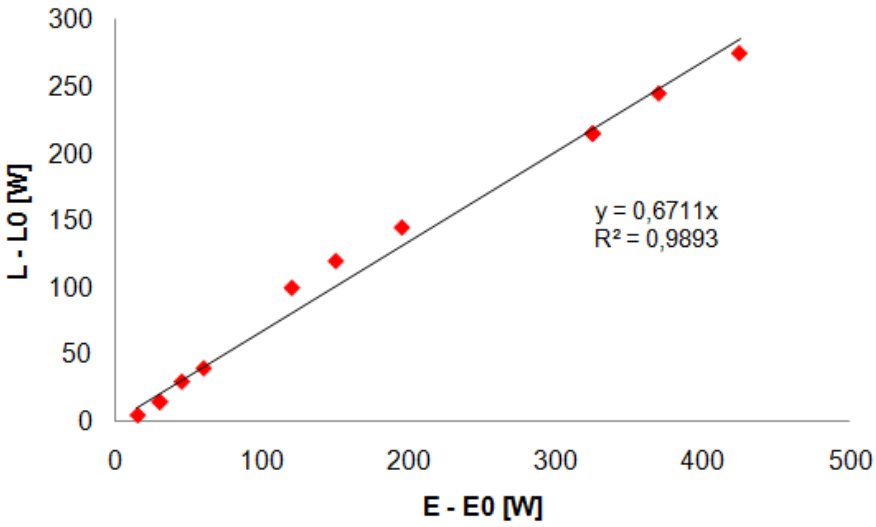

Figure 8: Occupant latent heat gain - Regression law

$$\dot{H}_{occ} = \dot{H}_{occ,0} + 0.6711 * (\dot{E}_{occ} - \dot{E}_{occ,0})$$

$$\dot{Q}_{occ} = \dot{E}_{occ} - \dot{H}_{occ}$$

Where

$\dot{E}_{occ}$ and $\dot{E}_{occ,0}$ (= 100 W) are the total metabolic rates in actual and rest conditions (in W)

$\dot{H}_{occ}$ and $\dot{H}_{occ,0}$ (= 40 W) are the latent heat gains in actual and rest conditions (in W)

$\dot{Q}_{occ}$ is the sensible heat gain in actual conditions (in W)

In addition to the radiative/convective split, other factors are considered to compute realistic heat gains due to artificial lighting:

- Special allowance factor (f_{sa}) representing the ratio of the lighting fixtures' power consumption (lamp and ballast) to the nominal power consumption of the lamps (ASHRAE Handbook F18). A value of 1 should be used for incandescent lights (no ballast). Values between 1.1 and 1.2 should be used for fluorescent lights with classical electromagnetic ballasts and between 0.9 and 0.95 for fluorescent lights with high efficiency electronic ballasts lowering the power consumption.
- Space fraction (f_{sp}) representing the fraction of the lighting heat gains that goes to the indoor ambiance. The remaining heat goes to the air extracted through the ceiling plenum (ASHRAE Handbook F18). Values of lighting gains space fraction highly depends on the use of ducted air returns (space fraction around 0.9) or non-ducted air returns (space fraction around 0.5).

Typical values of density and convection-radiation repartition factors are given in Table 3 for various types of heat gains and emitters (ASHRAE, 2009). More detailed information could be found in Hosni et al. (1999a and 1999b) and in the RTS method developed by Spitler et al. (1997).

Table 3: Internal Gains

Type of heat gain / emitter	Sensible heat	Latent heat	Rad. fraction
Occupant (seated at rest, 1 met)	60 W	40 W	0.3 to 0.6
Occupant (light work, 1.2 met)	80 W	50 W	
Occupant (active office work, 1.3 met)	80 W	60 W	
Fluorescent luminaire	9 to 15 W/m² floor area	0 W	0.4 to 0.8
Appliances	5.4 to 21 W/m² floor area	0 W	0.25 to 0.4

5.3. VENTILATION AND INFILTRATION

The infiltration rate can be fixed by the user in terms of Air-Change-per-Hour (ACH) or flow rate per square meter of facade (m³/h/m²). For office buildings, the infiltration rate usually varies from 0.2 to 0.8 ACH and from 2 to 3 m³/h/m².

The infiltration rate can also be estimated in a very simple way as a function of the wind speed and the indoor-outdoor temperature difference by means of the K1-K2-K3 method (ASHRAE, 1989).

The Air-Change-per-Hour is given by:

$$ACH_{K1-K2-K3} = K_1 + K_2 * |t_{out} - t_i| + K_3 * v_{wind}$$

Where

$ACH_{K1-K2-K3}$ is the infiltration rate (in ACH)

t_{out} is the outdoor temperature (in °C)

t_i is the indoor temperature (in °C)

v_{wind} is the wind speed (in m/s)

K_1, K_2 and K_3 are coefficients given in Table 4

Table 4: K1-K2-K3 method coefficients (ASHRAE, 1989)

Construction	K_1	K_2	K_3	Description
Tight	0.1	0.011	0.034	New building with special precautions
Medium	0.1	0.017	0.049	Use of conventional construction procedures
Loose	0.1	0.023	0.07	Poor construction on old building

The wind speed is generally provided in meteorological data in reference conditions (clear site, 10 meters above ground) but should be corrected to take the typology of the environment into account:

$$v_{wind} = a * v_{wind,0} * h^b$$

Where

$v_{wind,0}$ is the reference wind speed (in m/s)

v_{wind} is the corrected wind speed (in m/s)

h is the average building height (in m) (Bohler et al., 2000)

Table 5: Coefficients for describing the site and building height dependency of wind speed

Site	a	b
City centre medium to large town	0.21	0.33

Small town / suburban area	0.4	0.25
Country side	0.52	0.2
Clear site	0.68	0.17

Since cross ventilation and stack effects are not taken into account in the present model, the ACH is supposed to be equal in all the peripheral zones (in direct contact with the outdoor environment) and limited to $0.05h^{-1}$ in core zones (Stocki et al., 2007).

For the sake of simplicity, infiltration is supposed to be null in a zone which is mechanically ventilated (indoor zones are supposed to be over pressurized during ventilation operation).

In the case of a CAV ventilation system, the mechanical ventilation flow rate is specified by the user and stays constant. In the case of a VAV ventilation system, the air flow rate depends of the heating or cooling demands of the zone (see below). In both cases, the supply air temperature is fixed by the user (setpoint value) or determined as a function of the outdoor temperature (supply temperature reset).

The global (natural and mechanical) ventilation flow rate and the corresponding temperature are given by:

$$\dot{V}_{su} = \dot{V}_{vent} + \dot{V}_{inf}$$

$$t_{su} \approx \frac{\dot{V}_{vent} * t_{vent} + \dot{V}_{inf} * t_{inf}}{\dot{V}_{vent} + \dot{V}_{inf}}$$

Where

$\dot{V}_{vent}$ is the mechanical ventilation flow rate (in m^3/s)

$\dot{V}_{inf}$ is the infiltration flow rate (in m^3/s)

$\dot{V}_{su}$ is the global ventilation flow rate (in m^3/s)

t_{vent} is the mechanical ventilation supply air temperature (in °C)

t_{inf} is the infiltration air temperature = outdoor temperature (in °C)

t_{su} is the supply air temperature (in °C)

5.4. *ZONE THERMAL MODEL*

The simplified building zone model is based on the simple hourly method described in ISO13790-2007. The R5-C1 network is solved on an hourly basis (Figure 9) by means of the past-Euler's method. The simplicity of this implementation ensures an easy parameterization work (done in accordance with the ISO13786-2007), a high flexibility and an easy control of the level of details of the model. The use of Euler's method to solve the unique integration ensures quick and robust operation of the model.

Six types of walls are considered in this building zone model:

- External vertical opaque (massive) walls
- External horizontal opaque (massive) walls (i.e. roof)
- External vertical glazed (light) walls (windows)
- Adjacent and adiabatic vertical (massive) walls between adjacent buildings
- Internal and adiabatic vertical (massive) walls between zones
- Internal and adiabatic horizontal (massive) floor and ceiling slabs

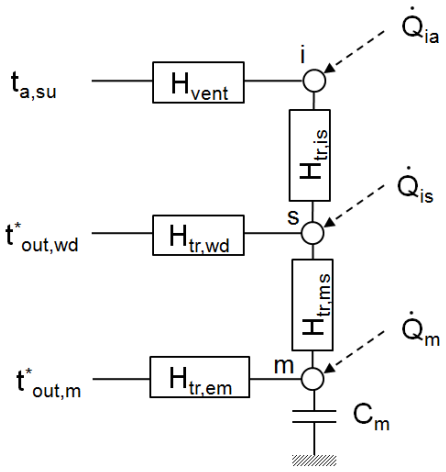

Figure 9: ISO13790 simple hourly method RC network

The three nodes of the RC network, "i", "s" and "m" respectively represent:

- the indoor air temperature,
- a "mix" between air indoor temperature and mean radiant temperature,
- the equivalent building thermal mass temperature.

Each building zone is described by three distinct temperatures nodes: an indoor air temperature node, an equivalent surface node (mean temperature between indoor temperature and mean radiant temperature) and a thermal mass temperature. Equivalent sol-air outdoor temperatures (t^*_{out}) are used to take into account solar radiation and infrared losses on opaque surfaces and infrared losses on glazed surfaces. A variable solar heat gain coefficient (function of the incidence angle) is used to describe glazed surfaces. Convective and radiation part of the heat fluxes related to entering solar gains, internal generated gains (lighting, appliances…) and sensible heating/cooling rates are computed and distributed over the three nodes.

5.4.1. Model parameters

The parameters of the building zone model include steady-state transmission and ventilation heat transfer coefficients (H) and dynamic thermal characteristics (building thermal mass, C) computed according to ISO13786 (2007) and ISO13789 (2007).

The heat transfer coefficient of windows ($H_{tr,wd}$) is given by:

$$H_{tr,wd} = A_{fr} * U_{fr} + A_{gl} * U_{gl}$$

Where

A_{fr} is the windows frame area (in m²)

U_{fr} is the windows frame U value (in W/m²-K)

A_{gl} is the glazing area (in m²)

U_{gl} is the glazing U value (in W/m²-K)

The heat transfer coefficient of (horizontal and vertical) heavy opaque walls ($H_{tr,op}$) is given by:

$$H_{tr,op} = A_{opw} * U_{opw}$$

Where

A_{opw} is the opaque walls total area (in m²)

U_{opw} is the opaque walls U value (in W/m²-K)

The heat transfer coefficient of heavy opaque walls is split into $H_{tr,em}$ and $H_{tr,ms}$ in accordance with clause 12.2.2 of ISO13790 (2007) as follows:

$$H_{tr,ms} = h_{ms} * A_m$$

$$H_{tr,em} = \frac{1}{\left(\frac{1}{H_{tr,op}} + \frac{1}{H_{tr,ms}}\right)}$$

Where

$H_{tr,ms}$ is the coupling conductance between the "s" and "m" nodes (in W/K)

$H_{tr,op}$ is the heat transfer coefficient of heavy opaque walls (in W/K)

h_{ms} is the heat transfer coefficient between "s" and "m" nodes (in W/m²-K, defined below)

A_m is the effective building mass area (in m², defined below)

The coupling conductance, $H_{tr,is}$, between the air node "i" and the surface node "s" is given by:

$$H_{tr,is} = h_{is} * A_{tot}$$

Where

$H_{tr,is}$ is the coupling conductance between the "i" and "s" nodes (in W/K)

h_{is} is the heat transfer coefficient between "i" and "s" nodes (in W/m²-K, defined below)

A_{tot} is the total area of all surfaces facing the building zone (in m²)

In the present simulation tool, the outdoor combined (radiation and convective) heat transfer coefficient (h_{out}) can be fixed to a constant value (generally between 17 and 23 W/m²-K) or computed as a function of the wind speed by means of the following equation:

$$h_{out} = a_1 + a_2 * v_{wind} + a_3 * v_{wind}^2$$

Where

h_{out} is the outdoor combined surface coefficient (in W/m²-K)

v_{wind} is the wind speed (in m/s)

a_1, a_2 and a_3 are polynomial coefficients given in Table 6 (Walton, 1983 in Judkoff and Neymark, 1995).

Table 6: Polynomial coefficients for describing wind speed dependency of outdoor surface coefficient

Material	a_1	a_2	a_3
Stucco	11.58	5.894	0.0
Brick	12.49	4.065	0.028
Concrete	10.79	4.192	0.0
Clear pine	8.23	4.0	-0.057
Plaster	10.22	3.1	0.0
Glass	8.23	3.33	-0.036

Heat transfer coefficients between the nodes "i", "s" and "m", h_{is} and h_{ms} (in W/m²-K) are defined in accordance to ISO15255 (2006):

$$h_{rs} = 1.2 * h_{r,i}$$

$$h_{ms} = h_{c,i} + h_{rs}$$

$$h_{is} = \frac{1}{\left(\frac{1}{h_{c,i}} - \frac{1}{h_{ms}}\right)}$$

Where

$h_{r,i}$ is the indoor radiative heat transfer coefficient, typically 5.1 W/m²-K

$h_{c,i}$ is the indoor convective heat transfer coefficient, typically 3.1 W/m²-K

The internal (or indoor-side) thermal capacity, C_m (in J/K), is defined as the sum of the internal thermal capacities of all the building elements in direct contact with the internal air of the zone:

$$C_m = A_{opw} * C_{opw} + A_{fl} * C_{fl} + A_{cl} * C_{cl} + A_{adj} * C_{adj} + A_{int} * C_{int}$$

Where

C is the internal capacity of the building element (in J/m²-K)

A is the building element area (in m²)

opw stands for external massive (vertical or horizontal) opaque walls

rf stands for (horizontal) roof

fl stands for floor

cl stands for ceiling

adj stands for adjacent walls

int stands for internal walls

The effective mass area, A_m (in m²), is defined by:

$$A_m = \frac{C_m^2}{A_{opw} * {C_{opw}}^2 + A_{fl} * {C_{fl}}^2 + A_{cl} * {C_{cl}}^2 + A_{adj} * {C_{adj}}^2 + A_{int} * {C_{int}}^2}$$

Indoor-side capacities of building elements are calculated by means of the Heat Transfer Matrix (HTM) method, according to ISO13786 (2007). The heat transfer matrix of each wall layer is computed as function of the material's properties. The surface-to-surface heat transfer matrix of the wall is obtained by multiplying the wall layers' HTMs and the boundary layers' HTMs:

$$Z = \begin{pmatrix} Z_{11} & Z_{12} \\ Z_{21} & Z_{22} \end{pmatrix} = Z_{s2} Z_N Z_{N-1} \dots Z_2 Z_1 Z_{s1}$$

The indoor-side capacity of the wall, C_{in} (in J/m²-K), is given by:

$$C_{in} = \frac{T}{2 * \pi} * \left| \frac{Z_{11} - 1}{Z_{12}} \right|$$

where T is the time period (in s).

If wall's composition and the exact dimensions of the building are not available, typical values of the global thermal mass C_m (in J/K) can be used. Default values are provided in Table 7 (ISO13790, 2007).

Table 7: Default values for dynamic parameters

Class	Am m²	Cm J/K
Very light	2.5 * A_{fl}[2]	80000 * A_{fl}
Light	2.5 * A_{fl}	110000 * A_{fl}
Medium	2.5 * A_{fl}	165000 * A_{fl}
Heavy	3.0 * A_{fl}	260000 * A_{fl}
Very heavy	3.5 * A_{fl}	370000 * A_{fl}

5.4.2. Main equations

Three algorithms are used to solve the building zone model:

1. The first algorithm (*ISO13790TEMP*) is used to compute the nodes temperatures by solving energy balances on each node. At each time step, the value of the mass temperature at the end of the time step ($t_{m,f}$, in °C) is computed from the mass temperature at the beginning of the time step ($t_{m,i}$, in °C) through the use of the Euler's method to solve the first order differential equation. Knowing the mass temperature, surface (t_s, in °C) and air (t_i, in °C) temperatures are computed. The operative temperature (in °C) is then given by:

$$t_{op} = \frac{1}{2} * \left(1 + \frac{h_{c,i}}{h_{r,s}}\right) * t_s + \left(1 - \frac{1}{2} * \left(1 + \frac{h_{c,i}}{h_{r,s}}\right)\right) * t_i$$

and the mean radiant temperature (in °C) is given by:

$$t_{rm} = 2 * t_{op} - t_i$$

2. The second algorithm (*ISO13790LOADS*) is used to compute the convective and radiative gains injected on the different nodes of the RC network.

$$\dot{Q}_{ia} = \dot{Q}_{c,ihg} + \dot{Q}_{c,sol,wd} + \dot{Q}_{c,heating} + \dot{Q}_{c,cooling}$$

$$\dot{Q}_m = P_{rm} * (\dot{Q}_{r,ihg} + \dot{Q}_{r,heating} + \dot{Q}_{r,cooling}) + P_{rm,sol} * \dot{Q}_{r,sol,wd}$$

$$\dot{Q}_{st} = P_{rs} * (\dot{Q}_{r,ihg} + \dot{Q}_{r,heating} + \dot{Q}_{r,cooling}) + P_{rs,sol} * \dot{Q}_{r,sol,wd}$$

Where P_{rm}, $P_{rm,sol}$, P_{rs}, $P_{rs,sol}$ are reparation factors for radiative gains between nodes s and m and are given by:

$$P_{rs} = \frac{A_{tot} - A_m - \frac{H_{tr,wd}}{h_{is}}}{A_{tot}}$$

[2] A_{fl} is the floor area (in m²)

$$P_{rm} = \frac{A_m}{A_{tot}}$$

$$P_{rs,sol} = \frac{A_{tot} - A_m - A_{wd} - \frac{H_{tr,wd}}{h_{is}}}{A_{tot} - A_{wd}}$$

$$P_{rm,sol} = \frac{A_m}{A_{tot} - A_{wd}}$$

3. The third algorithm (*ISO13790CALC*) is used to determine the actual indoor conditions and the corresponding heating/cooling needs calling several times the two first algorithms. Firstly, the temperatures are computed in "free-floating" conditions (no local heating/cooling). Secondly, depending on the value of the indoor temperature in "free-floating" conditions, the indoor temperature set point to maintain is determined:

   IF $t_{i,0} > t_{i,set,cooling}$ *THEN*

   $t_{i,set} = t_{i,set,cooling}$

   ELSE

   $t_{i,set} = t_{i,set,heating}$

   ENDIF

   Thirdly, the indoor temperature is computed for an arbitrary heating power of 10 W/m² of floor area. A linear interpolation is then used to determine the value of the actual heating/cooling power needed to maintain the temperature setpoint.

   Fourthly, if the heating/cooling power required to maintain the setpoint is higher than the heating/cooling capacity of the heating/cooling system, the heat/cold rate provided to the zone is limited and a new value of the temperature (different from the temperature setpoint) is computed. If the heating/cooling capacity is sufficient, the indoor temperature setpoint is maintained (supposing perfect temperature control).

   Two situations could be encountered: the heating/cooling capacity is fixed and constant (e.g. electrical heater) or dependent of the temperature difference between the heat/cold source (i.e. the emitter temperature) and the ambiance (Figure 10).

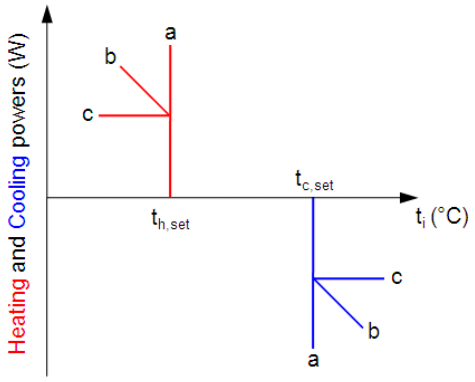

a: unlimited heating/cooling capacities
b: limited heating/cooling capacities depending on the indoor-source temperature difference
c: limited constant heating/cooling capacities

Figure 10: Heating/cooling Power vs indoor temperature

In a first time, only heat transfers between indoor and outdoor are considered. Internal partition walls (between two conditioned zones) or adjacent walls (between two conditioned buildings) are supposed to be adiabatic. ISO13790 (2007) proposes to integrate the heat transfer between adjacent zones with a time delay of one time step (typically one hour) to avoid any iteration. So, the heat flow between a zone and an adjacent zone is computed as function of the temperature of the adjacent zone at the previous time step and is integrated in the calculation of the corrected outdoor temperature according to ISO13790 – Appendix B. If this simplification leads to oscillations an iterative method has to be used.

5.5. *ZONE HUMIDITY MODEL*

The water capacitance method (Klein, 2007) is used to solve the humidity model (Figure 11) of the zone and takes the water flow rates related to occupancy, internal process, infiltration and ventilation into account.

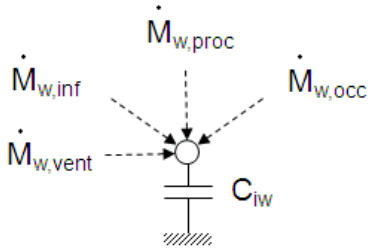

Figure 11: Zone humidity model

Once again, two distinct algorithms are used:

1. The first algorithm (WIN) is used to solve the first order differential equation by means of the past-Euler's method.
2. The second algorithm (WINCALC) computes the value of the supply humidity ratio needed to maintain the indoor conditions in the range determined by the humidification and/or dehumidification setpoints. The humidification and the dehumidification capacities are supposed to be sufficient to reach the setpoint in all conditions. The solving process is similar to the one applied for the sensible thermal zone model.

The water capacitance of the zone is equal to the mass of air present in the zone multiplied by an empirical factor varying between 1 to 10 (typically around 5) taking into account the moisture buffering effect of furniture and walls (Woloszyn, 1999).

5.6. *SENSIBLE BUILDING ZONE MODEL VALIDATION*

The level of detail required for the calculation of heating and cooling demands can be very different. For heating calculations, the major issues are a correct description of the building envelope and a reasonably accurate evaluation of the air renewal (including infiltration and ventilation). For cooling calculations, the fenestration area and orientation, the level and distribution of the internal gains, the ventilation rates and the geographical location and the usability of the thermal mass (if present and accessible) appear as critical issues.

The present implementation of this calculation method (only for sensible heat exchanges) has been validated through IEA-BESTEST (Judkoff and Neymark, 1995) comparative validation procedure in order to check its ability to handle the issues mentioned here above. This commonly used validation procedure uses a rectangular room as a basis for the various test cases.

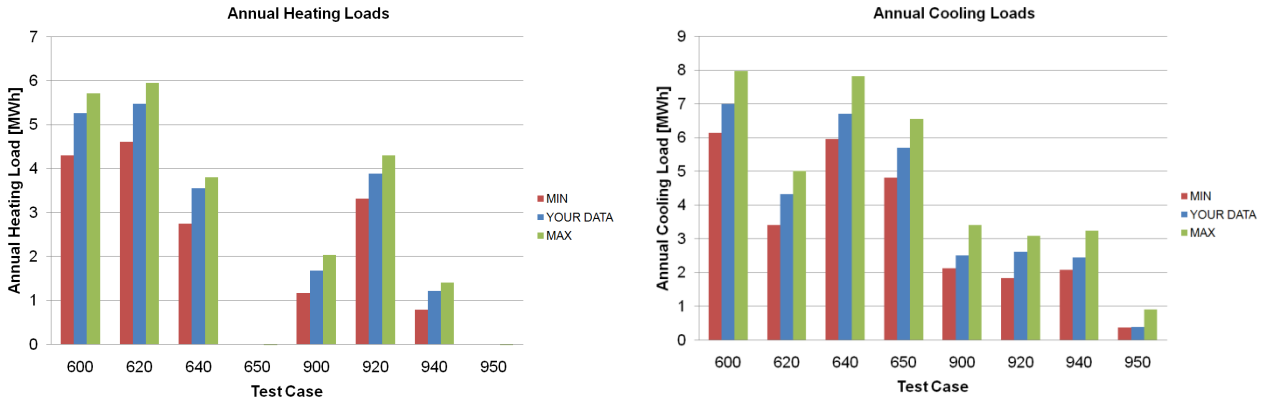

Figure 12. Yearly heating (left) and cooling (right) demands comparison - BESTEST

Figure 12 shows that this simple model is able to provide acceptable values of yearly heating and cooling demands for various conditions (schedule, setpoints, gains, ventilation), orientations and configurations (light or heavy envelope components). In both cases, the model provides results similar to the reference values or to the ones provided by more detailed simulation software (e.g. Trnsys and Energyplus). Taking Trnsys as a reference, the errors induced by the simplified model on the predicted annual heating and cooling demands is included between 1% and 7.9%. The error on the predicted peak heating load does not exceed 2% while the error on the predicted peak cooling load is about 10%. This last error can be explained by the fact that radiation-convective split of internal and solar gains is drastically simplified in the developed model.

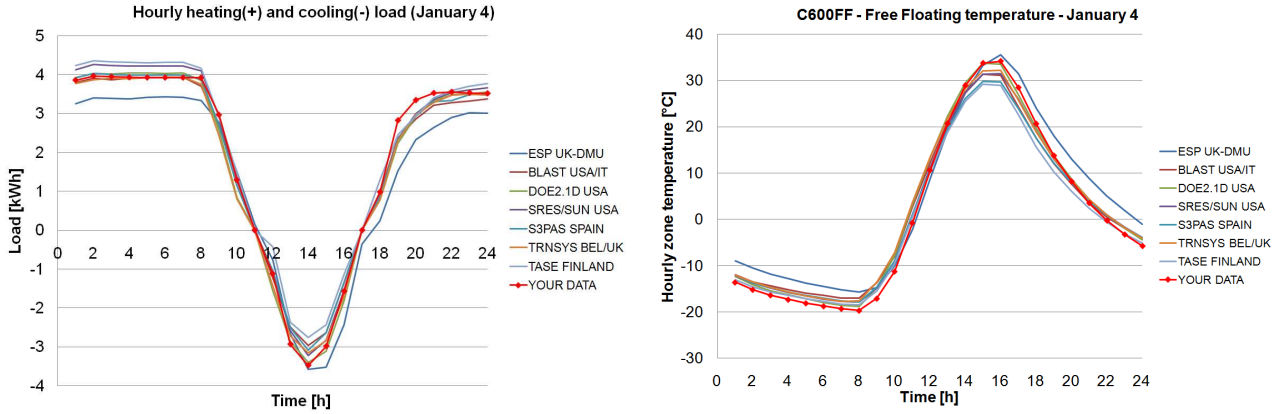

Figure 13. BESTEST hourly validation results C600: heating and cooling demands (left) and free floating temperature conditions (right).

Of course, such simplified model takes thermal mass effects into account in a very simplified way. Additional thermal mass of furniture is not taken into account and this simplified model should not be used to perform accurate prediction of indoor temperature variations.

However, if the considered building zone model is not aimed at providing accurate hourly values of temperatures and demands, it appears that the results are again in good accordance with the values provided by more detailed simulation software (Figure 13) and that this simplified model is accurate enough for the considered application.

6. SECONDARY HVAC SYSTEM MODEL

A whole secondary HVAC system model is connected to the zone model: it includes common CAV and VAV AHUs components (air recovery system, economizer, heating coils, cooling coil,

humidification system and fans) and terminal units (fan coil units, induction units, radiant systems, reheat boxes…).

The first step of the air handling system simulation consists in determining the required supply conditions in order to follow fixed temperature and humidity setpoints. In a second time, the air handling process is simulated in order to compute the corresponding heating, cooling and electricity demands.

6.1. AIR HANDLING UNIT MODEL

Only single duct air handling units are considered in the present work since dual duct systems are quite rare in Europe. Constant and variable flow systems are considered and can include the following components (Figure 14):

- Sensible or total heat recovery system
- Air economizer (mixer)
- Adiabatic humidification system (including pre-heating coil)
- Cooling coil (for temperature or humidity control)
- Post-heating coil
- Steam humidification system
- Supply and/or return fan

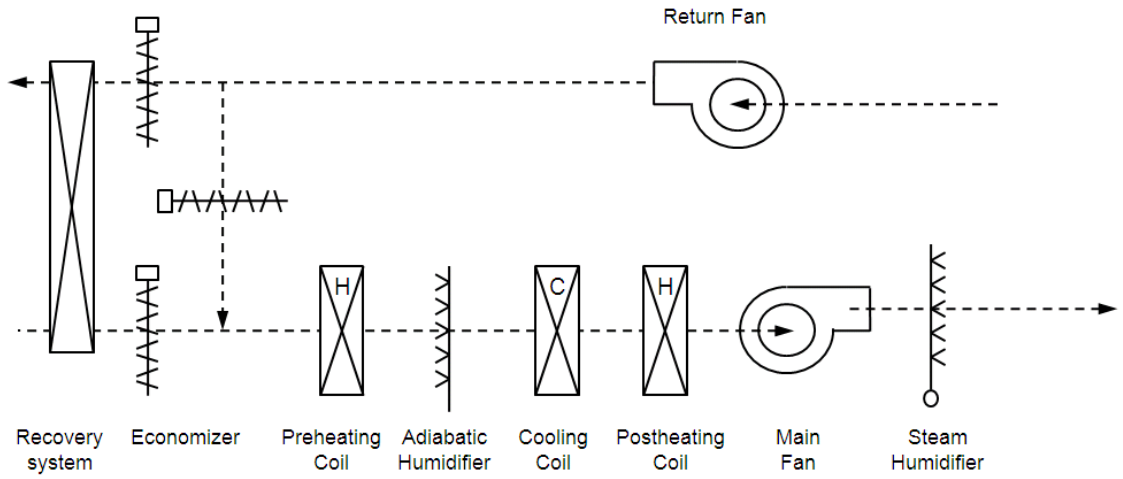

Figure 14: AHU Components

In the following, supply and exhaust subscripts correspond to the inlet port and outlet port of each component and do not correspond to supply and exhaust conditions of the zones.

6.1.1. Recovery system model

Only air-to-air heat exchangers are considered in the present model. Depending on the type of recovery heat exchanger, sensible and/or total heat exchanges are calculated by means of effective effectiveness'. Because the exhaust air flow rate is generally slightly inferior (generally 10% below) to the supply air flow rate (indoor zones over pressurized during ventilation operation), the specified effectiveness is corrected and replaced by an effective effectiveness (Klein, 2007 – Type 334).

$$\varepsilon_{sens,eff} = \frac{\dot{m}_{ret}}{\dot{m}_{fresh}} * \varepsilon_{sens}$$

$$\varepsilon_{lat,eff} = \frac{\dot{m}_{su}}{\dot{m}_{fresh}} * \varepsilon_{lat}$$

The exhaust conditions are given by:

$$t_{fresh,ex} = t_{fresh,su} + \varepsilon_{sens,eff} * \left(t_{ret,su} - t_{fresh,su}\right)$$

$$w_{fresh,ex} = w_{fresh,su} + \varepsilon_{lat,eff} * \left(w_{ret,su} - w_{fresh,su}\right)$$

The recovery systems can be equipped with a bypass for avoiding overheating and overcooling. If the bypass is activated, only the return air flow required to reach the setpoint flows through the recovery heat exchanger. The considered setpoint is arbitrary fixed to the supply air setpoint minus 2 K to take the air heating in the fan into account.

6.1.2. Economizer model

The air economizer (or mixer) can be operated in two ways: a constant fresh air fraction or a variable fresh air fraction determined by the following control objectives (Brandemuehl, 1993):

- Maintain mixed air temperature setpoint (arbitrary fixed 2 K below the supply air setpoint),
- Maintain minimum fresh air fraction (even in winter conditions),
- Reduce outside air to minimum when no beneficial for cooling.

After determining the optimal fresh air ratio, the mixed air conditions are given by:

$$t_{ex,econo} = \frac{\dot{M}_{recirc} * t_{ret} + \dot{M}_{fresh} * t_{fresh}}{\dot{M}_{recirc} + \dot{M}_{fresh}}$$

$$w_{ex,econo} = \frac{\dot{M}_{recirc} * w_{ret} + \dot{M}_{fresh} * w_{fresh}}{\dot{M}_{recirc} + \dot{M}_{fresh}}$$

Where

$\dot{M}$ is the air flow rate (in kg/s)

w is the air humidity ratio (in kg/kg)

t is the air temperature (in °C)

It is also possible to set scheduled full recirculation (at the start-up of the installation for example).

6.1.3. Heating coil model

The heating coil model consists in an “inversed model” used for both pre-heating and post-heating coils. Pre-heat in the pre-heating coil occurs when the operation of the adiabatic humidifier requires it. Re-heat in the post-heating (or re-heating) coil occurs when the coil supply temperature is below the supply air temperature setpoint.

The heat transfer rate is calculated as a function of the supply and exhaust (setpoint) temperature.

$$\dot{Q}_{heat} = \dot{M}_a * c_{p,a} * \left(t_{ex,set} - t_{su}\right)$$

Where

$\dot{M}_a$ is the air flow rate (in kg/s)

$c_{p,a}$ is the air specific heat (in J/kg-K)

$t_{ex,set}$ is the setpoint exhaust drybulb temperature (in °C)

t_{su} is the supply drybulb temperature (in °C)

Depending on the type of the coil (water, electrical or direct expansion), the corresponding hot water and electricity loads are computed.

$$\dot{W}_{heat} = \dot{W}_{aux} + \frac{\dot{Q}_{heat}}{COP}$$

$\dot{W}_{heat}$ is the heating coils electricity consumption (in W)

$\dot{W}_{aux}$ is the heating coils rating auxiliary (circulators) consumption and is about 0.5% of the nominal heating capacity of the coil (in W)

COP is the heating coil coefficient of performance (1 if electrical heating coil, >1 if direct expansion coil or not used in case of a hot water coil)

6.1.4. Adiabatic humidification system model

The adiabatic humidification system includes a pre-heating coil and an adiabatic humidifier (pulverization, evaporative or atomizing humidifiers). A post-heating (or re-heating) coil is also required to re-heat the air after the adiabatic cooling in the humidifier. The global heating load and the water consumption are computed in a simplified way (Klein, 2007 – Type 334). Knowing the supply conditions and the exhaust humidity setpoint, the corresponding heating load and the water consumption are easily computed.

The main equations used to describe the adiabatic humidification process are:

$$\varepsilon = 1 - e^{(-NTU)}$$

$$NTU = \frac{AU}{\dot{M}_a}$$

$$w_{ex} = w_{su} + \varepsilon * (w_{sat,su} - w_{su})$$

$$t_{ex} = t_{su} + \varepsilon * (t_{wb,su} - t_{su})$$

Where

ε is the adiabatic humidifier effectiveness

NTU is the number of transfer unit

AU is the equivalent heat transfer coefficient (in W/K)

$\dot{M}_a$ is the air flow rate (in kg/s)

w_{ex} is the exhaust humidity ratio (in kg/kg)

w_{su} is the supply humidity ratio (in kg/kg)

$w_{sat,su}$ is the supply humidity ratio at saturated conditions (in kg/kg)

t_{ex} is the exhaust drybulb temperature (in °C)

t_{su} is the supply drybulb temperature (in °C)

$t_{wb,su}$ is the supply wetbulb temperature (in °C)

The heat transfer coefficient is computed as a function of the actual air flow rate and the nominal air flow rate and heat transfer coefficients. This last value is determined as a function of the input value of the nominal adiabatic humidifier effectiveness.

In a first time, the equations given above are arranged in order to compute the value of the supply air temperature required to reach the humidity setpoint at the exhaust of the humidifier ($t_{adiabhum,su,set}$, in °C), as a function of the supply humidity ratio.

The computed supply air temperature corresponds to the exhaust temperature setpoint of the pre-heating coil. If this temperature is below the air temperature at the inlet of the pre-heating coil, the heating coil model is used to compute the corresponding heating load. If the temperature at the inlet of the pre-heating coil is already higher than the desired value, no heating is required and the adiabatic humidifier works as an "adiabatic cooling system" by cooling down the air by humidifying it.

IF $t_{adiabhum,su,set} > t_{prehc,su}$

Preheating is needed and the Heating Coil subroutine is called in order to compute the corresponding heating load ($\dot{Q}_{prehc}$*, in W).*

ELSE

No preheating is needed and there is no heating load.

END

This last operation occurs quite rarely since the humidity needs usually disappear when the outdoor air temperature increases (mid-season).

The auxiliary electricity consumption is given by:

$$\dot{W}_{adiabhum} = \dot{W}_{adiabhum,n}$$

Where

$\dot{W}_{adiabhum}$ is the adiabatic humidifier auxiliary (pump or motor) consumption (in W)
$\dot{W}_{adiabhum,n}$ is the adiabatic humidifier rating auxiliary (pump or motor) consumption (in W)

The auxiliary power highly depends on the type of humidifier user (pulverization, evaporative or atomizing humidifiers) and is usually about 5 to 20 W/kg/h.

6.1.5. Cooling coil model

The water cooling coil can be controlled for cooling (temperature control) or dehumidification (humidity ratio control) purposes. In case of temperature-based control, condensation can occur and must be taken into account to compute the final cooling need. In case of dehumidification control, the post-heating coil is used to re-heat the air after dehumidification. The present model is based on the work of Lebrun et al. (1990).

In both cases, perfect control is again supposed and the cooling coil is supposed to be able to reach the desired (temperature or humidity) setpoint. The main outputs of the model are the degree-of-freedom at the exhaust of the coil (humidity or temperature) and the corresponding total, sensible and latent cooling loads.

Firstly, the contact effectiveness (Lebrun et al., 1990) is computed as a function of the actual air flow rate:

$$AU_a = AU_{a,n} * \left(\frac{\dot{M}_a}{\dot{M}_{a,n}}\right)^{0.77}$$

$$NTU_c = \frac{AU_a}{\dot{M}_a * c_{p,a}}$$

$$\varepsilon_c = 1 - e^{(-NTU_c)}$$

Where

AU_a, $AU_{a,n}$ are the actual and nominal air side heat transfer coefficients (in W/K)

$\dot{M}_a$, $\dot{M}_{a,n}$ are the actual and nominal air flow rates (in kg/s)

NTU_c is the number of transfer units

ε_c is the contact effectiveness

If the cooling coil is controlled to maintain a determined exhaust humidity ratio, the exhaust humidity ratio matches the setpoint (perfect control and sufficient capacity) and the main unknown is the exhaust temperature. The contact humidity ratio is computed and used to determine the corresponding contact temperature and, finally, the exhaust temperature.

$$w_c = w_{su} + \frac{w_{ex} - w_{su}}{\varepsilon_c}$$

$$t_c = f(w_c)$$

$$t_{ex} = t_{su} - \varepsilon_c * (t_{su} - t_c)$$

$$\dot{Q}_{tot} = \dot{M}_a * (h_{su} - h_{ex})$$

$$\dot{Q}_{sens} = \dot{M}_a * c_{p,a} * (t_{su} - t_{ex})$$

$$\dot{Q}_{lat} = \dot{Q}_{tot} - \dot{Q}_{sens}$$

$$SHR = \dot{Q}_{sens}/\dot{Q}_{tot}$$

Where

w_{su}, w_{ex} are the supply and exhaust humidity ratios (in kg/kg)

t_{su}, t_{ex} are the supply and exhaust air temperatures (in °C)

h_{su}, h_{ex} are the supply and exhaust air enthalpies (in J/kg)

t_c, w_c are the contact temperature and humidity ratios (in °C and kg/kg)

$\dot{M}_a$ is the air flow rate (in kg/s)

$\dot{Q}_{tot}$ is the total heat transfer rate (in W)

$\dot{Q}_{sens}$ is the sensible heat transfer rate (in W)

$\dot{Q}_{lat}$ is the latent heat transfer rate (in W)

If the cooling coil is controlled to maintain a determined exhaust temperature, the exhaust temperature matches the temperature setpoint (perfect control and sufficient capacity) and the main unknown is the exhaust humidity ratio. The contact temperature is computed and used to determine the corresponding humidity ratio and, finally, the exhaust humidity ratio.

$$t_c = t_{su} + \frac{t_{ex} - t_{su}}{\varepsilon_c}$$

$$w_c = f(t_c)$$

$$w_{ex} = w_{su} - \varepsilon_c * (w_{su} - w_c)$$

If condensation does not occur, the exhaust humidity ratio is equal to the supply humidity ratio.

$$\dot{Q}_{tot} = \dot{M}_a * (h_{su} - h_{ex})$$

$$\dot{Q}_{sens} = \dot{M}_a * c_{p,a} * (t_{su} - t_{ex})$$

$$\dot{Q}_{lat} = \dot{Q}_{tot} - \dot{Q}_{sens}$$

$$SHR = \dot{Q}_{sens}/\dot{Q}_{tot}$$

6.1.6. Steam humidification system model

This subroutine computes the energy consumption of a dry steam injection humidifier as a function of the supply conditions and the humidification needs (exhaust humidity setpoint). The exhaust humidity ratio is of course limited by the saturated humidity ratio at exhaust temperature which is equal to the supply air temperature setpoint at the exhaust of the air handling unit.

The energy balance is given by:

$$\dot{M}_{steam} * h_{steam,su} = \dot{M}_a * (h_{a,ex} - h_{a,su})$$

$$\dot{M}_{steam} = \dot{M}_a * (w_{ex} - w_{su})$$

Where

$\dot{M}_{steam}$ is the steam flow rate (in kg/s)

$\dot{M}_a$ is the air flow rate (in kg/s)

w_{ex}, w_{su} are the exhaust and supply humidity ratios (in kg/kg)

$h_{steam,su}$ is the steam supply enthalpy (in J/kg)

$h_{a,ex}$, $h_{a,su}$ are the exhaust and supply air enthalpies (in J/kg)

The steam enthalpy flow rate is then computed and used to compute the heat flow required to produce the steam and the possible electricity consumption (in the case of a electrical steam generator).

$$\Delta h_{steamhum} = h_{steam,su} - h_{w,su}$$

$$\dot{Q}_{steam} = \dot{M}_{steam} * \Delta h_{steamhum}$$

$$\dot{W}_{steamgen} = \frac{\dot{Q}_{steam}}{\eta_{steamgen}}$$

Where

$\Delta h_{steamhum}$ is the water enthalpy variation (in J/kg)

$h_{w,su}$ is the initial water enthalpy (in J/kg)

$\dot{Q}_{steam}$ is the heat flow corresponding to the production of the steam flow (in W)

$\eta_{steamgen}$ is the electrical steam generator efficiency

$\dot{W}_{steamgen}$ is the electricity consumption of the steam generator (in W)

Steam is supposed to be produced at atmospheric pressure with a slight overheating of 10K and the initial temperature of the tap water is supposed to be equal to 10°C.

6.1.7. Fan model

To avoid a detailed calculation of pressure drops in air ducts, part load curves are used to compute the consumption of the ventilation fan as function of the air flow ratio (Brandemuehl, 1993). Of course, in case of a CAV, the ventilation fan consumption and flow rates are constant.

The fan consumption at maximal flow rate is defined by means of the Specific Fan Power (SFP) in W/m³/s as defined in EN13779-2007. Typical values of SFP for various fan classes are given in Table 8. Corrections should be applied when specific components are added (Table 9).

Table 8: Typical values of SFP (EN13779-2007)

Class	SFP W/m³/s
SFP 1	< 500
SFP 2	500 – 750
SFP 3	750 – 1250
SFP 4	1250 – 2000
SFP 5	2000 – 3000
SFP 6	3000 – 4500
SFP 7	> 4500

Table 9: example values of SFP corrections for some components (EN13779-2007)

Component	SFP W/m³-s
Additional filter	+ 300
High efficiency filter	+ 1000
Heat recovery exchanger	+ 300

The maximal fan consumption ($\dot{W}_{elec,n}$, in W) and the corresponding shaft power ($\dot{W}_{shaft,n}$, in W) are given by:

$$\dot{W}_{elec,n} = SFP * \dot{V}_{a,n}$$

$$\dot{W}_{shaft,n} = \dot{W}_{elec,n} * \eta_{mot}$$

Where

$\dot{V}_{a,n}$ is the nominal air flow rate (in m³/s)
η_{mot} is the (constant) motor efficiency

In operation, the part load ratio (PLR) is defined as the ratio of the actual volumetric flow rate to the nominal air flow rate:

$$PLR = \frac{\dot{V}_a}{\dot{V}_{a,n}}$$

The fraction of full load power (PFPLR) is calculated as a function of the part load ratio by means of the following polynomial curve:

$$PFPLR = a + b * PLR + c * PLR^2 + d * PLR^3$$

The actual shaft power ($\dot{W}_{shaft}$, in W) and the corresponding electrical consumption ($\dot{W}_{elec}$, in W) are given by:

$$\dot{W}_{shaft} = PFPLR * \dot{W}_{shaft,n}$$

$$\dot{W}_{elec} = \frac{\dot{W}_{shaft}}{\eta_{mot}}$$

The heat generated by the fan and exchanged with the blown air is given by:

$$\dot{Q}_{loss} = \dot{W}_{shaft} + \left(\dot{W}_{elec} - \dot{W}_{shaft}\right) * f_{mot,loss}$$

$$\dot{Q}_{loss} = \dot{V}_a * \rho_a * c_{p,a} * (t_{a,ex} - t_{a,su})$$

Where

$\dot{Q}_{loss}$ is the heat flow transmitted from the fan to the blown air (in W)

$f_{mot,loss}$ is the electrical motor loss factor, equal to 1 if the motor is located in the air stream or 0 if the motor is out of the air stream.

$t_{a,ex}$ is the fan exhaust temperature (in °C)

$t_{a,su}$ is the fan supply temperature (in °C)

So, knowing the desired exhaust temperature (determined in order to maintain the supply air temperature setpoint at the exhaust of the air handling unit), the required supply temperature can be computed and will be used as a corrected setpoint for the heating coils of the air handling unit.

Typical values of the coefficients of the polynomial curve used to describe the part load behavior of the fan are given in Table 10 depending on the type of part load control (discharge dampers, inlet vanes or variable speed drive). The PFPLR(PLR) curves are shown in Figure 15 for the three types of part load flow control. EN15241 (2007) provides also typical part load curves for different types of ventilation fans.

Table 10: Ventilation fans - regression coefficients (Brandemuehl, 1993)

Control	a	b	c	d
CAV	1	0	0	0
VAV - Discharge Dampers	0.3507123	0.3085	-0.54137	0.871988
VAV - Inlet Vanes	0.3707	0.9725	-0.3424	0.0
VAV - Variable Speed Drive	0.00153	0.005208	1.1086	-0.11635563

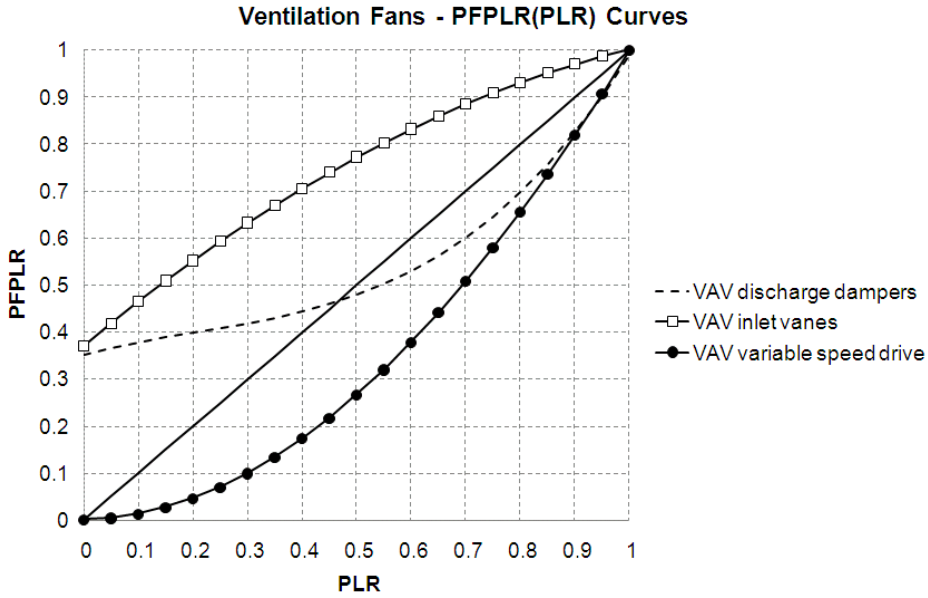

Figure 15: Ventilation fans - Fraction of full load power as a function of Part load ratio

6.2. TERMINAL UNIT MODEL

The terminal unit model consists in converting the sensible heating and cooling loads computed by means of the thermal zone model into hot water, chilled water and electricity demands. Condensation in cooling terminal units is not taken into account.

Six types of heating terminal units are considered in the present work:

- Fan coil unit
- Induction unit
- Light (not massive) radiant heating ceiling panels
- Light (not massive) radiant heating floor
- Radiators
- Terminal reheat boxes

Four types of cooling terminal units are considered in the present work:

- Fan coil unit
- Induction unit
- Light radiant cooling ceiling panels
- Light radiant cooling floor

When an auxiliary consumption is related to the operation of terminal unit (e.g. five speeds fans in fan coil units), its power is supposed to be proportional to the heating/cooling load. So, the part load ratio of the unit and the related electricity consumption are given by:

$$PLR_{tu} = \frac{\dot{Q}_{tu}}{\dot{Q}_{tu,max}}$$

$$\dot{W}_{tu} = PLR_{tu} * \dot{W}_{aux,n} + f_{elec} * \dot{Q}_{tu}$$

Where

$\dot{Q}_{tu}$, $\dot{Q}_{tu,max}$ are the actual heating/cooling power and capacity (in W)
PLR_{tu} is the part load ratio of the unit (defined in terms of power)
$\dot{W}_{aux,n}$ is the nominal auxiliary consumption
f_{elec} is the heating coil electrical factor (=1 if electrical heating coils or 0 if water heating coils)
$\dot{W}_{tu}$ is the terminal unit electricity consumption (in W)

Table 11 provides default values of auxiliary power normalized to the nominal heating/cooling capacity (in W_{el}/W_{th}) for different types of units (Figure 16).

Table 11: Specific Auxiliary Power for different types of terminal units

System	Heating	Cooling
Fan coil unit	0.015 – 0.02	0.02 - 0.03
Radiant ceiling panels	0.01	0.01
Radiant floor system	0.01	0.01
Terminal reheat box (if auxiliary fan)	0.02	-

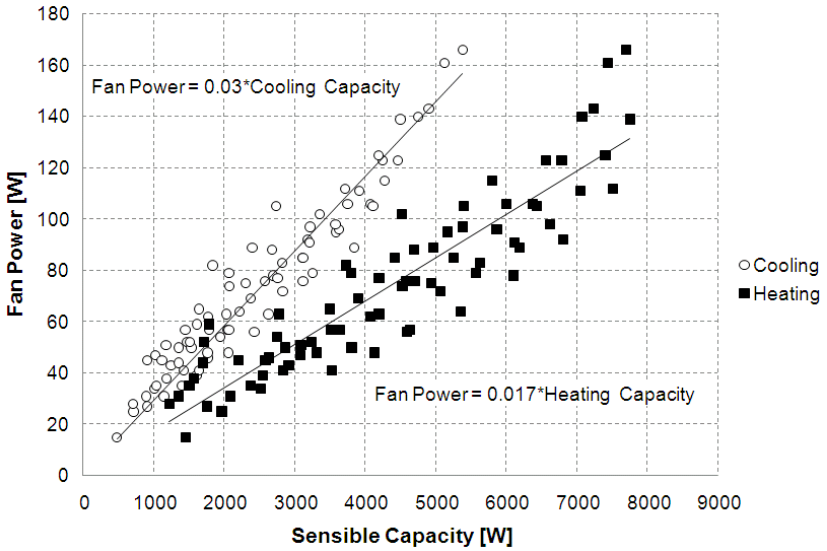

Figure 16: Relation between fan power and sensible heat transfer for fan coil units

In the case of water (heating or cooling) terminal units, the capacity is directly related to the heat source and heat sink temperatures (i.e. to the hot/chilled water temperature and to the indoor temperature). For the sake of simplicity, it has been decided to consider that the heating/cooling capacity of the unit is directly proportional to the temperature difference between the source and the sink.

$$\dot{Q}_{h,max} = \dot{Q}_{h,n} * \frac{t_{hs} - t_i}{t_{hs,n} - t_{i,n}}$$

Where

$\dot{Q}_{h,max}$ is the heating capacity of the unit (in W),

$\dot{Q}_{h,n}$ is the heating capacity of the unit in nominal ($t_{hs,n}$ and $t_{i,n}$) conditions (in W),

t_{hs} is the heat source temperature (typically the average hot water temperature, in °C),

t_i is the indoor air temperature (in °C).

Depending on the type of terminal unit in use, the radiative-convective split varies. For fan coil units, the heat transfer is (almost) purely convective. On the contrary, radiation can represent up to 80% of sensible heat transfer in radiant systems. Table 12 provides typical values of convective fraction for the considered terminal unit types.

Table 12: convective fraction for different types of terminal units

System	Heating	Cooling	Source
Fan coil unit	1	1	EN15255, Davies (2004)
Active induction unit	1	1	EN15255, Davies (2004)
Radiant ceiling panels	0.2	0.3 to 0.5	Conroy and Mumma (2001) Miriel et al. (2002) Fonseca (2009)
Radiant floor system	0.45	0.15	EN15255, Achermann (2003)
Radiator	0.8 to 0.9	-	Davies (2004)
Terminal reheat box	1	-	EN15255, Davies (2004)

7. PRIMARY HVAC SYSTEM MODEL

The primary HVAC system model includes various configurations of chillers (scroll, screw and centrifugal chillers; air and water condensers), water coolers (dry fluid cooler, direct and indirect contact cooling towers) and heat production systems (On-Off burners, High-Low-Off burners and Modulating burners boilers).

7.1. DISTRIBUTION SYSTEM MODEL

All auxiliaries (pumps, circulators and fans) related to the various primary HVAC components (cooling towers, boiler…) are also taken into account in a simplified way: default values of specific fan and pump powers based on manufacturers data are used to compute the related electricity use.

As a first approach, only constant flow pumps are considered. Pumps power consumption is directly linked to the fluid flow rate by defining a SPP ("Specific Pump Power") in W/kg/s.

ASHRAE Standard 90.1 (2007) directly provides values of SPP for classical hot and cold water networks (Table 13).

Table 13: Hydraulic network specific pump power

Type of hydraulic network	SPP	Source
Cold water network	350 W/(kg/s)	ASHRAE (2007)
Hot water network	300 W/(kg/s)	ASHRAE (2007)
Cooling water network (condenser pump)	300 W/(kg/s)	ASHRAE (2007)

Heat losses and gains along piping network are taken into account and occur when there is a heating/cooling demand. The heat loss/gain is arbitrarily computed as a fixed percentage of the heating/cooling capacity of the plant (e.g. 2.5% of the plant capacity) or estimated based on the characteristics of the building and the distribution network according to EN15316-2-3 (2006).

The nominal heat loss/gain of a water network is given by the following equation:

$$\dot{Q}_{loss/gain} = L_p * U_p * ABS(t_m - t_{amb})$$

Where

$\dot{Q}_{loss/gain}$ is the heat loss/gain of the network (in W),

L_p is the piping network length (in m),

U_p is the pipes linear heat transfer coefficient (in W/m-K),

t_m is the piping network average temperature (in °C),

t_{amb} is the ambient temperature (in °C).

The length of a two-pipes distribution network with shafts inside the building is given in Table 14 according to EN15316-2-3 (2006).

Table 14: Pipe length calculation

L_V - Between generators and shafts	**L_S - Pipes in shafts**	**L_A - Connection pipes to the emission system**
Unheated space (Ambient temp: 13°C)		Heated space (Ambient temp: 20°C)
$2 * L + 0.0325 * L * B + 6$	$0.025 * L * B * n * h$	$0.55 * L * B * n$

Where

L is the building length (in m),

B is the building width (in m),

n is the number of floors,

h is the floor height (in m).

Default values of linear heat transfer coefficient provided in EN15316-2-3 (2006) are given in Table 15.

Table 15: Linear heat transfer coefficient of distribution pipes

Age class of the installation	**Pipes in unheated space** W/m-K	**Pipes in heated space** W/m-K
Old installation (before 1980)	0.4	0.4
1980 to 1995	0.3	0.4
From 1995	0.2	0.3

7.2. HEATING PLANT MODEL

Only hot water boilers are considered in the present model. The model is based on performance curves given by Stan (1995) and in EN15316-4-1 (2006).

The water temperature dependency of the boiler performance is represented by the following law:

$$\eta_{cor,FL} = (\eta_{nom,FL} + f_{cor} * (t_{test} - t_{w,avg}))$$

Where

$\eta_{cor,FL}$ is the corrected efficiency of the boiler at full load (in %),

$\eta_{nom,FL}$ is the rating efficiency of the boiler at full load (in %),

f_{cor} is the correction factor (given in EN15316-4-1, 2006),

t_{test} is the boiler average water temperature at test conditions for full load (given in EN15316:2006, in °C),

$t_{w,avg}$ is the boiler average water temperature in operating conditions (in °C),

Table 16: Default values for full load correction factor (EN15316-4-1, 2006)

Boiler type	**Correction factor [-]**	**Test temperature [°C]**
Standard boiler	0.04	70°C (avg temperature)
Low-temperature boiler	0.04	70°C (avg temperature)

Gas condensing boiler	0.2	70°C (return temperature)
Oil condensing boiler	0.04	70°C (return temperature)

The part-load variation of the thermal performance of the boiler is given by the following equation:

$$\eta_{actual} = \eta_{cor,FL} * \eta^*_{PL}$$

$$\eta^*_{PL} = \left(a + b * \frac{1}{PLR} + c * PLR + d * PLR^2\right)$$

Where

η_{actual} is the actual efficiency of the boiler (in operating conditions, in %),

η^*_{PL} is the normalized part load efficiency of the boiler, defined as a ratio between the actual efficiency in given operating conditions and the nominal efficiency of the boiler

a, b, c, and d are regression coefficients,

PLR is the part load ratio.

The regression coefficients a, b, c and d have been identified for various types and generations of boilers and burners. The specific boiler method proposed in EN15316-4-1 (2006) has been implemented and run at various part load conditions in order to generate the desired part load curves (Figure 17).

The part load ratio is defined by the ration between the actual heat demand and the nominal capacity of the boiler:

$$PLR = \frac{\dot{Q}_{boiler}}{\dot{Q}_{boiler,FL}}$$

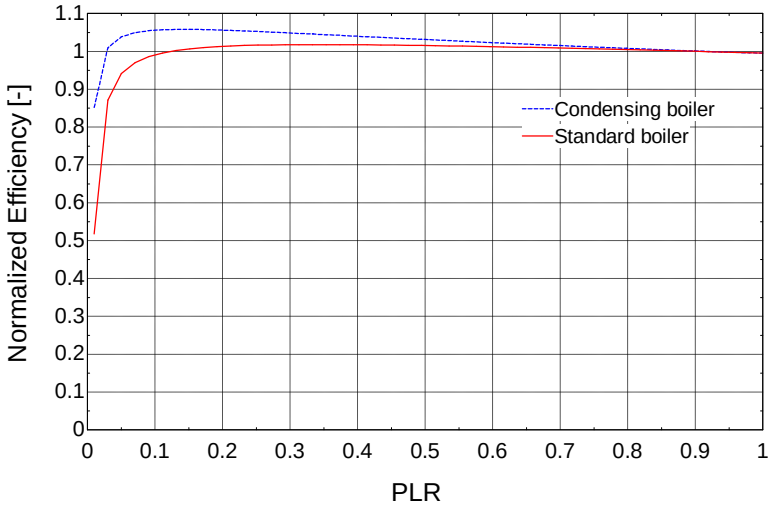

Figure 17: Part load dependency of the boiler efficiency

Stand-by losses are estimated based on the nominal capacity of the boiler. Default values of the nominal-to-stand-by power ratio are given in Table 17 according to EN15316-4-1 (2006).

Table 17: Default values of stand-by losses ratio

Boiler type	**Burner Type**	**Stand-by losses** [% of nominal capacity]

Standard	Atmospheric	0.6 to 0.7%
	Forced draught	0.6 to 0.7 %
Low Temperature	Atmospheric	0.6 to 0.7%
	Forced draught	0.6 to 0.7%
Gas Condensing	All	0.2 to 0.6 %
Oil Condensing	All	0.2 to 0.6 %
Change fuel	All	1.1 to 1.2 %

Two options are available to simulate multiple boilers plants:

- Ideal cascade: Boilers are started one after the other as function of the load. When "n" boilers operate, "n-1" boilers operate at full load and only the last one operates at part load.
- Realistic cascade: Boilers are started one after the other but the load is shared. When "n" boilers operate, the "n" boilers operate at the same load rate.

7.3. COOLING PLANT MODEL

7.3.1. Chiller model

The chiller model uses performance curves identified based on manufacturer data (Bohler et al., 2002). Like the DOE-2 model (Hydeman and Gillespie, 2002), the "Consoclim" model uses three basic functions usable to predict the chiller consumption over a range of operating conditions:

- Chiller capacity as a function of the operating conditions (secondary fluids temperatures) at full load;
- Electric power demand as a function of the operating conditions (secondary fluids temperatures) at full load;
- Electric power ratio as a function of part-load ratio.

The chiller full load capacity is given by:

$$\dot{Q}_{FL} = \dot{Q}_n * \left[1 + D_1 * \left(t_{su,cd} - t_{su,cd,n}\right) + D_2 * \left(t_{ex,ev} - t_{ex,ev,n}\right)\right]$$

Where

$\dot{Q}_{FL}$, $\dot{Q}_n$ are the actual full load capacity in actual conditions and the full load capacity in nominal conditions (in W)

$t_{su,cd}$, $t_{su,cd,n}$ are the actual and nominal condenser secondary fluid supply temperature (in °C)

$t_{ex,ev}$, $t_{ex,ev,n}$ are the actual and nominal evaporator secondary fluid exhaust temperature (in °C)

D_1, D_2 are parameters of the model.

The chiller full load power demand is given by:

$$\dot{W}_{FL} = \dot{Q}_{FL} * \frac{\dot{Q}_n}{\dot{W}_n} * (1 + C_1 * \Delta t + C_2 * \Delta t^2)$$

Where

$\dot{W}_{FL}$, $\dot{Q}_{FL}$ are the actual full load power demand and capacity in actual conditions (in W)

$\dot{W}_n$, $\dot{Q}_n$ are the actual full load power demand and capacity in nominal conditions (in W)

C_1, C_2 are parameters of the model.

The non-dimensional temperature difference, Δt, is given by:

$$\Delta t = \frac{t_{su,cd}}{t_{ex,ev}} - \frac{t_{su,cd,n}}{t_{ex,ev,n}}$$

Where

$t_{su,cd}$, $t_{su,cd,n}$ are the actual and nominal condenser secondary fluid supply temperatures (in [2] K)

$t_{ex,ev}$, $t_{ex,ev,n}$ are the actual and nominal evaporator secondary fluid exhaust temperatures (in K)

The original part load curve is given by:

$$EIRFPLR = K * PLR + (1 - K) * PLR^2$$

Where

EIRFPLR (Energy Input Ratio as a function of the Part Load Ratio) represents the part load behavior of the chiller

PLR is the part load ratio of the chiller, defined as the ratio of the actual cooling load to the full load capacity in actual operating conditions

K is a parameter of the model.

Parameters D1, D2, C1, and C2 are identified based on 3 full load data points and K can be estimated based on part load data analysis.

A modified EIRFPLR law is used in the present model. The original law gives a “lens” shape not fully representative of the actual part load behavior of vapor compression chillers. Indeed, such shape gives similar chiller performance at very low part load rate (below 20%) and at high load rate (over 90%). Degradation of performance intervenes only at medium load (50-60%).

The modified law is given by:

$$EIRFPLR = K_1 + (K_2 - K_1) * PLR + (1 - K_2) * PLR^2$$

A set of parameters estimated based on a chiller market survey are given in Table 18 (Dupont, 2006) for five configurations of air cooled reciprocating, scroll and screw chillers and for water cooled reciprocating and scroll chillers. Unfortunately, only the original part load law (one parameter) was used in this work. A new market survey would allow identifying typical values of the parameters of the proposed part load law (Figure 18). Manufacturer data collected for water cooled screw and centrifugal chillers have been used to complete the set of default values and identify typical values of the full load and part load parameters for 26 water cooled screw chillers, 95 constant speed centrifugal chillers and 47 variable speed centrifugal chillers (Bertagnolio et al., 2010).

Table 18: Chiller model default values

Condenser	Compressor	C1	C2	D1	D2	K1	K2
air	reciprocating	4.5	-0.04	-0.014	0.034	0	1.04
air	scroll	8.15	24.15	-0.01	0.033	0	0.82
air	screw	8.15	24.15	-0.01	0.033	0	1.12
water	reciprocating	6.92	21.9	-0.01	0.032	0	0.82

water	scroll	8.93	69.74	-0.01	0.032	0	0.8
water	Screw (inlet vanes)	8.5	25.5	-0.0034	0.03	0.19	0.71
water	Centrifugal (inlet vanes)	8.712	44.6	-0.014	0.0667	0.22	0.55
water	Centrifugal (VSD)	8.712	44.6	-0.014	0.0667	0.14	0.25

Of course, when available, manufacturer data of the installed chiller should be used to identify these coefficients instead of using typical/average values. In the case of a lack of manufacturer data, another possibility is to use a detailed (or "reference") chiller model (Lemort, 2008), calibrated to measurements or using similarity laws, to generate these performance curves and identify the parameters of the regression based model. Nominal performances have to be provided according to EN14511 (2008).

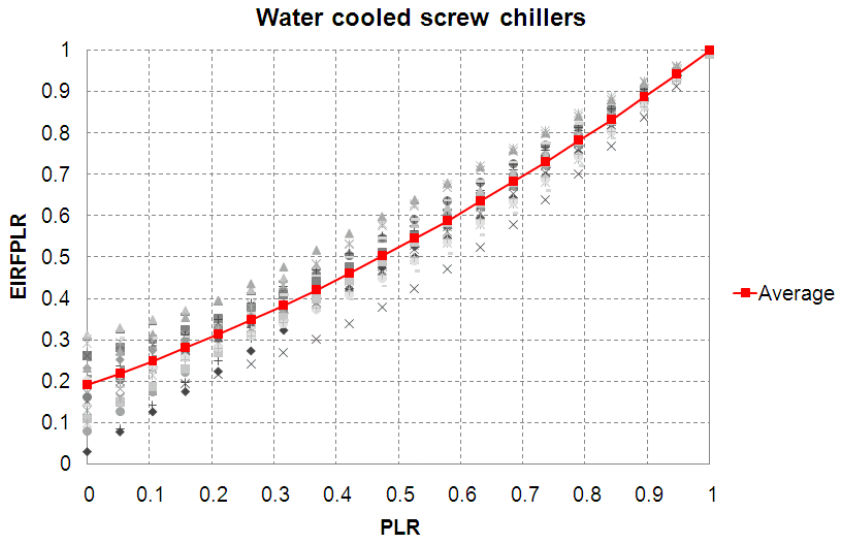

Figure 18: Water cooled screw chiller part load curve

7.3.2. Cooling tower model

The cooling tower model is based on the work of Bourdouxhe et al. (1999) and Lebrun et al. (2002) and uses a modified epsilon-NTU method to simulate the performance of a cooling tower. Only classical direct and indirect contact cooling towers are considered. Hybrid indirect contact cooling towers with operation in dry regime at low load are not taken into account. A brief market survey allowed identifying regression laws used to estimate the installed auxiliary power (pumps and fans) and the nominal air flow rate as function of the nominal capacity for indirect contact (ICCT, Figure 19 and Figure 20) and direct contact (DCCT, Figure 21 and Figure 22) cooling towers.

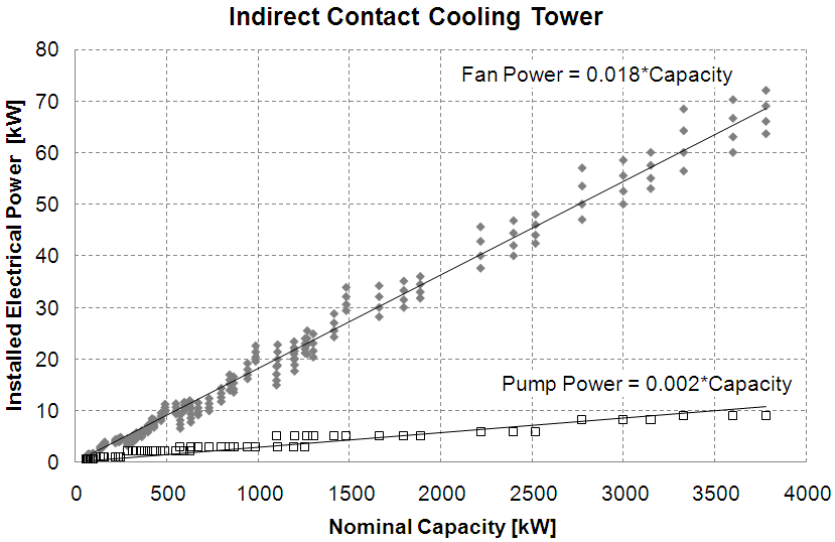

Figure 19: ICCT - Installed Auxiliary power

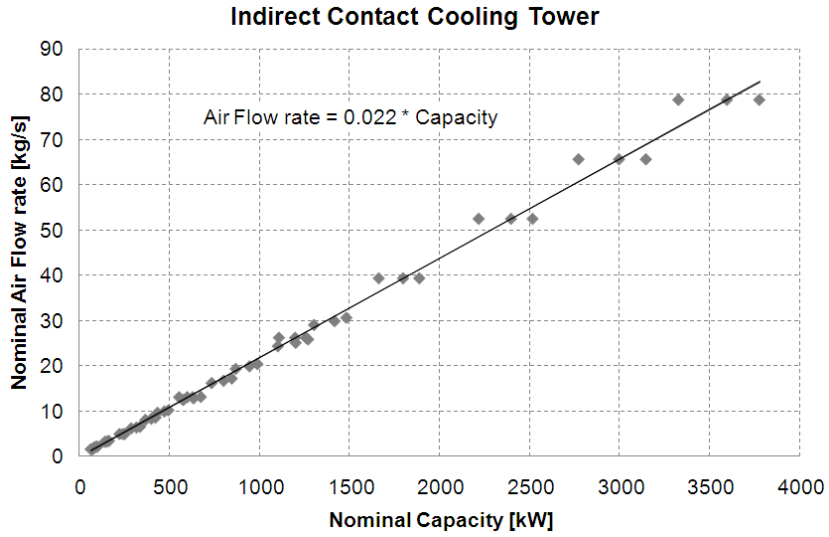

Figure 20: ICCT - Nominal air flow rate

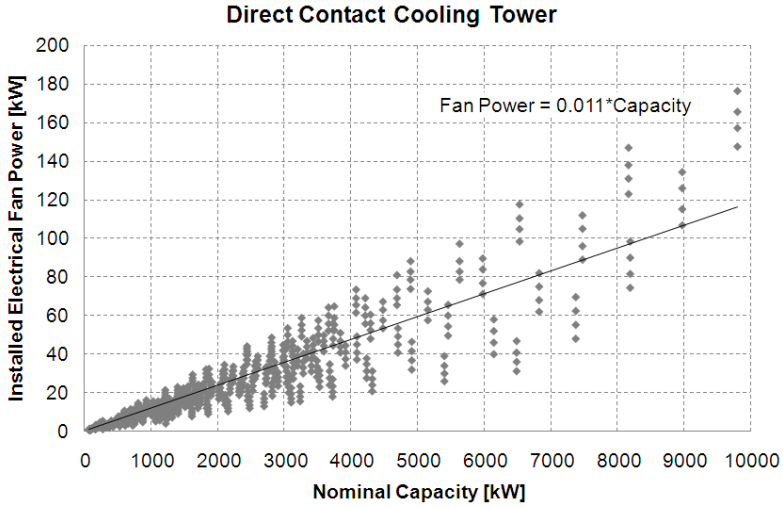

Figure 21: DCCT – Installed auxiliary power

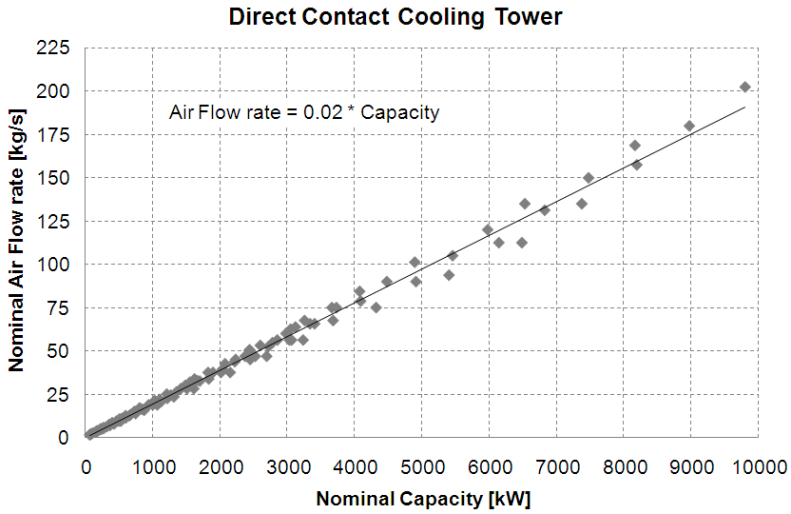

Figure 22: DCCT – Nominal air flow rate

The other parameters of the simulation model are the air-side and water-side heat transfer coefficients are identified by means of the following equations.

Knowing the nominal capacity, air and water supply conditions (specified by the user) and the corresponding air and water flow rates (fixed range determined by the user) and supposing saturated air at the exhaust of the tower, the exhaust air conditions (temperature and humidity) can be computed.

The logarithmic mean temperature difference method is then used to estimate the global heat transfer coefficient (AU, in W/K) and its air-side – water-side repartition (only for indirect contact cooling towers).

$$\Delta t_{ln} = \frac{\left(t_{w,su} - t_{wb,ex}\right) - \left(t_{w,ex} - t_{wb,su}\right)}{ln\left(\frac{t_{w,su} - t_{wb,ex}}{t_{w,ex} - t_{wb,su}}\right)}$$

As proposed by Bourdouxhe et al. (1999), the moist air is replaced by a fictitious perfect gas characterized by its wetbulb temperatures. This leads to the definition of a effective specific heat (in J/kg-K) and the corresponding global heat transfer coefficient (in W/K).

$$c_{p,f} = \frac{h_{a,ex} - h_{a,su}}{t_{wb,ex} - t_{wb,su}}$$

$$AU_{f,n} = \frac{1}{R_{f,n}} = \frac{\dot{Q}}{\Delta t_{ln}}$$

In indirect contact cooling towers, air and water are not directly in contact and the global thermal resistance can be splitted up into three thermal resistances connected in series: an air-side (convective) resistance (R_a), a metal (conductive) resistance and a (convective) water-side resistance (R_w). As proposed by Lebrun et al. (2002), the conductive thermal resistance is neglected and only convective resistances are considered. As two operating points are necessary to evaluate both resistances, a default value of the repartition key (k_R) is used to limit the quantity of data asked to the user.

$$R_{a,n} = \frac{R_{f,n}}{\left(\frac{c_{p,a}}{c_{p,f}} + \frac{1}{k_R}\right)}$$

$$R_{w,n} = \frac{R_{a,n}}{k_R}$$

$$R_{ct,n} = R_{a,n} + R_{w,n} = \frac{1}{AU_{ct,n}}$$

In direct contact cooling towers, Lebrun et al. (2002) proposes to use a unique global heat transfer coefficient to represent the heat and mass transfer.

$$AU_{ct,n} = AU_{f,n} * \frac{c_{p,a}}{c_{p,f}} = \frac{1}{R_{ct,n}}$$

The simulation of the cooling tower is done in two steps:

- First, the full load (maximal air and water flow rates) performance and capacity of the cooler are computed in the actual operating conditions (entering air temperature and humidity and water temperature);
- Secondly, part load curves are used to compute the actual electricity consumption of the cooler as function of the part load ratio.

An iterative process is used to determine the exhaust wetbulb temperature. The effective specific heat is then computed and used to determine the actual value of the heat transfer coefficient to be used to compute the heat exchange effectiveness.

$$c_{p,f} = \frac{h_{a,ex} - h_{a,su}}{t_{wb,ex} - t_{wb,su}}$$

$$\dot{C}_f = \dot{M}_a * c_{p,f}$$

As the cooling tower is supposed to operate at full load (maximal air and water flow rates), actual values of thermal resistances are equal to nominal values.

$$R_w = R_{w,n}$$

$$R_a = R_{a,n}$$

$$R_{ct} = \frac{1}{AU_{ct}} = R_{ct,n}$$

For indirect contact cooling towers, the global thermal resistance is computed as the sum of the water-side thermal resistance and the corrected air-side thermal resistance.

$$R_{a,f} = R_a * \frac{c_{p,a}}{c_{p,f}}$$

$$R_f = R_{a,f} + R_w = \frac{1}{AU_f}$$

For direct contact cooling towers, the fictitious global heat transfer coefficient is given by:

$$AU_f = AU_{ct} * \frac{c_{p,f}}{c_{p,a}}$$

In both cases, supposing counterflow heat exchange, the effectiveness is given by the following set of equations:

$$\dot{C}_{min} = MIN(\dot{C}_f, \dot{C}_w)$$

$$\dot{C}_{max} = MAX(\dot{C}_f, \dot{C}_w)$$

$$\omega = \frac{\dot{C}_{min}}{\dot{C}_{max}}$$

$$NTU = \frac{AU_f}{\dot{C}_{min}}$$

$$\varepsilon = \frac{1 - e^{(-NTU*(1-\omega))}}{1 - \omega * e^{(-NTU*(1-\omega))}}$$

The cooling capacity (at full load) and the corresponding minimal exhaust water temperature are given by:

$$\dot{Q}_{max} = \varepsilon * \dot{C}_{min} * (t_{w,su} - t_{wb,su})$$

$$t_{w,ex,min} = t_{w,su} - \frac{\dot{Q}_{max}}{\dot{C}_w}$$

The actual water exhaust temperature is equal or superior to the minimal exhaust temperature calculated above. If the capacity limit of the cooling tower is not reached, the water exhaust temperature is supposed to be equal to the temperature setpoint (perfect control).

$$t_{w,ex,ac} = MAX(t_{w,ex,min}, t_{w,ex,set})$$

The corresponding cooling power is given by:

$$\dot{Q}_{ac} = \dot{C}_w * (t_{w,su} - t_{w,ex,ac})$$

The part load ratio (varying between 0 and 1) is defined as the ratio of the actual cooling power and the maximal cooling capacity. A regression curve is then used to compute the electrical input ratio (EIRFPLR) and the actual fan consumption as function of the part load ratio (Figure 23). In the case of an indirect contact cooling tower, the auxiliary pump is supposed to operate when the cooling tower is operated. Nominal fan and pump powers are identified by means of the regressions given above (Figure 19 to Figure 22).

$$PLR = \frac{\dot{Q}_{ac}}{\dot{Q}_{max}}$$

$$\dot{W}_{fan} = EIRFPLR(PLR) * \dot{W}_{fan,n}$$

$$\dot{W}_{pump} = \dot{W}_{pump,n}$$

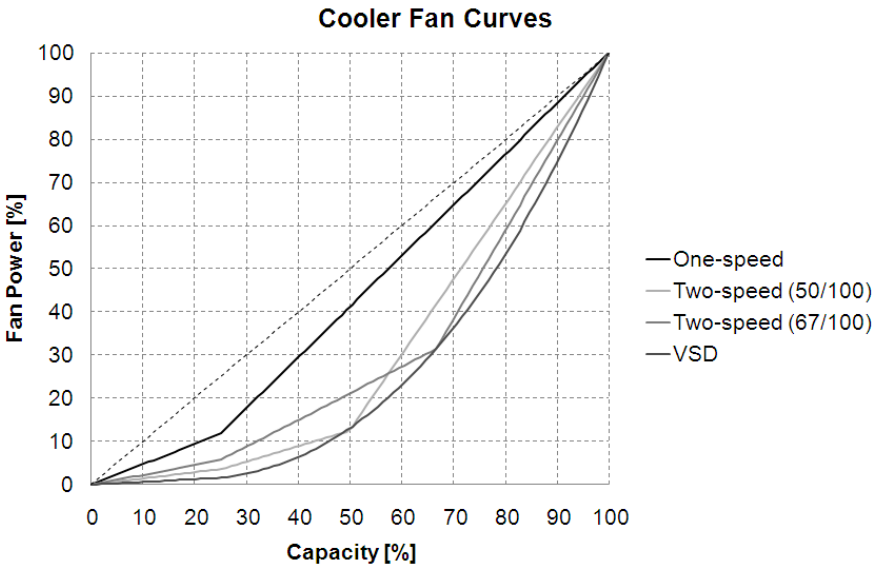

Figure 23: Cooling tower part load curves (Hydeman et al., 2002)

7.3.3. Dry fluid cooler model

Dry fluid coolers are simulated as classical counterflow heat exchangers. The epsilon-NTU method is used to compute the exhaust air and water temperatures. Once again, a market survey allowed identifying a relationship between the installed fan power, the nominal air flow rate and the dry cooler nominal capacity (Figure 24 and Figure 25). The other parameters of the model are identified by means of equations similar to the ones used in the cooling tower model. The simulation is done in two steps:

- First, the full load (maximal air and water flow rates) performance and capacity of the cooler are computed in the actual operating conditions (entering air temperature and humidity and water temperature);
- Secondly, part load curves are used to compute the actual electricity consumption of the cooler as function of the part load ratio.

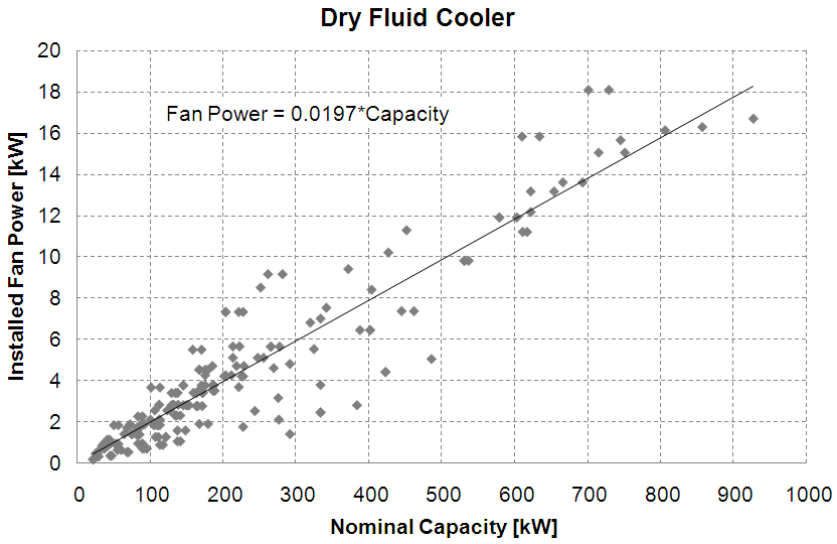

Figure 24: DFC – Installed auxiliary power

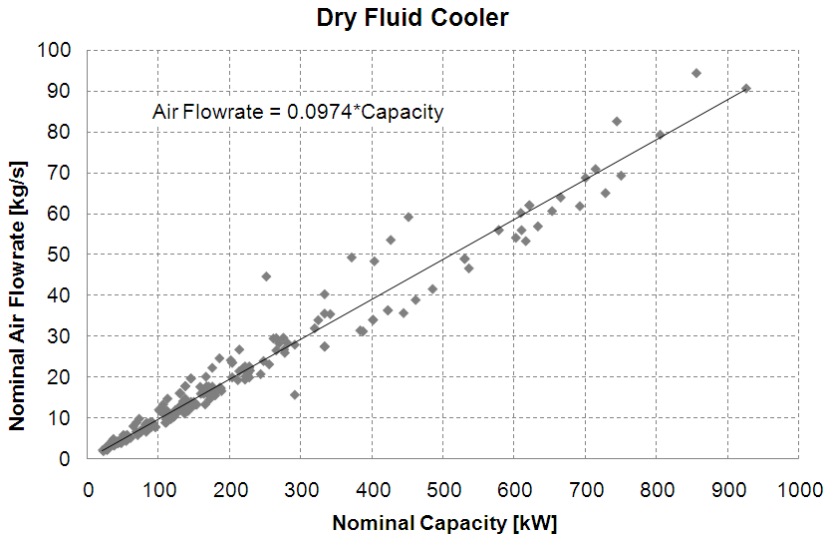

Figure 25: DFC – Nominal air flow rate

8. MOIST AIR PROPERTIES

Classical methods are used to compute the main moist air properties. Sometimes, regression laws are used to avoid iterations. The wetbulb temperature is computed as a function of drybulb temperature and humidity ratio by means of the classical procedure given in ASHRAE (2009). An iterative process is needed to compute the wetbulb temperature. Other moist air properties, such as enthalpies, temperatures and humidity ratios are given in Table 19 and are computed at normal atmospheric pressure (101325 Pa).

Table 19: Moist air properties calculation

Humidity ratio of saturated air as a function of the wetbulb temperature	C_0=0.00388691 C_1=0.0659728 w_s_twb=C_0*exp(C_1*t_wb)
Wetbulb temperature of saturated air as a function of humidity ratio	C_0=0.00388691 C_1=0.0659728 t_wb_ws=LN(w_s/C_0)/C_1
Wetbulb temperature as function of enthalpy	t_wb_h=-5.96424758E+00+6.55925194E-04*h-4.14785613E-09*h^2+1.17408543E-14*h^3
Enthalpy as function of wetbulb temperature	h_twb=9.74400569E+03+1.65233377E+03*t_wb+1.74032625E+01*t_wb^2+9.22867149E-01*t_wb^3
Enthalpy of saturated air as function of the humidity ratio	h_sat=-2.96730126E+04+1.63024862E+07*w_sat-1.83742266E+09*w_sat^2+ 9.15354155E+10*w_sat^3
Enthalpy as function of the drybulb temperature and the humidity ratio	h_t_w=c_p_a*t+(h_fg0+c_p_g*t)*w
Drybulb temperature as function of the enthalpy and the humidity ratio	t_w_h=(h-h_fg0*w)/(c_p_a+w*c_p_g)
Relative humidity as function of drybulb temperature and humidity ratio	p_w=(p_atm*w)/(0.62198+w) p_w_s=exp((17.438*t/(239.78+t))+6.4147) RHUM=MAX(1E-6,MIN(1,p_w/p_w_s))
Humidity ratio as function of drybulb temperature and humidity ratio	p_w_s=exp((17.438*t/(239.78+t))+6.4147 HUMRATIO=(p_w*0.62198)/(p_atm-p_w)
Temperature as function of humidity ratio and relative humidity	p_w=p_atm*w/(0.62198+w) p_w_s=p_w/RH t=(239.78*(log(p_w_s)-6.4147))/(17.438-(log(p_w_s)-6.4147))

9. AUTOMATED PRE-SIZING

An automated pre-sizing of the HVAC system is done to estimate the main parameters of the model (heating and cooling capacities and corresponding flow rates, heat transfer coefficients...). This calculation is based on a static heating energy balance and a static cooling energy balance computed in the nominal winter and summer conditions specified by the user (outdoor temperature, humidity and solar radiation). This first calculation allows identifying the main parameters of the model while reducing to the minimum the quantity of data specified by the user. Correction factors (or multipliers)

can be used to adjust the sizes of the components of the system (e.g. heating and cooling capacities of terminal units, boilers, chillers...). By default, the oversizing is generally estimated to 10 to 20%.

10.IMPLEMENTATION

This simplified BES model has been developed in an equation Solver (Klein, 2010). This implementation increases the flexibility of the model and makes it easily readable and understandable for the user. To decrease the calculation time, increase the numerical performance of the model and make automated calibration possible, it is now implemented in Matlab (2009).

11.SUMMARY

In this chapter, a simulation tool dedicated to energy-use analysis has been presented. The developed simulation tool relies on the use of simple normative or semi-empirical sub-models using physically meaningful parameters. The main advantages of such tool is that it does not require particular modeling expertise since it follows a set of modeling rules that produce a standard measure of energy performance.

The present whole building simulation model is able to simulate various configurations of buildings and systems and include main envelope, HVAC and control issues in order to allow easier calibration and assessment of numerous energy conservation opportunities.

It has been shown that the simple building zone model was able to predict hourly heating and cooling loads (as wells as annual heating and cooling demands) with an acceptable accuracy. This light-weight (generic) quasi-steady state model is able to scale up to large sets of buildings.

12.REFERENCES

Achermann, M., Zweifel, G. 2003. Radtest – Radiant heating and cooling test cases. International Energy Agency – Solar Heating and Cooling Programme Task 22 “Building Energy Analysis Tools”.

Alessandrini, J.M., Fleury, E., Filfi, S., Marchio, D. 2006. Impact de la gestion de l’éclairage et des protections solaires sur la consommation d’énergie des bâtiments de bureaux climatisés. Proceedings of the Climamed Conference, 2006.

ASHRAE, 1989. Handbook Fundamentals. Atlanta: American Society of Heating, Refrigerating and Air-Conditioning Engineers, Inc.

ASHRAE. 2002. ASHRAE Guideline: Measurement of energy and demand savings. ASHRAE Guideline 14-2002.

ASHRAE. 2007. ANSI/ASHRAE/IESNA Standard 90.1-2007, Energy Standard for Buildings Except Low-Rise Residential Buildings. Atlanta: American Society of Heating, Refrigerating and Air-Conditioning Engineers, Inc.

ASHRAE, 2009. Handbook Fundamentals. Atlanta: American Society of Heating, Refrigerating and Air-Conditioning Engineers, Inc.

Bertagnolio, S., Andre, P., Lemort, V. 2010. Simulation of a building and its HVAC system: Application to audit. Building Simulation: An International Journal. Vol 3. DOI 10.1007/s12273-010-0204-z

Bliss R (1961). Atmospheric radiation near the surface of the ground: a summary for engineers. Solar Energy. 5: 103-120.

Bohler, A., Casari, R., Collignan, B., Fleury, E., Marchio, D., Millet, J.R., Morisot, O. 2000. Méthode de calcul des consommations d’énergie des bâtiments climatisés « Consoclim ». Report CSTB ENEA/CVA-99.176R

Bourdouxhe, J.-P., Grodent, M., Lebrun, J., Saavedran C. 1999. ASHRAE HVAC1 Toolkit : A Toolkit for Primary System Energy Calculation. Atlanta : American Society of Heating, Refrigerating and Air-Conditioning Engineers, Inc.

Brandemuehl, M.J. 1993. HVAC 2 Toolkit : A toolkit for secondary HVAC system energy calculations. RP-629. Atlanta: American Society of Heating, Refrigerating and Air-Conditioning Engineers, Inc.

Cho, S., Haberl, J. 2008b. Validation of the eCalc commercial code-compliant simulation versus measured data from an office building in a hot and humid climate. Proceedings of the 16th Annual Symposium on Improving Building Energy Efficiency in Hot and Humid Climates, Plano, Texas.

Conroy C., Mumma S. 2005. Ceiling Radiant Cooling Panels as a viable distributed Parallel Sensible Cooling Technology integrated with dedicated Outdoor air Systems. ASHRAE transactions, 107(1).

CSTB 2008. Annexe à l'arrêté portant approbation de la méthode TH-C-E ex. Paris, France.

Davies, M.G. 2004. Building heat transfer. John Wiley and Sons, Ltd Editors. University of Liverpool, UK.

Duffie, J.A., Beckman, W.A. 1980. Solar Engineering of Thermal Processes. John Wiley & Sons, NY.

Dupont, M. 2006. Energy saving potential of energy services – Experimentation on the life cycle of energy conversion equipments. PhD thesis, Ecole des Mines de Paris, France.

EN 13779:2007. Ventilation for non-residential buildings – Performance requirements for ventilation and room-conditioning systems. International Standard Organization, Geneve, Suisse.

EN 14511-2-2008 Air conditioners, liquid chilling packages and heat pumps with electrically driven compressors for space heating and cooling – Part 2: test conditions. International Standard Organization, Geneve, Suisse.

EN 15241:2007. Ventilation for buildings — Calculation methods for energy losses due to ventilation and infiltration in commercial buildings. International Standard Organization, Geneve, Suisse.

EN 15255:2007. Thermal performance of buildings – Sensible room cooling load calculation – General criteria and validation procedures. International Standard Organization, Geneve, Suisse.

EN 15265:2007. Thermal performance of buildings – Calculation of energy needs for space heating and cooling using dynamic methods – General criteria and validation procedures. International Standard Organization, Geneve, Suisse.

EN15316-2-3: 2006. Heating systems in buildings – Method for calculation of system energy requirements and system efficiencies. Space heating distribution systems. International Standard Organization, Geneve, Suisse

EN 15316-4-1:2006. Heating systems in Buildings – Method for calculation of system energy requirements and system efficiencies – Part 4.1: Space heating generation systems, combustion systems. International Standard Organization, Geneve, Suisse

Fels, M. 1986. Prism: An introduction. Energy and Buildings, 9: 5-18

Fonseca Diaz, N. 2009. About the use of Radiant Ceiling Simulation Models as Commissioning Tools. PhD Dissertation, University of Liège.

Hosni, M.H., Jones, B.W., Xu, H. 1999a. Experimental results for heat gain and radiant/convective split from equipments in Buildings. ASHRAE Transactions. 105(2): 503-515.

Hosni, M.H., Jones, B.W., Xu, H. 1999b. Measurements of heat gain and radiant/convective split from equipments in Buildings. ASHRAE Research Project 1055-RP. Atlanta: American Society of Heating, Refrigerating and Air-Conditioning Engineers, Inc.

Hydeman, M., Gillespie, K.L. 2002. Tools and Techniques to Calibrate Electric Chiller Component. Models. ASHRAE Transactions. 108(1): 733-741.

Hydeman, M., Taylor, S.T., Winiarski, D. 2002. Application of Component Models for Standards Development. ASHRAE Transactions. 108(1): 742-750.

ISO 7730: 2005 Moderate Thermal Environments - Determination of the PMV and PPD Indices and the Specifications of the Conditions for Thermal Comfort - International Standard Organization, Geneve, Suisse

ISO13789 :2007. Thermal performance of buildings – Transmission and ventilation heat transfer coefficients – Calculation method. International Standard Organization, Geneve, Suisse

ISO/FDIS 13790:2007. Energy performance of buildings – Calculation of energy use for space heating and cooling. International Standard Organization, Geneve, Suisse

ISO 13786:2007. Thermal performance of building components – Dynamic thermal characteristics – calculation methods. International Standard Organization, Geneve, Suisse

Katipumala, S., Claridge, D.E. 1993. Use of simplified system models to measure retrofit energy savings. Journal of Solar Energy Engineering, vol. 115, pp. 57-68.

Judkoff, R., Neymark, J. 1995. International Energy Agency Building Energy Simulation Test (BESTEST) and Diagnostic Method. National Renewable Energy Laboratory, U.S. D.O.E.

Kissock, J.K., Haberl, J.S., Claridge, D.E. 2002. Development of a toolkit for calculating linear, change-point linear and multiple-linear inverse building energy analysis models. Final Report, ASHRAE 1050-RP.

Klein, S.A., 2007. TRNSYS 16 Program Manual. Solar Energy Laboratory, University of Wisconsin, Madison, USA

Klein., S.A. 2010. EES: Engineering Equation Solver, User manual. F-chart software. Madison: University of Wisconsin, Madison, USA.

Krarti, M. 2000. Energy Audit of Building Systems; An Engineering Approach. CRC Press, Florida. U.S.

Laustsen, J.B., Svendsen, S. 2002. Calculation tool for determining the net energy gain through windows. Proceedings of the 6th Sympoisum on Building Physics in the Nordic Countries, Trondheim, Norway.

LBNL. 1980. DOE-2 User Guide, Ver. 2.1. Lawrence Berkeley Laboratory and Los Alamos National Laboratory, LBL Report No. LBL-8689 Rev. 2; DOE-2 User Coordination Office; LBL, Berkeley, CA.

LBNL, 2010. Window 5.2a. Lawrence Berkeley National Laboratory, Berkeley, CA.

Lebrun, J., X. Ding, J.-P. Eppe, and M.Wasac. 1990. Cooling Coil Models to be used in Transient and/or Wet Regimes. Theoritical Analysis and Experimental Validation. Proceedings of SSB 1990. Liège:405-411

Lebrun, J., Aparecida Silva, C., Trebilcock, F., Winandy, E. 2002. Simplified models for direct and indirect contact cooling towers and evaporative condenser. Proceedings of the 6th International Conference on System Simulation in Buildings, Liège, Belgium.

Lemort, V. 2008. Contribution to the characterization of scroll machines in compressor and expander modes. PhD Dissertation, University of Liège.

Liu, M., Song, L., Wei, G., Claridge, D.E. 2004. Simplified building and air-handling unit model calibration and applications. Journal of Solar Energy Engineering. Vol. 126, pp. 601-609.

Lydberg, M.D. 1987. Source book for energy auditors. International Energy Agency – Energy Conservation in Buildings and Community Systems Programme Annex 11 “Energy Auditing” final report.

Masy, G. 2008. Definition and validation of a simplified multi-zone dynamic building model connected to heating system and HVAC unit. PhD Dissertation, University of Liège.

MATLAB, 2009. Matlab user manual, The Mathworks Inc., http://www.mathworks.com, Natick, USA.

Miriel, J., Serres, L. ,Trombe, A. 2002. Radiant ceiling panel heating-cooling systems: experimental and simulated study of the performances, thermal comfort and energy consumptions. Applied Thermal Engineering, Vol. 22; pp. 1861-1873.

Purdy, J., Beausoleil-Morrison, I. 2001. The significant factors in modeling residential buildings. Proceedings of the seventh International IBPSA conference, Rio de Janeiro, Brazil.

Reddy, T.A., Deng, S., Claridge, D.E. 1999. Development of an inverse method to estimate overall building and ventilation parameters of large commercial buildings. Journal of Solar Energy Engineering. Vol 121. pp. 40-46

Reddy, T.A., Maor, I. 2006. Procedures for reconciling computer-calculated results with measured energy data. ASHRAE Research Project 1051-RP. Atlanta: American Society of Heating, Refrigerating and Air-Conditioning Engineers, Inc.

Reddy, T.A. 2011. Discussion at ASHRAE Winter Conference, Las Vegas, NV.

Spitler, J.D., Fisher, D.E., Pedersen, C.O. 1997. The radiant time series cooling load calculation procedure. ASHRAE Transactions. 103(2): 503-515.

Stan, S. 1995. Maîtrise et calcul des installations de climatisation dans le secteur tertiaire. PhD thesis, Ecole des Mines de Paris.

Stocki, M., Curcija, D.C., Bhandari, M.S. 2007. The development of standardized whole-building simulation assumptions for energy analysis for a set of commercial buildings. ASHRAE Transactions. 113(2): 422-428.

Thevenard, D., Haddad, K. 2006. Ground reflectivity in the context of building energy simulation. Energy and Buildings, 38, pp. 972-980.

US-DOE. 2009. EnergyPlus Energy Simulation Software, U.S. Department of Energy. Available at: http://apps1.eere.energy.gov/buildings/energyplus/

Walton, G. 1983. Thermal Analysis Research Program Reference Manual (TARP). NBSIR 83-2655. Washington D.C.: National Bureau of Standards.

Westphal, F.S., Lamberts, R. 2005. Building Simulation Calibration using Sensitivity Analysis. Proceedings of the 9th IBPSA Building Simulation Conference, Montréal, Canada.

Woloszyn, M. 1999. Moisture-Energy-Airflow modelling of multizone buildings. PhD Dissertation. CETHIL Laboratory, INSA Lyon, France.

CHAPTER 3 SIMULATION-BASED WHOLE-BUILDING ENERGY PERFORMANCE ANALYSIS METHODOLOGY

CHAPTER 3: SIMULATION-BASED WHOLE-BUILDING ENERGY PERFORMANCE ANALYSIS METHODOLOGY 2
1. PREVIOUS WORK AND EXISTING CALIBRATION METHODOLOGIES 2
1.1. Manual calibration methods 2
1.2. Graphical and statistical methods 5
1.3. Automated calibration methods 7
1.4. Accuracy of calibrated BES models 9
2. DATA GATHERING 12
2.1. Weather Data Collection 12
2.2. Energy Use Data Collection 13
2.3. Accuracy of the available data 16
3. BES MODEL OUTPUTS AND UNCERTAINTY 16
4. SIMULATION-BASED ENERGY USE ANALYSIS METHODOLOGY 18
4.1. Data Collection and Analysis 20
4.2. As-built Input File Construction and Preliminary Sensitivity Analysis 21
4.3. Evidence-based Calibration Method 22
4.4. Energy Use Analysis and ECOs Evaluation 26
5. SUMMARY 26
6. REFERENCES 28

CHAPTER 3: SIMULATION-BASED WHOLE-BUILDING ENERGY PERFORMANCE ANALYSIS METHODOLOGY

1. PREVIOUS WORK AND EXISTING CALIBRATION METHODOLOGIES

The calibration of a forward building energy simulation program, involving numerous input parameters, to common building energy data is a highly under-determined problem that would result in a non-unique solution (Carroll and Hitchcock, 1993). As noticed by Kaplan et al. (1990), it will never be possible to identify the exact solution to the calibration problem and sensitivity issues may be of primary importance in the calibration field. A second constrain relies on the fact that calibration requires a dynamic matching over one year between computed and measured values and not a static one at one condition (Reddy and Maor, 2006). These elements make the calibration of building energy simulation models challenging.

The most common calibration methods can be classified as proposed by Reddy (2006):

- Manual iterative calibration based on the user's experience and consisting in an adjustment of inputs and parameters on a trial-and-error basis until the program output matches the known data;
- Calibration based on specific graphical representations and comparative displays of the results to orient the calibration process;
- Calibration based on special tests and analytical procedures involving specific intrusive tests and measurements, such as the PSTAR method (Subbarao, 1988a) described below;
- Analytical and mathematical calibration methods involving use of optimization algorithms.

Of course, all these methods are not exclusive and could be coupled (e.g. use of graphical and statistical analysis methods to support iterative manual calibration, semi-automatic procedures coupling mathematical and heuristic manual methods).

1.1. MANUAL CALIBRATION METHODS

Manual methods are the most commonly used. Numerous authors and practitioners use this kind of methods to adjust the parameters of detailed BES models. **Unfortunately, these methods are highly dependent on the user's experience and rarely applied in a systematic way**.

Kaplan et al. (1990) presented a methodology to evaluate the ECOs (Energy Conservation Opportunities) already implemented in a monitored building. This was done by calibrating a DOE2.1 model to recorded data and deriving a "baseline" (or pre-retrofit) model without ECOs. This work is one of the first successful calibrations of a detailed simulation model.

The manual iterative calibration performed by the authors involves 9 steps to tune the model within the specified tolerances. Unfortunately, the authors provide only general guidelines and rules to perform the calibration. The changes and adjustments between two iterations are purely subjective and based on user's experience.

Another typical example of manual iterative calibration is the one presented by Pan et al. (2007).The paper presents the calibration of an e-Quest (DOE2 based simulation tool) model of a commercial building located in Shanghai. Building geometry and zoning were simplified to save calculation time.

The calibrated model is then used for energy-use breakdown and ECOs evaluation. The model was calibrated in four steps:

- Replacement of TMY weather data by actual 2004 weather data for Shanghai;
- Refining HVAC system operating schedules according to measurements and site survey;
- Refining internal loads according to on-site measurements;
- Adjusting infiltration rate according to on-site observations.

Even if some explanations of the remaining errors are proposed, this typical calibration of a commercial code to monthly billing data does not satisfies all the tolerances prescribed by common calibration standards (ASHRAE Guideline 14-2002, IPMVP and FEMP). Moreover, the calibration performed here is fully heuristic and is not based on any systematic or logical calibration procedure. Unfortunately, no consideration on sensitivity of the model is given by the authors.

Pedrini et al. (2002) present a general calibration methodology based on three major steps:

- simulation from building documentation;
- walk-through audit;
- and end-use energy measurements.

The proposed methodology is successfully applied to calibrate a DOE2.1 model to several case studies buildings but stays very general and is not as systematic as it could be. The authors affirm reaching a final error of about 0.2 % on annual energy consumption which can be highly questionable. Indeed, this is equivalent to try “answering a 10% question with a 1% answer” (Waltz, 2000). Once again, **the importance of coupling the calibration work to a sensitivity analysis is noticed but not developed**.

Westphal et al. (2005) present a calibration method similar to the one proposed by Pedrini et al. (2002). This method is applied to the EnergyPlus software and combines energy audit techniques and sensitivity analysis. This calibration method starts with the adjustment of lights and plug loads, followed by a very short sensitivity analysis (using design days simulations) allowing identifying the most influential parameters to adjust in priority. The main advantage of this sequential approach is the integration of a simple sensitivity analysis into the calibration process. The approach does not follow the classical way to perform energy audit and studies building base loads before its envelope and HVAC system. Moreover, numerous hypotheses (on the building and the equipments) are needed at the beginning of the calibration process and make the methodology not easily reproducible.

In his paper, Lunneberg (1999) describes how short-term monitoring of key internal loads (measurement of key electrical end-uses and hourly load profiles) was successfully applied to DOE-2 simulation of an existing commercial office building located in California. Even if the author does not integrate this technique into a systematic calibration process, some very interesting findings and conclusions are highlighted:

- Monthly, weekly and daily schedules are important and should be monitored.
- Using schedules provided by the building operating staff or standardized schedules can lead to large over/under-estimation of energy use;
- Care must be taken when considering a behavior, a schedule, an area or any tenant as “typical” and representative of the building under study.

Yoon et al. (2003) provide a systematic manual iterative calibration methodology of the DOE 2.1E code based on a so-called “base load analysis approach” combining analysis of monthly billing and sub-metered data commonly available in Korean buildings (watt meters are commonly installed in

Korean buildings to monitor the various electricity end use). The purpose of this study is to use a calibrated model in the frame of an energy audit procedure to evaluate ECO's.

This approach includes seven steps:

- Base case modeling (basing on available documentation);
- Base load consumption analysis using data analysis techniques such as the signature method described by Lyberg et al. (1987);
- Swing-season calibration
- Site interview and measurements
- Heating and cooling seasons calibration
- Validation of calibrated base model using graphical and statistical techniques
- Application of the calibrated model to evaluate ECO's

Classical statistical indexes (MBE: Mean Bias Error; CV(RMSE): Coefficient of Variation of the Root Mean Square Error) and gas and electricity signatures are used to validate the calibration. Due to the large cooling demands commonly encountered in Korea, the electricity signature allowed to identify the base load consumption quite easily. Moreover, the fifteen watt meters already present in the buildings were used to disaggregate the electricity consumption and quantify the electricity end uses. As an example, during the typical week day considered for "base load analysis", it was found that the fraction of the global electricity consumption due to lighting, HVAC, plug load and elevators were, respectively, 31%, 16%, 41% and 12%.

This first systematic manual method highlights interesting issues, such as the **usefulness of electricity end-use measurements and manual data analysis to identify some parameters of the model**. Unfortunately, this procedure cannot be directly transposed for European applications due to the impossibility to identify base load and HVAC electricity consumptions from whole-building electricity data (specific energy meters are not commonly installed in European Building).

Raftery et al. (2011) developed a calibrated model to allow the building manager to optimizing the operation of the HVAC system using a "key factors" methodology (Costa et al., 2009). The proposed calibration methodology is intended to be applied to the EnergyPlus program and is based on three core principles:

- Use of a detailed BES model that represents the real building as closely as possible;
- Application of a reproducible and scientific method;
- Obtain and use (sub-)hourly sub-utilities level measurements from energy monitoring systems (EMS) and building automation systems (BAS)

This classical manual iterative calibration methodology includes measurements issues and tries to **keep the calibration process as systematic and "evidence-based" as possible**. In this frame, the BES model being calibrated should be used to investigate possible further measurements. Data gathering is fully integrated to the iterative calibration process and includes short-time step and very component-level measurements.

An initial "as-built model" is built and is supposed to be similar to a very detailed BES model created at the design stage. A very detailed zone typing and HVAC system description based on extensive design data (Building Information Model, As-built drawings, Operation & Maintenance manuals...) is used by the authors.

Due to this very detailed description of the building, the manual iterative calibration process requires the installation and use of an important number of energy monitoring systems and the gathering of an important quantity of measurements. Till now, the calibration method has been applied to a real office

building located in Ireland but, unfortunately, no sensitivity issues have been included in the calibration process even if the importance of this issue is mentioned several times by the authors. Moreover, the use of such detailed model and monitoring is generally out of the scope of an energy efficiency service process.

1.2. GRAPHICAL AND STATISTICAL METHODS

Bou-Saada and Haberl (1995) propose a calibration method including bin analysis on different time-scales and statistical indices such as MBE and CV(RMSE) to analysis the goodness-of-fit of the model. This procedure was used to calibrate a DOE2 model of a building located in Washington D.C. to hourly whole-building electricity (WBE) data.

In addition to classical time-series plots and scatter plots, the authors use binned box-whisker-mean plots displaying maximum, minimum, mean, median and percentile points for each data bin for a given period (Figure 1). This new graphical method allows the author to view and analyze the weather and schedule dependent hourly energy use. 3D surface plots and statistical indices are also used to have a global view of the differences between measured and computed hourly values to help in identifying seasonal or daily patterns in the comparisons (Figure 2).

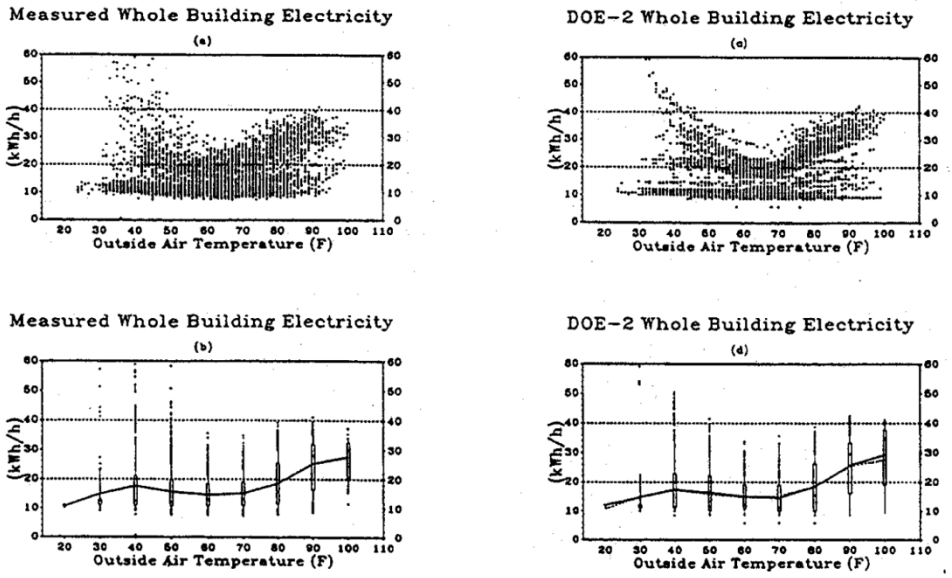

Figure 1: Scatter and box-whisker mean plots (Bou-Saada and Haberl, 1995)

McCray et al. (1995) propose another graphical method to calibrate a DOE2.1 model to an entire year of hourly or 15 minute metered whole-building energy use. The Visual Data Analysis (VDA) method allows quickly comparing the results and reviewing the parameters of the model during a calibration process. Once again, the accuracy criteria is based on classical statistical indices (MBE and CV(RMSE)).

The graphical methods proposed by Bou-Saada and Haberl (1995) and McCray et al. (1995) suit well with the calibration of simulation models to hourly measured data. With only whole-building monthly data, these advanced graphical methods are of less help and a very systematic and logical calibration method has to be applied to limit the number of simulation runs and make the calibration process efficient.

Wei et al. (1998) found that calculating, normalizing and plotting the difference between measured and predicted heating and cooling consumptions as function of the outdoor temperature was useful to help in calibrating building energy simulation models. This “signature method”, based on daily

heating and cooling energy consumptions, has been extended to other climates and types of HVAC system by Liu et al. (2003). The signatures provided in these reports have been generated by means of the "AirModel" tool (Liu, 1997). This simulation model has been developed by the Energy Systems Laboratory (ESL) at Texas A&M Univesity in the 1990's and is based on the ASHRAE Simplified Energy Analysis Procedure (SEAP, Knebel, 1983).

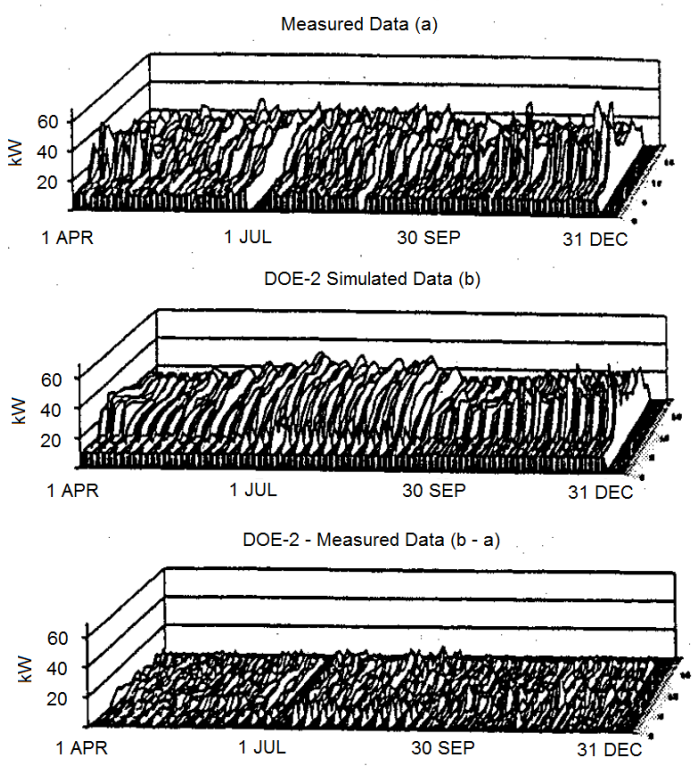

Figure 2: 3D surface plots (adapted from Bou-Saada and Haberl, 1995)

Liu et al. (2004) presented another example of use of this method to calibrate simplified building and AHU energy consumption models. The simplified model used consists in a two-zone (interior – exterior) building model coupled to a consolidated AHU model.

The two-level calibration method focuses on the weather dependence of the model (1st level) and on the time schedule dependency (2nd level) and uses measured hourly values of heating and cooling energy consumptions.

For a given system type (CAV, VAV…) and climate, the "calibration signature" (graph of the difference between measured and computed data as a function of outdoor temperature) has a characteristic shape that depends on the reason for the difference (Figure 3).

$$Residual = Simulated\ consumption - Measured\ consumption$$

$$Calibration\ signature = \frac{Residual}{Maximum\ measured\ consumption} * 100\%$$

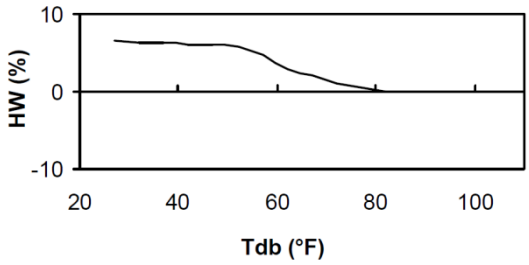

Figure 3: Example of a heating calibration signature (Liu et al., 2003)

So, "characteristic signatures" can be generated and plotted for different systems and climates by varying important parameters one-at-a-time and plot the % of variation of the hot/chilled water use as function of the outdoor temperature (Figure 4). Then, the comparison of the "calibration signature" to this "characteristic signature" can help in performing the calibration of the model.

$$Characteristic\ signature = \frac{Change\ in\ energy\ consumption}{Maximum\ energy\ consumption} * 100$$

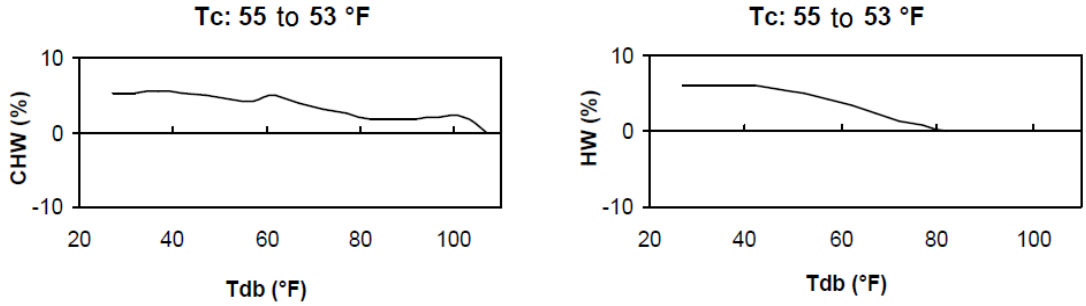

Figure 4: Example of cold deck temperature characteristic signatures (Liu et al., 2003)

The method is easy to follow and generalize but is actually based on data currently not available (hourly or daily hot water and chilled water consumptions).

Unfortunately, the authors recognize that this signature method cannot be transposed to more common cases where only whole-building monthly consumption data are available (Liu, 2011). In a more recent paper (Liu and Liu, 2011), the authors mention the integration of sensitivity issues as a possible improvement for the method.

Heo (2011) proposes an interesting Bayesian approach to calibrate a simple normative simulation model based on CEN standards. The author characterized the few parameters of the model by a "best-guess / initial" value and some probability ranges. Such ranges were used to, firstly, perform a screening analysis (in order to identify the most-influential parameters) and, secondly, quantify the uncertainty on model's outputs.

1.3. AUTOMATED CALIBRATION METHODS

Carroll and Hitchcock (1993) summarized the work done by the team of LBNL onto the development of automatic calibration methods for the RESEM (Retrofit Energy Saving Estimation Model) tool (Carroll et al., 1989) based on the ASHRAE modified bin method (Knebel, 1983). A semi-automatic numerical calibration algorithm has been developed and implemented. The calibration is performed by minimizing an objective function constructed as a weighted sum of the difference between computed and recorded data. Model's parameters are categorized in "high-level" and "low-level" characteristics. In a first time, the user is allowed to select the "high-level" characteristic suspected to be the source of the discrepancies, then, the calibration algorithm tunes the "low-level" parameters related to this

characteristic. The proposed method is applied to calibrate the RESEM tool to yearly data but could be adapted to be used with smaller time scales (as monthly or weekly data). The existence and uniqueness of solutions issues are already discussed in this paper. Since minimization algorithm are more efficient with a limited amount of parameters, **the authors suggest also to begin a calibration with a heuristic selection of most influential parameters (basing on sensitivity analysis and experience of the user) to limit the calibration time and the number of simulation runs**.

More recently, Lee and Claridge (2003) have presented another automatic calibration of a simplified building energy simulation model based on the ASHRAE Simplified Energy Analysis Procedure (Knebel, 1983) to measured data. This automatic calibration is performed by means of a commercial optimization program used to minimize the error between measured and computed hot water and chilled water consumptions. For the studied case, the model was calibrated to simulation data to which a small amount of white noise has been added. Five parameters have been considered: cooling coil leaving air temperature, room temperature, heat transfer coefficient of the building envelope, supply-air volume and outdoor-air flow fraction. The optimization algorithm used by the authors is able to provide objective free of local-minima.

The calibration method used here seems to be efficient and very promising. However, it must be noticed that this type of calibration is, most of the time, applied to simplified calculation method (such as the ASHRAE modified bin method) rather than detailed simulation models. Such numerical algorithms involve the use of a large number of parameters and simulation runs and cannot be easily adapted to dynamic hourly simulation tools.

The calibration method developed in the frame of the ASHRAE RP-1051 research project by Reddy and Maor (2006) is based on the same approach as the one proposed by Carroll and Hitchcock (1993) but uses a detailed hourly simulation code (DOE2.1), perform calibration to monthly billing data and include sensitivity analysis issues to identify a plausible set of solutions instead of an hypothetical unique solution.

A, even very good (satisfying all the accuracy criteria as the ones recommended by ASHRAE), calibration to the utility bill will not guarantee accurate fit at the end and may yield very bad and unsatisfactory prediction accuracy when using the calibrated model for energy and economic evaluation of ECO's. For that reason, Reddy and Maor (2006) consider that using a small number of most plausible solutions is more robust than using only one feasible calibration solution to make predictions. In the frame of the ASHRAE RP1051, the authors have developed a calibration procedure based on the DOE2 model and using only monthly billing data. This calibration procedure involves heuristic steps (definition of a set of influential parameters basing on walk-through audit and inspection), advanced mathematical methods (Monte-Carlo method, use of optimization algorithms…) and numerous trials and simulation runs. This sophisticated and partially "black-box" calibration method allows identifying a subset of most plausible solutions to this under-determined problem. However, this method is also heavy to handle due to the multiple steps and can be confusing for non-experimented users (Reddy, 2011).

Lavigne (2009) has developed a semi-automatic calibration procedure implemented in DOE2.1 software. This calibration process involves common engineering rules and optimization algorithms and requires monthly electricity consumption, electricity peak demand and real local weather data. This methodology has been successfully applied to two existing buildings, using electricity as a unique energy source, resulting in maximal errors of less than 14%.

Two steps are involved in this calibration process:

- Pre-calibration, requiring no simulation run but simply analyzing the available recorded billing data to extract useful information (building heating and cooling global heat transfer coefficients, base load consumption...) and identifying critical parameters (ventilation rate, envelope performance...). A five-variable energetic model is used (ASHRAE Fundamentals, 2001) for this first analysis.
- Calibration, involving a Marquardt-Levenberg optimization method in order to minimize an objective function defined as a sum of differences between measured and computed data.

Combining intuitive and mathematical methods to calibrate detailed BES models is certainly an attractive solution to the calibration problem and an interesting compromise between black-box methods and full manual iterative processes. These methods are particularly interesting when having to fit simultaneously to various sources and important amounts of measurement data.

However, it seems difficult to integrate such methods with local/additional measurements issues and to make the calibration process as reproducible and flexible as a manual method. Indeed, some hypotheses on the available data have to be done when developing such a methodology and some parameters (as schedules) cannot be easily adjusted during the automated calibration. Moreover, optimization-based methods have limited potential when using global monthly billing data to check the accuracy of the calibration. Indeed, as recently confirmed by Reddy (2011), utility billing data are generally too global to allow "direct" (automated) adjustment of the parameters because of the amount of influences integrated in such values and the large amount of parameters to calibrate.

1.4. ACCURACY OF CALIBRATED BES MODELS

A calibration process consists in adjusting the parameters of a model through several iterations until it agrees with recorded data within some predefined criteria. The definition of these criteria is a complex issue and, to date, it is impossible to determine how close a tolerance needs to be to fulfill the calibration objective (Kaplan et al., 1990).

Usually, the authors (Yoon et al., 2003; Pan et al., 2007; ASHRAE, 2002) recommend using Mean Bias Error (MBE), Root Mean Square Error (RMSE) and Coefficient of Variation of the Root Mean Square Error (CV(RMSE)) to evaluate calibration accuracy.

$$MBE = \frac{\sum_{i=1}^{n}(Q_{pred,i} - Q_{data,i})}{(n-p) * \overline{Q}_{data}}$$

$$RMSE = \sqrt{\frac{\sum_{i=1}^{n}(Q_{pred,i} - Q_{data,i})^2}{n}}$$

$$CV(RMSE) = \frac{RMSE}{Q_{data}} = \frac{\sqrt{\frac{\sum_{i=1}^{n}(Q_{pred,i} - Q_{data,i})^2}{n-p}}}{\overline{Q}_{data}}$$

Where

$Q_{pred,i}$ is the predicted value during the ith period

$Q_{data,i}$ is the measured value during the ith period

$\overline{Q}_{data}$ is the measured average during the period

n is the number of available data points (or periods)

p is a correction parameter

This multiple variable analysis allows preventing any calibration error due to errors compensation. Indeed, the common Mean Bias Error (MBE) approach is an important measure of calibration but has the disadvantage that large compensating errors (i.e. positive and negative errors) can lead to a zero MBE (Yoon et al., 2003). Using CV(RMSE) in addition to MBE to describe the variability of the results allows preventing this compensation problem.

For calibrated simulations, it is suggested that the MBE and CV(RMSE) indices should be used, respectively, with p=0 and p=1 (Reddy and Maor, 2006). The authors justify this choice by particularities of the calibration problem (not clearly defined number of "degrees of freedom").

Figure 5 illustrates a typical situation where the MBE (about 1%) would indicate an accurate and successful calibration. However, the CV(RMSE) is largely bigger (about 15%) and proves that the calibration is not completed. Of course, plotting the curves would have also permitted to indentify directly the discrepancy.

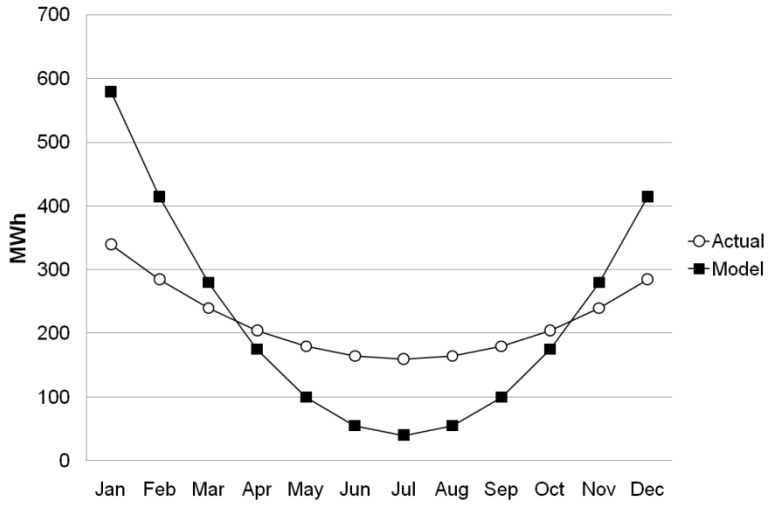

Figure 5: Example of comparison between actual and predicted values

Waltz (2000) considers that a maximal difference of 5% between annual recorded and computed energy consumption is a realistic objective for BES model calibration.

The three standards dealing with calibration (ASHRAE, 2002; EVO, 2007; US-DOE; 2008) provide also numerical criteria (Table 1) to calibrate BES models to building energy use data. The values proposed by ASHRAE Guideline 14-2002 and FEMP are the same but very different from the ones proposed by IPMVP.

Table 1: Commonly used calibration tolerances

Index	Waltz (2000)	ASHRAE 14	IPMVP	FEMP
MBEyear	± 5%			
MBEmonth		± 5%	± 20%	± 5%
CV(RMSE)month		± 15%	± 5%	± 15%
MBEhourly		± 10%		
CV(RMSE)hourly		± 30%		

Instead of a unique set of tolerances, Kaplan et al. (1990) have proposed different tuning tolerances (Table 2) depending on the energy uses (lighting, cooling, heating, fans…) and tuning periods (monthly, daily, hot period, cold period…).

Table 2: End-use specific tolerances (Kaplan et al., 1990)

End-Use	Tuning Period Weather Type	Monthly End-Use Tolerances	Daytype Profile Tolerances
Indoor lighting	All	± 5%	± 15%
Outdoor lighting	All	± 5%	± 15%
DHW	All	± 5%	± 15%
Plug loads	All	± 5%	± 15%
Heating	Cold	± 15%	± 25%
	Temperate	± 25%	± 35%
Cooling	Hot	± 15%	± 25%
	Temperate	± 25%	± 35%
Ventilation fans	Hot, Cold	± 15%	± 25%
	Temperate	± 25%	± 35%
Whole-building	All	± 10%	± 15%

Reddy (2011) considers the ASHRAE criteria as “too cool” and advices to investigate the possibility to compute the above mentioned statistical indexes on a monthly bases or on a floating period. Of course, this would require having shorter time step data (e.g. daily consumption data). These possibilities have not been investigated yet. **However, Kaplan (1990) considers that “investigation to date on the calibration tolerance required to fulfill the research objectives indicates that this is probably unanswerable” because of the very high under-determination degree of the calibration problem.**

Statistical indices should not be the unique way to evaluate the accuracy of the calibration (Waltz, 2000) and could lead to a “blind” calibration missing numerous influences (weather, occupancy, operation…). Indeed, even if the “net effect” of all the “knobs” yields to a simulated output close to the measured one, there is no guarantee that all individual “knobs” are properly tuned.

Figure 6 shows a typical example of comparison between computed and measured electricity demand for a summer day. Once again, because the two curves correspond to similar energy uses, the difference between the simulation and actual situation cannot be observed by means of aggregated data (such as daily values).

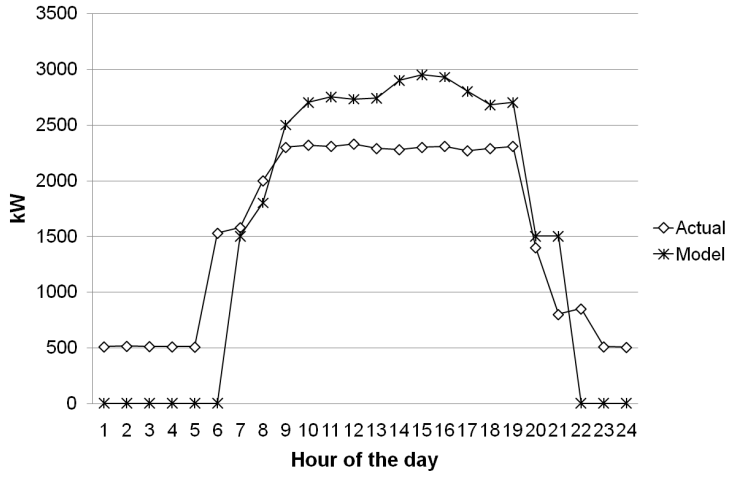

Figure 6: Electricity demand comparison (adapted from Waltz, 2000)

Thus, because the selected statistical indexes and the corresponding tolerances have been defined in an arbitrary way and are not fully reliable, other (more practical) accuracy criteria should be imagined.

For example, in addition to the mathematical criteria defined above, the following accuracy issues should be considered when looking at the simulation results:

1. Peak heating and cooling loads should be checked and compared to installed heating/cooling capacities (taking into account the possible over/under-sizing)
2. Computed and measured seasonal (monthly) energy use profiles should be visually compared to identify any seasonal pattern in the difference between simulated and recorded values
3. Simulated daily/hourly energy use profiles (concerning internal gains, system operation, chiller load,...) should be checked, criticized and confronted to the operating patterns observed (or measured) during the inspection phase
4. End-use energy consumption should be faithfully allocated (use short-term measurements to check the end-use energy consumption)

Some of the graphical methods and tools described earlier (Bou-Saada and Haberl, 1995; McCray et al., 1995; Liu et al., 2003) can also be used as calibration quality estimators.

2. DATA GATHERING

2.1. WEATHER DATA COLLECTION

It appears that gathering of weather data is still a problem for analysts having to calibrate a BES model. ASHRAE (2002) considers that collecting hourly weather data corresponding to the same time period as the energy data used for calibration is a minimal requirement to perform calibration. Sometimes, modern buildings are equipped with their own weather station. Even if this is very useful, weather data are rarely complete and some values are often missing (e.g. solar radiation) and should be completed from other sources of data. Moreover, in most cases, actual weather data is not available and should be obtained from another source.

To simplify modelling and prevent this lack of data, Liu et al. (2004) treat solar radiation as a linear function of the outdoor drybulb temperature. Even if this approach can be envisaged to be used with simplified calculation methods, such as the ASHRAE modified bin method (Knebel, 1983) used by Liu et al. (2004), this hypothesis can lead to large errors when studying largely glazed commercial

buildings, strongly influenced by solar gains. The related error is even larger when applying this hypothesis to hourly BES models.

Typical weather data, such as TRY or TMY data, is sometimes used to perform calibration. This requires normalizing energy consumptions (by means of signatures) to allow comparison. However, the use of average data to perform calibration can induce important errors and ASHRAE Guidelines 14-2002 strongly discourages this approach.

Hopefully, in our countries, recent actual hourly weather data are generally available for at least a few weather stations. When having to perform calibration, hourly weather data from the nearest location should be used when actual local weather data is not available. This allows performing a better calibration than the one performed by mean of, sometimes poorly representative, TRY or TMY weather data. However, whatever the origin, some uncertainties remain because of measurement errors, incomplete sets of data...etc

2.2. ENERGY USE DATA COLLECTION

Burch et al. (1990) categorizes the monitoring methods in two classes:

- Macrostatic methods based on time-integration of the building energy balance, such as classical utility bill analysis or long-term or short-term energy measurements. These techniques are the most commonly used;
- Macrodynamic methods combining identification methods (such as the PSTAR method, developed by Subbarao, 1988a) and use of the building's dynamic energy balance. These techniques are generally employed in residential buildings.

Most commonly available data are utility billing data. Whole-building monthly gas and electricity consumptions are generally made available for at least one complete year by the energy management team. A special attention has to be paid to possible corrections applied to the provided values. It is also often possible to obtain electricity peak demands on a quarter-hour basis from the electricity provider. However, the data available when starting an energy audit may vary a lot from case to case.

In some buildings, one can find separate energy or power meters measuring local or end-use (e.g. lighting, HVAC, chiller...) electricity consumptions and demands. The use of these meters is not mandatory in the European tertiary building sector but is more common in some countries, such as Korea (Yoon et al., 1999; Yoon et al., 2003).

Cooling and heating energy or demand meters can also be encountered. Once again, these meters are not common in Europe (except for very large buildings) but can be often encountered in the U.S.

Building Energy Management Systems (BEMS) are also very useful when performing an inspection. BEMS programs can often be used to perform measurements without requiring any additional sensor. Of course, the quality of the measurements has to be checked and evaluated before analyzing the results. Open source BEMS programs are also of a great help to identify the control laws as the basis for operating the HVAC system.

Of course, the data available when starting the audit process (for example) can be completed by means of short-term or spot measurements. These measurements are generally achieved by means of (portable or not) data loggers and can help in quantifying some specific energy uses (e.g. lighting power density, fan power...), check some operation parameters (e.g. supply air temperature and flow rate) or patterns (e.g. ventilation schedule). The decision to perform these measurements is generally taken as function of the needs of the auditor/inspector and depends mainly of his own experience.

Other specific measurements and tests, developed for residential applications (e.g. blower door, dynamic tests), can be used to determine and quantify critical parameters such as infiltration rate and thermal inertia. However, these measurements are more intrusive and, most of the time, not feasible in existing non-residential buildings.

The PSTAR (Primary and Secondary Term Analysis and Renormalization) method (Subbarao, 1988a) is a short term monitoring method which has been developed at the end of the 80's for residential applications. It includes measurement protocols and provides a simplified (static or dynamic) model to calibrate.

This method aims at estimating the parameters of a realistically complex building model basing on the data obtained during an inspection (or audit) and short term (typically a few days) monitoring data. Each zone of the studied building is described by an air energy balance expressed as a sum of heat flows. One particularity of the method is the great freedom allowed to the user in defining the terms of this energy balance to take into account. Each heat flow may be a primary unknown (firstly estimated by a simple audit calculation and secondly renormalized by means of monitoring data), a secondary one (obtained by calculation only) or a measured one (obtained by direct measurement only). Once the model described, a test plan has to be constructed to allow identifying the parameters of the model.

Typical measurements used when applying the PSTAR method are:

- Outdoor, indoor and supply air temperature measurements;
- Incident solar radiation measurement;
- Lighting and plug loads power measurements;
- Ventilation rate measurement;
- Infiltration rate measurement (blower door test);
- Supply and return air flows diffusion measurement (tracer gas);

In addition with these measurements, some specific tests have to be realized to force each "primary" term to become dominant in the energy balance during a short period (e.g. make the steady-state conduction term dominant by suppressing the night setback for one or more nights).

After "renormalization" (or calibration), the model can be used for long-term extrapolation, energy savings evaluation, fault detection, HVAC operation optimization…

Since its development, the PSTAR method has been applied several times to residential buildings (Subbarao et al., 1988b; Carrillo et al., 2009) but very rarely to office buildings. Only a few examples exist, as the one described by Burch et al. (1990) which have applied the PSTAR method to a 12000 m² office building. Even if this method is more adapted to residential buildings because of the measurement techniques involved, the PSTAR method has the advantage to fully integrate measurement issues within the calibration process.

The time-period, the time-step and the accuracy of the gathered measurement data are also very important issues. Usually, monthly data for a whole year can be collected at the beginning of the process and are used to perform calibration. Kaplan et al. (1990) use three "snapshot" periods instead of an entire year of data. A hot, a cold and a temperate month are extracted from monitored data in order to calibrate a DOE2 model.

It is easy to admit that the shorter the measurement time step, the more useful are the measurements. Indeed, compared to long time step data (e.g. monthly records) short time step data (e.g. daily or hourly measurements) allow correlating energy use with weather and operating schedules (distinction between week and weekend days, more accurate correlation between outdoor temperature and gas consumption…) and identifying operating patterns (e.g. electricity base load). Averaged recorded data

(e.g. billing data) is less useful and tend to smooth weather and operation influences. It is impossible to deduce any schedule or operating profiles from such data. Lunneberg (1999) affirms that, in mild climates, large non-residential buildings are often internal load-dominated rather than weather-dominated. This observation indicates a large dependence of the building energy use to operating and occupancy schedules and confirms the need to properly estimate occupancy and operating schedules (Pedrini et al., 2002).

As mentioned before, measurements accuracy has also to be considered before any analysis. Indeed, errors of approximately 5% are common when working with data recorded manually because of approximate recording periods. When using short term measurements equipments, the accuracy of the data logger has to be taken into account when analyzing the results.

Reddy and Maor (2006) proposed to distinguish different levels of calibration as a function of the level of effort (and related costs) needed to gather and analyze the data (Table 3).

Table 3: Calibration levels as a function of input data available (adapted from Reddy and Maor, 2006)

Calibration levels	Building description and performance data available for calibration					
	Utility bills (one year)	As-built data	Site visit or inspection	Detailed audit	Short-term monitoring	Long-term monitoring
Level 1	x	x				
Level 2	x	x	x			
Level 3	x	x	x	x		
Level 4	x	x	x	x	x	
Level 5	x	x	x	x	x	x

The first level consists in using only the information available in the as-built file as well as at least one year of consumption data. The second level adds a on-site visit (or inspection) while information available in the as-built file could be cross-checked (by means of interview of the building manager…) and completed by the reading of the nameplate information of the main components of the installation. The third level, referred to as “detailed audit”, involves taking nameplate information and spot on-site measurements (clamp-on meters…) at different periods of the day (morning, afternoon, night) or the week (weekdays or weekend). The fourth level needs the installation of loggers and energy-counters for a short period (typically a few weeks) to allow collection of data (such as powers, thermal loads, temperatures…) at short intervals (hourly or less) for certain end-use equipments. The last (and highest) level involves long-term monitoring and the collection of similar data for the whole installation and for an entire year. This last level presumes that specific and sufficient budgets have been planned for that purpose.

Level 1 calibration is certainly weak since the modeler has no contact with the installation and its operators/users. A serious calibration work can be expected starting from level 2.

In the frame of the present work, the minimal data requirements will consist in monthly gas and electricity bills for a complete year. Peak electricity loads on a quarter-hour basis will also be used when available. On-site visit and inspection are considered as mandatory and will be integrated in the calibration process. The planning and the use of short-term and spot measurements will also be considered. Very detailed long-term monitoring data will not be studied in details since they are usually out of the scope of the setup of an energy efficiency service process (but could be envisaged after its implementation). In other terms, calibration levels 2, 3 and 4 will be covered in this study.

2.3. ACCURACY OF THE AVAILABLE DATA

An important issue when discussing calibration accuracy is related to the accuracy of the available data. For example, utility billing data often contains distinct outliers due to improper meter-reading, temporary equipment dysfunction, arbitrary (and sometimes not clear) correction of the original data by the building owner/energy provider or manager. Moreover, utility bills do not necessarily correspond to calendar months. This makes again the use of mathematical criteria questionable. Sonderegger (1998) proposes to exclude some unsuitable billing data points before starting developing the baseline model in order to keep the calibration process as robust as possible. Indeed, since the available amount of data is very limited (12 or 24 data points of monthly data), even one or two biased values can lead to not-representative values of the statistical indexes used to characterize the goodness of fit (GOF).

It is difficult to define fixed criteria for such selection/rejection since the origin of the problem can vary a lot from cases to cases (unknown billing periods, temporary malfunctioning or manual operation of the system…). Reddy and Maor (2006) estimate automated outliers detection methods as not adapted to the present application (due to the small amount of data points to analyze and the amount of possible reasons for the deviations of the data) and advice to use simple visual inspection methods. Biased data points can generally be easily identified by means of simple and classical billing data analysis (such as energy signatures).

3. BES MODEL OUTPUTS AND UNCERTAINTY

Criticizing simulation results is certainly an important issue. Considering the highly under-determined problem which is calibration, baseline calibrated model results have to be analyzed carefully. Moreover, it is important to consider uncertainty issues when trying to evaluate energy conservation opportunities or provide information about predicted energy performance (e.g. for energy contracting purposes). Unfortunately, information about evaluation of uncertainty on energy savings is quite rare in the literature. Most of papers on the topic focus on uncertainties at the design stage.

Sources of uncertainty can be categorized into four groups: (a) scenario uncertainty, (b) physical/operational uncertainty, (c) model inadequacy and (d) observation error ().

Table 4: Sources of uncertainty (adapted from Heo, 2011)

Category	Factors
Scenario uncertainty	- Outdoor weather conditions - Building usage/occupancy schedule
Building physical/operational uncertainty	- Building envelope properties - Internal gains - HVAC systems - Operation and control settings
Model inadequacy	- Modeling assumptions - Simplification in the model algorithm - Ignored phenomena in the algorithm
Observation error	- Metered data accuracy

Scenario uncertainty refers to external environment (e.g. weather conditions) and the use of the considered building (e.g. impact of occupants). Building physical and operational uncertainty refers to envelope characteristics, HVAC system characteristics and control settings, as well as internal gains densities. Model inadequacy is directly related to the resolution of the model and to the level of

abstraction of the physical phenomena occurring in reality. This source of uncertainty has already been discussed in Chapter 2 and has been partly quantified by validating the different components of the considered simulation tool. Observation errors depend on the quality of the metered data used to study the behaviour of the studied system and to calibrate the simulation model. Uncertainties on investment costs and utility costs should be added to the list when the calibrated model is used to evaluate ECO's.

Reddy and Maor (2006) argue that defining arbitrary calibration criteria, as done in ASHRAE (2002) is too naïve. It is necessary to consider the uncertainties introduced by the fact that numerous assumptions/approximations have been done during the modelling and the adjustment of the parameters and not only the overall calibration accuracy. To solve this problem the authors propose to identify a set of plausible solutions (i.e. a series on input files for the calibrated model) instead of only one in order to define the "boundaries" of the "real" solution. Despite its robustness, such method highly increases the number of simulation runs and make the calibration and ECO evaluation processes very heavy.

ASHRAE Guideline 14-2002 provides mathematical method to evaluate the savings uncertainty in the case where utility bills are the source of the energy use data and weather data are used as the only independent variable. This approach, adapted to regression models, is extended to the calibrated simulation approach. Basing on the CV(RMSE) and on the Student's t-distribution, it is proposed to compute the saving uncertainty (U), applying to the totals savings determined for a meter, by means of the following formula:

$$U = t \times \frac{1.26 \times CV(RMSE)}{F} \times \sqrt{\frac{n+2}{n \times m}}$$

Where,

U: relative uncertainty in a reported energy saving

t: Student's t distribution (available in Statistics textbooks)

CV(RMSE): post-calibration Coefficient of Variation of the Root Mean Square Error

F: computed fraction (%) of the baseline energy use that is saved for a given period (m)

m: number of periods

n: number of data points or periods in the baseline period

For example, a monthly energy saving of 20% on the whole-building electricity consumption computed by means of a baseline calibrated BES model resulting in a CV(RMSE) of 12% leads to an uncertainty of 32.1% (90% confidence level) on the estimated saving. So, the savings should be included between 13.6 and 26.4 % (90% confidence level). Unfortunately this method is not perfect since it considers only the value of CV(RMSE) to quantify the uncertainty on the savings.

This uncertainty evaluation method is often considered as arbitrary and not sufficiently robust. Heo (2011) considers that the error on the savings should be derived from a probabilistic distribution. Moreover, such method is not able to quantify the impact of uncertainties associated with the proposed ECMs (since it considers only the post-calibration CV(RMSE) value). Indeed, using this method leads to the same magnitude of risk for any retrofit option although some options may be characterized by smaller uncertainties than others.

A more general approach to address uncertainty issues is the one proposed by Reddy and Maor (2006). Their method is based on the use of a series (e.g. of ten) sets of parameters, representing the best possible solutions to the calibration problem, to evaluate the ECOs. This method is certainly more

robust than the one proposed by ASHRAE (2002) but remains heavy and sometimes confusing for the user due to the manipulation of several possible sets of inputs.

Another approach would consist in using an uncertainty analysis method similar to the ones used to quantify uncertainty during the design phase (Struck and Hensen, 2007; Hopfe and Hensen, 2011; Corrado and Mechri, 2009). For ECO evaluation as well as energy use analysis purposes, the output of the calibration process would consist in a final (best) set of (calibrated) input parameters accompanied by uncertainty ranges corresponding to a certain level of confidence (e.g. 95%) for all the parameters. **This would allow the final user of the calibrated model to run a global uncertainty analysis (using a Monte Carlo method) to quantify the uncertainty on each output (from whole-building annual energy consumption to specific energy use).**

When evaluating an ECO, the modified value of the input parameter(s) (for example, chiller EER in the case of a chiller replacement) would be integrated within the model, as well as the uncertainty range of this parameter (i.e. the uncertainty on the new chiller's EER) at the given level of confidence. Running again the uncertainty analysis would allow identifying both saving value and saving uncertainty at the same time. The validity and the robustness of this last approach are difficult to proof without actual pre-retrofit and post-retrofit data but this method is safer than the arbitrary "U-t method" proposed in ASHRAE Guideline 14-2002 and described above since it allows a true quantification of the propagation of the uncertainty from the model's inputs to the outputs.

4. SIMULATION-BASED ENERGY USE ANALYSIS METHODOLOGY

As mentioned above, the present work focuses on the use and the calibration of whole-building energy simulation models to support an energy efficiency services process consisting in:

- Energy end use breakdown and analysis at inspection and audit stages;
- ECOs evaluation and post-retrofit performance M&V;
- Building-level on-going/continuous commissioning.

Focus will be given to the setup of this process (i.e. to the first step of the energy diagnosis) but the results available at the end of these initial steps will be directly usable for the next stages of the process (ECOs evaluation and on-going commissioning).

An integrated simulation-based energy performance analysis methodology is developed hereunder. This methodology makes an intensive use of building energy simulation models at every stage of the analysis process and integrates a complete calibration process including the main issues discussed above (i.e. sensitivity and uncertainty issues). Indeed, as discussed before, calibration cannot be avoided when pretending applying a BES model to an existing building.

As pointed by Liu et al. (2004), numerous authors have calibrated detailed simulation models (DOE-2, EnergyPlus, Trnsys…), developed calibration procedures and attempted to compile calibration guidelines and manuals. Various calibration methods already exist, including manual iterative methods (Kaplan et al., 1990; Yoon et al., 2003; Liu et al., 2004), graphical methods (Bou-Saada and Haberl, 1995; McCray et al., 1995; Liu et al., 2003), methods based on specific tests (Subbarao, 1988a; Burch et al., 1990) and automatic methods (Carroll and Hitchcock, 1993; Lee and Claridge, 2003; Reddy and Maor, 2006).

Fully automatic methods are very attractive but are generally heavy to handle and limited because of their reduced flexibility (pre-defined required data and impossibility to integrate specific monitoring data in the calibration process).

Moreover these methods may lead to unrealistic calibrated models if not well controlled and understood by the user. Indeed, because of the high level of underdetermination of the calibration problem (large amount of parameter s and very limited available data such as monthly energy bills), it is not realistic to imagine that an automated method would be able to find the exact solution: numerous local optima exist and make impossible the use of an optimization method at the early stage of a calibration process.

Existing semi-automatic method involving heuristic and automatic steps are attractive but don't generally suit very well with the energy efficiency service process (where available data and measurements can vary a lot from cases to cases) and a more adapted method should be imagined.

Methods relying with specific monitoring tests, such as the PSTAR method (Subbarao, 1988a), have been developed for residential applications and are not well adapted to non-residential office buildings where the required intrusive tests cannot be easily realized.

Methods combining manual iterations and graphical/statistical tools seem to be well adapted to energy audit purposes. These methods are very flexible and could be adapted to most cases. Moreover, these methods allow the auditor identifying, visualizing and apprehending the behavior of the building under study during the calibration process. However, attention should be paid to keep the calibration method systematic and reproducible and to integrate sensitivity issues. Indeed, because the calibration stays a highly under-determined problem, sensitivity, accuracy and uncertainty issues have also been pointed out as important issues by the authors.

Considering these facts, it is believed that a manual but systematic calibration methodology is more adapted when the available amount of data is limited (as-built and billing data). The present methodology will rely on a flexible but systematic evidence-based calibration methodology able to fit with the varying constrains encountered by energy analysts (varying amount and quality of available data, varying time and money constraints…). The analysis methodology will integrate the notion of hierarchy between influential and non-influential parameters and between high and low quality sources of information (as-built files, on-field inspection, BEMS recording, spot and short-term measurements…) and will include the following stages (Figure 7):

1. As a first step of the diagnosis methodology and as a pre-requisite of the calibration process, the modeling work will be preceded by a complete analysis of both as-built and energy use data (plotting of energy signatures, etc) in order to allow cross-checking between the information coming from different sources and to flag outlier (non-significant) data points.
2. The distinction between influential and non-influential parameters (or screening) will be assisted by an integrated sensitivity analysis whose results will help the analyst in identifying critical issues and starting the calibration process.
3. As whole-building spot or short-term measurements are often required and handled during such energy performance diagnosis, the calibration method has to integrate additional measurement issues. So, the proposed methodology will also help the user in identifying the potentially useful measurements AND in valorizing the gathered data within the calibration process. In the present methodology, the calibration (and the calibrated model) should not be only seen as an end in itself but also as a mean to perform efficient and advanced energy diagnosis. Since it is difficult to define general calibration criteria, both statistical and graphical assessment methods will be used to assess the validity of the calibration.
4. The exploitation of the outputs of the calibrated model for energy use analysis and evaluation of ECOs will be accompanied by an uncertainty analysis based on the Latin Hypercube Monte Carlo (LHMC) method.

The different steps of the global simulation-based energy performance analysis methodology proposed in this work are detailed below.

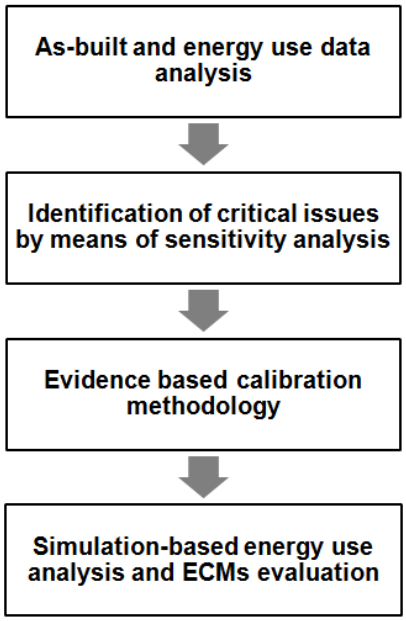

Figure 7: Simulation-based energy performance analysis methodology

Optimization-based adjustment of the model's parameters should not been abandoned. However, for the reasons explained above, it is believed that such type of "blind" adjustment method should be envisaged only as a last resort, when all the evidence-based issues have been investigated.

4.1. DATA COLLECTION AND ANALYSIS

A first and critical data collection issue concerns the weather data. The availability of weather data is highly dependent on the location (presence or not of a weather station, quality/accuracy and/or cost of the data made available by a local or national organism…) and the analyst has generally very little control over this aspect. However, the uncertainty on the weather data set used to run simulations and the impact of this uncertainty on the simulation results has to be considered during the analysis.

In addition to actual weather data, basic data collection will consist in gathering as-built data files and whole-building monthly energy billing data for a complete year (Figure 8). Usually, separate values are provided for heating (fuel-oil or natural gas energy bills) and other energy-uses (whole building electricity bills). If possible, this basic data set, required in order to start the analysis and the modeling work, can be completed by the whole-building electricity load provided on a quarter-hour basis by the energy provider.

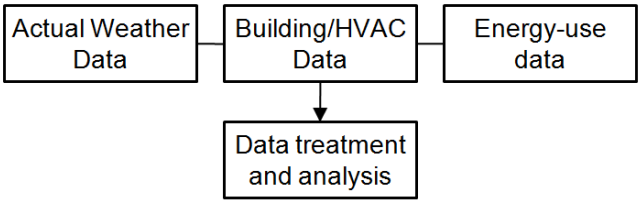

Figure 8: Step 1 - Data collection and analysis

On-site visit/inspection is also mandatory to complete and check the information available in the as-built file. This visit helps the analyst to have a first representation of the main uses of the building

(offices, meetings, conferences, restaurant, library…). As mentioned in Chapter 1, numerous inspection procedures are available in the literature (Knight, 2010).

The first step of the analysis will consist in classifying all the equipments of the facility in order to give a first definition of the zones that will be considered during the modeling phase. The characteristics of the main building and HVAC components have to be checked on-site. Basic information about building and HVAC use and operation schedules has to be obtained from the building manager and/or from the BEMS.

Secondly, (thermal and electrical) energy signatures are constructed and analyzed with regards to the information collected on the main energy consumers of the building (HVAC system, lighting, plug-loads…). Simple cross-checking can be realized by evaluating the global heat transfer coefficient of the building (see for example Bertagnolio et al., 2010) or the electricity consumption due to lighting, plug-loads, ventilation fans, etc; and comparing such values to the recorded energy bills.

The distinctions between peak and off-peak hours consumptions are also helpful in order distinguish base and variable electrical loads.

Finally, if made available, the quarter-hour electricity load profile can be used in order to distinguish base electrical load and time-varying loads. The comparative analysis between such data and the information available about main electricity loads and the corresponding operating/use schedules allow a new cross-checking of the gathered data.

4.2. As-built Input File Construction and Preliminary Sensitivity Analysis

The first step of the modeling phase consists in constructing a so-called “as-built input file”. This initial input file includes all the information resulting of the data collection and analysis step.

This as-built input file will also be used as a base for the sensitivity analysis phase (Figure 9).

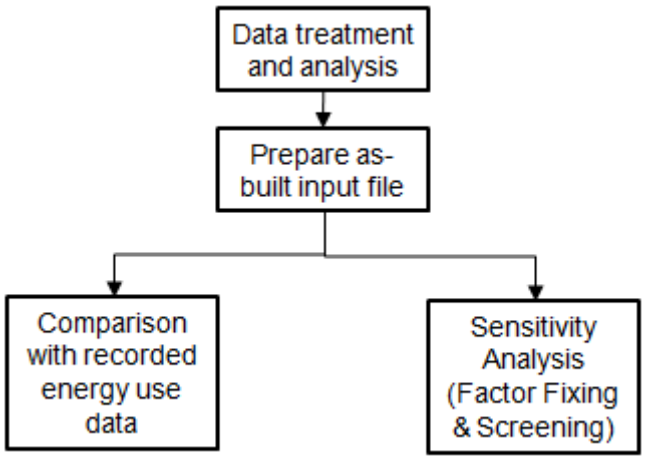

Figure 9: Step 2a - As-built input file and 1st simulation run

A preliminary sensitivity analysis is run in order to proceed to (Figure 10):

- Factor fixing setting
- Parameters screening

The first objective is to rank the parameters by order of influence and to reduce the dimension of the calibration problem by fixing the weak influential parameters to their most likely value without

significantly affecting the system prediction(s). This objectives is generally known as “factor fixing” setting.

The second objective of this preliminary sensitivity analysis is to provide a first hierarchy between the most influential parameters (in terms of seasonal or monthly fuel/gas, electricity and heating and cooling needs) in order to catch the eye of the user on the aspects needing further investigations, such as additional measurements, and to be considered in priority during the calibration phase. This second objective is similar to the, so-called, “experimental design” process, generally used to select the measurement equipments that have to be installed when designing an experimental test rig.

Typical ranges of variation are provided for each parameter of the model. However, the ranges of variation of the input parameters have to be adjusted in order to reflect the “uncertainty” of the user on the values defined in the as-built input file. As an example, if the exact value of the glazing U-value is unknown (e.g. missing data in the as-built file) but the type of glazing is known (e.g. glazing have been identified as “double glazing” during inspection), the range of variation for this parameter can be reduced from [1.53; 5.91] W/m²-K (range covering simple to triple glazing, ASHRAE, 2009) to [1.70; 2.50] W/m²-K (range covering old double glazing to recent high-performance double glazing). The impact of the range of variation will be studied in details in a following chapter.

While most influential parameters are listed, less influential parameters can be fixed to guessed values. The guess value has to be selected according to the information available in the as-built file and to guidance that could be found in the literature such as scientific papers, model user’s manual or standards/guidelines (ASHRAE, 2007, ASHRAE, 2009…). Typical values for most of the input parameters of the model have been given in Chapter 2.

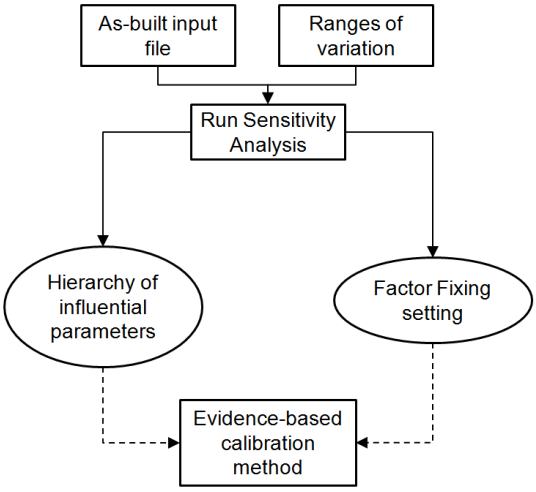

Figure 10: Step 2b - Preliminary sensitivity analysis

4.3. EVIDENCE-BASED CALIBRATION METHOD

Once the as-built input file is constructed and the preliminary sensitivity analysis is run, one can proceed to the calibration of the simulation model. The steps of the calibration process will be dedicated to the identification of the source of discrepancy between the simulation and the real situation and to the adjustment of the values of the most influential parameters previously identified.

This will be done by applying the evidence-based calibration method described below. This calibration method is fully integrated into the energy diagnosis process and relies on some interactions between the on-desk modeling work and the on-field inspection.

The initial as-built input file is used again to run a first simulation run. The results of this first simulation run are compared to the billing data used to evaluate the quality of the calibration. Generally, this first simulation run provides results with an accuracy of about 30% (Ahmad and Culp, 2006) in terms of annual energy use. At this stage, whatever the results of such comparison (satisfying the criteria or not), the model is supposed as not valid. Indeed, even if it is not likely, the accuracy criteria could be satisfied by chance.

Is there any measurable parameter?

In the iterative calibration process, the first question to be answered concerns the input parameters to calibrate (Figure 11). It is necessary to know if there are still opportunities to identify some influential parameters by means of physical on-site (spot or short-term, direct or indirect) measurements. Starting by answering this question, forces the user to consider physical measurements in priority. Indeed, as discussed above and considering the data available to evaluate the quality of the calibration, (blind, manual or automated) iterative adjustment methods should be used as a last resort only and could lead only to a temporary calibrated model (whose adjustment would have to be checked by means of physical measurements for instance).

What is the source of discrepancy? Which parameter/issue should be investigated?

At this stage, three situations can occur: (1) the source of discrepancy appears as evidence for the (experienced) user (e.g. influential parameter set to a default value for example) who knows what is the first priority, (2) the source of discrepancy is not trivial, or (3) the first most influential parameters of the list have already been identified/estimated with “acceptable” accuracy (e.g. based on observations or measurements). In these two last situations, the parameter to be considered is the next one by order of influence (as defined in the results of the sensitivity analysis).

Because of the potential non-linearity of the model, there may exist a need to include the sensitivity process in the iterative calibration process, or, at least, re-run the sensitivity process after having adjusted one or some of the most influential parameters. However, using a global sensitivity analysis method should allow taking into account the potential non-linearity of the model (i.e. the interactions between parameters). Sensitivity issues will be discussed in detail in the next chapter.

On-site measurement and update of the simulation model

After having been identified as a critical parameter, the value of the concerned parameter has to be estimated/refined. If practically feasible, spot (SpotM) or short-term (STeM) monitoring has to be considered in priority and added to the list of the tasks of the field-study. Various direct or indirect measurement techniques can be used for that purpose (e.g. direct indoor or supply temperature measurement or indirect estimation of the operating profiles by means of short-term monitoring of some lighting or appliances consumption measurements). When short-term (typically daily or weekly) measurements are performed, collected profiles (e.g. electrical load profile) can also be compared to the simulation results in order to check the validity of the model on an hourly (or sub-hourly) basis.

Of course, during the data collection process, redundant data could be collected. In that case, the “higher quality” information (i.e. the information judged as the more representative of the usual operation/behavior of the building) should be used to specify the value of the parameter. However, the other values should not be neglected and should be used to cross-check the available information and verify their validity.

A typical example of cross-verification has been encountered during the case study and is presented in Chapter 6. The initial information on the ventilation fans operation was obtained by analyzing the schedules implemented in the BEMS. A cross-verification consisted in monitoring the fan

consumption and their operating time. These measurements confirmed the fact that the fans were operated in the way prescribed by the BEMS.

If the physical measurement is not possible for a given reason (e.g. because of money or time constraints), it is suggested to study the next parameter by order of influence. Once again, proceeding in such a way ensures that the procedure is "evidence-based" and that priority is given to physical measurement and not to highly questionable "tuning" of the parameter.

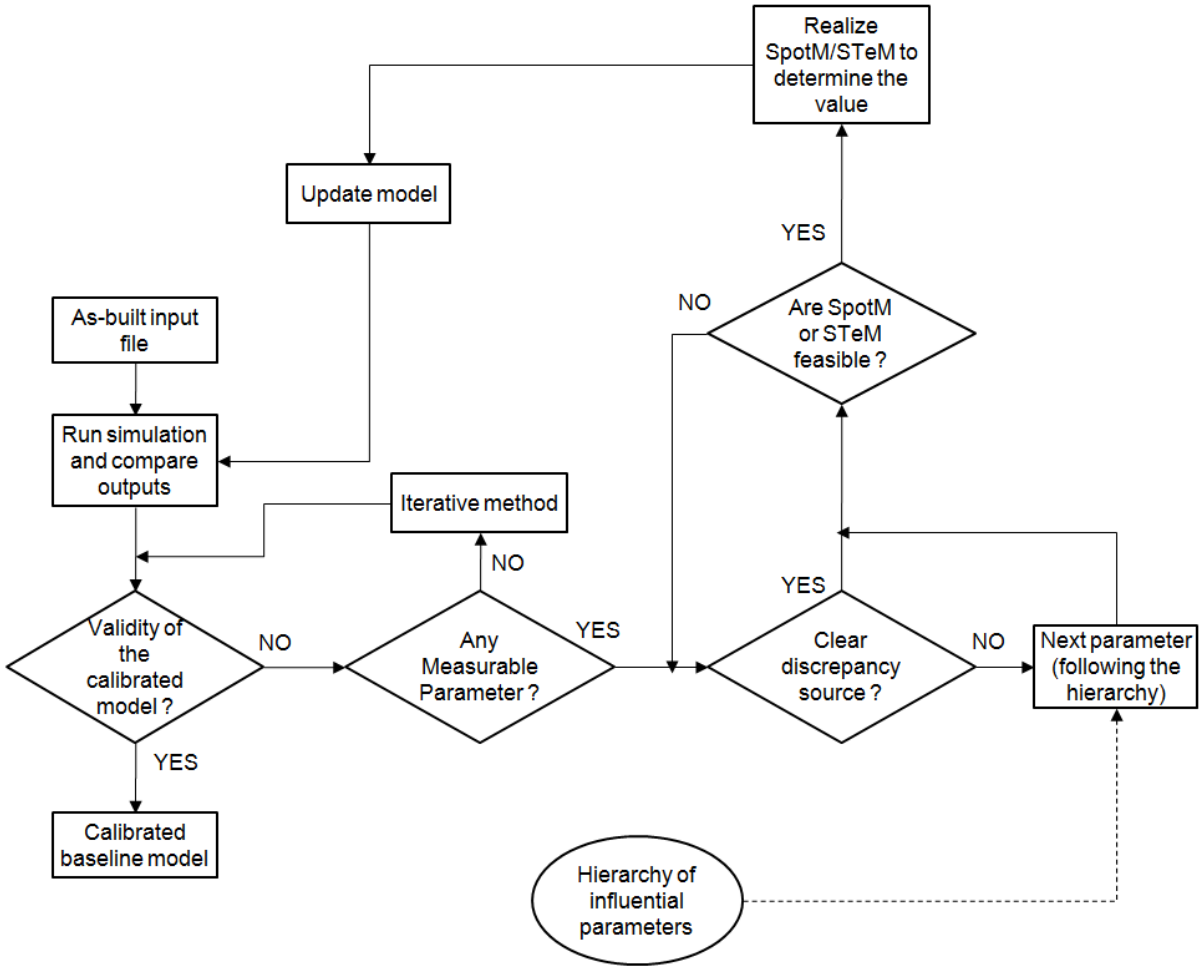

Figure 11: Step 3 - Evidence-based calibration methodology

When the measurements are available and analyzed, an updated version of the input file is issued and a second iteration can start**. The update of the input file will consist in updating the best-guess value of the concerned parameter, as-well as the corresponding probability/uncertainty range.** If some influential parameters still have to be adjusted after a few iterations and no measurement is possible to allow accurate quantification (because of time, money or physical constraints), a classical (manual or automated) iterative method can be used in order to adjust the last parameters. Of course, this adjustment work is not related to the practical reality of the building under study but can help to refine the value of some critical parameters which cannot be easily measured. Such logic allows making clear distinction between "measurable" and "non-measurable" parameters, so that adapted adjustment methods can be used for each category. Moreover, it allows characterizing the quality of the source of information considered to adjust the value of the input parameter. **In every case, priority is given to physical measurements and observation.**

Blind iterative adjustment of the parameter is considered only as a last possibility. Indeed, if the most of the influential parameters have been calibrated, the dimension of the calibration problem is largely reduced and the definition of a well mathematically conditioned optimization problem becomes possible. In the frame of the present work, focus will be given to evidence-based steps of the process and to sensitivity and uncertainty issues. The use of an automated method to finalize the calibration won't be studied.

It has to be noticed that, in general, it is advised to follow a "conservative" approach when adjusting the values of the parameters and the corresponding probability range. Indeed, it is often preferable to underestimate the real energy performance of the building (and so, use "pessimistic" values of the parameters, from an energy efficiency point of view) instead of overestimating it. The same conservative approach should be applied when specifying uncertainty ranges. Indeed, it is preferable to overestimate the uncertainty on a parameter and underestimate it.

When all the influential parameters have been considered for calibration and when the calibration criteria are satisfied, the model can be considered as "calibrated". It is critical to consider all influential parameters, even if, by chance, the calibration criterion is satisfied before the end of the inspection phase. Indeed, some "compensation" effects can occur and hide remaining discrepancies. The only way to avoid such trap is to consider each influential parameter one after the other in a very systematic approach and to stick to an "evidence-based" approach.

As a summary, one can consider as a general rule of the proposed evidence-based process that **the value of a parameter and the corresponding probability range can be determined only if the selected values have a physical meaning (i.e. obtained by means of observation, measurements…).**

Calibration quality criteria

As discussed above, it is delicate (if not impossible) to define a general criterion, ensuring proper calibration of a given building energy simulation model to a given existing situation.

As a first approach, it is proposed to consider the commonly used criteria proposed by ASHRAE-14 (2002) as well as proceeding to additional calibration quality verifications. This criterion, based on two statistical indexes (MBE and CV(RMSE)) evaluated on a monthly or hourly basis is one of the most robust among the criteria usually considered in practice. In addition to this mathematical criterion, it is necessary to consider the following points to check the validity of the calibration:

1. Computed peak heating and cooling loads have to be in good accordance with the installed heating/cooling capacities;
2. If available, the recorded whole-building hourly electricity load should be compared to the computed values;
3. Simulated daily/hourly energy use profiles (concerning internal gains, system operation, chiller load,...) should be visually checked, criticized and confronted to the operating patterns observed (or measured) during the inspection phase;
4. End-use energy consumption should be faithfully allocated (use short-term measurements to check the end-use energy consumption)

4.4. ENERGY USE ANALYSIS AND ECOS EVALUATION

Once calibrated, the baseline model can be used to evaluate some selected ECOs, envisage continuous performance verification and diagnosis, etc. The selection of ECOs remains purely heuristic and results from the analysis and observations. Typical weather data sets (Typical Reference or Mean Years, TRY or TMY) should be used to evaluate the ECOs after their implementation in the baseline model.

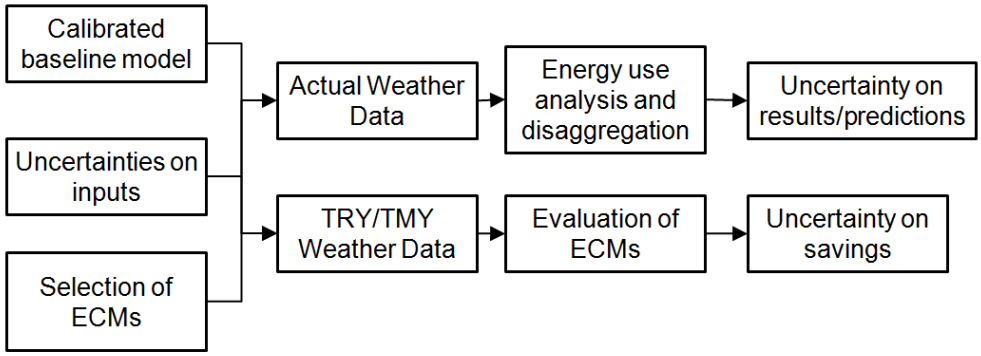

Figure 12: Step 4 - Use of the calibrated baseline model for energy use analysis and ECOs evaluation

Continuous performance verification (or on-going commissioning) will consist in periodically comparing predicted values of the whole-building energy performance to the corresponding values recorded on the existing installation. This process can be based on monthly energy bills but can be improved by using additional energy meters installed in the facility.

In both situations, uncertainty issues will be tackled in the same way. It is proposed to accompany the final set of input parameters with uncertainty ranges in order to allow performing an uncertainty analysis (Figure 12). Of course, uncalibrated and approximated/guessed parameters are characterized by wider variation ranges (higher uncertainty) than identified (or measured) parameters (lower uncertainty).

As an example, normal distributions characterized by mean values (the calibrated baseline value or best-guess value) and corresponding standard deviation values (defining the uncertainty on the adjusted value and representing the “measurement” error on the considered value) can be used to characterize calibrated parameters. For uncalibrated/unknown parameters, a uniform distribution between two realistic limits could be used to characterize uncertainty. Once the range of variation and the probability distribution are defined, the selected sampling method (e.g. Latin Hypercube Monte Carlo) is used to quantify the uncertainty on the model’s outputs.

5. SUMMARY

The calibration of a forward building energy simulation model remains a complex and highly underdetermined problem. Even if a special attention has been paid to select easily identifiable parameters with a physical meaning, the number of parameters to calibrate remains important in comparison with the limited amount of available data (e.g. monthly energy bills). In practice, even if the “net effect” of all the “knobs” yields to a simulated output close to the measured one, there is no guarantee that all individual “knobs” are properly tuned.

Because of the complexity of the problem, the three following issues are considered as crucial when performing a calibration:

- Sensitivity issues, consisting in distinguishing influential and non-influential parameters
- Uncertainty issues, consisting in characterizing or quantifying the final uncertainty on the model's outputs
- Accuracy issues, related to the definition of the calibration criterion that will be used to estimate the quality of the calibrated model

In practice, manual iterative (heuristic) calibration methods are the most popular ones. Unfortunately, these methods are generally highly dependent on the user's experience and skills and not systematic or easily reproducible. Moreover, such methods rarely include sensitivity and uncertainty issues.

Numerous automated methods have been developed in the past. In general, these methods are quite attractive because they propose to use an optimization algorithm to automatically adjust the values of the parameters of the model. However, because the calibration problem is highly underdetermined, it is hard (if not impossible) to define a well conditioned optimization algorithm (and the corresponding objective function) able to find the correct answer to the problem (i.e. the actual values of the parameters). Moreover, such methods are generally not flexible enough to be adapted to situations characterized by variable degree of complexity, variable amount of available billing or monitoring data…

The question of the definition of a criterion to assess the quality of a calibration has been studied by several authors. It appeared that it is delicate (if not impossible) to define a general criterion, ensuring proper calibration of a given simulation model to a given existing situation. Usually, statistical criteria computed on annual or monthly basis (MBE and CV(RMSE)) are used as calibration criteria. However, such criteria are often considered as too cool or not representative enough of the quality of the calibrated model. Currently, it seems that the best way to evaluate the quality of a calibrated model is to conduct additional visual verifications to check the ability of the model to predict the energy use behavior of the building.

In the present work, a systematic evidence-based method making intensive use of sensitivity and (non-intrusive) measurement issues is developed. This new calibration methodology relies on the definition of two types of hierarchy:

- A hierarchy between influential and non-influential parameters: sensitivity analysis is used to distinguish influential and non-influential parameters (non-influential parameters are then fixed to their best-guess value following a factor fixing approach) and to classify the influential parameters by order of importance (screening)
- A hierarchy between the source of information exploited to identify the parameters: Priority is given to physical observation and measurements. the adjustment of a parameter is done only if the value consists in an "improvement" of the quality of the model (i.e. the updated value has a physical meaning and has been obtained from a more reliable source of information than the previous one).

After the end of the evidence-based process (i.e. the "physical" identification of the most influential parameters), iterative (manual or automated) adjustment is envisaged only as a last possibility to refine the calibration of the model and to adjust the values of the parameters that have not been calibrated (because of the impossibility to measure them during the evidence-based process)

Finally, three categories of parameters can be defined:

- Non-influential parameters set to their "best-guess" value at the beginning of the calibration process and not adjusted during the calibration process
- Influential parameters concerned by a (evidence-based) calibration based on collected information (as-built, metering…)
- Non-calibrated parameters subject to iterative adjustment in order to refine and finalize the calibration of the model

Specifying (and updating/narrowing) probability/uncertainty ranges for the parameters all along the calibration allows characterizing the quality of the calibrated model at each step of the process (since specified ranges "translate" the quality of the information used to adjust the value of the parameter). At the end of the calibration, an uncertainty analysis is run to quantify the final uncertainty on the model's output.

6. REFERENCES

Adam, C., André, P., Hannay, C., Hannay, J., Lebrun, J., Lemort, V., Teodorese, I.V. 2006. A contribution to the audit of air-conditioning system: modelling, simulation and benchmarking. Proceedings of the 7th System Simulation in Buildings conference, SSB 2006, Liège, Belgium.

Ahmad, M., Culp, C.H. 2006. Uncalibrated Building Energy Simulation Modeling Results. HVAC&R Research, vol. 12, Nr. 4, pp. 1141-1155.

ASHRAE. 2002. ASHRAE Guideline: Measurement of energy and demand savings. ASHRAE Guideline 14-2002. American Society of Heating, Refrigerating and Air-Conditioning Engineers, Inc.

ASHRAE. 2004. Procedures for Commercial Building Energy Audit. American Society of Heating, Refrigerating and Air-Conditioning Engineers, Inc.

ASHRAE. 2007. ASHRAE Standard 90.1 - 2007: Energy standard for buildings except low-rise residential buildings. American Society of Heating, Refrigerating and Air-Conditioning Engineers, Inc.

AuditAC. 2007. AuditAC project : field benchmarking and market development for audit methods in air conditioning. AuditAC Final report. Intelligent Energy Europe programme.

Bertagnolio, S., Lebrun, J., Hannay, J., Aparecida Silva, C. 2008a. Simulation – assisted audit of an air conditioned building. 8th International Conference for Enhanced Building Operations, Berlin, Germany.

Bertagnolio, S., Lebrun, J. 2008b. Simulation of a building and its HVAC system with an equation solver: Application to benchmarking. Building Simulation: An International Journal. Vol 1, pp.234-250.

Bou-Saada, T.E.,Haberl, J. (1995). An improved procedure for developing calibrated hourly simulation models. Proceedings of the 5th IBPSA Building Simulation Conference, Madison, Wisconsin, USA.

Burch, J., Subbarao, K., Lekov, A., Warren, M., Norford, L. 1990. Short-term energy monitoring in a large commercial building. ASHRAE Transactions x(y): 1459-1477.

Carrillo, A., Dominguez, F., Cejudo, J.M. 2009. Calibration of an EnergyPlus simulation model by the STEM-PSTAR method. Proceedings of the 11th IBPSA Conference, Glasgow, UK.

Carroll, W.L., Hitchcock, R.J. 1993. Tuning Simulated Building Descriptions to match actual utility data: methods and implementation. ASHRAE Transactions, 99(y): 928-934.

Chen, C., Pan, Y., Huang, Z., Wu, G. 2006. Energy consumption analysis and energy conservation evaluation of a commercial building in Shanghai. Proceedings of the 6th International Conference on Enhanced Building Operation, Shenzhen, China.

Cho, S., Haberl, J. 2008a. Development of a simulation toolkit for the selection of high-performance systems for office buildings in hot and humid climates. Proceedings of the third National Conference of IBPSA-USA, Berkeley, California.

Cho, S., Haberl, J. 2008b. Validation of the eCalc commercial code-compliant simulation versus measured data from an office building in a hot and humid climate. Proceedings of the 16th Annual Symposium on Improving Building Energy Efficiency in Hot and Humid Climates, Plano, Texas.

Cho, S., Haberl, J.S. 2009. Development of a high-performance office building simulation model for a hot and humid climate. Proceedings of the 11th IBPSA Conference, Glasgow, UK.

Corrado, V., Eddine Mechri, H. 2009. Uncertainty and Sensitivity Analysis for Building Energy Rating. Journal of Building Physics, 33(2), pp. 125-156.

Costa, A., Keane, M., Raftery, P., O'Donnell, J. 2009. Key factors – Methodology for enhancement and support of building energy performance. Proceedings of the 11th IBPSA Conference, Glasgow, UK.

Efficiency Valuation Organization. 2007. International Performance Measurement and Verification Protocol (IPMVP). Concepts and Options for Determining Energy and Water Savings – Volume 1.

Fels, M. 1986. Prism: An introduction. Energy and Buildings, 9: 5-18

Friedman, H., Claridge, D., Choinière, D., Milesi Ferretti, N. 2010. Commissioning Cost-Benefit and Persistence of Savings. IEA-ECBCS Annex 47 Report. National Institute of Standards and Technology, and Natural Resources Canada (2010). Available at: www.ecbcs.org

Hopfe, C., Hensen, J. 2011. Uncertainty Analysis in Building Performance Simulation for Design Support. Energy and Buildings 43, pp. 2798-2805.

Jagpal, R. 2006. International Energy Agency – Energy Conservation in Buildings and Community Systems Annex 34 : Computer Aided Evaluation of HVAC System Performance. Synthesis Report.

Kaplan, M.B., McFerran, J., Jansen, J., Pratt, R. 1990. Reconciliation of a DOE2.1c model with monitored end-use data for a small office building. ASHRAE Transactions. 11 (1):981-993.

Kissock, J.K., Haberl, J.S., Claridge, D.E. 2003. Inverse modeling toolkit: numerical algorithms. ASHRAE Transactions x(y): xx-yy.

Kissock, J.K., Haberl, J.S., Claridge, D.E. 2002. Development of a toolkit for calculating linear, change-point linear and multiple-linear inverse building energy analysis models. Final Report, ASHRAE 1050-RP.

Klein, S.A., 2007. TRNSYS 16 Program Manual. Solar Energy Laboratory, University of Wisconsin, Madison, USA

Klein, S.A., 2009. EES Engineering Equation Solver. F-Chart Software, University of Wisconsin, Madison, USA

Knebel, D.E. 1983. Simplified energy analysis using the modified bin method. American Society of Heating, Refrigeration and Air-Conditioning Engineers, Atlanta, GA.

Knight, I. 2010. HarmonAc project : Harmonizing Air Conditioning Inspection and Audit Procedures in the Tertiary Building Sector. Intelligent Energy Europe programme.

Krarti, M. 2000. Energy Audit of Building Systems; An Engineering Approach. CRC Press, Florida. U.S.

Kreider, J.F., Haberl, J.S. 1994. Predicting hourly building energy use: The great energy predictor shootout – Overview and discussion of results. OR-94-17-7. Pp 1104-1118

Lavigne, K. 2009. Assisted calibration in building simulation-algorithm description and case studies. Proceedings of the 11th IBPSA Conference, Glasgow, UK.

LBL. 1980. DOE-2 User Guide, Ver. 2.1. Lawrence Berkeley Laboratory and Los Alamos National Laboratory, LBL Report No. LBL-8689 Rev. 2; DOE-2 User Coordination Office; LBL, Berkeley, CA.

Lebrun, J., Liebecq, G. 1988. International Energy Agency – Energy Conservation in Buildings and Community Systems Annex 10: Building HVAC System Simulation. Synthesis Report.

Lebrun, J., Wang, S. 1993. International Energy Agency – Energy Conservation in Buildings and Community Systems Annex 17: Building Energy Management Systems – Evaluation and Emulation Techniques. Synthesis Report.

Liu, M. 1997. User's manual for air side simulation programs (AirModel). Energy Systems Laboratory, Texas A&M University, College Station, TX.

Liu, M., Claridge, D.E. 1998. Use of calibrated HVAC system models to optimize system operation. Journal of Solar Energy Engineering. 120:131-138

Liu, M., Claridge, D.E., Bensouda, N., Heinemeier, K., Lee, S.U., Wei, G. 2003. Manual of Procedures for calibrating simulations of building systems. HPCBS#E5P23T2b. California Energy Commission, Public Interest Energy Research Program.

Liu, M., Song, L., Wei, G., Claridge, D.E. 2004. Simplified building and air-handling unit model calibration and applications. Journal of Solar Energy Engineering. Vol. 126, pp. 601-609.

Liu, M. 2011. Discussion at ASHRAE Winter Conference, Las Vegas, NV.

Lunneberg, T.A. 1999. Improving simulation accuracy through the use of short-term electrical end-use monitoring. Proceedings of the 7th IBPSA Building Simulation Conference, Kyoto, Japan.

Lydberg, M.D. 1987. Source book for energy auditors. International Energy Agency – Energy Conservation in Buildings and Community Systems Programme Annex 11 "Energy Auditing" final report.

McCray, J.A., Bailey, P.L., Parker, J.L. (1995) Using data visualization tools for the calibration of hourly DOE-2.1 simulations. Proceedings of the 5th IBPSA Building Simulation Conference, Madison, Wisconsin, USA.

Pan, Y., Huang, Z., Wu, G. 2007. Calibrated building energy simulation and its application in a high-rise commercial building in Shanghai. Energy and Buildings. Vol. 39, pp. 651-657.

Pedrini, A., Westphal, F.S., Lamberts, R. (2002). A methodology for building energy modeling and calibration in warm climates. Building and Environment. 37: 903-912.

Raftery, P. Keane, M., Costa, A. 2009. Calibration of a detailed simulation model to energy monitoring system data: a methodology and case study. Proceedings of the 11th IBPSA Conference, Glasgow, UK.

Reddy, T.A., Deng, S., Claridge, D.E. 1999. Development of an inverse method to estimate overall building and ventilation parameters of large commercial buildings. Journal of Solar Energy Engineering. Vol 121. pp. 40-46.

Reddy, T.A. 2006. Literature review on calibration of building energy simulation programs: uses, problems, procedures, uncertainty and tools. ASHRAE Transactions, 112(1): 226-240.

Reddy, T.A., Maor, I. 2006. Procedures for reconciling computer-calculated results with measured energy data. ASHRAE Research Project 1051-RP. Atlanta: American Society of Heating, Refrigerating and Air-Conditioning Engineers, Inc.

Reddy, T.A. 2011. Discussion at ASHRAE Winter Conference, Las Vegas, NV.

Spitler, J.D. 2006. Building performance simulation: the now and the not yet. HVAC&R Research 12(3a): 711-713.

Struck, C., Hensen, J. 2007. On Supporting Design Decisions in Conceptual Design Addressing Specification Uncertainties Using Performance Simulation. Proceedings of the 10th IBPSA Building Simulation Conference, Beijing, China.

Subbarao, K., Burch, J.D., Hancock, C.E., Lekov, A., Balcomb, J.D. 1988a. Short-Term Energy Monitoring (STEM): Application of the PSTAR method to a residence in Fredericksburg, Virginia. SERI/TR-254-3356, Solar Energy Research Institute, Golden, CO.

Subbarao, K. 1988b. PSTAR – Primary and Secondary Terms Analysis and Renormalization. A unified approach to building energy simulations and short-term monitoring. SERI/TR-254-3175, Solar Energy Research Institute, Golden, CO.

US DOE. 2008. M&V Guidelines: Measurements and Verification for Federal Energy Projects, version 3.0

US-DOE. 2009. EnergyPlus Energy Simulation Software, U.S. Department of Energy. Available at: http://apps1.eere.energy.gov/buildings/energyplus/

Visier, J.C., Jandon, M. 2004. International Energy Agency – Energy Conservation in Buildings and Community Systems Annex 40: Commissioning of Building HVAC Systems for Improved Energy Performances. Synthesis Report.

Waltz, J.P. 2000. Computerized building energy simulation handbook. Lilburn, GA: Fraimont Press.

Wei, G., Liu, M., Claridge, D.E. (1998) Signatures of heating and cooling energy consumption for typical AHUs. Proceedings of the Eleventh Symposium on Improving Building Systems in Hot and Humid Climates, Fort Worth, TX.

Westphal, F.S., Lamberts, R. 2005. Building Simulation Calibration using Sensitivity Analysis. Proceedings of the 9th IBPSA Building Simulation Conference, Montréal, Canada.

Yoon, J., Lee, J.E. 1999. Calibration procedure of energy performance simulation model for a commercial building. Proceedings of the xxth IBPSA Conference, Eindhoven, Netherlands.

Yoon, J., Lee, J.E., Claridge, D.E. 2003. Calibration procedure for energy performance simulation of a commercial building. Journal of Solar Energy Engineering. 125:251-257

CHAPTER 4 INTEGRATING SENSITIVITY AND UNCERTAINTY ISSUES WITHIN THE CALIBRATION PROCESS

CHAPTER 4: INTEGRATING SENSITIVITY AND UNCERTAINTY ISSUES WITHIN THE CALIBRATION PROCESS 2
1. INTRODUCTION 2
2. SENSITIVITY AND UNCERTAINTY ANALYSIS IN BUILDING SIMULATION 2
3. SELECTION OF A SENSITIVITY ANALYSIS METHOD 4
3.1. Implementation of the Morris Method 6
3.2. Parameters and Outputs Selection 12
4. APPLICATION OF THE MORRIS METHOD 13
4.1. Base Case Buildings Description 13
4.2. Basecase Energy Use 17
4.3. Ranges of Variation 18
4.4. Results 20
5. SENSITIVITY AND UNCERTAINTY ISSUES IN THE CALIBRATION PROCESS 26
5.1. Example of Preliminary Sensitivity Analysis 27
5.2. Post-Calibration Uncertainty Analysis 30
6. CONCLUSION 32
7. REFERENCES 34

CHAPTER 4: INTEGRATING SENSITIVITY AND UNCERTAINTY ISSUES WITHIN THE CALIBRATION PROCESS

1. INTRODUCTION

Statistics textbooks generally recommend that mathematical modeling of a given system should be coupled to a "sensitivity analysis" (Saltelli and Annoni, 2010). In practice, within the global concept of "sensitivity analysis" one can distinguish:

- Uncertainty analysis (UA) aimed at characterizing the empirical probability density function and the confidence intervals of a given model output. This corresponds to measurement error for physical experiments.
- Sensitivity analysis (SA) aimed at identifying factors which are the source of the uncertainty in the prediction.

These two tasks, while having different objectives, are often coupled and called by the generic term: "sensitivity analysis".

As a prerequisite of the calibration process, a comprehensive sensitivity analysis is carried out in the present chapter. The implication in the development of the calibration methodology is explained. The application of this sensitivity analysis method to a synthetic case and its integration within the calibration process are presented below. Finally, the problem of the uncertainty on the outputs of the calibrated model is also tackled.

2. SENSITIVITY AND UNCERTAINTY ANALYSIS IN BUILDING SIMULATION

Simulation models can be used in practical applications when they are within acceptable ranges of reliability, accuracy and repeatability (Corson, 1992). These three characteristics are directly related to program sensitivity which depends of three factors: the investigated building, the modeling approach and the considered simulation software. Even if modeler interpretations and choices commonly appear to be the most significant factor influencing simulation results (Diamond et al., 1985; ASHRAE, 1994), sensitivity analysis of a given building energy simulation model is needed for the user, (1) to evaluate how confident he can be with the results and, (2) to identify the most influential parameters that should be given particular attention. Moreover, such an analysis will contribute to add to the user's understanding of the building energy simulation model, which is a critical factor to perform accurate simulation work (Waltz, 1992).

Sensitivity analysis is commonly used for design optimization (Lam and Hui, 1996; Roujol et al., 2003) and assessment of ECMs (Mottillo, 2001; Lam et al., 2008). However, sensitivity, accuracy and uncertainty issues have also been pointed out as important issues by Reddy and Maor (2006). Because the calibration remains a highly undetermined problem, sensitivity analysis should be coupled to the calibration process in order to identify the most influencing parameters. Finally, calibration should result in a plausible solution where the most influential parameters are addressed. Of course, uncertainty analysis methods are also useful to quantify the uncertainty on the results predicted by the calibrated model.

Westphal et al. (2005) present a calibration method applied to the EnergyPlus software, combining audit techniques and sensitivity analysis. This calibration method starts with the adjustment of lights and plug loads, followed by a short sensitivity analysis (using design days simulations) allowing identifying the most influential parameters to adjust in priority. The main advantage of this sequential approach is the integration of a simple sensitivity analysis into the calibration process.

Corson (1992) has evaluated the sensitivity of 5 simulation software (from bin-type programs to hourly simulation programs) to 25 input variables for 2 difference base cases (one small and one large office building), resulting in 10 building energy models. Surprisingly, considering that BES models have been originally devoted to accurate evaluation of building loads rather than system consumptions, it appeared that HVAC&R issues (HVAC components performance, set points, operating profiles…) are more likely to impact the results than building envelope characteristics. This confirms that BES models adapted to energy audit and ECMs evaluation should not neglect neither envelope nor HVAC&R issues but should integrate all these influences into an homogeneous way.

Sensitivity analysis has also been used for optimizing design of office buildings (Lam and Hui, 1996). More than 400 simulation runs have been performed with a DOE-2 model of a typical all-electric base case building located in Hong Kong. The impact and the correlation between input design variables and selected outputs have been examined. Building envelope characteristics and some control set-points (supply air temperature and chilled water temperature set-points) and HVAC components efficiencies (fan efficiencies and chiller EER) have been identified as having significant impact on the whole electricity consumption.

The building energy simulation software Consoclim (Bolher et al., 1999), based on the simplified lumped dynamic building model described in ISO13790 (2007), has been developed for design purposes and submitted to a sensitivity analysis (Roujol et al., 2003). The impact of 20 parameters on chiller electricity consumption has been studied assuming Gaussian distribution and relative uncertainties at 90% of level of confidence. The most influential input variables appear to be the indoor set-point temperature, the glazing solar factor, the internal gains density, the part load performance and the rating EER of the chiller. Ventilation rate, infiltration rate and walls U-values had no significant impact on the cooling demand and chiller consumption.

Mottillo (2001) has performed a sensitivity analysis using a DOE-2 based Canadian code compliant program applied to 10 different all-electric base case buildings. 14 parameters (from envelope characteristics to HVAC system rating performance and operation) have been investigated to identify the most sensitive parameters (and so, the less and the most efficient ECMs).The walls thermal resistances, internal gains densities and minimum outdoor rate were found to have the largest impact on predicted energy savings. The less influential parameters are orientation, building thermal mass and supply air flow rate.

Lam et al. (2008) have applied sensitivity analysis techniques to a set of 10 DOE-2 calibrated models in order to study implications for energy conservation measures (ECMs). These models have been manually calibrated to 10 office buildings located in Hong Kong by following the ASHRAE (2002) criteria. Only global monthly electricity uses were considered to perform the calibration. 10 key design parameters were selected to perform sensitivity analysis by means of the calibrated models. The total electricity consumptions computed given more than 420 simulation runs were examined. It was possible to see that the influence of some input variables (e.g. building envelope parameters) was largely different from case to case and for a same parameter, no clear general pattern could be identified. The results of this sensitivity analysis were then used to assess 4 different energy conservation measures.

It appears that some findings provided by the various sensitivity analyses mentioned above are similar whatever the initial objective (design optimization, ECMs evaluation or calibration). However, it is still difficult to draw some general conclusions applicable to the entire office building stock, all over the world. Indeed, the results of a sensitivity analysis seem to be highly dependent to the model used to run simulations, the type of building and HVAC system considered as "base case", the location (and the weather) of the considered base case building, the sampling method used to perform the analysis, and, once again, the modeler's skills. So, considering the high number of variables and influences occuring in such an analysis, it seems rational to integrate some sensitivity issues in each building simulation work, including calibration.

3. SELECTION OF A SENSITIVITY ANALYSIS METHOD

Various sensitivity analysis methods are available in the literature. The selections of a sensitivity method, as well as the sensitivity measure have to be suited to the goal of concern in order to provide relevant information about the relative influence of the parameters.

One can distinguish local and global sensitivity analysis methods:

- Local methods, relying on one-at-a-time sampling, estimate the sensitivity indices (such as the influence coefficient IC) at a single data point in the parametric space (i.e. the set of possible combinations between the potential values of the considered parameters), known as "baseline" value. These techniques are efficient in terms of computing time but do not provide any information about the part of the parametric space which remains unexplored unless the model is proven to be linear (Saltelli and Annoni, 2010). Indeed, varying the values of the considered parameters from a pre-defined base case does not allow to identify the potential interactions between them (i.e. the non-linearities of the model)
- Global methods are generally preferred if the property of the model is a-priory unknown. Such methods generate sampled points in the whole parametric space (hypercube) according to a given sampling strategy, such as, for instance, Latin Hypercube Monte Carlo sampling method (LHMC) or "elementary" factorial sampling methods.

In the field of building performance simulation, the two most common methods are:

- The "local" Differential Sensitivity Analysis (DSA) method: each parameter is varied, one at a time. Results can be expressed in terms of various dimensional or non-dimensional influence coefficients.
- "Global" Monte Carlo Analysis (MCA): all parameters are varied simultaneously (in accordance with a pre-defined distribution, generally a normal distribution) for each simulation run

Lomas and Eppel (1992) have applied the DSA and MCA to three detailed BES models. It is shown that both DSA and MCA methods can be applied to a wide range of BES models (from simple steady-state models to complex dynamic models). Compared to MCA, DSA produces both individual (influence of variations in each individual input on predictions) and total (due to variations in all input data) sensitivities. DSA is often used in the frame of validation and uncertainty analysis but also to identify most influential parameters in building energy simulation models. It is interesting to note that the results obtained by the authors using MCA and DSA were in good agreement even if the results of the MCA method are considered as more accurate since they include the potential interactions between parameters. In their study, Lam and Hui (1996) have compared different forms of sensitivity coefficients. For building energy studies, the most useful one appears to be the non-dimensional influence coefficient (also known as elasticity):

$$IC = \frac{\frac{\Delta OP}{OP_{bc}}}{\frac{\Delta IP}{IP_{bc}}} \qquad (1)$$

OP: output

IP: input

bc: base case

For limited ranges of inputs, building energy simulation models are often roughly considered as linear and the value of the influence coefficient is generally considered as representative of the "average" sensitivity of the model to the considered input (Lomas and Eppel, 1992), in the considered range. Generally, the linear regression coefficient (R^2) is also computed in order to check the validity of this hypothesis.

However, when considering larger variation ranges (e.g. when having to calibrate a totally unknown parameter), the hypothesis of linearity is highly questionable, and interactions have to be considered. Moreover, Saltelli and Annoni (2010) have shown that OAT (One-at-A-Time) methods are often inadequate because of their "local" characteristics. Indeed, reverting to the baseline point in order to compute any effect is the reason of the poor efficiency of such methods and the inability to explore the parametric space in a satisfying way. Local OAT methods may be attributed to (Campolongo et al., 2007):

- A lack of knowledge about other and more sophisticated sampling techniques;
- The lower computational cost;
- The simplicity of the sampling design.

MCA methods are commonly applied to BES models and allow exploring all the parametric space, taking into account individual and interaction effects. The main drawback of such methods is related to the fact that they require to pre-define the probability density function for each parameter. Moreover, unlike local OAT methods, MCA-based methods do not allow deriving individual sensitivities and separately assessing the effects of the different parameters. However, these methods present the advantage to be considered as "quantitative" since they allow determining the combined impact of input uncertainties on the model outputs uncertainties (Struck and Hensen, 2007).

A better application of the OAT principle used in "local" methods would consist in defining trajectories, i.e. varying each parameter one after the other without coming back to the baseline value. This is the principle of "Elementary Effects" methods, such as the "Morris" screening method (Morris, 1991). This last method has been applied a few times to building performance simulation codes (De Wit, 1997; Heiselberg and Brohus, 2007) in order to support design process but its applications are still rare in the literature (Campolongo et al., 2007). Corrado and Mechri (2009) applied both MCA and OAT-EE methods to simplified building simulation software. Probability density functions were assigned to 129 parameters grouped into three sets: climatic data, envelope data and building use data. MCA was used in order to quantify the uncertainty on the predicted energy performance class while the OAT-EE method was used to identify the 10 most influential parameters responsible of the main part of the computed uncertainties.

The screening method proposed by Morris was found to be suitable for identifying the most influential parameters of BES models by De Wit (1997) since it is not dependent on the properties of the model and does not require any assumption regarding linearity or correlations between the inputs and the outputs of the model. Heiselberg and Brohus (2007) also highlighted other advantages:

- The method can handle large number of parameters and requires a relatively limited amount of simulation runs;
- The parameters are varied globally within the range and the whole parametric space can be explored without pre-defining the probability density function of each parameter;
- The results are easily interpreted and visualized graphically as prescribed by Morris (1991).

The sensitivity of the output is characterized by a value called "Elementary Effect". The effect of a given parameter is calculated several times, at randomly selected points of the parametric space. The mean value of the effect is then compared to the dispersion (standard deviation) in order to allow the selection of the most influential parameters and the distinction of parameters with linear effects from parameters with nonlinear effects (i.e. interactions). A drawback of the Morris analysis is that it does not allow uncertainty analysis due to the fact that it does not take the shape of the probability density function of the parameters into account (De Wit et al., 2002). Indeed, the method cannot be considered as quantitative and the value of its measures can only be used to rank the studied parameters by order of influence and characterize the structure (i.e. the interactions) of the model but cannot be interpreted as percentages of the output variance.

Ideally, a sensitivity analysis used in the frame of calibration methodology should have the following properties:

- Being global in order to explore the whole parametric space and lead to significant results and sensitivity measures representative of the model behavior;
- Being flexible, reproducible and model-free in order to allow providing significant results whatever the model structure (linear or non-linear, monotonic or non-monotonic…);
- Being appropriated for factor fixing, meaning that the results should help in distinguishing non-influential parameters from critical ones and should allow to appreciate individual effects and first and higher-order interactions;
- Being reasonably cheap in terms of computation time.

For these various reasons, the Morris method is evaluated as the most interesting method for supporting factor fixing setting. Indeed, the Morris method is often considered as one of the best screening method when having to screen a subset of influent factors among a large number of variables contained in a model. Since it is still very commonly used in practice, the DSA method will also be applied and results of both methods will be analyzed and compared.

3.1. IMPLEMENTATION OF THE MORRIS METHOD

The "Elementary Effects" method proposed by Morris (1991) is based on the OAT sampling principle. This method initially aims at recognizing a few important parameters among a larger amount of parameters using two sensitivity measures: the mean and the standard deviation of the computed Elementary Effect (EE). Later, Campolongo (2007) improved the sampling strategy proposed by Morris and refined the definition of the sensitivity measures.

3.1.1. Elementary Effects

Considering a parametric space where the k parameters X_i (i=1,…,k) are uniformly distributed in between 0 and 1 following the set {0, 1/(p-1), 2/(p-1),…,1}, the region of experimentation Ω of the Morris method is defined as a part of the parametric space that is a k-dimensional p-level grid (Figure 1).

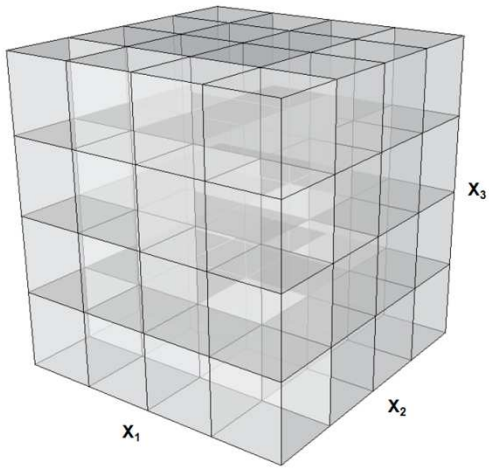

Figure 1: 3D graphical representation of the parametric space (k=3; p=5)

The "Elementary Effect" (EE) of the i[th] parameter X_i at a given point ($\underline{X}^j$) is defined as:

$$EE_i(\underline{X}^j) = \frac{Y(X_1^j, \dots, X_{i-1}^j, X_i^j + \Delta, X_{i+1}^j, \dots, X_k^j) - Y(\underline{X}^j)}{\Delta}$$

where Y is the system output evaluated before and after the variation of the i[th] parameter, Δ is an incremental effect that is a multiple of 1/(p-1) and where $(X_1^j, \dots, X_{i-1}^j, X_i^j + \Delta, X_{i+1}^j, \dots, X_k^j)$ and $\underline{X}^j$ are particular points in the region of experimentation Ω.

3.1.2. Sensitivity Measures

By computing the value of elementary effect EE_i of each of the k parameters at r random points $\underline{X}^j$ (j=1, …, r) of the region of experimentation, one obtain a sample of r values of EEi for each of the k parameters.

Based on that sample of values, Morris proposes to compute the mean μ_i and the standard deviation σ_i of each of the k distributions of values of EE_i. The mean (μ_i) is a measurement of the overall effect of the input X_i on the output Y while the standard deviation, σ_i, is an expression of the interactions effects (i.e. high-order or curvature effects).

$$\mu_i = \frac{\sum_{j=1}^{r} EE_i(\underline{X}^j)}{r}$$

$$\sigma_i = \sqrt{\frac{\sum_{j=1}^{r} [EE_i(\underline{X}^j) - \mu_i]^2}{r}}$$

Because of the possible compensation (cancellation) of positive and negative values of the elementary effect (EE_i) of a given parameter X_i, the mean value is not always a reliable measure. Indeed, in non-monotonic models, parameters characterized by alternatively positive and negative effects on the output Y can lead to low μ values. However, parameters having non-monotonic effects will be characterized by a high standard deviation.

Both mean and standard deviation values are then used to rank the parameters by order of importance. Morris proposed to graphically represent the results by plotting the measures of each parameter in the (σ, μ) plane (Figure 2).

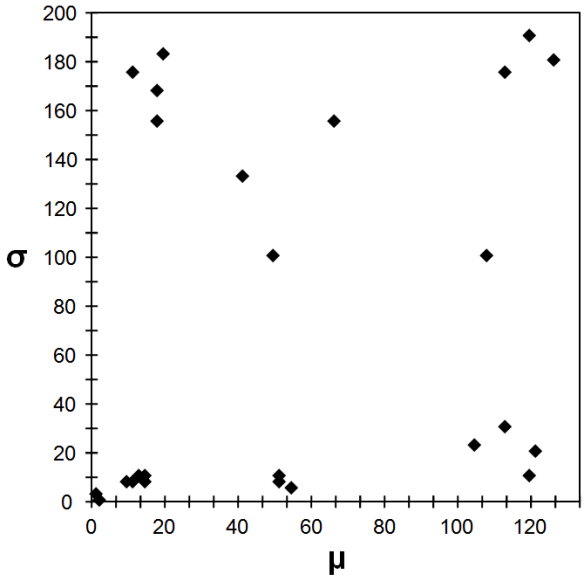

Figure 2: Example results of a Morris experiment plotted in the (σ, μ) plane

The zone "B" represented in Figure 3 includes the parameters characterized by high mean and standard deviation values. Those parameters appear as critical for the calibration problem: they have a high influence on the considered output and are characterized by important interactions with other parameters since their influence is highly dependent of the value of the other parameters.

The parameters located in the zones "C" and "D" are characterized by low standard deviation values (i.e. low high-order effects) but, high and low mean values, respectively. During a calibration process, for instance, the first ones will have to be considered as important parameters while the other ones could be fixed to estimated values without altering the capabilities of the model.

The parameters located in the zone "A" are also important parameters since they are characterized by high standard deviation values. The low mean value is due to the cancellation of the positive and negative values of EE_i due to the non-monotonic behavior of the model with respect to the considered parameter.

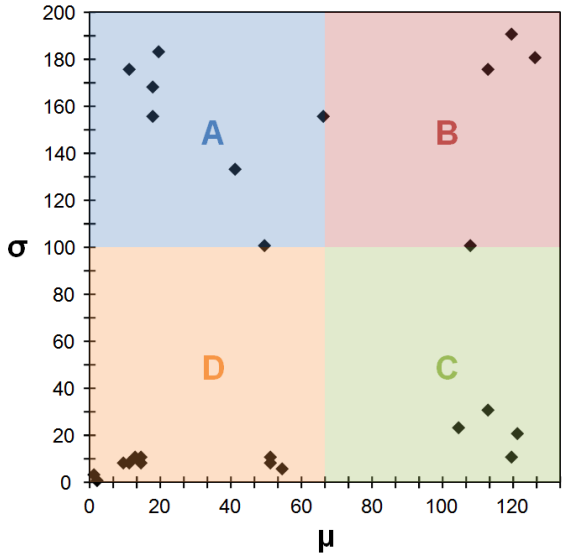

Figure 3: Example analysis of the results of a Morris experiment

In addition to the two first sensitivity measures, σ and μ, Campolongo et al. (2007) proposed to calculate a revised version of the second one, denoted μ^*, consisting in the mean value of the distribution of the absolute values of EE_i.

$$\mu_i^* = \frac{\sum_{j=1}^{r} \left| EE_i(\underline{X}^j) \right|}{r}$$

Unlike the original mean, μ, μ^* is a reliable measure of the importance of the parameter since the cancellation effect is avoided. Moreover, the comparison between the two mean values (Figure 4) is useful to study the effect of the sign changing of the computed elementary effects. Equal or almost equal values of both values correspond to a monotonic behavior of the model with respect to the considered parameter while different values correspond to a non-monotonic behavior.

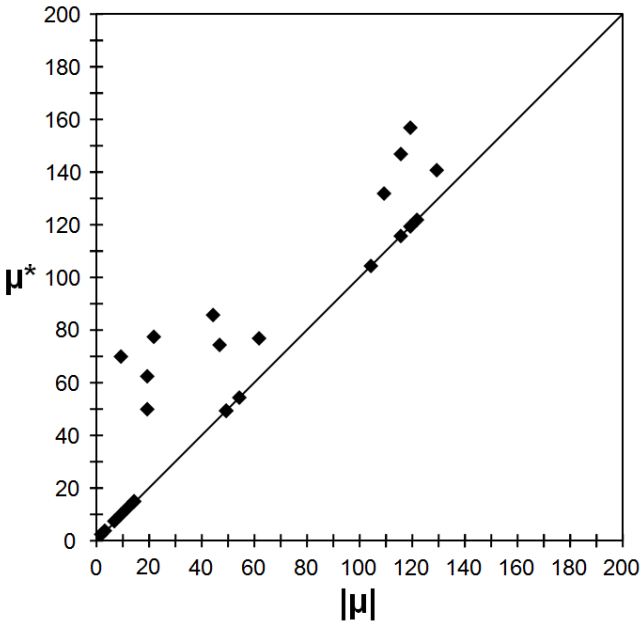

Figure 4: Example results of a Morris experiment plotted in the (μ, μ*) plane

Finally, three sensitivity measures should be considered when analyzing the results of the Elementary Effects method (or Morris method). The main effect of a given parameter, as well as its interactions with the other parameters (i.e. the high order or curvature effects) or the monotonic behavior of the model can be highlighted by means of μ, μ^* and σ.

3.1.3. Sampling Strategy

As mentioned above, the sampling strategy proposed by Morris (1991) is based on an OAT design. When studying the effect of *k* parameters on the output *Y*, a series of *r* "trajectories" (generally 10 to 20 trajectories) of *(k+1)* steps are randomly generated within the parametric space Ω with the property that two consecutive points differ in only one component by an elementary variation of ±Δ (Figure 5). The computational cost is then of *r*(k+1)* runs.

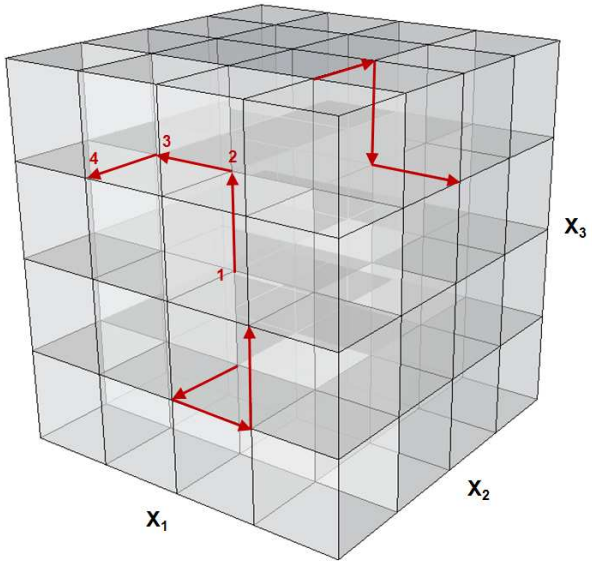

Figure 5: 3D graphical representation of a series of 3 trajectories generated within the parametric space Ω (k=3; p=5)

As explained above, it is crucial to ensure a high level of exploration of the parametric space in order to highlight first-order and higher-order influences, without involving a too high number of model evaluations (especially in models with a high number of parameters). Campolongo et al. (2007) proposed to improve the original sampling strategy of Morris (1991) by selecting the *r* "highest spread" trajectories among a larger number, *M*, of randomly generated trajectories. As explained hereunder, the spread of the selected trajectories is characterized by a specific metric, such as the Euclidian distance or the Manhattan distance.

The first step of the selection of the best series of r trajectories among the M generated trajectories consists in constructing the C_M^r combinations of trajectories. Following Campolongo et al. (2007), the best combination is the one that maximizes the root mean square *D* of the Euclidian distances d_{ij} between the trajectories *i* and *j*.

The Euclidian distance between two trajectories is defined as:

$$d_{ij} = \sum_{l=1}^{k+1} \sum_{m=1}^{k+1} a_{lm}$$

where a_{lm} is the geometric distance between the point *l* of the i^{th} trajectory and the point *m* of the j^{th} trajectory (Figure 6).

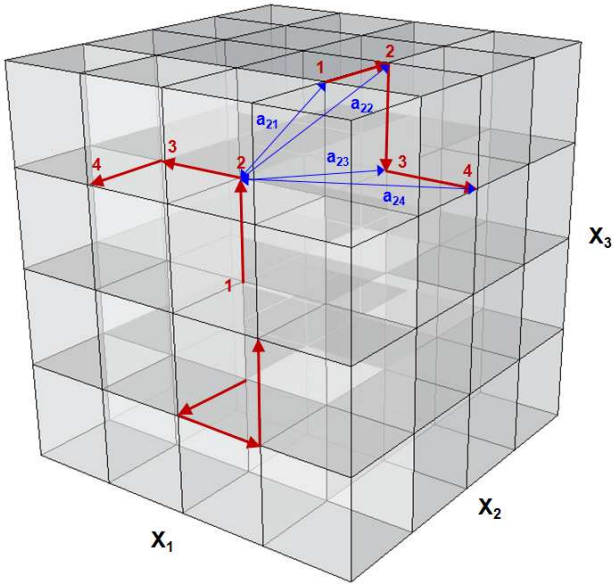

Figure 6: 3D graphical representation of the distance between two trajectories (k=3; p=5)

As an example, when selecting the best 4 trajectories ($r = 4$) among 10 randomly generated trajectories ($M = 10$), the best combination corresponds to the maximal value of the $C_{10}^{4} = 210$ values of the root mean square distance D, defined as:

$$D_{1,2,3,4} = \sqrt{\frac{d_{12}^2 + d_{13}^2 + d_{14}^2 + d_{23}^2 + d_{24}^2 + d_{34}^2}{6}}$$

The improvement due to the use of the "Campolongo" sampling strategy instead of the original strategy of Morris has been highlighted (Campolongo et al., 2007) by comparing the empirical distributions for 4 inputs parameters obtained after the selection of 20 trajectories among a very high number of generated trajectories (500 to 1000).

Morris (1991) and Campolongo et al. (2007) provide some guidance to define the parameters p, Δ and r. It has been judged as convenient to fix the parameter p to an even value and Δ to $\frac{p}{2*(p-1)}$. Of course, the size of the sample of trajectories, r, is linked to the value of p since. If p has a high value, a high number of trajectories is needed to explore a sufficient number of points within the considered p-level grid.

Saltelli et al. (2008) mention that the following values have proved to produce valuable results: $p = 4$, $\Delta = 2/3$ and $r = 10$ to 20. These values of the parameters will be used in the following.

3.1.4. Implementation of the Method

The implementation of the enhanced Morris method has been made on MATLAB (2009) and includes the following steps.

Construction of the M random trajectories

The enhanced design of Morris is based on the construction of M random trajectories with the key property that, within each of them, two consecutive points differ in only one component by $\pm\Delta$.

Morris (1991) proposes the following formula for the *(k+1)-by-k* dimensional orientation matrices *B** including the values of the *k* parameters for the *k+1* points of a given trajectory.

$$B = \left[J_{k+1,1}x^* + \left(\frac{\Delta}{2}\right)\left(\left(2B - J_{k+1,k}\right)D^* + J_{k+1,k}\right)\right]P^*$$

Where

- x^* is a random point of the parametric space Ω whose components belong to the set $\left\{0, \frac{1}{p-1}, \ldots, 1-\Delta\right\}$;
- $J_{i,j}$ is a unitary *i-by-j* matrix;
- *B* is a strictly lower *(k+1)-by-k* rectangular unitary matrix;
- *D* is a *k-by-k* diagonal matrix in which each diagonal element is either 1 or -1;
- *P* is a *k-by-k* random permutation matrix in which each row and column contain one element equal to 1 (the other ones being equal to 0).

Calculation of the C_M^r values of the root mean square distance D

A brute force approach (consisting in generating all the possible combinations and comparing two-by-two) is used to compute the values of D and allow for the selection of the best trajectories (Campolongo et al., 2007). The C_M^r of the root mean square distance *D* defined above are computed for all the possible combinations of *r* trajectories out of the *M* randomly generated trajectories.

The main drawback of this implementation relies on the use of the brute force method to solve the combinatorial optimization problem of finding the best combination of trajectories. Indeed, values of M = 100 and r = 10 lead to 1.7E13 values of D.

Recovery of the r best trajectories

The combination of *r* trajectories corresponding to the maximal value of *D* is selected.

Going from the unit hypercube to the orthotope of the real parametric space

The unit hyper-cube used to design the sampling is then converted into the hyper-rectangle corresponding to the real parametric space by dilatation, contraction or translation according to the imposed variation ranges of all the parameters.

Computation of the sensitivity measures μ, μ^* and σ

For each of the *r*(k+1)* simulation run, the elementary effect value (*EE*) is computed for each considered output (e.g. annual whole-building electricity consumption…etc) using the following equation:

$$EE = \frac{\dfrac{\Delta OP}{\Delta IP}}{(IP_{max} - IP_{min})}$$

The values of *EE* are stored in an *r-by-k* matrix in order to allow computing the previously defined sensitivity measures for the *k* parameters on the available sample of *r* values.

3.2. PARAMETERS AND OUTPUTS SELECTION

The general procedure used by Lam and Hui (1996) is used in the present study. It includes:

- Describing a base case reference;
- Identifying parameters of interest and ranges of variation;
- Determining what simulation outputs are to be investigated;
- Introducing perturbations to the selected parameters;
- Studying the corresponding effects of the perturbations;
- Expressing the sensitivity for each parameter.

As the present sensitivity analysis is performed in view of a calibration method, a careful selection of the considered parameters and outputs has to be done.

The outputs to investigate are the factors which are commonly encountered and essential to perform good quality model calibration. So, it has been decided to study impact of the selected input variables on the outputs that are directly used to check the validity of the calibration (i.e. energy billing data) and on the intermediate heating and cooling loads (generally unknown during the calibration process) in order to see if the set of influential parameters is the same for both global consumptions and intermediate loads.

So, the following outputs will be considered during the sensitivity analysis described below:

- annual and monthly whole-building peak and off-peak electricity consumption (in kWh);
- annual and monthly fuel oil/natural gas consumption (in kWh);
- annual and monthly whole-building annual heating and cooling demands (in kWh);
- Electricity, heating and cooling peak loads (in kW).

4. APPLICATION OF THE MORRIS METHOD

4.1. BASE CASE BUILDINGS DESCRIPTION

Studied input variables can be classified into three main groups (Lam and Hui, 1996): building characteristics (including construction characteristics), HVAC system performance and building use (internal loads, occupancy, system control and operation). Building location (Uccle, Belgium) and orientation (Table 1), weather data (TMY Uccle weather data provided by IWEC), building geometry and basic HVAC system configuration will be considered as fixed (i.e. known) for both base case buildings.

Table 1: Base case buildings general characteristics

	BC1	**BC2**
Location	Uccle (Belgium)	
Climate	Energy Plus IWEC	
Latitude	50.8° N	
Longitude	4.333 °E	
Main orientation	N/S	E/W
Building footprint	36 x 25 = 900 m²	75 x 12 = 900 m²
Number of storeys	10	5
Ceiling height	3 m	

Both base case buildings have been defined in order to be representative of the actual building stock. The geometry, as well as the floor area distribution and the envelope and HVAC system characteristics have been fixed based on field observations made on medium-size office buildings case studies (Andre et al., 2010) and on survey data collected for Flemish office buildings (BBRI, 2001) in order to obtain realistic energy use behavior.

4.1.1. Geometry

In a first step, two building types and two types of HVAC systems have been considered. Figure 7 shows a typical floor of each building type:

- BC1 building has a double corridor “core-peripheral” configuration on 10 floors for a total net floor area of 9000 m² (Table 2). Offices are located in peripheral zones. Central zones are storages/archives and meeting rooms. Circulations include stairs and elevators.
- BC2 building has a single corridor configuration on 5 floors (for a total net floor area of 4500 m²) with offices on the two main facades only.

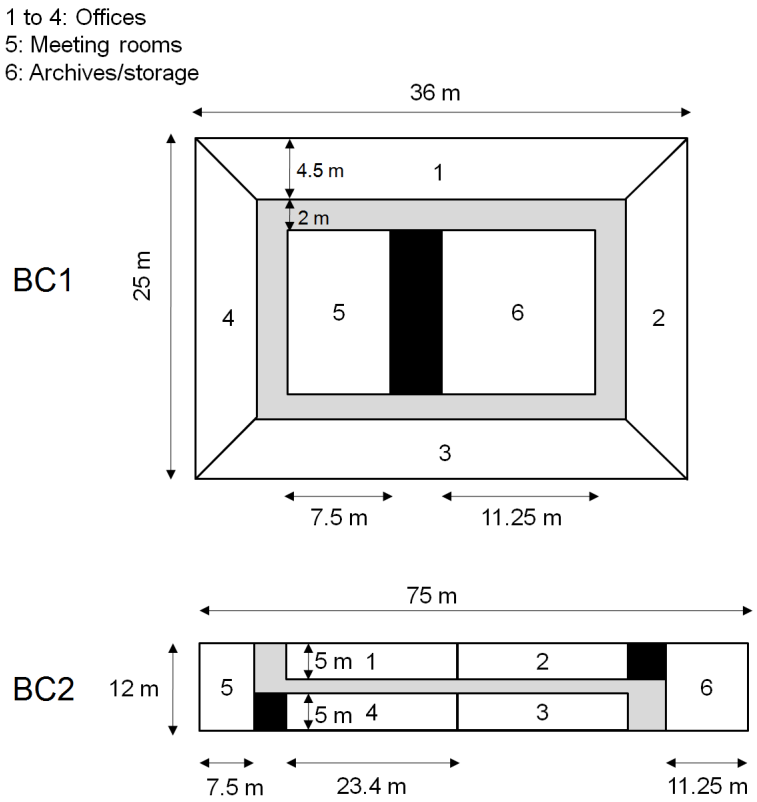

Figure 7: Building Types BC1 and BC2

Table 2: Base case buildings floor area distribution

Type	Use	BC1		BC2	
		Floor surface area (m²)	% of total	Floor surface area (m²)	% of total
Usable floor area	Offices	4680	52	2340	52
	Meeting	900	10	450	10
Functional floor area	Archives/Storage/Print	1350	15	675	15
	Other (no AC)	510	5.67	236.25	5.25
Circulations		1560	17.33	798.75	17.75
Net floor area		9000	100	4500	100

4.1.2. Envelope

The main envelope characteristics are given in Table 3. Base case values of the various input variables have been determined according to available guidelines and standards (ASHRAE, 2009, ISO13790:2007, Hauglustaine and Simon., 2006).

Table 3: Base case buildings envelope and environmental characteristics

Building characteristic	Value
Window-to-Wall ratio	0.5
Frame-to-Window ratio	0.1
Opaque walls U-value	1 W/m²-K
Roof slab U-value	0.6 W/m²-K
Glazing U-value	2.83 W/m²-K
Normal SHGC	0.75
Frame U-value	2.3 W/m²-K
Specific thermal mass	165 kJ/m²-K
Infiltration rate (night only)	0.4 ACH
Exfiltration rate (operating hours)	0.1 ACH
Walls emissivity	0.9
Walls absorbance	0.6
Outdoor combined heat transfer coef.	23 W/m²-K
Indoor radiation heat transfer coef.	5.13 W/m²-K
Indoor convective heat transfer coef.	3.16 W/m²-K
Ground albedo	0.2

4.1.3. Internal loads and building operation

Internal loads densities and operation profiles have been selected according to ASHRAE (2009) and based on rule of thumb values (Table 4 and Table 5).

Table 4: Base case buildings internal loads

Load	Density
Occupants density – Offices	12.5 m²/occ
Occupants density – Meeting	2.5 m²/occ
Occupants – Metabolic rate	1.2 met (50% convective)
Lighting Power Density – Offices	12 W/m² (40% convective)
Lighting Power Density – Meeting	14 W/m² (40% convective)
Lighting Power Density – Archives	9 W/m² (40% convective)
Lighting Power Density – Circulations	6 W/m² (40% convective)
Lighting Power Density – Other	10 W/m² (40% convective)
Plug Loads Density – Offices	10 W/m² (75% convective)
Plug Loads Density – Meeting	10 W/m² (75% convective)

Table 5: Base case buildings - operation profiles

Item	Schedule
HVAC system operation time	7:00 – 21:00
Maximal occupancy rate – Offices	75%
Maximal occupancy rate – Meeting	50%
Minimal occupancy rate	0%
Occupants presence time – Offices	8:00-18:00
Occupants presence time – Meeting	14:00-17:00
Minimal lighting rate – Offices/Meeting	10%

Minimal plug-loads rate – Offices/Meeting	10%

As proposed by Reddy and Maor (2006), occupancy and operation/use schedules are defined by the four values given in Figure 8. The A and B values represent the day-time and night-time operation rates respectively. The night-time rate is maintained constant during the weekend too. The parameter C represents the day-time operation in hours per day, centred on noon. The last parameter (D) corresponds to a time shift (in hours) with respect to noon. In the present study, HVAC system operation is supposed to be set within the BEMS, independently from the occupancy. Lighting and appliances gains in offices and meeting rooms are supposed to be directly related to the occupancy, except for the night-time rate which represents the fraction of appliances/lighting fixtures which are not switched off at the end of the day.

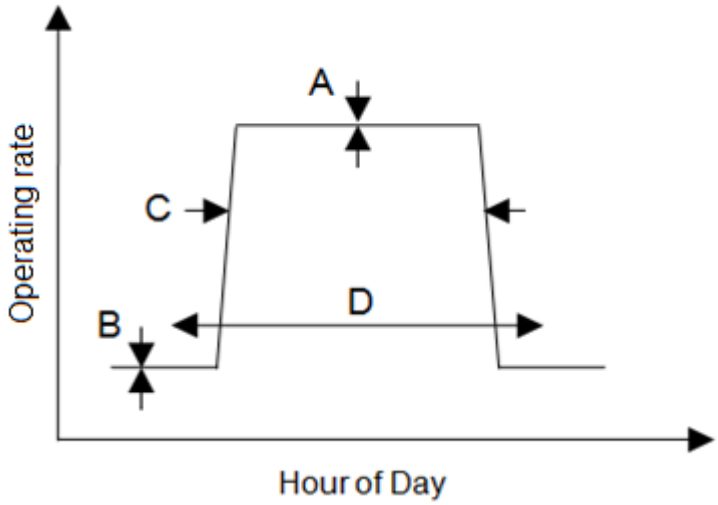

Figure 8: Typical operation/use schedule

4.1.4. HVAC System

Two arbitrary types of HVAC systems have been considered:

- CAV system + Fan Coil Units (FCU) = AHU (heating, cooling and adiabatic humidification) + Terminal unit (heating and cooling fan coil units)
- VAV system + Terminal Reheat = AHU (with air economizer, heating, cooling and electrical steam humidification) + (water) Terminal reheat boxes

Hot water production is ensured by a natural gas boiler in both cases. Chilled water production is ensured by a large plant composed of water cooled screw chillers and indirect contact cooling towers in BC1. A scroll air cooled chiller ensures chilled water production in BC2 (Table 6).

Temperature, humidity and ventilation needs have been determined according to recent standards and guidelines (EN15251:2007, ASHRAE, 2008). HVAC components performance has been defined based on typical performance data (Eurovent, 2001, ASHRAE 90.1, 2007, EN15316:2006).

Table 6: Base case buildings HVAC system main characteristics

Building case	1	2
HVAC system type	VAV + terminal reheat	CAV + fan coil units
Heating indoor setpoints	16/21 °C – 50%	16/21 °C – 50%
Cooling indoor setpoints	24°C	24°C
Maximal ventilation rate – Offices	15 ACH	1.2

Minimal ventilation rate – Offices	3 ACH[1]	1.2 (45 m³/h/occ)
Maximal ventilation rate – Meeting	6 ACH	4
Minimal ventilation rate – Meeting	4 ACH	4 (30 m³/h/occ)
Maximal ventilation rate – Archives	5 ACH	1
Minimal ventilation rate – Archives	1 ACH	1
Humidification system efficiency	85 % (electrical steam generator)	85 % (adiabatic)
Nominal specific fan power	1625 W/m³/s	1625 W/m³/s
Fan drive efficiency	75 %	75 %
Supply air temperature at 5°C outdoor	18°C	18°C
Supply air temperature at 15°C outdoor	14°C	18°C
Boiler type	Natural gas boiler (forced draught)	
nominal efficiency	90%	90%
Boiler standby losses	1%	1%
Chiller type	Water cooled screw chiller	Air cooled scroll chiller
Chiller nominal EER	4	2.5
Hot water pump specific power	300 W/l/s	300 W/l/s
Chilled water pump specific power	350 W/l/s	350 W/l/s
Condenser pump specific power	300 W/l/s	-
Hot water network thermal losses	3%	3%
Chilled water network thermal losses	3%	3%

4.2. BASECASE ENERGY USE

The energy consumptions computed for the two base case buildings are given below. As expected, the base cases considered in the present work are characterized by very typical energy performance and end-use (Figure 9), in good accordance with values available in the literature (Adnot et al., 2007; Perez-Lombard et al., 2008). Annual electricity (WBE: Whole-Building Electricity) and natural gas (WBG: Whole-Building Gas) consumptions (Table 7) are very similar to sector average values in Belgium (between 70 and 150 kWh/m²/yr of fuel/gas and electricity; BBRI, 2001).

Table 7: Base case buildings energy use

	BC1		**BC2**	
	WBE	**WBG**	**WBE**	**WBG**
	kWh	kWh	kWh	kWh
Jan	115361	206962	25158	109871
Feb	109186	174675	22081	94082
Mar	105223	135202	24484	73757
Apr	91306	97212	24873	51430
May	86942	57673	27874	30807
June	75172	36511	30627	10720
July	74520	39190	29104	12457
Aug	81847	39385	31358	10935
Sep	66938	38638	26673	10265
Oct	70210	88974	25084	41411
Nov	92626	158722	23783	83482

[1] Due to technical limits, the inferior boundary for the minimal flow rate corresponds to 20% of the maximal flow rate

Dec	107826	209145	23821	111692
Total [kWh/m²]	**120**	**143**	**70**	**142**

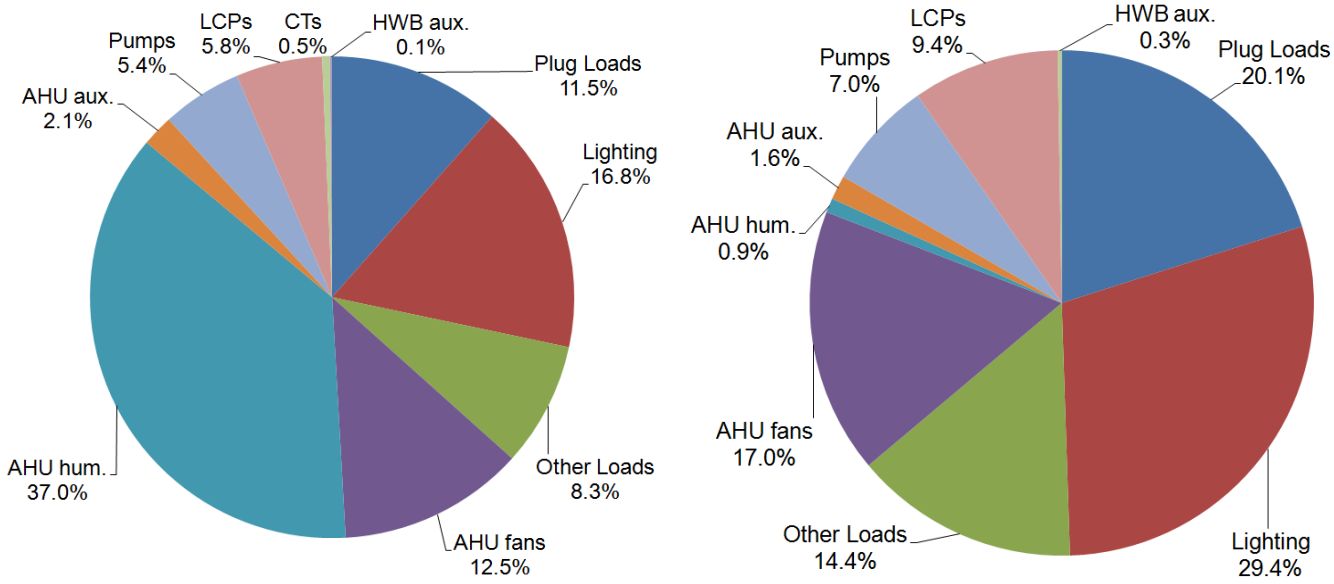

Figure 9: Whole Building Electricity Consumption Disaggregation (BC1 & 2)

Computed gas and electricity signatures also show typical patterns (Figure 10). For the first base case building, the use of electrical steam humidification leads to an electricity signature with a negative slope. The slope of the electricity signature of the second base case is slightly positive due to the operation of the liquid chilling packages in summer.

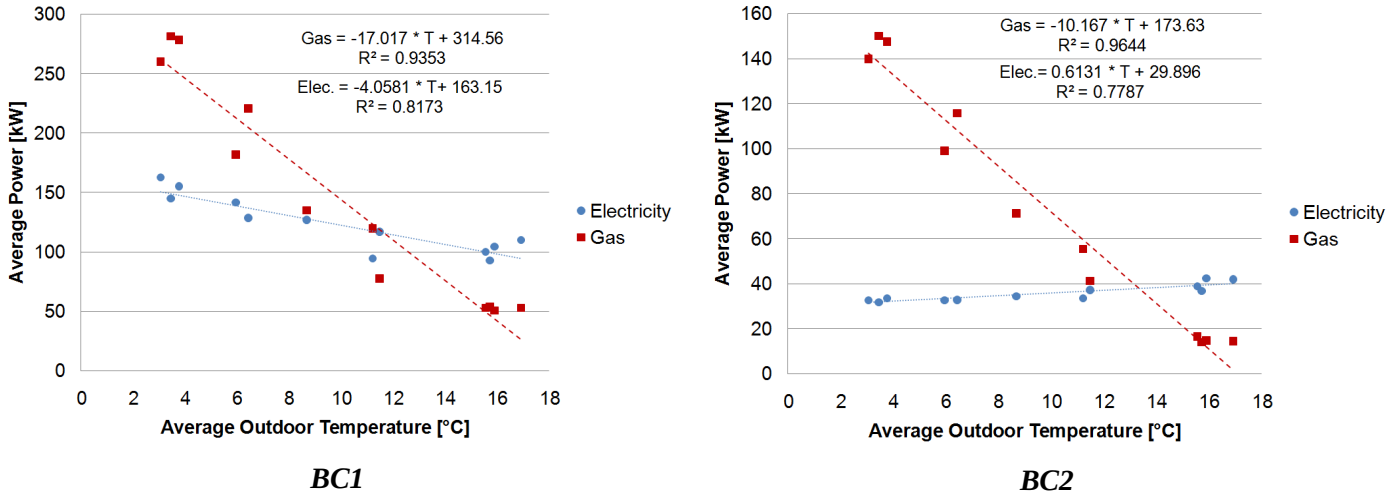

Figure 10: Gas and Electricity Signatures (BC1 & 2)

4.3. *RANGES OF VARIATION*

More than fifty parameters will be considered for the present sensitivity analysis. This set of parameters includes parameters usually considered for calibration (such as walls U-value and main HVAC equipments performance and schedules) as well as parameters characterized by an important uncertainty (surface heat transfer coefficients, albedo...). Since the two configurations are supposed to be known, the climate, the geometry of the building and the composition of the HVAC system do not vary.

As shown in Table 8, some of the parameters have been normalized in order to be able to use the same variation matrix for both building cases and sensitivity methods (e.g. P5: relative walls U-value).

The ranges of variations for the considered parameters are given in Table 8. These ranges have been defined according to the information available in the literature. In this preliminary sensitivity analysis, extremely wide variation ranges (e.g. albedo between 0.05 and 0.9) are used in order to cover most of the possible cases and to lead to the most generic conclusions.

Parameters #1 to #15 are characteristics of the building it-self (envelope physical characteristics and air-tightness) and of the location of the building (albedo). In order to evaluate their influence, combined heat transfer coefficients are considered as parameters in this sensitivity study and are not computed by means of the empirical correlations mentioned in Chapter 2. Parameters #16 to #22 are related to the use of the two buildings (occupancy and internal gains). Parameters #23 to #27 include temperature, humidity and ventilation setpoints and describe the comfort level of the buildings. Parameters #28 to #43 correspond to the nominal performance of the HVAC components. Parameters #44 to #52 deal with the operation/use of the considered buildings. In the present cases, lighting and appliances loads during occupancy hours are supposed to be directly related to the occupancy rate (parameters #46 and #47).

Table 8: Ranges of variation for the parameters considered for SA

#	Variable	Description	Unit	Min	Max	Reference
1	$h_{out,m}$	Outdoor combined surface heat transfer coef.(massive walls)	W/m²-K	16.7	33.3	ASHRAE 2009
2	$h_{out,wd}$	Outdoor combined surface heat transfer coef. (windows)	W/m²-K	16.7	33.3	ASHRAE 2009
3	$h_{r,i}$	Indoor radiation heat transfer coef.	W/m²-K	0.57	4.56	ASHRAE 2009; IEA-BESTEST 1995
4	$h_{c,i}$	Indoor convective heat transfer coefficient	W/m²-K	1.57	3.73	ASHRAE 2009; IEA-BESTEST 1995
5	k_{Um}[2]	Massive walls U-value multiplication factor	-	0.2	1.8	Hauglustaine, 2006
6	U_{gl}	Glazings U-value	W/m²-K	1	5.9	Hauglustaine, 2006
7	$SHGC_0$	Glazings Solar Heat Gain Coef.	-	0.13	0.86	ASHRAE 2009
8	p_{SHGC}	Solar Heat Gain Coef. exponent	-	2.37	4.06	ASHRAE 2009
9	U_{fr}	Windows frame U-value	W/m²-K	1.8	6	Hauglustaine, 2006
10	$k_{\varepsilon,ir}$[3]	Walls emissivity multiplication factor	-	0.95	1.05	Lomas and Eppel 1992
11	k_{α}[4]	Walls absorbance multiplication factor	-	0.75	1.25	Lomas and Eppel 1992
12	C_{m/m^2}	Specific thermal mass	J/m²-K	80000	370000	ISO13790
13	Albedo	Ground albedo	-	0.05	0.9	Lomas and Eppel 1992
14	ACH_{inf}	Infiltration rate	ACH	0.1	0.8	ASHRAE
15	X_{exfil}	Exfiltrated fraction of supply ventilation flow	-	0	0.2	Estimation

[2] Multiplication factor used to vary the value of the parameter in the same proportion for the different zones
[3] Multiplication factor used to vary the value of the parameter in the same proportion for the different zones
[4] Multiplication factor used to vary the value of the parameter in the same proportion for the different zones

16	$k_{IGFR,light}$[5]	Lighting density multiplication factor	-	0.75	1.25	ASHRAE 2009
17	$k_{IGFR,appl}$[6]	Appliances density multiplication factor	-	0.5	1.5	ASHRAE 2009
18	$k_{m^2,occ}$[7]	Occupancy density multiplication factor	-	0.8	1.2	EN15251
19	Met_{occ}	Occupants metabolic rate	met	1	2.1	ASHRAE 2009
20	$f_{c,light}$	Lighting gain convective fraction	-	0.1	0.6	ASHRAE 2009
21	$f_{c,appl}$	Appliances gain convective fraction	-	0.6	1	ASHRAE 2009
22	$f_{c,occ}$	Occupancy gain convective fraction	-	0.4	0.8	ASHRAE 2009
23	$T_{i,set,h,occ}$	Indoor heating setpoint temperature	C	21	23	EN15251; ASHRAE 2007
24	$T_{i,set,h,nocc}$	Indoor heating setpoint temperature (non-occupancy hours)	C	16	18	EN15251; ASHRAE 2007
25	$T_{i,set,c,occ}$	Indoor cooling setpoint temperature	C	23	25	EN15251; ASHRAE 2007
26	RH_{min}	Indoor humidification setpoint	-	0.3	0.5	ASHRAE 2007
27	$k_{ACH,out}$	Air renewal rate multiplication factor	-	0.5	1.5	EN15251
28	$\varepsilon_{hum,n}$	Humidifier efficiency	-	0.75	0.95	Estimation
29	$\eta_{drive,fan,n}$	Ventilation fans drive efficiency	-	0.5	0.86	EN13779
30	SFP_{fan}	Ventilation fans specific power	W/m³-s	500	4500	EN13779
31	$T_{a,ex,AHU,set,max}$	Supply air temperature setpoint (winter)	°C	18	22	Energie Plus RW
32	$T_{a,ex,AHU,set,min}$	Supply air temperature setpoint (summer)	°C	12	16	Energie Plus RW
33	$T_{hw,max}$	Hot water temperature setpoint	°C	60	80	Energie Plus RW
34	$\eta_{hwboiler,n}$	Hot water boiler nominal efficiency	-	0.8	0.97	EN15316
35	$f_{hwboiler,sbloss}$	Hot water boiler standby losses factor	-	0.005	0.02	EN15316
36	$T_{cw,min}$	Chilled water temperature setpoint	C	7	10	Estimation
37	$k_{EER,chiller,n}$[8]	Chiller nominal EER multiplication factor	-	0.75	1.25	Eurovent 2011
38	SPP_{hw}	Hot water pumps specific power	W/kg/s	200	400	ASHRAE 90.1
39	SPP_{cw}	Chilled water pumps specific power	W/kg/s	250	450	ASHRAE 90.1
40	SPP_{cd}	Condenser water pumps specific power	W/kg/s	200	400	ASHRAE 90.1
41	SPP_{ct}	Cooling tower water pumps specific power	W/kg/s	200	400	ASHRAE 90.1
42	f_{hloss}	Hot water network loss factor	-	0.01	0.05	Estimation
43	f_{closs}	Chilled water network loss factor	-	0.01	0.05	Estimation
44	$C_{sched,AHU}$	AHU daily operation time	h/day	12	15	Estimation
45	$C_{sched,set}$	H&C system daily operation time	h/day	12	15	Estimation
46	$k_{A,sched,occ}$[9]	Occupancy rate multiplication factor	-	0.667	1.333	Estimation
47	$C_{sched,occ}$	Daily occupancy time	h/day	8	11	Estimation
48	$B_{sched,light}$	Lighting operation rate (night time)	-	0	0.2	Estimation
49	$B_{sched,appl}$	Appliances operation rate (night time)	-	0	0.2	Estimation
50	$A_{sched,addload}$	Additional loads operation rate (day-time)	-	0.5	1	Estimation
51	$B_{sched,addload}$	Additional loads operation rate (night-time)	-	0	0.5	Estimation
52	$C_{sched,addload}$	Additional loads daily operation rate	h/day	12	15	Estimation

4.4. RESULTS

The variations of the selected outputs computed by applying the DSA method are studied in terms of influence coefficient (IC; Lam et al., 2008) and also displayed as bar charts (Lomas and Heppel,

[5] Multiplication factor used to vary the value of the parameter in the same proportion for the different zones
[6] Multiplication factor used to vary the value of the parameter in the same proportion for the different zones
[7] Multiplication factor used to vary the value of the parameter in the same proportion for the different zones
[8] Multiplication factor used to vary the value of the parameter in the same proportion for the different chillers
[9] Multiplication factor used to vary the value of the parameter in the same proportion for the different zones

1992). The results of the Morris method will be studied using the three sensitivity measures described above (μ, μ* and σ).

The parameters of the Morris method were fixed as proposed by Saltelli et al. (2008): r=10 to 20 and p=4. Two samples of 10 trajectories (r=10) and one sample of 20 trajectories (r=20) have been generated and used to perform the analysis. The three sets of results were found similar and only the last one is detailed below (r=20). This confirms a fair adjustment of the value of r to the imposed value of p.

4.4.1. DSA Method

The influence coefficient (IC) used to analyze the results of the DSA method has been defined in order to provide normalized results (in %/%):

$$IC = \frac{\frac{\Delta OP}{OP_{bc}}}{\frac{\Delta IP}{IP_{bc}}}$$

The influence of temperature setpoints (#23, #24, #25, #31, #32, #33 and #36) cannot be expressed in %/% and are given in %/K:

$$IC_{temp} = \frac{\frac{\Delta OP}{OP_{bc}}}{\Delta IP}$$

4.4.1.1. Base Case Nr 1

The main results provided by the DSA method for BC1 are shown below (Figure 11).

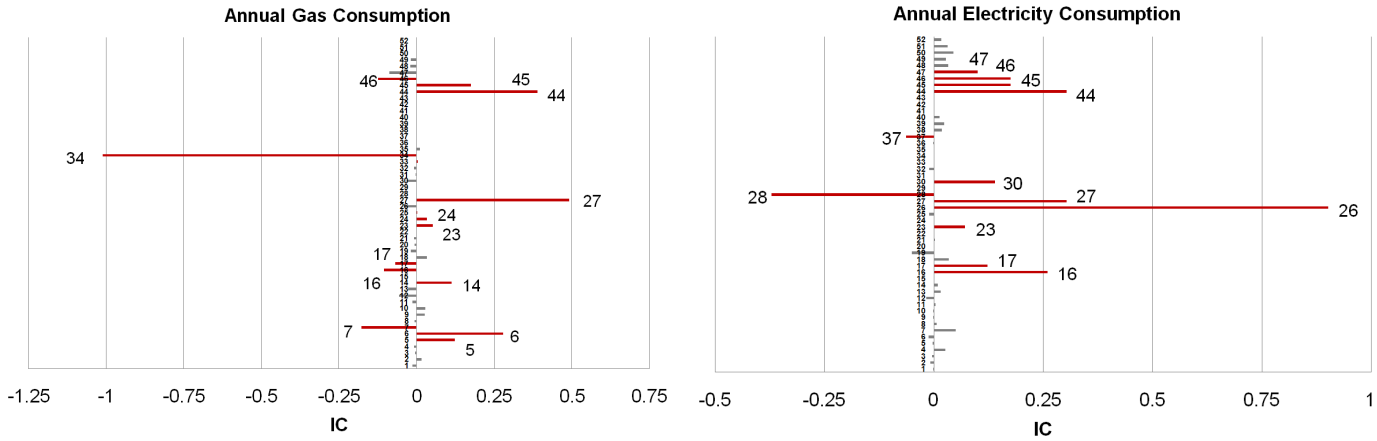

Figure 11: DSA results for BC1

As expected, the whole building gas consumption is directly influenced by the main envelope characteristics (#5, #6, #7 and #14). Indoor temperature, humidity and ventilation setpoints and schedules have also a direct influence on the annual gas consumption (#23, #24, #27, #44 and #45). The most influential parameter is the hot water boiler efficiency (#34). Due to its link with the internal heat gains, the occupancy rate has also a direct influence on the heating demand (#46).

Because of the important ventilation rates and the use of electrical steam humidification, humidifier and ventilation system setpoints (#26 and #27), performance (#28 and #30) and schedules (#44 and #45) have a major influence on the electricity consumption. Internal gains densities and schedules

have also a direct impact on the whole-building electricity consumption (#16, #17, #46 and #47). The heating temperature setpoint has also a non-negligible impact on the electricity consumption. This effect could be explained by the physical link existing between the relative humidity level (and so, the humidification needs) and the temperature of the indoor air.

4.4.1.2. Base Case Nr 2

The main results provided by the DSA method for BC2 are shown below (Figure 12).

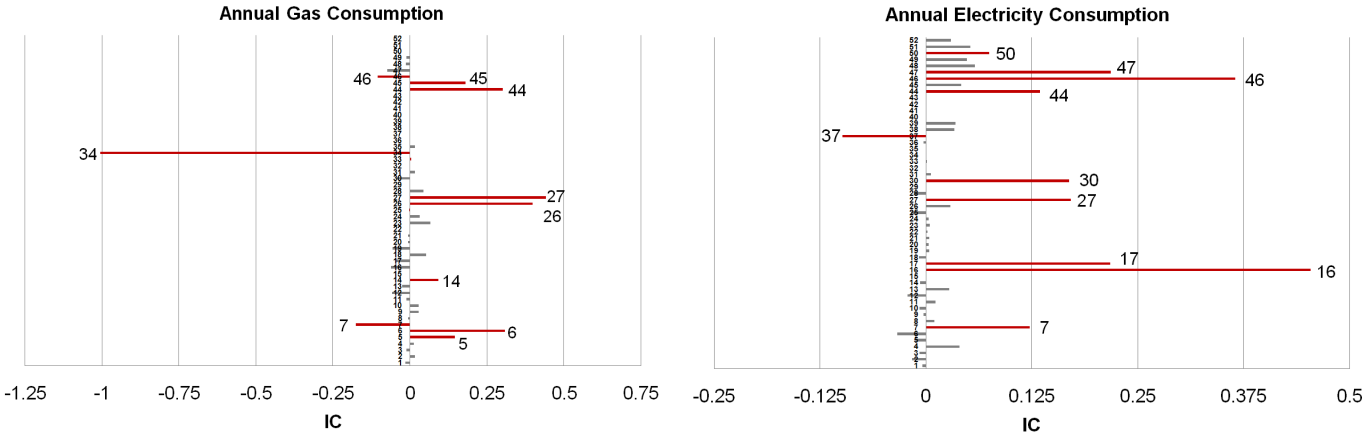

Figure 12: DSA results for BC2

Influences noticed for BC2 are similar to the ones observed for BC1. The main difference is related to the HVAC system configuration: due to the use of adiabatic humidification system, the humidification system performance (#28) and setpoint (#26) no longer influence the electricity consumption in an important manner but have an impact on the natural gas consumption.

4.4.2. Morris Method

4.4.2.1. Base Case Nr 1

The results of the Morris method for the annual gas consumption are plotted in Figure 13. The Morris method confirms the first list of influential parameters evidenced by means of the DSA method. However, additional parameters, previously considered as less influential, are also highlighted.

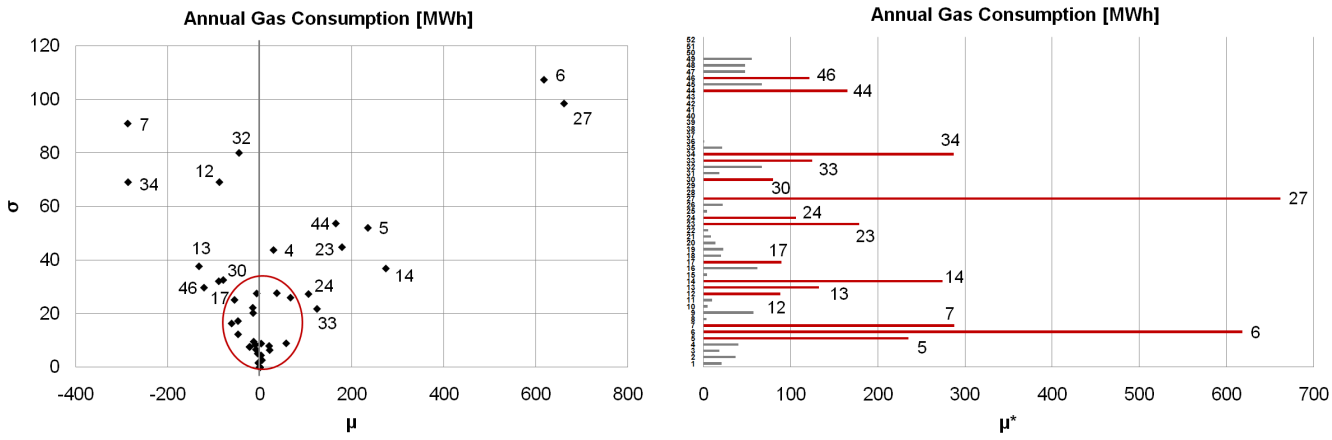

Figure 13: Morris results for BC1 - Gas consumption

The results shown in Figure 13 clearly show that the use of the sensitivity measure μ* is convenient when trying to identify the important factors out of a set of parameters.

As already shown by the DSA method, walls thermal characteristics (#5, #6 and #7) have an important influence. The infiltration rate (#14) has also a considerable impact on the gas consumption. In addition to those parameters, the present method also highlights the building thermal mass (#12) and the ground albedo (#13) as important parameters.

Indoor temperature, humidity and ventilation setpoints and schedules have once again a direct influence on the annual gas consumption (#23, #24, #27 and #44).

The (σ, μ) plot is also of a great help for identifying interactions and non-linearity. It appears the most influential parameters (high values of μ*, #6, #7, #27 and #34) are characterized by the highest values of standard deviation (σ). This appears more clearly in Figure 14 where most of the parameters lies around a straight line what demonstrates that there is a link between the level of influence of a parameter and its involvement in the curvature effects. It is also important to note that none of the influential parameters have purely linear effect on the outputs since the standard deviation is always strictly positive.

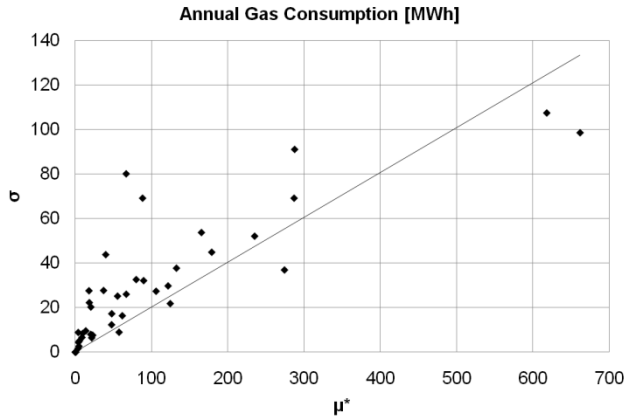

Figure 14: Morris results for BC1 - Gas consumption - (σ, μ*) plane

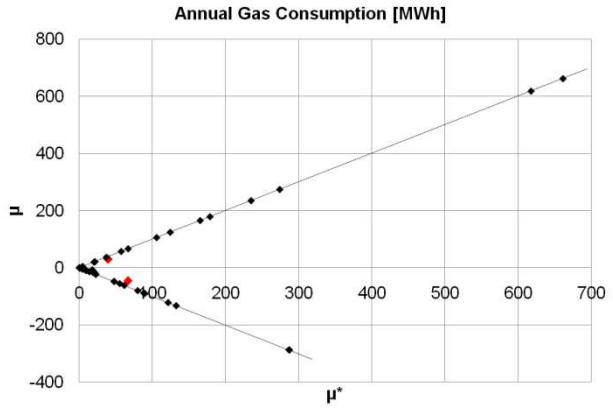

Figure 15: Morris results for BC1 - Gas consumption - (μ, μ*) plane

Parameters #4 (indoor convective coefficients) and #32 (minimal supply air temperature) have reduced average impact (small μ and μ* values) but higher standard deviation values. This indicates that these two parameters can have important effects in some particular situations. It is also interesting to note that these two parameters are involved in non-monotonic effects since their values of μ and μ* are significantly different (red points in Figure 15). All the other parameters (including the most influential ones) are characterized by a monotonic behavior in the considered experimental plan.

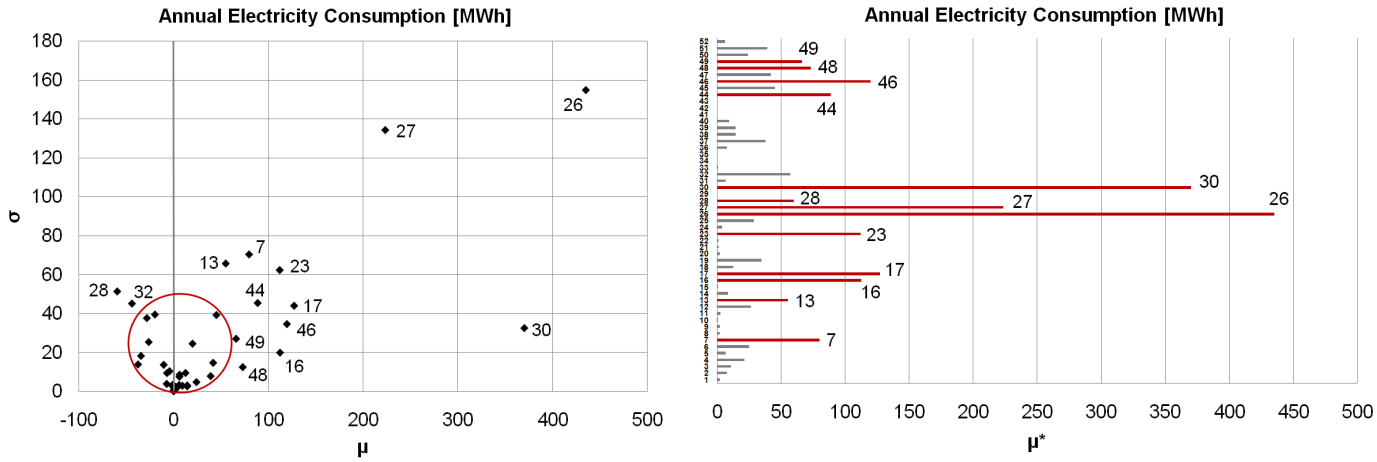

Figure 16: Morris results for BC1 - Electricity consumption

When studying the variations of the whole-building electricity consumption, the trends identified by means of the DSA method are again reproduced (Figure 16):

- Humidifier and ventilation system setpoints (#26 and #27), performance (#28 and #30) and schedules (#44 and #45) are among the most influential parameters
- Internal gains densities and schedules have also a direct impact on the whole-building electricity consumption (#16, #17 and #46)
- The indoor heating temperature setpoint (#23) has an impact on the electricity consumption due to its influence on the humidification needs.

Comparing to the results of the DSA method, additional parameters can be added to the list of the influential parameters:

- The solar heat gain coefficient (#7) and the ground albedo (#13) have direct impacts on the electricity consumption due to their effect on the calculation of solar gains,
- Night-time operation rates of lighting fixtures and electrical appliances (#48 and #49) have a non-negligible impact on the global electricity consumption.

It is interesting to check if the parameters influencing the most the final energy consumptions have a similar effect on the intermediate heating and cooling demands.

Since the natural gas consumption is directly related to the hot water use, simulation results for gas and hot water demands are very similar (Figure 17). Of course, the only differences rely with the characteristics of the distribution and production system which has no influence on the hot water demand.

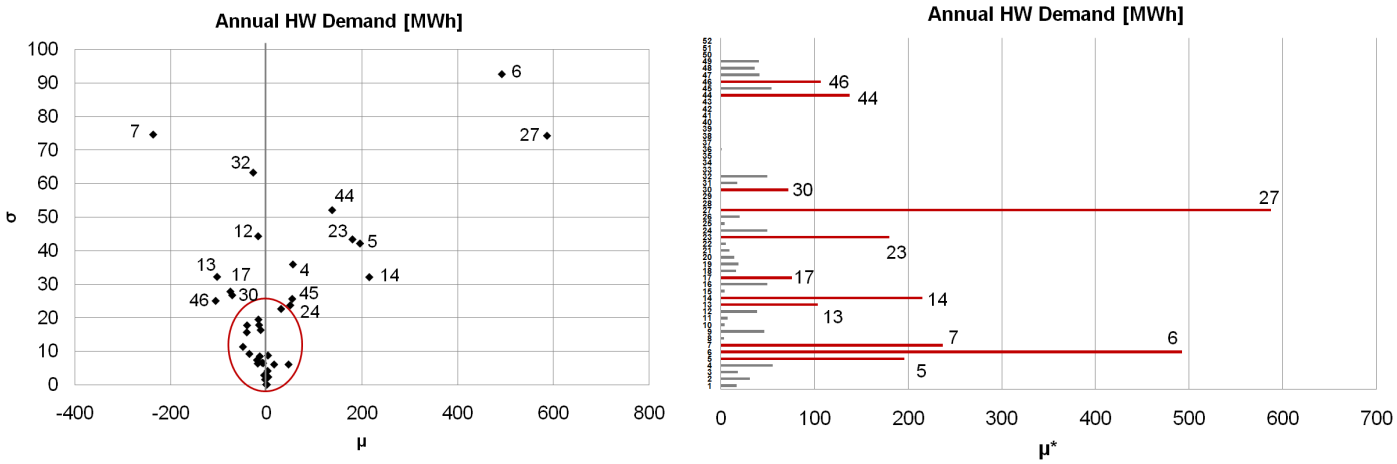

Figure 17: Morris results for BC1 – Hot water demand

It is believed that the situation can be significantly different when looking at the chilled water demand. Indeed, since the relative importance of the chilled water production system is quite limited (chiller consumption is about 6% of the whole-building electricity consumption), once can expect that some important influences have not appeared when looking at the final energy consumption.

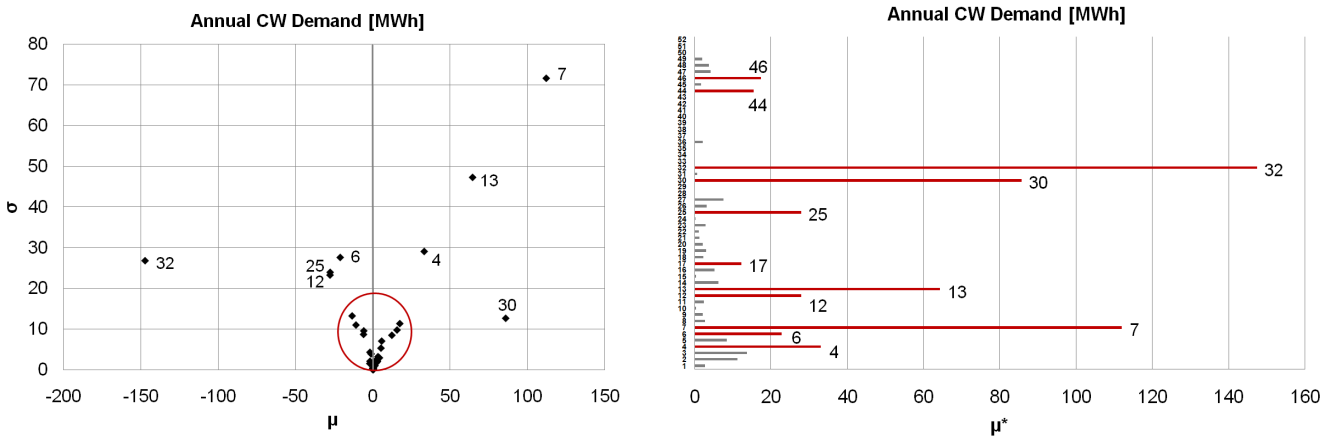

Figure 18: Morris results for BC1 – Chilled water demand

While the impact of the parameters #7 and #13 on the solar gains (and so, on the cooling load) was already identified by looking at the whole-building electricity consumption, this is not true for all the parameters influencing the chilled water demand (Figure 18).

Indeed, it appears that some envelope characteristics (such as walls U-values, #5 and #6) have a direct impact on the chilled water consumption but only a reduced impact on the whole-building electricity consumption. Looking specifically to the chilled water consumption allows also to highlight the impact of the building thermal mass (#12), indoor cooling temperature setpoint (#25) and supply air temperature summer setpoint (#32).

4.4.2.2. Base Case Nr 2

As observed with the DSA, the results for both cases are very similar and the main differences rely on the fact that the HVAC system configuration is different between BC1 (electrical steam humidifier) and BC2 (adiabatic humidifier). In other words, the sensitivity to the parameters related to the humidification of the indoor air (#26: humidity setpoint, #28: humidifier efficiency and #24: indoor air temperature setpoint in a second time) is "transferred" from the electricity consumption to the "natural gas consumption".

Except this fact, most of observations made for BC1 are still valid, as shown in Figure 19, Figure 20, Figure 21 and Figure 22.

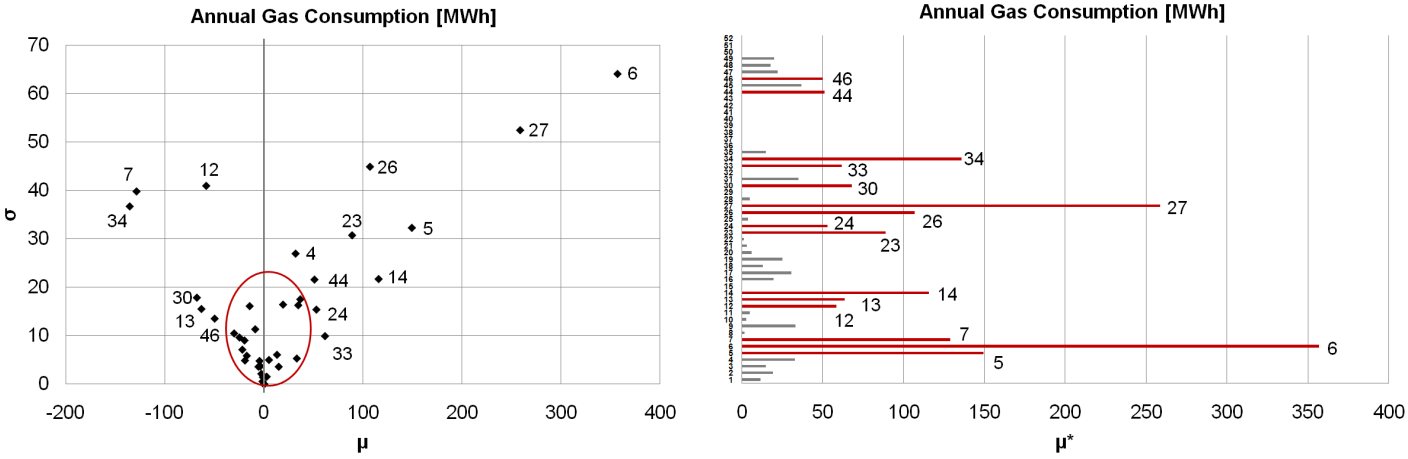

Figure 19: Morris results for BC2 - Gas consumption

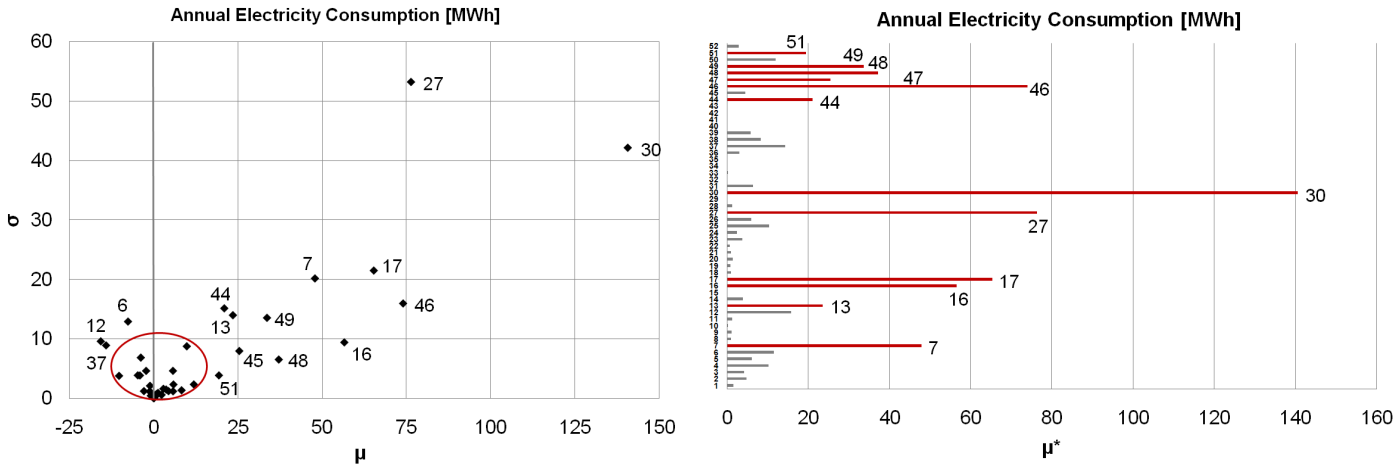

Figure 20: Morris results for BC2 - Electricity consumption

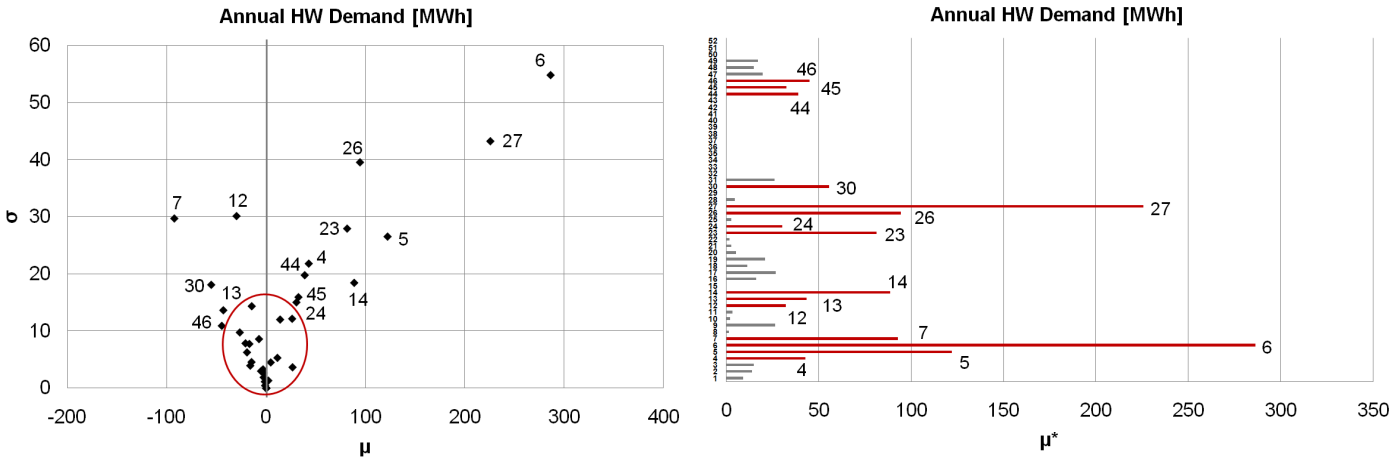

Figure 21: Morris results for BC2 – Hot water demand

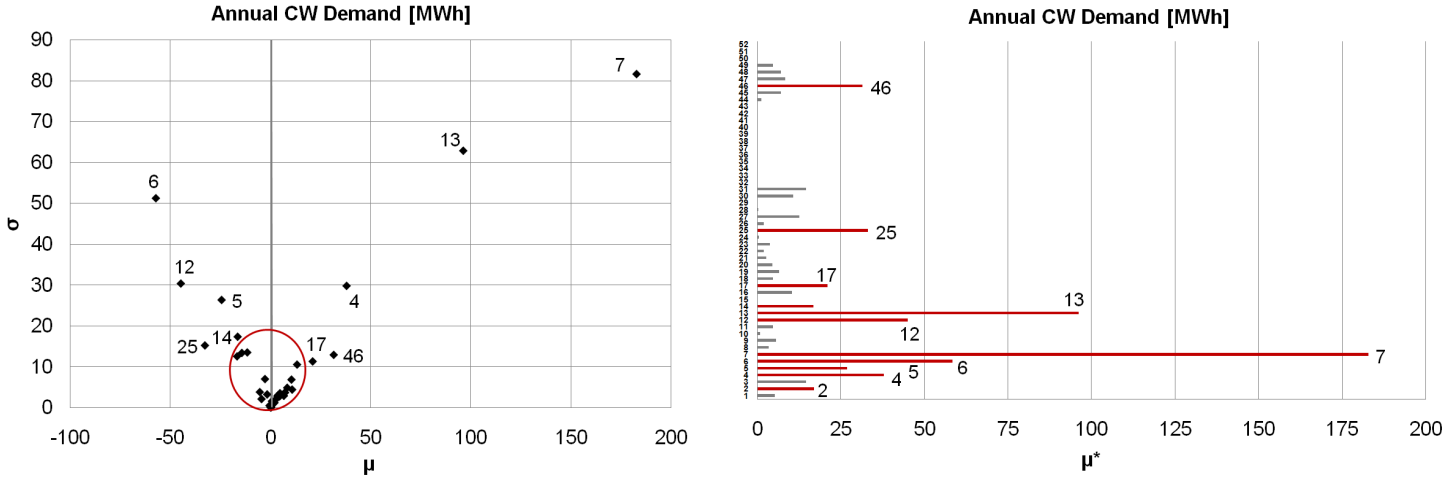

Figure 22: Morris results for BC2 – Chilled water demand

5. SENSITIVITY AND UNCERTAINTY ISSUES IN THE CALIBRATION PROCESS

As discussed before, during an energy service process, complementary data on the building under study can be progressively obtained by means of as-built data analysis, site inspections, energy management staff interviews, spot or short-term measurements... Progressing in data collection and in

the analysis of the building allows narrowing the probable range of variations of the parameters to be calibrated.

The example presented hereunder illustrates how sensitivity and uncertainty issues can be addressed in the frame of a calibration process. Probable ("reasonable") ranges of variations have been arbitrary set for a series of 19 parameters considered for adjustment in order to represent an intermediate step in a given calibration process (Table 9).

5.1. *EXAMPLE OF PRELIMINARY SENSITIVITY ANALYSIS*

Table 9: Ranges of variation for considered parameters

#	Variable	Unit		Min	Max
1	U_hopw	W/m²-K	Vertical walls	0.8	1.2
		W/m²-K	Roof slab	0.48	0.72
2	**U_gl_w**	**W/m²-K**		**0.68**	**5.9**
3	**SHGC_gl_0**	**-**		**0.13**	**0.86**
4	**p_SHGC**	**-**		**2.37**	**4.06**
5	C_mm2_user	J/m²-K		115500	214500
6	ACH_inf_user	-		0.2	0.6
7	IGFR_light	W/m²	Offices	9	15
		W/m²	Meeting	10.5	17.5
		W/m²	Storage	6.75	11.25
8	IGFR_appl	W/m²		7.5	12.5
9	t_i_set_h_occ	°C		19	23
10	t_i_set_c_occ	°C		22	26
11	RH_min	-		0.4	0.6
12	ACH_vent	-	Offices	1.08	1.32
		-	Meeting	3.6	4.4
		-	Storage	0.9	1.1
13	SFP_sufan	W/m³-s		1218.75	2031.25
14	eta_hwb_n	-		0.828	0.972
15	EER_lcp_n	-		2.125	2.875
16	C_sched_AHU	h		13	16
17	C_sched_set	h		13	16
18	C_sched_light	h		9	12
19	C_sched_appl	h		9	12

The present example is based on the second building case presented above (BC2) and focuses on the calibration of the building model parameters related to glazing:

- Parameter #2: The glazing U-value in W/m²-K
- Parameter #3: The glazing normal solar heat gain coefficient ($SHGC_0$)
- Parameter #4: The glazing solar heat gain coefficient angular dependency coefficient (p_{SHGC})

While the data collection progresses, more detailed information are made available about the characteristics of the glazing and it is possible to narrow the ranges of variation of the parameters #2,

#3 and #4. The values given in Table 10 are based on the glazing data library available in ASHRAE (2009).

Table 10: Levels of investigation of glazing type

Step	Glazing type	U-value (W/m^2-K)	$SHGC_0$	p_{SHGC}
A	Unknown	0.68 – 5.9	0.13 – 0.86	2.37 – 4.06
B	Double glazing	1.26 – 3.12	0.13 – 0.76	2.52 – 3.89
C	Double glazing 3-12.7-3 (air)	1.7 – 2.73	0.41 – 0.76	2.98 – 3.34
D	Double glazing 3-12.7-3 (air) + low-e coating	1.7 – 1.99	0.41 – 0.7	2.98 – 3.13
E	Exact glazing type: 21c3 (ASHRAE, 2009)	1.82 +/- 5%	0.6 +/- 5%	3.13 +/- 5%

Initially, no information is available on the glazing type (step A) and large ranges of variations are used in order to cover all the possibilities (from single to high performance triple glazing systems). Progressively, as more detailed information is collected about the glazing type (e.g. by means of on-site inspections), ranges of variations are narrowed (steps B to D). The final variation range (step E) corresponds to the final estimation of the glazing characteristics based on the data provided by the glazing manufacturer. These last values include an arbitrary uncertainty range that will be considered for studying uncertainty issues on the predicted results (i.e. 5% in the present case).

In order to illustrate how sensitivity issues can be handled in the frame of a calibration process, the Morris method will be applied five times with the ranges of variation given in Table 10. The ranges of variation the other parameters will be maintained constant (Table 9). A sample of 10 Morris trajectories has been judged as sufficient and used to limit the number of simulation runs to 200.

Since two different Morris samples are randomly generated, two application of the Morris sampling method can lead to different values of the Elementary Effects. Even if different tests have shown that the main conclusion stay true (i.e. hierarchy of influential and non-influential parameters), different results make direct comparison difficult. Therefore, to allow highlighting effects of the ranges of variation and of interactions between parameters in a univocal way, a unique Morris unitary orientation matrix (or hypercube) has been generated and adapted to the varying ranges of variation given in Table 10.

Figure 23 shows the results for the step A. Reference numbers of the parameters correspond to the list given in Table 9.

As expected, results are similar to the ones obtained previously even if the variation ranges have been narrowed. Two of the three parameters related to the characteristics of glazing appear as highly influential. This can be explained the large variation ranges considered at this stage (step A). The angular dependency of the SHGC does not seem to be an influential parameter and the adjustment of this parameter is not crucial.

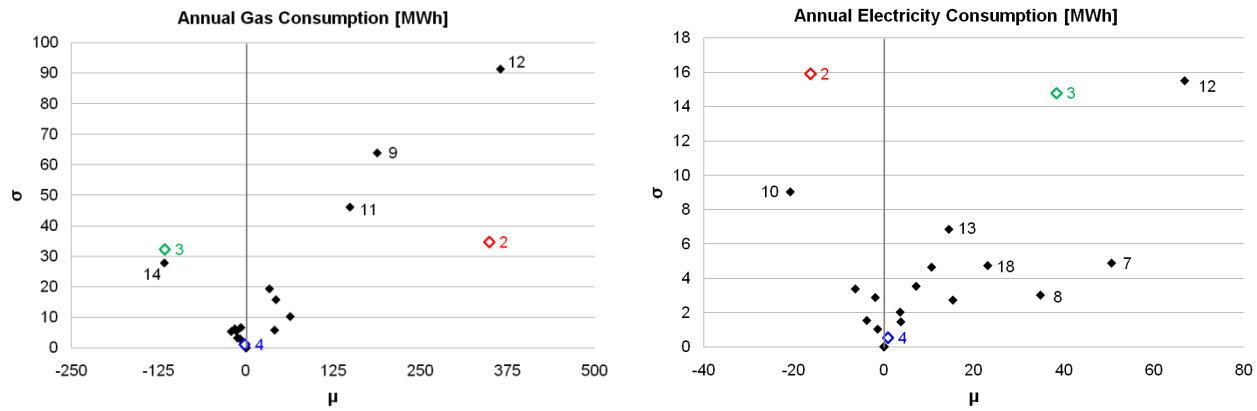

Figure 23: Morris method results - step A

Figure 24 shows the results of the Morris method in the (σ, μ) plan for the five steps detailed in Table 10. As expected, narrowing the range of variation leads to a decrease of the effect of the considered parameters in terms of both σ and μ values. It appears that few parameters (#9, #10, #12 and #14) seem to be involved in interactions with the parameters related to glazing characteristics. When looking at the effects on the annual electricity consumption, the most important interaction is the one with the indoor temperature cooling setpoint (#10). Despite of the identified interactions, it is interesting to notice that, in the present case, the results of the initial screening (Figure 23) stay valid and that the other parameters are not displaced in the (σ, μ) plan in an important manner.

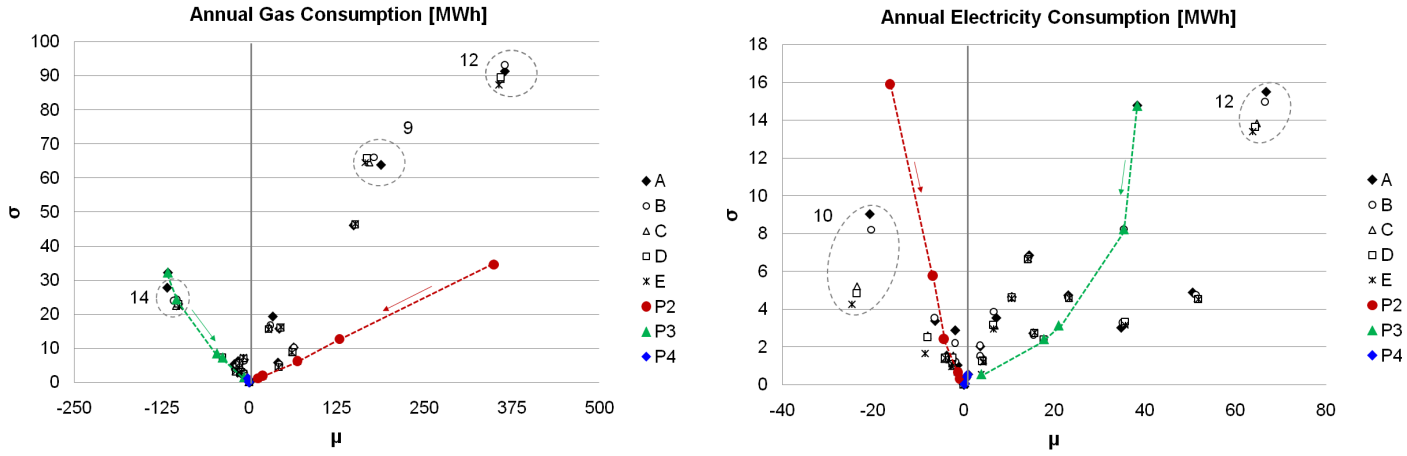

Figure 24: Morris method results - steps A to E

Once the glazing type is known and the corresponding parameters are adjusted, the user can focus on another influential parameter such as the ventilation rate (#12) or the indoor temperature cooling setpoint (#10).

5.2. POST-CALIBRATION UNCERTAINTY ANALYSIS

As proposed above, at the "end" of the calibration process, when all the most influential parameters are judged as satisfactorily adjusted, the updated uncertainty ranges can be used to perform a global uncertainty analysis and to quantify the potential error on the energy consumptions and demands predicted by the calibrated model. Two types of uncertainties can be distinguished:

- Uncertainty on the predicted performance resulting from the approximation errors induced by the model itself.
- Uncertainty on the predicted performance resulting from the uncertainties/errors on the identified input data.

The first type of uncertainty can be estimated during a validation process where the accuracy of the model is analyzed by means of perfectly known parameters and the corresponding reference output values.

At the present stage, in the frame of a calibration process, the model is considered as a reference (able to accurately represent the considered situation) and the uncertainty analysis is dedicated to the quantification of the second type of uncertainty. In other words, the computed uncertainty corresponds to the effect of propagation of uncertainties on the parameters.

Of course, specifying uncertainty on a given parameters is often arbitrary and the estimation of the uncertainty range has to be based on user's experience, measurement device accuracy, etc.

In the present work, it has been decided to use the Latin Hypercube Monte Carlo (LHMC) sampling (Figure 25). This method has the advantage that large amounts of uncertainties can be represented with relatively small samples (and so limited computational expense).

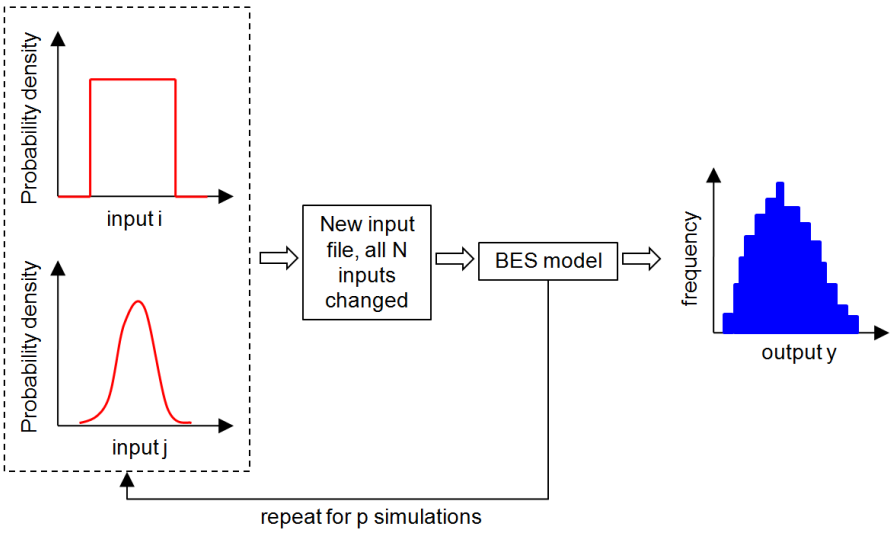

Figure 25: LHMC sampling

In the LHMC method, the sample size depends on the accuracy of the output standard deviation. Figure 26 shows the evolution of the standard deviation of computed annual gas and electricity consumptions as a function of the size of the Monte Carlo Analysis (MCA) sample. Lomas and Eppel (1992) state that only marginal improvements in accuracy can be achieved after 60 to 80 simulations, independently of the number of variables/uncertainties considered for the analysis. In the present case, increasing the size of the sample from 80 to 100 runs, cause variations of the standard deviation of less than 5% for both considered outputs. Variations are less than 1% when increasing the size of the sample from 100 to 200 runs. Based on this analysis, the size of the sample has been set to 100 runs.

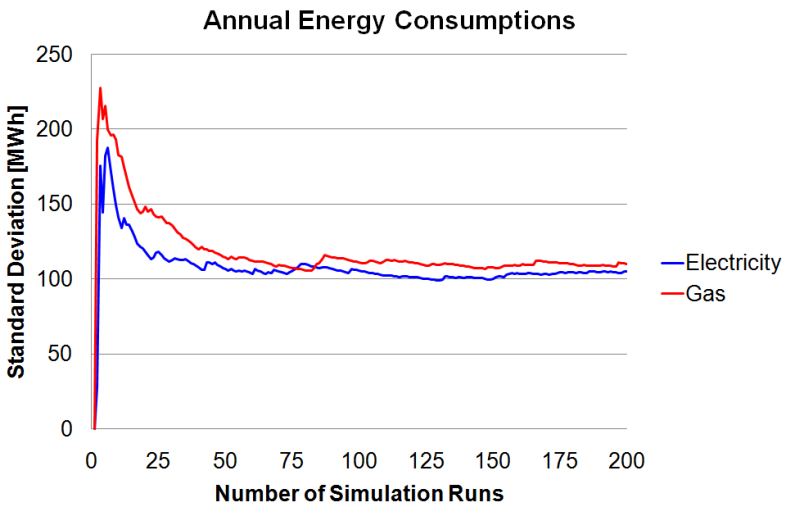

Figure 26: Accuracy assessment – Relationship between Standard Deviation and number of Monte Carlo Simulations

Normal or uniform probability density functions can be used in the present implementation. However, since the set up of the uncertainty range and the selection of the probability distribution is generally arbitrary, it is proposed to use uniform distributions and consider the estimated uncertainty range to fix the boundaries of the distribution of each parameter.

Example of uncertainty ranges for monthly gas and electricity consumptions are shown in Figure 27. Blue bars represent the mean value while the dotted lines represent the min/max intervals for the considered sample.

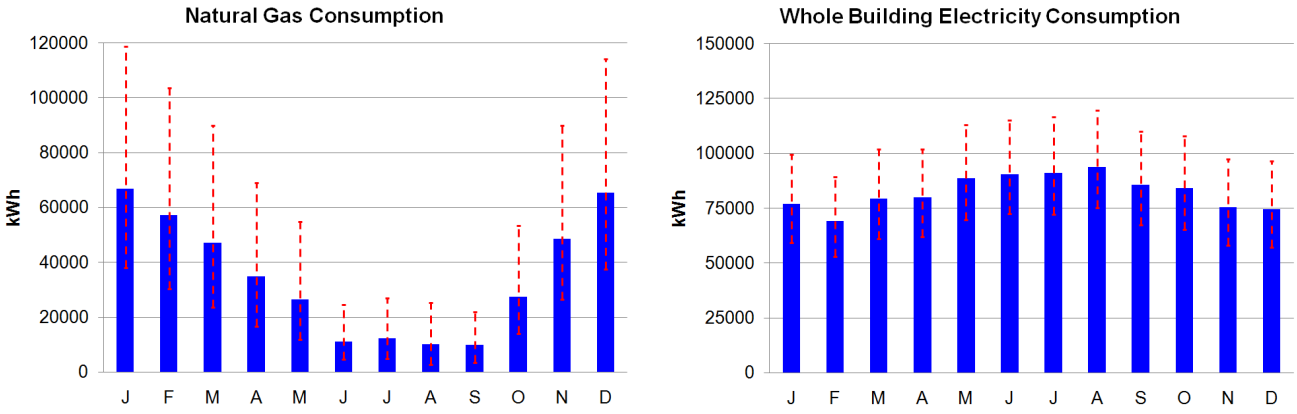

Figure 27: Uncertainty on computed monthly gas and electricity consumptions for BC-2

6. CONCLUSION

Major influences have been highlighted by the DSA method but it is delicate to consider these results as representative since they do not take into account the non-linearities of the model. Even if the model is not highly non-linear, the interaction effects have to be characterized in order to provide good guidance for calibration. Moreover, the IC defined above and usually used to characterize the results of a DSA analysis do not allow for a direct comparison between the influences of all the parameters: temperature parameters and others have to be studied separately. To this end, the (global) Morris sensitivity analysis method has been applied to the two considered cases.

All the parameters highlighted by the DSA method have been identified as influential by the Morris method and both methods provide similar results. However, the Morris method was able to highlight additional influences and to characterize interactions between parameters. For the considered cases and range of variations, interactions (high-order effects) were non-negligible.

The results of the sensitivity analyzes detailed above are in good accordance with expectations and results generally encountered in the literature (e.g. Westphal and Lamberts, 2005). Natural gas consumption is directly related to all the parameters influencing the heating demand of the building (walls thermal characteristics, air renewal rate and indoor setpoints). As expected, the electricity consumption is mainly influenced by the parameters related to the main electricity consumers: internal gains densities (lighting and appliances) and HVAC system performance. Depending on the type of humidification system, humidifier performance and setpoints can influence either gas or electricity consumptions. **Behavioral issues have also been highlighted as influential parameters**. Occupant's use of artificial lighting and appliances has a direct effect on final energy consumptions. It is fair to assume that behavioural issues may have more complex and intensive effects in buildings equipped with manual shading systems or allowing windows opening, etc.

While **natural gas consumption is generally a good representation of the heating needs of the building** (no major difference was observed between the variations of gas consumption and hot water demand), the previous analysis confirms that **the electricity consumption is a too global index to allow clear distinction of all the influences and to analyze the impact of some parameters on the cooling demand**.

The results of the present sensitivity analyzes should not be taken directly as general conclusions or guidance for calibration since the results described above could be case specific and not necessarily representative of the whole building stock. Numerous additional simulation runs, for various building cases, sets of parameters and variation ranges would be necessary to provide exhaustive conclusions about model sensitivity. However, interesting points related to sensitivity and calibration issues have been highlighted:

- The considered variation ranges are quite wide and can lead to a high dispersion of the results (i.e. artificially high values of σ and μ). Indeed, the effect of ground albedo (#13) or indoor convective heat transfer coefficient (#4) on the results is certainly artificially increased due to the wide variation ranges considered for these two parameters. However, it is interesting to consider that, **despite the fairly wide variation range considered for the analysis, some parameters have very little influence on final and intermediate energy demands (e.g. outdoor combined heat transfer coefficients, internal gains radiation-convective split, walls absorbance…)**. For the targeted work (energy use analysis), such parameters should certainly not been considered as a priority when

proceeding to calibration and could be ignored during further parameters adjustment works[10].

- Since the results of the Morris method are highly dependent of the selected ranges of variation, **it is recommended to pay a special attention to the selection of parameters to vary and to the corresponding range of variations when proceeding to sensitivity analysis as a pre-requisite of a calibration process**. These range of variations should represent the actual "probability range" (or "confidence interval") for the considered parameter.
- **Interactions between influential parameters could make the calibration process more complex**. It has been shown that the adjustment of a given parameter can modify the impact that other parameters have on the model outputs. Ideally, the sensitivity analysis should be run as soon as a variation range is adapted during the calibration process. This would allow updating the ranking of influential parameters and characterizing the interactions between them at every time. However, in practice, it is not realistic to run such sensitivity analysis an important number of times for each parameter. This would lead to perform thousands of simulation runs and would lengthen the calibration process in an unacceptable way. Moreover, despite of the interactions highlighted above, it is fair to believe that **the "hierarchy" between influential and non-influential parameters is quite stable** when adjusting progressively a parameter (i.e. narrowing its range) and that the top of the ranking stays valid. It is so recommended to perform a new screening with updated variation ranges after having adjusted some of the most influential parameters (e.g. the 5 first parameters by order of influence).

  These non-linearities of the model also make difficult the application of any local automated adjustment method to such a large set of parameters. Indeed, a too early "blind" iterative adjustment of a given parameter could lead to erroneous value and bad calibration because of such interactions. This confirms that the notion of "hierarchy" between the sources of information is also a crucial issue when adjusting the value of a given parameter. **It is believed that blind adjustment of the parameter has to be considered as a last resort, when the probability ranges of the most influential parameters have already been narrowed. To this end other adjustment possibilities based on reliable sources of information (inspection, interviews, surveys, measurements…) have to be considered in priority.**
- In the frame of a calibration process, in order to make the best use of the commonly available data (monthly energy bills), it would be interesting to express the results of such sensitivity analysis in terms of seasonal consumptions/demands. Moreover, a separated analysis of the variations of both peak-hours and offpeak-hours electricity consumptions would also allow fully exploiting the available information. Such issues will be studied when applying the proposed calibration methodology to a synthetic and a real building case.

Finally, it has been shown how the final estimated probability ranges of each parameter can be used to run a global uncertainty analysis. The LHMC sampling method has been used in order to allow accurate quantification of the uncertainty on the predicted energy consumptions.

[10] In the frame of more specific studies (such as local comfort analysis and modeling), the influence of indoor convective and radiation heat transfer coefficients is important and should not be neglected.

7. REFERENCES

Adnot, J. et al. 2007. Field benchmarking and Market development for Audit methods in Air Conditioning (AUDITAC) final report.

Andre, P., Fabry, B., Bertagnolio, S., Franck, P.Y. 2010. Development of an Evidence-Based Calibration Methodology Dedicated to Energy Audit of Office Buildings. Part 2: Application to a typical office building in Belgium. Proceedings of the 10th REHVA World Congress Clima 2010, Antalya, Turkey. Available at: http://hdl.handle.net/2268/10874

ASHRAE. 1994. Predicting Hourly Building Energy Use – The Great Energy Predictor Shootout. J.Haberl, editor, ASHRAE Technical Data Bulletin, Vol. 10, No. 5.

ASHRAE. 2002. ASHRAE Guideline: Measurement of energy and demand savings. ASHRAE Guideline 14-2002.

ASHRAE. 2007. ANSI/ASHRAE/IESNA Standard 90.1-2007, Energy Standard for Buildings Except Low-Rise Residential Buildings. Atlanta: American Society of Heating, Refrigerating and Air-Conditioning Engineers, Inc.

ASHRAE, 2008. Handbook HVAC Systems and Equipment. Atlanta: American Society of Heating, Refrigerating and Air-Conditioning Engineers, Inc.

ASHRAE, 2009. Handbook Fundamentals. Atlanta: American Society of Heating, Refrigerating and Air-Conditioning Engineers, Inc.

BBRI. 2001. Kantoor2000: Study of Energy Use and Indoor Climate in Office Buildings.

Campolongo, F., Cariboni, J., Saltelli, A., Schoutens, W. 2004. Enhancing the Morris Method. Proceedings of the 4th International Conference on Sensitivity Analysis of Model Output, Santa Fe, NM.

Corrado, V., Eddine Mechri, H. 2009. Uncertainty and Sensitivity Analysis for Building Energy Rating. Journal of Building Physics, 33(2), pp. 125-156.

Corson, G.C. 1992. Input-Output sensitivity of building energy simulations. ASHRAE Transactions. 98(2): 618-626.

De Wit, M.S. 1997. Identification of the Important Parameters in Thermal Building Simulation Models. Journal of Statistical Computation and Simulation, 57:1-4, pp. 305-320.

De Wit, S., Augenbroe, G. 2002. Analysis of Uncertainty in Building Design Evaluations and its Implications. Energy and Buildings, 34, pp. 951-958.

Diamond, S.C., Hunn, B.D., Cappiello, C.C. 1985. The DOE-2 validation. ASHRAE Journal 27(11): 22-32.

EN15251:2007. Indoor environmental input parameters for design and assessment of energy performance of buildings addressing indoor air quality, thermal environment, lighting and acoustics. International Standard Organization, Geneve, Suisse

EN 15316-4-1:2006. Heating systems in Buildings – Method for calculation of system energy requirements and system efficiencies – Part 4.1: Space heating generation systems, combustion systems. International Standard Organization, Geneve, Suisse

Eurovent. 2011. Eurovent certification database. Available at : http://www.eurovent-certification.com/

Hauglustaine, J.M., Simon, F. 2006. La conception globale de l'enveloppe et l'énergie. Guide pratique pour les architectes. Ministère de la Région Wallone, Belgium.

Heiselberg, P., Brohus, H. 2007. Application of Sensitivity Analysis in Design of Sustainable Buildings. Proceedings of the International Conference on Sustainable Development in Building and Environment, Chongqing, China.

ISO/FDIS 13790:2007. Energy performance of buildings – Calculation of energy use for space heating and cooling. International Standard Organization, Geneve, Suisse

Lam, J.C., Hui, S.C. 1996. Sensitivity analysis of energy performance of office buildings. Building and Environment, Vol. 31, No. 1, pp. 27-39.

Lam, J.C., Wan, K.K., Yang, L. 2008. Sensitivity analysis and energy conservation measure implications. Energy conversion and management, Vol. 49, pp. 3170-3177.

Lomas, K.J., Eppel, H. 1992. Sensitivity analysis techniques for building thermal simulation programs. Energy and Buildings, Vol. 19, pp. 21-44.

MATLAB, 2009. Matlab user manual, The Mathworks Inc., http://www.mathworks.com, Natick, USA.

Mottillo, M. 2001. Sensitivity analysis of energy simulation by building type. ASHRAE Transactions. 107(2): 722-732.

Morris, M. 1991. Factorial Sampling Plans for Preliminary Computational Experiments. Technometrics 33(2), pp. 161-174.

Perez-Lombard, L., Ortiz, J., Pout, C. 2008. A review on buildings energy consumption information. Energy and Buildings 40, 394-398.

Reddy, T.A., Maor, I. 2006. Procedures for reconciling computer-calculated results with measured energy data. ASHRAE Research Project 1051-RP. Atlanta: American Society of Heating, Refrigerating and Air-Conditioning Engineers, Inc.

Roujol, S., Fleury, E., Marchio, D., Millet, J.R., Stabat, P. 2003. Testing the energy simulation building model of Consoclim using Bestest method and experimental data. Proceedings of the eighth International IBPSA conference, Eindhoven, Netherlands.

Saltelli, A., Ratto, M., Andres, T., Campolongo, F., Cariboni, J., Gatelli, D., Saisana, M. and Tarantola, S. 2008. Global Sensitivity Analysis. The Primer. John Wiley & Sons, New York, USA.

Saltelli, A., Annoni, P. 2010. How to Avoid Perfunctory Sensitivity Analysis. Environmental Modelling & Software, 25, pp. 1508-1517.

Westphal, F.S., Lamberts, R. 2005. Building Simulation Calibration using Sensitivity Analysis. Proceedings of the 9th IBPSA Building Simulation Conference, Montréal, Canada.

CHAPTER 5 ASSESSMENT OF THE CALIBRATION METHOD USING A VIRTUAL TEST BED

CHAPTER 5: ASSESSMENT OF THE CALIBRATION METHOD USING A VIRTUAL TEST BED 2
1. INTRODUCTION 2
2. VIRTUAL CALIBRATION TEST BED (VCTB) 4
2.1. Base Case Building 4
2.2. Building model 4
2.3. Lighting, Appliances and Occupancy Gains 7
2.4. Secondary HVAC System Model and Control 9
2.5. Primary HVAC System Model 11
3. SYNTHETIC DATA 13
4. APPLICATION OF THE CALIBRATION METHODOLOGY 17
4.1. Data Collection and Calibration Levels 17
4.2. Calibration Process 19
5. CONCLUSION 46
6. REFERENCES 50
7. APPENDIX 52
7.1. Walls Composition 52
7.2. Building Floor Geometry 52
7.3. Fan Coil Unit Simulation Model 52
7.4. Air Handling Unit Simulation Model 54
7.5. Chilled and Hot water Pumps 54
7.6. Level 3a – Identified Internal Loads Operating Profiles 54

CHAPTER 5: ASSESSMENT OF THE CALIBRATION METHOD USING A VIRTUAL TEST BED

1. INTRODUCTION

The assessment of a calibration method is very different of simulation model validation process. In the frame of simulation model (comparative) validation (Figure 1), the complete set of inputs and parameters is known beforehand and used to set the values of the inputs/parameters of the reference model (assumed to be valid and validated) and of the simplified model (to be calibrated). Simulation results are then compared in order to assess the accuracy of the simplified model.

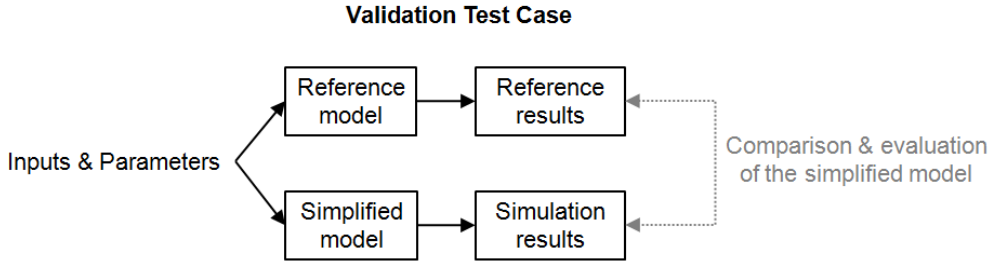

Figure 1: Typical comparative simulation model validation process

The assessment of calibration methods is generally achieved by means of a synthetic building case (Figure 2) or a real building case. **The use of real building cases in order to evaluate the robustness of a calibration process is a complex problem. Since the "true" solution is not known beforehand and can only be approached by means of numerous and detailed measurements, only a partial assessment of the calibration process is possible**. Indeed, the satisfaction of an arbitrary criterion does not necessarily guarantee the robustness and the accuracy of the method. Moreover, in the case of operated/occupied building, many variables cannot be controlled and/or measured (occupancy, infiltration…).

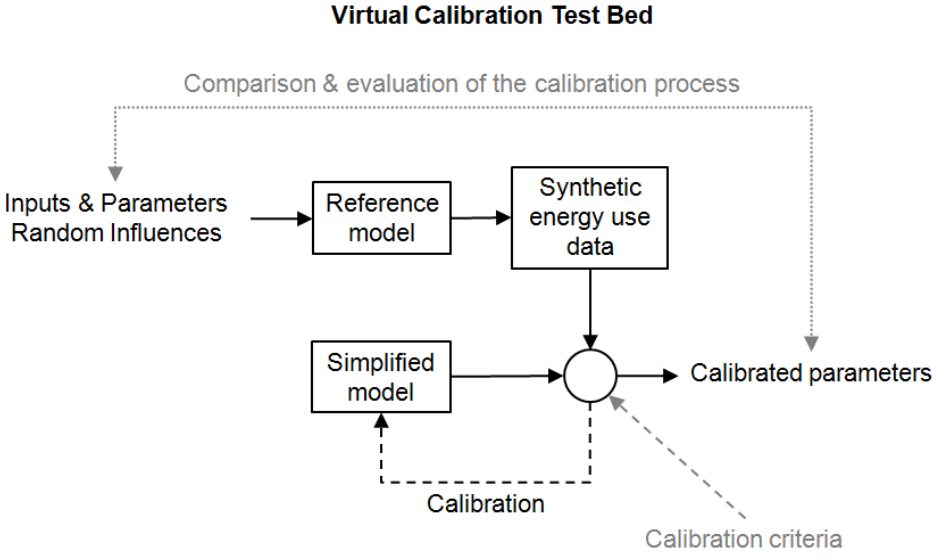

Figure 2: Assessment of a calibration method using a VCTB

Using synthetic cases to evaluate calibration methods consist in defining a typical building and specifying its various construction and equipment characteristics as well as its operating conditions and profiles. In general, the "(synthetic) measured data" used to perform the calibration are simulation data to which a certain amount of white noise has been added (Lee and Claridge, 2002; Reddy and Maor, 2006). The second step of the evaluation process consists in applying the calibration method to the original BES tool (Figure 3, Left) used to generate the synthetic data and where perturbations in the parameters have been added. **Since the "true" solution of the calibration problem is known beforehand, the accuracy and the robustness of the calibration process can be evaluated by determining how the calibrated model fits the generated energy use data**. However, the use of such type of synthetic case does not allow evaluating all types of calibration procedures. Indeed, even if such method can be used to perform preliminary assessment of automated calibration algorithms/methods, it does not allow evaluating manual iterative or graphical methods since the preliminary knowledge of the case by the user would bias the evaluation. Moreover, numerous influences and perturbations encountered in practice are generally not included in the synthetic case which is generally far from reality so that it is difficult to trust the validity of the calibration process even after evaluation.

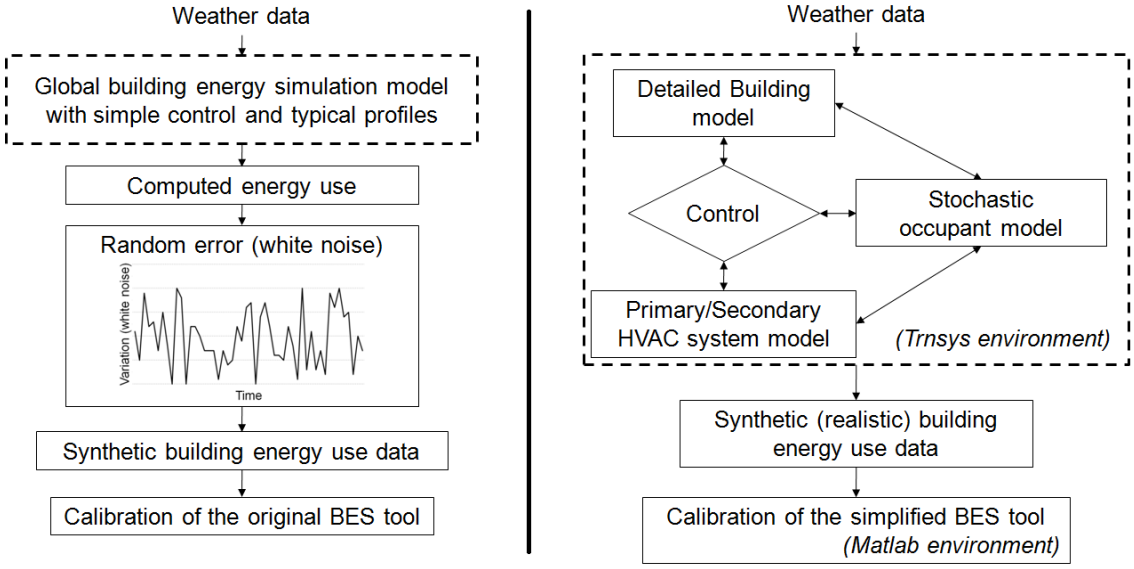

Figure 3: Calibration method evaluation by means of a classical synthetic case (left) and the proposed virtual calibration test bed (right)

In the present chapter, a virtual test bed dedicated to the **evaluation of calibration method** presented earlier (Chapter 3) is developed and used. Such test bed consists in a detailed model of a typical building, its envelope and its HVAC system implemented in Trnsys (Klein, 2010). Various influences and perturbations generally neglected in simple building energy models are included by means of probabilistic or deterministic models (e.g. stochastic occupancy profiles, varying infiltration rates and surface heat transfer coefficients, realistic PI controllers…) or arbitrary random perturbations (e.g. assuming a random distribution of thermal bridges) in order to represent the behavior of a real building and its highly variable energy use. Unlike classical synthetic cases (Figure 3, left), perturbations and variability is taken into account in a realistic way, at the input level (Figure 3, right). Moreover, a very detailed simulation model is used to include an important number of physical influences.

This virtual calibration test bed (VCTB) will be used as a fictitious building case to which a BES model would be calibrated. Fictitious measurements will then be performed to generate the synthetic data required for the calibration of the simplified model (billing data, specific and local measurements…). Similar virtual test beds are often used to develop and test control algorithms, strategies and systems (Mansson & McIntyre, 1997; Wetter, 2011).

Finally, the main objectives of the use of the VCTB developed and used hereunder are:

- To assess the robustness of the calibration methodology presented in Chapter 3 and integrating the sensitivity and uncertainty issues, as described in Chapter 4;
- To study the evolution of the values of the statistical indexes used to evaluate the quality of a calibration (MBE and CV(RMSE)) and the robustness of the criteria used in practice (e.g. as in ASHRAE, 2002);
- To check how physical measurement can help the parameters adjustment process in practice and see if some measurements are more useful or meaningful than others (i.e. such as in a "experimental design" process).

2. VIRTUAL CALIBRATION TEST BED (VCTB)

2.1. BASE CASE BUILDING

Once again, the base case building consists in a typical office building as frequently encountered in Europe. General characteristics (envelope, HVAC system and floor area distribution) have been defined based on survey data collected for office buildings in Belgium (BBRI, 2000).

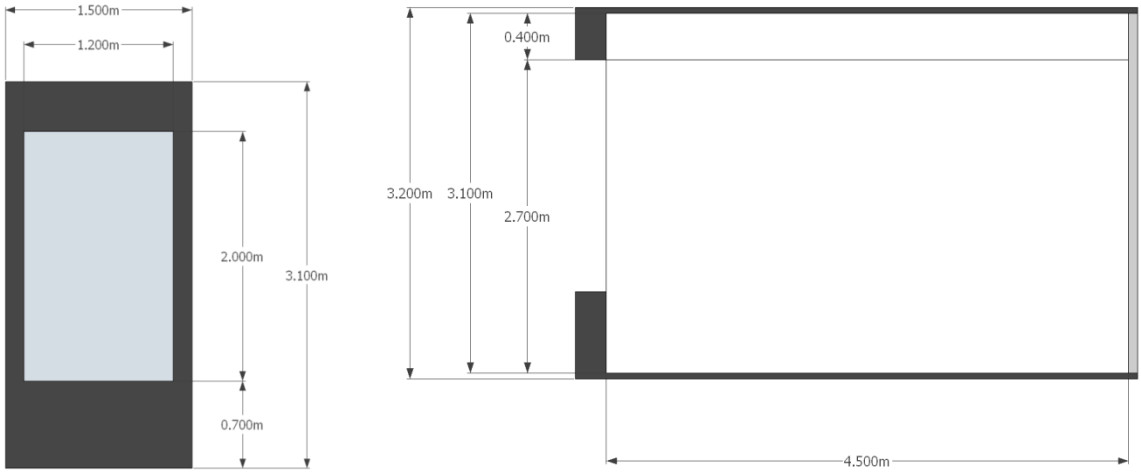

Figure 4: Facade module geometry (left) and office zone cross section (right)

The building is a five-storey building located in Paris (TMY Paris Montsouris weather file). All the façades are made of precast concrete modules of 1.5m large and 3.2m high (Figure 4) integrating 2cm of extruded polystyrene (0.034 W/m-K thermal conductivity). Each module includes a double glazed window of 2.4 m² (U = 2.83 W/m²-K; $SHGC_0$ = 0.755; p = 3; $SHGC_{hemis}$=0.655) mounted on an aluminum frame (U=2.27 W/m²-K) whose area is 15% of the total window area.

Detailed walls compositions are provided in the Appendix.

2.2. BUILDING MODEL

The building model has been built in Trnsys (Klein, 2006). Only one single typical floor has been represented by 12 peripheral zones, 7 core zones and 1 circulation zone (Figure 5) and will be simulated 5 times in order to generate whole-building consumption data. The top floor and the lobby

have not been simulated so that roof and slab effects are not taken into account. The geometrical description of the floor layout is provided in the Appendix.

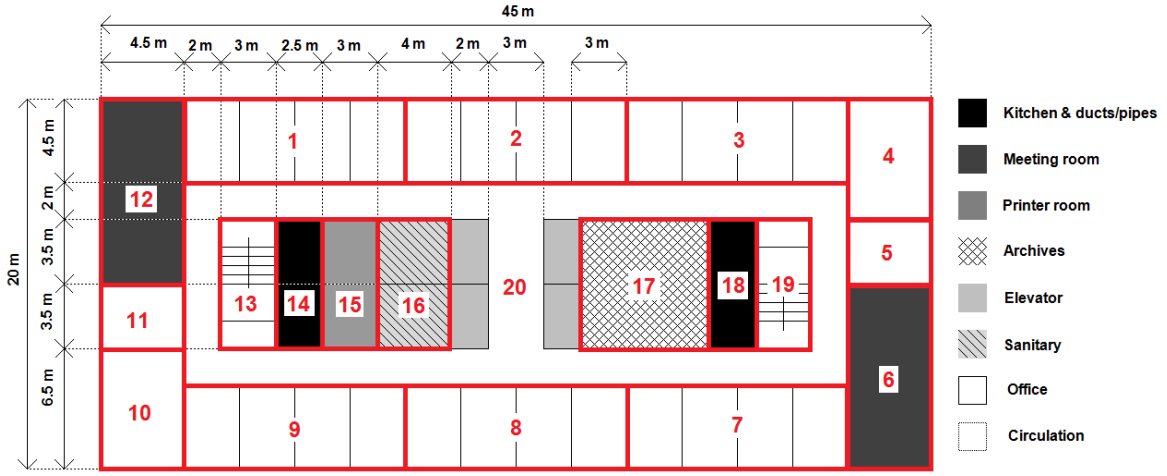

Figure 5: Base Case building - internal layout

Thermal bridges have been represented by a fictitious increase of the opaque wall area of the peripheral zones. The opaque wall areas of the peripheral zones have been artificially increased by 50% in average with a +/- 25% variation supposing a uniform distribution between zone. This arbitrary correction leads to an artificial increase of approximately 10% of the design global AU value of the floor (Figure 6). Such correction allows taking into account thermal bridges in an easy way (without modifying walls compositions). Unfortunately, this artificial increase of the opaque wall area also leads to an over-estimation of the absorbed solar radiation. However, it is considered that such influence (supplemental absorbed heat gain) has a limited impact on the building energy use in comparison with heat losses through walls and solar gains through windows.

Table 1: Fictitious increase of the opaque walls area

Zone	Initial opaque wall area m²	Corrected opaque wall area m²
1	18	25.17
2	18	30.79
3	18	22.89
4	18.85	29.93
5	4.5	6.14
6	23.35	32.58
7	18	28.27
8	18	24.15
9	18	27.35
10	18.85	31.27
11	4.5	7.12
12	23.35	32.24

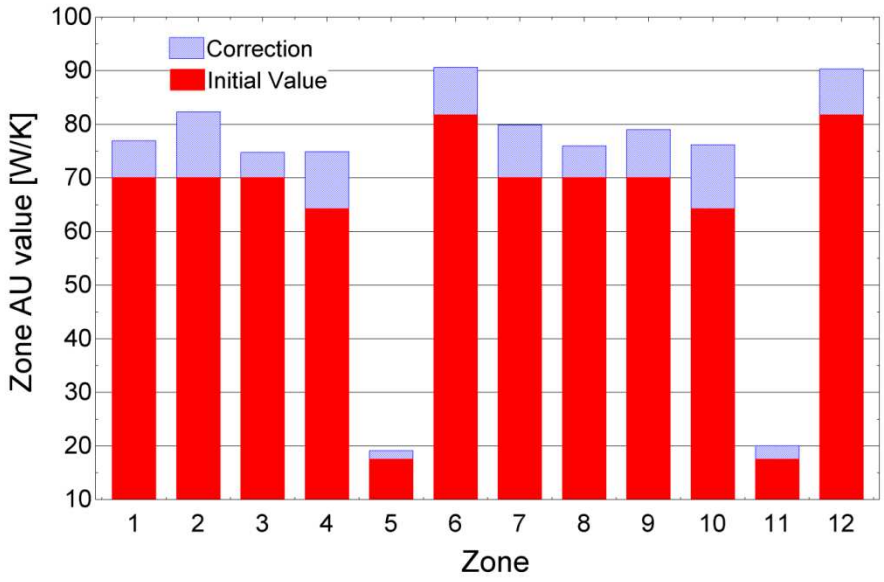

Figure 6: Random thermal bridges distribution between zones

The combined (radiation-convective) and convective heat transfer coefficients of the outdoor glazed and opaque surfaces are computed as function of the wind speed by means of the correlations provided by Walton (1983).

$$h_{out,combined} = a_1 + a_2 * v_{wind} + a_3 * {v_{wind}}^2 \quad (W/m^2 - K)$$

$$h_{out,conv} = h_{out,combined} - 5.1 \quad (W/m^2 - K)$$

Table 2: Coefficients of the Walton's correlation (1983)

	a_1	a_2	a_3
Concrete	10.79	4.192	0
Glass	8.23	3.33	-0.036

Type571 is used to compute infiltration rate of each peripheral zone as function of the wind speed and the indoor-outdoor temperature difference by means of the K1-K2-K3 method (ASHRAE, 1981) during non-operating hours. Infiltration rate is assumed to be null the rest of the time (guessing a slight overpressure of the building due to the operation of the mechanical ventilation system). The values of the 3 coefficients have been chosen to correspond to a medium quality construction.

$$ACH = K_1 + K_2 * |T_{in} - T_{out}| + K_3 * v_{wind}$$

Table 3: Coefficients of the K1-K2-K3 method

Construction	K_1	K_2	K_3	Description
Medium	0.10	0.017	0.049	Building constructed using conventional construction procedures

Infiltration rate in the core zones is arbitrarily imposed to 0.05 ACH.

2.3. *LIGHTING, APPLIANCES AND OCCUPANCY GAINS*

Design lighting power densities, plug loads and occupancy loads in the different zones are given in Table 4.

Table 4: Nominal internal gains

	Occ.[1]	**Lighting (conv. Part)**	**Appliances (conv. Part)**	**Profile**
	m²/occ	W/m²	W/m²	-
Offices	15	12 (40%)	8.89 (80%)	Behavioral (Parys et al., 2011)
Meeting	3.5	14 (40%)	10 (100%)	Behavioral
Archives	0	9 (40%)	0	Fixed
Copy room	0	10 (40%)	110 (100%)	Behavioral
Kitchen	0	14 (40%)	10	Fixed
Sanitary	0	5 (40%)	0	Fixed
Circulations	0	5 (40%)	0	Fixed
Stairs	0	5 (40%)	0	Fixed

A complete behavioral model (Figure 7) integrating occupant's presence, lighting and appliances use has been used to generate stochastic internal gains profiles following the methodology proposed by Parys et al. (2011). Firstly, occupancy pattern and daylight levels in the zones are computed with a 5-minutes time step. Two parameters are used to introduce some variability in the occupancy profiles:

- The turn-up (T) multiplies the cumulative arrival probability and has been set to 0.9 for "normal" working days (i.e. a peak occupancy rate of 90% during a normal weekday). High turn-up rates leads to higher occupancy rates in the zone (Figure 8).
- The mobility (M) multiplies the probability of temporary absence and influences the number of state transitions during the day (arrival-departure) and has been set to 0.4 (Figure 8).

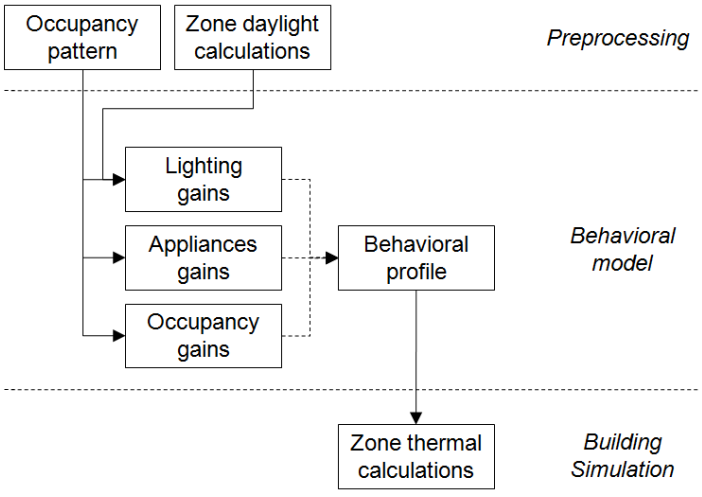

Figure 7: Schematic overview of the behavioral model (adapted from Parys et al., 2011)

These two parameters are critical since occupant control decisions are generally made at arrival or departure. So, the main outcomes of this occupancy model are the number of state transitions during the day and the total amount of time spent in the zone by the occupant. Holidays have been taken into

[1] Occupant's total metabolic rate is supposed to be 150W (50% sensible; 50% latent). A diversity between occupants is considered by defining a normal distribution with a 20% standard deviation.

account by varying the turn-up parameter (T) from 0 (Sunday and holidays) to 0.9 (normal working days).

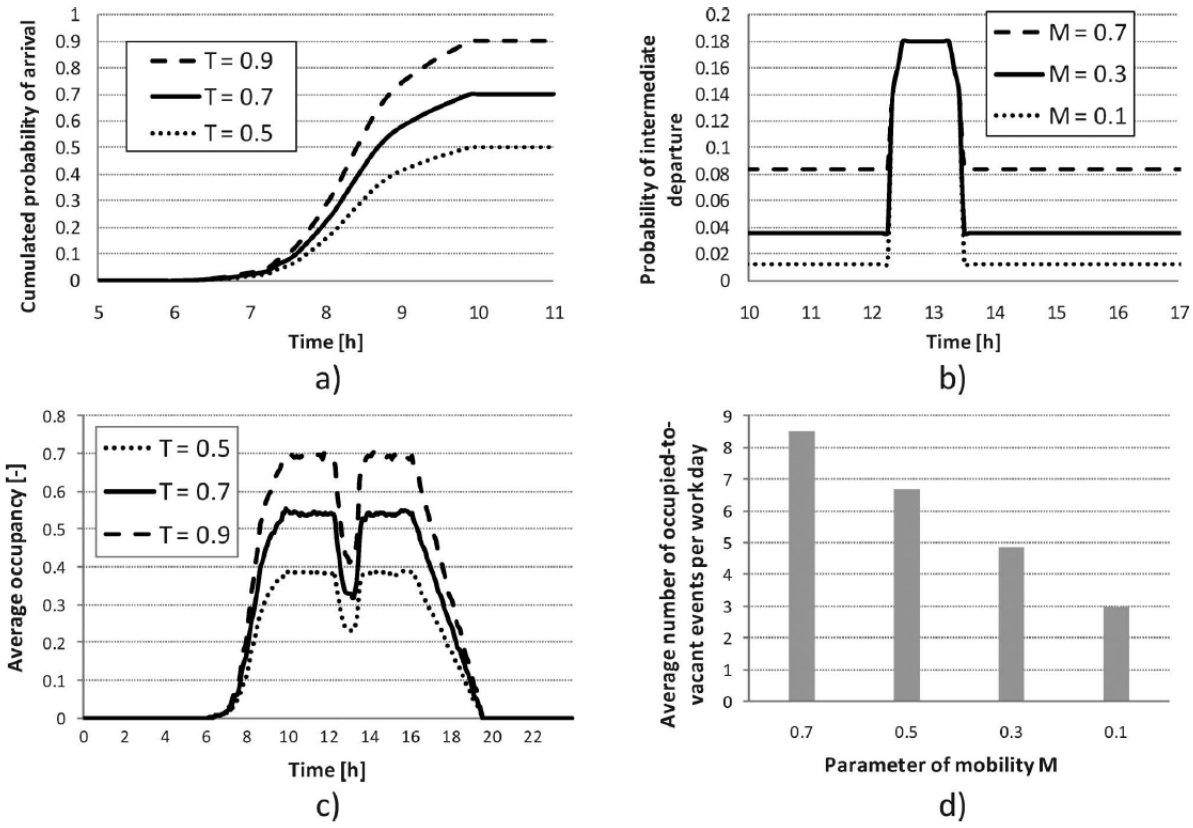

Figure 8: (a) Cumulated probability of arrival for different values of parameter of turn-up. (b) Probability of intermediate departure for different values of parameter of mobility. (c) Mean occupancy level for 10,000 runs of the occupancy model. (d) Mean number of occupied-to-vacant events for 10,000 runs of the occupancy model (from: Parys et al., 2011).

Then, the lightswitch-2002 model from Reinhart (2004) is used to calculate artificial lighting gains and related energy consumption. Finally, the generated profiles are used as inputs in Trnsys.

It should be noticed that most of the behavioral models available in the literature concern only occupant's presence and lighting use in single office cells. A few global behavioral mobility/space utilization models exist in the literature but are complex to implement and use (e.g. the USSU model described in Hoes et al., 2009). So, some assumptions have been done in order to generate realistic behavioral or fixed profiles for lighting use in meeting rooms and common zones (sanitaries, circulation…) and for appliances.

The average nominal appliances load density is defined to 8.89 W/m² in offices. To add some variability in the profiles, the value is sampled from a normal distribution (with a standard deviation of 1 W/m² around the nominal value) every occupied day; this value is maintained constant throughout the working day. At the end of the day, a certain percentage remains. This percentage is also sampled from a normal distribution (average 15% of nominal load with a 10% stdev).

The printer room is supposed to be equipped with two copiers, two laser printers and one fax. Each device is supposed to be in operation about 5% of occupancy time (Parys et al., 2011) which corresponds to about 30 minutes of operation per day. The devices are in idle (standy-by) mode the rest of the time. Each operation is supposed to take at least 2 minutes. An example of profile for one day is shown in Figure 9.

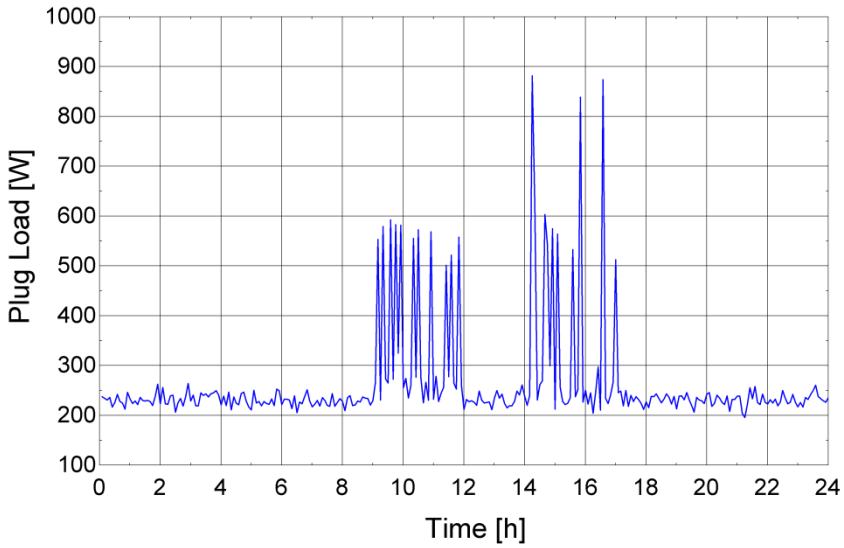

Figure 9: Appliances stochastic operation profile in print room for a given day

Lighting and appliances use in meeting rooms are supposed to be directly proportional to the occupancy rate. Stochastic occupancy profiles in meeting rooms are defined by assuming that meetings can start between 9:00-12:00 and 14:00-17:00 during normal "working days" (Monday to Friday). Meeting duration is sampled from a normal distribution with an average of 90 minutes and a standard deviation of 20 minutes. The "participation rate" of each meeting is sampled from a normal distribution with an average of 50% and a standard deviation of 25%. A 100% participation rate corresponds to the capacity of the meeting room. As an example, occupancy rates of both meeting rooms are shown in Figure 10 for two consecutive days.

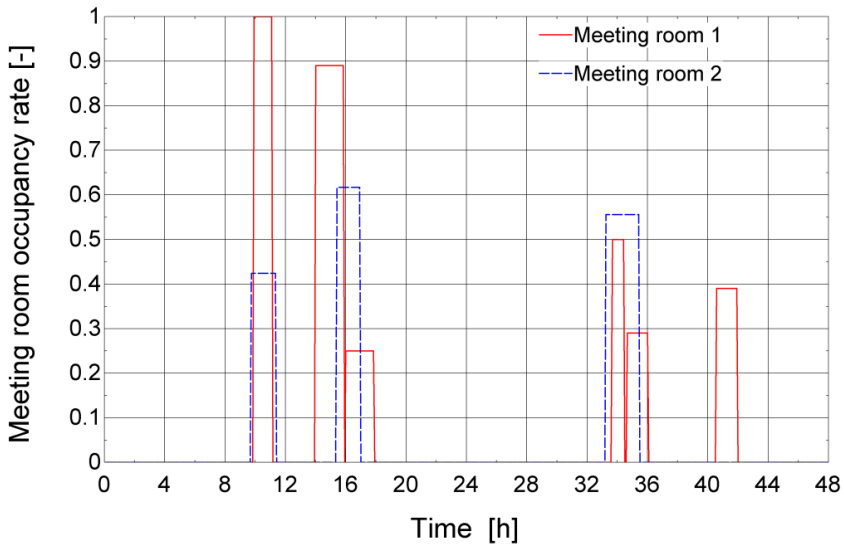

Figure 10: Meeting rooms stochastic occupancy profiles for two consecutive days

2.4. SECONDARY HVAC SYSTEM MODEL AND CONTROL

The temperature in peripheral zones and archives are locally controlled by means of heating/cooling 4-pipes fan coil units. The hygienic ventilation in these zones is ensured by a constant volume system supplying air at desired temperature (water heating and cooling coils) and humidity (electrical steam humidification system). Hot water and chilled water productions are ensured by two natural gas boilers and one air cooled chiller respectively.

The building is equipped with an air-water heating/cooling system. The 4-pipes terminal heating and cooling fan coil units (FCU) have been sized in order to have one unit per facade module as it is generally encountered in real buildings (to maximize internal space availability and flexibility). Indoor conditions in the core zones of the building are not controlled except for the archives room (zone Nr. 17).

The FCU model relies on the coupling of the Trnsys building model (Type56) and its built-in indoor temperature controller and some Type581 (Multi-dimensional interpolation) components and takes into account the effect of potential condensation on the cooling coil in cooling operation. Details about the FCU simulation model are given in the appendix.

Primary indoor temperature and humidity setpoints are fixed by the BEMS system to 16°C/22°C (Night/Day) in heating mode, 24°C (Day) in cooling mode. Two random variations have been added to this FCU model in order to represent a more realistic (and non-perfect) control. First, it is considered that the user is allowed to locally adjust the daytime temperature setpoint in a limited way (i.e. +/- 1.5°C around a fixed setpoint). So, a normal distribution with a standard deviation of 0.75°C has been defined on a zone basis to represent users' sensitivity and preferences in terms of indoor temperature. A minimal dead band between heating and cooling setpoints has been fixed to 2°K to ensure robustness and avoid cycling. A second random effect has been added to represent the effect of the inaccuracy and the sensitivity of the temperature sensor installed in the unit and consists in a correction of the setpoint of each zone at each time step following a normal distribution with a standard deviation of 0.25°C. As an example, users-defined local heating temperature setpoints in zones 1, 2 and 3 are shown in Figure 11 for a given day (zone1: 15/23.3°C; zone2: 15/22.3°C; zone3: 15/20.6°C).

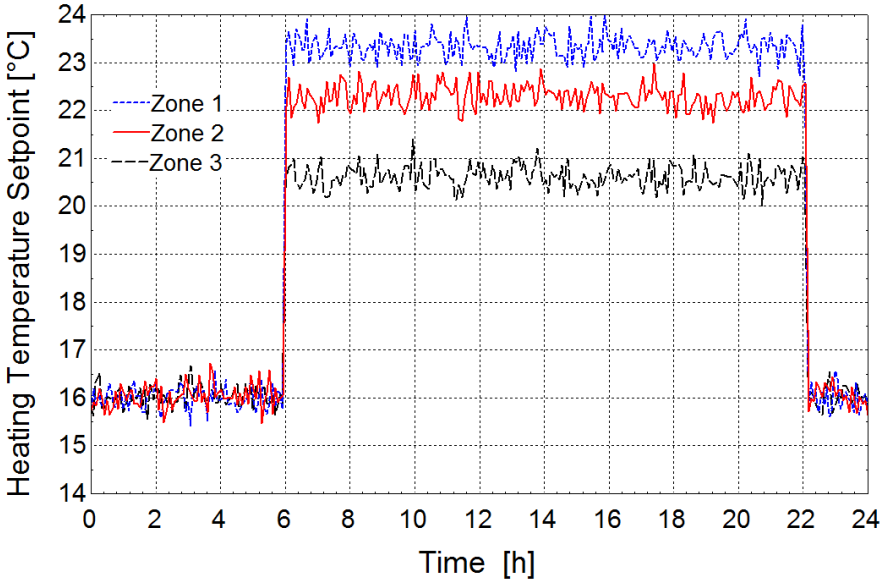

Figure 11: Heating temperature setpoints for three zones

The central ventilation system consists in a simple constant volume Air Handling Unit (AHU) providing heated/cooled/humidifier air by means of one water cooling coil, one water heating coil and one electrical steam humidifier. Design flow rates have been fixed according to EN15251 as shown in Figure 12. Non-polluted zones (offices, meeting rooms and circulations) and polluted zones (copy room, kitchen and sanitaries) have been distinguished and have separated extraction systems. The exfiltration flow is supposed to be 10% of the supply air flow. All the supply and return flows vary at each time step following a normal distribution centered on the design flow rate with a standard deviation of 2.5%. Such arbitrary random variation allows representing slight flow rate variations

induced by pressure variations between the zone and the system (e.g. due to doors opening and closing) without integrating a complex airflow model of the building. Other influences (such as leakages, fouling…) are not taken into account in the present model.

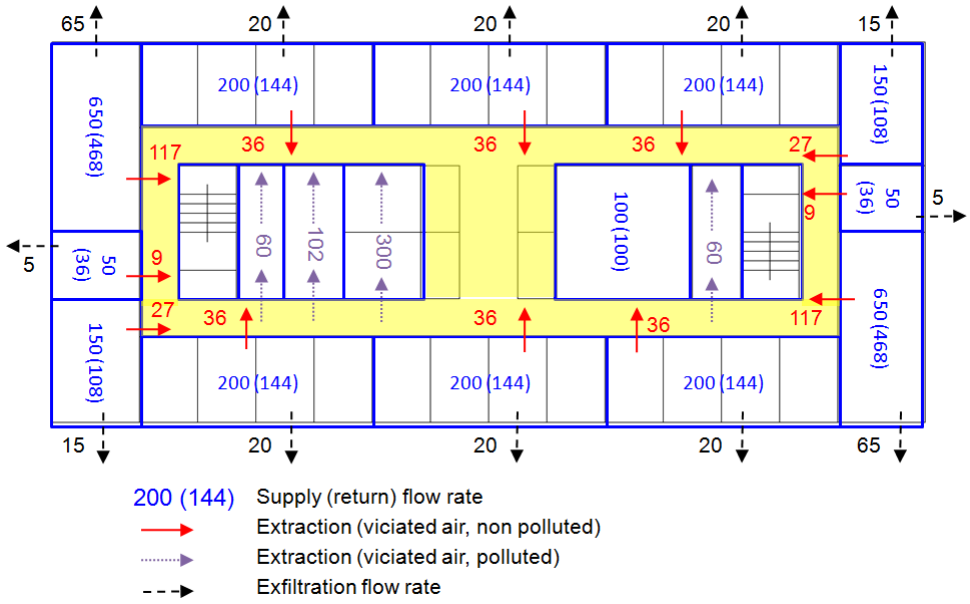

Figure 12: Design ventilation air flows in cubic meters per hour

Ventilation fan electrical power demands have been imposed to represent medium class equipment (EN13779). Because the ventilation system is a constant flow system, no accurate airflow model is used in the present model and pressure distribution and interactions between ventilation system and window and doors opening/closing are not represented. Thus, the model does not account for the interactions between the fan and the building pressure/air flow rates and equations establishing the location of the fan running point are skipped. For each fan, the motor nameplate value (i.e. the value usually available in the as-built file) of the power has been supposed to be rounded up. In the present case, the name plate value of the electrical power is about 15% higher than the actual power consumption. AHU components characteristics and models are described in the Appendix.

Heat losses/gains in air ducts are computed by means of the Type709. Ducts dimensions have been estimated based on the exterior dimensions of the building. The ambient temperature in technical rooms and shafts is equal to a weighted average of the outdoor temperature and the average building indoor temperature.

2.5. *Primary HVAC System Model*

Chilled water production is ensured by one air-cooled chiller of 540 kW cooling capacity and with a rating EER (including fan power at LWT 7°C and EAT 35°C) of 3.1. Extended performance maps used in Type655 have been generated by means of a detailed semi-empirical model of the chiller developed in EES (Lemort and Bertagnolio, 2010) and calibrated by means of part load and full load data provided by the manufacturer.

In a first time, the very simple Type751 boiler model (tabulated values of efficiency) is used to simulate the performance of the hot water production system because the lack of manufacturer data does not allow using a more advanced (physical) model.

A detailed semi-empirical model of the boiler implemented in EES (Bourdouxhe et al., 1999) has been used in order to generate the performance map to be used by the Type751 model. The plant includes

two identical natural gas boilers (with a 92% LHV efficiency at 60/80°C) connected in parallel and controlled by means of an ideal cascade algorithm (no hysteresis) for a total installed capacity of 490 kW.

Hot and chilled water distribution and production systems have also been modelled. It is supposed that the AHU, the FCU of the North and East façades and the FCUs of the South and West façades are supplied using separated circuits connected to main hot water and chilled water collectors (Figure 13).

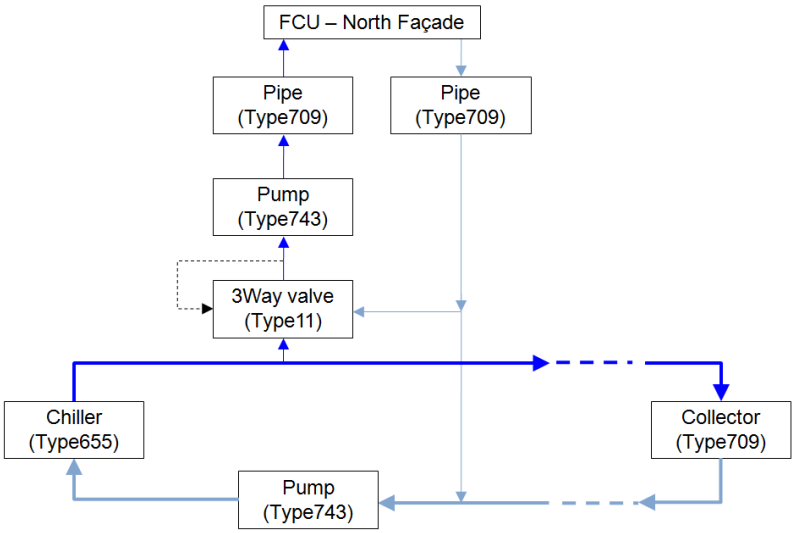

Figure 13: Chilled water distribution and production system

Two different non-dimensional pumping power curves are used for pumps with nominal power smaller than 375W (considered as "circulators") or greater than 375W. These curves simulate the variations of the pumping power when hot and chilled water vales open and close. These curves are used to compute the normalized power as function of the normalized flow rate (Figure 14) and have been identified based on the work of Sfeir et al. (2005) supposing pumps with flat characteristic curve and medium efficiency.

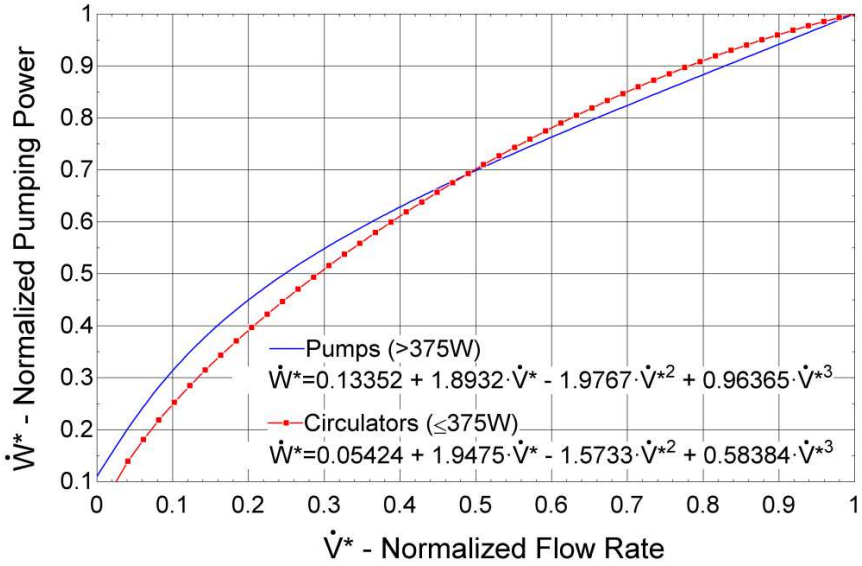

Figure 14: Non-dimensional Pumping Power Curves

All the pumps and circulators have been sized based on rule of thumb values (in-line pressure drops estimated to 400 Pa/m, circuits lengths estimated based on building main dimensions) and

manufacturer data (local pressure drops in coils, chiller, boiler…). The main pumps and circulators of the system are listed in the Appendix. As done for ventilation fans, the nameplate value of the pump power is a rounded value and is about 15% higher than the actual nominal power demand.

3. SYNTHETIC DATA

After selecting a building and specifying its various construction and equipment parameters as well as its operating schedules, Trnsys has been used to generate synthetic billing and measurement data. Some example simulation results of the Virtual Calibration Test Bed (VCTB) are presented below. These selected results correspond to data generally available (billing data) or measurable (electrical power demand, indoor conditions…) in real buildings. In order to evaluate the impact of the stochastic influences implemented in the model, a comparison is done with simulation data obtained by means of the same model whose variable input profiles would have been replaced by standard "sharp" profiles (with constant weekly starting/ending schedules and rates) for occupancy, lighting, appliances and system operation. These standard profiles have been derived from the stochastic ones in order to keep equivalent levels of supplied energy due to internal gains and air volume due to infiltration and ventilation on an annual basis.

Table 5: Synthetic building - Monthly consumption data

Month	Natural Gas	Peak Electricity	Offpeak Electricity
	MWh	MWh	MWh
J	63.58	37.63	7.23
F	45.50	33.64	7.12
M	30.42	35.88	6.99
A	14.34	33.51	6.54
M	7.19	33.18	6.47
J	3.19	29.74	6.69
J	1.42	30.08	6.92
A	1.60	30.97	6.48
S	3.90	25.36	6.56
O	14.45	29.45	5.69
N	41.42	32.98	6.36
D	58.43	32.99	7.90
Total	285.43	385.40	80.94
Year	Natural Gas	Electricity	
	kWh/m²	kWh/m²	
Total	63.43	103.63	

Normalized synthetic whole building gas and electricity consumptions are within the ranges generally encountered in practice for this category of building: 63 kWh/m²/yr of gas consumption and 104 kWh/m²/yr of electricity consumption.

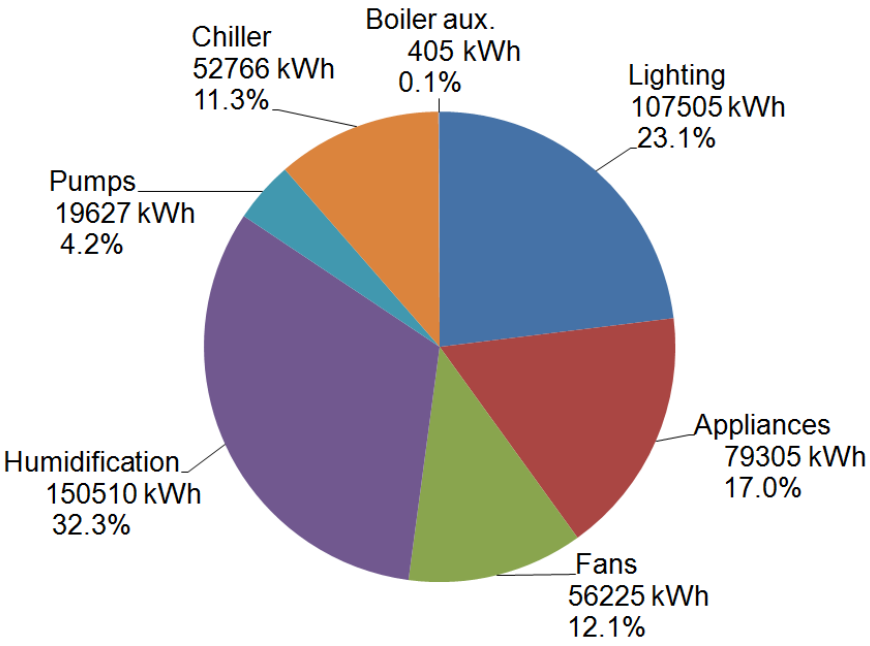

Figure 15: Synthetic building - Whole building electricity consumption disaggregation

The disaggregation of the whole-building electricity consumption (Figure 15) is typical for this type of building:

- Lighting and appliances parts are of the same order of magnitude (about 20% each)
- Electrical Steam Humidification part is about 30%
- Chiller part is between 10 and 15%

Synthetic monthly billing data are shown in Figure 16 and Figure 17 and compared. Whole building gas and electricity consumption have been used to generate normalized thermal and electrical signatures. Both synthetic signatures are quite similar to "real" signatures generally encountered in practice. It is interesting to note that the linear regression coefficients (R^2) are quite high (around 87% for gas consumption) regarding the values that could be encountered in practice (50 to 70%).

The slope variation between the "stochastic" and "standard" synthetic signatures is mainly related to the calculation of the infiltration rate (variable in the first case, constant in the second one) and the different time distributions of lighting gains (higher in winter in the case of behavioral profiles).

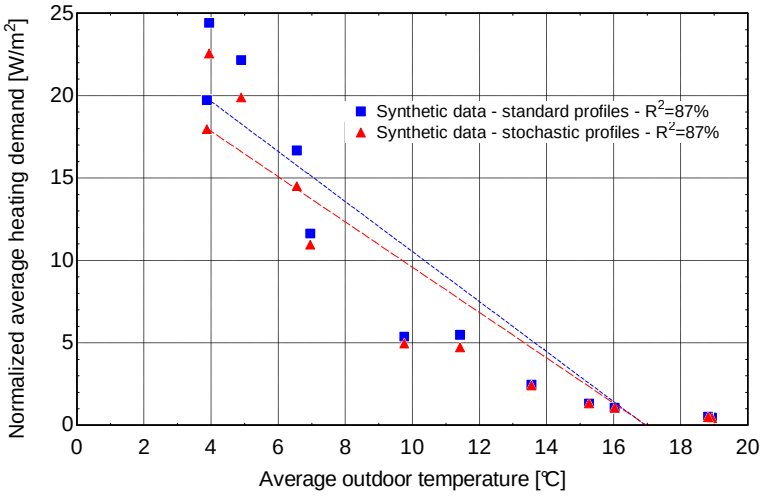

Figure 16: Thermal Signature

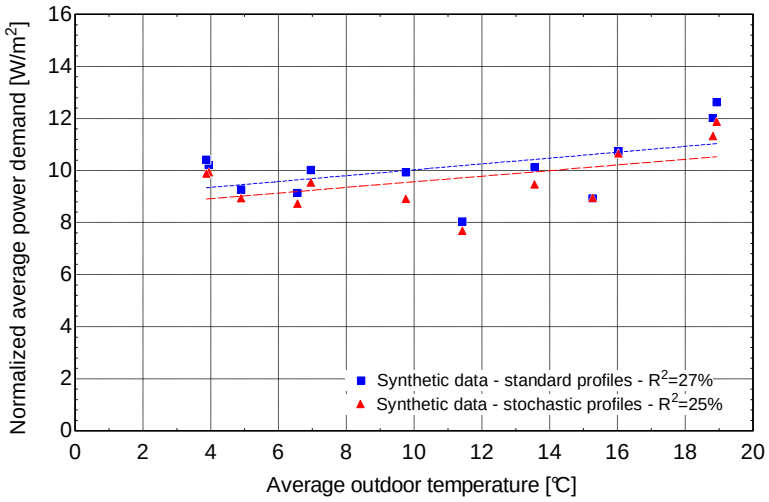

Figure 17: Electrical Signature

The same observation can be made for electricity data. As it is often encountered in practice, the electrical signature has a very flat shape and a poor correlation coefficient in all the cases. Comparing to natural gas consumption, a very non-significant decrease of the linear regression coefficient can be observed when using stochastic profiles (from 27 to 25%).

So, despite of the use of a validated building and HVAC system simulation platform, able to take into account most of the influences intervening in heating and cooling loads calculation in a very detailed way (solar gains, internal gains, building dynamics…), the dispersion of monthly data is not well represented. This leads to the following observations:

- The use of stochastic profiles does not lead to large dispersion of the data when looking at integrated billing data (on a monthly or yearly basis). Indeed, signatures and data dispersion are very similar when using standard or stochastic occupancy profiles. Indeed, for equivalent injected quantities of energy, the stochastic and standard profiles lead to very similar values of linear regression coefficient.
- The dispersion of the data identified in practice (lower values of linear correlation coefficients) would mainly be due to variations in the operation of the HVAC system (e.g. arbitrary switches from automatic to manual operating mode for technical or comfort reasons) or errors in the recorded values (exact billing periods are badly known)

However, the effect of variable and stochastic operation/occupancy profiles appears more clearly when looking at the mean and standard deviation values of the electrical power demand (Table 6). The impact of stochastic variations on the HVAC-system consumption is limited but the variability of the in-zone electricity consumption (especially during operating hours) is increased by using variable profiles.

Table 6: Synthetic building - Electrical power demand

Electrical power demand (avg ± stdev) in kW	Stochastic profiles	Standard profiles
Peak hours	77.5 ± 31.3	78.1 ± 26.5
Off-peak hours	15.5 ± 20.5	15.8 ± 19.4
HVAC System	21.3 ± 15.3	21.4 ± 14.4
In-zone consumptions (lighting and appliances)	37.6 ± 31.1	39.4 ± 26.1

Figure 18 shows illustrate the impact of variable profiles when looking at the electrical power demand for one floor for a given winter period. This “fictitious measurement” (which could be realized in

practice by logging directly on the main electrical panel of the floor) includes lighting and appliances consumptions for the whole floor. The two curves have very similar shapes but variations due to the use of the behavioral profile are much more realistic.

Peak demands predicted by means of stochastic and standard profiles are very different mainly because of the seasonal variations in the artificial lighting use that are taken into account by the stochastic profiles and not by the standard profile (constant, all year long).

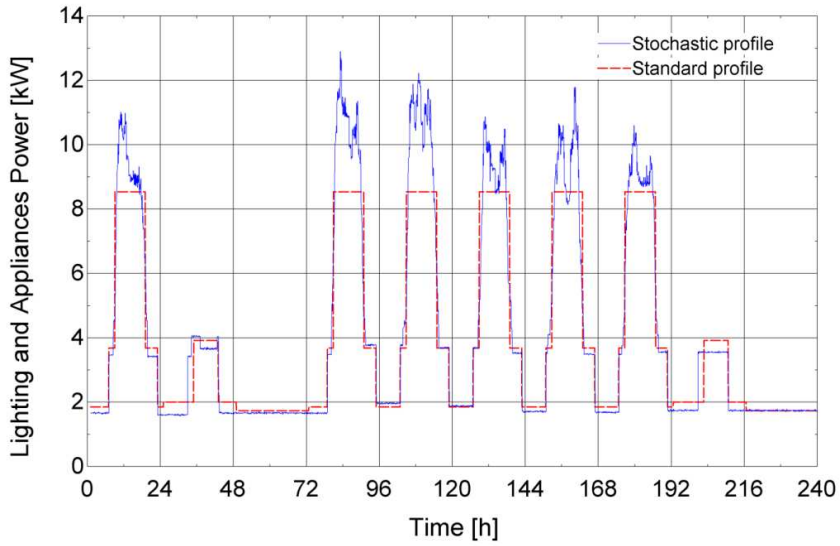

Figure 18: Synthetic whole building electricity consumption data

Another "fictitious measurement" could consist in local temperature and humidity measurements performed in one office cell in order to identify the actual indoor conditions ensured by the HVAC system (Figure 19). Bold curves represent the original simulation data provided by the synthetic case. Variations observed on these curves are due to the interactions between the dynamic building model, the HVAC system model and the controllers. Thin curves have been obtained by adding a filtering in order to represent the resolution (e.g. +/- 0.5°C and +/- 5%) of the "fictitious" temperature and humidity logger. Those two last curves are the ones to use when assessing a calibration procedure.

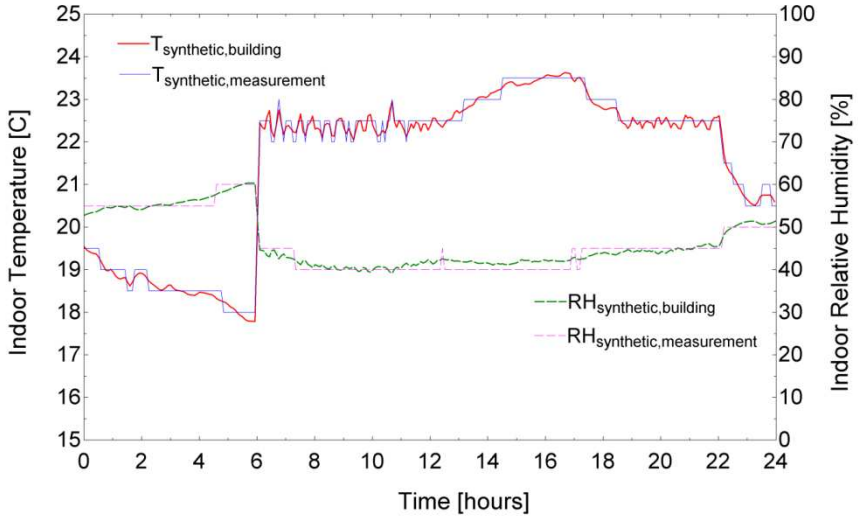

Figure 19: Synthetic temperature and humidity measurements

Other "fictitious/synthetic" measurements could be performed in the synthetic building, such as:

- Artificial lighting operation time in offices by means of lighting loggers
- Appliances power consumption in offices by means of plug-in loggers
- Pumps and fans operation time by means of magnetic field loggers
- Air temperature and humidity measurements at AHU exhaust and in ventilation ducts by means of temperature and humidity loggers
- HVAC system components electricity consumption by means of electrical loggers
- Air and water flow rates measurements

The use of such measurement data is illustrated below.

4. APPLICATION OF THE CALIBRATION METHODOLOGY

The proposed calibration methodology is evaluated using synthetic data generated by means of the synthetic building case described above.

Comparing to a real application of the calibration process, the use of a synthetic case allow avoiding some parasitic influences such as:

- The uncertainty on the weather data used to run simulation: in the present case, the same weather data set will be used to generate the synthetic data and to run the simplified model to be calibrated;
- No measurement uncertainty can bias the calibration process (no error on the billing periods, etc.)
- The uncertainty on building system operation: possible interferences due to temporary modification of the system operation by the building owner/manager (e.g. switch from automatic to manual operation of the ventilation system during short periods…)
- The change/variation of building operation/use between the (past) "reference period" used to develop the calibrated model and the (present) current operation period while the energy service process is going on

No iterative calibration method will be applied to the present case and only "evidence-based" (i.e. data and information collection), sensitivity and uncertainty issues will be studied. The main objectives of this application of the calibration methodology consist in:

- Assessing the robustness of the proposed systematic calibration methodology and checking its "applicability";
- Showing how sensitivity and uncertainty issues can be handled in the frame of a calibration process by defining realistic probability ranges (or "confidence intervals") for the parameters of the model;
- Characterizing the possible levels of calibration by studying how existing measurement techniques (from spot to short-term measurements) can help at the different stages of a calibration process. This first objective can be seen as a first tentative for the definition of an experimental design;
- Characterizing the accuracy of the calibration process by studying quality criteria issues for the different levels of calibration.

4.1. DATA COLLECTION AND CALIBRATION LEVELS

As discussed in a previous chapter, the notion of "hierarchy" between the sources of information is a critical issue when adjusting the value model's parameters. So, it was decided to define calibration levels, characterizing the information availability and quality all along the calibration process.

Four levels of calibration can be considered depending on the availability of building, system and measurement data. The four levels (Table 7) have been defined according to the classification proposed by Reddy and Maor (2006).

Table 7: Calibration levels as a function of input data available (adapted from Reddy and Maor, 2006)

Calibration levels	Building description and performance data available for calibration					
	Utility bills (one year)[2]	WBE demand[3]	As-built data	Inspection	Spot/Short-term monitoring	Long-term monitoring
Level 1	x	x	x			
Level 2	x	x	x	x		
Level 3	x	x	x	x	x	
Level 4	x	x	x	x	x	x

The basic energy data set is common to the four calibration levels and includes monthly energy bills and hourly values of the whole-building electricity demand (in kW) for one year.

The first level corresponds to the initial "as-built" model of the installation. This version of the model is based on available as-built data (plans, schemes and nameplate data of main HVAC components…) and will be used for parameters screening (by means of the Morris sensitivity analysis method). This model cannot be considered as calibrated since important data (e.g. operation schedules…) are missing.

The second level involves on-site inspection (e.g. complete inventory of installed appliances and lighting powers) and BEMS analysis (setpoints, schedules…). The data collected at this stage correspond to the information that can be expected when proceeding to an energy audit/inspection of an installation.

The third level involves spot and short-term measurements that can be realized as part of a detailed audit (e.g. short term monitoring of power consumption of some parts of the installation…). The use of short-term monitoring data allows identifying some "average" trends such as indoor night and day temperature setpoints, HVAC components power demands, etc.

The last level relies on a detailed measurement campaign and involves longterm measurements, occupants' behavior survey… allowing to better identifying schedules and utilization/operation patterns. This last calibration level will not be considered in the present work since it can be seen as an improvement of Level 3 calibration or as an evolutionary/on-going calibration. Special attention is paid below to the early development of a calibrated model (i.e. to the three first levels) as it can be done in the frame of an energy service process.

Table 8: Calibration levels

Level	Data availability
1	- Complete geometrical description - Maximal number of occupants and "typical" schedules for occupants and systems - Nominal powers for main HVAC system components (chiller and boilers) - Default values for fans and pumps powers - Nominal (design) ventilation flow rate

[2] Natural gas, peak-hours and offpeak-hours electricity consumption (in kWh) provided on a monthly basis

[3] WBE demand : whole-building electricity demand (in W) provided by the electricity provided on a quarter-hour basis for a complete year

2	- Detailed envelope composition - Survey of installed lighting and appliances loads densities - Complete inventory of installed powers of auxiliaries (pumps and fans) - Analysis of the BEMS (setpoints and schedules)
3	Spot and short-term monitoring: - Local temperature and humidity measurements in the zones - Lighting and appliances electricity consumption measurement (zone level) - Secondary and primary HVAC components electricity consumption measurement
4	Long-term monitoring of: - Chiller electricity consumption - Pumps electricity consumption - Boiler gas consumption - Hot and chilled water temperature and flow rates

4.2. CALIBRATION PROCESS

The calibration process is described below for each of the first three calibration levels mentioned above. The simplified building energy simulation model described in Chapter 2 is applied and calibrated to the synthetic case described above. Synthetic energy use data generated by means of the virtual test bed implemented in Trnsys will be used to perform calibration. The update of the model as the calibration progresses is detailed hereunder. Data gathering, sensitivity, accuracy and uncertainty issues are discussed for each level. At each stage, the validity of the calibrated model will be checked by means of commonly available data (monthly energy bills and whole-building electricity demand). In a second time, predicted and synthetic energy end-use data will be compared in order to characterize the accuracy of the calibrated model.

4.2.1. Level 1

The first level of calibration consists in constructing the "as-built input file" of the building under study (Calibration Level 1). A simple division of the building is proposed in Figure 20 and Table 9. This definition of the building in six zones relies on a compromise between model complexity, building geometry and orientation and configuration of the HVAC system. Offices are consolidated into zones A and C. Due to their different occupancy/operation, meeting rooms are simulated separately (zones B and D). Due to its "core" location and its ventilation/heating/cooling, the storage room is simulated as an individual zone. The last zones which are part of the core zone of the building (kitchen, restrooms, circulations…) are aggregated and form zone F.

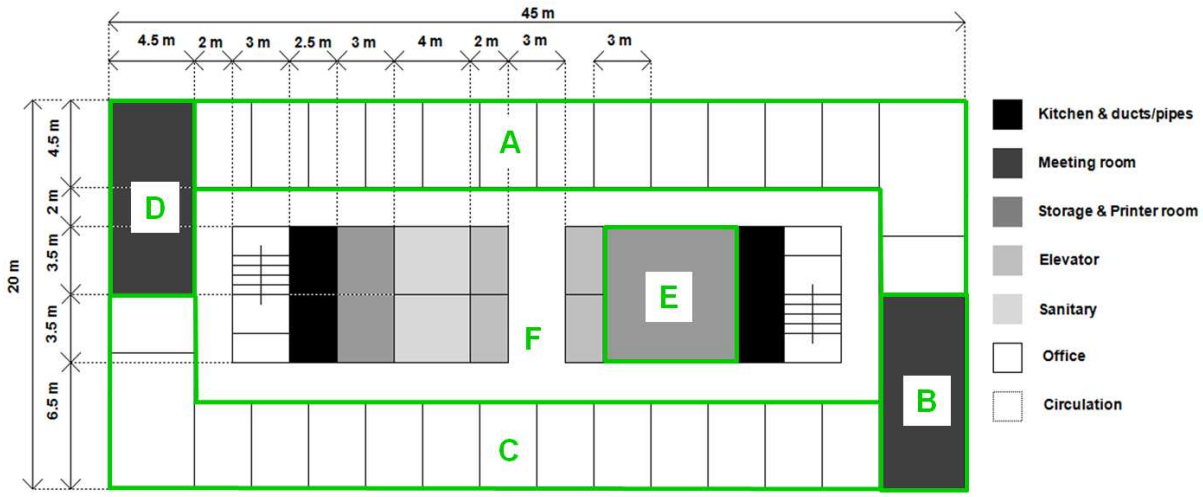

Figure 20: Simple zoning for the Matlab model

Table 9: Simple zoning for the Matlab model

Zone	Floor area m²	Wall	Orientation	External wall area m²	Window area m²
A	1035	1	N	303.75	324
		2	E	83	72
B	225	1	E	83	72
		2	S	33.75	36
C	1035	1	S	303.75	324
		2	W	83	72
D	225	1	W	83	72
		2	N	33.75	36
E	245	-	-	-	-
F	1735	-	-	-	-

Table 10 lists the 36 input parameters that are deemed influential for the considered simple office building case. In accordance with the conclusions of the previous chapter, the other parameters (e.g. ground albedo, radiation-convective split of internal gains…) are supposed to be of a secondary influence and have been estimated or set to default values following a "factor fixing" approach. These "secondary" parameters will not be considered for sensitivity/uncertainty analysis and calibration. Table 10 also includes the "best guess" values and the estimated range of variation (representing the "uncertainty" on the given parameter) for the considered parameters. Since, the present case is a synthetic case, uncertainty ranges have been quite arbitrarily defined in order to be able to highlight the use of sensitivity and uncertainty analyses methods and the effect of the narrowing of the uncertainty of the ranges as the calibration progresses.

The first calibration level relies on the use of available consumption and as-built data. This first description of the building corresponds to the information that could be found in basic as-built files, prior to any on-site visit.

The complete geometrical description of the building has been done but no detailed information about walls compositions is available. Information on the HVAC system was limited to the type of components (i.e. CAV ventilation system, four-pipes fan coil units…) and nominal capacities of hot

and chilled water production devices (i.e. nominal capacity of the air cooled chiller and of the gas boilers). The limited amount of available data and the poor quality of this information (e.g. non-necessarily up-to-date information available in the as-built file) justifies the relatively broad ranges of variations considered for envelope (parameters #1 to #6) and HVAC system characteristics (parameters #13 to #26).

Default values (and relatively broad variation ranges) are used to describe building loads (i.e. occupancy, lighting and appliances loads densities and schedules; parameters #7, #8 and #29 to #36) and HVAC&R system operation (i.e. setpoints and schedules; parameters #9 to #12; #27 and #28) and performances (e.g. fans and pumps powers; humidifiers, boilers and chiller efficiencies…) since no information about building and system operation are available.

Table 10: List of influential parameters – Calibration Level 1

#	Variable	Unit	Description	Level 1	Min	Max
1	U_{hopw}	W/m²-K	Vertical walls U-value	2.25	0.6	2.25
2	$U_{gl,w}$	W/m²-K	Glazing U-value	3.12	1.26	3.12
3	$U_{fr,w}$	W/m²-K	Window frame U-value	4	1	4
4	$SHGC_{gl,0}$	-	Glazing normal SHGC	0.76	0.13	0.76
5	$C_{m/m²}$	J/m²-K	Thermal capacity	165000	110000	260000
6	ACH_{inf}	-	Infiltration rate	0.4	0.2	0.8
7	$IGFR_{light}$	W/m²	Lighting – Offices	12	10	14
		W/m²	Lighting – Meeting	12	10	14
		W/m²	Lighting – Storage	12	6	12
		W/m²	Lighting – Circulations + others	12	6	12
8	$IGFR_{appl}$	W/m²	Appliances – Offices	10	6	14
		W/m²	Appliances – Meeting	10	6	14
9	$T_{i,set,h,occ}$	°C	Heating indoor setpoint	21	19	23
10	$T_{i,set,h,nocc}$	°C	Heating indoor setpoint (night)	15	14	18
11	$T_{i,set,c,\ occ}$	°C	Cooling indoor setpoint	24	23	27
12	RH_{min}	-	Humidification indoor setpoint	0.5	0.4	0.6
13	ACH_{out}	-	Ventilation rate – Offices	1.25	1.1875	1.3125
		-	Ventilation rate – Meeting	4.66	4.427	4.893
		-	Ventilation rate – Storage	0.66	0.627	0.693
14	$\varepsilon_{hum,n}$	-	Humidifier efficiency	0.85	0.75	0.95
15	SFP_{sufan}	W/m³-s	Supply fan specific power	1750	500	3000
16	SFP_{retfan}	W/m³-s	Return fan specific power	1750	500	3000
17	$T_{a,ex,AHU,set,max}$	°C	Supply temperature setpoint	16	16	20
18	$k_{h,loss}$	-	Hot water network loss coefficient	0.01	0	0.02
19	$k_{c,loss}$	-	Chilled water network loss coefficient	0.025	0	0.05
20	$T_{hw,set}$	°C	Hot water temperature setpoint	80	60	80
21	$\eta_{hwboiler,n}$	-	Boiler efficiency	0.85	0.8	0.95
22	$f_{hwboiler,sbloss}$	-	Boiler standby losses coef.	0.005	0.001	0.01
23	SPP_{hw}	W/l-s	Hot water pump power	300	150	450
24	$T_{cw,set}$	°C	Chilled water temperature setpoint	7	6	10
25	$EER_{lcp,n}$	-	Chiller efficiency	3	2.5	3.5
26	SPP_{cw}	W/l-s	Chilled water pump power	350	175	525

27	$C_{sched,AHU}$	h	AHU daily operation time	12	10	14
28	$C_{sched,set}$	h	H&C system daily operation time	12	10	14
29	$A_{sched,occ}$	-	Occupancy rate (day time)	1	0.5	1
30	$C_{sched,occ}$	h	Daily occupancy time	10	8	12
31	$A_{sched,light}$	-	Lighting operation rate (day time)	1	0.5	1
32	$B_{sched,light}$	-	Lighting operation rate (night time)	0	0	0.5
33	$C_{sched,light}$	h	Lighting daily operation time	10	8	12
34	$A_{sched,appl}$	-	Appliances operation rate (day time)	1	0.5	1
35	$B_{sched,appl}$	-	Appliances operation rate (night time)	0	0	0.5
36	$C_{sched,appl}$	h	Appliances daily operation time	10	8	12

Accuracy and Calibration Criteria

The results of this first version of the model are presented below. Computed energy use data shown in Figure 21 corresponds to the "best guess" values given in Table 10. Both monthly natural gas and whole-building electricity consumptions are already quite well represented. Seasonal effect on the natural gas consumption is well represented by the model but the electricity consumption is underestimated, especially in summer.

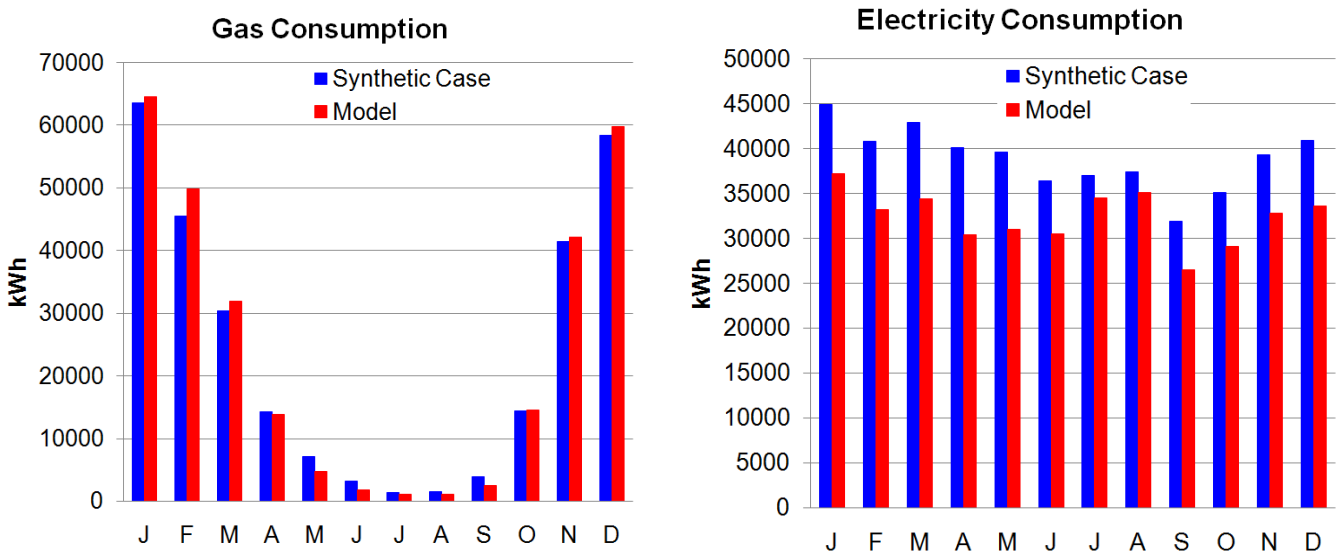

Figure 21: Level 1 - Consumption data comparison

Classical calibration accuracy indexes (MBE and CV(RMSE)) have been computed based on monthly data for whole-building gas, electricity, peak hours electricity and off-peak hours electricity consumptions. The two indexes have also been computed on a hourly basis for one winter week, one summer week and the whole year of whole-building electricity demand data (Table 11).

The values of the CV(RMSE) index confirms the good match between seasonal trends of synthetic and computed consumption data and satisfy the ASHRAE-14 (2002) criteria (15%). However, the MBE is over the tolerated value (5%). MBE and CV(RMSE) values for hourly electricity demand profiles are also over the tolerated values (respectively, 10% and 30%).

As suggested previously, it is also interested to evaluate these criteria based on monthly off-peak and peak electricity consumptions. The comparison of the four values shows that peak-electricity is relatively well predicted (low MBE and CV(RMSE) values) but of the off-peak electricity is largely underestimated (large negative value of MBE).

Table 11: Level 1 - Calibration errors

Errors	Monthly billing data				Whole-building hourly power demand		
	Gas	Electricity	Peak Electricity	Off-peak Electricity	Week 3 Electricity	Week 26 Electricity	1 year Electricity
	%	%	%	%	%	%	%
MBE	0.82	-16.73	-1.17	-90.79	-13.03	-26.09	-16.73
CV(RMSE)	7.47	18.42	6.83	95.00	65.81	73.02	80.18

The comparison of the synthetic and computed whole-building electricity demand profiles on an hourly basis is shown in Figure 22. Several observations can be made when looking at the average synthetic and predicted hourly profiles (respectively, the blue and red bold curves):

- Off-peak hours electricity demand is underestimated
- Considered operating schedules seem to be wrong since daily demand increases and decreases do not match
- Peak power demands are overestimated in winter and relatively well estimated in summer
- Electricity consumption on Saturday is not represented by the model

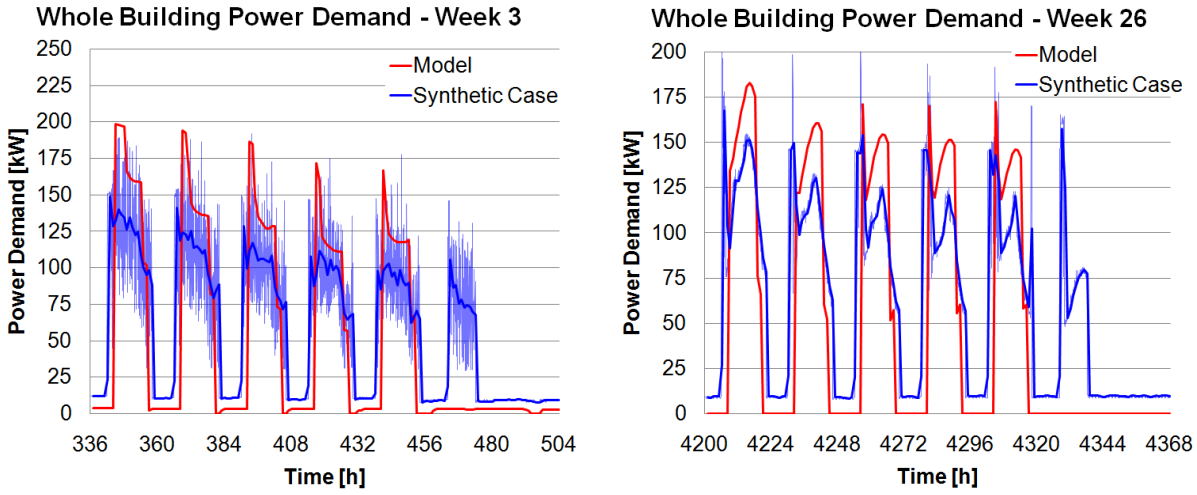

Figure 22: Level 1 - Whole building power demand comparison - Weeks 3 & 26

Simulation Results and Validity of the Calibrated Model

Despite of the low accuracy of this first version of the model and the high uncertainty on the input parameters, it is interesting to have a look to the simulation results and especially to the electricity consumption disaggregation (Figure 23). However, the lighting consumption seems to be overestimated comparing to the other items (36%). On the contrary, in temperate climates, the part of electricity consumption due to steam humidification is generally higher than 16%.

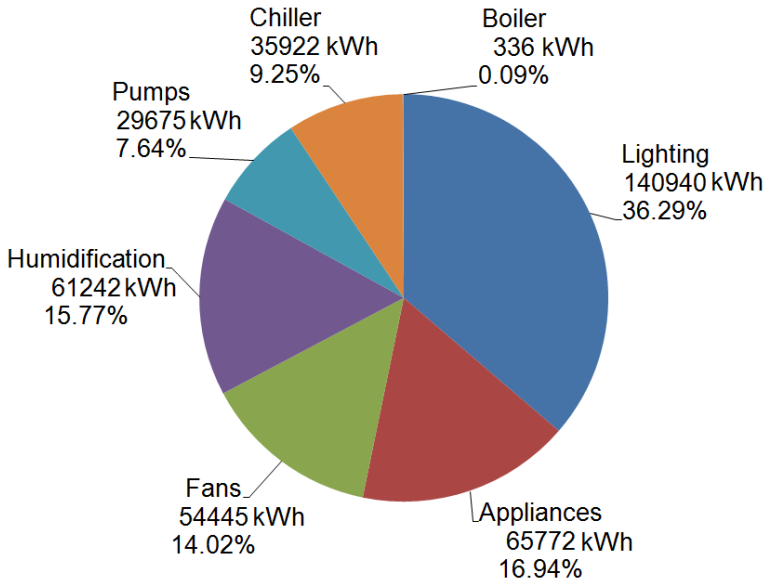

Figure 23: Level 1 – Annual electricity consumption disaggregation

Looking at the values given in Table 12 confirms such observations. Indeed, this initial version of the model tends to underestimate the chiller and humidifiers electricity consumptions in an important way. On the contrary, lighting consumption is largely overestimated comparing to the synthetic data.

Table 12: Level 1 - Electricity end-use

Use	Synthetic data kWh	Level 1 kWh	Deviation %
Lighting	107505	140940	31.10%
Appliances	79305	65772	-17.06%
Fans	56225	54445	-3.17%
Humidification	150510	61242	-59.31%
Pumps	19627	29675	51.19%
Chiller	52766	35922	-31.92%
Boiler aux.	405	336	-17.04%

Uncertainty on simulation outputs

The uncertainty on the results is quantified by means of Monte Carlo simulations. A LHMC (Latin Hypercube Monte Carlo) sampling is generated based on the range of variations given in Table 10. Uniform probability density functions have been arbitrarily considered for each parameter. As expected, the relatively broad ranges of variation lead to considerable uncertainties on the computed energy consumptions. Results are represented in box whisker mean plots (Figure 24 and Figure 25). Green bars correspond to the synthetic values generated by means of the test bed (Trnsys model). Blue stars correspond to the values predicted by the Matlab model under calibration already shown in Figure 21.

The results obtained by means of the LHMC uncertainty analysis are summarized as boxes and whiskers. Upper and lower edges of the blue boxes correspond to the 25th and 75th percentiles. The red line corresponds to the median value of the generated sample of values. The whiskers (dotted lines) extend to the most extreme values without considering outliers. Outliers are plotted separately (red

crosses). A data point is considered as an outlier if it is larger than $y^{75th} + 1.5*(y^{75th} – y^{25th})$ or lower than $y^{25th} – 1.5*(y^{75th} – y^{25th})$.

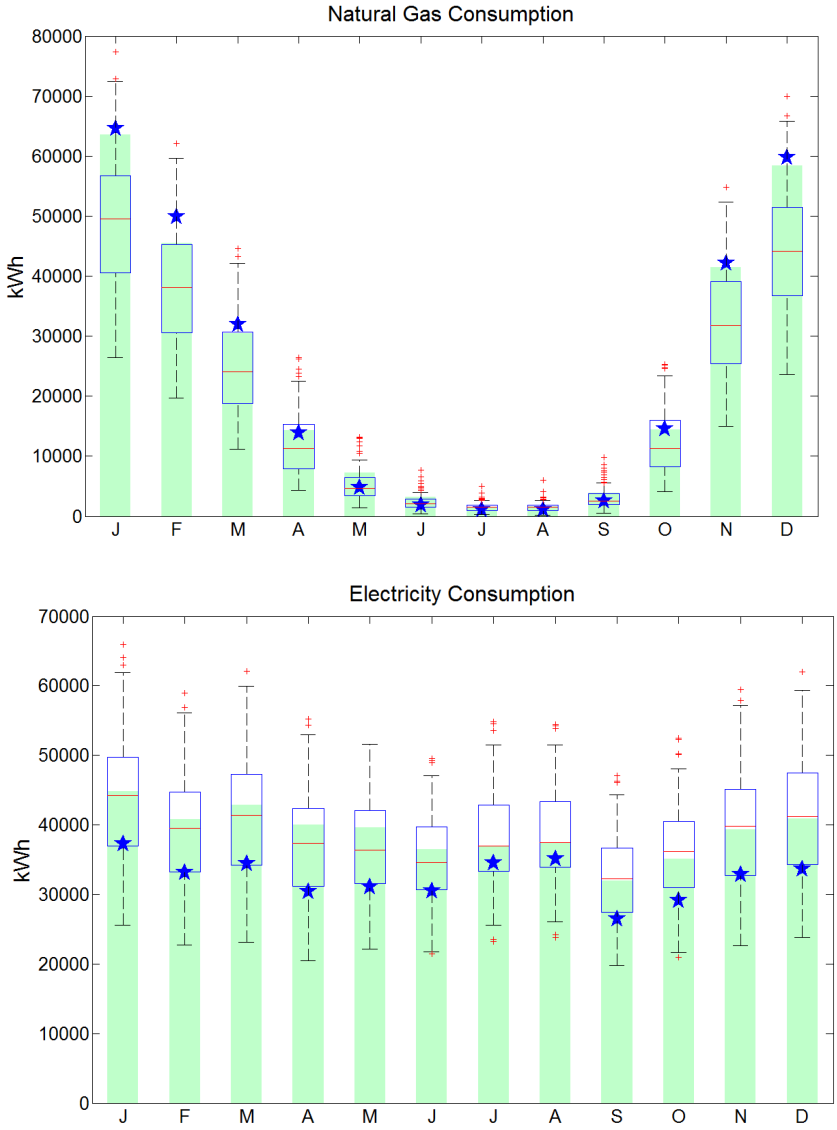

Figure 24: Level 1 - Uncertainty on predicted monthly gas and electricity consumptions

As expected, uncertainty ranges on the predicted values are quite large. Because of the non-linearity of the model and the fact that variation ranges of the considered parameters are not symmetric, the “best-guess” values (blue star) is sometimes quite far of the median.

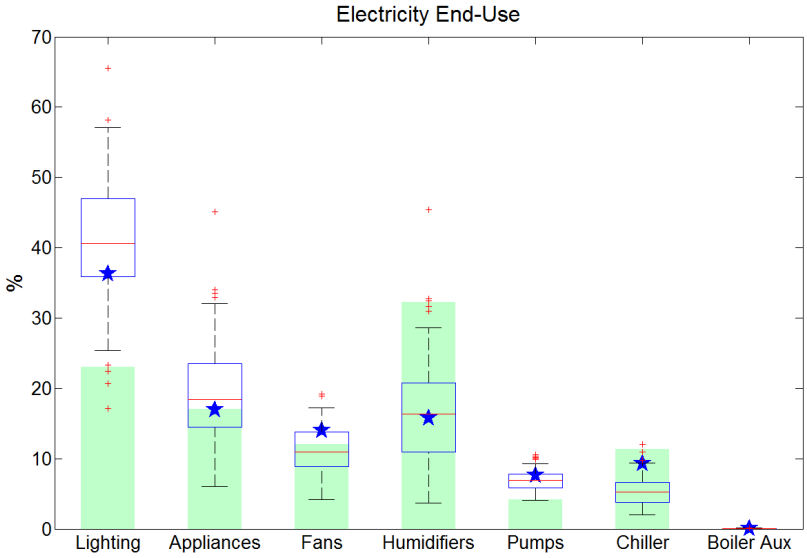

Figure 25: Level 1 - Uncertainty on predicted electricity consumption disaggregation

The results shown in Figure 25 confirm that this version of the model leads to a very high uncertainty on the predicted results. The quality of such results is clearly insufficient to allow accurate or meaningful analysis.

4.2.2. Level 2

The second level of calibration corresponds to on-site inspection. No physical measurements are done in the building but information about building and system operation and performance can be obtained by means of observations, surveys and interviews.

Before starting collecting additional data and exploiting it for calibration, it is needed to identify the most influential parameters requiring special attention and priority adjustment. The variation ranges resulting of the construction of the “as-built input file” (Calibration Level 1) will be used as a reference to generate a sample and run a sensitivity analysis. As explained before, the intent of such sensitivity analysis is two-fold:

- Reduce the dimensionality of the calibration by identifying strong and weak variables
- Identify and characterize the variables involved in high-order (non-linear) effects (i.e. interactions)

Preliminary Sensitivity Analysis

The results of the initial sensitivity analysis are shown below (Figure 26). Elementary effects of the influential parameters have been expressed in terms of seasonal gas and electricity consumptions (summer: April to September; winter: January to March and October to December) by means of the uncalibrated MATLAB model (Calibration Level 1 version). Influential categories of parameters have been highlighted. Envelope characteristics, ventilation flow rate, indoor heating temperature setpoint, heating plant characteristics and building use and system operation schedules have significant influence on the natural gas consumption. Winter electricity consumption is highly influenced by ventilation rate and humidity setpoint. Summer electricity consumption is directly related to cooling plant performance, glazing’s SHGC and indoor temperature setpoint. Internal loads densities and schedules have similar impact on both winter and summer consumptions.

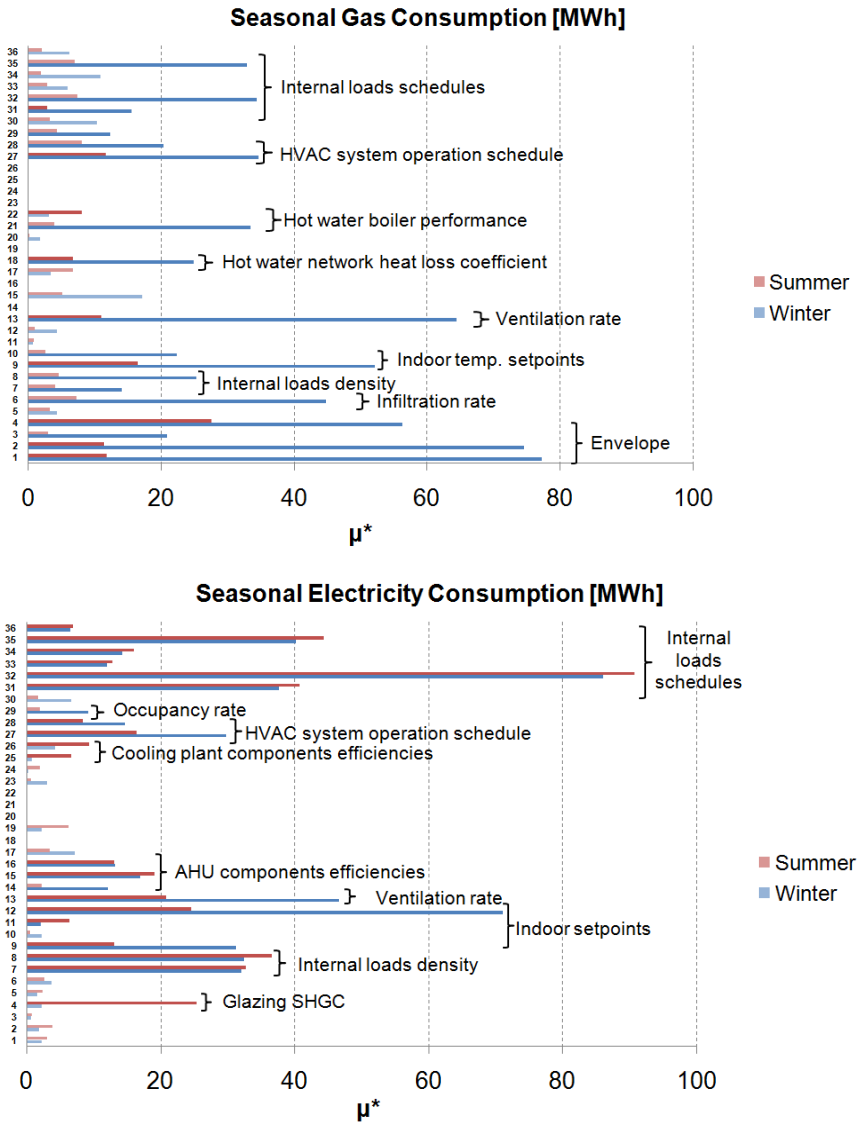

Figure 26: Results of the preliminary sensitivity analysis (Morris Method)

Regarding these conclusions, it appears that the identification of the ventilation rate, and to a lesser extent of the infiltration rate, are crucial issues. Unfortunately, these parameters are one of the most difficult to adjust since it is hard (if not impossible) to accurately measure the actual supply flow rate, to estimate duct leakages, flow rate distribution, infiltration… So, the current best guess value (corresponding to the design flow rate and an estimation of the infiltration rate) and actual range of variation (+/- 10% around the best guess value for the ventilation rate and +/- 50% for the infiltration rate) will not be updated during the calibration process.

Calibration process

During Level 2 calibration, the adjustment of the model's parameters will be done in four steps and will focus on the parameters highlighted by the sensitivity analysis (Figure 26):

- Firstly, the envelope characteristics will be collected and embedded in the model.
- Secondly, a detailed survey of the actually installed lighting and appliances powers will be done. Collected information will be used to update the internal loads densities.
- Thirdly, the analysis of the BEM system will allow to get accurate values of the operating schedules and conditions of the HVAC system and of some of the lighting fixtures (e.g. in the

circulations where lighting are directly controlled by the BEMS). Occupancy and building use schedules will also be updated.

- Fourthly, the collection of nameplate information and/or manufacturer data of some HVAC system components will allow specifying more accurate values of some parameters related to HVAC components performance (e.g. steam humidifier efficiency, chiller and boiler nominal efficiencies, etc.)

2a: envelope

At this level, the first step consists in collecting detailed envelope data. Such information can be obtained by collecting detailed architectural plans or by physical checking at different places in the building. The data provided in Table 24 have been used in order to identify the values of the ISO13790-2007 model as prescribed in ISO13786-2007 and ISO13789-2007.

Table 13: Walls characteristics

Wall	U W/m²-K	$C_{m,ISO13786}$ J/m²-K	SHGC -
External wall	0.97	81884	-
Floor slab	3.49	73430	-
Heavy internal wall	2.80	66823	-
Light internal wall	2.32	59912	-
Glazing	2.83	-	0.755 (p=3)
Frame	2.27	-	-

It is supposed that an arbitrary uncertainty of about +/- 10% remains on these values because of possible measurement errors on layers thicknesses in case of physical verification or bad practical implementation of wall layers prescribed on the architectural plans.

2b: envelope + internal loads

The second step consists in collecting information on load densities in the different zones of the building. The values proposed in Table 14 are based on corrected nameplate information and do not necessarily correspond to actual consumptions. As an example, desktops and screens installed in zone 1 have a total nameplate value of about 900W by workstation. As advised by Hosni and Beck (2008), the actual consumption in normal operation has been estimated to 10 to 15% of the nameplate value (i.e. 135W by work station) which gives a load density of 9.8 W/m².

The calculation of the installed lighting density is more direct and should include both fluorescent tube and ballast powers.

Table 14: Internal loads densities

Zone	Occupants	Lighting		Appliances	
		W/m²	Control	W/m²	Control
1	75	12	Manual	9.8	Manual
2	65	14	Manual	10	Manual
3	75	12	Manual	9.8	Manual
4	65	14	Manual	10	Manual
5	0	9	Automatic	0	-
6	0	6.15	Automatic	2.6	Manual

The uncertainty of the values given in Table 14 is supposed to be about +/- 5%. Of course, a larger uncertainty remains on the operating profiles of lighting fixtures and appliances in office and meeting rooms (zones 1 to 4) but no detailed information on the actual occupants' behavior are available at this stage.

2c: envelope + internal loads + BEMS

The analysis of the BEMS allows identifying actual ventilation and heating/cooling schedules and setpoints (Table 15). Lighting operating schedule in circulations is also imposed by the BEMS. The night-time lighting operating rate in this zone corresponds to 36% of the installed power density.

Lighting and appliances operating schedules in office and meeting rooms (zones 1 to 4) can only be estimated based on information collected during visits and interviews of the building manager/occupants. Appliances operation rate during night has been estimated to about 10% of the daily rate because of standby consumption.

Uncertainties on supply temperature and indoor humidity are related to the accuracy of the sensors connected to the BEMS. Probability ranges for indoor temperature setpoints in the occupied zones during occupancy hours are wider because of the authorized local temperature adjustment of +/- 1.5°C around the "base" setpoint imposed by the BEMS.

Table 15: Operating conditions and occupancy schedules

Item	Week	Saturday	Sunday	Uncertainty	Source
Ventilation	06:00 to 22:00	08:00 to 18:00	-	0	BEMS
Supply setpoint	18°C		-	+/- 0.5°C	BEMS
Heating/Cooling	06:00 to 22:00	08:00 to 18:00	-	0	BEMS
Heating setpoint	16/22°C 50%		16°C	+/- 0.5°C / +/- 1.5°C +/- 5%	BEMS
Cooling setpoint	24°C		-	+/- 1.5°C	BEMS
Occupancy	08:00 to 18:00	-	-	+/- 1h	Hypothesis
Appliances	08:00 to 18:00	-	-	+/- 1h	Hypothesis
Lighting	08:00 to 18:00	08:00 to 18:00	-	+/- 1h	Hypothesis/BEMS

2d: envelope + internal loads + BEMS + HVAC components characteristics

Survey of nameplates and manufacturer data sheets of HVAC system components are useful to identify nominal characteristics and performance indexes. Unfortunately, only nominal capacities and performance are usually available and the use of such values can lead to an overestimation of the related energy consumption. Moreover, at this stage, no information is generally available about part load performance.

Table 16: HVAC system components nominal characteristics

HVAC component characteristic	Unit	Value
Supply fan specific power	W/m³-s	1680
Return fan specific power	W/m³-s	1316
Hot water pump power	W/l-s	293
Chilled water pump power	W/l-s	376
Humidifier efficiency	-	0.82
Boiler efficiency	-	0.91
Chiller efficiency	-	3.1

A residual uncertainty of about +/-5% has been considered for the values given in Table 16. The final complete input file with the uncertainty range of each parameter is given in Table 17. Values noticed in bold have been adjusted during this phase of the calibration process. The values and the probability range of the other parameters have not been updated since Level 1.

Table 17: Level 2d - Input file with uncertainties

#	Variable	Unit	Description	Level 2	Min	Max
1	**U_{hopw}**	**W/m²-K**	**Vertical walls U-value**	**0.97**	**0.873**	**1.067**
2	**$U_{gl,w}$**	**W/m²-K**	**Glazing U-value**	**2.83**	**2.547**	**3.113**
3	**$U_{fr,w}$**	**W/m²-K**	**Window frame U-value**	**2.27**	**2.043**	**2.497**
4	**$SHGC_{gl,0}$**	**-**	**Glazing normal SHGC**	**0.755**	**0.6795**	**0.8305**
5	**C_{m/m^2}**	**J/m²-K**	**Thermal capacity**	**Table 13**	**-10%**	**10%**
6	ACH_{inf}	-	Infiltration rate	0.4	0.2	0.8
7	**$IGFR_{light}$**	**W/m²**	**Lighting – Offices**	**12**	**11.4**	**12.6**
		W/m²	**Lighting – Meeting**	**14**	**13.3**	**14.7**
		W/m²	**Lighting – Storage**	**9**	**8.55**	**9.45**
		W/m²	**Lighting – Circulations + others**	**6.15**	**5.84**	**6.46**
8	**$IGFR_{appl}$**	**W/m²**	**Appliances – Offices**	**9.8**	**9.31**	**10.29**
		W/m²	**Appliances – Meeting**	**10**	**9.5**	**10.5**
		W/m²	**Appliances – Circulations + others**	**2.6**	**2.47**	**2.73**
9	**$T_{i,set,h,occ}$**	**°C**	**Heating indoor setpoint**	**22°C**	**20.5°C**	**23.5°C**
10	**$T_{i,set,h,nocc}$**	**°C**	**Heating indoor setpoint (night)**	**16°C**	**15.5°C**	**16.5°C**
11	**$T_{i,set,c,\ occ}$**	**°C**	**Cooling indoor setpoint**	**24°C**	**22.5°C**	**25.5°C**
12	**RH_{min}**	**-**	**Humidification indoor setpoint**	**0.5**	**0.45**	**0.55**
13	ACH_{out}	-	Ventilation rate – Offices	1.25	1.1875	1.3125
		-	Ventilation rate – Meeting	4.66	4.427	4.893
		-	Ventilation rate – Storage	0.66	0.627	0.693
14	**$\varepsilon_{hum,n}$**	**-**	**Humidifier efficiency**	**0.96**	**0.936**	**0.984**
15	**SFP_{sufan}**	**W/m³-s**	**Supply fan specific power**	**1680**	**1428**	**1932**
16	**SFP_{retfan}**	**W/m³-s**	**Return fan specific power**	**1316**	**1118.6**	**1513.4**
17	**$T_{a,ex,AHU,set,max}$**	**°C**	**Supply temperature setpoint**	**18**	**17.5**	**18.5**
18	$k_{h,loss}$	-	Hot water network loss coefficient	0.01	0	0.02
19	$k_{c,loss}$	-	Chilled water network loss coefficient	0.025	0	0.05
20	$T_{hw,set}$	°C	Hot water temperature setpoint	80	79	81
21	**$\eta_{hwboiler,n}$**	**-**	**Boiler efficiency**	**0.92**	**0.874**	**0.966**
22	$f_{hwboiler,sbloss}$	-	Boiler standby losses coef.	0.005	0.001	0.01
23	**SPP_{hw}**	**W/l-s**	**Hot water pump power**	**293**	**249.05**	**336.95**
24	$T_{cw,set}$	°C	Chilled water temperature setpoint	7°C	6	8
25	**$EER_{lcp,n}$**	**-**	**Chiller efficiency**	**3.1**	**2.945**	**3.255**
26	**SPP_{cw}**	**W/l-s**	**Chilled water pump power**	**376**	**319.6**	**432.4**
27	**$C_{sched,AHU}$**	**h**	**AHU daily operation time**	**16**	**16**	**16**
28	**$C_{sched,set}$**	**h**	**H&C system daily operation time**	**16**	**16**	**16**
29	$A_{sched,occ}$	-	Occupancy rate (day time)	1	0.5	1

30	**$C_{sched,occ}$**	**h**	**Daily occupancy time**	**10**	**9**	**11**
31	$A_{sched,light}$	-	Lighting operation rate (day time)	1	0.5	1
32	$B_{sched,light}$	-	Lighting operation rate (night time)	0	0	0.5
33	**$C_{sched,light}$**	**h**	**Lighting daily operation time**	**10**	**9**	**11**
34	$A_{sched,appl}$	-	Appliances operation rate (day time)	1	0.5	1
35	$B_{sched,appl}$	-	Appliances operation rate (night time)	0.1	0	0.5
36	**$C_{sched,appl}$**	**h**	**Appliances daily operation time**	**10**	**9**	**11**

Accuracy and Calibration Criteria

The evolution of the monthly error indexes (MBE and CV(RMSE)) for each stage are shown in Table 18 and Figure 27.

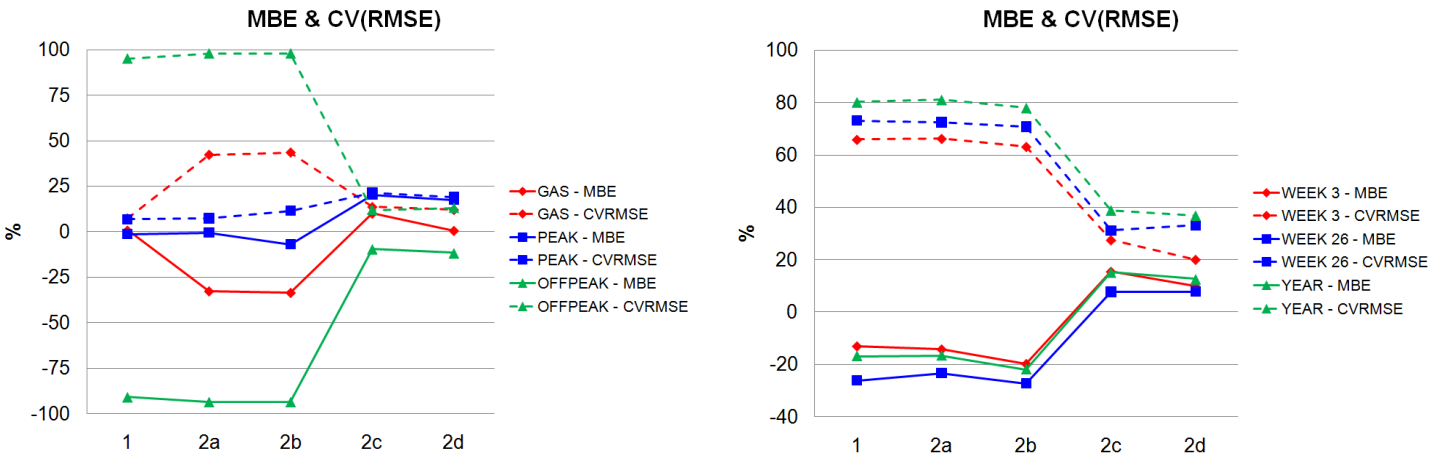

Figure 27: Levels 1 and 2 - Variations of the errors

As the data collection and the calibration of the model progress, most of the error indexes decrease. The evolution of the error indexes confirms the importance of the operating schedules. Indeed, progressing from step 2b to 2c (adjustment of operating and occupancy/use schedules) leads to a significant decrease of the errors between computed and actual (synthetic) monthly energy consumptions and hourly whole-building power demand profiles.

It is also interesting to notice the importance to consider each influential parameter, one after the other! **The successive increases and decreases of the error indexes highlight the non-linearities of the model and the possible compensation that can be encountered during the adjustment of the model's parameters. The use of a non-systematic or non-evidence-based methodology could lead to erroneous parameter adjustment and bad representation of the building under study.**

At the end of the Level 2 (2d), computed consumption data well matches with synthetic billing data. Only the mean bias error (MBE) of the natural gas consumption is above the criteria specified by ASHRAE-14 guideline (2002). The error indexes regarding recorded and predicted whole-building hourly electricity power demands are also within an acceptable range (less or about 10%).

Table 18: Levels 1 and 2 - Calibration errors

Step	Errors	Gas	Electricity	Peak Electricity	Off-peak Electricity	Week 3 Electricity	Week 26 Electricity	Hourly Electricity
		%	%	%	%	%	%	%
1	MBE	0.82	-16.73	-1.17	-90.79	-13.03	-26.09	-16.73
	CV(RMSE)	7.47	18.42	6.83	95.00	65.81	73.02	80.18
2a	MBE	-32.66	-16.55	-0.40	-93.44	-14.21	-23.33	-16.55
	CV(RMSE)	42.18	18.56	7.43	97.81	66.18	72.35	81.08
2b	MBE	-33.50	-21.84	-6.80	-93.47	-19.81	-27.24	-21.84
	CV(RMSE)	43.41	24.23	11.54	97.84	63.12	70.73	77.94
2c	MBE	10.13	15.22	20.42	-9.52	15.51	7.63	15.22
	CV(RMSE)	13.72	16.25	21.62	11.94	27.42	31.30	38.76
2d	MBE	0.63	12.60	17.70	-11.71	9.77	7.76	12.60
	CV(RMSE)	12.18	13.68	19.11	13.10	19.94	33.17	36.76

As shown in Figure 28, seasonal variations of the global energy consumptions are quite well represented by the calibrated model.

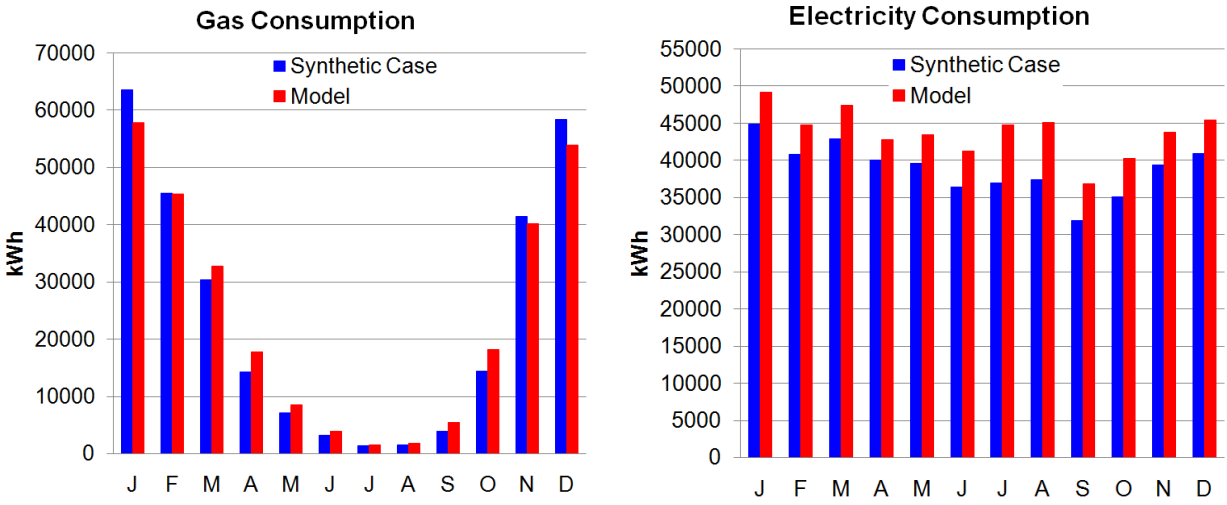

Figure 28: Level 2 - Consumption data comparison

The comparison of the electricity demand profiles (Figure 29) is also satisfying. The offpeak-hours electricity demand is well represented. The synchronization of the two profiles has also been largely improved comparing to Level 1 even if substantial differences remain when comparing peak values. The Saturday power demand is now represented by the model due to the correction of the operating profiles of lighting and HVAC systems.

In winter, the overestimation of the peak values can be due to an overestimation of the power demands of the HVAC components and an overestimation of the lighting and appliances operating rates. In summer, it is likely that the underestimation of the peak values is due to an underestimation of the cooling load (and consequently, of the chiller electricity consumption).

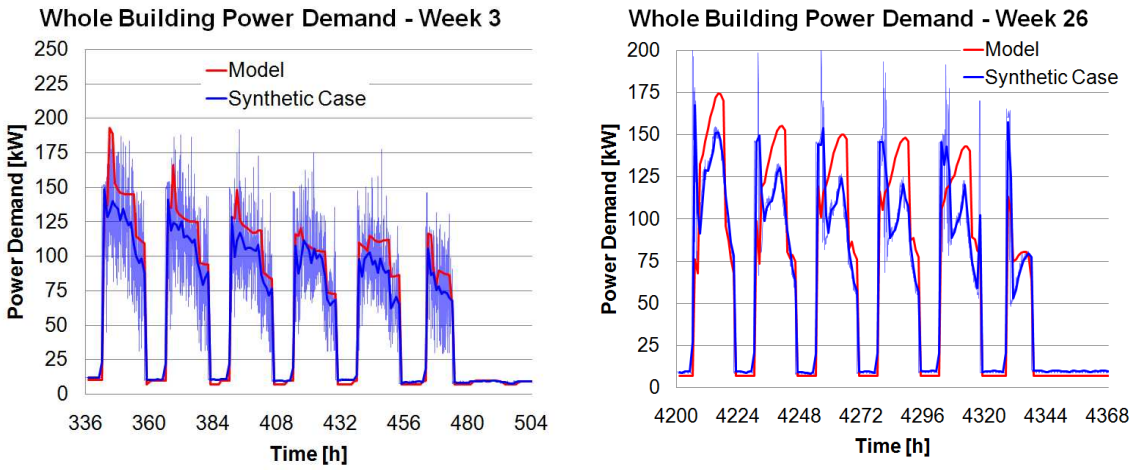

Figure 29: Level 2 - Whole building power demand comparison - Weeks 3 & 26

Simulation Results and Validity of the Calibrated Model

Once again, it is interesting to proceed to a post-calibration checking of the results by comparing the predicted end-use electricity consumptions to the synthetic data. The electricity disaggregation is now closer to the actual values (Figure 30), especially when looking at the humidifiers electricity consumption. However, it appears that even if the classical calibration criteria are (almost) satisfied, some substantial differences remain. Lighting, appliances, pumps and fans electricity consumptions are largely overestimated while humidifiers electricity consumption is largely underestimated (Table 19). These results are in good accordance with the conclusions of Westphal and Lamberts (2005) attesting that "rough" calibration lead to an acceptable representation of the global energy performance of the building but a bad prediction of the energy end-use.

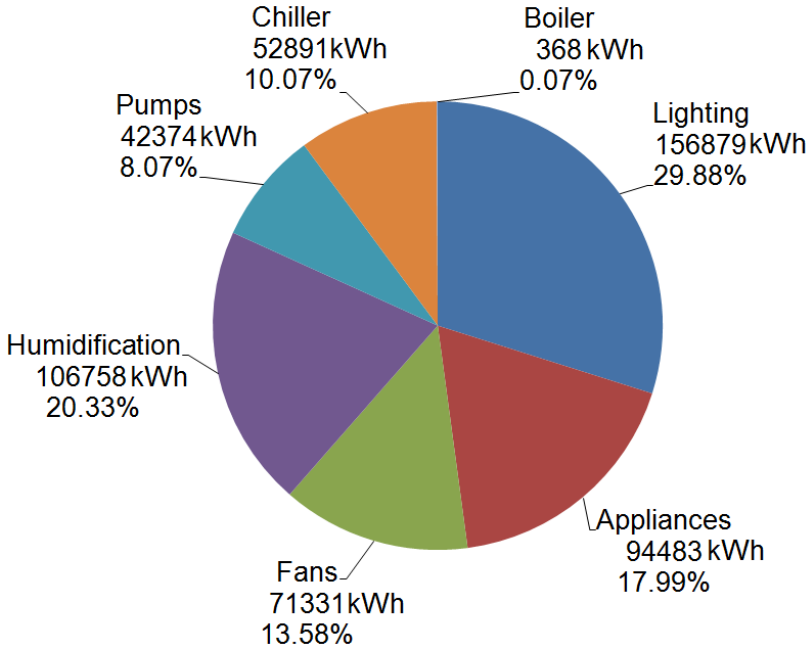

Figure 30: Level 2 - Electricity consumption disaggregation

Table 19: Level 2 - Electricity end-use

Use	Synthetic data kWh	Level 2d kWh	Deviation %
Lighting	107505	156879	45.93%
Appliances	79305	94483	19.14%
Fans	56225	71331	26.87%
Humidification	150510	106758	-29.07%
Pumps	19627	42374	115.90%
Chiller	52766	52891	0.24%
Boiler aux.	405	368	-9.14%

Uncertainty on simulation outputs

The LHMC sampling method has been applied to the probability ranges given in Table 17. As expected, the narrower probability ranges of some influential parameters lead to a reduction of the uncertainties on predicted consumptions (Figure 31 and Figure 32). However, the uncertainties remain significant and express an important variability of the calibrated model. Even if the model seems to be able to represent the main trends of the energy-use behavior of the considered building, the accuracy of the model is too limited to allow for accurate prediction of the energy performance of the building and accurate quantitative evaluation of Energy Conservation Measures (ECMs).

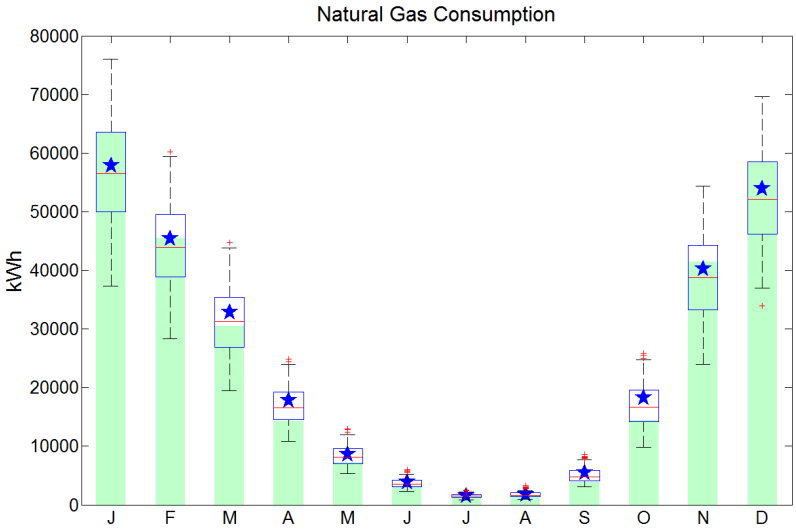

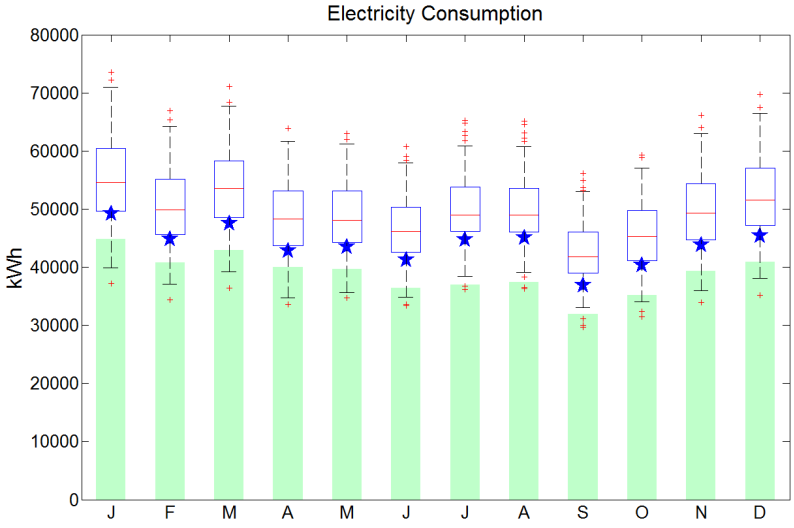

Figure 31: Level 2 - Uncertainty on predicted monthly gas and electricity consumptions

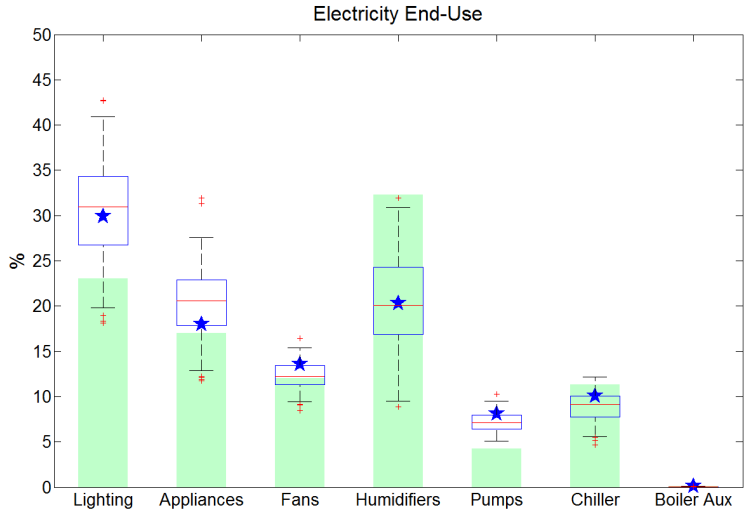

Figure 32: Level 2 - Uncertainty on predicted electricity consumption disaggregation

4.2.3. Level 3

The third calibration level corresponds to detailed audit. Additional physical measurements are conducted in the building in order to obtain detailed information about building and system operation and performance.

New sensitivity analysis

Since the values of numerous parameters have been updated during the second level of calibration, it is interesting to run a new sensitivity analysis with updated ranges of variations. A new Morris design has been constructed based on the values given in Table 17 in order to study the evolution of the hierarchy between most influential parameters (i.e. of the results of the screening process) during the calibration process. Running this new sensitivity analysis leads to the results shown in Figure 33.

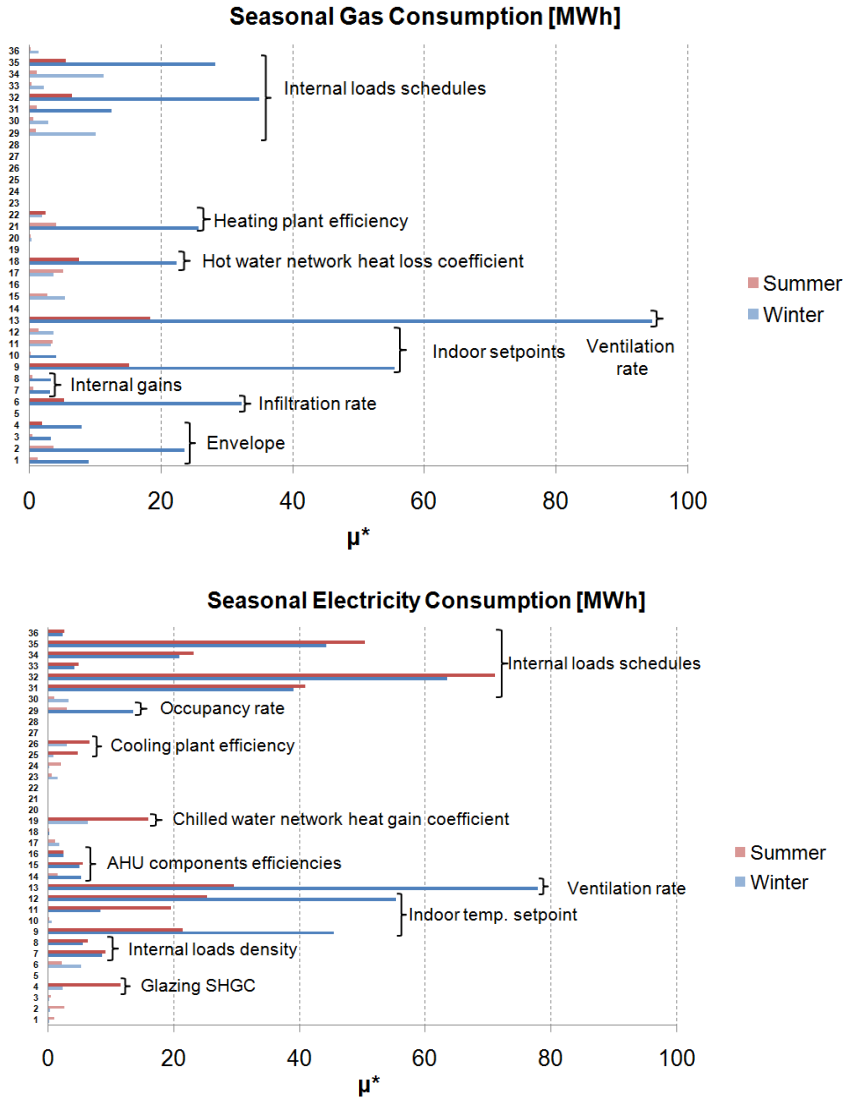

Figure 33: Results of the second sensitivity analysis (Morris Method)

Despite of the update of the variation ranges, the hierarchy between the parameters remains stable. Parameters initially identified as important still have a major impact on the predicted energy consumptions. Unsurprisingly, mechanical ventilation and infiltration rates have significant influences on the final energy consumption. Internal gains schedules and densities have a large impact on winter gas consumption and on both winter and summer electricity consumptions. Indoor temperature and humidity setpoints have also considerable influence. The last influential parameters

are the characteristics of hot and cold distribution networks and the performance of HVAC system components (fans, pumps, boilers and chiller). Envelope characteristics have now a more limited impact due to narrowed probability ranges.

Calibration process

Based on the results of the preliminary sensitivity analysis, the adjustment of the model's parameters during Level 3 calibration will be done in three steps and will focus on the parameters highlighted by the sensitivity analysis:

- Firstly, internal loads operating rates and schedules will be adjusted based on the analysis of power sub-metering data.
- Secondly, local temperature and humidity measurement data will be used to adjust the values of internal temperature and humidity setpoints
- Thirdly, HVAC components performance will be analyzed based on sub-metering data.

3a: Occupancy and operating rates and schedules

Power metering at floor level during the third week of the year gives the power curves shown in Figure 34. This measurement includes lighting and appliances consumptions only. Three distinct periods have been identified:

- 8 :00 to 18 :00 : Occupancy period – average power demand is about 10.6 kW
- 6 :00 to 8 :00 and 18 :00 to 22 :00 : pre and post-occupancy periods – average power demand is about 3.5 kW
- 22:00 to 6:00: night period – average power demand is about 1.7 kW

Base consumption during night period is supposed to be due to lighting fixtures controlled by the BEMS and to stand-by consumption of appliances. Pre and Post-occupancy periods corresponds to starting and ending times of the remaining lighting fixtures located in core zones. The increase of the electricity consumption during occupancy period is supposed to be directly linked to the occupants of the building (use of lighting and appliances in offices and meeting rooms). Based on installed power densities identified at Level 2, hourly operating rates have been identified and are given in the Appendix.

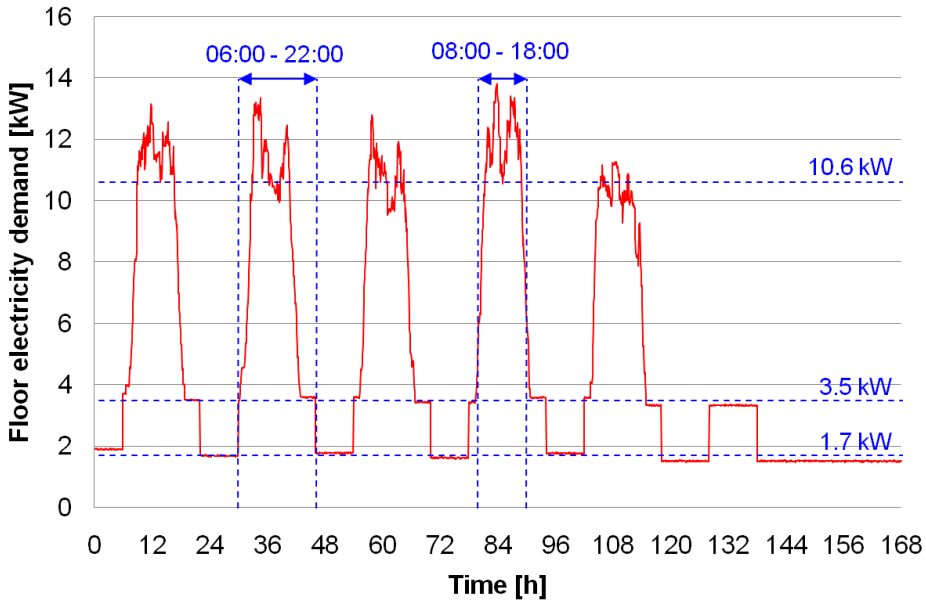

Figure 34: Synthetic power sub-metering at floor level (week 3)

Implementing the values given in the appendix and the corresponding schedules give the global power demand profile shown in Figure 35.

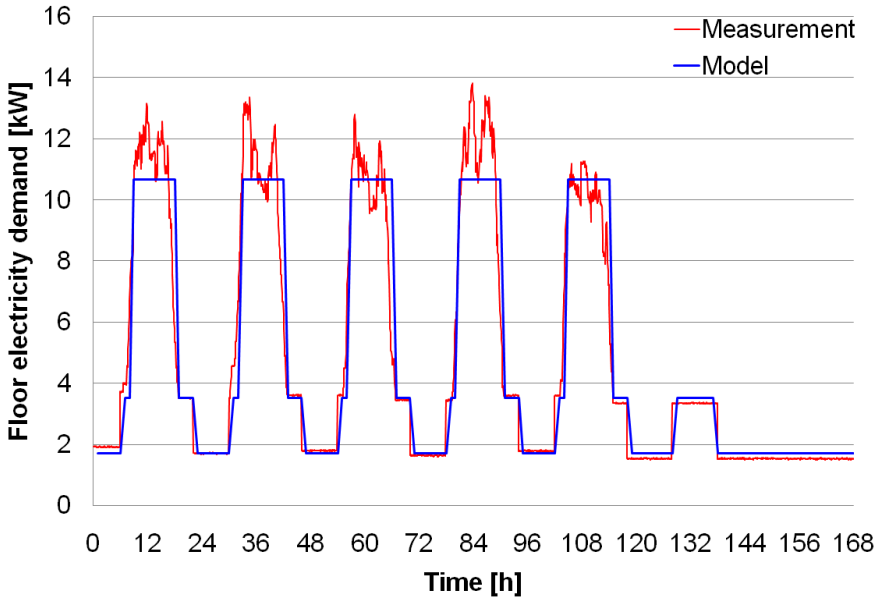

Figure 35: Comparison between measured and identified electricity demands at floor level (week 3)

Since starting and ending times have been fixed, no uncertainty is considered on time values. The maximal uncertainty on operating rates is supposed to be about +/- 15%. This uncertainty remains quite important because of the use of a unique (and arbitrarily selected) week of data to estimate these parameters. Moreover, the use of winter data does not allow estimating the impact of natural lighting on the use of artificial lighting in offices and meeting rooms. Such identification of the lighting use rates should lead to an overestimation of the total annual lighting electricity consumption.

3b: Indoor temperature and humidity setpoints

Local short-term measurements of temperature and relative humidity allow identifying achieved comfort in building zones. In order to identify both heating and cooling setpoints, measurements have been conducted on week 3 and week 26 (Table 20). Examples of measurements are shown in Figure 36. The blue curve is the “synthetic” value of the indoor temperature of room 1 (included in the Zone A in the simplified model). The red curve represents the “fictitious” measurement done with a resolution of 0.5°C.

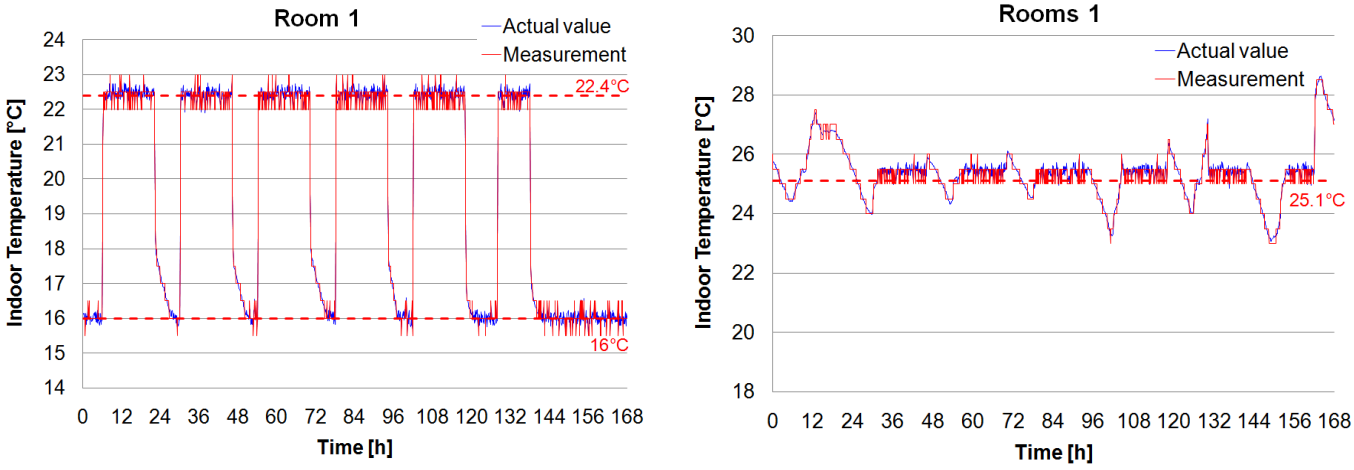

Figure 36: Indoor temperature synthetic measurements. Left: week3; Right: week 26

The measured values are summarized in Table 20. The final uncertainty on measured temperatures is supposed to be +/- 0.5°C.

Table 20: Identified heating and cooling setpoints

Zone	Winter (heating) setpoints	Summer (cooling) setpoints
	Temperature	Temperature
1	16 / 22.4 °C	25.1 °C
2	16 / 21.3 °C	24.9 °C
3	16 / 22.3 °C	24.4 °C
4	16 / 22.5 °C	24.6 °C
5	16 / 22.4 °C	23.8 °C

3c : puissances composants (ventilos et pompes)

Local (specific) power metering allows indentifying some performance indexes of some components of the HVAC plant. Global power demand of the AHU during a winter week includes supply and returns fans and steam generator. Regarding the synthetic measurements shown in Figure 37, two distinct power levels can be highlighted. The low power demand (9.6 kW) corresponds to the total power demand of the two constant-speed fans. Knowing the nameplate power of the supply fan and of the return fan (7 kW and 4 kW, respectively), and assuming that the actual-to-nameplate power ratio is similar for both components, the following ratios can be computed:

- Supply fan actual (estimated) power demand: $\frac{9.6}{11} * 7 = 5.98\ kW$ → 1436 W/m³-s (for a nominal flow rate of 15000 m³/h instead of the previous value of 1680 W/m³-s)
- Return fan actual (estimated) power demand: $\frac{9.6}{11} * 4 = 3.42\ kW$ → 1125 W/m³-s (for a nominal flow rate of 10940 m³/h instead of the previous value of 1316 W/m³-s)

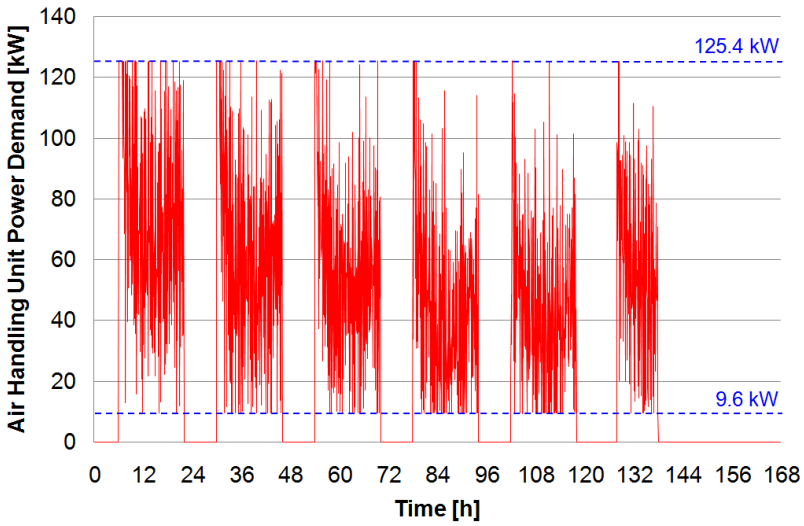

Figure 37: AHU power demand synthetic measurement – Week 3

Assuming that the nameplate-to-actual power ratio is similar for the additional extraction fan (extracting vitiated air from the core zones), the actual power demand of this last component is supposed to be: $\frac{9.6}{11} * 1 = 0.86\ kW$.

The high level power demand (125.4 kW) corresponds to the full load operation of the steam humidifier. In these conditions, the actual power demand of 115.8 kW (125.4 – 9.6 kW) should

correspond to a maximal (nominal) steam flow rate of 150 kg/hr. These values correspond to value of the wire-to-steam efficiency of 95%, which is in fair agreement with the nominal (nameplate) value considered above.

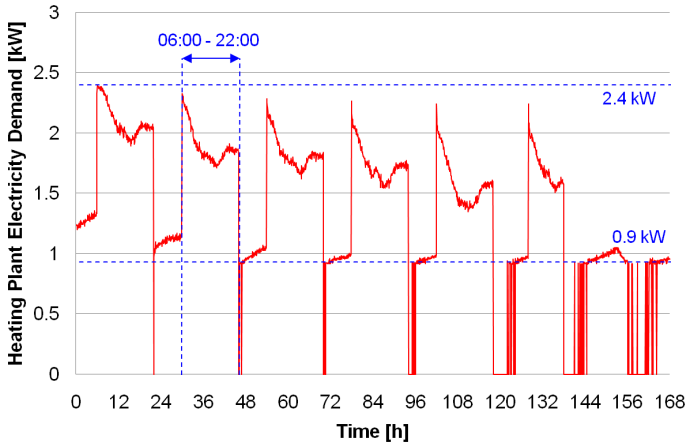

Figure 38: Heating plant power demand synthetic measurement – Week 3

The metering of the heating plant power demand includes the burners' auxiliaries (fans) and the primary and secondary hot water pumps (Figure 38). Considering that the two burners' fans consume about 400W each, the maximal pumping power demand corresponds to about 1600W (and so to a global specific pumping power of 273 W/kg-s for a primary water flow rate of 5.85 kg/s). Such an estimation of the pumping power demand will certainly lead to an overestimation of the annual pumping consumption. However, a more detailed description and metering of the plant would be required to perform more detailed (and accurate) calculations. Using global power metering as done here does not allow going further in details.

Similar (synthetic) measurements can be performed on the cooling plant side (Figure 39). The separated metering of chiller and plant power demands allows distinguishing chiller and pumping consumptions. The average power demand for pumping is estimated to 6.8 kW. Considering a primary chilled water flow rate of 25.83 kg/s, this leads to a global specific pumping power of 263 W/kg-s.

Since no measurement of the cooling load is performed, it is not possible to deduce any information about the chiller performance at this stage.

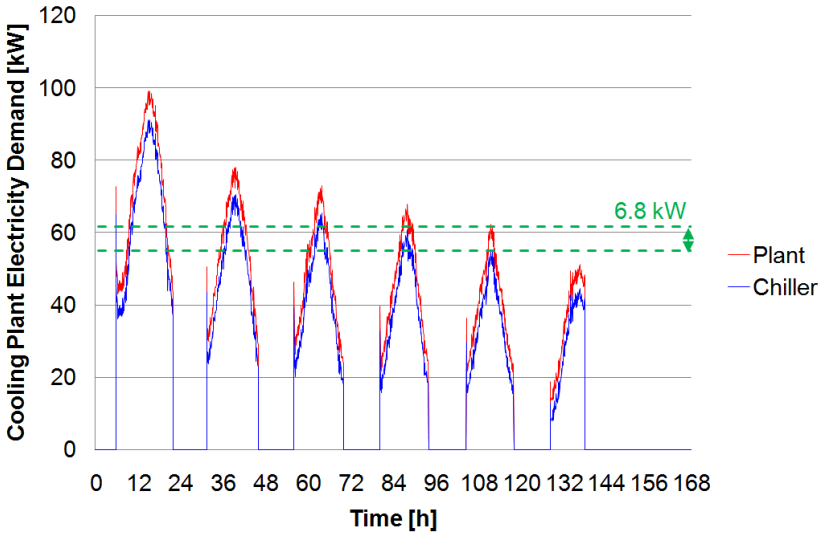

Figure 39: Cooling plant power demand synthetic measurement – Week 26

The final uncertainty on the estimated values is supposed to be about +/- 5% because of the measurement error and of the assumptions introduced to analyze the recorded data (estimation of specific values based on non-measured values of air and water flow rates, etc.).

The final Level 3 input file with the corresponding uncertainty range of each parameter is given in Table 21. Values noticed in bold have been adjusted during this phase of the calibration process. The values and the probability ranges of the other parameters have not been updated since Level 2.

Table 21: Level 3c - Input file with uncertainties

#	Variable	Unit	Description	Level 3c	Min	Max
1	U_{hopw}	W/m²-K	Vertical walls U-value	0.97	0.873	1.067
2	$U_{gl,w}$	W/m²-K	Glazing U-value	2.83	2.547	3.113
3	$U_{fr,w}$	W/m²-K	Window frame U-value	2.27	2.043	2.497
4	$SHGC_{gl,0}$	-	Glazing normal SHGC	0.755	0.6795	0.8305
5	$C_{m/m²}$	J/m²-K	Thermal capacity	Table 13	-10%	10%
6	ACH_{inf}	-	Infiltration rate	0.4	0.2	0.8
7	$IGFR_{light}$	W/m²	Lighting – Offices	12	11.4	12.6
		W/m²	Lighting – Meeting	14	13.3	14.7
		W/m²	Lighting – Storage	9	8.55	9.45
		W/m²	Lighting – Circulations + others	6.15	5.84	6.46
8	$IGFR_{appl}$	W/m²	Appliances – Offices	9.8	9.31	10.29
		W/m²	Appliances – Meeting	10	9.5	10.5
		W/m²	Appliances – Circulations + others	2.6	2.47	2.73
9	**$T_{i,set,h,occ}$**	**°C**	**Heating indoor setpoint**	**Table 20**		
10	**$T_{i,set,h,nocc}$**	**°C**	**Heating indoor setpoint (night)**			
11	**$T_{i,set,c,occ}$**	**°C**	**Cooling indoor setpoint**			
12	**RH_{min}**	**-**	**Humidification indoor setpoint**			
13	ACH_{out}	-	Ventilation rate – Offices	1.25	1.1875	1.3125
		-	Ventilation rate – Meeting	4.66	4.427	4.893
		-	Ventilation rate – Storage	0.66	0.627	0.693
14	**$\varepsilon_{hum,n}$**	**-**	**Humidifier efficiency**	**0.95**	**0.926**	**0.974**
15	**SFP_{sufan}**	**W/m³-s**	**Supply fan specific power**	**1436**	**1364**	**1508**
16	**SFP_{retfan}**	**W/m³-s**	**Return fan specific power**	**1125**	**1069**	**1181**
17	$T_{a,ex,AHU,set,max}$	°C	Supply temperature setpoint	18	17.5	18.5
18	$k_{h,loss}$	-	Hot water network loss coefficient	0.01	0	0.02
19	$k_{c,loss}$	-	Chilled water network loss coefficient	0.025	0	0.05
20	$T_{hw,set}$	°C	Hot water temperature setpoint	80	79	81
21	$\eta_{hwboiler,n}$	-	Boiler efficiency	0.92	0.874	0.966
22	$f_{hwboiler,sbloss}$	-	Boiler standby losses coef.	0.005	0.001	0.01
23	**SPP_{hw}**	**W/l-s**	**Hot water pump power**	**273**	**260**	**287**
24	$T_{cw,set}$	°C	Chilled water temperature setpoint	7°C	6	8
25	$EER_{lcp,n}$	-	Chiller efficiency	3.1	2.945	3.255
26	**SPP_{cw}**	**W/l-s**	**Chilled water pump power**	**263**	**250**	**276**
27	$C_{sched,AHU}$	h	AHU daily operation time	16	16	16
28	$C_{sched,set}$	h	H&C system daily operation time	16	16	16
29	**$A_{sched,occ}$**	**-**	**Occupancy rate (day time)**	**Table 28**		

30	**$C_{sched,occ}$**	**h**	**Daily occupancy time**	**Table 29**
31	**$A_{sched,light}$**	**-**	**Lighting operation rate (day time)**	**Table 30**
32	**$B_{sched,light}$**	**-**	**Lighting operation rate (night time)**	
33	**$C_{sched,light}$**	**h**	**Lighting daily operation time**	
34	**$A_{sched,appl}$**	**-**	**Appliances operation rate (day time)**	
35	**$B_{sched,appl}$**	**-**	**Appliances operation rate (night time)**	
36	**$C_{sched,appl}$**	**h**	**Appliances daily operation time**	

Accuracy and Calibration Criteria

The evolution of the calibration error indexes is shown in Table 22 and Figure 40. The evolution of the error indexes between steps 2d and 3a confirms the large impact of the internal loads schedules on the quality of the calibrated model. The two last steps (3b and 3c) allow reducing the uncertainty on indoor temperature setpoints and on the performance of the main HVAC components but do not lead to an important reduction of the errors. At the end of Level 3 (step 3c), all the error indexes are very low for both monthly consumptions and hourly demands and the criteria defined in ASHRAE 14-2002 are satisfied (except the natural gas consumption MBE slightly over 5%). The calibrated model seems able to reproduce the energy behavior of the building in an acceptable way at seasonal, monthly, daily and hourly levels.

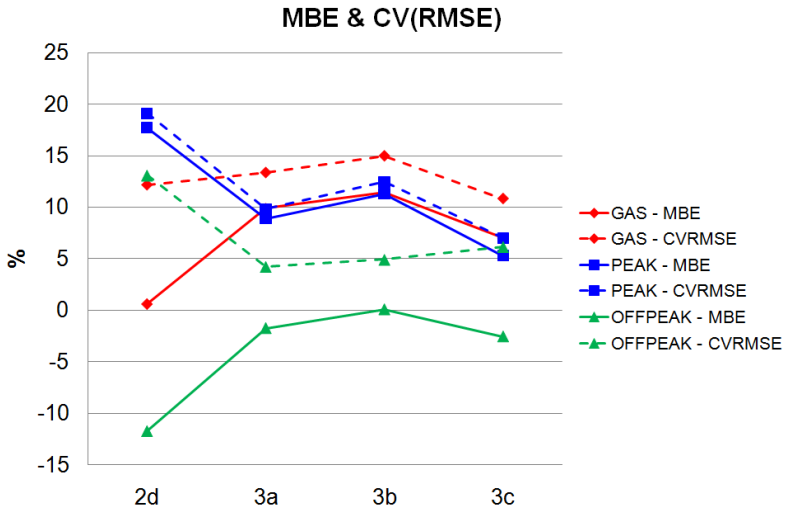

Figure 40: Levels 2 and 3 - Variations of the errors

Table 22: Levels 2 and 3 - Calibration errors

Step	Errors	Gas	Electricity	Peak Electricity	Off-peak Electricity	Week 3 Electricity	Week 26 Electricity	Hourly Electricity
		%	%	%	%	%	%	%
2d	**MBE**	0.63	12.60	17.70	-11.71	9.77	7.76	12.60
	CV(RMSE)	12.18	13.68	19.11	13.10	19.94	33.17	36.76
3a	**MBE**	9.90	7.09	8.94	-1.71	8.57	2.27	7.08
	CV(RMSE)	13.37	7.99	9.84	4.22	16.93	25.42	25.63
3b	**MBE**	11.43	9.34	11.28	0.11	12.50	4.58	9.34
	CV(RMSE)	15.00	10.62	12.51	4.91	20.81	25.03	26.83
3c	**MBE**	**7.02**	**3.94**	**5.30**	**-2.52**	**8.40**	**-2.28**	**3.94**
	CV(RMSE)	**10.83**	**6.05**	**7.05**	**6.16**	**17.50**	**23.33**	**24.22**

Both monthly gas and electricity consumptions are well represented by the model (Figure 41). In both case, the calibrated model leads to a slight over-estimation of the gas consumption, especially in winter. This might be due to a bad estimation of the infiltration flow rate (not measured).

The remaining errors should be put in perspective with the discrepancy noticed between the simplified model and detailed simulation models during the validation of the former (see Chapter 2). As reminder, the prediction errors on predicted heating and cooling demands were of a few percents (2 to 8%).

The electricity consumption is also overestimated during cold months (e.g. January to March) and hot periods (July and August). These overestimations can be explained by the rough estimation of the pumping electricity consumption (more important during the months requiring intensive operation of heating and cooling systems), by the supposed constant use of artificial lighting and by the lack of information about actual building occupancy (no information about holidays…etc).

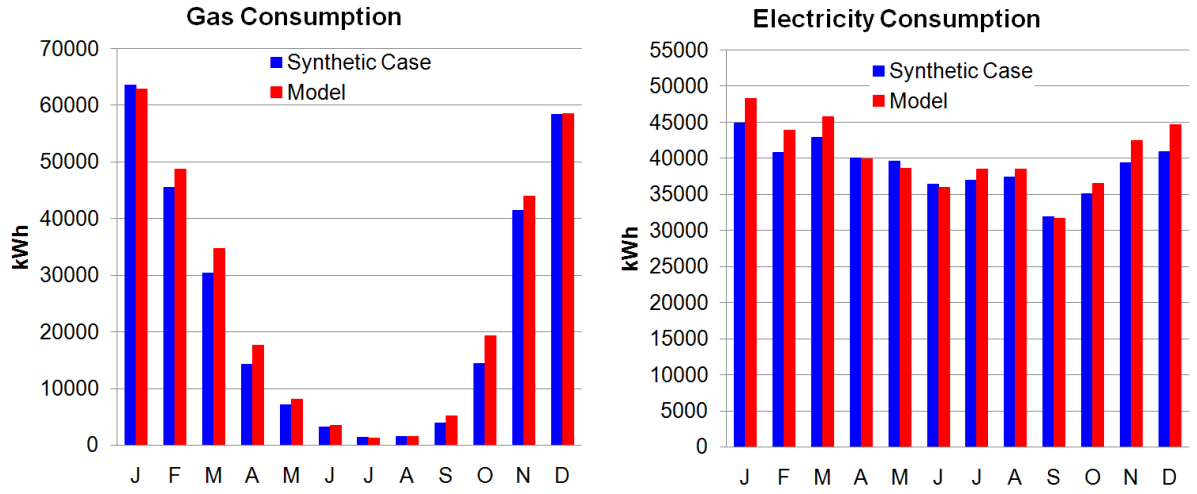

Figure 41: Level 3 - Consumption data comparison

Whole-building power demand profiles are satisfyingly reproduced by the calibrate model. In winter (week 3), peak electricity consumption is slightly overestimated and the MBE is about 8%. In summer (week 26), the agreement is better and the MBE is below 3%.

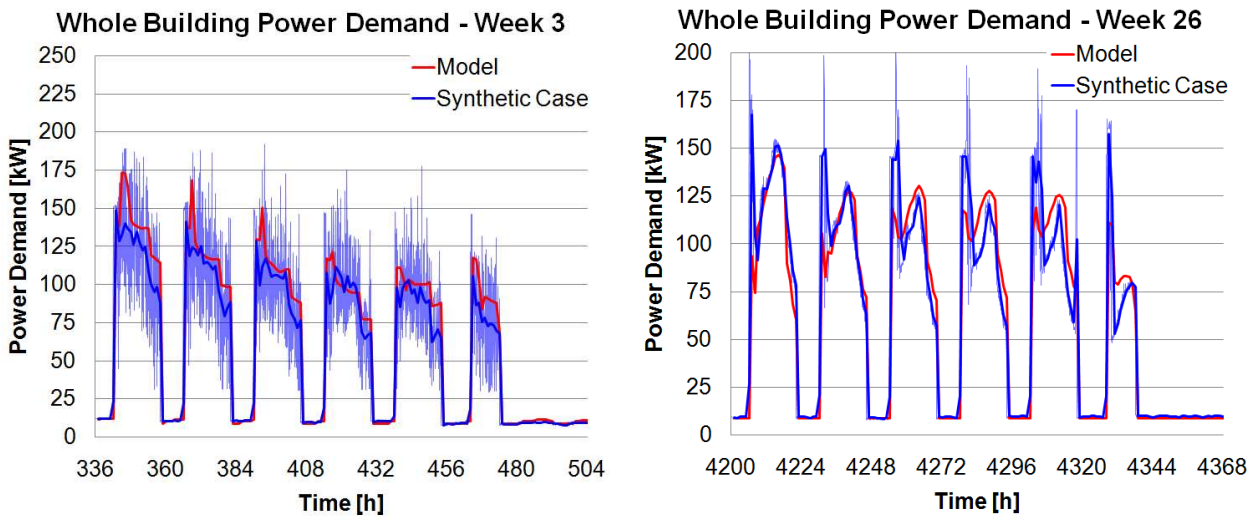

Figure 42: Whole building power demand comparison - Weeks 3 & 26

Simulation Results and Validity of the Calibrated Model

The post-calibration checking of the results is shown in Figure 43 and Table 23. The electricity disaggregation is again closer to the actual values.

As mentioned above, an overestimation of the lighting electricity consumption remains due to the use of a constant lighting use profile, not taking into account of the less intensive use of artificial lighting during summer. Appliances, fans and boilers auxiliaries consumptions are in a fair agreement. Humidifier and chiller electricity consumptions are now quite well estimated (errors of 10 and 13%, respectively). As expected, the adjustment of the pumping powers allowed reducing the gap between actual and predicted consumptions. However, the deviation remains significant and can mainly be explained by the very simple pump model used in the Matlab code (use of constant Specific Pump Power values and no simulation of the pumping curves). A better adjustment would need more detailed and specific monitoring in order to identify actual power consumptions and operating behavior of each pump. These results also confirm that an evaluation of the uncertainty of the model's outputs is absolutely necessary.

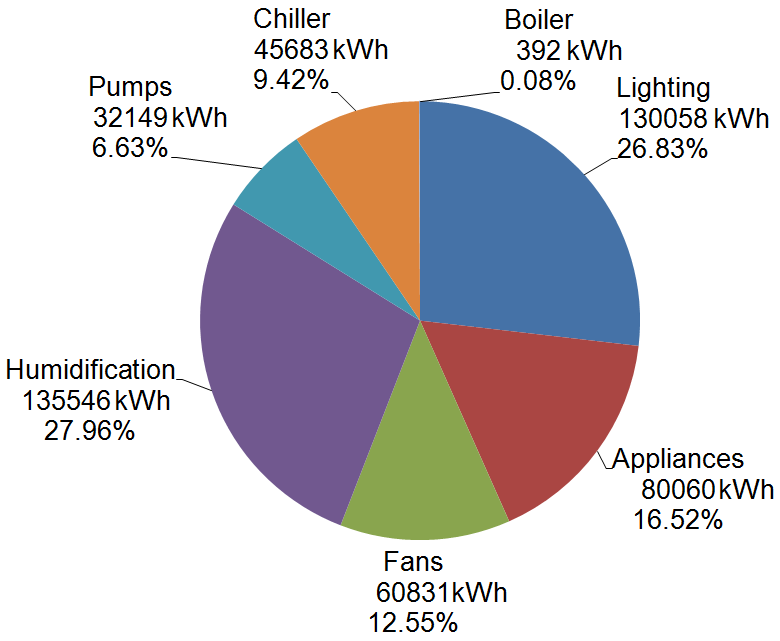

Figure 43: Level 3 - Electricity consumption disaggregation

Table 23: Level 3 - Electricity end-use

Use	Synthetic data kWh	Level 3c kWh	Deviation %
Lighting	107505	130058	20.98%
Appliances	79305	80060	0.95%
Fans	56225	60831	8.19%
Humidification	150510	135546	-9.94%
Pumps	19627	32149	63.80%
Chiller	52766	45683	-13.42%
Boiler aux.	405	392	-3.21%

Uncertainty on simulation outputs

At this stage, it is hoped that uncertainties on predicted energy use is small enough to allow considering the model as able to predict the energy consumptions of the building and to allow accurate enough evaluation of some ECO's. Error ranges estimated by means of the LHMC method and using uniform probably density functions and the uncertainty ranges given in Table 21 are shown in Figure 44 and Figure 45. In general, computed uncertainty ranges are approximately two times smaller than the ones estimated at Level 1.

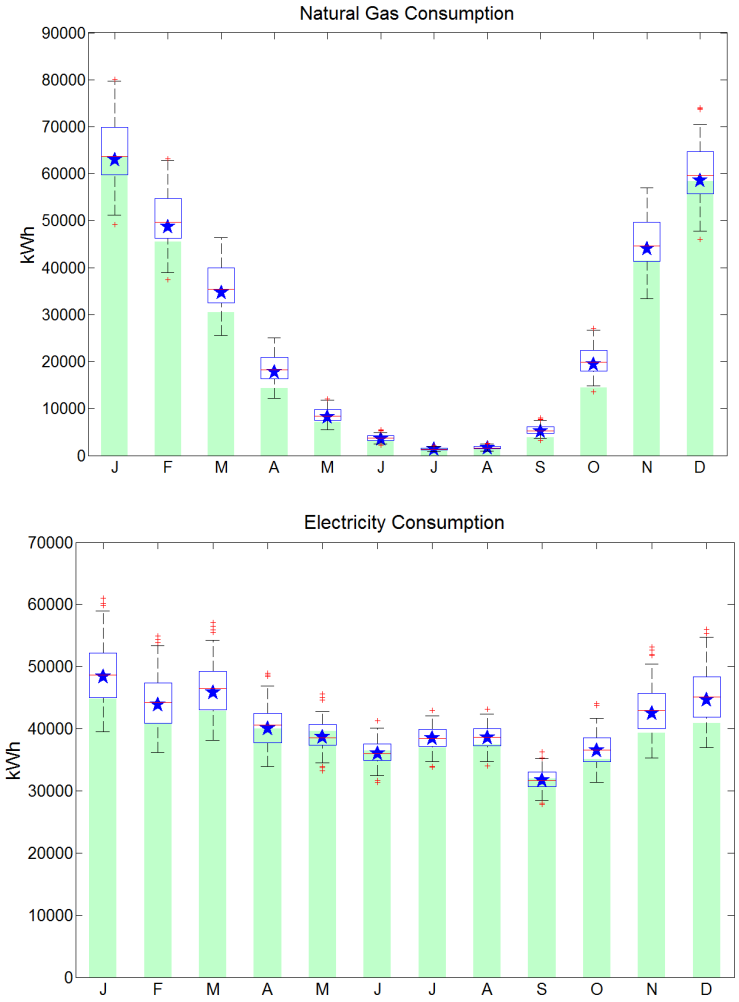

Figure 44: Level 3 - Uncertainty on predicted monthly gas and electricity consumptions

When looking at Figure 45, it appears that the actual pumping consumption is not within the predicted range. This can be explained by the very simplified representation of the pumps operation integrated in the simplified model used to perform calibration (pumps are consolidated and supposed to operate as soon a heating/cooling demand appears). So, it appears that the considered uncertainty range is too small and that the variability of the pumping power is higher than expected in the present case.

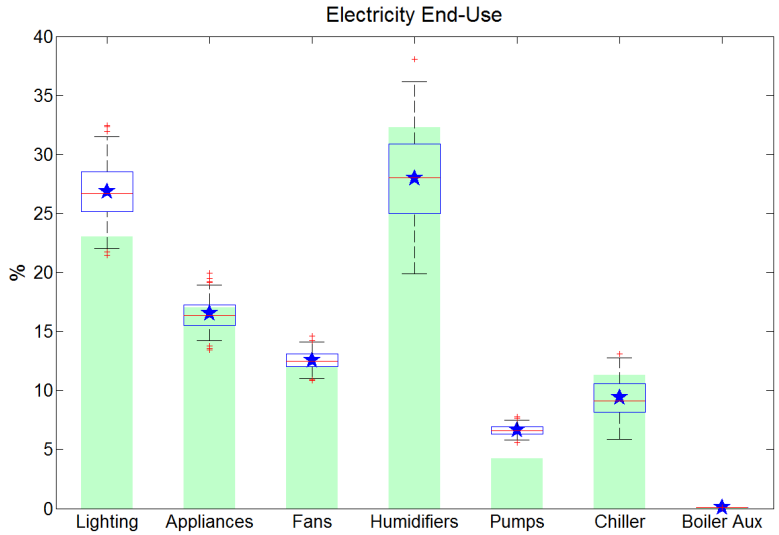

Figure 45: Level 3 - Uncertainty on predicted electricity consumption disaggregation

As mentioned in a previous chapter, such error ranges are quite pessimistic because of the use of uniform probability density functions. Indeed, at this stage, the best guess values (represented by the blue stars) might be considered as the mean of a normal distribution. In order to set the shape of the normal distribution, the uncertainty ranges of each parameter could be supposed, for example, to correspond to 99.7% confidence intervals.

5. CONCLUSION

Advantages and limits of the Virtual Calibration Test Bed

The development of a virtual calibration test bed has been detailed in the present chapter. Such synthetic case is dedicated to the evaluation and the improvement of the calibration methodology described in Chapters 3 and 4. A detailed sub-hourly dynamic building simulation model including numerous influences (variable infiltration rate, thermal bridges…) is coupled to a detailed HVAC system model controlled by realistic control loops. Variable stochastic internal gains and operation profiles have been generated and supply the simulation model in order to obtained realistic energy use profiles.

Synthetic energy use profiles have been compared and standard energy use profiles (generated by the same model supplied with standard “sharp” operation profiles). It was interesting to note that the detailed simulation model was able to reproduce realistic energy consumption data, whatever variable stochastic profiles were used or not. **Variable stochastic profiles appeared to be very useful in order to generate realistic sub-hourly energy use profiles but have very little influence on globalized energy consumption data (e.g. monthly energy bills)**. It should be noticed that it is believed that occupancy and operating profiles are much more chaotic in reality.

Using such synthetic case to evaluate a calibration method allowed avoiding some parasitic influences which are often encountered in practice such as:

- The uncertainty on the energy billing/recorded data
- The uncertainty on the weather data (the same weather data file were used in both models)
- Potential (manual/stochastic) changes in the operation of the building/HVAC system

Other issues that have to be tackled in general rely on the control of the HVAC system that has been modeled in an ideal way in the present virtual test bed (e.g. no hysteresis, etc.).

Finally, we have to keep in mind that the results generated by such virtual test bed remain synthetic and are not physical/actual data. However, whatever the number of influences and variations taken into account, the data generated by means of such test bed can be considered as representative of a given reality that it intends to emulate, even if the generated data are exactly similar to the ones that could be collected in real building under operation.

Quality of the calibration and data collection issues

Errors between predicted and actual monthly energy consumptions have been significantly reduced all along the calibration progress**. The initial as-built model (Level 1) already produced interesting results but was not reliable.**

The Level 2 calibration produced also an acceptable representation of the energy behavior of the building but uncertainties remained too important to allow true quantitative analysis of the building energy use. At this stage (corresponding to a typical energy audit/inspection), it was estimated that the calibrated model was not able to allow accurate quantitative evaluation of ECOs but was able to represent the main trends of the energy behavior of the building.

Additional (synthetic) measurements performed to build the Level 3 model were useful and allowed refining the values of some critical parameters. **At the end of this third calibration level, the calibrated model was able to predict the building energy performance with a satisfying accuracy.**

It is also important to note that, in real buildings, the base load consumption is generally higher than in the present synthetic case, so that uncertainties on variable loads (weather and occupancy dependent loads) have less influence on the final energy consumption.

Even if the Level 3 model provides satisfyingly reliable results, it has to be mentioned that some influences initially integrated in the virtual test bed were not detected during the calibration process. Thermal bridges and condensation in terminal units had a too limited impact to be highlighted by means of the available information and measurement data. However, such influences are “integrated” within the uncertainty ranges.

It is interesting to note that even if classical error indexes were useful to characterize the quality of the calibrated model at the beginning of the calibration process (steps 1 to 2c or 2d), these too global indexes were not helpful when having to refine the adjustment of the model. Indeed, as soon as these global criteria are satisfied (acceptable values of the errors since step 2d), the trends (increase or decrease of an error indexes comparing to another) were no more significant in the last steps of the calibration process. Indeed, even if the classical/global statistical indexes were low, it was shown that the predicted energy performance (electricity consumption disaggregation) was not in good agreement with the (synthetic) reality. **This can be explained by the definitions of the two indexes themselves. Indeed, with a very limited amount of data points (12 monthly in the present case), the information provided by the CV(RMSE) is not “rich” enough to characterize the accuracy of the model.** However, the study of these indexes stay relatively interesting when working with more values (24 or 36 monthly values or 8760 hourly values).

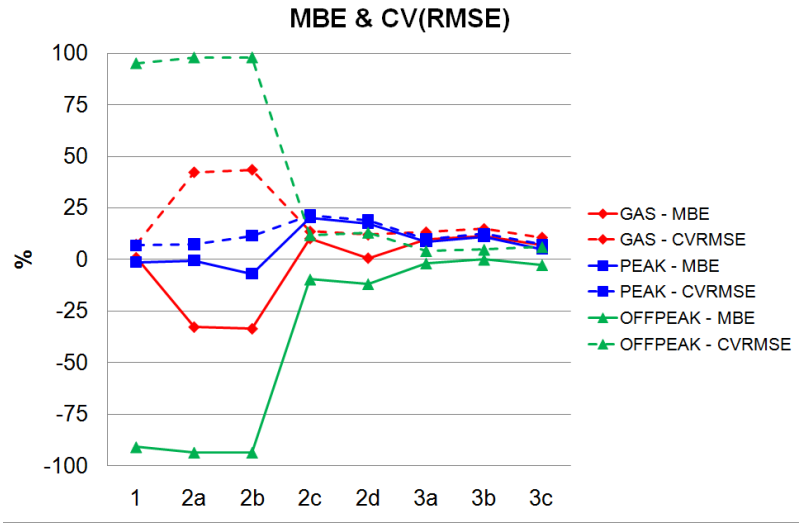

Figure 46: Levels 1 to 3 - Variations of the errors (monthly consumptions)

This confirms that, in addition to such global/statistical criteria, additional practical/direct comparisons, verifications and critical analyses of the predicted results are needed to assist the modeler and characterize the quality of the calibrated model.

The study of the whole-building electricity demand profile (generally provided on a quarter-hourly or hourly basis) was of a great help to check the quality of the calibrated model. Even if seasonal effects on this demand profile are generally limited (the larger part of the demand is generally due to lighting, appliances and base loads), the use of such profile is very helpful to check the good adjustment of operating schedules (steps 2b to 2c and 2d to 3a) and to identify potential discrepancies (such as in Figure 22 at Level 1) between the model and the reality.

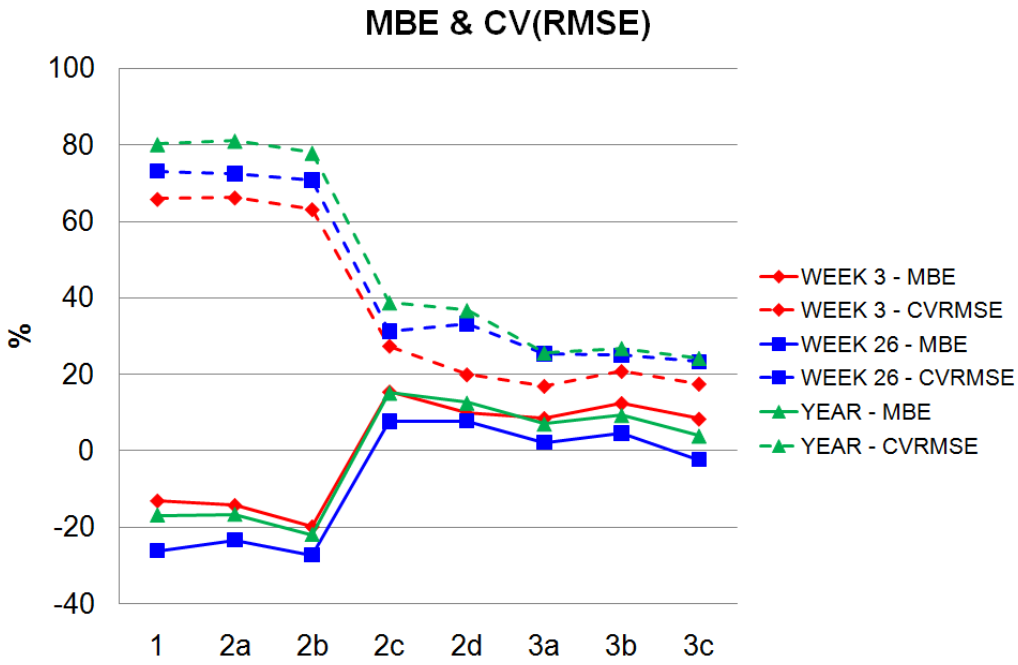

Figure 47: Levels 1 to 3 - Variations of the errors (WBE demand profiles)

Additional/local measurements were also of a great help to identify more accurate values of some parameters of the model and to allow verification of the simulation results produced by the calibrated model. Local electricity demand metering at floor level was a very valuable measurement

since it allowed identifying more accurately building occupancy/use schedules and operating rates. Local temperature measurements were also helpful and led to a better representation of the achieved levels of temperature and humidity.

Sensitivity and uncertainty issues

In general, one can say that, in parallel with quantitative mathematical evaluations of the calibrated model, modeler's experience remains important. Whatever the mathematical criteria used to quantify the quality of the calibration, it appears as crucial to criticize the outputs of the model in order to identify discrepancies.

However, in order to avoid exclusively relying on modeler's knowledge and experience, it was shown that the use of a sensitivity analysis (or screening) method such as the Morris method was of a great help to guide the user during this complex process. At the beginning of the calibration process, the first application of the sensitivity method was very helpful in order to screen the model parameters and identify influential ones. As the calibration process progressed, the uncertainty ranges were narrowed and it was possible to up-date the classification between influential and less-influential (secondary) parameters. **The conclusions of these sensitivity analyzes were very helpful to focus on critical issues and orient the data collection work**. It is also interesting to note that, despite of the narrowing of the range as the calibration was progressing; **the main conclusions of the screening method remained valid all along the process.**

Specifying uncertainty ranges for the parameters also allowed applying the LHMC method in order to compute the global uncertainty on the simulation results. At the end of each stage, it was possible to run an uncertainty analysis by considering a probability distribution for each parameter. It was decided to consider the most pessimistic situation and to use uniform distribution. Indeed, since the final uncertainty ranges are (almost) symmetric around the identified "best guess" values, it could be convenient to consider that the uncertainty is normally distributed around this value. In this case, the boundaries of the uncertainty range could be seen as the boundaries of the 95 or 99.7% confidence intervals. Of course, following such idea, the computed uncertainties are smaller than the ones obtained by means of uniform distributions.

Finally, this calibration exercise allowed highlighting the complexity and the limits of calibration as it is used today. Global energy consumption data do not allow satisfying adjustment of relatively detailed dynamic building energy simulation models**. Influences and interactions are aggregated in such a way that very global data (monthly final energy bills) cannot be used to study the energy behavior of the installation under study. Accurate enough calibrated models can be developed only after additional measurements and significant efforts and work**.

Further work

Next improvements of the test bed would consist in replacing some of the arbitrary stochastic profiles (e.g. random correction of indoor temperature setpoints, meeting room occupancy and use) used in the present model by deterministic or probabilistic behavioral models (e.g. occupant's comfort model). However, only little information is available in the literature. Other improvements could consist in adding physical effects such as ducts and pipes fouling, more realistic and detailed dynamic boiler and chiller models… A better representation of the air flows in the building (by means of a dynamic interzonal flow model) would also help in representing heat and mass transfers between zones in a more realistic manner.

A fourth calibration level might be investigated and could consist in a continuous improvement of the model developed at Level 3. This fourth level could be helpful to refine some parameters by means of continuous monitoring of lighting, appliances and HVAC components consumptions. More specific

metering should be envisaged at this stage (such as water flow measurements) in order to check the performance of some HVAC components (chiller, boilers…). This last stage is out of the scope of this work since it has been decided to focus on the initial development of a calibrated model.

Finally, it could be envisaged to express the calibration criteria on shorter periods by collecting energy consumption data at a higher frequency (weekly or daily). **Short-time step energy metering and data should allow to check the validity of the calibrated model in a more accurate way** but require long-term and more detailed monitoring that could be out of scope of the first steps of an energy efficiency service process.

The definition of new calibration criteria could be study in parallel with the possibility to implement an automatic adjustment process in order to refine the calibration of the model at the end of the evidence-based process. Indeed, **the application of the evidence-based process (steps 1 to 3c) allowed to considerably reducing the dimension of the calibration problem** so that **the use of an optimization-based method** to adjust the values of the influential but non-measurable (or not "easily" measurable) parameters **could be envisaged**.

6. REFERENCES

ASHRAE. 1981. ASHRAE Handbook Fundamentals – Chapter 26. American Society of Heating, Refrigerating and Air-conditioning Engineers, Inc., Atlanta.

ASHRAE. 2002. ASHRAE Guideline: Measurement of energy and demand savings. ASHRAE Guideline 14-2002. American Society of Heating, Refrigerating and Air-Conditioning Engineers, Inc.

BBRI, Kantoor2000: Study of Energy Use and Indoor Climate in Office Buildings, 2001.

Bertagnolio, S., Andre, P. 2010. Development of an Evidence-Based Calibration Methodology Dedicated to Energy Audit of Office Buildings. Part 1: Methodology and Modeling, in: 10th REHVA World Congress Clima 2010. Available at: http://hdl.handle.net/2268/29291

Bourdouxhe, J.-P., Grodent, M., Lebrun, J., Saavedran C. 1999. ASHRAE HVAC1 Toolkit : A Toolkit for Primary System Energy Calculation. Atlanta : American Society of Heating, Refrigerating and Air-Conditioning Engineers, Inc.

EN-15251. 2007. Indoor environmental input parameters for design and assessment of energy performance of buildings addressing air quality, thermal environment, lighting and acoustics.

Hensen, J.L.M., Clarke, J.A. 2000. State-of-the-art and future work in building and system simulation, Proc. Simulace Budov**,** Prague, Czech Republic.

Hoes, P., Hensen, J.L.M., Loomans, M., de Vries, B., Bourgeois, D. 2009. User behavior in whole building simulation, Energy and Buildings 41.

Klein, S.A. 2008. EES: Engineering Equation Solver, User manual. F-chart software. Madison: University of Wisconsin-Madison, USA.

Klein, S.A., 2010. TRNSYS 16 Program Manual. Solar Energy Laboratory, University of Wisconsin, Madison, USA.

Lee, S., Claridge, D. 2002. Automatic calibration of a building energy simulation model using a global optimization program. ICEBO 2002.

Lemort, V., Rodriguez, A., Lebrun, J. 2008. Simulation of HVAC Components with the Help of an Equation Solver. IEA SHC Task 34 / ECBCS Annex 43 – Subtask D report.

Lemort, V., Bertagnolio, S. 2010. A Generalized Simulation Model of Chillers and Heat Pumps to be Calibrated on Published Manufacturer's Data. International Symposium on Refrigeration Technology, Zhuhai, China.

Liu, M., Claridge, D.E., Bensouda, N., Heinemeir, K., Lee, S.U., Wei, G. 2003. Manual of Procedures for calibrating simulations of building systems, HPCBS#E5P23T2b. California Energy Commission, Public Interest Energy Research Program.

Mansson, L.G., McIntyre, D. 1997. Technical Synthesis Report. A Summary of IEA Annexes 16 and 7. Building Energy Management Systems. International Energy Agency Energy Conservation in Building and Community Systems Programme. http://www.ecbcs.org/annexes/annex17.htm

MATLAB, 2009. Matlab user manual, The Mathworks Inc., http://www.mathworks.com, Natick, USA.

Morisot, O., Marchio, D. 2002. Simplified Model for the Operation of Chilled Water Cooling Coils Under Nonnominal Conditions. HVAC&R Research 8(2): 135-158.

Parys, W., Saelens, D., Hens, H. 2011. Coupling of dynamic building simulation with stochastic modeling of occupant behavior in offices – a review-based integrated methodology. Journal of Building Performance Simulation. First published on: 11 February 2011 (iFirst).

Purdy, J., Beausoleil-Morrison, I. 2011. The significant factors in modeling residential buildings. Proceedings of the seventh International IBPSA conference, Rio de Janeiro, Brazil.

Reddy, T.A., Maor, I. 2006. Procedures for reconciling computer-calculated results with measured energy data. ASHRAE Research Project 1051-RP.

Reinhart, C.F. 2004. "Lightswitch 2002: A model for manual control of electric lighting and blinds", Solar Energy 77:1 pp. 15-28.

Sfeir, A., Bernier, M., Million, T., Joly, A. 2005. A Methodology to Evaluate Pumping Energy Consumption in GCHP Systems. ASHRAE Transactions OR-05-7-3.

Subbarao, K. Burch, J.D., Hancock, C.E., Lekov, A., Balcomb, J.D. 1988. Short-Term Energy Monitoring (STEM): Application of the PSTAR method to a residence in Fredericksburg, Virginia. SERI/TR-254-3356, Solar Energy Research Institute, Golden, CO.

Walton, G. 1983. Thermal analysis research program reference manual (TARP). NBSIR 83-2655. Washington, D.C.: National Bureau of Standards. In Judkoff, R., Neymark, J. 1995. IEA Building Energy Simulation Test and Diagnostic Method. NREL, U.S. D.O.E.

Westphal, F.S., Lamberts, R. 2005. Building Simulation Calibration using Sensitivity Analysis. Proceedings of the 9th IBPSA Building Simulation Conference, Montréal, Canada.

Wetter, M. 2011. Co-simulation of building energy and control systems with the Building Control Virtual Test Bed. Journal of Building Performance Simulation, vol. 3 (4).

Yoon, J., Lee, J.E., Claridge, D.E. 2003. Calibration procedure for energy performance simulation of a commercial building, Journal of Solar Energy Engineering 125, 251-257.

7. APPENDIX

7.1. WALLS COMPOSITION

Table 24: Walls layers (outside to inside)

Wall	Layer	thickness m	Cond. W/m-K	Spec. heat J/kg-K	Density kg/m³
External wall	Light concrete	0.07	0.37	840	1200
	Extruded polystyrene	0.02	0.034	1470	35
	Reinforced concrete	0.15	2.2	840	2400
	Plaster	0.01	0.42	840	1200
Heavy internal wall	Plaster	0.01	0.42	840	1200
	Reinforced concrete	0.15	2.2	840	2400
	Plaster	0.01	0.42	840	1200
Light internal wall	Plaster	0.08	0.42	840	1200

7.2. BUILDING FLOOR GEOMETRY

Table 25: Building floor geometry

#	Type	Floor area m²	Volume m³	Ext. Wall area m²				Window area m²			
				N	E	S	W	N	E	S	W
1	Office	54	167.4	18	-	-	-	19.2	-	-	-
2	Office	54	167.4	18	-	-	-	19.2	-	-	-
3	Office	54	167.4	18	-	-	-	19.2	-	-	-
4	Office	31.5	97.65	6.75	12.1	-	-	7.2	9.6	-	-
5	Office	13.5	41.85	-	4.5	-	-	-	4.8	-	-
6	meeting	45	139.5	-	16.6	6.75	-	-	14.4	7.2	-
7	Office	54	167.4	-	-	18	-	-	-	19.2	-
8	Office	54	167.4	-	-	18	-	-	-	19.2	-
9	Office	54	167.4	-	-	18	-	-	-	19.2	-
10	Office	31.5	97.65	-	-	6.75	12.1	-	-	7.2	9.6
11	Office	13.5	41.85	-	-	-	4.5	-	-	-	4.8
12	meeting	45	139.5	6.75	-	-	16.6	7.2	-	-	14.4
13	stairs	21	65.1	-	-	-	-	-	-	-	-
14	kitchen	17.5	54.25	-	-	-	-	-	-	-	-
15	copy	21	65.1	-	-	-	-	-	-	-	-
16	sanitaries	28	86.8	-	-	-	-	-	-	-	-
17	storage	49	151.9	-	-	-	-	-	-	-	-
18	kitchen	17.5	54.25	-	-	-	-	-	-	-	-
19	stairs	21	65.1	-	-	-	-	-	-	-	-
20	circulation	221	685.1	-	-	-	-	-	-	-	-

7.3. FAN COIL UNIT SIMULATION MODEL

The FCU model relies on the coupling of the Trnsys building model (Type56) and its built-in indoor temperature controller and some Type581 (Multi-dimensional interpolation) components. This

solution has been preferred to a detailed physical FCU model coupled to external controllers in order to ensure robustness and reasonable computation time. A detailed heating coil model (Lemort et al., 2008) and a detailed cooling coil model (Morisot et al., 2002) implemented in EES (Klein, 2011) have been calibrated by means of manufacturer data in order to simulate the full load performance (maximal air and water flows) of the two coils. Figure 48 shows some example results of the calibrated water cooling coil model. Then, a realistic FCU control algorithm (with simultaneous fan speed and water valve control) has been implemented in order to generate performance tables covering large range of part load operation. The inputs of this sub-model are the heating and cooling loads and the supply air and water conditions. The main outputs of the model are (1) the latent heat transfer rate due to possible condensation in cooling mode, (2) the required hot or chilled water flow (opening of the valve), (3) the return hot or chilled water temperature and the (4) fan consumption (Figure 49). Due to the relatively high temperature of the supply chilled water (10°C), the impact of condensation remains limited and represents about 5 to 10% of the integrated total cooling load of the FCU's.

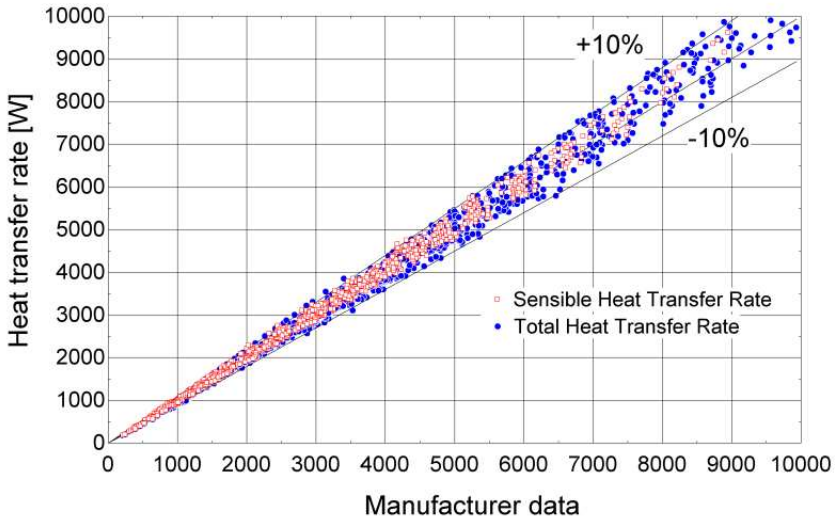

Figure 48: FCU Cooling Coil Detailed Model Calibration

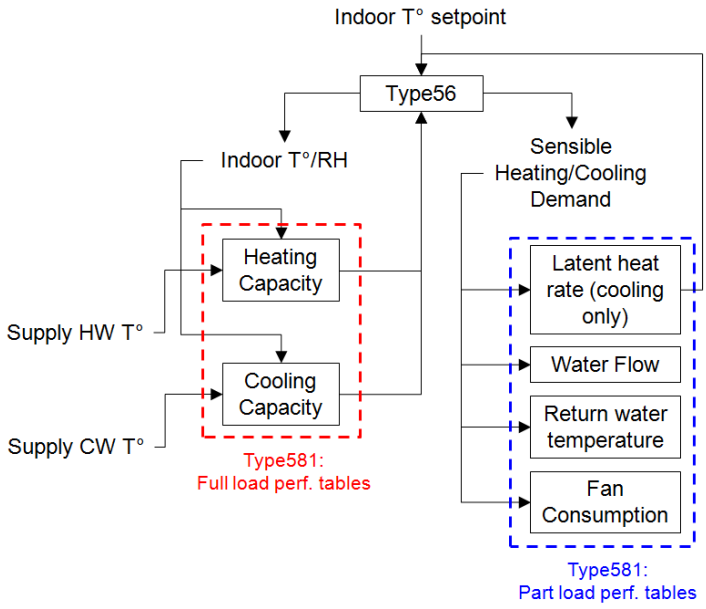

Figure 49: FCU model principle

7.4. AIR HANDLING UNIT SIMULATION MODEL

Realistic controllers are used to control the components of the Air Handling Unit (AHU). Iterative feedback controllers (Type22) have been used to control the supply water flow of the water cooling coil (Type697) and the water heating coil in order to respect the supply air temperature setpoint (18°C). A PI controller (Type23) has been used to control the steam flow injected in the ventilation air to reach a 50% relative humidity on the return side. Once again, additional random variations (normal distributions with standard deviations of 0.25°C or 2.5%) have been used to emulate the sensitivity of the sensors connected to these controllers. Temperature sensors are supposed to be installed at the outlet of the coils but the humidifier is controlled in order to maintain a constant relative humidity in the main return duct (collecting the return flows coming from the non-polluted zones). The nominal characteristics of the main AHU components are given in Table 26.

Table 26: AHU nominal characteristics

Building Supply Air Flow	m³/h	15000
Building Return Air Flow	m³/h	10940
Building Extraction Air Flow	m³/h	2610
Building Exfiltration Air Flow	m³/h	1450
Supply Fan Actual Power Demand	W	6200
Return Fan Actual Power Demand	W	3400
Extraction Fan Actual Power Demand	W	830
Supply Fan Motor (nameplate) Electrical Power	W	7000
Return Fan Motor (nameplate) Electrical Power	W	4000
Extraction Fan Motor (nameplate) Electrical Power	W	1000
Heating Coil Water Flow	m³/h	7.5
Cooling Coil Water Flow	m²/h	17.4
Steam Humidifier Flow	kg/h	150
Steam Humidifier Efficiency	%	96

The performance maps used to simulate the behavior of the water coils have been generated by means of similar models as the one used for the FCU model calibrated using real manufacturer data.

7.5. CHILLED AND HOT WATER PUMPS

Table 27: Chilled and Hot Water Pumps

Pump	Nominal Power Demand W	Nominal Flow rate m³/h	Nameplate Power W
Chilled Water – AHU	990	17.4	1100
Chilled Water – FCU (North)	1860	30.32	2000
Chilled Water – FCU (South)	2130	34.66	2400
Chilled Water – Chiller	3920	93	4200
Hot Water – AHU	315	7.5	400
Hot Water – FCU (North)	315	5.1	400
Hot Water – FCU (South)	360	5.81	450
Hot Water – Boiler (2x)	445	10.55	500

7.6. LEVEL 3A – IDENTIFIED INTERNAL LOADS OPERATING PROFILES

Table 28: Internal loads operating rates - night-time period

Zone	Floor area	Installed power				Operation	
		Lighting		Appliances		Lighting power	Appliances Power
	m²	W/m²	W	W/m²	W	W	W
1	207	12	2484	9.8	2029	0	**0.16***2029 = 325
2	45	14	630	10	450	0	**0.16***450 = 72
3	207	12	2484	9.8	2029	0	**0.16***2029 = 325
4	45	14	630	10	450	0	**0.16***450 = 72
5	49	9	441	0	0	0	0
6	347	6.15	2134	2.6	902	**0.36***2134 = 768	**0.16***902 = 144
Total power demand						**1706 W**	

Table 29: Internal loads operating rates - pre/post-occupancy period

Zone	Floor area	Installed power				Operation	
		Lighting		Appliances		Lighting power	Appliances Power
	m²	W/m²	W	W/m²	W	W	W
1	207	12	2484	9.8	2029	0	**0.16***2029 = 325
2	45	14	630	10	450	0	**0.16***450 = 72
3	207	12	2484	9.8	2029	0	**0.16***2029 = 325
4	45	14	630	10	450	0	**0.16***450 = 72
5	49	9	441	0	0	**1***441 = 441	0
6	347	6.15	2134	2.6	902	**1***2134 = 2134	**0.16***902 = 144
Total power demand						**3513 W**	

Table 30: Internal loads operating rates - occupancy period

Zone	Floor area	Installed power				Operation	
		Lighting		Appliances		Lighting power	Appliances Power
	m²	W/m²	W	W/m²	W	W	W
1	207	12	2484	9.8	2029	**0.67***2484 = 1664	**0.67***2029 = 1359
2	45	14	630	10	450	**0.67***630 = 422	**0.67***450 = 302
3	207	12	2484	9.8	2029	**0.67***2484 = 1664	**0.67***2029 = 1359
4	45	14	630	10	450	**0.67***630 = 422	**0.67***450 = 302
5	49	9	441	0	0	**1***441 = 441	0
6	347	6.15	2134	2.6	902	**1***2134 = 2134	**0.67***902 = 604
Total power demand						**10674 W**	

CHAPTER 6 APPLICATION TO A BUILDING CASE STUDY

CHAPTER 6: APPLICATION TO A BUILDING CASE STUDY 2
1. INTRODUCTION 2
2. BUILDING DESCRIPTION 2
2.1. Geometry and Orientation 2
2.2. Building Facades 3
2.3. Internal Layout 5
3. HVAC&R SYSTEM DESCRIPTION 7
3.1. Ventilation System 7
3.2. Local Heating and Cooling 10
3.3. Heat Production 11
3.4. Cold Production 13
4. BUILDING USE AND OCCUPANCY 14
4.1. Occupancy 14
4.2. Lighting 15
4.3. Appliances 16
4.4. Building Systems Operation 17
5. ENERGY BILLING DATA 19
6. MONITORING CAMPAIGN: EQUIPMENT AND DATA COLLECTION 24
7. AVAILABLE WEATHER DATA 29
8. CALIBRATION PROCESS 32
8.1. LEVEL1: Initial As-Built Input File 35
8.2. LEVEL2: Inspection Phase 46
8.3. LEVEL3: Monitoring Phase 52
8.4. LEVEL 4: Occupancy Survey 66
8.5. LEVEL 5: Prospective Iterative Adjustment 75
9. CONCLUSION 77
10. REFERENCES 79
11. APPENDIX 80
11.1. Envelope Composition 80
11.2. Energy Performance Certificate 82
11.3. HVAC System 83
11.4. Occupancy Survey 84
11.5. Zones Geometry 87

CHAPTER 6: APPLICATION TO A BUILDING CASE STUDY

1. INTRODUCTION

The whole calibration methodology presented earlier is applied to a real office building located in the city center of Bruxelles, Belgium. The building was built in the 70's and was largely refurbished in 1998. The refurbishment includes a complete modification of the HVAC system and a renovation of the facade and of the indoor space. The building was recently awarded with an energy performance certificate (see Appendix) with a mark of D+ (i.e. just above the average for similar buildings in Brussels area), corresponding to an annual primary energy consumption of about 316 kWh/m²/yr.

Figure 1: Case study building (South-West façade)

In 2008, the as-built data and some energy performance data for the last few years have been collected and analyzed as a pre-requisite of an energy audit of the building and its installation. During the inspection, detailed information on building use and operation (control laws, installed internal loads densities and schedules...) were collected. This study has been carried out in cooperation with an engineering company based in Bruxelles. In December 2009, a detailed monitoring campaign was started in order to extend the analysis initiated the year before.

Main results and conclusions of Chapter 4 and 5 will be used to make the calibration process as efficient as possible.

2. BUILDING DESCRIPTION

2.1. GEOMETRY AND ORIENTATION

The net floor area of the building is about 10100 m², distributed over 9 floors and includes mainly office cells and meeting rooms. The building has an (exterior) foot print of about 54.8m * 22.9m and a ground-to-roof height of 30.9m. The fully enclosed area (including the three levels of basement and parking of about 2534 m² each, the 9 levels dedicated to occupancy and the technical rooms of about 750 m² located at the roof level) is about 18700m². The main orientation of the building is near SW-NE.

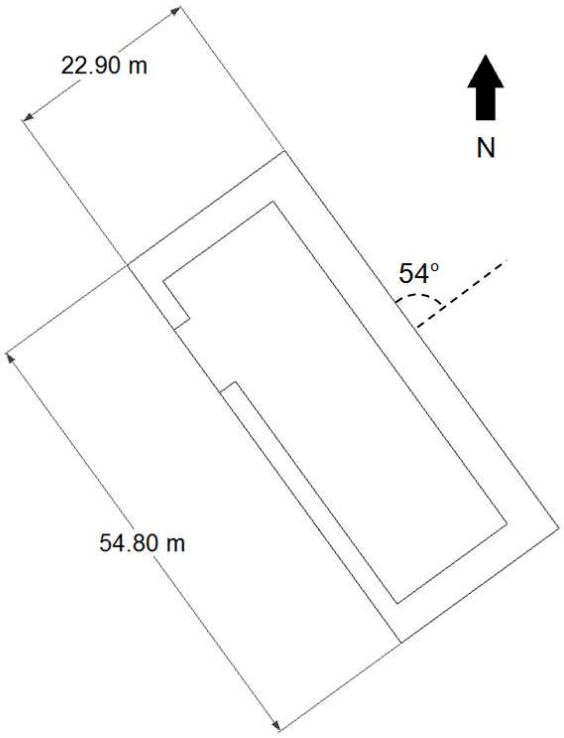

Figure 2: Building external dimensions and orientation

The effect of the shading from the urban surrounding are relatively limited. The SW and SE facades are poorly influenced by the surrounding buildings since they are quite small (1 or 2 storeys houses) and distant. A similar building surrounds the NW façade and a small hill surrounds the NE façade.

2.2. BUILDING FACADES

Building facades are composed of 6 types of precast façade modules. Figure 3 and Figure 4 show schematic representations of the front façade and of type1 façade module. As described in Table 1, opaque parts of the façades vary in both concrete and insulation thicknesses.

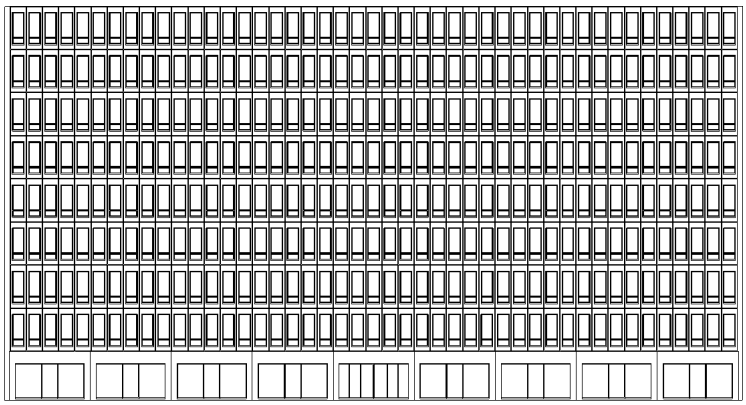

Figure 3: Case study building front façade (SW)

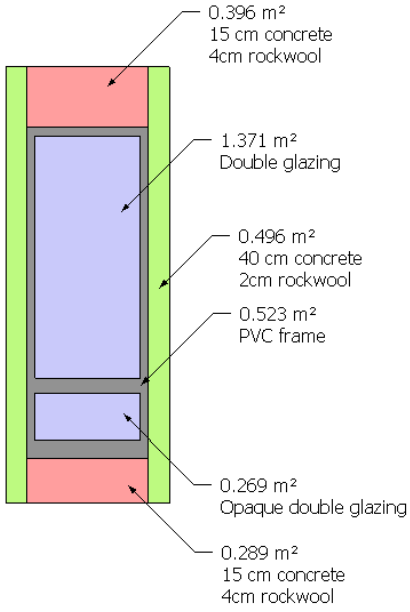

Figure 4: Type 1 façade (window) module

Figure 5: Glazed module with external shading (left) and glazed opaque panel (right)

Glazed modules are composed of a clear surface and an opaque surface. Manual external textile screens can be operated by the occupants (Figure 5). The bottom of the window sill is partly insulated on the indoor side to reduce thermal bridges (Figure 6).

Figure 6: Window sill (indoor)

The composition of the four façades of the building and the characteristics of the different types of façades modules are given in Table 1 and Table 2.

Table 1: Case study buildings facades modules characteristics

Façade module	**Composition**		**Surface area m²**
Type 1	Double glazing		1.37
	Opaque double glazing		0.27
	Frame	PVC	0.52
	Heavy opaque (side)	0.4 m concrete + 0.02 m rockwool	0.99
	Heavy opaque (top – bottom)	0.15 m concrete + 0.04 m rockwool	0.69
	Total		3.84

Type 2	Glazed		12.40
	Frame	PVC	1.02
	Heavy opaque	0.5 m concrete + 0.05 m rockwool	8.56
	Total		21.97
Type 3	Glazed		12.10
	Frame	PVC	1.47
	Heavy opaque	0.5 m concrete + 0.05 m rockwool	8.33
	Total		21.90
Type 4	Glazed		3.82
	Frame	PVC	0.47
	Heavy opaque (center)	0.15 m concrete + 0.02 m rockwool	10.24
	Heavy opaque (side)	0.5 m concrete + 0.04 m rockwool	7.38
	Total		21.90
Type 5	Heavy opaque	0.4 m concrete + 0.03 m rockwool	5.36
	Total		5.36
Type 6	Heavy opaque	0.4 m concrete + 0.03 m rockwool	6.11
	Total		6.11

Table 2: Case study building facades composition

Facade	Floor level	Type 1	Type 2	Type 3	Type 4	Type 5	Type 6
SW (front)	0	0	8	1	0	0	0
	1 to 8	45	0	0	0	0	0
SE (lateral)	0	15	0	0	0	0	2
	1 to 8	15	0	0	0	2	0
NE (back)	0	0	0	0	9	0	0
	1 to 8	45	0	0	0	0	0
NW (lateral)	0	15	0	0	0	0	2
	1 to 8	15	0	0	0	2	0

Manufacturer data of the glazing have been obtained. These glazing are composed of 2 glazing layers and include Argon. Since the exact thickness of the Argon layer is not known, a small uncertainty remains about the actual performance of the glazing. The considered glazing should correspond to type 1 or type 2 glazing given in Table 3.

Table 3: Glazing characteristics

Type	Composition	U – W/m²K	SHGC - %
1	4 – 15 (Ar 90%) – 4	1.3	67
2	4 – 12 (Ar 90%) – 4	1.5	67

The roof slab is composed of approximately 0.5m of concrete and 0.04m of rockwool.

2.3. INTERNAL LAYOUT

Basement levels mainly include parking areas. The ground floor mainly includes the entrance hall, a library, some meeting rooms and offices. Levels +1 to +8 mainly include office cells. At each level,

the core zone is split in two parts and has a similar composition and includes some utility areas (stairs, elevators, sanitary, storage, kitchen, copy rooms…). Peripheral zones are separated by light walls (plaster boards) while core zones walls are mainly heavy concrete walls.

The gross internal surface area of each level is about 1121 m².

The entrance hall of the ground floor is about 142 m² of floor area. At this level, the remaining circulation area (corridors and elevators area) represents about 134 m². The peripheral zones (including meeting rooms, offices and library) of the ground floor represent a floor area of about 683 m² (Figure 7). The two core zones including utility rooms (sanitaries, kitchen, technical rooms…) represent about 162 m². The total indoor height is 3.55 m. Lighting fixtures and technical components (pipes and ducts) are hidden behind ceiling panels installed at 2.8 m from the floor.

Figure 7: Ground floor layout (Level 0)

Levels +1 to +8 include about 217 m² of circulations (corridors and elevators area) and 159.8 m² of utility areas located in the two core zones (Table 4). Two additional storage/archives rooms of 25.2 m² each are also attached to the core zones.

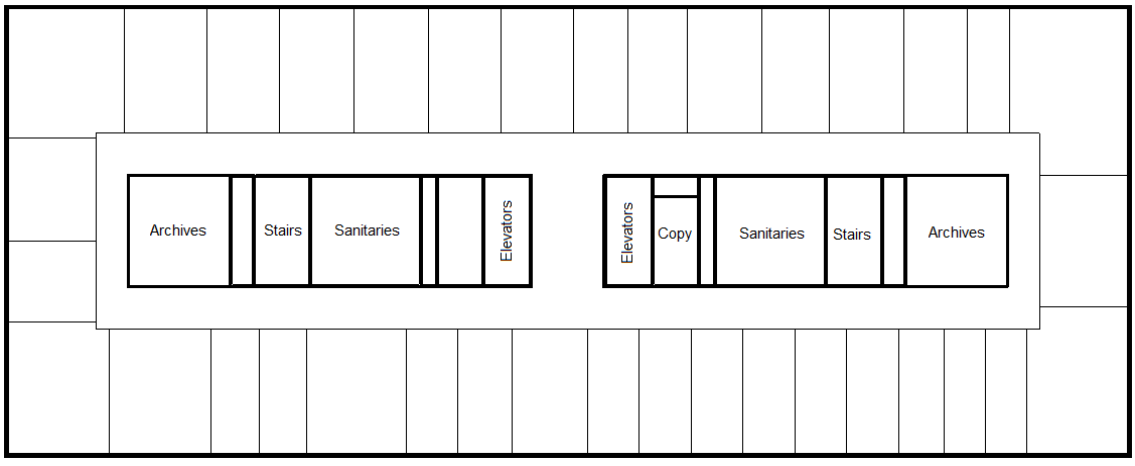

Figure 8: Typical intermediate floor layout (Level 5)

The remaining floor area is dedicated to office cells of various sizes (depending of the number and status of employees occupying the considered office) and is about 723 m² (Figure 8). A typical office cell encloses two window modules and is therefore 2.4 m wide and 5.95 m deep. The total indoor height is 3.2 m while the ceiling height is 2.65 m.

Table 4: Core zone composition

Core zone	Unitary area – m²	Number	Total – m²
Archives	25.2	2	50.4
Sanitaries + kitchen	26.8	2	53.6
Stairwells	13.4	2	26.8
Copy	8.8	1	8.8
Elevators	11.1	2	22.1
Technical 1	3.1	2	6.2
Technical 2	4.9	2	9.9
Technical 3	10.8	1	10.8
Technical 4	1.8	1	1.8
Total area			190.4

3. HVAC&R SYSTEM DESCRIPTION

HVAC components equipping the buildings have been installed in 1998. A classical BEMS system is used to manage the whole technical installation of the building (from lighting to heating, cooling and ventilation).

3.1. VENTILATION SYSTEM

Five main Air Handling Units (AHUs) serve the three main conditioned zones of the building (Figure 9):

- The Entrance hall
- The ground floor peripheral zones (meeting zones, offices and library)
- The offices located at Levels +1 to +8

Office cells located at levels +1 to +8 are served by AHUs #1 and #2. Both units are Constant Air Volume (CAV) units and include an adiabatic humidification system, a cooling coil, a postheating coil, a supply fan and a return fan. A fraction of the air extracted by these two units is sent back to the parking levels -1 and -3. The AHUs #3 and #4 are Variable Air Volume (VAV) units and serve the peripheral zones located at the ground floor. The fifth AHU (#5), serving the entrance hall, consists in a small ventilation unit supplied with vitiated air extracted from the zone and a small fraction of fresh air coming from the AHU3.

AHU #	Scheme
1 and 2	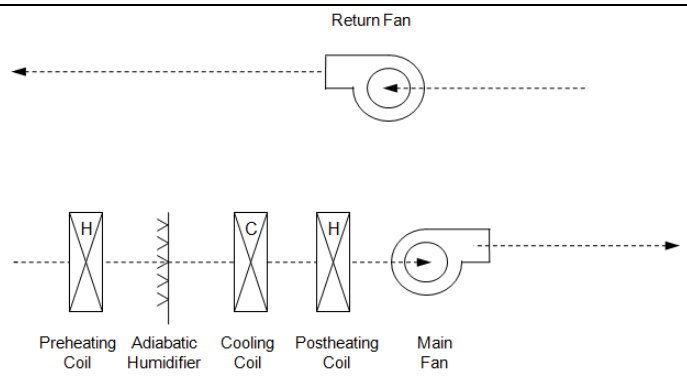

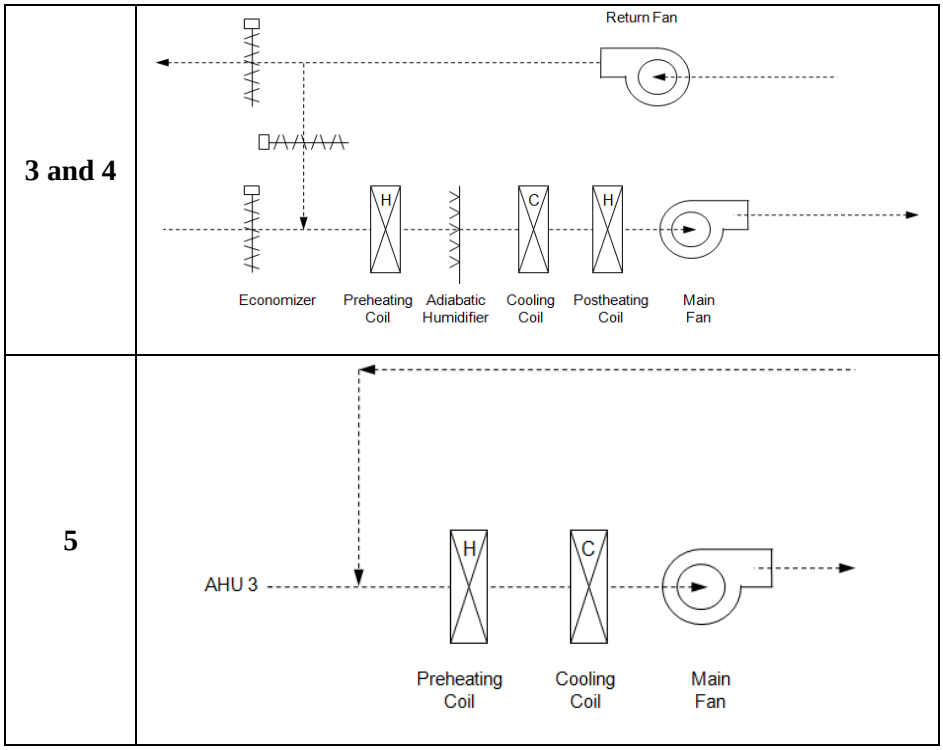

Figure 9: Composition of the main AHUs

Nominal supply and exhaust air flow rates of the nine ventilation units are summarized in Table 5. In addition to the five main AHUs shown in Figure 9, four ventilation units work in extraction mode only. About 8200 m³/h are extracted from sanitaries of levels 0 to +8 by means of AHU #6. The AHU #7 extracts a mix of vitiated and fresh (infiltrated) air from the three parking levels in order to maintain them at an acceptable temperature and air quality level. The intermediate parking level (-2) is also equipped with two large hot water fan coil units (70.5 kW each) in order to avoid freezing risk of the fire safety piping system (Figure 10).

Figure 10: Parking fire savety piping network

Figure 11: AHU #1

The small AHU #8 is used only to ventilate the high tension transformer with fresh outdoor air and is directly controlled by a thermostat. The AHU #9 is totally dedicated to the printshop located at the ground floor.

Table 5: AHUs setpoints

AHU	Zone	Type	SuFlow	ExFlow	Min Fresh	Tsu -10	Tsu +10	RH
			m³/h	m³/h	%	°C	°C	%
1	Offices	CAV	12660	9000	100	25	20	50
2	Offices	CAV	12480	8960	100	25	20	50
3	Ground floor	VAV	12565	8430	30	25	19	50
4	Ground floor	VAV	11890	10250	30	25	19	50
5	Hall	CAV	3500	3500	6 (AHU3)	Thermostat (min. 16°C)		-
6	Sanitaries	CAV	0	8200	0	-	-	-
7	Parking	CAV	0	37600	0	-	-	-
8	Elec. Box	CAV	-	-	100	-	-	-
9	Printshop (0)	CAV	0	2700	0	-	-	-

The main characteristics of the AHUs components available in the as-built documents are summarized in Table 6.

Table 6: Air handling unit components and sizes

AHU	ExFan	Econo	PreH	Humid.	Cool	PostH	SuFan
	kW	-	kW	-	kW	kW	kW
1	2.2	No	182.5	85% eff.	98.5	23	5.5
2	2.2	No	180	85% eff.	97	23	5.5
3	2.2	Yes	25.5	85% eff.	64	20	5.5
4	3	Yes	23	85% eff.	60	20	5.5
5	No	No	No	No	14	17.5	1.1
6	2.2	No	No	No	No	No	No
7	11	No	No	No	No	No	No
8	0.5	No	No	No	No	No	No
9	0.75	No	No	No	No	No	No
Total	**24.05**	**-**	**411**	**-**	**333.5**	**86**	**23.1**

3.2. LOCAL HEATING AND COOLING

The peripheral zones located at the ground floor are equipped with VAV boxes controlling the supply air flow rate. Hot water convectors are installed all along the external walls (one per 2.4m of façade) to provide local heating to the peripheral zones. Cooling of the zones is ensured by increasing the supply air flow. In a few zones, some electrical reheat boxes have been added to ensure backup heating if the capacity of the hot water convectors is insufficient. It has to be noticed that these additional electrical coils operate a very limited number of hours per year.

Table 7: Ground floor VAV boxes

VAV Boxes Ground floor	AHU	Supply			Exhaust			Electrical coil	
		Min	Max	Nbr	Min	Max	Nbr	Pwr	Nbr
		m³/h	m³/h	-	m³/h	m³/h	-	W	-
Office 1	3	28	280	1	23.2	232	1	-	-
Office 2	3	139	1390	2	115.5	1155	2	-	-
Meeting 30	3	202	2020	2	167.5	1675	2	4000	2
Office 3	3	26.5	265	1	22	220	1	-	-
Printshop	3	120	1200	2	-	-	-	-	-
Storage 1	3	222	2220	1	195	1950	1	-	-
Storage 2	3	60	600	1	50	500	1	-	-
Office 4	3	67.5	675	1	56	560	1	-	-
Total		**1326 – 13260 m³/h**			**912.2 - 9122 m³/h**			**4000**	**2**
Meeting 40	4	121	1210	1	106	1060	1	2500	1
		182	1820	2	160	1600	2	4000	2
Meeting 20	4	222	2220	1	195	1950	1	4500	1
Meeting	4	165	1650	1	145	1450	1	-	-
Meeting	4	67.5	675	1	59	590	1	1500	1
Meeting	4	67.5	675	1	59	590	1	1500	1
Meeting	4	162	1620	1	142	1420	1	-	-
Total		**1169 - 11690 m³/h**			**1026 - 10260 m³/h**			**18000**	**6**

Peripheral zones at levels +1 to +8 are equipped with vertical concealed 4-pipes heating/cooling fan coil units (one per façade module of 1.2m width).

Figure 12: Concealed vertical fan coil unit

3.3. *HEAT PRODUCTION*

Hot water production is ensured by three natural gas boilers (Table 8) of 465 kW each. Two classical boilers (#1 and #2) provide hot water to the AHUs heating coils and to the two air heaters located in the parking space. The third boiler is a condensing boiler and provides hot water to all the FCUs installed in the office zones (levels +1 to +8). In normal operation, the two hot water networks are decoupled (Figure 14) and the isolating valves are closed. Boilers nominal efficiencies are given in Table 8. Since the manufacturer provides only ranges, the average value will be used as a best-guess value but the ranges will be used for sensitivity and uncertainty analyses.

Table 8: Hot water boilers

Name	Fuel	Brand	Type	Nominal Pwr	LHV Effic.
Boiler 1	Natural gas	Ygnis	Optimagaz E465 - Classical	465 kW	92 – 95%
Boiler 2	Natural gas	Ygnis	Optimagaz E465 - Classical	465 kW	92 – 95%
Boiler 3	Natural gas	Ygnis	TBT E465 - Condensing	465 kW	96 – 104%

The characteristics of all the hot water pumps are summarized in Table 9. Once again, the manufacturer provides different values of the absorbed power depending on the operation of the pump (speed level 1, 2 or 3). At the beginning, these values will be used to define the probability range of the installed pumping power. Later (i.e. during the monitoring campaign), these values will be measured.

Figure 13: Hot water production plant

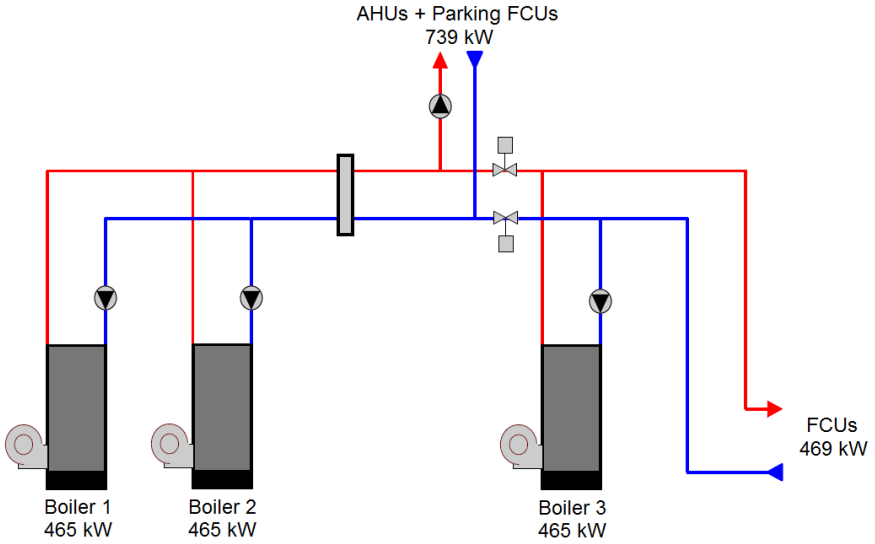

Figure 14: Hot water production plant components

Table 9: Heating plant water pumps

Name	Type	Flowrate (m³/h)	Power (W)	Description
PC1	WILO TOP-S 50/7	22.2	375-470-610	Boiler 1
PC2	WILO TOP-S 50/7	22.2	390-500-650	Boiler 2
PC3	WILO TOP-S 50/10	22.2	495-660-850	Boiler 3
PC4	WILO TOP ED 40/1-10	10.2	30-570	FCUs
PC5	WILO TOP ED 40/1-10	10	100-600	FCUs
PC6	WILO TOP-S 65/13	32	1450	AHUs & others
PC7	WILO TOP-S 30/10	9.67	205-290-395	AHU1 PreH coil
PC8	WILO TOP-S 30/10	9.46	205-290-395	AHU2 PreH coil
PC10	WILO RS25/50 r	1.12	38-48-60-74	AHU3 PreH coil
PC11	WILO TOP SD 32/7	2.05	90-130-200	Convectors (0)
PC12	WILO RS25/50 r	1.03	18-31-48	AHU4 PreH coil
PC13	WILO TOP SD 32/7	1.6	90-130-185	Convectors (0)

3.4. COLD PRODUCTION

Chilled water production is ensured by two water cooled chillers of 512.4 kW of cooling capacity each (Figure 15). The nominal EER of these components is about 4.27 (Table 10). Two indirect contact cooling towers equipped with two speeds fans ensure the cooling on the condenser side (Figure 16). The main characteristics of all the pumps and circulators ensuring chilled water circulation are given in Table 11.

Table 10: Cooling plant components

Name	Brand	Type	Compressor / Fan Power	Temperatures	Nominal Power	Absorbed Power
Chiller 1	Trane	RWTA 215	2 x Screw	7/12°C 29/34°C	512.4	120.1
Chiller 2	Trane	RWTA 215	2 x Screw	7/12°C 29/34°C	512.4	120.1
Tower 1	BAC	Balticare VFL 963-O	Two speeds	34/29°C	665 kW	7/30 kW
Tower 2	BAC	Balticare VFL 963-O	Two speeds	34/29°C	665 kW	7/30 kW

Figure 15: Water-cooled chilling package

Table 11: Cooling plant water pumps

Name	Type	Flowrate (m³/h)	Power (W)	Description
PF1	WILO IPn 100/200-3/4	87.5	3100	Chiller 1 – Evaporator
PF2	WILO IPn 100/200-3/4	87.5	3100	Chiller 2 – Evaporator
PF3	WILO IPn 100/160-7.5/2	123.8	7500	Chiller 1 - Condenser
PF4	WILO IPn 100/160-7.5/2	123.8	7500	Chiller 2 – Condenser
PF5	WILO IPE 65/4-20	55.4	3900	FCUs
PF6	WILO IPE 65/4-20	49.9	3800	FCUs
PF7	WILO IPE 80/125-3/2	49.7	3800	AHUs
PTR1	Balticare	87.12	2200	CT1 – spray pump
PTR2	Balticare	87.12	2200	CT2 – spray pump

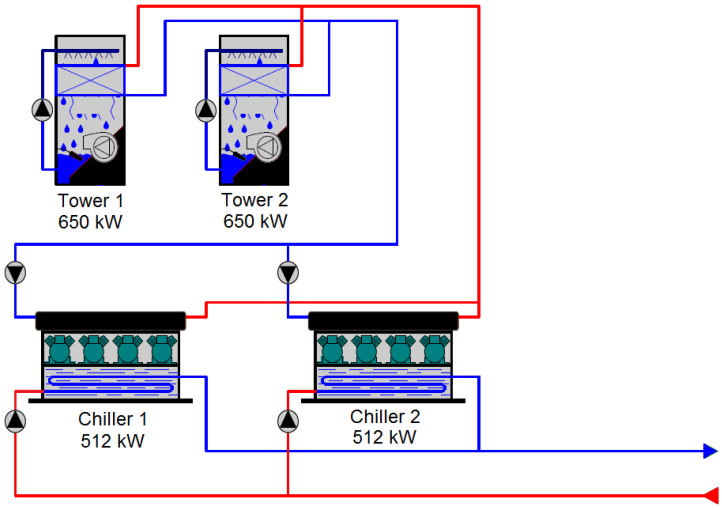

Figure 16: Chilled water production plant components

4. BUILDING USE AND OCCUPANCY

During the inspection of the building, the different floors of the building were scouted around to visually find and note down electrical appliances and lighting fixtures. This building contains several hundred office cells, and therefore, to make this work faster and more effective, the observations/inspection were/was limited to the first floor, the ground floor and the parking levels. Because occupants are not always available, many offices were not scouted. Assumptions had therefore to be made. A relation between visited offices and number of occupants, computers and lighting fixtures seemed to emerge (Figure 17):

- For each window module on the façade, there are 2 lighting fixtures;
- There is one occupant per 1.5-2 window modules;
- There is (at least) one computer with a flat screen per occupant.

Figure 17: Typical office cell (1sth floor)

4.1. OCCUPANCY

The total number of occupants of the building is approximately 350. Numerous office cells are shared by two, three or four employees. No official information is available on the occupancy rate of the

building and indirect estimation methods (lighting and appliances consumption measurement) will have to be used to tackle this issue.

4.2. LIGHTING

Lighting fixtures installed at the first floor are listed in Table 12. The computed average lighting power densities are typical for this kind of building. In the offices, lighting fixtures are manually controlled by the occupants by means of two separate switches: one for the lighting fixtures on the window side and one for the lighting fixtures on the corridor side.

Lights in the elevators area and circulations are fully automated and controlled by the BEMS and lead to a global lighting power density of about 9.98 W/m².

At the ground floor, the lighting power density in entrance hall is similar to the one in the circulation area (8.7 W/m²). These lighting fixtures are also controlled by the BEMS.

Table 12: List of lighting fixtures in use at the first floor

Zone	Area m²	Type	#	Average Density W/m²	Operation
Offices (peripheral zones)	712	Fluorescent tube TL5 – 38W	192	10.25	Occupants
Archives/Storage and utility rooms (core)	95.2	Fluorescent tube TL5 – 38W	12	7.82	Occupants
		Fluorescent tube TL5 – 36W	2		Occupants
		Economic lamp – 36W	6		BEMS
Archives/Storage and utility rooms (core)	95.2	Fluorescent tube TL5 – 38W	12	7.82	Occupants
		Fluorescent tube TL5 – 38W	2		Occupants
		Economic lamp – 36W	6		BEMS
Circulation	200	Economic lamp – 36W	36	7.83	BEMS
		Emergency lighting – 18W	15		ON
Elevators area	18.5	Fluorescent tube TL5 – 38W	6	33.13	BEMS
		Economic lamp – 36W	8		BEMS
		Spotlight – 7W	14		BEMS

Each of the three parking levels is lighted by about 88 lighting fixtures of 39W each (i.e. 10296W in total). These lights are controlled by the BEMS and operate between 06:00 and 22:00, from Monday to Friday.

Figure 18: Lighting fixtures in elevators area (left) and circulations (right)

4.3. APPLIANCES

Electrical appliances are present in offices (computers, screens and printers), in the copy room (copiers, printers…) and in the kitchen. All the equipments are listed in Table 13. All these appliances are controlled manually. Average power demands given in Table 13 (and the corresponding power densities) have been estimated based on available literature and/or manufacturer data. Such hypotheses can be cross checked by means of local monitoring.

Table 13: List of electrical appliances in use on the first floor

Zone	Area m²	Appliance	Nameplate Power W	Average Power W	#	Total Power	Power Density W/m²
Copy room	8.8	Fax Lanier 4560	-	80 [1]	1	80	89.10
		HP laser 8150DN	685	110	1	110	
		Xerox 8560	230 [2]	80	1	80	
		Nashuatec MP7500	1850 [3]	305	1	305	
		Nashuatec MP2500	1450 [4]	135	1	135	
		Lexmark 7654DN	740 [5]	74	1	74	
Kitchen	26.8	Microwave	1150 [6]	11	2	22	3.58
		Coffee machine	1450 [7]	15	2	30	
		Water boiler	2400 [8]	24	1	24	
		Fridge	-	20 [9]	1	20	
Offices	712	Computer	-	60 [10]	57	3420	11.15
		Computer screen	-	65	66	4290	
		Fax machine	-	80	1	80	
		Laser printer	520	50	3	150	

[1] http://h10010.www1.hp.com
[2] http://www.office.xerox.com
[3] http://www.copiersuk.com
[4] http://gg.nashuatec.com
[5] http://www1.lexmark.com
[6] http://www.samsung.com
[7] http://www.senseo.be
[8] Http://shop.philips.be
[9] http://www.beko.co.uk
[10] Hosni et al. (1999)

The building also includes four IT rooms whose the total installed electrical power is about 30kW. These rooms are cooled by means of fan coil units supplied by chilled water produced in the neighbor building.

4.4. BUILDING SYSTEMS OPERATION

Most of the technical equipments (lighting fixtures and HVAC&R components) of the building are controlled by a central BEMS system.

The lighting fixtures installed in the occupancy zones (offices and meeting rooms) can be switched ON and OFF by the occupants during the following "switch-on allowance period":

- Between 06:00 and 22:00, from Monday to Friday,
- Between 10:00 and 19:00, during weekends and holidays.

Out of these periods, the BEMS does not allow the lights of the offices to be switched ON. During the "switch-on allowance period" defined for the offices, the lights that are not controlled by the occupants (i.e. installed in circulations and common areas) are switched ON. Lighting fixtures near the elevators area are supposed to be switched ON all the time (24h/day and 7days/week) while only a fraction (about 16 fixtures on 36) of the lighting fixtures located in the circulation stay on during non-occupancy periods. This information should be checked during the monitoring campaign.

In the entrance hall, the lights are totally automated and are switched ON:

- Between 06:00 and 22:00, from Monday to Friday,
- Between 10:00 and 19:00, during weekends and holidays.

All the AHUs are controlled by the BEMS system. AHU #5 (entrance hall) operates between 6:00 and 22:45 from Monday to Friday and from 10:00 to 19:00 on Saturday, Sunday and holidays. The AHU #8 (electrical box) is directly controlled by a thermostat located in the high tension transformer. The other AHUs (#1 to 4, 6, 7 and 9 supplying offices, meeting rooms, sanitaries, parking lots and the print shop) operate between 08:00 and 20:00 five days a week and are switched off the rest of the time (i.e. during weekends and holidays).

The adiabatic humidifiers equipping AHUs #1, 2, 3 and 4 and serving the offices (levels +1 to +8) and the occupancy zones of the ground floor are controlled to maintain a relative humidity of 50% on the return side. Supply temperature setpoints vary as a function of the outdoor temperature (temperature reset between -10°C and +10°C outdoor temperature) according to the values given in Table 5.

The two large air heaters (70.5 kW each) installed in the partially opened parking area operate once the outside temperature goes below 2°C in order to maintain a temperature of 12°C within the area. Due to the location of the temperature sensor, the setpoint temperature cannot be reached and the two air heaters operate at full load as soon as the outdoor temperature is below 2°C.

The operation of the fan coil units (FCUs) installed at the levels +1 to +8 is controlled by the BEMS following the setpoints given Table 14 but allow a local adjustment of the temperature of +/-1.5°C around the setpoint. In each zone, the temperature sensor is located on the bottom of each unit.

Table 14: Indoor local heating/cooling setpoints

Zone	Heating setpoint (°C)		Cooling setpoint (°C)	
	Occupancy hours	Night-setback	Occupancy hours	Night-setback
Offices (+1 to +8)	21.4	15	23	-

Ground floor	21.4	15	23	-
Entrance hall	17	15	26	-

The “occupancy” indoor setpoints given in Table 14 are maintained between 08:00 and 20:00, five days a week except in the entrance hall where the heating/cooling is ensured by the AHU #5 operating following an extended schedule (06:00 to 22:45 from Monday to Friday and 10:00 to 19:00 during weekend and holidays). These values were obtained by averaging the values implemented and measured by the BEMS (Figure 19).

Figure 19: Print screen of the BEMS software for the left side of the first floor (temperature measurements)

The supply hot water temperature is controlled on both circuits as function of the outdoor temperature (Figure 20). The heating plant is stopped when outdoor temperature goes over 16°C (summer limit temperature). The three boilers and all the circulators and pumps are started (24/7) when outdoor temperature goes below 3°C to avoid freezing.

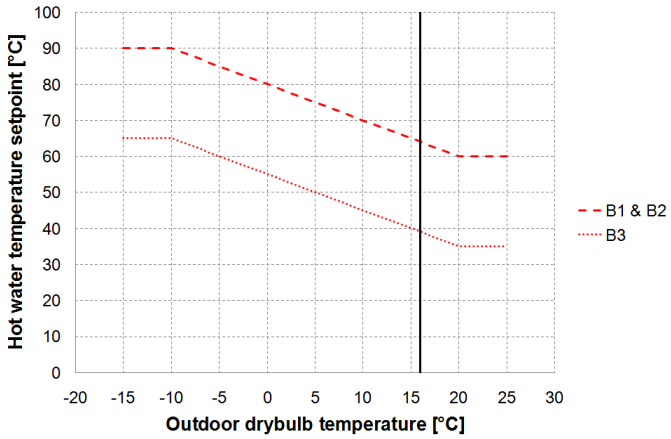

Figure 20: Hot water temperature setpoints

The cooling plant is automatically switched off as soon as the outdoor temperature is below 14°C. The chilled water network is constant and set to 9°C while the temperature setpoint at the exhaust of the cooling towers is set to 29°C. The two water chilling packages operate in cascade, as well as the two cooling towers.

An “optimizer” algorithm is implemented in the BEMS in order to control the re-start of the installation during very cold and very hot periods in order to ensure proper indoor conditions achievements in the morning. Re-starts of the installation may occur during weekend or during night.

Except the main control laws, it was not possible to determine the exact operation and identify the algorithms composing this so-called "optimizer".

5. ENERGY BILLING DATA

Monthly natural gas and electricity bills are available from January 2008 to, respectively, November and September 2011. The electricity bills provide also distinct values for peak and off-peak periods. The original energy bills were used to check the billing periods. Billing periods for electricity consumption correspond to the calendar months while billing periods for gas consumption vary.

Normalizing the annual consumptions by means of the net indoor area (about 10100 m²) give the values provided in Table 15. The natural gas consumption varies between 74.7 and 90.8 kWh/m²/yr while the total electricity consumption is included between 103.9 and 107.5 kWh/m²/yr. These values are very near the average values provided at the regional and national levels for the tertiary sector (Gas: 40 to 150 kWh/m²/yr and Electricity: 100 to 160 kWh/m²/yr; BBRI, 2001).

Table 15: Monthly electricity billing data

	2008		2009		2010		2011	
	PK[11]	OP[12]	PK	OP	PK	OP	PK	OP
	MWh	MWh	MWh	MWh	MWh	MWh	MWh	MWh
Jan	64 288	29 440	60 687	31 185	60 368	32 172	60 245	27 411
Feb	60 864	26 580	57 642	25 777	58 468	24 993	56 898	23459
Mar	52 953	28 670	62 114	28 052	66 256	25 747	67 297	25 135
Apr	61 490	24 895	60 021	24 435	62 394	24 837	57 053	24 281
May	61 446	27 874	55 685	26 320	57 654	27 951	63 773	24 718
June	68 992	26 161	71 042	27 250	78 053	23 298	60 731	23 814
July	71 988	25 869	75 909	27 114	78 421	26 558	57 193	25 436
Aug	60 326	27 878	71 261	32 158	63 068	24 429	60 472	23 786
Sep	70 269	24 502	71 135	23 876	65 711	25 032	67 658	23 303
Oct	67 329	25 831	64 589	24 819	59 531	26 485		
Nov	55 741	31 760	56 101	26 636	54 826	27 837		
Dec	55 857	27 913	61 249	31 725	60 903	28 022		
TOT	751.54	327.37	767.44	329.35	765.65	317.36		
kWh/m²	72.40	31.54	73.93	31.73	73.76	30.57		

Table 16: Natural gas billing data and corresponding mean outdoor temperature

Billing period		Consumption[13]	Mean Outdoor Temperature[14]
Start	**End**	**kWh**	**°C**
4/01/2008	23/01/2008	88544	7.70
24/01/2008	20/02/2008	142340	5.10
21/02/2008	19/03/2008	118125	7.63
20/03/2008	24/04/2008	143141	7.32
25/04/2008	21/05/2008	21149	15.41
22/05/2008	19/06/2008	11514	15.88
20/06/2008	23/07/2008	10978	16.88
24/07/2008	26/08/2008	5412	18.52
27/08/2008	24/09/2008	17860	15.16

[11] Peak-hours electricity consumption
[12] Offpeak-hours electricity consumption
[13] HHV kWh
[14] Mean outdoor temperature in Uccle (Belgium) for the corresponding billing period

25/09/2008	24/10/2008	34678	11.63
25/10/2008	20/11/2008	90954	8.45
21/11/2008	18/12/2008	174073	2.61
19/12/2008	22/01/2009	249767	1.35
23/01/2009	19/02/2009	195818	2.19
20/02/2009	25/03/2009	142618	6.53
26/03/2009	23/04/2009	56054	11.48
24/04/2009	22/05/2009	26635	13.04
23/05/2009	29/06/2009	14799	16.43
30/06/2009	29/07/2009	5001	18.97
30/07/2009	20/08/2009	1255	19.60
21/08/2009	22/09/2009	9215	16.87
23/09/2009	30/10/2009	48621	12.05
31/10/2009	20/11/2009	65183	9.80
21/11/2009	4/01/2010	259940	4.21
5/01/2010	26/01/2010	177551	0.50
27/01/2010	19/02/2010	179061	0.72
20/02/2010	24/03/2010	145317	5.83
25/03/2010	27/04/2010	75012	9.69
28/04/2010	25/05/2010	44869	11.51
26/05/2010	23/06/2010	12942	15.39
24/06/2010	3/08/2010	1246	20.45
4/08/2010	23/08/2010	3524	17.60
24/08/2010	30/09/2010	19608	14.47
1/10/2010	22/10/2010	36866	11.44
23/10/2010	26/11/2010	116708	7.63
27/11/2010	27/12/2010	227077	-1.04
28/12/2010	27/01/2011	165124	4.51
28/01/2011	22/02/2011	133605	4.22
23/02/2011	30/03/2011	128206	7.19
31/03/2011	26/04/2011	30943	14.02
27/04/2011	27/05/2011	18914	14.60
28/05/2011	30/06/2011	13541	16.65
1/07/2011	20/07/2011	6088	16.36
21/07/2011	29/08/2011	12973	16.96
30/08/2011	27/09/2011	17229	16.00
28/09/2011	27/10/2011	42523	12.62
28/10/2011	28/11/2011	69169	9.38

As shown in Figure 21, the electricity consumption vary in a very limited way and the 48 monthly values (4 years of data) are included within +/-16% around an average consumption of 90 MWh per month. Off-peak consumptions are not characterized by significant variations either (27 MWh +/-20%). It is hard (even almost impossible) to deduce a significant seasonal behavior from this profile. This consumption behavior is typical for this type of buildings where an important part of the whole-building electricity consumption is due to normal building operation (lighting, appliances, ventilation system…) and not strongly related to the outdoor climate.

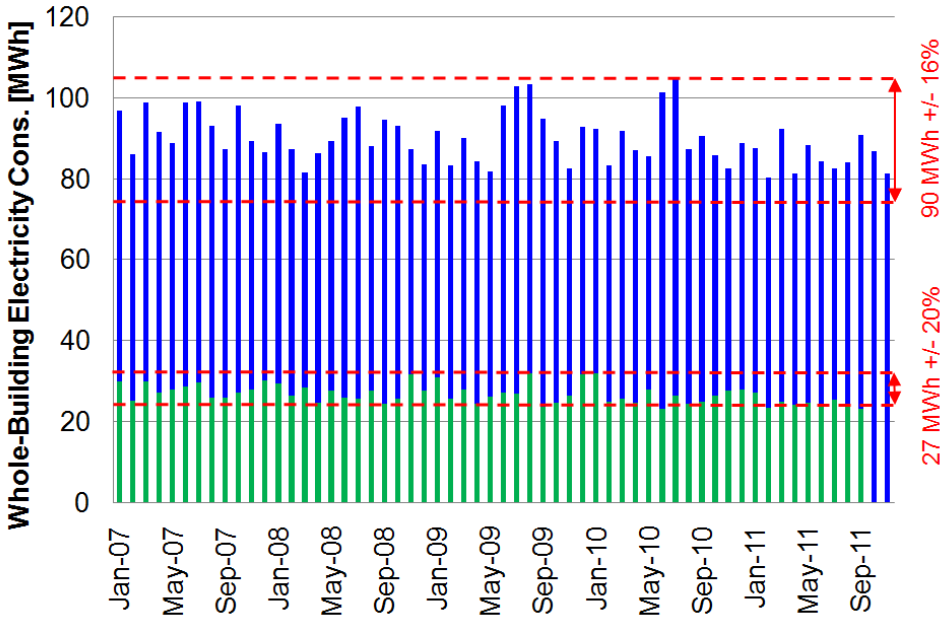

Figure 21: Whole-building monthly electricity consumption (green: offpeak)

The original files (i.e. from the energy provided) of whole-building electrical power demand are available on a quarter-hour basis from 2008 to 2010. Quarter-hourly profile of the whole building electricity consumption may also be of a great help during calibration since it allows to checking if the calibrated model is able to represent:

- The nighttime electricity demand (base load);
- The daytime winter and summer peak demands;
- The starting and ending time of operation of the main electricity consumers in the building.

The demand profile shown in Figure 22 has been modified in order to hide the shift due to summer/winter time change. This profile allows to clearly identifying different daily or weekly operation periods (e.g. from 06:00 to 22:45 and from 08:00 to 20:00 from Monday to Friday). As expected, winter daytime peak consumption is quite constant from weeks to weeks and is between 200 and 250 kW. The summer daytime peak consumption is directly related to cooling plant operation and reaches about 400 kW.

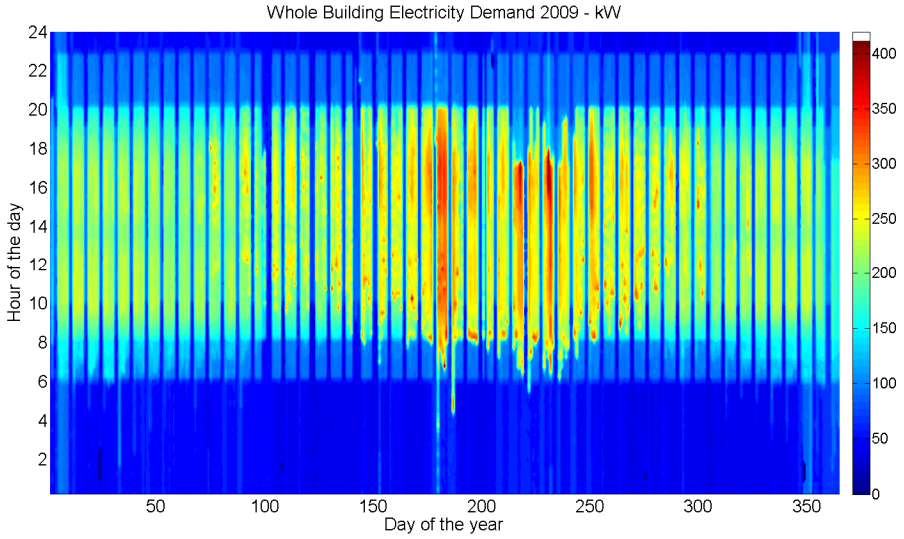

Figure 22: Whole-building electricity demand (2009)

Figure 23 shows the recorded values of the natural gas consumptions. These values are not actual "monthly" consumptions since the billing period may be shorter or longer than the corresponding calendar month. Despite this fact, the trend is very clear and the natural gas consumption is strongly related to the outdoor climate. The seasonal effect is very clear: peak consumptions occur in December/January while the summer consumptions (July/August) are almost null.

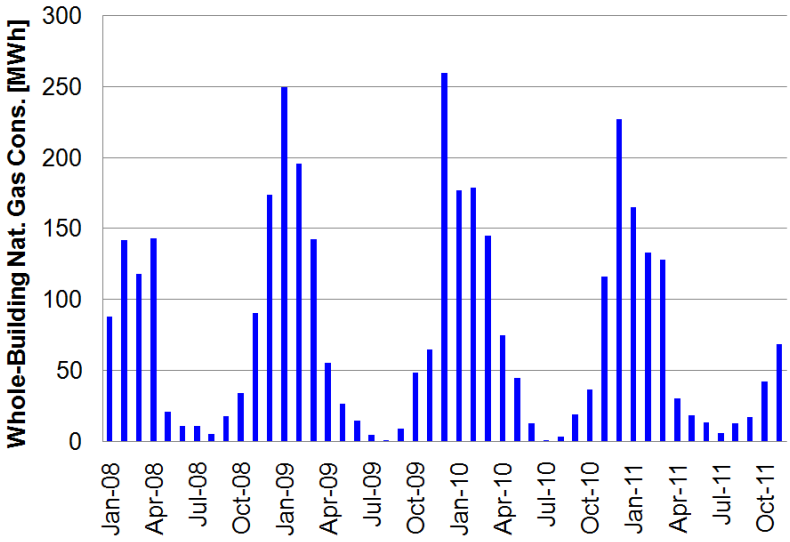

Figure 23: Whole-building (not corrected) monthly natural gas consumption

The values given in Table 16 have been used to generate the thermal signature shown in Figure 24. A HHV to LHV ratio of 90.28% and an average heat generation (LHV) efficiency of 95.6% were used to compute the mean values of the heating demand shown in Figure 24. It is important to notice that a first signature had been built using the same consumption values but supposing that billing periods corresponded to calendar months. This led to a very different slope coefficient (-16.31 kW/K instead of -21.61kW/K) and a larger dispersion of the points (correlation coefficient of about 83% instead of 96%). This confirms that it is crucial to check the validity and the accuracy available billing data prior to any analysis or modeling work.

After the adjustment of the billing periods, the curve shown in Figure 24 was obtained. The data are separated in two groups: data points corresponding to a period with a mean outdoor temperature above 15°C and points corresponding to a period with a mean outdoor temperature below 15°C.

Below 15°C, the dispersion of the points around the linear regression is quite limited (high correlation coefficient: 96%). This confirms the very strong correlation existing between the natural gas consumption and the outdoor climate. Above 15°C, the consumption is very low and corresponds to an average (and almost constant) heating demand of about 10.8 kW.

It is hard to identify a global loss coefficient for the building and compare it to the slope of the thermal signature; however, the following verification is possible. For a mean outdoor temperature of -10°C, the total heating demand can be computed as given in Table 17.

Table 17: Building peak heating demand

Contribution	Calculation	Corresponding demand
Heating (levels 0 to 8)	AU value (walls and roof): 7006 W/K Average indoor temp.: 17.1°C[15]	189.9 kW

[15] 21°C during 60 hours per week and 15°C rest of the time

	Temperature difference: 27.1 K	
Heating (level 0)	AU value (floor slab): 7840 W/K Average indoor temp.: 17.1°C[16] Temperature difference: 7.1 K[17]	55.7 kW
Parking (level -2)	Parking air heaters: 141 kW	141 kW
Ventilation	Fresh air flow rate: 32500 m³/h[18] Supply temperature: 21°C	120.5 kW
Humidification	Fresh air flow rate: 32500 m³/h[19] Supply conditions: 21°C/50%	61.7 kW
Total Heating Demand		**568.8 kW**

This value can be compared with the value "predicted" by the thermal signature generated by means of the billing data. For a mean outdoor temperature of -10°C, the thermal signature gives a total heating demand of about 556.5 kW. The fact that the two values are in a fair agreement (difference of less than 3%) confirms that the global heating demand of the building consumption is mainly due to heating and humidification.

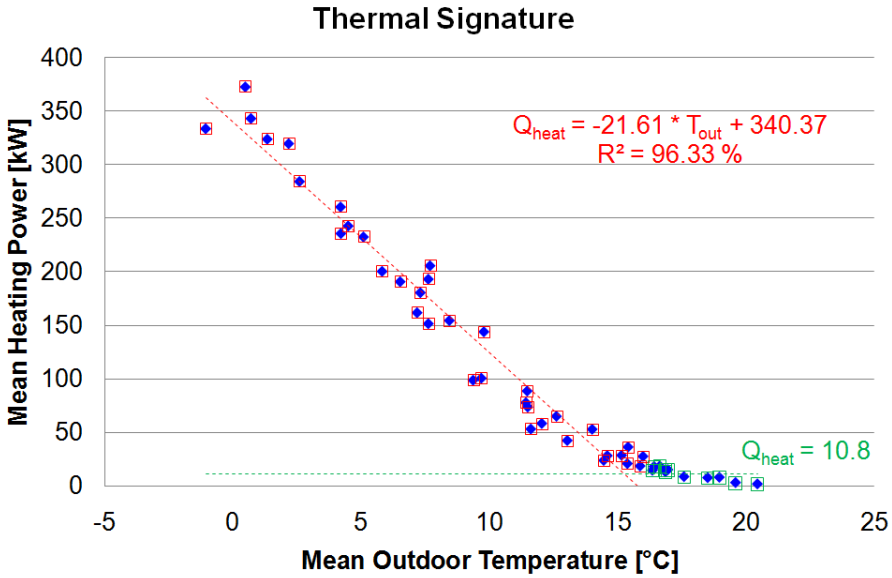

Figure 24: Thermal Signature (2008-2011)

[16] 21°C during 60 hours per week and 15°C rest of the time
[17] Average temperature in the first basement level supposed to be of about 10°C
[18] Ventilation is operating 60 hours per week and is off rest of the time → operation factor: 60/168 = 0.357
[19] Ventilation is operating 60 hours per week and is off rest of the time → operation factor: 60/168 = 0.357

6. MONITORING CAMPAIGN: EQUIPMENT AND DATA COLLECTION

The study of the present building involved on-site measurements. The objective was to refine the values of the parameters of the computer-based simulation tool by collection and analysis of actual data about building operation and consumptions.

For logistical simplicity, self-recording loggers were used. A “logger” as such can be any kind of sensor or measuring tool delivered with built-in memory. In this way, this relatively small object can be placed alone anywhere to measure and record data, which can be transferred later to a computer for analysis. The loggers which were used are described below.

In a building like the present one, with hundreds of office booths with different climates and internal loads, as well as operation, it is not reasonably feasible in a study of this kind to place loggers everywhere. Therefore, to gather as much representative and data as possible, the monitoring campaign was realized progressively, according to the needs of the calibration process. Available monitoring equipment and data collection techniques are presented below. Measurement results will be presented in a following section, during the calibration process.

6.1.1. Power Loggers

Three-phase power loggers can be installed on several electrical panels (Figure 25) to measure the electrical power demand at different levels (one or several floors, groups of components of the HVAC system…). The data logging system include one logger (including built-in memory and battery), 3 current clamps (one per phase) and four croc clips dedicated to voltage measurement. The local network is supposed to be balanced and the current through the common line is supposed to be negligible.

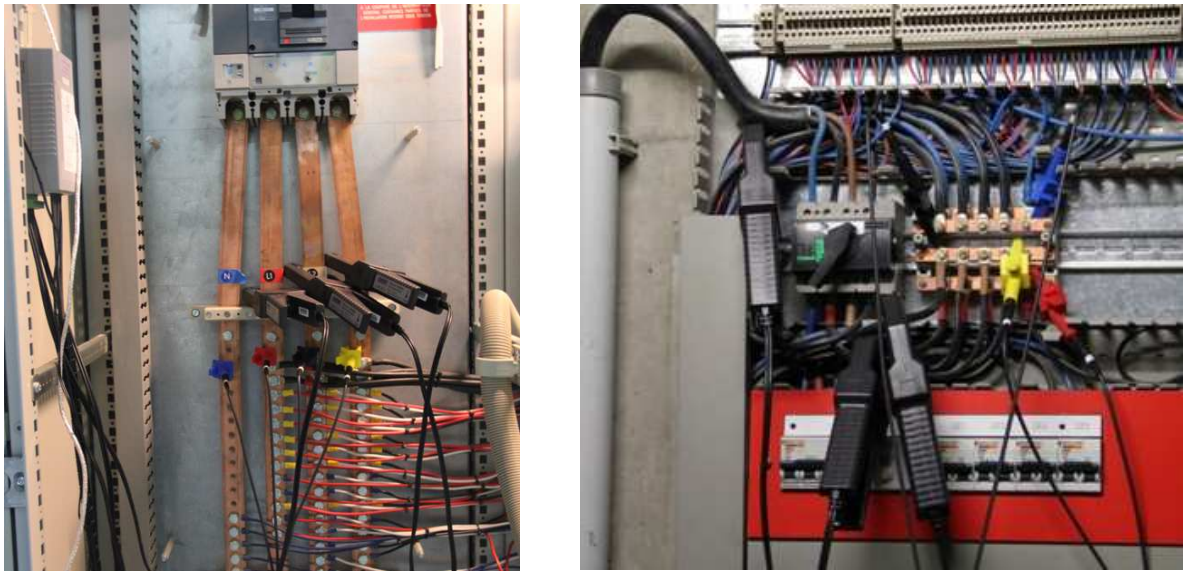

Figure 25: Power loggers installed on two electrical panels

Brand and model:	DENT ElitePro
Quantity:	2
Measurements:	true-RMS 3-phases AC electrical power and energy (actual, reactive and apparent), power factor, frequency
Range:	0-500 or 1000 A, depending on the current clamps in use
Record time step:	5 or 10 minutes

Usage: power and energy usage of main electrical panels
Error: less than 1% on reading and ~0.2% for sensors.

6.1.2. Plug-load loggers

Plug-load loggers are socket-mounted loggers (Figure 26) used to measure voltage, current, actual and apparent power of one or several classical appliance (e.g. computer, copiers…). Data is available with a 1 minute time step and stored on a SD memory card. Such loggers can be used to estimate the actual consumption of some typical appliances.

Figure 26: Socket plug load logger

Brand and model: Voltcraft Energy Logger 4000F
Quantity: 5
Measurements: voltage, current, frequency, power factor, actual and apparent power consumptions
Range: 1.5-3500 W
Record time step: 1 minute
Usage: placed in series with the appliances on the wall socket (Figure 26), they record their power consumption as a function of time.
Error: 1 to 2%

6.1.3. Local Temperature and Humidity Loggers

Temperature and humidity loggers (Figure 27) can be installed in various locations and are able to measure temperature and relative humidity with a 5-minutes time step. Measured values can be compared to the values of temperatures and humidity provided by the BEMS in order to check the accuracy and the influence of the location of the sensors used to control the HVAC system.

Figure 27: Indoor temperature and humidity logger

Brand and model: Lascar EL-USB-2-LCD+

Quantity: 6
Measurements: temperature (°C) and relative humidity (%)
Range: -35 to 80°C, 0 to 100% RH
Record time step: 5 minutes
Usage: measure the indoor comfort and cross-check the temperature in offices with the Building Energy Management System (BEMS)
Error: temperature error is of the order of 0.3°K and resolution is 0.5°K, humidity error can reach 4 points% but is typically of 2 points%

6.1.4. Lighting and appliances operating time loggers

Lighting loggers (Figure 28) do not provide a measure of the lighting intensity but record the time when the surrounding lighting intensity goes below or above a predefined level. These loggers are very useful to check the operation of artificial lighting fixtures. However, the location and the sensitivity level of the sensor have to be carefully defined to obtain exploitable results.

Figure 28: Lighting operating time logger (left) installed in the elevators area (right)

Brand and model: DENT Lighting SMARTLoggers
Quantity: 5
Measurements: on-time and on/off transitions of artificial lights
Sensitivity: manually adjusted to react to artificial lighting only
Record time step: on/off transitions only
Usage: check when lights are on or off in the offices and other rooms of the building
Error: Sensitivity is manually adjusted. The error will depend on the adjustment and whether the logger sees other sources of light (natural or artificial) than the one intended

Magnetic field loggers (Figure 29) operate in a similar way than lighting loggers. These loggers are very useful to check the operation of electric appliances (such as pumps, fans, motors, computers…). Once again, the location and the sensitivity level of the sensor have to be carefully defined to obtain exploitable results.

Figure 29: Magnetic field logger (left) installed to monitor the operating time of a pump (right)

Brand and model:	DENT Mag SMARTLoggers
Quantity:	5
Measurements:	on-time and on/off transitions of magnetic fields
Sensitivity:	minimum 40 mGauss – 4 µT
Record time step:	on/off transitions only
Usage:	Check when electric motors (fan, pumps) are on or off on the HVAC system.
Error:	Sensitivity is set manually at its minimal level to make sure the logger only "feels" the field it monitors.

6.1.5. Building Energy Management System (BEMS)

The Building Energy Management System (BEMS) control the operation of the HVAC system and the lighting system. To successfully achieve these tasks, temperature, humidity and operation (e.g. valve opening sensors) sensors are placed in many strategic points of the HVAC systems operation.

Most of these values can be easily recorded by BEMS software and then, compared to the physical measurements realized by means of the monitoring equipment described above. In the end, BEMS data can be confronted to:

- Theoretical (supposed) operation in order to check that the system is working according to the implemented schedules and setpoints.
- Loggers measurements in order to check that measured temperatures, humidity values and operating times correspond to actual (measured) values.

6.1.6. Occupancy Survey

Energy monitoring can be used in order to characterize HVAC systems, on one hand, and internal loads (lighting, appliances...), on the other hand. Both aspects, and especially the second one, are greatly influenced by the occupant's behavior. Measurements may quantify the impact of the actions of the occupants on the building systems, but are limited to some aspects (appliances use, lighting use...), and to a small sample of offices.

In regard to that, the establishment of an occupant's survey can be considered as a way of gathering data that could not be measured with the available loggers, such as actual daily occupancy of the building, but it is also a way to virtually extend the amount of offices that were monitored.

One of the expected results of such survey is the proportion of active and passive occupants, whether he/she interacts with the artificial lighting, window blinds, the fan coil units' thermostats on a regular basis.

The first step to submitting a survey to the occupants was to pin-point the data that are expected from it. Understanding the building operation from an occupant's point of view is a first stage to figuring out what he/she has control over (e.g. lighting fixture in his/her office, local thermostat...) and how his/her behavior can affect energy and power consumption.

In the present case, a questionnaire designed in the frame of the IEA-ECBCS Annex 53 project was designed and sent to the building's occupants. Indoor air quality, space and comfort, as well as lighting quality are not considered relevant issues in order to limit the length of the questionnaire. Indeed, a compromise has to be found between information needs and survey length. As many questions as possible, questions have to be merged and simplified to be answered more quickly. So, the questionnaire designed in the frame of this study (and given in the Appendix) focuses on occupants' presence, lighting use, appliances use and local thermostat setting.

6.1.7. Measurements uncertainty

The uncertainty on the available monitoring data is directly related to the accuracy of the sensors. However, the sampling error (amount of inaccuracy in estimating the value a given parameter based only on a limited amount of data) is also important and can be due to:

- A partial monitoring of the installation (e.g. monitoring of the lighting consumption of a unique floor in order to estimate the global lighting consumption of the building);
- A time-limited monitoring period (e.g. estimation of the winter indoor temperature setpoint based on 3 or 4 weeks of measurements);
- Non-measured seasonal variations (e.g. estimation of the lighting use rate in offices based on measurements performed during winter period).

In order to reduce the sampling error (or estimation error), it is necessary to:

- Carefully select the components/parts of the installation that will be monitored and to make sure that the selected components/parts are representative of the actual situation in order to allow extending the conclusions of the monitoring data analysis.
- Carefully choose (if possible) the monitoring periods (e.g. winter, summer or swing season) in order to catch the variations of the time-behavior (e.g. seasonal variations of lighting use, setpoints change…) of the monitored system.

Both measurement and sampling errors will be taken into account when updating the uncertainty ranges during the calibration process.

7. AVAILABLE WEATHER DATA

Several sets of weather data are available to perform this case study and are summarized in Table 18. These sets of data are characterized by:

- The geographical location of the measurement equipment,
- The availability of the data (starting date, ending data and data frequency),
- The measured values (temperature, humidity, solar radiation, atmospheric pressure, wind…).

Table 18: Weather data sets

Réf.	Location	Coordinates	Elevation	Source	Type[20]	Availability
M1	Mons	50.46°N 4.0°E	63 m	Werner Krenn meteo-mons.nival.be	DB, RH, ATM, GLOB	2006 – 60min
B1	Bruxelles	50.90°N 4.53°E	58 m	Bruxelles (EBBR) www.wunderground.com	DB, RH, ATM	1997 – 30min
B2	Bruxelles	50.93°N 4.53°E	16 m	Bruxelles (IVLAAMSG7) www.wunderground.com	DB, RH, ATM, GLOB	2008 – 15min
B3	Bruxelles	50.83°N 4.33°E	192 m	SODA *www.soda-is.com*	GLOB, DIFF	2005 – 30min
CS	Bruxelles	50.83°N 4.38°E	67 m	28 rue Demot, Bruxelles *Station Vantage Pro 2*	DB, RH, ATM, GLOB	2011 – 15min

Complete hourly measurements of temperature, humidity, atmospheric pressure and global solar radiation are freely available for Mons (data set M1), a city located about 52km SSW of Bruxelles. Data sets B1 and B2 are freely available data sets for Bruxelles but no guarantee is provided on the quality of the data. Moreover, about 5% of the values are missing and it is not possible to have a complete year of data.

The data set B3 only includes values of global and diffuse solar radiations. These values are based on the HC3v3 data base. Solar radiation at the ground level is computed by means of the Heliosat method. On this base, a mathematical method developed by Ruiz-Arias (2009) is applied to derive the values of diffuse radiation. Such values could be used to complete data set B1 or B2 which include partial or no information about solar radiation. However, when analyzing this data set, it appeared that the provided values of the diffuse radiation were particularly low comparing to other data.

In 1982, Erbs developed a correlation based on numerous measurements made in the US. The aim of this correlation was to estimate the part of diffuse radiation based on the clearness of the sky. The clearness of the sky is characterized by the clearness index (ratio between actual global radiation and theoretical global radiation) and used to predict the diffuse-to-global solar radiation ratio.

$$R_1 = 1 - 0.09 * k_T$$

$$R_2 = 0.9511 - 0.1604 * k_T + 4.388 * k_T^2 - 16.638 * k_T^3 + 12.336 * k_T^4$$

$$R_3 = 0.165$$

$$\frac{I_{diff,h}}{I_{glob,h}} = \begin{cases} R1 \; if \; k_T \leq 0.22 \\ R2 \; if \; 0.22 < k_T \leq 0.8 \\ R3 \; if \; k_T > 0.8 \end{cases}$$

[20] DB : Drybulb temperature ; RH : Relative Humidity; ATM: Atmospheric Pressure; GLOB: Global Horizontal Radiation; DIFF: Diffuse Horizontal Radiation

Where

k_T is the clearness index

$I_{diff,h}$ is the diffuse radiation on an horizontal surface, in W/m²

$I_{glob,h}$ is the global radiation on an horizontal surface, in W/m²

Figure 30 shows a comparison between the values of diffuse radiation given in typical data sets of Bruxelles (TMY data from Meteonorm and IWEC). The correlation coefficient in both cases is above 93%.

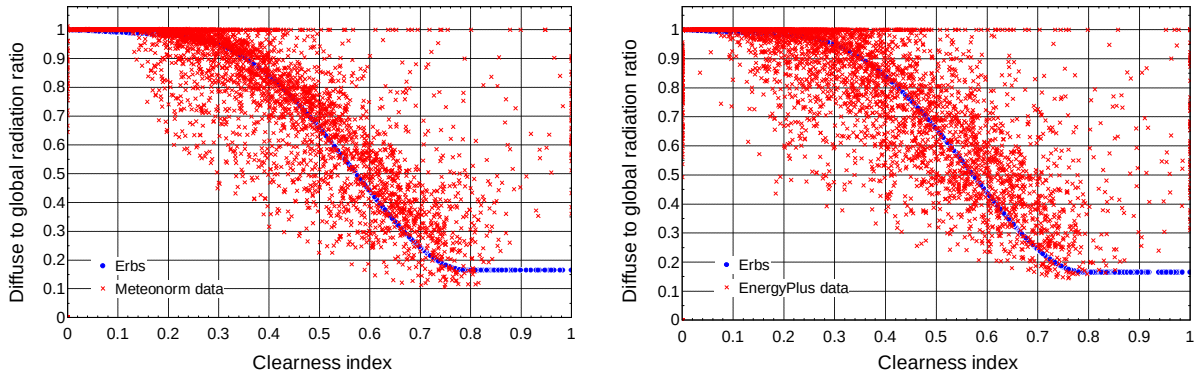

Figure 30: Comparison between Erbs correlation and Typical weather data sets (left: Meteonorm; right: IWEC)

Applying the Erbs correlation mentioned above to the B3 data set gives the results shown in Figure 31. As mentioned above, the values of diffuse radiation provided by SODA (B3 data set) seem surprisingly low. So, it was decided to reject this data set. Obviously, this also excludes the data set B1 which includes no information about solar radiation.

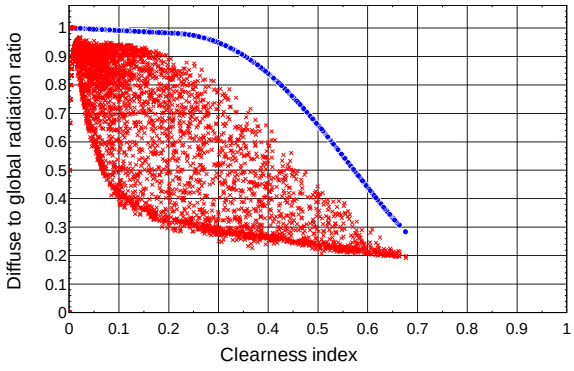

Figure 31: Comparison between B3 data set (red dots) and Erbs Correlation (blue dots)

In March 2011, a weather station "Vantage Pro 2 Plus" has been installed on the roof of the case study building (Figure 32) and would allow the collection of complete sub-hourly onsite measurements. Unfortunately, such data is not available yet to perform model calibration on a complete year.

Brand and model: Davis Wireless Vantage Pro 2 Plus
Quantity: 1 (available 10/02/11)
Measurements: precipitations, temperature, relative humidity, pressure, wind speed and direction, solar radiation
Range: - precipitations: maximum 2438 mm/hr
- temperature: -40 to 65°C
- relative humidity: 0 to 100%

- pressure: 540 to 1100 hPa
- wind speed: 1.5 to 79 m/s
- solar radiation: 0 to 1800 W/m²

Record time step: 15 minutes

Usage: gather precise local weather data (mainly temperature, humidity and solar radiation)

Error:
- precipitations: highest value from 5% or 1 mm/hr
- temperature: 0.5°C
- relative humidity: 3 % (4% above 90% RH)
- pressure: 1 hPa
- wind speed: highest value from 5% or 1 m/s
- solar radiation: 5% of full scale

Figure 32: Weather station installed on building rooftop

No complete data set is available for the surrounding of the building (Figure 33). Indeed, it appears that only the weather data set of Mons is fully complete. Available data for Bruxelles or Bruxelles suburbs are not complete (yet) and cannot be used in the frame of the present study. Since measured on-site are not complete neither, it was decided to use the weather data sets available for Mons.

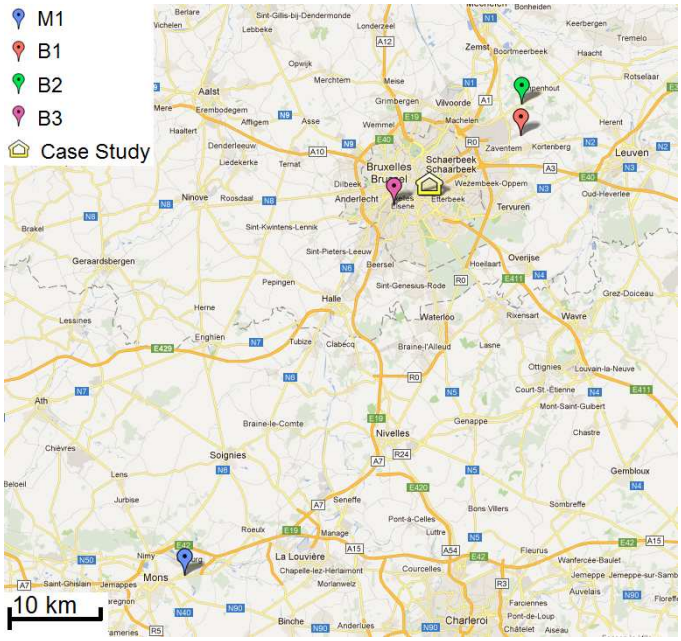

Figure 33: Weather data collection locations

Mons and Uccle (city located in the suburbs of Bruxelles) climates are compared in terms of Heating Degree Days in Table 19 in order to estimate the bias related to the use of Mons weather data for the further simulation work.

Table 19: Heating Degree Days for Uccle and Mons

HDD 16.5	2008	2009	2010	Average 1961-2010
Mons	2305.08	2317.93	2770.62	-
Uccle	2214.57	2224.77	2700.41	2446 +/- 229

Data from Mons and region of Bruxelles (B1) for 2010 had also been compared on an hourly basis. Comparison of measured Drybulb temperature, Dewpoint temperature and Atmospheric Pressure led to RMS error values of 1.7 °K, 1.3°K and 1.54 hPa, respectively.

Regarding these comparisons, it appears that the climates of both regions are quite similar. However, it is also interesting to try to estimate the impact of the urban heat island effect. Indeed, except the data collected on-site, other data do not take this effect into account since all the corresponding weather stations are located in the country-side or in suburbs areas.

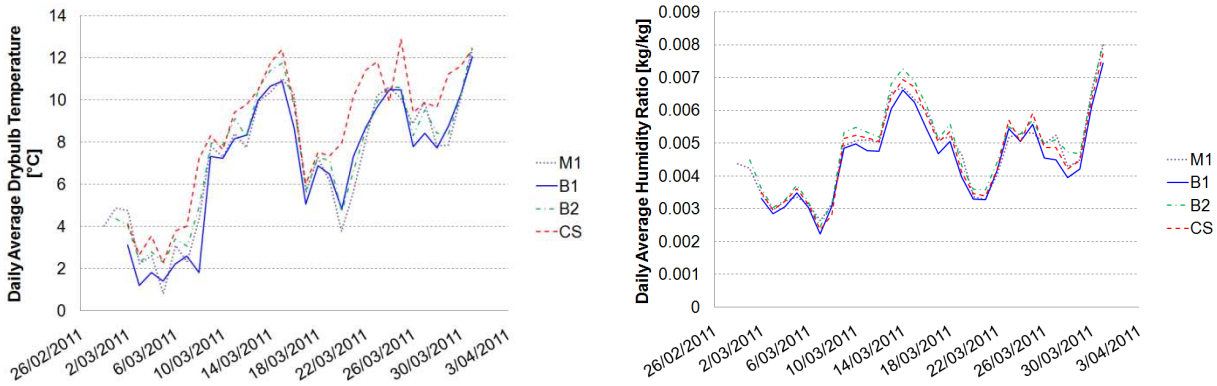

Figure 34: Comparison of drybulb temperature and humidity ratio - March 2011

The data shown in Figure 34 confirm that values of humidity ratio are very similar for all the data sets. However, one can observe a clear offset between the drybulb temperatures measured on-site (CS) and the other data-sets. The RMS deviation between B2 and CS drybulb temperatures on the considered period (March 2011) is about 1.5°K.

Regarding the available data, the data sets from Mons will be used since they include the required data with a sufficient time step (one hour) for several years. Even, if the climate in the region of Mons is similar to the one in the region of Bruxelles, the urban heat island effect should be taken into account during the analysis. So, the Mons weather data sets will be used as they are but an additional uncertainty will be added to the drybulb temperature to perform the uncertainty analysis.

Since only global solar radiation is available, the Erbs correlation (1982) mentioned earlier will be used to derive the diffuse solar radiation.

Table 20: Uncertainty on weather data

	Uncertainty	Urban heat island effect	Final Uncertainty
Drybulb temperature	+/- 0.5°C	+/- 1.5°C	+/- 2°C (abs)
Humidity Ratio	+/- 10%		+/- 10% (rel)
Global and Diffuse Solar Radiation	+/- 10%		+/- 10% (rel)

8. CALIBRATION PROCESS

Regarding the availability of the weather data (see section 0) and billing data (see section 5), it has been decided to evaluate the accuracy of the calibration by computing the classical calibration criteria (in terms of MBE and CVRMSE calculated on a monthly basis for natural gas, peak and offpeak electricity consumptions) from 4th January 2008 to 27th December 2010. In addition to these relatively soft criteria, recorded and predicted hourly peak demand profiles for the three years will also be compared to check the accuracy of the calibrated model.

The first stage of the modeling process will consist in building the “as-built” input file based on the data provided in sections 2 and 3 (Table 21). This first input file will be used as a base case for the preliminary sensitivity analysis. During this sensitivity analysis, special attention will be paid to the most influential parameters highlighted in chapters 4 and 5. As it was observed in chapter 5, it is not

mandatory to run a new sensitivity analysis at each step of the calibration process. Indeed, it was shown that despite of the narrowing of the range as the calibration was progressing; the main conclusions of the screening method remained valid all along the process (i.e. the hierarchy between influential and less-influential parameters remained valid). So, in the present case, the results of this preliminary sensitivity analysis will be used all along the calibration process and to orient the data collection work.

In a second step, three successive calibration levels will be considered in the following as a function of the type/category of information which is available (i.e. as-built information, observations made during on-site inspection, monitoring data…). These calibration levels correspond to different stages of the data collection process (from data collected during on-site inspection to detailed energy metering and occupancy survey). At each level, the evidence-based calibration process described in Chapter 3 (Figure 35) will be followed.

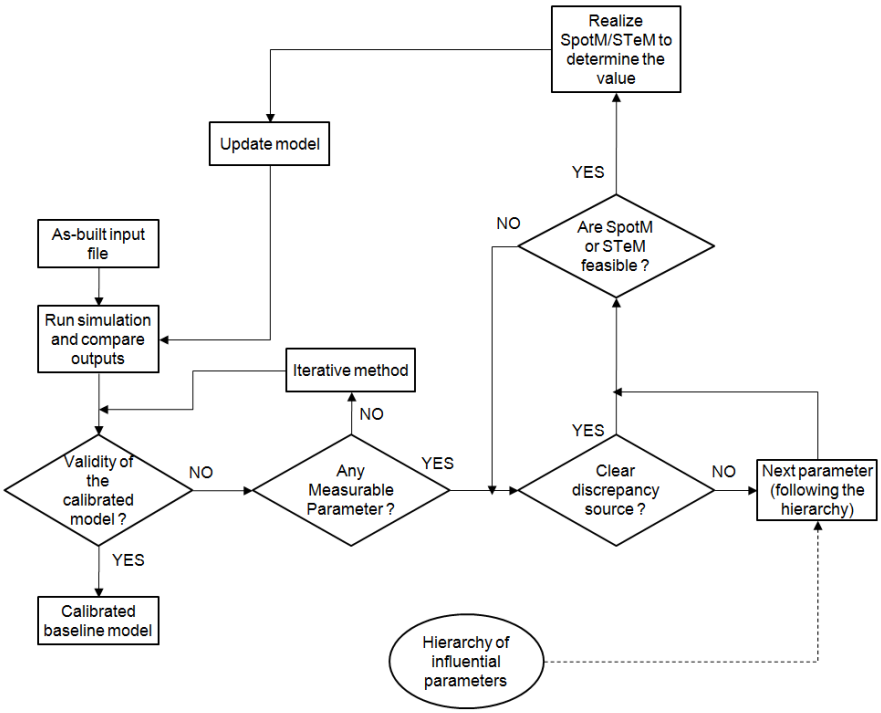

Figure 35: Evidence-based calibration process

The distinction between influential and non-influential parameters and the hierarchy between the most-influential parameters established are based on the results of the preliminary sensitivity analysis. At each step of the calibration process, it will be tempted to identify the best-guess values of the influential parameters by means of the available information (as-built file, inspection results, BEMS records, spot and short-term measurements data…). A probability range will also be considered in order to allow a quantification of the uncertainty on the final energy use predicted by the calibrated model. As explained in previous chapters, the best guess values will be adjusted and probability ranges will be narrowed as the calibration will progress and the information on the building and its use will become more detailed and accurate.

The calibration level 2 corresponds to the “inspection phase” and information about building and system operation are made available by means of a direct (“on-screen”) analysis of the BEMS system. At this stage, no verification of the data provided in the BEMS is done (e.g. no verification about the achievement of the specified setpoints…) and no measurement/recording is done but the information collected during the inspection of the building and summarized in section 4 is used to adjust the

parameters of the model and to define the probability range of each parameter according to the estimated quality of the information.

The next calibration level (3) will make an intensive use of BEMS records and of the monitoring data collected on-site by means of the measurement equipment described in sections 6.1.1 to 6.1.5. At this stage, the probability ranges depend on the accuracy of the sensors, loggers and recorders.

The fourth level (level 4) will include the information derived from the analysis of the answers to the survey presented in section 6.1.6.

Finally, a last level could consist in an iterative adjustment of some uncalibrated parameters. A prospective manual adjustment will be performed in order to investigate potential improvements of the models and orient future data collection work.

Table 21: Calibration levels

Calibration levels		**Building description and performance data available for calibration**					
		Utility bills[21]	WBE demand[22]	As-built data	Inspection	Spot/Short-term monitoring	Occupancy survey
Evidence-based process	**Level 1**	x	x	x			
	Preliminary Sensitivity Analysis						
	Level 2	x	x	x	x		
	Level 3	x	x	x	x	x	
	Level 4	x	x	x	x	x	x
	Final simulation results and uncertainty on the predicted energy use						
Final adjustment	**Level 5**	Iterative adjustment of uncalibrated parameter					

In order to stay “conservative”, probability ranges will always be set to their wider values. At the first calibration level, uniform probability distribution functions will be used to generate the samples used for sensitivity and uncertainty analyses. Later (during the calibration process), normal probability density function will be used to characterize variations of the parameters which will be identified by physical measurements (resulting in average and standard deviation values of the considered parameters).

At each step of the calibration process, the simulation results that would be considered for analysis are the ones that correspond to the “best-guess” set of parameters. The classical calibration criteria (MBE and CVRMSE) will be evaluated based on the available consumption data (monthly gas and electricity consumptions and hourly power demand). Visual analysis and comparison of the simulation results will also help in estimating the accuracy of the calibrated model. Finally, performing an uncertainty analysis will help in quantifying the final uncertainty on the predicted energy consumptions.

[21] Natural gas, peak-hours and offpeak-hours electricity consumption (in kWh) provided on a monthly basis
[22] WBE demand : whole-building electricity demand (in W) provided by the electricity provided on a quarter-hour basis

8.1. LEVEL1: INITIAL AS-BUILT INPUT FILE

8.1.1. Available data and parameters adjustment

The initial input file is built based on the as-built information (sections 2 and 3) but does not include any information about actual building use or operation (section 4). The ground floor is divided in 5 distinct zones (Figure 36). The zone 3 corresponds to the entrance hall. The four other zones include offices, meeting rooms and library. In order to reduce the computation costs, thermal behavior of core zones and circulations is not simulated since the indoor climate in those zones is not controlled (no heating/cooling/humidification/air supply). The effects of heat and mass transfer between the simulated (peripheral) zones and the core/circulation areas on building energy demands are neglected.

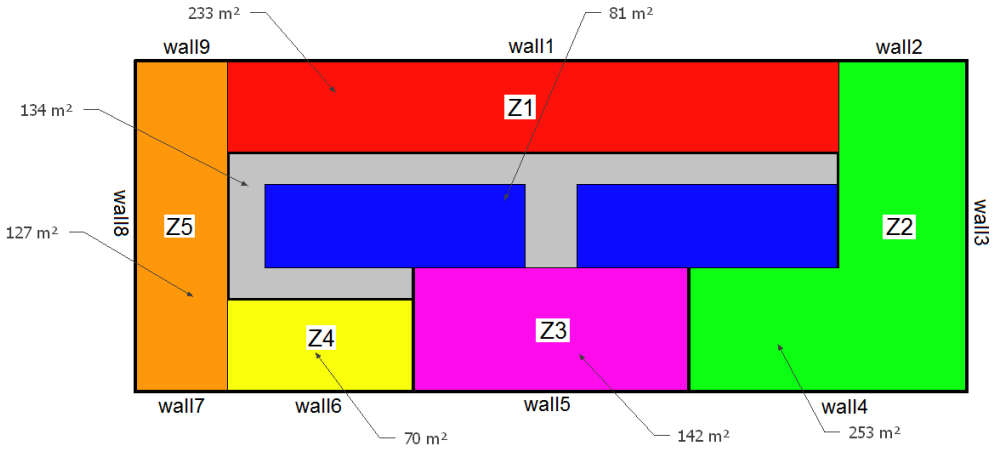

Figure 36: Ground floor – definition of thermal zones

The 8 office levels are divided in four peripheral zones (zone 6 to zone 9, Figure 37). For the reasons explained above, core and circulation areas are not considered for simulation.

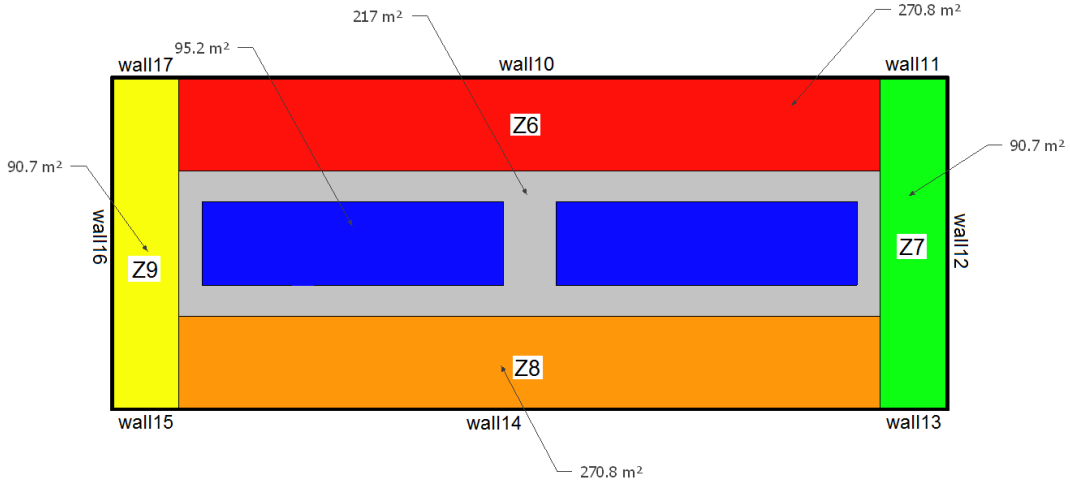

Figure 37: Floors 1 to 8 – definition of thermal zones

Regarding the location of the building, no shading masks are taken into account on SW and SE façades. Shading masks on NE and NW façades have been taken into account by estimating the angular height of the obstructing element (surrounding building or small hill) but have very limited influence on the calculation of incident solar radiation.

The entire HVAC system has been modeled. The as-built information given in sections 3.1 to 3.4 have been used to set the parameters of the model. Since they have similar components and operation, the

main AHUs have been consolidated two by two (AHUs 1&2 and 3&4) following the rules proposed by Liu et al. (2004) mentioned in Chapter 2.

The manufacturer data about the two chillers are used to identify the parameters of the chiller model (Figure 38). As shown in

Table 22, identified values are very similar to the default values available for similar configurations (water-cooled screw chiller). Part load data are not available so a default part load curve will be used to simulate the performance of the chiller at low loads.

Table 22: Chiller model parameters – Full load characteristics

Chiller model parameters	C1	C2	D1	D2
Default values	8.5	25.5	-0.0034	0.03
RTWA215	7.522	32.11	-0.003846	0.05769

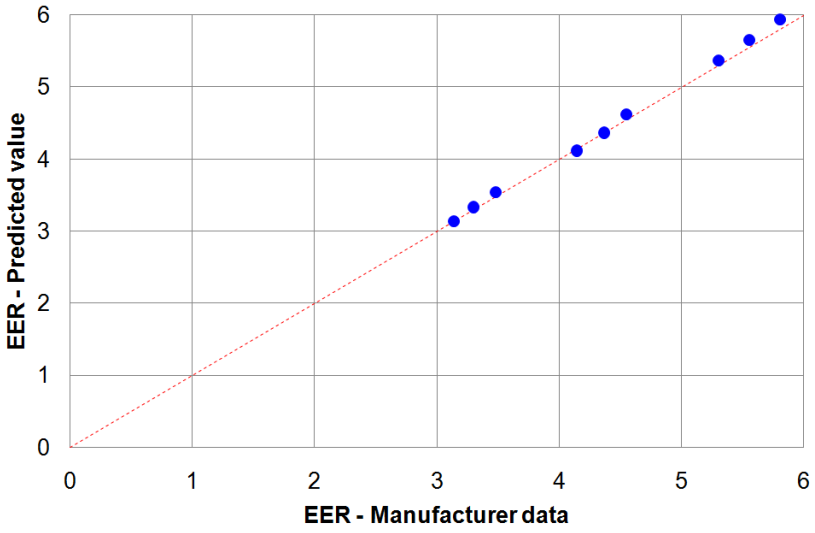

Figure 38: Chiller model parameters identification – Full load data

The main parameters of the model are summarized below. Only the parameters concerned by the calibration process are given in Table 23. The selection of the 45 "likely influential" parameters is based on the results of the sensitivity analysis's performed in Chapters 4 and 5. Best-guess values have been set for every parameters based on the as-built information described above.

Variation ranges have also been set based on the (qualitative) uncertainty related to the source of the information in order to allow running uncertainty and sensitivity analyses. Conservative hypotheses have been made in order to define relatively large uncertainty ranges.

Regarding wall compositions, the as-built information were quite complete and allowed identifying relatively accurate "best-guess" values of envelope components characteristics (e.g. U-values). The remaining uncertainty is related to the potential differences between the as-built file and the realization (presence of thermal bridges…). Larger uncertainties remain regarding the composition of the light opaque window components (P2) and on building thermal capacity (P6). Indeed, the composition of the light opaque walls (window sill) is not well known (uncertainty on the presence and thickness of insulation) and it was not possible to accurately estimate the "accessible" part of the global thermal capacity of the building's structure (because of a lack of information about composition of building's internal walls and structure).

Since no information was available about the use of manual external shadings, the nominal glazing SHGC value (P5) was used as a "best-guess" (supposing no impact of the solar shading system on envelope performance and subsequent energy consumptions) but a larger uncertainty interval of [-50%; +5%] was considered. Such uncertainty range allows taking into account the accuracy of available manufacturer data (+5%) and a relatively intensive use of the shading system (decrease of the glazed surface exposed to solar radiation of-50% in average).

The infiltration rate (P7) was estimated based on values commonly used in practice for this type of building (i.e. fixed frames and slight over-pressure during ventilation system operation periods) but an important uncertainty remains.

At this level, no information is available regarding the building use and operation. So, internal gains and corresponding schedules (parameters 8, 9, 10 and 35 to 45) are set to default/typical values and characterized by large probability ranges (+/- 50%). It has to be noticed that no "IT" power demand was considered since no information about IT rooms was available in the as-built file. A similar remark can be done for building/HVAC operation parameters (P11 to P14, P19, P20, P23, P27, P29, P33 and P34): default values and corresponding large probability ranges are considered for setpoints and operating schedules.

Since only as-built/nameplate values were available to characterize ventilation fans and circulation pumps (P17, P18, P26, P30, P31 and P32); relatively large ranges of variation have been considered (+/- 25%) in order to take into account the possible overestimation of the actual absorbed power of these components.

The other parameters, such as chiller nominal EER (P28), are characterized by small variations ranges since the available information for such components was quite detailed (complete manufacturer data…).

Table 23: Level 1 - Input parameters values and uncertainty ranges

#	Variable	Unit	Description	Level 1	Min[23]	Max
1	U_{hopw}	W/m²-K	Vertical heavy opaque walls U-value	1.01	-10%	+10%
2	U_{lopw}	W/m²-K	Vertical light opaque walls U-value	2.65	-50%	+0%
3	$U_{gl,w}$	W/m²-K	Glazing U-value	1.4	-7%	+7%
4	$U_{fr,w}$	W/m²-K	Window frame U-value	2.27	-10%	+10%
5	$SHGC_{gl,0}$	-	Glazing normal SHGC	0.67	-50%	+5%
6	$C_{m/m²}$	J/m²-K	Thermal capacity	165000	-33%	+33%
7	ACH_{inf}	-	Infiltration rate	0.4	-50%	+50%
8	$IGFR_{light}$	W/m²	Lighting power density – Offices/meeting	12	-50%	+50%
		W/m²	Lighting power density – Circulation	5	-50%	+50%
		W/m²	Lighting power density – Utility rooms	12	-50%	+50%
		W/m²	Lighting power density – Parking	5	-50%	+50%
9	$IGFR_{appl}$	W/m²	Appliances power density – Offices	10	-50%	+50%
		W/m²	Appliances power density – Utility rooms	10	-50%	+50%
10	$IGFR_{addload}$	kW	Appliances power – IT rooms	0	-	-
11	$T_{i,set,h,occ}$	°C	Heating setpoint – Offices/meeting	21°C	-2°C	+2°C
			Heating setpoint – Entrance hall	21°C	-2°C	+2°C
12	$T_{i,set,h,nocc}$	°C	Heating setpoint (night) – Offices/meeting	15°C	-2°C	+2°C

[23] In this table and in the following, values in % are relative values. Others are absolute values.

			Heating setpoint (night) – Entrance hall	15°C	-2°C	+2°C
13	$T_{i,set,c,\ occ}$	°C	Cooling setpoint – Offices/meeting	25°C	-2°C	+2°C
			Cooling setpoint – Entrance hall	25°C	-2°C	+2°C
14	RH_{min}	-	Humidification indoor setpoint	0.5	-20%	+20%
15	ACH_{out}	-	Average ventilation rate	1.85	-5%	+5%
16	$\varepsilon_{hum,n}$	-	Humidifier effectiveness	0.85	-5%	+5%
17	SFP_{sufan}	W/m³-s	Average supply fan specific power	1442	-25%	+25%
18	SFP_{retfan}	W/m³-s	Average return fan specific power	942	-25%	+25%
19	$T_{a,ex,AHU,set,max}$	°C	Maximal supply temperature setpoint	19	-2°C	+2°C
20	$T_{a,ex,AHU,set,min}$	°C	Minimal supply temperature setpoint			
21	$k_{h,loss}$	-	Hot water network loss coefficient	0.02	-50%	+50%
22	$k_{c,loss}$	-	Chilled water network loss coefficient	0.02	-50%	+50%
23	$T_{hw,set}$	°C	Hot water temperature setpoint	80/60	-10°C	+10°C
24	$\eta_{hwboiler,n}$	-	Boiler efficiency	0.955	-2.6%	+2.6%
25	$f_{hwboiler,sbloss}$	-	Boiler standby losses coef.	0.005	-100%	+100%
26	PP_{hw}	W	Hot water pump power	6023[24]	-25%	+25%
27	$T_{cw,set}$	°C	Chilled water temperature setpoint	7°C	-3°C	+3°C
28	$EER_{lcp,n}$	-	Chiller efficiency	4.27	-5%	+5%
29	$T_{ct,set}$	°C	Cooling tower setpoint	26°C	-3°C	+3°C
30	PP_{cw}	W	Chilled water pump power	17700[25]	-25%	+25%
31	PP_{cd}	W	Condenser pump power	15000[26]	-25%	+25%
32	PP_{ct}	W	Cooling tower pump power	4400[27]	-25%	+25%
33	$C_{sched,AHU}$	h	AHU daily operation time	14	-2h	+2h
34	$C_{sched,set}$	h	H&C system daily operation time	14	-2h	+2h
35	$A_{sched,occ}$	-	Occupancy rate (day time)	1	-0.5	+0
36	$C_{sched,occ}$	h	Daily occupancy time	10	-2h	+2h
37	$A_{sched,light}$	-	Lighting operation rate (day time)	1	-0.5	+0
38	$B_{sched,light}$	-	Lighting operation rate (night time)	0	-0	+0.5
38	$C_{sched,light}$	h	Lighting daily operation time	10	-2h	+2h
40	$A_{sched,appl}$	-	Appliances operation rate (day time)	1	-0.5	+0
41	$B_{sched,appl}$	-	Appliances operation rate (night time)	0	-0	+0.5
42	$C_{sched,appl}$	h	Appliances daily operation time	10	-2h	+2h
43	$A_{sched,addload}$	-	IT equipment operation rate (day time)	1	-0.5	+0
44	$B_{sched,\ addload}$	-	IT equipment operation rate (night time)	0	-0	+0.5
45	$C_{sched,\ addload}$	h	IT equipment daily operation time	10	-2h	+2h

[24] Total installed power as given in Table 9
[25] Total installed power as given in Table 11
[26] Total installed power as given in Table 11
[27] Total installed power as given in Table 11

8.1.2. Calibration and accuracy criteria

First of all, it is interesting to notice that the classical criteria (MBE_{month}<5% and $CV(RMSE)_{month}$<15%; ASHRAE, 2002) computed for monthly natural gas (Table 24) are almost satisfied. A priori, this could mean that implementing complete as-built information with realistic occupancy/operating profiles in the model is sufficient to approximate the heating demand of the building and represent the main seasonal variations (Figure 39), even if no detailed information about building use/operation is taken into account. These results are in good accordance with the results obtained for "as-built models" by Ahmad and Culp (2006): annual global consumptions predicted with a +/- 30% deviation.

However, it is important to notice that statistical criteria are far from being satisfied when looking at global, peak and offpeak electricity consumptions (MBE reaching 11.3% for peak consumption and 89% for offpeak consumption). The graphical analysis of the monthly values (Figure 40) allows highlighting the compensation effect: the underestimation of the offpeak consumption partially compensates the overestimation of the peak consumption. This compensation explains the intermediate values of MBE obtained for the total electricity consumption (MBE of -18.8%).

Table 24: Level 1 - Calibration accuracy indexes

1 - %	2008 to 2010	
	MBE	CV(RMSE)
Gas	-3.1	17.9
Elec	-18.8	20.2
Peak	11.3	13.5
Offpeak	-89.3	91.1
Hourly	-18.8	63.4

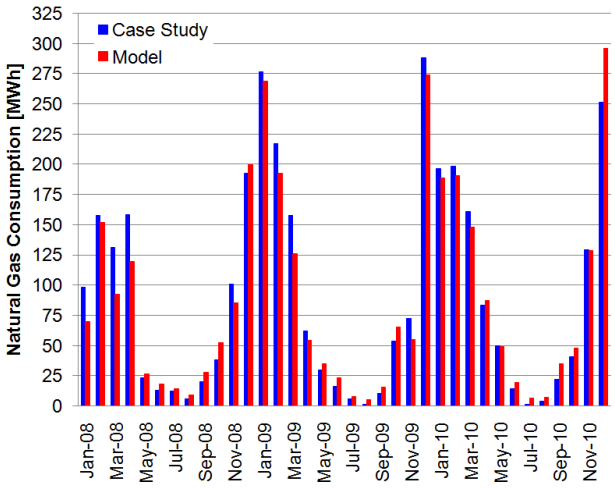

Figure 39: Level 1 - Monthly Gas Consumption Comparison

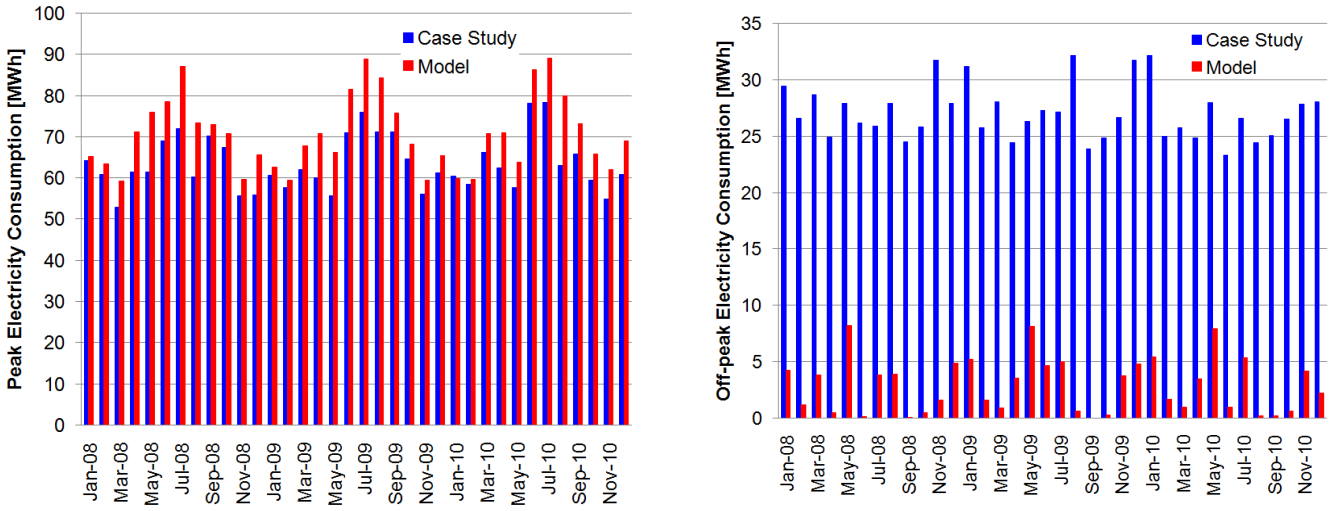

Figure 40: Level 1 - Monthly Peak (left) and Offpeak (right) Electricity Consumptions Comparison

The value of the mean bias error (MBE[28]) is quite important (18.8%) when comparing recorded and predicted hourly power demand profiles. This can be explained by some internal loads which are not or badly taken into account in the model and by the use of hypothetic operating profiles. The values of the CV(RMSE) is high (63.4%) because of bad representations of the daily variations, the base load (0 to 1 kW instead of 50 kW in reality), the peak demands (270 kW instead of 240 kW in reality) and the variations of the power demand during weekends (Figure 41). Deviations are even more important when looking at a summer week when the effect of the cooling demand of the building is visible on the power demand profile.

This confirms that it is still too early to consider the model as "properly calibrated".

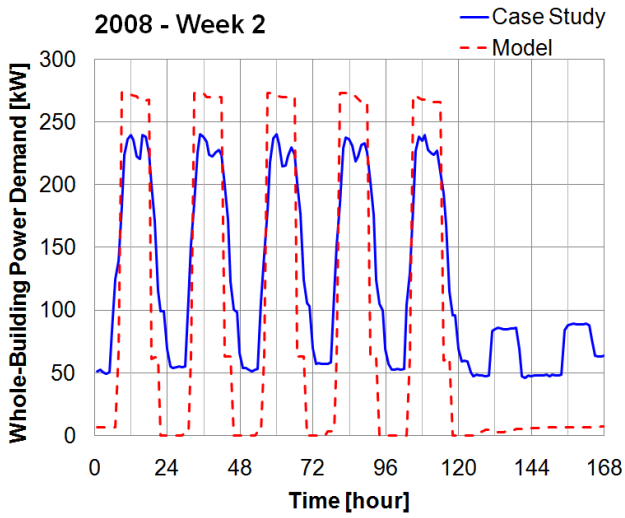

Figure 41: Level 1 - Predicted and recorded whole-building power demand (2008 - week 2)

8.1.3. Uncertainty analysis

As mentioned before, an uncertainty analysis is performed by means of the LHMC method. A sample of 100 simulation runs is built basing on the probability/uncertainty ranges given in Table 23 by means of the Monte Carlo method described in Chapter 4. Uniform probability distributions have been used (conservative hypothesis).

[28] Criteria: MBE_{hour}<10% and $CV(RMSE)_{hour}$<30% (ASHRAE, 2002)

Once again, the results obtained by means of the LHMC uncertainty analysis are summarized as boxes and whiskers. Upper and lower edges of the blue boxes correspond to the 25th and 75th percentiles. The red line corresponds to the median value of the generated sample of values. The whiskers (dotted lines) extend to the most extreme values without considering outliers. Outliers are plotted separately (red crosses). A data point is considered as an outlier if it is larger than $y^{75th} + 1.5*(y^{75th} – y^{25th})$ or lower than $y^{25th} – 1.5*(y^{75th} – y^{25th})$. Best guess values are represented as blue stars and do not correspond necessarily to the average result value because all the probability ranges specified for the studied parameters are not symmetric and the model includes some high-order effects.

As shown in Figure 42, uncertainty ranges on the simulation results are quite large. Standard deviations for gas and electricity consumptions vary between 14% and 37% and 19 and 22%, respectively. Recorded monthly consumptions are within the ranges of the consumptions predicted by the simulation model. This reassures the user on the hypotheses made to estimate the uncertainty ranges given in Table 23.

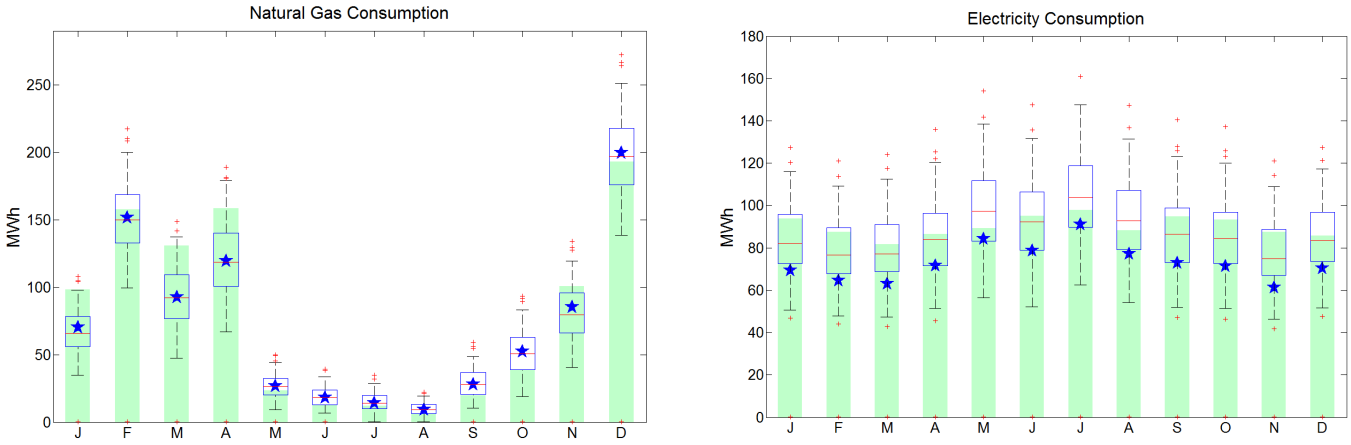

Figure 42: Level 1 - Uncertainty on predicted final energy consumptions

The resulting uncertainty on electricity end-use (Figure 43) is also significant and confirms the poor quality of the simulation results at this stage of the calibration process. Looking at the error bars shown in Figure 43, it seems to be difficult to draw meaningful conclusions about the energy use in the building.

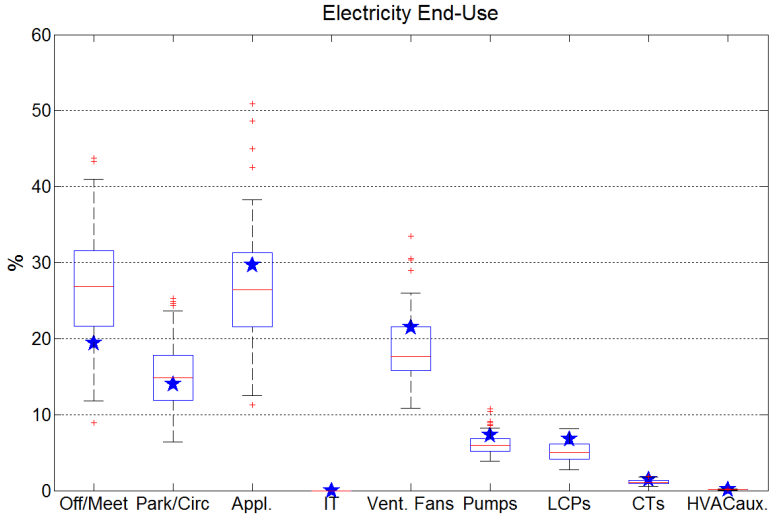

Figure 43: Level 1 - Uncertainty on electricity disaggregation

8.1.4. Preliminary Sensitivity Analysis

As expected, the conclusions that can be drawn basing on the results of the preliminary sensitivity analysis (Figure 44 and Figure 45) are similar to the conclusions drawn during previous analyses performed on similar buildings in Chapters 4 and 5.

Since the uncertainty on the main characteristics of the envelope components (P1 to P4 and P6) is relatively limited (maximum +/- 10%, thanks to the detailed architectural plans and as-built file), the impact of these parameters is reduced and focus should be given to more influential parameters. However, the larger uncertainty on the SHGC value due to the unknown use of external shadings has a non negligible impact on winter gas consumption and summer electricity consumption.

Despite of the limited probability range (+/- 5%) set for the ventilation rate (P15); this parameter has a major influence on natural gas consumption and a non-negligible impact on the electricity consumption. However, the measurement of this parameter is hard to implement and the as-built values will be conserved (lack of a better) as “best-guess values” during the first steps of the calibration process (at least). The infiltration rate (P7) has also an important influence on gas consumption but is impossible to measure in a building in operation.

Heating (P11, P12) and humidification (P14) indoor setpoints and cooling (P13) indoor setpoint have a considerable influence on the winter natural gas and the summer electricity consumption, respectively.

HVAC system operating schedules (P33 and P34) as well as some HVAC components performance indexes (ventilation fans efficiencies, P17 and P18; heating plant efficiency, P24 and P25; cooling plant efficiency, P27 and P28) have also an important influence on the model’s outputs.

Finally, internal loads densities (P8 to P10) and corresponding schedules (P35 to P45) have a major impact on winter gas consumption and on both winter and summer electricity consumptions.

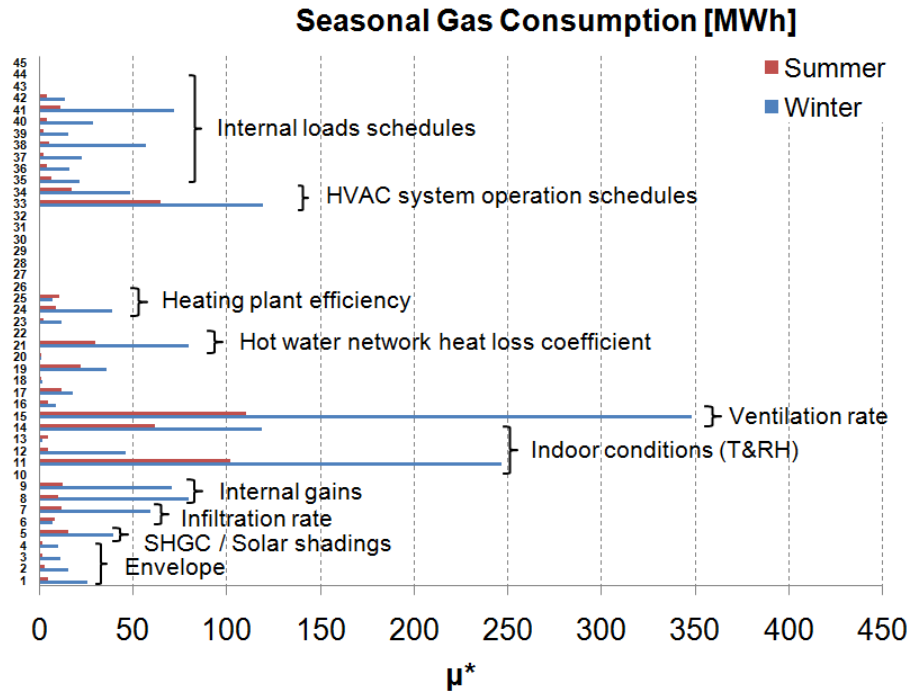

Figure 44: Preliminary Sensitivity Analysis – Seasonal natural gas consumption (μ* values)

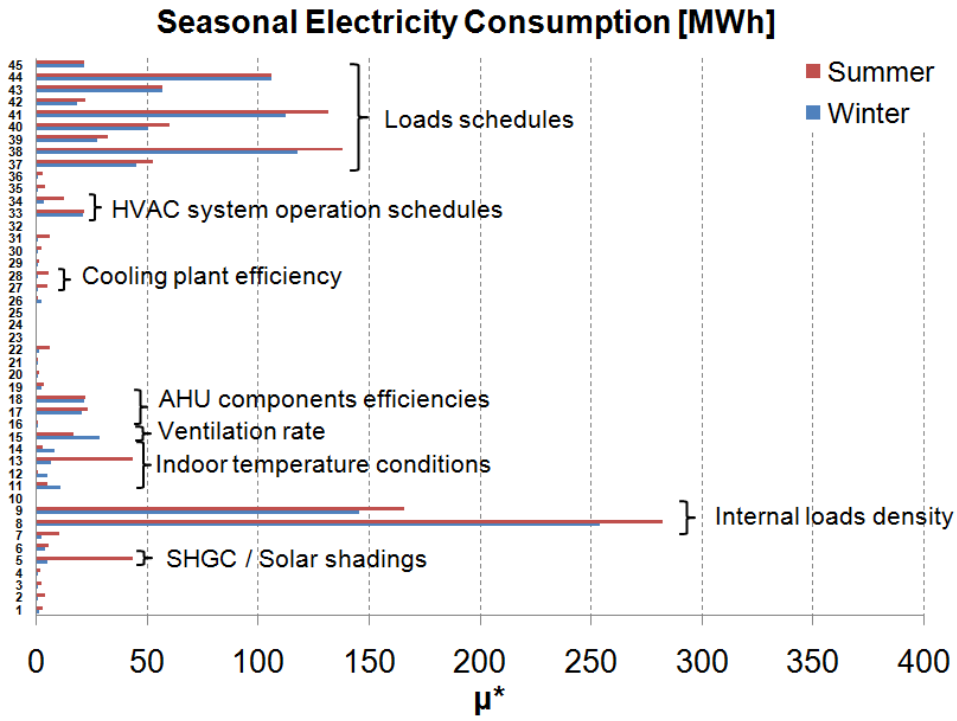

Figure 45: Preliminary Sensitivity Analysis – Seasonal electricity consumption (μ* values)

In order to identify the parameters that have to be calibrated to allow a good representation of heating and cooling needs, elementary effects of the 45 studied parameters on hot and chilled water needs are plotted in Figure 46. As observed in a previous chapter, gas consumption and heating needs are directly correlated. It is also interesting to notice that, in the present case, parameters influencing cooling needs (indoor cooling setpoint, glazing SHGC and internal gains) have already been identified by studying the effects on electricity consumption even if the hierarchy between these parameters is slightly different (higher impact of SHGC and cooling setpoint).

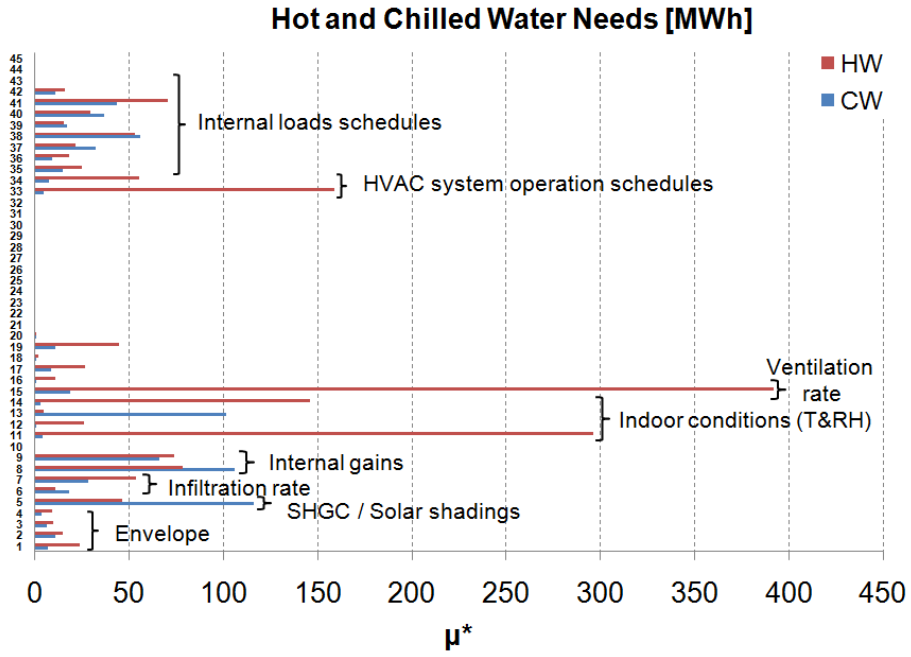

Figure 46: Preliminary Sensitivity Analysis - Annual Hot and Chilled Water Needs

Figure 47 and Figure 48 show the (σ,μ*) representation of the results of the preliminary sensitivity analysis. It is interesting to notice that most of the parameters having a considerable impact on natural gas consumption are characterized by high-order interactions (e.g. P8, P11, P15, P33…). This representation of the results also allows identifying the supply air temperature setpoint as an influential parameter (high σ value despite of a low μ value).

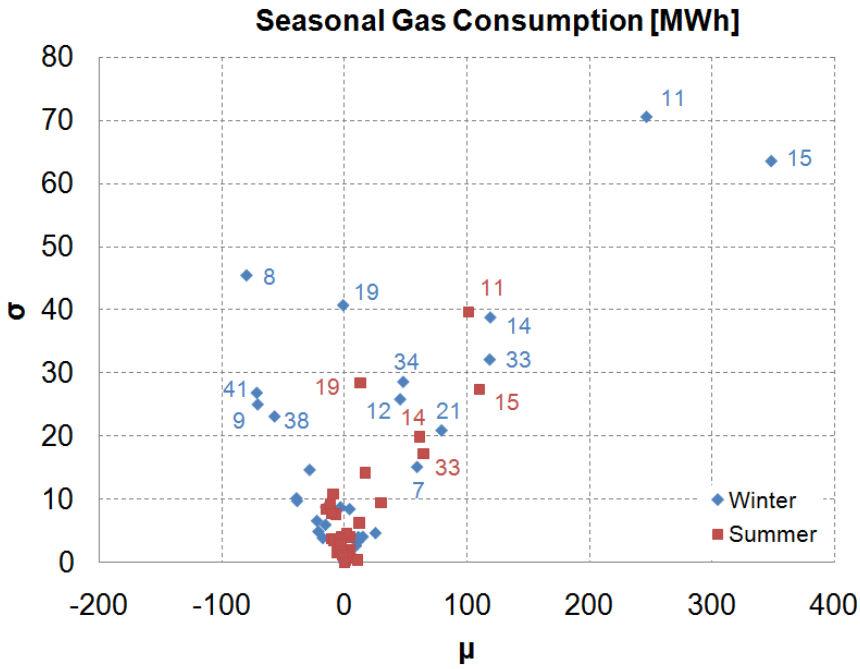

Figure 47: Preliminary Sensitivity Analysis – Seasonal natural gas consumption in (σ,μ) plan

The results plotted in Figure 48 confirm that internal loads densities and schedules are the major influence on the final electricity consumption and show that these parameters are involved in high-order effects.

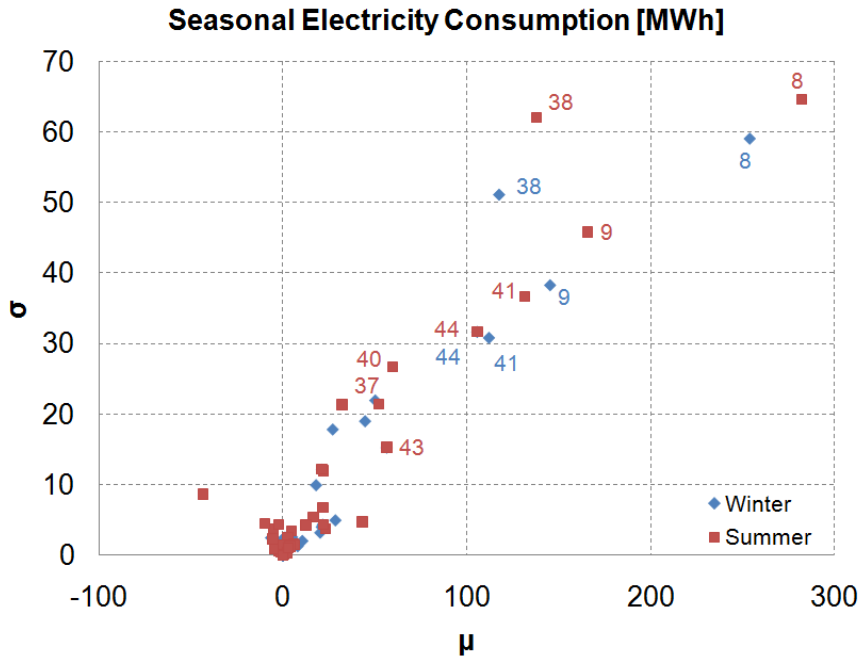

Figure 48: Preliminary Sensitivity Analysis – Seasonal electricity consumption in (σ,μ) plan

These confirms that applying a mathematical (i.e. optimization based) calibration method at this initial stage could be hazardous and lead to an unrealistic or non-physical set of parameters. Indeed, influences are numerous and most of them are high-order effects. An evidence-based methodology seems more adapted to adjust the parameters of the simulation model to the present situation.

The results of the present sensitivity analysis will be used to guide the data collection process (sort of "experimental design") during the next steps of the calibration process. Indeed, it has already been shown (see Chapter 5) that it was hard (almost impossible) to only base a calibration process on the comparison and the analysis of predicted and recorded consumption indexes such as (too global) monthly final energy consumptions.

Table 25 summarizes the data collection process that will be followed in the frame of the present study. Based on the results of the sensitivity analysis and the hierarchy between influential parameters, available evaluation methods (depending on the calibration level) are defined. As the calibration progresses, collected data can be used:

- to update the value of the given parameter if the new information is more reliable than the previous one (e.g. physical measurements vs default value; short-term monitoring vs BEMS recordings);
- to (cross-)check the current value of the parameter if the quality level of the new information is lower (e.g. observation vs measurement; spot vs short-term monitoring data) or similar (e.g. spot monitoring performed at different moments).

Table 25: Data collection process

Influence	Parameter	Level 1	Level 2	Level 3	Level 4	Level 5
		As-built	Inspection	Monitoring	Questionnaire	Iterative adjustment
	**Ventilation rate**	Design value	-	-	-	Adjustment
	Internal loads densities	Default values	Survey	Local power measurements	-	-
	Internal loads schedules	Default values	Default values	Local power measurements	-	-
	Occupancy schedules	Default values	Default values	Deduced from internal loads	Questions: holidays? Presence?	-
	Achieved indoor conditions	Default values	BEMS	Local T/RH measurements/records	-	-
	HVAC system operation schedules	Default values	BEMS	Checking	-	-
	HVAC system setpoints	Default values	BEMS	Local T/RH measurements/records	-	-
	Solar shadings use (SHGC)	No use	-	-	-	Adjustment

Most of the influential parameters listed in Table 25 can be subjected to direct or indirect measurements. Unfortunately, ventilation rate and solar shadings use (and its impact on the SHGC)

cannot be monitored and the best guess values will be used during the calibration process. An iterative adjustment of these last parameters will be envisaged at the end of the evidence-based process.

8.2. LEVEL2: INSPECTION PHASE

8.2.1. Available data and parameters adjustment

During the inspection phase, no physical measurement was performed in the building or the system but several visits have been organized. These visits were very helpful to refine influential parameters identified above by:

- Characterizing internal loads densities and schedules (Table 26)
- Analyzing the control laws implemented in the BEMS and obtain more accurate information about the indoor setpoints and HVAC system operation (Table 27)

Thanks to a detailed survey of the installed lighting fixtures and appliances in the different zones of the building, both values and uncertainty ranges of lighting and appliances power densities (P8 and P9) were adjusted (Table 26; according to the information given in section 4: BUILDING USE AND OCCUPANCY). In addition, the installed power of the IT rooms was estimated (based on installed cooling capacity in those rooms and nameplate information) and a remaining uncertainty of +/-10% was considered (P10).

Since no information was available about the occupancy and lighting/appliances operation schedules and rates in offices were available, the schedules parameters were not adjusted (P35 to P45).

Table 26: Level 2 – Internal loads (values and uncertainty ranges)

8	$IGFR_{light}$	W/m²	Lighting power density – Offices/meeting	10.25	-5%	+5%
		W/m²	Lighting power density – Circulation	9.36	-5%	+5%
		W/m²	Lighting power density – Utility rooms	7.82	-5%	+5%
		W/m²	Lighting power density – Parking	3.0	-5%	+5%
9	$IGFR_{appl}$	W/m²	Appliances power density – Offices	11.15	-5%	+5%
		W/m²	Appliances power density – Utility rooms	4.70	-5%	+5%
10	$IGFR_{addload}$	kW	Appliances power – IT rooms	30	-10%	+10%
35	$A_{sched,occ}$	-	Occupancy rate (day time)	1	-0.5	+0
36	$C_{sched,occ}$	h	Daily occupancy time	10	-2h	+2h
37	$A_{sched,light}$	-	Lighting operation rate (day time)	1	-0.5	+0
38	$B_{sched,light}$	-	Lighting operation rate (night time)	0	-0	+0.5
38	$C_{sched,light}$	h	Lighting daily operation time	10	-2h	+2h
40	$A_{sched,appl}$	-	Appliances operation rate (day time)	1	-0.5	+0
41	$B_{sched,appl}$	-	Appliances operation rate (night time)	0	-0	+0.5
42	$C_{sched,appl}$	h	Appliances daily operation time	10	-2h	+2h
43	$A_{sched,addload}$	-	IT equipment operation rate (day time)	1	-0	+0
44	$B_{sched,\ addload}$	-	IT equipment operation rate (night time)	1	-0	+0
45	$C_{sched,\ addload}$	h	IT equipment daily operation time	24	-0h	+0h

Using the values available in the BEMS, it was possible to adjust the parameters summarized in Table 27. Uncertainty ranges were adjusted to represent the estimated accuracy of the BEMS sensors (+/-1°C and +/-5% RH). Of course, schedules (P33 and P34) imposed by the BEMS are known and no remaining uncertainty exist at this stage.

Table 27: Level 2 – HVAC system operation (values and uncertainty ranges)

11	$T_{i,set,h,occ}$	°C	Heating setpoint – Offices/meeting	21.4°C	-1°C	+1°C
			Heating setpoint – Entrance hall	17°C	-1°C	+1°C
12	$T_{i,set,h,nocc}$	°C	Heating setpoint (night) – Offices/meeting	15°C	-1°C	+1°C
			Heating setpoint (night) – Entrance hall	16°C	-1°C	+1°C
13	$T_{i,set,c,\ occ}$	°C	Cooling setpoint – Offices/meeting	23°C	-1°C	+1°C
			Cooling setpoint – Entrance hall	23°C	-1°C	+1°C
14	RH_{min}	-	Humidification indoor setpoint	0.5	-10%	+10%
19	$T_{a,ex,AHU,set,max}$	°C	Maximal supply temperature setpoint	Table 5	-1°C	+1°C
20	$T_{a,ex,AHU,set,min}$	°C	Minimal supply temperature setpoint			
23	$T_{hw,set}$	°C	Hot water temperature setpoint	Figure 20	-1°C	+1°C
27	$T_{cw,set}$	°C	Chilled water temperature setpoint	9°C	-1°C	+1°C
29	$T_{ct,set}$	°C	Cooling tower setpoint	29°C	-1°C	+1°C
33	$C_{sched,AHU}$	h	AHU daily operation time	12	-0h	+0h
34	$C_{sched,set}$	h	H&C system daily operation time	12	-0h	+0h

During the different visits, it was observed that only very little use was done of the external blinds. Indeed, it appeared that only a few users used the blinds to avoid visual discomfort. After speaking with a few users, it appeared that external blinds were rarely used because they usually don't need them (rare visual comfort problems) and because their operation was too slow. Because no objective information was available, no adjustment of the SHGC (P5) value was done at this stage.

The "optimizer" mentioned earlier has not been implemented in the simplified building energy simulation tool since the operation of the former was not known with sufficient details. So, at this stage, it is proposed to consider that the interventions of this "optimizer" (controlling the re-starts of the installation) do not cause important energy consumptions.

8.2.2. Calibration and accuracy criteria

Integrating the information available about actual building use and operation should lead to a better representation of the final energy consumption of the building. However, the values of statistical indexes for natural gas and peak electricity consumptions are higher than the ones obtained at Level 1. It is also visible on Figure 49 that the representation of the natural gas consumption is less good.

On the contrary, the values of the statistical indexes for global and offpeak electricity consumptions have been reduced. A similar observation can be done when looking at the MBE and CV(RMSE) values for hourly power demand profiles (e.g. MBE is now 14.7% instead of 18.8% as given in Table 24).

Table 28: Level 2 - Calibration accuracy indexes

2 - %	2008 to 2010	
	MBE	CV(RMSE)
Gas	-14.4	23.9
Elec	14.7	16.9
Peak	22.6	24.4
Offpeak	-3.7	12.0
Hourly	14.7	47.8

	Large degradation comparing to previous calibration step (variation > 5%)
	Small degradation comparing to previous calibration step (variation < 5%)
	Small improvement comparing to previous calibration step (variation < 5%)
	Large improvement comparing to previous calibration step (variation > 5%)

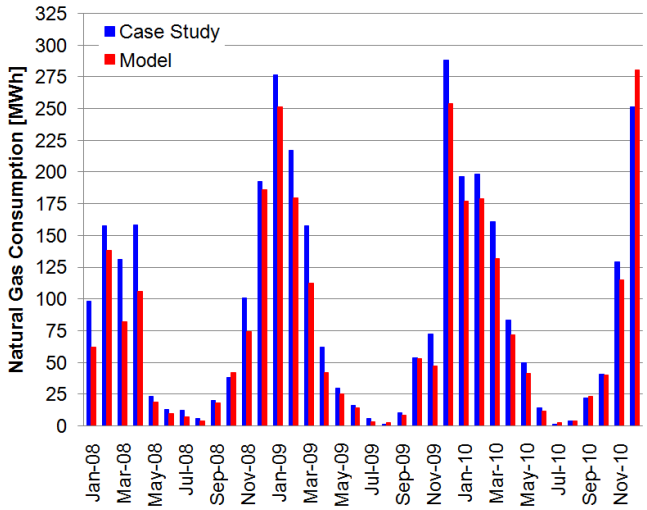

Figure 49: Level 2 - Monthly Gas Consumption Comparison

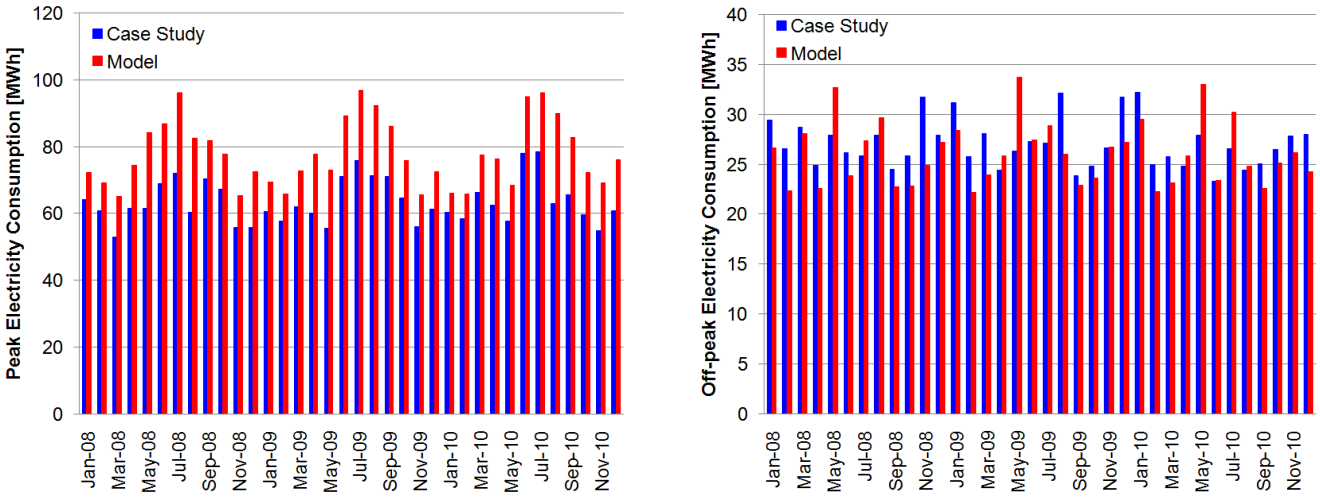

Figure 50: Level 2 - Monthly Peak (left) and Offpeak (right) Electricity Consumptions Comparison

Despite of the apparent degradation of the accuracy of the model (worst representation of the natural gas and electricity peak consumptions) in comparison with the previous calibration level, the model gives a more realistic representation of the day/night split of the electricity demand of the building. This observation is confirmed by visually comparing predicted and recorded power demand profiles for a winter week (Figure 51). Indeed, the nighttime (50 kW) and weekend demands are now better represented even if the daytime peak demand is still overestimated (280 kW instead of 240 kW). This overestimation of the whole-building power demand can be due to the fact that the building is not fully occupied during working hours (at this stage, a 100% occupancy rate is considered in the simulations) but also to an overestimation of the actual absorbed power of some lighting fixtures, appliances or HVAC components.

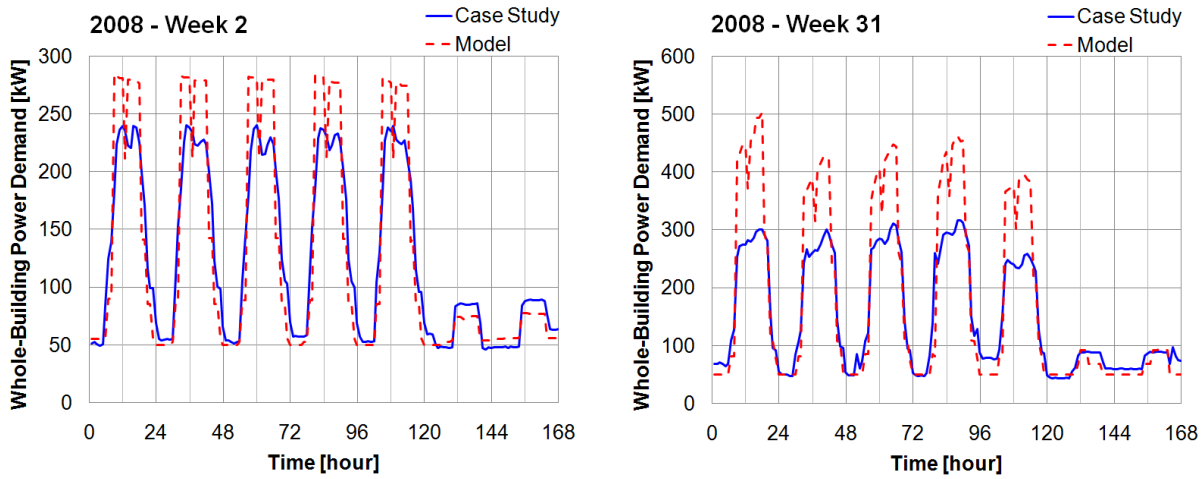

Figure 51: Level 2 - Predicted and recorded whole-building power demand (left: 2008 - week 2; right: 2008 – week 31)

In summer, the overestimation of the daytime peak demand is more important (500 kW instead of 300 kW; Figure 51). This additional error on the representation of the power demand profile can be due to other reasons:

- Less intensive use of artificial lighting fixtures due to a higher level of natural lighting,
- Partial occupancy of the building during summer periods (holidays),
- Wrong cooling indoor setpoints,
- …

On the other side, the underestimation of the natural gas consumption could be explained by underestimated heating and humidification setpoints during winter period, as well as underestimated ventilation/infiltration rate.

At this stage, it is impossible to get additional information and to answer these questions. So, these issues, among others, will have to be addressed at the next calibration level.

8.2.3. Analysis of the simulation results

Even if the quality of the calibration is not satisfying, it is interesting to take a first look at the simulation results in order to get a first idea and some orders of magnitude of the relative importance of the main energy consumers present in the building.

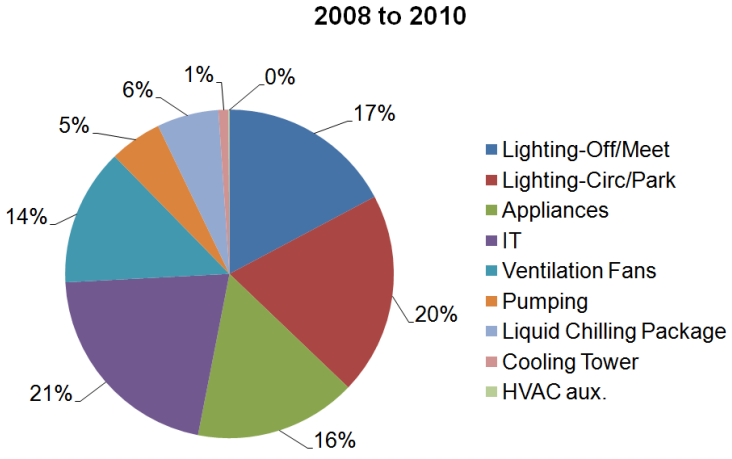

Figure 52: Level 2 - Whole-building electricity consumption disaggregation

The analysis of the power demand during a winter week allows identifying the main electricity consumers without any influence of the weather. Base load power demand is largely due to the consumption of the IT rooms (about 30 kW on 50 kW; Figure 53) which represent about 21% of the annual electricity consumption (Figure 52). In total lighting represents about 37% of the annual consumption and more than the half of this consumption is due the lighting fixtures installed in non-occupancy zones (parking and circulations). In total, HVAC represents about 26% of the annual electricity consumption. These results are in good accordance with values usually encountered in practice for final energy end-use (Adnot et al., 2007; BBRI, 2001).

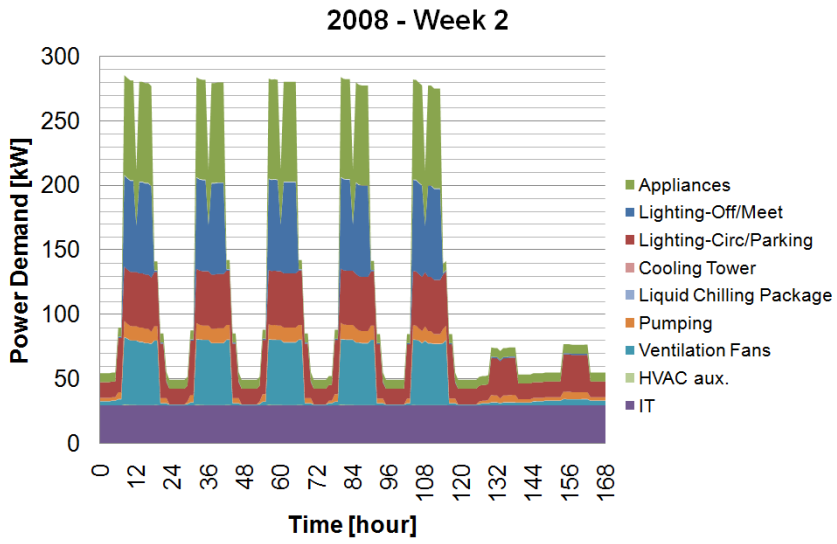

Figure 53: Level 2 - Whole-building power demand disaggregation (2008 – week 2)

During daytime, about the half of the total power demand (140 kW on 280 kW) is due to lighting and appliances in offices and meeting rooms. Since the uncertainty on other electricity consumers is less important (absorbed power of the main HVAC components as well as lighting operation schedules in circulation and parking are relatively well known), one can estimate that the demand of offices lighting and appliances is mainly responsible of the overestimation of the building power demand. However, without any physical measurements (i.e. evidence), it is not possible to consider this as a fact and to reduce the uncertainty on the parameters of the model in order to improve its quality.

8.2.4. Uncertainty on the simulation outputs

As expected, adjusting the values of the parameters and narrowing the probability ranges led to a reduction of the uncertainty on the final simulation results. Even if the quality of the model is not yet satisfying, simulation results seem to be more representative of the reality (Figure 54).

Indeed, the improvement since the previous calibration level is significant: standard deviations for gas and electricity consumptions vary between 13% and 27%, and 8% and 9%, respectively. However, some consumption recordings are still out of the 25-75th percentile range of the simulation results and correspond to “outliers” (not plotted). This can be explained by an under-estimation of the uncertainty ranges and means that significant refinement of the model’s parameters is still needed

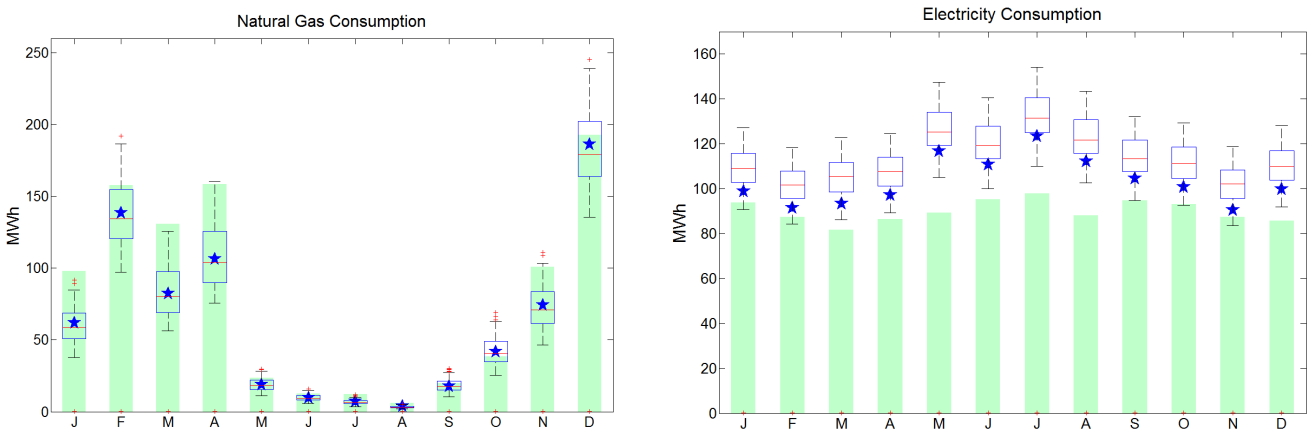

Figure 54: Level 2 - Uncertainty on predicted final energy consumptions

As shown in Figure 55, error bars on electricity end-use have been significantly reduced. The results do not allow an accurate quantification of the relative importance of the different electricity consumers present in the building but some trends are already appearing:

- Artificial lighting in occupancy zones, in circulations, appliances and IT equipments each represent between 15 and 20% of the total electricity consumption,
- All together, HVAC components represent between 20 and 30% of the total electricity consumption.

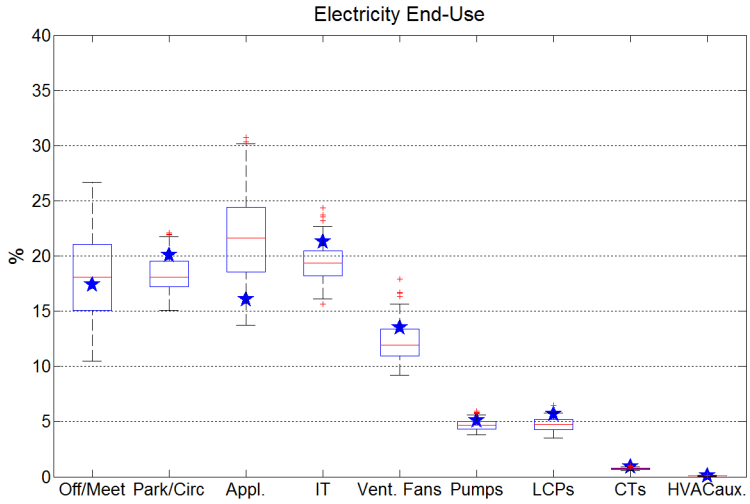

Figure 55: Level 2 - Uncertainty on electricity disaggregation

In the frame of a classical calibration process (i.e. non evidence-based), the user would be tempted to adjust the parameters of the model by means of an iterative process in order to fit better to the available consumption data and to satisfy the statistical criteria mentioned earlier.

Such iterative and totally blind adjustment could easily lead to a bad representation of the energy performance of the building and bias conclusions about the current energy performance of the installation under study. For instance, in order to decrease the winter daytime peak demand, numerous options would be available to the user, such as (among others):

- Adjust the lighting power density in the whole building or only in some chosen zones,
- Adjust the appliances power density in the whole building or only in some chosen zones,
- Adjust lighting and appliances operation profiles together or separately,
- Adjust seasonal occupancy and building use rates,

- Adjust the absorbed power of all or part of the HVAC components,
- Adjust heating, humidification and cooling setpoints in an arbitrary way,
- …

In the next section (8.3. LEVEL3: Monitoring Phase), a special attention will be paid to these critical issues. Focus will be given to the physical quantification (by means of spot and short-term monitoring) of the influential parameters and to the study of the issues discussed here above.

8.3. LEVEL3: MONITORING PHASE

As shown above, physical measurements are needed to continue adjusting the model's parameters and improving the quality of the model. Focus will be given to the most influential issues (identified by means of the sensitivity analysis) and characterized by broad uncertainty ranges. The analysis of the Level 2 simulation results also confirmed that a special attention should be paid to:

- Power density and operation schedules of internal loads (lighting and appliances),
- Indoor heating, cooling and humidification setpoints,
- HVAC components performance.

Specific and global electricity consumption measurements have been performed at the first level of the building (+1). The total electricity consumption (including lighting and plug loads) of the about half of the floor level has been monitored continuously during several weeks. At the same time, lighting and plug loggers have been used to record the operation of the lighting fixtures and the energy consumption of computers, printers…

Measurements were performed in circulation (orange area, Figure 56), shared offices (blue zones, Figure 56), single offices (green zones, Figure 56) and print room (red zone, Figure 56). The selection of this sample of rooms was done in order to be representative of the floor but was also limited by practical constrains (availability of the occupant, agreement to install loggers in his office, number of available loggers…).

These measurements allowed to:

- Check the operation schedules of lighting fixtures installed in circulation area
- Qualify the actual use of artificial lighting in single and shared offices and estimate the occupancy schedule
- Quantify the actual plug loads densities and schedules in offices and print room

Figure 56: Floor 1 layout - Monitoring campaign

Temperature and humidity have also been measured in different offices in order to determine the level of comfort achieved in occupancy areas. Some HVAC components have also been monitored in order to determine their power consumption and their operation.

At this stage, it was supposed that the conclusions of this measurement campaign (realized between December 2010 and April 2011) could be extended to the whole studied period (2008 to 2010). Indeed, it is considered that the building and system use and performance have not been strongly modified since 2008.

8.3.1. Monitoring data analysis

8.3.1.1. Lighting use monitoring in occupied offices

The data collected by the lighting loggers installed on the lighting fixtures of the circulation area is shown in Figure 57. This confirms that approximately two fixtures (A and B) out of three stay switched on all the time. The third fixture (C) is on between 06:00 and 22:00 from Monday to Friday and between 10:00 and 19:00 during weekends. Recording performed in the elevators area confirmed that these lighting fixtures are switched on all the time.

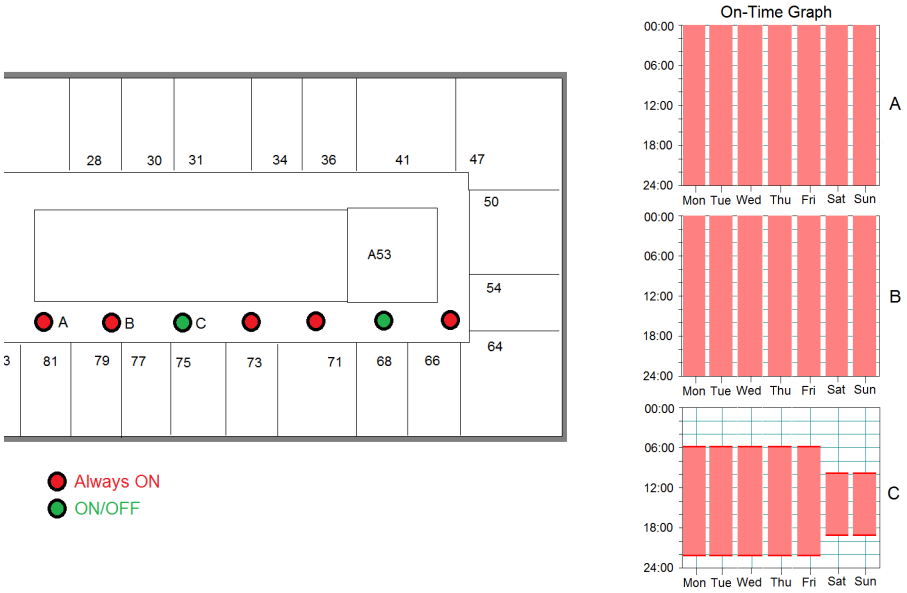

Figure 57: Circulation lighting operation recording

In offices, lighting fixtures can be switched on/off by the occupants during the “switch-on allowance period” defined above. So, artificial lighting use rates can vary a lot from one occupant to another and from one day/week/month to another.

Lighting use time has been monitored during more than 4 weeks in 5 occupied offices of the first floor (at least one per façade). Averaging the use rate on these 5 offices allowed generating an average workday lighting use profile as shown in Figure 58. Such profile corresponds to offices that are occupied in a regular manner from Monday to Friday and should also reflect, in an indirect way, the occupancy rate of the considered offices (average occupancy peak is 90%). The average relative standard deviation is approximately 6%. As expected, lighting use in offices during weekend is null since it is not allowed by the BEMS.

The limited amount of lighting sensors did not allow studying the impact of the orientation or of the seasonal effect (less intensive use of artificial lighting during summer) on lighting use.

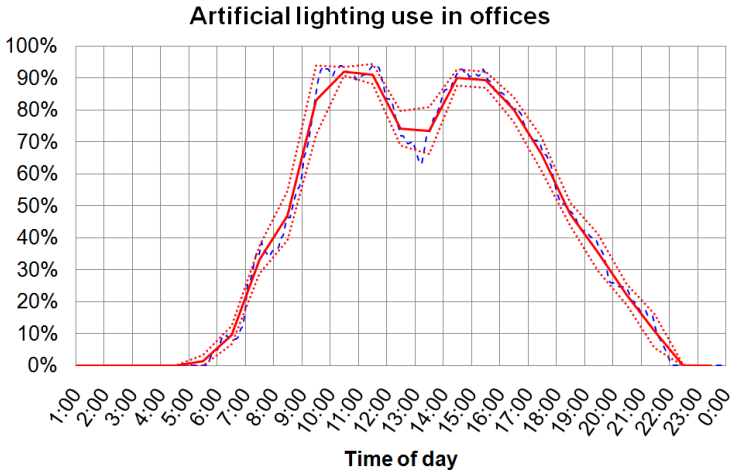

Figure 58: Average (weekday) lighting use sub-hourly profile in offices (blue) and derived hourly profile (red) +/- standard deviation (dotted red lines)

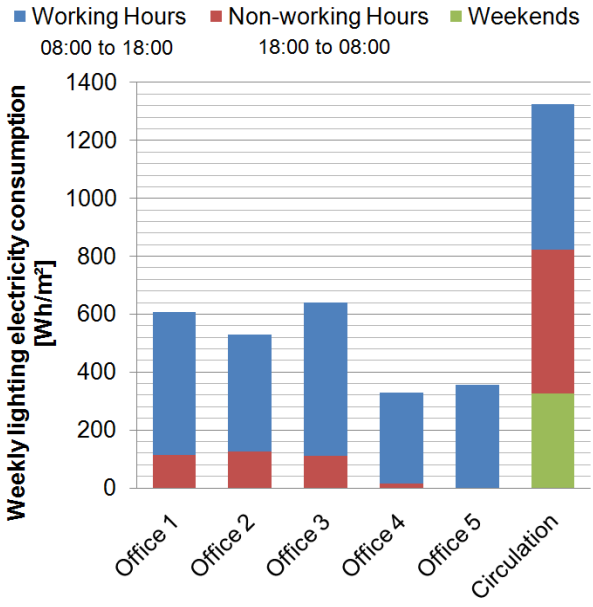

Figure 59: Estimated weekly lighting electricity consumption

It is also interesting to have a look to the estimated lighting consumption for the zones were measurements have been performed. Recorded operation times have been multiplied by the observed installed lighting power (Figure 59).

In offices, about 18% of the consumption is due to operation of the lighting fixtures out of the normal working period (08:00 to 18:00, Monday to Friday). It is likely that this consumption is mainly due to forgetting switching off the lights at the end of the day so that the lighting stays on till the automatic switch off at 22:00. In the circulation area, it is interesting to note that only 38% of the related consumption occurs during normal working period (08:00 to 18:00, Monday to Friday). The remaining consumption occurs during nights and weekends.

8.3.1.2. Appliances use monitoring in occupied offices and copy room

Appliances electricity consumption has been monitored during 5 weeks in 6 (daily) occupied offices and in the copy room. Average normalized consumption profiles have been derived from these data and are shown in Figure 60. As expected, the power density in the copy room is largely higher than in offices and reaches 35 W/m². Peak power density in offices is largely dependent on the zone and can vary approximately between 3 to 10W/m².

Considering the nominal power densities given above (section 4.3), distinct normalized average daily operation profiles have been identified for the operation of electrical appliances in offices and copy room, during weekdays and weekends. The relative standard deviation around the derived average profiles is approximately 25%.

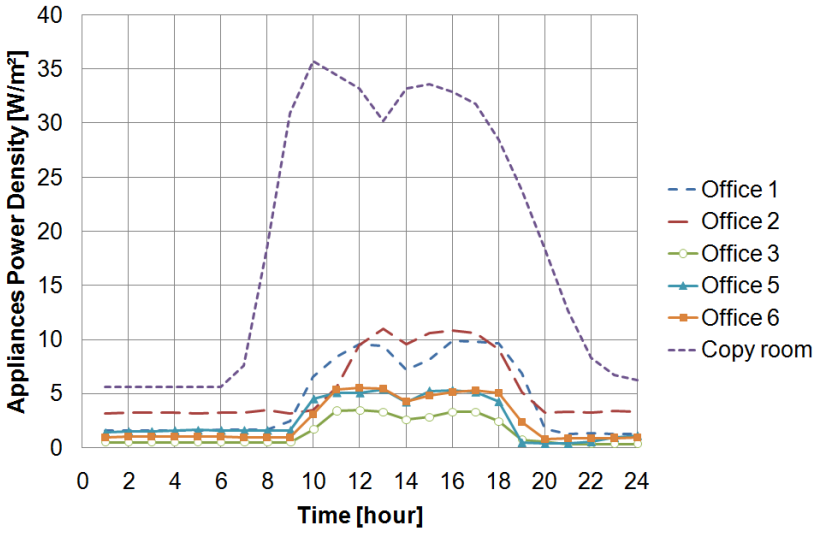

Figure 60: Average appliances power density in several zones

8.3.1.3. Floor level electricity consumption monitoring

The electricity consumption of a fraction of the first floor has been monitored during 7 weeks between January and March. These measurements were performed by means of a power meter installed on one of the two electrical panels of the floor. This power demand includes all the lighting fixtures and appliances of the left part of the floor (approx. 52% of the installed power) and all the lighting fixtures installed in the circulation area. An average weekly consumption profile based on these 7 weeks of measurement data is shown in Figure 61.

It appears that the five weekdays are characterized by similar profiles:

- The peak demand occurs generally in the morning
- A less intensive use of lighting and appliances around noon (lunch break) already observed when looking at the data collected in occupied zones shown in Figure 58 and Figure 60
- The night power demand is almost constant all week long (approximately 1.5 kW) and is due to safety/emergency lighting in circulations and standby appliances.
- Power demand on Saturday and Sunday follows exactly the operating schedules of the BEMS during these days (10:00 to 19:00).

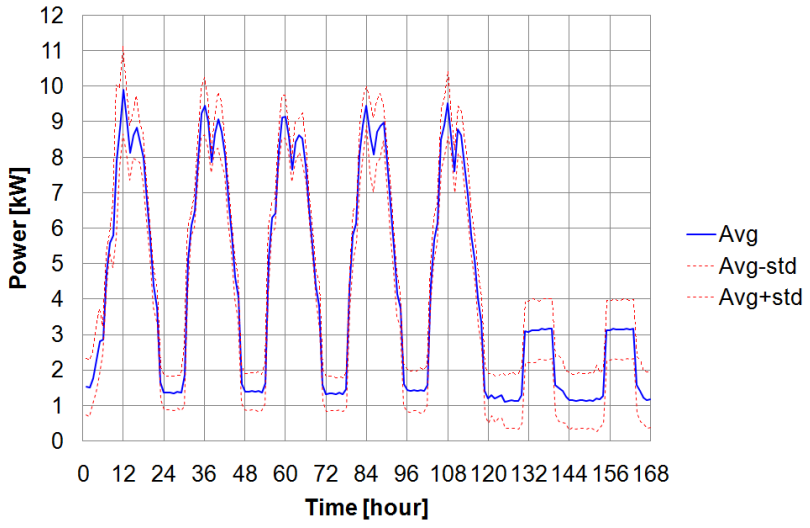

Figure 61: Average floor power demand (including lighting and appliances)

Average weekday and weekend day profiles have been derived and are shown in Figure 62 (blue curve). Standard deviations had also been represented (red dotted lines). The specific average operating profiles identified for lighting fixtures (see paragraph 8.3.1.1) and appliances (see paragraph 8.3.1.2) have been used, summed and extended to the whole floor (i.e. multiplied by the total installed lighting and appliances powers, supposing a 100% occupancy of the floor; "Non-adjusted" profile in Figure 62) in order to allow comparison with the global average recorded power demand ("Avg" blue curve and "Avg+/-std").

Both night-time and day-time demands are overestimated when supposing a 100% occupancy ("Non-adjusted" bold red curve in Figure 62). An average use rate of 85% has been supposed in order to adjust the power demand profile (green dotted curve) and to fit to the recorded (average) power demand profile. Of course, this adjustment only concerns the consumptions which are directly related to the occupancy rate (i.e. lighting and appliances use in offices). The other parts of the power demand profile (e.g. circulation and common zones lighting) are not concerned by this adjustment since their use is imposed by the BEMS and is independent of the building use/occupancy rate.

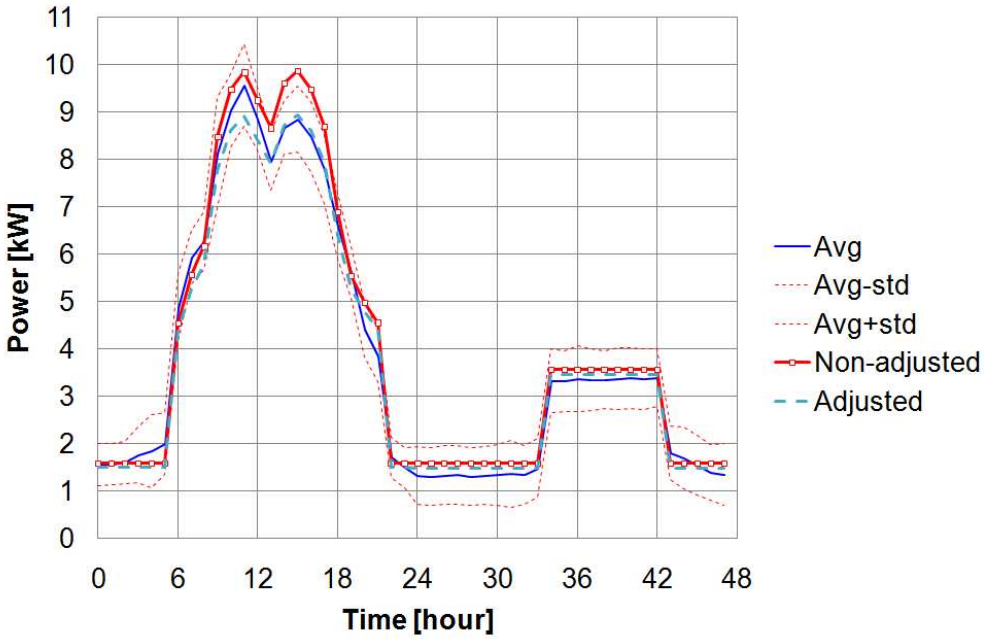

Figure 62: Average weekday (0 to 24h) and weekend day (25 to 48h) power demand (floor level)

The final operation profiles for the internal gains occurring at the floor level are shown in Figure 63. These profiles will be directly implemented in the model.

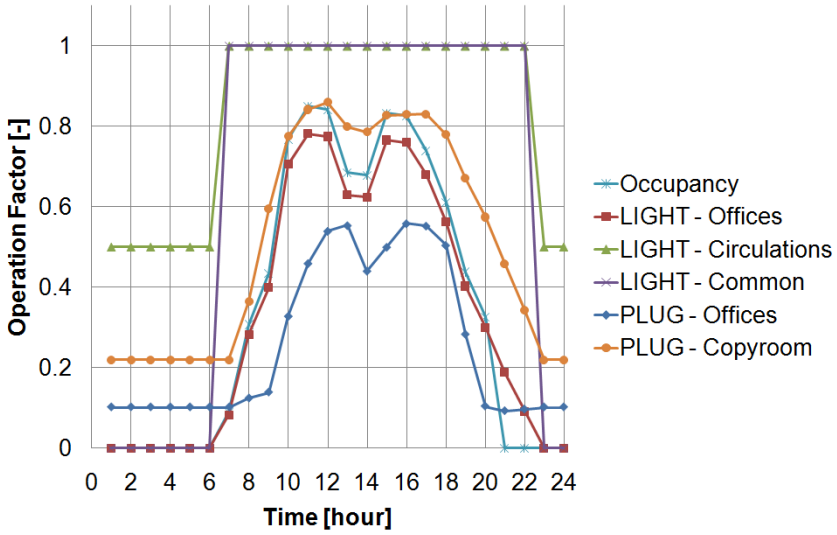

Figure 63: Adjusted normalized operation profiles for internal gains (typical weekday)

8.3.1.4. Indoor temperature and humidity monitoring

Indoor temperature and humidity have been measured during more than five weeks in nine offices of different sizes and orientations. These measurements allowed identifying achieved temperature and humidity levels during HVAC system operating hours and during night.

A first interesting fact was observed when comparing the temperatures measured in the offices (using temperature/humidity loggers described above) and the values of the temperature recorded by the BEMS system in the same rooms. Some examples of this comparison are shown in Figure 64. In average, the measured temperature is approximately 1.0°C to 1.2°C higher than the value recorded by the BEMS. This offset can be explained by the location of the temperature sensor, installed below the fan coil unit, very near the non-insulated window sill. Considering the whole period of monitoring, the average indoor heating setpoint temperature during HVAC system operating hours (08:00 to 20:00) is estimated to 22.65°C (+/- 0.25°C standard deviation) while the average value of the night-setback is 16.7°C (+/- 0.30°C standard deviation). This last value was estimated by averaging the indoor temperature measured on Sunday, after stabilization. Indeed, during the week, the effect of thermal inertia does not allow identifying properly the night setback temperature (Figure 65).

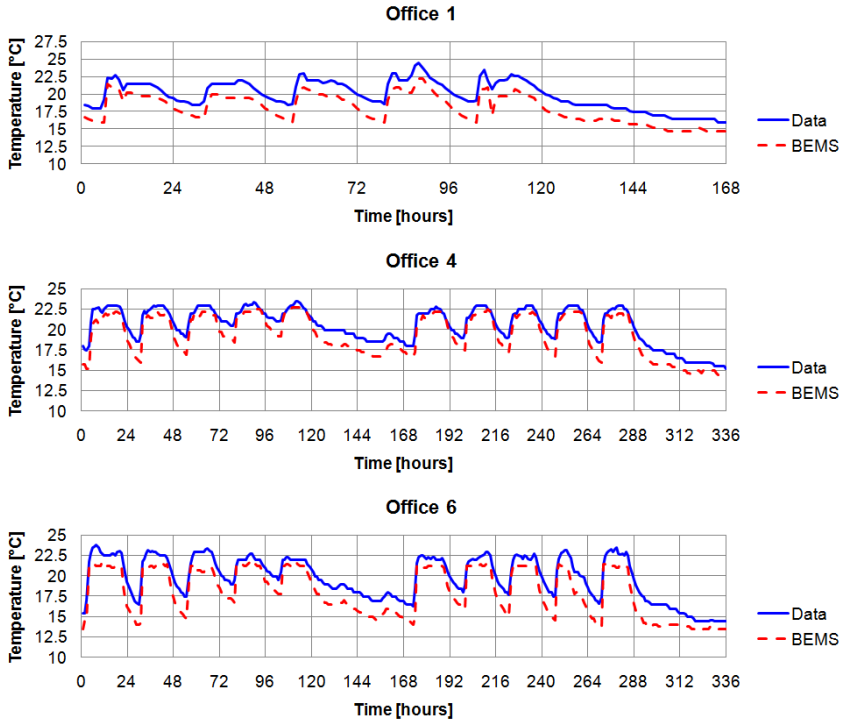

Figure 64: Measured (loggers) and recorded (BEMS) values of the indoor drybulb temperature

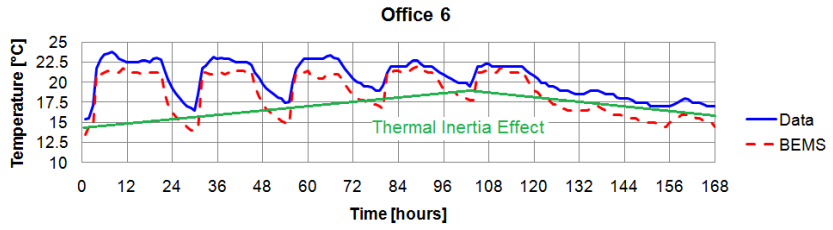

Figure 65: Thermal inertia effect

To allow an easier comparison, measured values of relative humidity have been converted into humidity ratio values. As set by the BEMS, the relative humidity setpoint for return ventilation air is 50% for both AHUs supplying the offices (AHUs 1 and 2).

The average measured relative humidity in the zones is approximately 42% (i.e. humidity ratio of about 0.0071 kg/kg). The difference between these values and the RH setpoint imposed by the BEMs can be due to the slight cooling of the return air that can occur within the return ducts bringing the air from the rooms to the AHUs. As shown in Figure 66, the temperature difference between supply and exhaust of the return ducts is in average of about 1.2°C during operating hours (08:00 to 20:00). During non-operation periods, the temperature measured at the exhaust of the return duct (AHU1 return) is decreasing to stabilize at the temperature of the technical room (approx. 12.5°C).

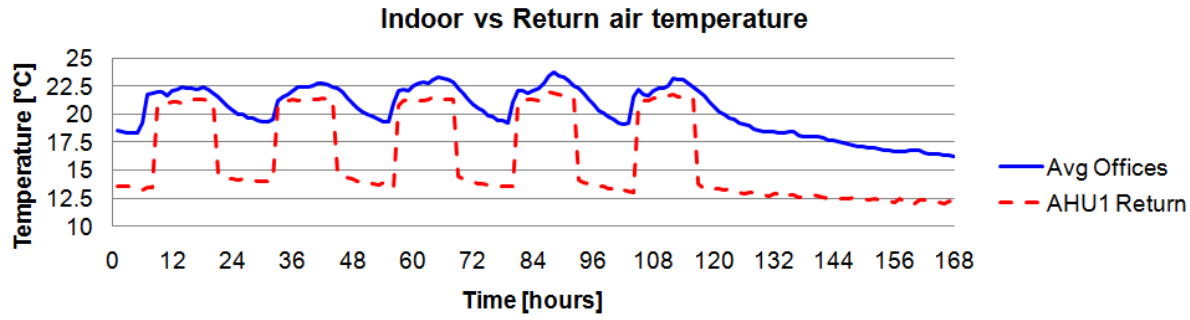

Figure 66: Office indoor temperature and return air temperature

It also appears that two groups of rooms can be distinguished when looking at the measured values of humidity ratio (Figure 67). Achieved levels of humidity are higher in the rooms supplied by the AHU1 (average humidity ratio of 0.0081 kg/kg during occupancy hours corresponding to a 46% relative humidity) while humidity is lowers in the rooms supplied by AHU2 (average humidity ratio of 0.0062 kg/kg during occupancy hours corresponding to a 37% relative humidity). This can be due to a malfunction of the relative humidity sensor of AHU2. In average, the achieved level of humidity is 42% +/- 4% standard deviation (which is slightly above the current standards for thermal comfort).

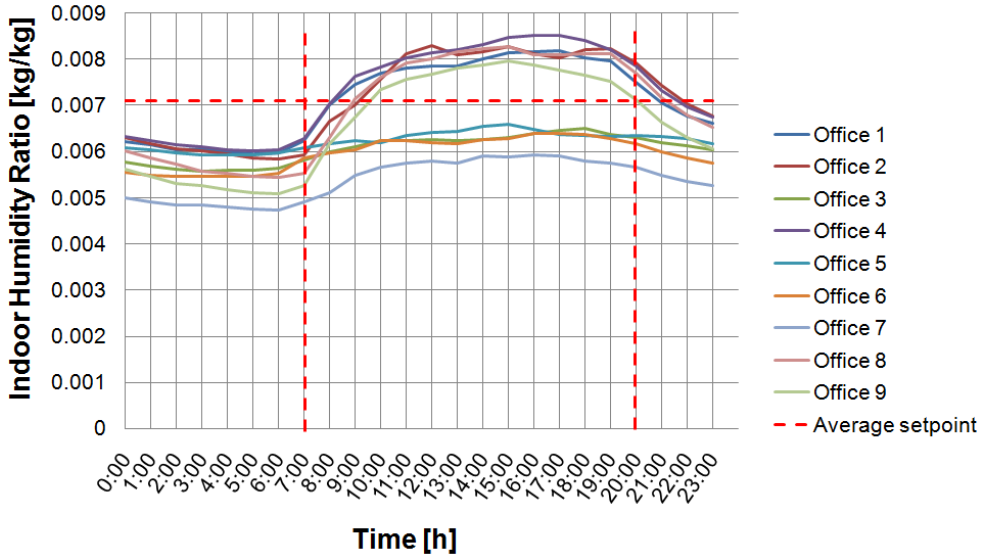

Figure 67: Achieved average humidity ratio levels in offices

Temperature in the entrance hall has been monitored too and is in average about 17.7°C between 06:00 and 22:00.

Similar measurements were conducted at the beginning of the cooling season (beginning of Spring) but sensors were lost or destroyed and no information was finally available about the temperature and humidity levels achieved in the zones during cooling season.

8.3.1.5. HVAC system operation monitoring

Power measurements and operation time recordings, as well as BEMS data recordings have been performed on the HVAC system. Figure 68 shows the power demand of three AHUs operating between 08:00 and 20:00, five days a week. These data have been obtained by monitoring the control panel of a part of the HVAC plant during a winter week. A power demand of approximately 1 kW remains constant all the time. It is supposed that this consumption corresponds to the standby consumption of the control system.

The total (nominal) absorbed power of the monitored (constant speed) ventilation fans (AHUs 1, 2, 6 and 7) is about 28.6 kW. During operation time, the power consumption related to the operation of these ventilation fans is about 23.3 kW, i.e. 82% of the nominal power. A second verification made only with AHUs 1 and 2 gave a similar ratio (about 81%). So, it was considered that the actual power demand of the ventilations fans is, in general, approximately 82% of the nominal absorbed power given in the as-built file.

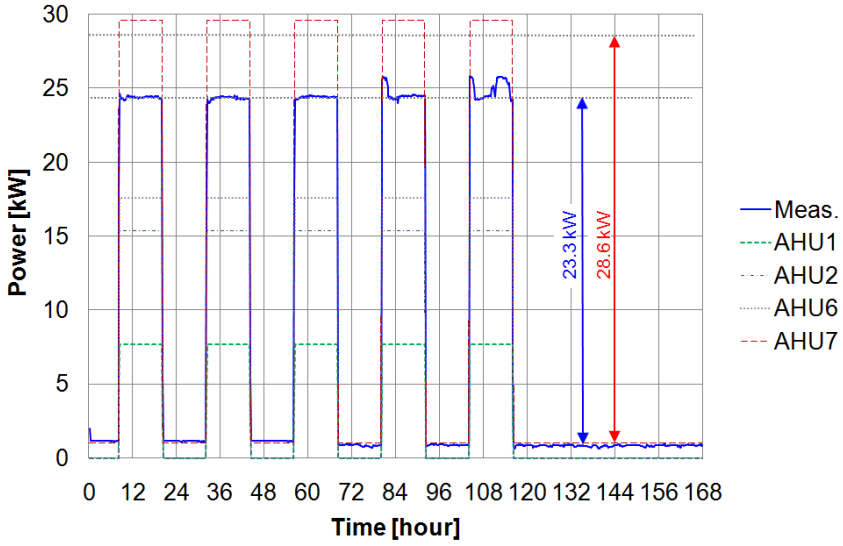

Figure 68: AHUs power demand

The lack of data about ducts pressure drops did not allow identifying the operation point of the fan and estimating its efficiency.

AHUs supply and return conditions during a winter week are shown in Figure 69. The variations of the supply temperature are directly related to the outdoor temperature. As seen on Figure 70, the recorded supply temperature follows pretty well the law implemented in the BEMS (Table 5). The deviation between the setpoint and the achieved temperature can be partly explained by the fact that the values of the outdoor temperature recorded by the BEMS were not available and that the curve had been built using Mons weather data.

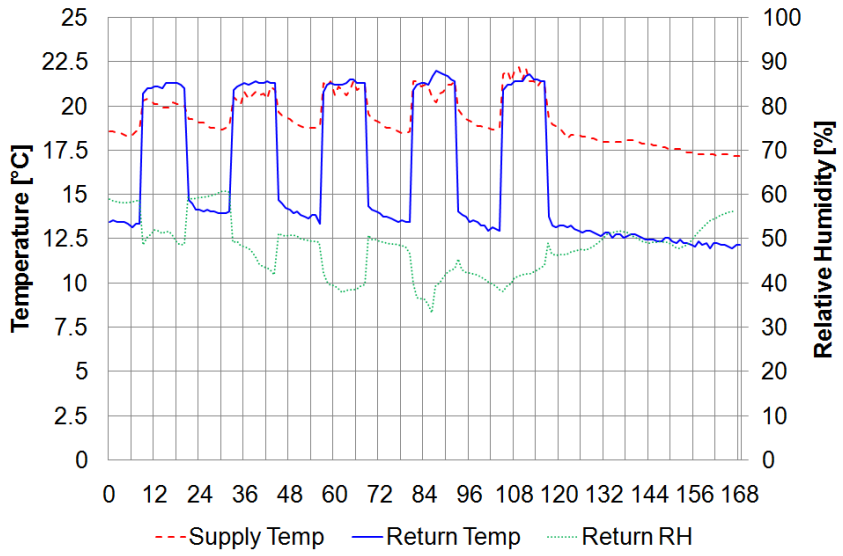

Figure 69: AHU1 supply and return air conditions

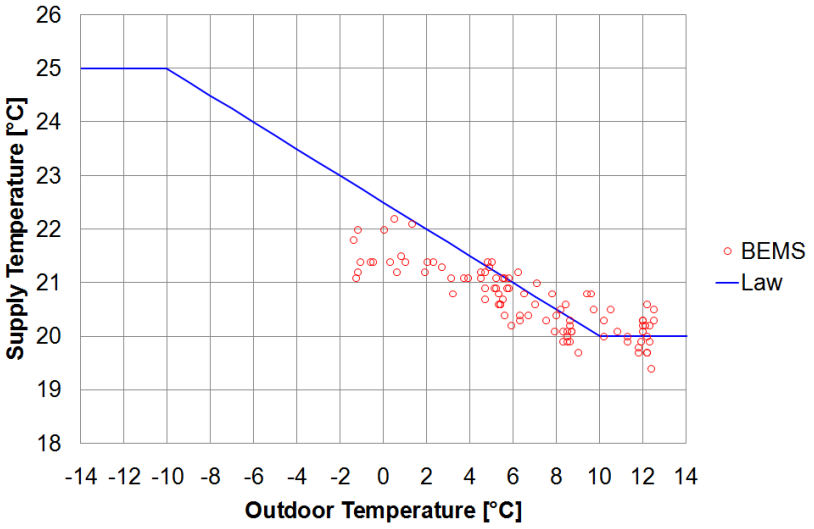

Figure 70: AHU1 supply temperature

The recording of the AHUs supply temperature during a summer week also confirms this fact since the average temperature during operating hours was included between 19.5°C and 20.8°C (setpoint imposed by the BEMS: 20°C).

Figure 71 shows a comparison between measured (blue curve) and predicted (red and green curve) power demand for a part of the HVAC plant. The red curve corresponds to the operation of the AHUs already considered in Figure 68 (AHUs 1, 2, 6 and 7). Magnetic loggers were used to record the operation periods of the main chilled water pumps. By summing the corrected power demand of the ventilation fans (cf. Figure 68) and the nominal power demand of the chilled water pumps in operation, it was possible to represent the total power demand of the considered part of the HVAC plant. On the first day, chilled water pumps supplying AHUs, FCUs, chillers evaporators and condensers are successively switched on-off depending on the demand. On the second day, only the fans and pumps supplying the heating coils of the AHUs 1 and 2 are operating.

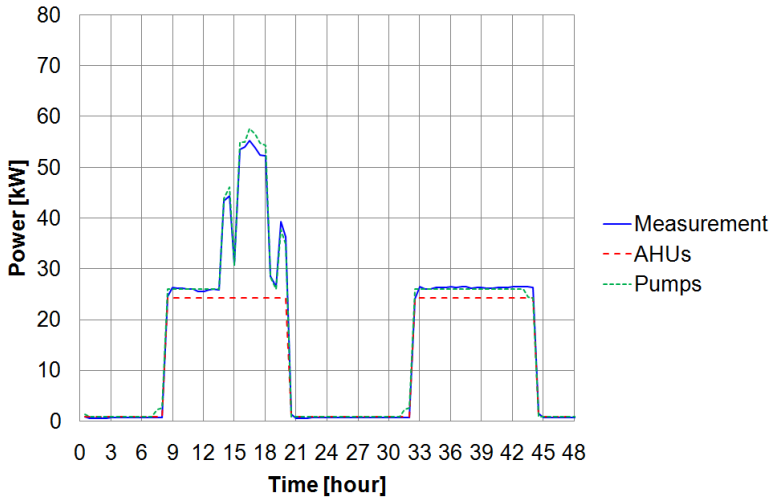

Figure 71: AHUs and chilled water pumps consumption

Additional BEMS recordings were useful in order to check the chiller and cooling towers setpoints. As shown in Figure 72, the chilled water setpoint temperature is approximately 9.7°C while the cooling towers setpoint temperature is approximately 28.7°C. These two values are in good accordance with the setpoints mentioned above (respectively, 9°C and 29°C).

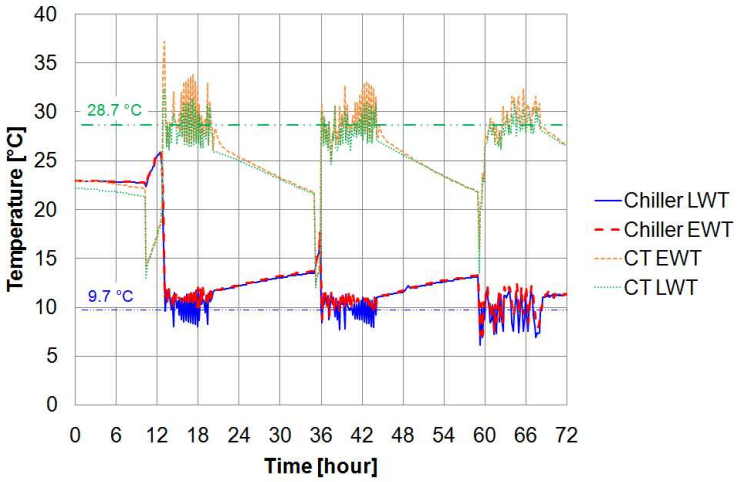

Figure 72: Cooling plant operating conditions

During the monitoring campaign, the effects of the "optimizer" were not highlighted. Indeed, only very few re-starts of the installation were noticed during nights and weekends. So, it was decided to neglect these effects and the corresponding energy consumptions.

8.3.2. Parameters adjustment

The parameters of the model will be adjusted step by step, by following the data collection process. The three steps (3a to 3c) are described below.

8.3.2.1. Step 3a: Lighting and appliances use

The measurement data analyzed in sections 8.3.1.1, 8.3.1.2 and 8.3.1.3 were used to adjust the parameters (Table 29) related to internal loads densities (P8 and P9) and operation (P35 to P42). Best-guess values, as well as uncertainty ranges, have been defined according to the results of the analysis of the available monitoring data. It is important to notice that the values of schedules parameters (P35 to P42) given in Table 29 are average values only shown to illustrate the adjustment of the parameters and the modification of the uncertainty range. Operating profiles used in the model are hourly values of operation factors (between 0 and 1) and not simple synthetic profiles characterized by two or three parameters (A, B and C).

Table 29: Level 3a - Internal loads parameters

8	$IGFR_{light}$	W/m²	Lighting power density – Offices/meeting	10.25	-2%	+2%
		W/m²	Lighting power density – Circulation	9.36	-2%	+2%
		W/m²	Lighting power density – Utility rooms	7.82	-2%	+2%
		W/m²	Lighting power density – Parking	3.0	-2%	+2%
9	$IGFR_{appl}$	W/m²	Appliances power density – Offices	11.15	-5%	+5%
		W/m²	Appliances power density – Utility rooms	4.70	-5%	+5%
35	$A_{sched,occ}$	-	Occupancy rate (day time)	0.78	-0.05	+0.05
36	$C_{sched,occ}$	h	Daily occupancy time	10	-1h	+1h
37	$A_{sched,light}$	-	Lighting operation rate (day time)	0.78	-0.05	+0.05
38	$B_{sched,light}$	-	Lighting operation rate (night time)	0	-0	0
38	$C_{sched,light}$	h	Lighting daily operation time	10	-1h	+1h
40	$A_{sched,appl}$	-	Appliances operation rate (day time)	0.56	-0.14	+0.14
41	$B_{sched,appl}$	-	Appliances operation rate (night time)	0.09	-0.005	+0.005
42	$C_{sched,appl}$	h	Appliances daily operation time	9	-1h	+1h

8.3.2.2. Step 3b: Indoor conditions

Indoor setpoints have also been adjusted based on the analysis of the measurement data presented in section 0. Since monitoring campaign was handled during winter period, no additional information was collected about cooling setpoints and the parameter P13 has not been adjusted since the previous calibration level (Table 30).

Table 30: Level 3b - Indoor setpoints parameters

11	$T_{i,set,h,occ}$	°C	Heating setpoint – Offices/meeting	22.6°C	-0.75°C	+0.75°C
			Heating setpoint – Entrance hall	18°C	-0.8°C	+0.8°C
12	$T_{i,set,h,nocc}$	°C	Heating setpoint (night) – Offices/meeting	16.7°C	-0.8°C	+0.8°C
			Heating setpoint (night) – Entrance hall	16°C	-0.8°C	+0.8°C
13	$T_{i,set,c,\ occ}$	°C	Cooling setpoint – Offices/meeting	23°C	-1°C	+1°C
			Cooling setpoint – Entrance hall	23°C	-1°C	+1°C
14	RH_{min}	-	Humidification indoor setpoint	0.42	-10%	+10%

8.3.2.3. Step 3c: HVAC components operation and performance

The last step of the adjustment consisted in extracting values of the HVAC system parameters from the monitoring data analyzed in section 8.3.1.5. By means of these data, it was possible to adjust the values and/or the uncertainty range of the parameters presented in Table 31.

Table 31: Level 3c - HVAC components performance and operation parameters

17	SFP_{sufan}	W/m³-s	Average supply fan specific power	1185	-2%	+2%
18	SFP_{retfan}	W/m³-s	Average return fan specific power	772	-2%	+2%
19	$T_{a,ex,AHU,set,max}$	°C	Maximal supply temperature setpoint	Table 5	-1°C	+1°C
20	$T_{a,ex,AHU,set,min}$	°C	Minimal supply temperature setpoint			
26	PP_{hw}	W	Hot water pump power	6023[29]	-2%	+2%
27	$T_{cw,set}$	°C	Chilled water temperature setpoint	9.7°C	-1°C	+1°C
29	$T_{ct,set}$	°C	Cooling tower setpoint	28.7°C	-1°C	+1°C
30	PP_{cw}	W	Chilled water pump power	17700[30]	-2%	+2%
31	PP_{cd}	W	Condenser pump power	15000[31]	-2%	+2%
32	PP_{ct}	W	Cooling tower pump power	4400[32]	-2%	+2%

8.3.3. Calibration and accuracy criteria

The values of the statistical indexes have been computed at each step of the adjustment process and are given in Table 32, Table 33 and Table 34.

The implementation of adjusted operation profiles for internal loads (lighting and appliances) allowed decreasing the values of all the indexes. Classical criteria are now almost satisfied for the electricity consumptions and demand. A substantial bias remains for the natural gas consumption but it is likely that this problem will be solved by adjusting the values of the heating and humidification indoor setpoints.

[29] Total installed power as given in Table 9
[30] Total installed power as given in Table 11
[31] Total installed power as given in Table 11
[32] Total installed power as given in Table 11

Table 32: Level 3a - Calibration accuracy indexes

3a - %	2008 to 2010	
	MBE	CV(RMSE)
Gas	-9.7	19.9
Elec	3.4	7.6
Peak	6.7	9.6
Offpeak	-4.1	11.0
Hourly	3.4	30.5

As expected, implementing more realistic values of achieved levels of temperature and humidity in the building allowed improving the quality of the model and led to values below 10% for most of the statistical indexes. At this stage, all the criteria as specified by ASHRAE (2002) are satisfied.

Table 33: Level 3b - Calibration accuracy indexes

3b - %	2008 to 2010	
	MBE	CV(RMSE)
Gas	-1.8	15.0
Elec	3.5	7.4
Peak	6.7	9.6
Offpeak	-3.8	10.5
Hourly	3.5	30.5

The final step of the calibration process consisted in adjusting the parameters related to the operation of the HVAC system (operating schedules and setpoints). Once again, most of the statistical indexes were reduced and the global quality of the model was improved.

Table 34: Level 3c - Calibration accuracy indexes

3c - %	2008 to 2010	
	MBE	CV(RMSE)
Gas	-1.1	14.8
Elec	2.3	6.8
Peak	4.6	8.0
Offpeak	-2.6	10.0
Hourly	2.3	29.3

As shown in Figure 73, the calibrated model is now able to represent the seasonal variations of both natural gas and electricity consumption. The split between daytime and nighttime electricity consumption is also well represented since most of the statistical indexes are below the limits imposed by the classical criteria.

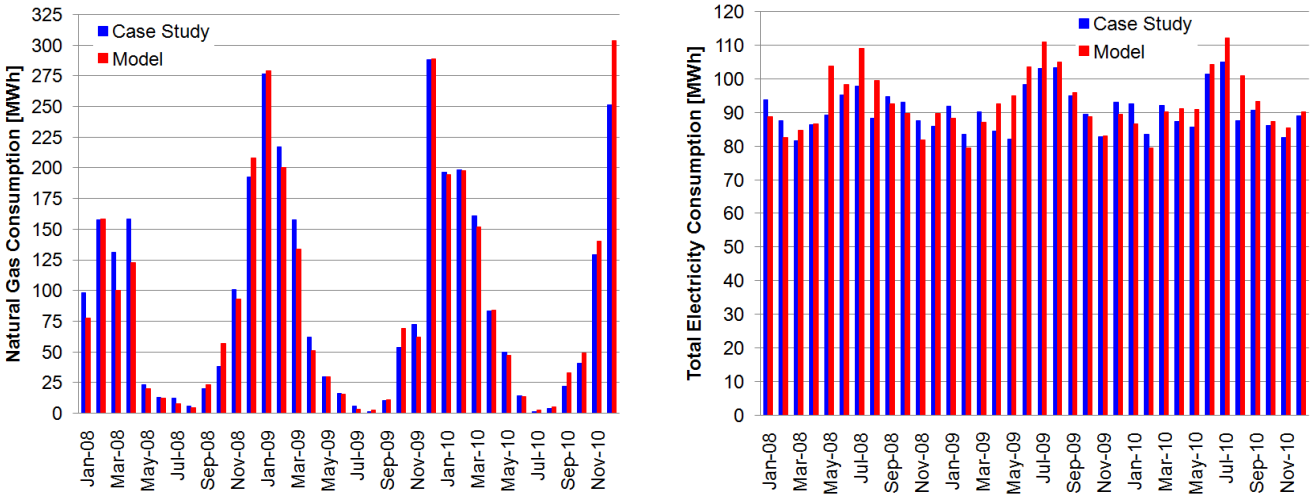

Figure 73: Level 3c - Monthly Gas (left) and Peak Electricity (right) Consumptions Comparison

It is also interesting to take a look to hourly power demand profiles. It is encouraging to notice that the model is able to represent the whole-building demand during a winter week with a good accuracy (Figure 74 – left).

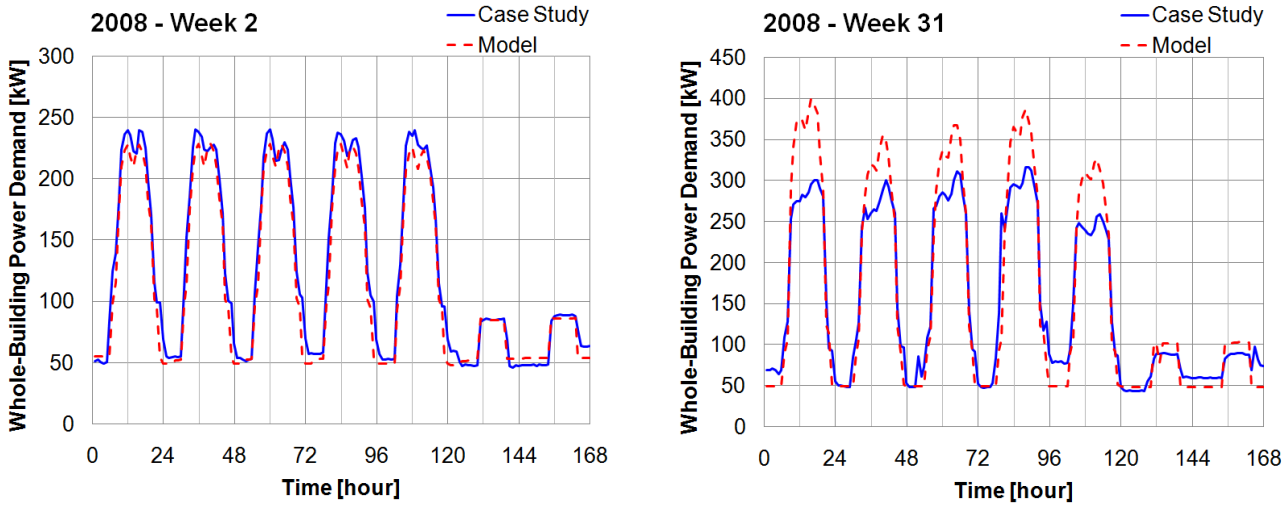

Figure 74: Level 3c - Predicted and recorded whole-building power demand (left: 2008 - week 2; right: 2008 – week 31)

However, some larger deviations can be observed when looking at summer electricity consumptions (Figure 73 – right) and demand (Figure 74 - right). Such deviations could be explained by:

- An overestimation of the consumption related to the operation of the cooling equipment because of a bad representation of its operation (e.g. wrong setpoints) or its performance (e.g. lack of information about chillers and cooling towers performance),
- The underestimation of the impact of the use of manual external shadings by the occupants
- An overestimation of the occupancy rate of the building (and/or of the corresponding energy use intensity) during summer period.

Since additional measurements on the HVAC system were not possible because of time and practical constrains, priority was given to the third option and some questions about holiday period were asked to a sample of the occupants of the building. These results are presented in the next section.

8.4. LEVEL 4: OCCUPANCY SURVEY

8.4.1. Available data and parameters adjustment

About 160 occupants answered the survey. This approximately corresponds to half of the occupants of the building. All the information collected during the occupancy survey won't be analyzed here. Attention will be paid to the questions related to holidays.

Based on the survey results, it is estimated that occupants take, in average, about 15 days off during summer (i.e. three weeks). These holidays are supposed to be equally distributed over July and August. The occupancy and operating factors of offices lighting and appliances have been adapted accordingly. Legal holidays (such as Eastern, Labor Day, etc.) were also integrated in the model. During these days the building is operated in "weekend mode".

The survey also allowed characterizing (in a qualitative way) the use of external blinds. It appeared that about 40% of the occupants use the blinds in summer to adjust lighting level in their office during the day. Some authors (Reinhart and Voss, 2003; Hunt, 1980) also observed similar behavior by office buildings' occupants (i.e. interaction between outdoor luminance and blinds or artificial lighting use). However, other authors (Yun et al., 2012) observe the contrary (i.e. almost no influence of outdoor luminance on occupants' behavior) and it is hard to extract general rules on this topic at the moment.

Since it seems hazardous (because highly dependent of the building configuration and of the uses of the occupants) to integrate such behavioral issue in the model, the initial best-guess value and the uncertainty range of the SHGC (P5) will be conserved.

8.4.2. Calibration and accuracy criteria

The adjustment of holiday occupancy rate (and related lighting and appliances use rates in offices) during holiday periods allowed improving the quality of the model and decreasing the discrepancy between predicted and recorded electricity consumptions and demand during summer period (Table 35). No significant variation of the computed natural gas consumption was observed.

Table 35: Level 4 - Calibration accuracy indexes

%	2008 to 2010	
	MBE	CV(RMSE)
Gas	-2.1	14.9
Elec	-2.2	5.6
Peak	-0.9	7.4
Offpeak	-5.1	9.7
Hourly	-2.2	24.4

As expected, the prediction of the summer hourly peak demand is improved and the predicted curve matches better the recorded values (Figure 75).

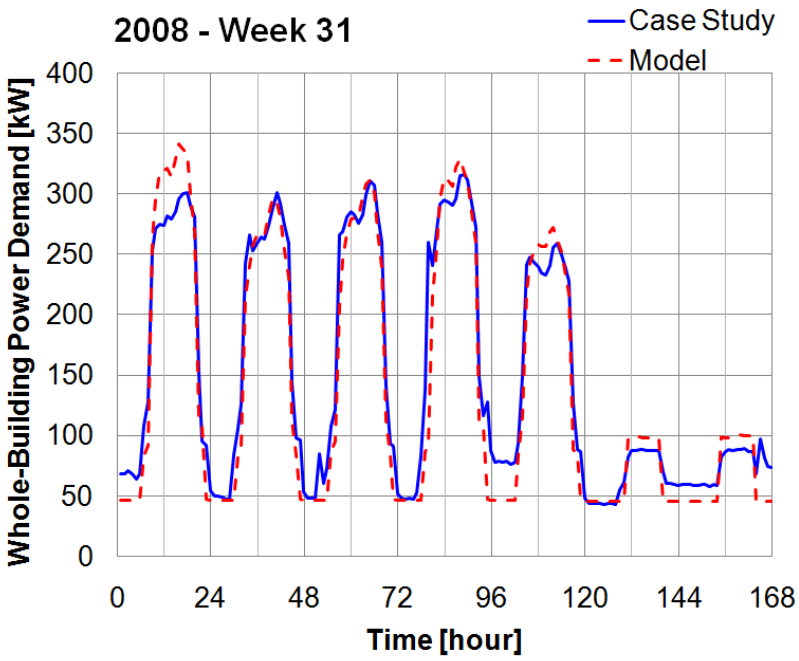

Figure 75: Level 4 - Predicted and recorded whole-building power demand (2008 – week 31)

It is interesting to notice that some discrepancies remain when looking at the monthly electricity consumption profile (Figure 76). These discrepancies are generally higher during the cooling period (between May and September).

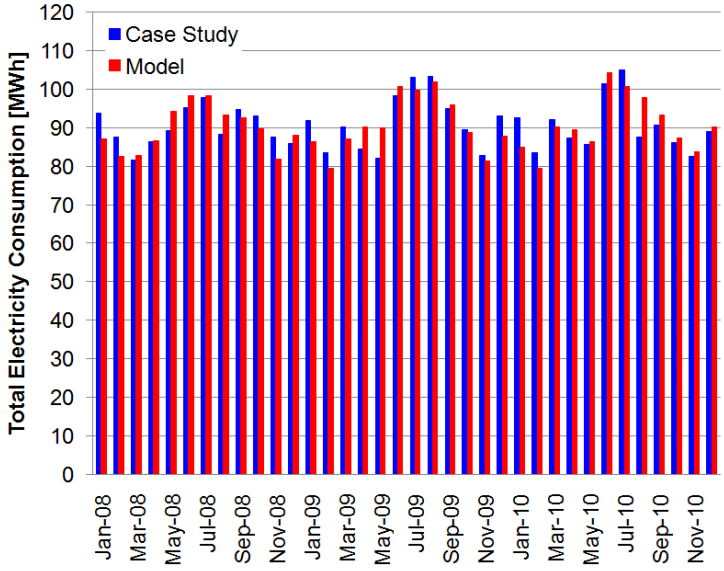

Figure 76: Level 4 - Monthly Electricity Consumption Comparison

Despite of this last adjustment, some discrepancies remain between predicted and recorded summer power demands.

The scatter plots shown in Figure 77 represent the recorded (left – blue) and predicted (right – red) hourly electrical power demands as a function of the outdoor temperature. Different strata can be observed on both graphs but the recorded data form a more continuous and homogeneous scatter.

The different strata (or layers) represent the various operating modes of the building. Horizontal layers represent nights (around 50 kW), weekends (around 70 to 110 kW) and winter days (200 to 250 kW). Summer days (cooling period) form an oblique scatter covering power levels from (approx.) 250 to

350 kW. Intermediate power levels (150 to 200 kW) observed in the simulation results (right) correspond to morning starting and evening shut-off of the HVAC installation (components controlled by the BEMS, such as fans). The more continuous distribution of intermediate power levels observed in the recorded data (left) can partly be explained by the operation of the "optimizer" implemented in the BEMS, controlling the nights and weekends re-start of the installation during very cold and very hot periods, but also by non-simulated power users (elevators) and by a higher dispersion of the actual power demand (due to occupants behavior, random use of lighting and appliances…etc).

The break observed at 14°C in the simulation data is due to the minimal outdoor temperature for cooling plant operation. This may indicates that the overestimation of summer power demand is related to the operation of the cooling system and may be due to an overestimation of the cooling needs (due to the non-representation of the shadings used, the over-estimation of artificial lighting use and of the indoor cooling temperature setpoint).

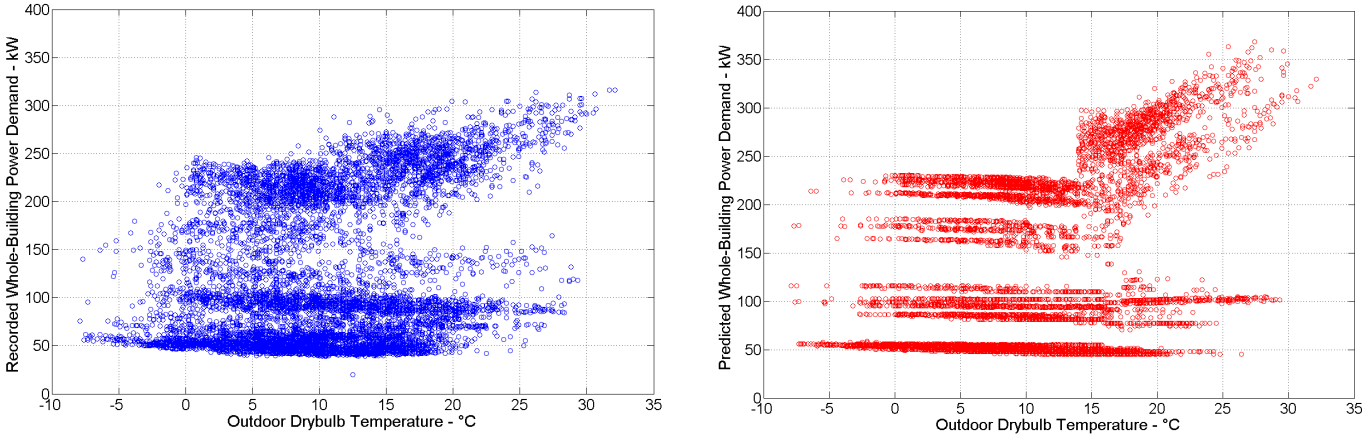

Figure 77: Level 4 - Recorded (left) and predicted (right) hourly whole-building power demand as a function of the outdoor drybulb temperature (2008)

The low-power strata identified above are clearly visible when comparing directly predicted and recorded whole-building power demands (Figure 78). These strata represent offpeak hours operation and include nights (for all year), winter weekends and summer weekends (during which some cooling is necessary in the entrance hall). Remaining blue points represent peak hours (between 7:00 and 22:00, from Monday to Friday) and include system starting and stopping periods, winter operation and summer operation.

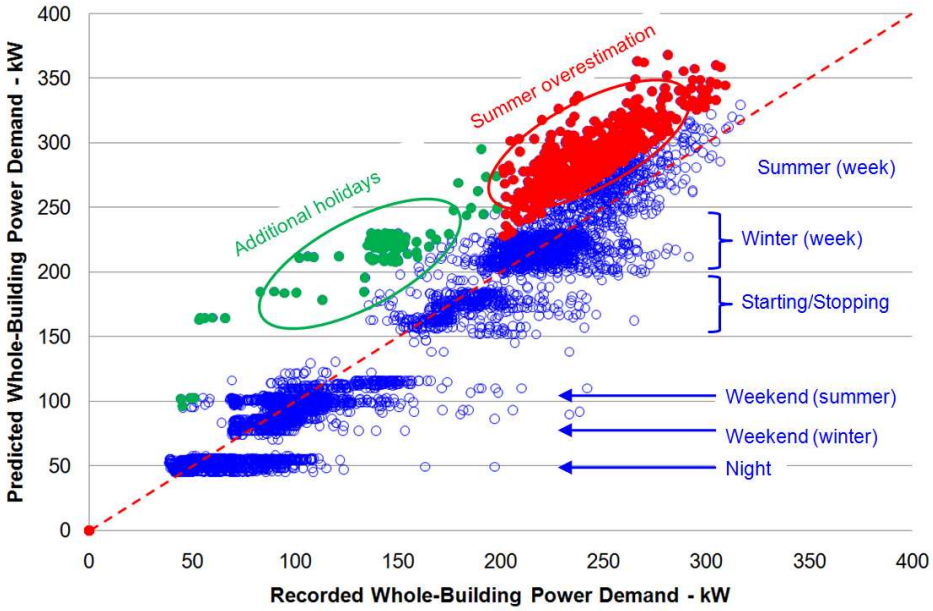

Figure 78: Level 4 - Predicted VS Recorded whole-building power demand (2008)

Green points represents additional holidays identified by comparing predicted and computed whole-building profiles and correspond, among others, to 30th and 31st of December… The model can be easily corrected to integrate this new information but this adjustment (concerning 5 or 6 days, depending of the year) has very small impact on the final results and on the performance of the model.

The summer peak demand (over 250 kW) overestimation is again visible and is highlighted by red points. These overestimations occur at the beginning of summer (June and first half of July) and at the end of summer (end of August and beginning of September).

Figure 79 shows the average whole-building electricity power demand (and the corresponding standard deviation) as a function of the outdoor drybulb temperature. These curves have been obtained by grouping (by outdoor temperature intervals) and averaging recorded and predicted values of the hourly total power demand.

It appears clearly that the model tends to slightly underestimate the winter power demand (1 to 2% error in average during the winter period) while the summer power demand is more largely overestimated (about 10 to 15%). This confirms that the main reasons of the overestimation of the power demand are dependent of the season.

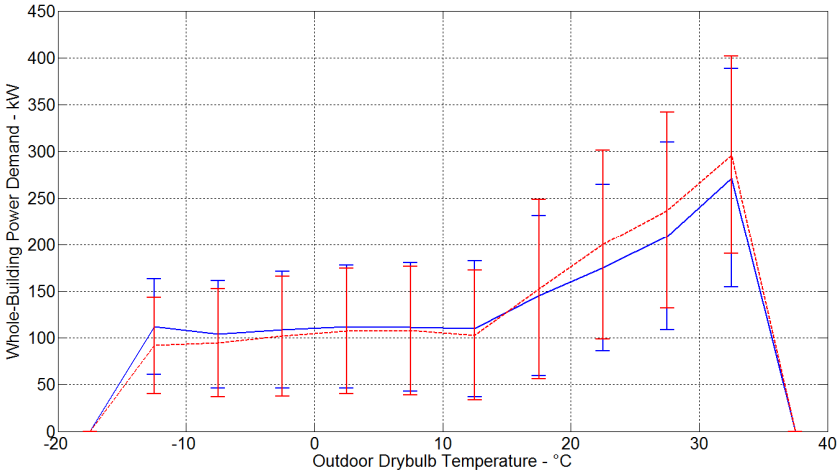

Figure 79: Level 4 - Predicted (red-dotted curve) and recorded (blue curve) average power demands

Even if the adjustment of the summer holiday period leads to an improvement of the model when evaluating the quality of the calibration (statistical indexes and visual verification), regular inspection and physical measurements during summer period would be very helpful and would allow verifying the hypothesis made about the summer operation of the building and the HVAC system. Indeed, other issues (such as less intensive use of artificial lighting, more intensive use of external shadings, overestimation of cooling needs or underestimation of cooling plant performance) could explain the remaining discrepancies.

Finally, it is interesting to have a look at the evolution of the major statistical indexes all along the calibration process. As observed earlier (Chapter 5), the impact of the adjustment of the parameters on the MBE and CV(RMSE) indexes is very clear during the first stages of the calibration process. After a certain time (step 3a in the present case), the improvement of the quality of the model is not well translated anymore by the mathematical indexes computed using the available monthly data (Figure 80) and visual verification becomes the most valid way to check the quality of the model. This can be explained by the fact that at this stage of the calibration process (step 3a and following), the adjustment of the model is done in order to fit to smaller time-scale data (i.e. monitoring data and whole-building power demand). At this moment, monthly global indexes become unable to catch the improvement of the model.

On the contrary, the evolution of the statistical indexes computed for hourly power demands (Figure 81) represents the progressing improvement of the model. However, these values reflect in priority the effect of the adjustment of the parameters having a direct and strong impact on the whole-building power demand.

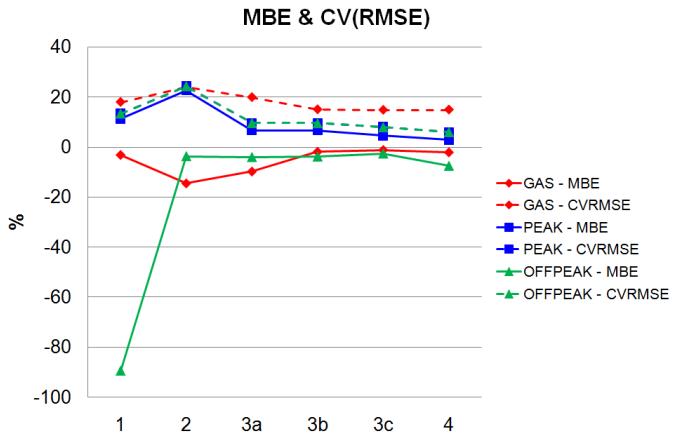

Figure 80: Levels 1 to 4 - Calibration accuracy indexes

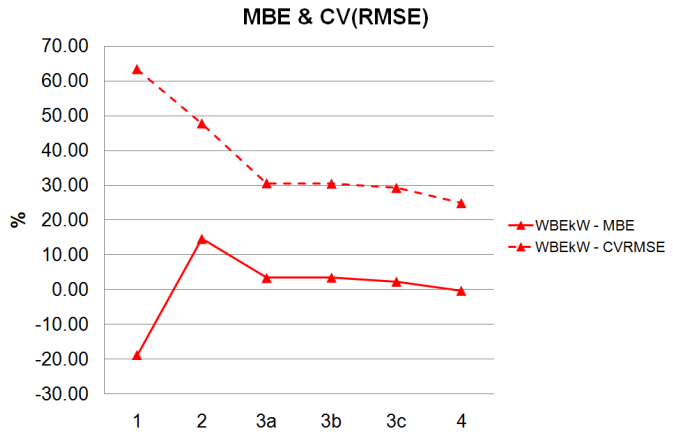

Figure 81: Levels 1 to 4 - Statistical indexes for hourly whole-building power demand

Regarding the remanent uncertainties on the available consumption data (used to compute the values of the statistical indexes), the uncertainties introduced by the use of the simplified model (a few percents in comparison with Trnsys, see Chapter 2) and the uncertainties on some inputs of the model (e.g. weather data), it seems not meaningful to try to continue reducing the values of these indexes. Moreover, the visual analysis of the simulation results done here above confirmed the ability of the model to represent the main trends of the energy consumption behavior of the building under study. The model is now considered as sufficiently accurate to be used in the next steps of an energy efficiency services process (e.g. energy use analysis, selection and comparative evaluation of ECOs).

8.4.3. Analysis of the simulation results

The final simulation results are presented below. The final electricity consumption disaggregation is presented in Figure 82. About 33% of the total electricity consumption is due to artificial lighting. Only one third of this part of the consumption is due to lighting in occupancy zones. Offices appliances (computers, printers…) represent about 16% of the total consumption while almost one quarter of the total consumption is due to IT rooms. Ventilation fans are responsible of about 14% of the consumption. The hot and chilled water production and distribution equipments represent about 13% of the total consumption. Some electricity users (such as elevators) have not been taken into account in the modeling and cannot be quantified by the simulation model. However, as shown above, the main energy users installed in the building have been taken into account during the modeling phase and the energy use of the neglected ones does not represent more than a few percents of the total energy consumption and is of the same order of magnitude as the final calibration error.

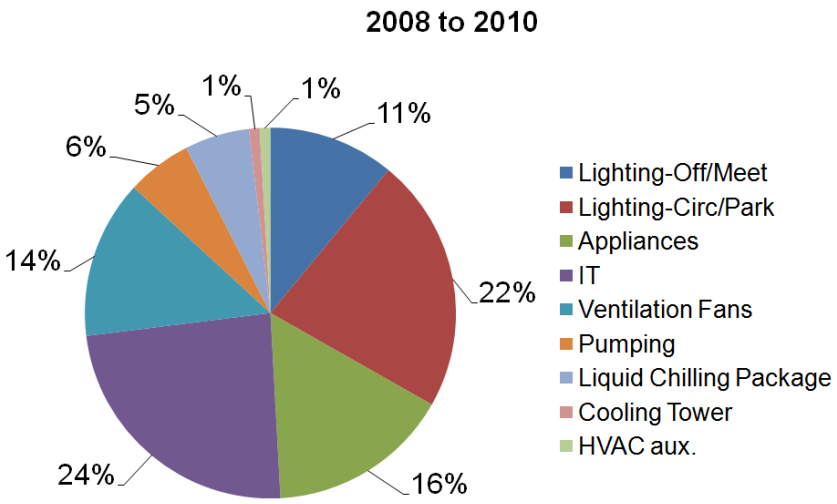

Figure 82: Level 4 - Whole-building electricity consumption disaggregation

During a typical winter week, the base load is mainly due to the constant power demand of the IT rooms (30 kW). The power demand profile is quite regular and only little variations appear from days to days, because of some variations in the HVAC system consumption (Figure 83). The daytime peak is about 180 kW (230 kW peak – 50 kW base load) during weekdays and is mainly due to internal loads in occupancy zones (offices lighting and appliances, approximately 45 kW each) and circulations (circulation and parking lighting, approximately 40 kW). The last 50 kW are due to ventilation fans and water pumps.

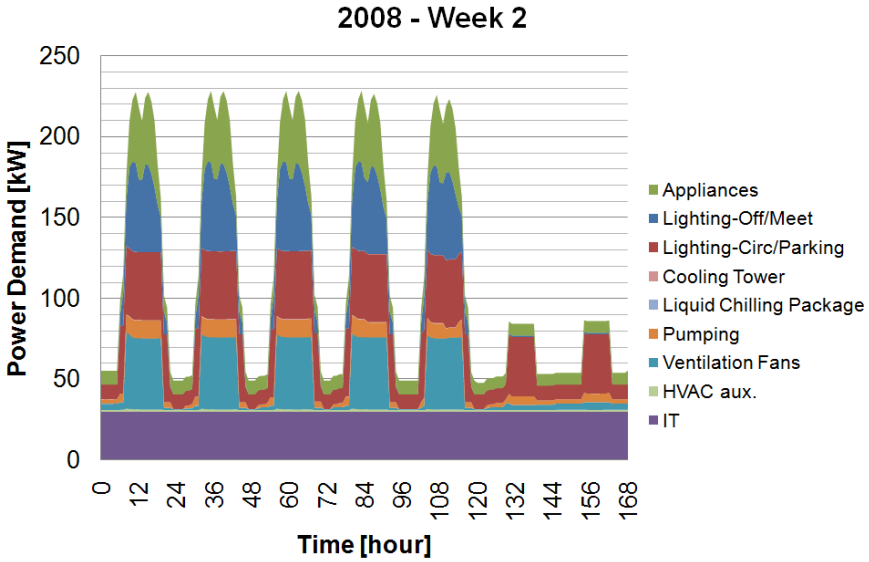

Figure 83: Level 4 - Whole-building power demand disaggregation (2008 – week 2)

As expected, the distribution of the power demand profile is less regular during a summer week. Even if the power demand of IT rooms, internal loads and air and water circulation devices (fans and pumps) remains quite constant, the profile is highly influenced by the chillers and cooling towers power demands (Figure 84).

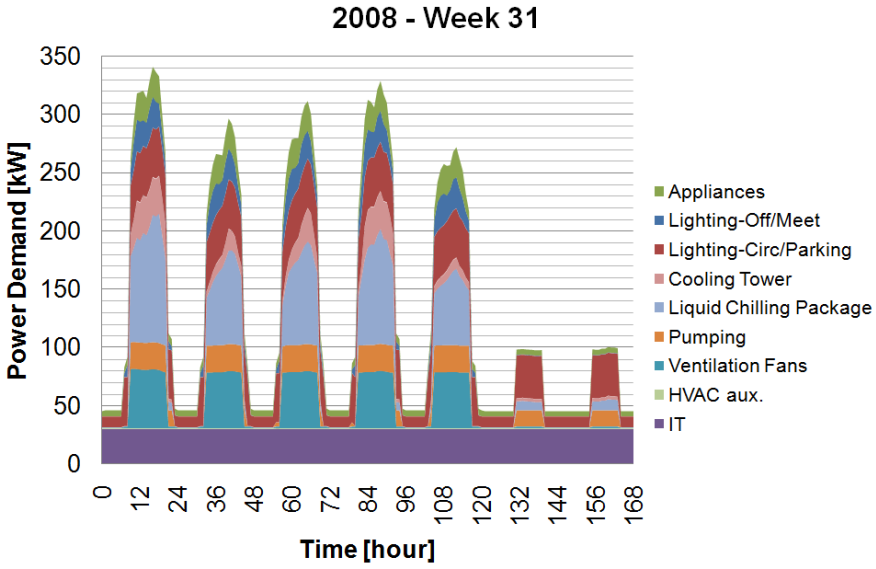

Figure 84: Level 4 - Whole-building power demand disaggregation (2008 – week 31)

The calibrated model can only be used to generate some annual energy balances. Figure 85 shows the disaggregation of the annual heating and cooling demands. On the heating side, it appears that the heating of the parking level (-2) is responsible of about 16% of the total hot water demand (and so, about 16% of the natural gas consumption). About 33% of the hot water demand is due to local zone heating by the fan coil units. Only a limited part (14%) of the total hot water demand is due to humidification of the supply ventilation air by adiabatic humidifiers. The relatively high supply air temperature setpoints (between 20°c and 25°C) explain why supply air reheat is the most important hot water consumer.

Considering these results, the following options should be studied to reduce the hot water demand (and the related natural gas consumption):

- Rationalize (i.e. reduce) both indoor and supply temperature setpoints in order to decrease FCU's and AHU's hot water demands,
- Replace the parking heating system by a tracing system preventing any freezing risk for the water safety distribution system.

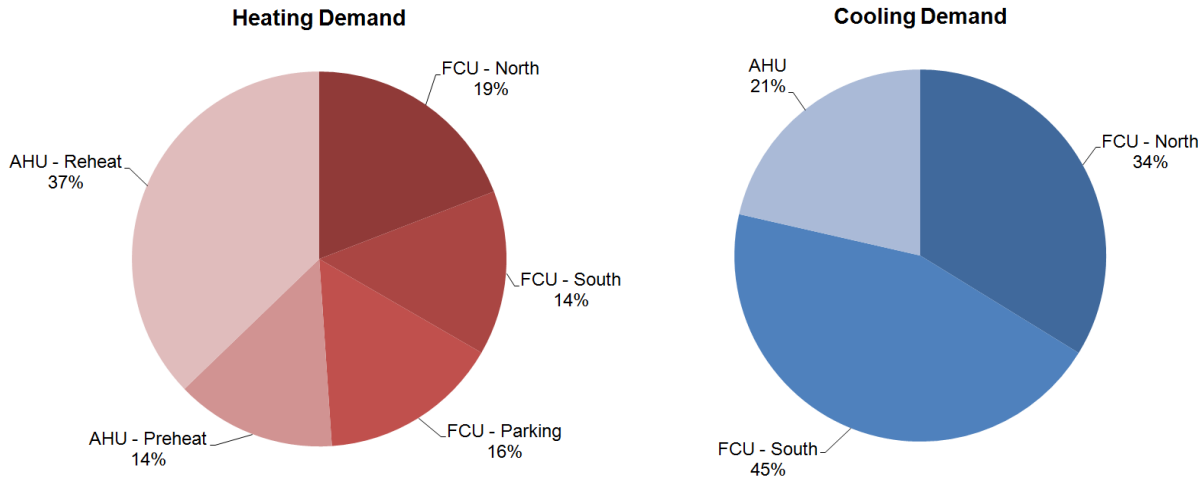

Figure 85: Heating and Cooling Demands Disaggregation

Conclusions are a bit different when looking at the cooling demand disaggregation:

- AHUs cooling demand is relatively limited because of the high supply temperature setpoints during summer (20°C minimum),
- Local zone cooling by means of the FCUs represent about 80% of the total chilled water demand.

Regarding the relative influence of the cooling plant in the final energy balance of the building (i.e. about 6%, as shown in Figure 82), no urgent renovation seems to be needed to reduce the related energy consumption. Focus should be given to other electricity consumers (e.g. lighting in non-occupancy zones and/or during non-occupancy periods) and to non-rational natural gas consumers (e.g. parking heating).

8.4.4. Uncertainty on the simulation outputs

As expected, the uncertainty on the final outputs is again decreased (Figure 86). The standard deviation for monthly gas consumption varies between 11 and 22% while the standard deviation for electricity consumption is included between 2 and 3%.

Even if the uncertainty on electricity consumption has been substantially decreased, the uncertainty on gas consumption remains significant. This can be explained by the fact that the values and corresponding probability ranges of some influential parameters, such as the ventilation rate, have not been updated. Indeed, since this parameter cannot be measured by available measurement equipment, it was decided to keep the as-built value and the original probability range all along the calibration process. The only way to reduce the remaining uncertainty would consist in setting a detailed, heavy (and expensive) monitoring campaign. Moreover, the simple signature analysis made above confirmed that the gas consumption was strongly related to the heating, humidification and ventilation demands. Since the uncertainties on the two first issues have been drastically decreased (by means of physical measurements) and since the final input file (Level 4 version of the model) leads to a good representation of the monthly gas consumption profile, it is believed that the use of the as-built value of the ventilation rate is a satisfying hypothesis. Considering that the as-built ventilation rate is a good approximation of the reality, the final version of the calibrated model can be trusted until additional and more accurate information could be collected.

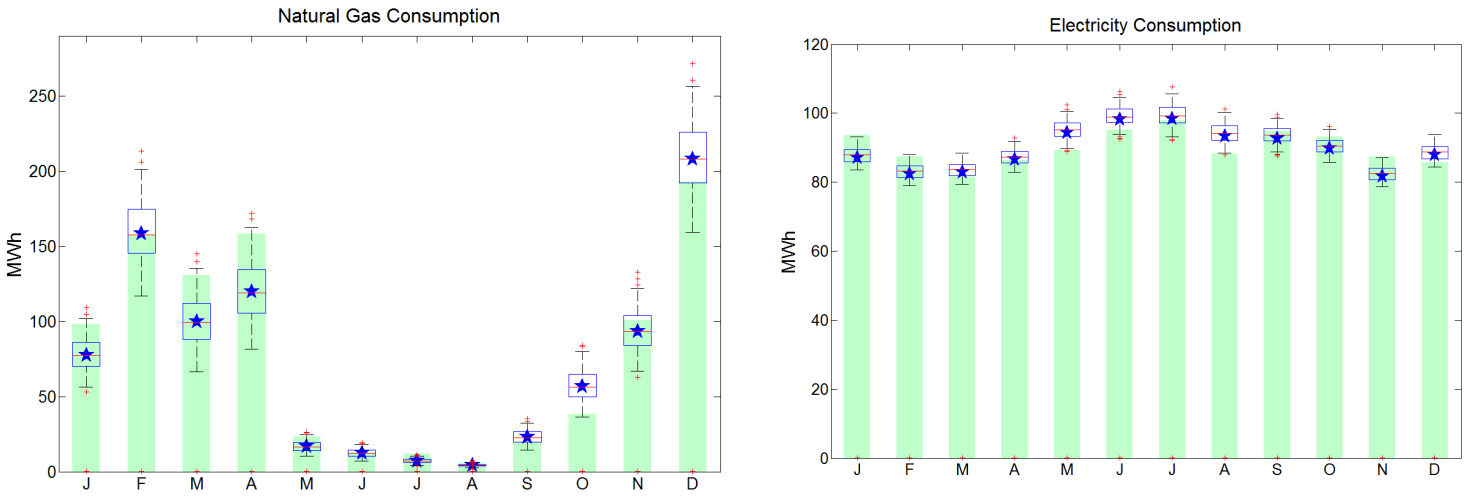

Figure 86: Level 4 - Uncertainty on predicted final energy consumptions (2008)

On the other side, the numerous electrical measurements performed during the monitoring phase allowed substantially reducing the uncertainty on the whole-building electricity consumption and on the specific (end-use) consumptions (Figure 87).

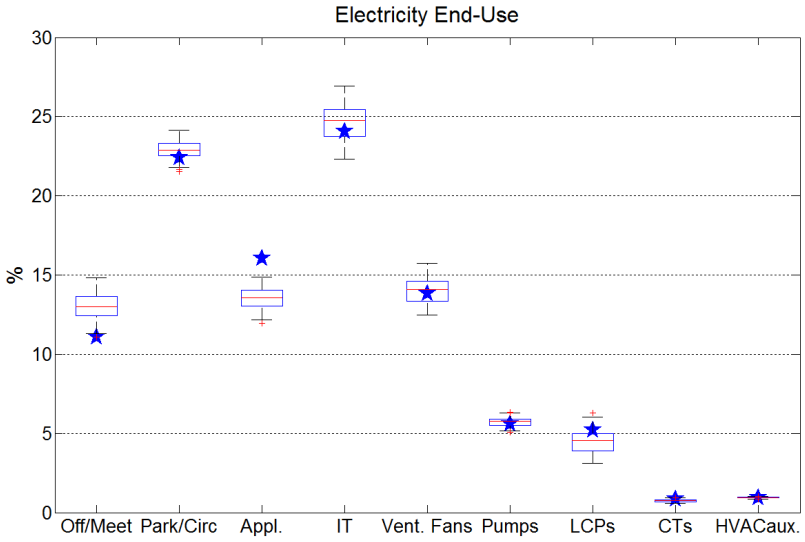

Figure 87: Level 4 - Uncertainty on electricity disaggregation

It is interesting to note that the final share of the electricity end-use is not that far from the trends identified at the calibration Level 2. Moreover, thanks to the application of an evidence-based calibration method including sensitivity issues, the data collection process and the monitoring phase were focused (in priority) on the identification/quantification of the main energy consumers (lighting, appliances and ventilation fans). Only IT rooms were not monitored since the corresponding electrical panels were not accessible (for safety reasons) and the available information was already reliable.

The relative uncertainty (standard deviation) on predicted energy end-use is included between 2.5% and 17%. Lowest uncertainties (between 2.5% and 6%) correspond to internal gains, which have been subject to monitoring (and are characterized by narrowed uncertainty ranges). The energy uses of non-monitored electricity consumers (chillers, cooling towers…) or related to non-monitored energy needs (cooling needs) are characterized by higher uncertainties (between 6% and 17%).

The relative standard deviation on predicted hot water demands (Figure 85 left) varies between 14% and 19% except for preheat heat demand which is characterized by a relative uncertainty of about 37%. This higher uncertainty can explain that AHU's preheat is the only hot water consumer influenced by humidity setpoint and humidifier effectiveness in addition to temperature setpoints, ventilation rate…

The relative standard deviation on predicted chilled water demands (Figure 85 right) of fan coil units varies between 16% and 18%. For the reasons mentioned hereabove, the relative uncertainty (standard deviation) on cooling coil chilled water demand is higher and is about 31%.

8.5. LEVEL 5: PROSPECTIVE ITERATIVE ADJUSTMENT

As shown above, some errors remain when trying to predict summer electricity consumptions and demands.

Because the monitoring campaign was mainly held during winter period, it was not possible to check the achieved level of temperature in offices during the cooling period. An easy trial would consist in adjusting the cooling temperature setpoint in order to improve the prediction of the summer power demand.

Figure 88 shows the average (and corresponding standard deviation) whole-building electricity power demand as a function of the outdoor drybulb temperature. The modification of the cooling temperature setpoint value (increase from 23°C to 24°C) leads to a better representation of the summer power

demand and the maximal discrepancy between average predicted and recorded summer demands is decreased from 15% (Level 4) to about 10%.

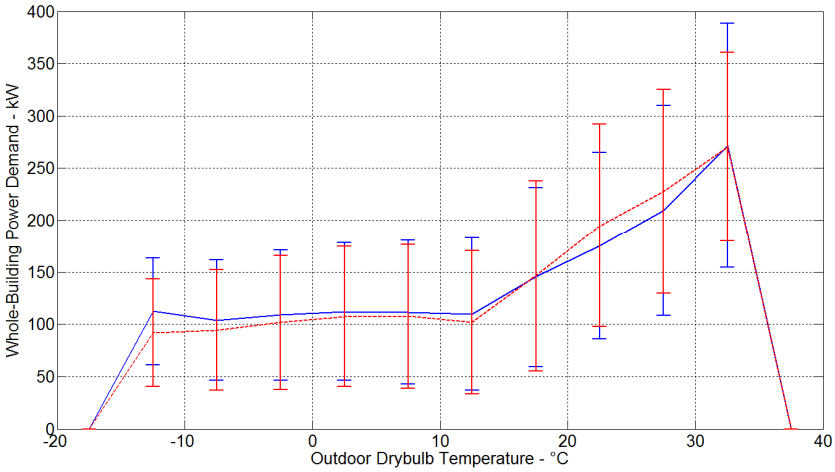

Figure 88: Level 5 - Comparison of predicted (red-dotted curve) and recorded (blue curve) average WB power demands for an indoor cooling setpoint temperature of 24°C

Another possible adjustment would concern the SHGC (P5). Indeed, taking into account a given percentage of use of shadings during the year would lead to a decrease of the summer electricity consumption. The effect of a constant decrease of the SHGC of about 20% (i.e. supposing that solar shadings cover 20% of the glazed area in average, all year long) is similar to the one obtained by correcting the indoor setpoint temperature (error is decreased approx. from 15% to 10%). However, this adjustment also leads to a slight increase of the winter gas consumption (due to less important solar gains) and tends also to reduce the underestimation of the natural gas consumption and improve the predictive abilities of the model during winter period also.

Varying these uncalibrated parameters confirm than an optimum could be reached. Considering that the number of influential parameters that have not been calibrated/adjusted is quite reduced (SHGC, ventilation rate, cooling setpoints, lighting use rate during summer…), a well mathematically-conditioned automated calibration method could certainly be developed and would help in reaching this optimal set of parameters.

One should remind that the accuracy of the model (compared to a detailed commercial simulation software) is about a few percents (see Chapter 2) when predicting annual heating and cooling demands. Moreover, the simulation model remains an abstraction of the reality and it is not realistic to try to reach a perfectly accurate model (e.g. with a 1% accuracy). Continuing the adjustment of the model's parameters too far would actually consist in "modeling" the error induced by the use of a simulation model. Such adjustment can be useful to investigate the potential sources of discrepancies between the reality and the model but should not be considered as evidence or proof of any "physical effect".

However, since physical measurements are still possible (indoor temperature measurement during summer etc.) and because the calibration process developed in this work is, first of all, an evidence-based process: it is proposed to first focus on the physical identification of these last parameters by means of the available monitoring equipment (e.g. measurement of the indoor cooling setpoint, measurement/recording of the chiller performance) and envisage iterative adjustment of the remaining parameters (ventilation rate and solar shadings use) in a second time.

9. CONCLUSION

The simplified dynamic hourly simulation tool described in Chapter 2 and the associated calibration methodology presented in Chapters 3 and 4 have been applied to a case study building located in Brussels.

After having developed the as-built simulation model, a set of potentially influential parameters was defined and some best-guess values and probability ranges were defined. A sensitivity analysis was performed based on the specified probability ranges by means of the Morris screening method. The results of this preliminary sensitivity analysis were used to orient the data collection work. During the next steps of the calibration process, focus was given to the most influential parameters and the model was progressively calibrated as the information and data were collected/available. Finally, the simulation results were analyzed and an uncertainty analysis based on the LHMC method was performed in order to quantify the uncertainty on the final simulation results.

All along the calibration process, a special attention was paid, of course, to the adjustment of the parameters but also to the definition and the update of corresponding probability ranges. Specifying such ranges allowed performing useful sensitivity and uncertainty analyzes in order to orient the calibration work and criticize the model's outputs.

The application of an evidence-based methodology as the one proposed in this work allowed making some interactions between the field-study and the simulation/calibration work. Indeed, analyzing intermediate simulation results was useful in order to confirm the information obtained from the sensitivity analysis and orient further inspection and data collection work (e.g. analysis of the Level 2 simulation results before starting the monitoring campaign of Level 3).

During the calibration process, it was also possible to identify some patterns in the energy use of the building and to refine these results as the adjustment of the process was progressing (e.g. approximate electricity disaggregation at Level 2 and refinement of these results at Level 4).

This case study confirmed that it is possible to calibrate a simplified hourly simulation model by means of a relatively little amount of physical measurements if focus is given to critical issues and a systematic and efficient approach is followed.

The progress of the calibration process confirmed the main conclusions and observations of Chapter 5:

- Calibration accuracy indexes (MBE and CV(RMSE)) followed similar evolution and the "saturation" effect was noticed as soon as model was able to represent the seasonal energy use behavior of the building;
- Preliminary sensitivity analysis was useful to orient the data collection and the parameters adjustment works;
- Some well-chosen measurements can help a lot in improving the quality of the model;
- Uncertainty analysis was useful to quantify the impact of partially or not adjusted parameters (characterized by large confidence/uncertainty ranges) on the model's outputs.

Unfortunately, it was not possible to perform all the desired measurements. Indeed, for practical reasons (loss or unavailability of monitoring equipment), it was not possible to perform indoor conditions measurements during summer.

The data collection could be continued by means of:

- Additional spot and short-term monitoring (e.g. ventilation rate measurement, infiltration rate measurement, hot water and chilled water needs measurements…);

- Set up long term monitoring to allow measuring seasonal variations of the energy use because (e.g. cooling system performance monitoring during summer, seasonal variations of the artificial lighting use…)
- Complementary survey to derive clear occupants' behavioral patterns and cross-check the identified patterns with the available physical measurements.

In the present study, the calibrated model was used to disaggregate the final energy use and to identify the intermediate energy flows in the buildings (specific heating and cooling demands per zone and/or HVAC component) but other applications are possible and will be envisaged in the next step of this case study:

- Selection and evaluation of Energy Conservation Opportunities,
- Continuous performance verification on a monthly/weekly/daily basis,
- …

In a near future, the next steps of this case study will consist in:

- Perform spot and short-term monitoring during the cooling period to identify the achieved levels of temperature in the zones;
- Setting up online long-term monitoring of the performance of the cooling system (in the frame of the iServ project, Knight 2011);
- Using the calibrated model to make continuous performance verification (realizing and sending monthly report on the actual performance of the building to the building energy manager);
- Evaluation of the impact of some modifications of the HVAC system and comparison with reality (e.g. study of the impact on the energy consumptions of the replacement, for technical reasons, of adiabatic humidifiers by electrical steam humidifiers at the beginning of 2012).

The diversity of the buildings composing the non-residential building stock makes hard to derive a general automated methodology that could fit all the cases encountered in practice. For the following reasons, it is, more than ever, believed that a flexible evidence-based calibration is required during the initial steps of such process (i.e. use of building simulation tools as a support for energy services):

- Inspection and monitoring needs could vary a lot from case to case, depending on the initial uncertainties on the building/system description;
- Various sources and types of data have to be collected (field observations, BEMS analysis, various types of loggers…) and treated to allow translation into parameters values;
- Statistical indexes that could be used to express an objective function in the frame of an optimization-based calibration approach are to global to reflect all the influences and interactions involved in the model;

However, the set up of an automated adjustment method could be envisaged to finalize the calibration work. Indeed, after having collected a maximal amount of data (taking into account time and money constrains) to allow "physical" identification of the most influential parameters, an optimization-based approach could be used to refine the values of the last (non-adjusted) influential parameters. Since the dimension of the problem should have been drastically reduced by following the evidence-based approach (e.g. at the end of the evidence-based approach only 3 or 4 influential parameters have not been identified by means of direct or indirect measurements), it is believed that a well-conditioned optimization problem could be built and solved. Such improvement should be envisaged in further works.

10.REFERENCES

Adnot, J. et al. 2007. Field benchmarking and Market development for Audit methods in Air Conditioning (AUDITAC) final report.

ASHRAE. 2001. International Weather for Energy Calculations (IWEC Weather Files) Users Manual and CD-ROM, Atlanta: ASHRAE

ASHRAE. 2002. ASHRAE Guideline: Measurement of energy and demand savings. ASHRAE Guideline 14-2002.

BBRI. 2001. Kantoor2000: Study of Energy Use and Indoor Climate in Office Buildings.

Meteonorm, Meteotest, http://www.meteotest.ch.

Erbs, D.G., Klein S.A., Duffie, J.A. 1982. Estimation of the diffuse radiation fraction for hourly, daily and monthly-average global radiation. Solar Energy Vol. 28, No. 4, pp. 293-302.

Hosni, M.H., Jones, B.W., Xu, H. 1999. Measurements of heat gain and radiant/convective split from equipments in Buildings. ASHRAE Research Project 1055-RP. Atlanta: American Society of Heating, Refrigerating and Air-Conditioning Engineers, Inc.

Hunt, D.R.G. 1980. The use of artificial lighting use: a method based upon observed patterns of behavior. Lighting Research and Technology Vol. 12, pp. 45-50.

International Energy Agency. 2010. IEA-ECBCS Annex 53: Total Energy Use in Buildings: Analysis and Evaluation Methods. http://www.ecbcs.org

Knight, I. 2011. Inspection of HVAC System through continuous monitoring and benchmarking. http://www.iservcmb.info

Liu, M., Song, L., Wei, G., Claridge, D.E. 2004. Simplified building and air-handling unit model calibration and applications. Journal of Solar Energy Engineering. Vol. 126, pp. 601-609.

Reinhart, C.F., Voss, K. 2003. Monitoring manual control of electric lighting and blinds. Lighting Research and Technology Vol. 35, pp. 243-260.

Ruiz-Arias, J.A. 2009. Modelization of the Terrain's morphology Influence on the Solar Radiation Field at the Earth's surface. Doctoral Thesis (PhD) eq. 4.34, University of Jaé, April 2009, 202 p.

Yun, G.Y., Kim, H., Kim, J.T. 2012. Effects of occupancy and lighting use patterns on lighting energy consumption. Energy and Buildings Vol. 46, pp. 152-158.

11. APPENDIX

11.1. ENVELOPE COMPOSITION

All the envelope components are described below.

Type 1 Window module	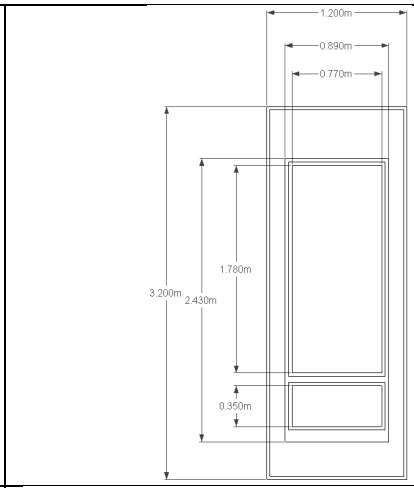	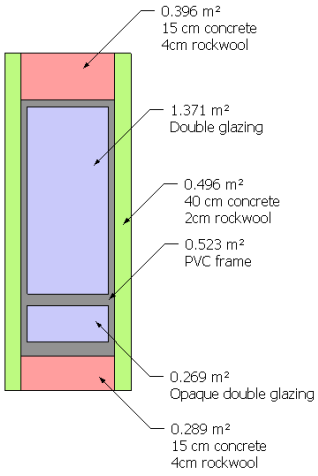
Type 2 Front façade module	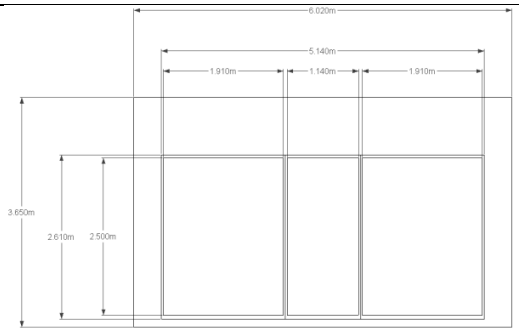	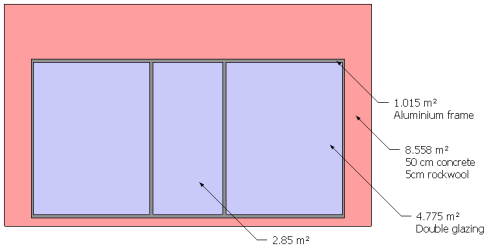
Type 3 Entrance module	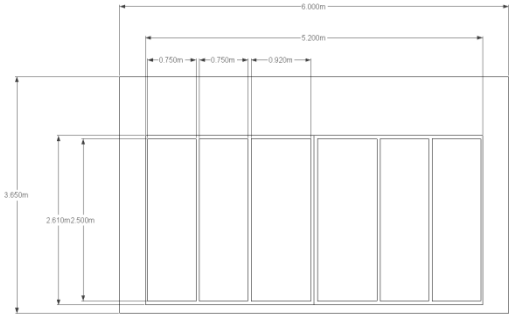	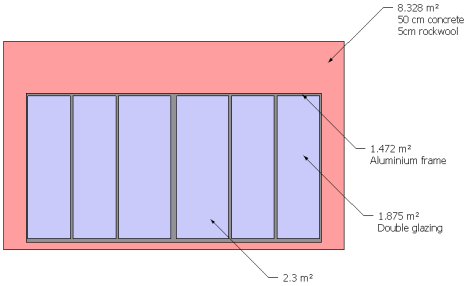
Type 4 Back façade module	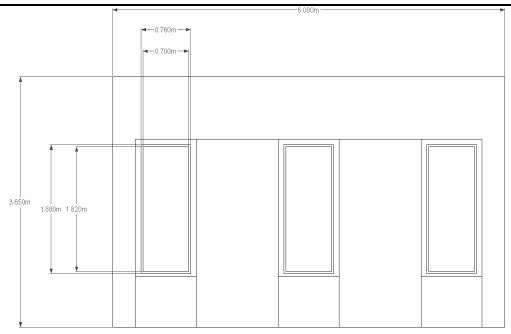	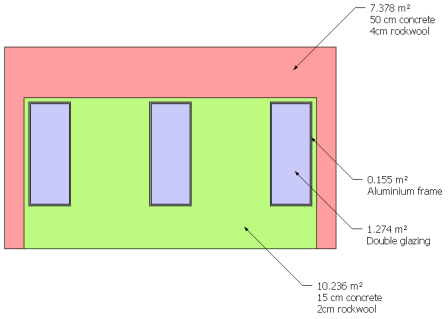

Type 5 & 6 Lateral façade module	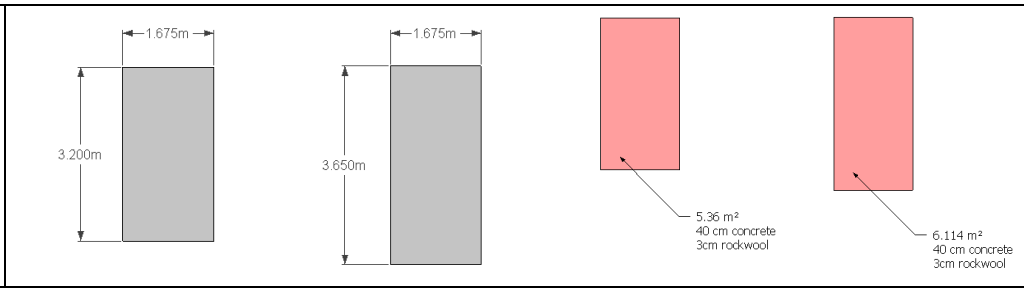

Drawings of building front, back and lateral façades are shown below.

Front Façade	**Back Façade**
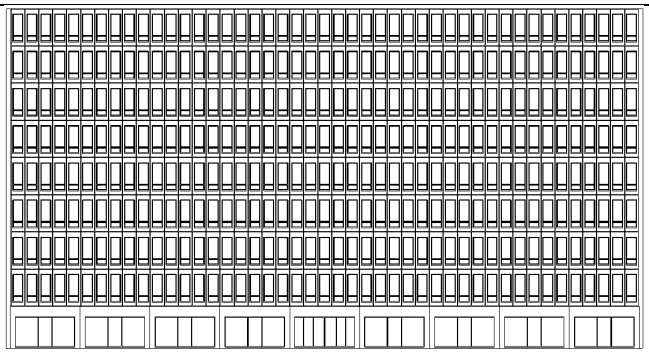	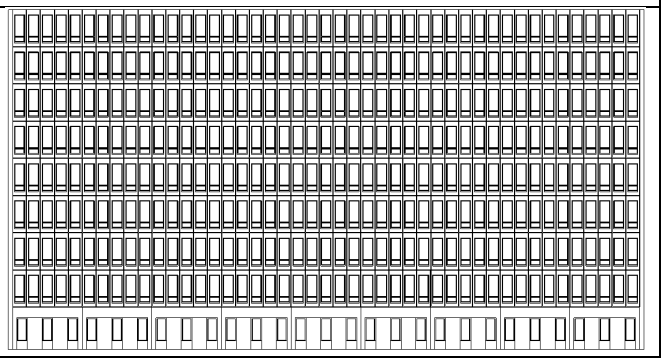

Lateral Façade

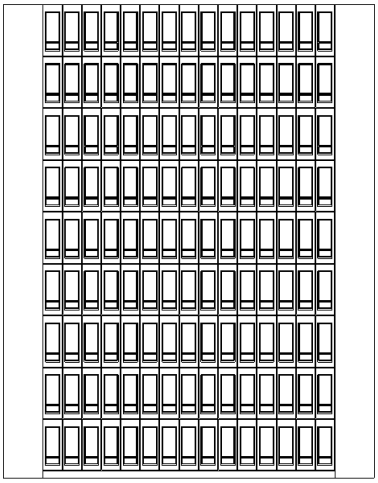

11.2. *ENERGY PERFORMANCE CERTIFICATE*

Energy performance certificate delivered in 2010.

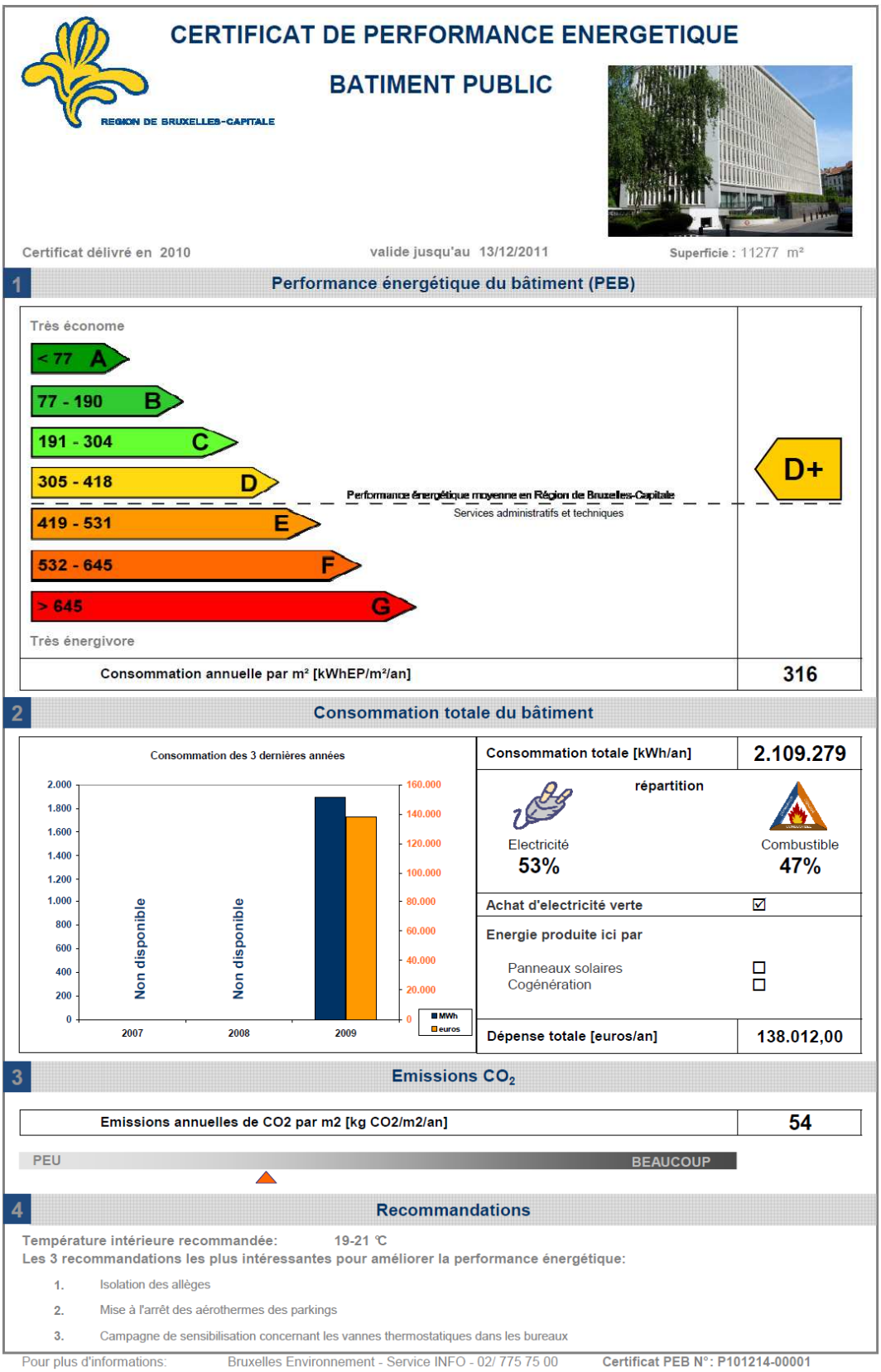

CERTIFICAT DE PERFORMANCE ENERGETIQUE

BATIMENT PUBLIC

REGION DE BRUXELLES-CAPITALE

Certificat délivré en 2010 — valide jusqu'au 13/12/2011 — Superficie : 11277 m²

1 Performance énergétique du bâtiment (PEB)

Très économe

< 77 A

77 - 190 B

191 - 304 C

305 - 418 D

Performance énergétique moyenne en Région de Bruxelles-Capitale
Services administratifs et techniques

419 - 531 E

532 - 645 F

> 645 G

Très énergivore

D+

Consommation annuelle par m² [kWhEP/m²/an]	316

2 Consommation totale du bâtiment

Consommation des 3 dernières années

Consommation totale [kWh/an]	2.109.279
répartition	
Electricité 53%	Combustible 47%
Achat d'électricité verte	☑
Energie produite ici par	
Panneaux solaires	☐
Cogénération	☐
Dépense totale [euros/an]	138.012,00

3 Emissions CO_2

Emissions annuelles de CO2 par m2 [kg CO2/m2/an]	54

PEU — BEAUCOUP

4 Recommandations

Température intérieure recommandée: 19-21 °C

Les 3 recommandations les plus intéressantes pour améliorer la performance énergétique:

1. Isolation des allèges
2. Mise à l'arrêt des aérothermes des parkings
3. Campagne de sensibilisation concernant les vannes thermostatiques dans les bureaux

Pour plus d'informations: Bruxelles Environnement - Service INFO - 02/ 775 75 00 — Certificat PEB N°: P101214-00001

11.3. HVAC SYSTEM

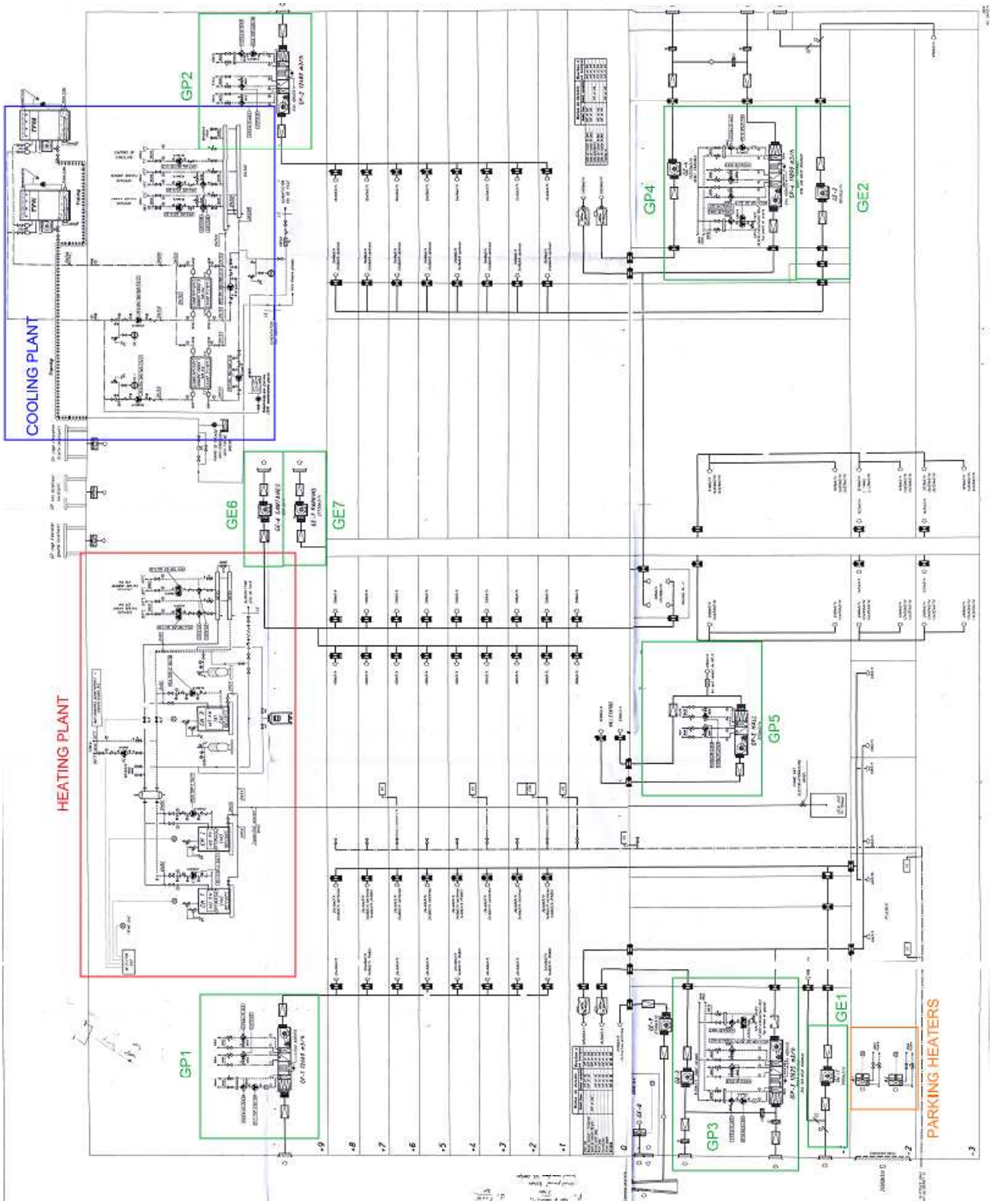

11.4. OCCUPANCY SURVEY

The final version of the survey is presented below, and practical use of the results is introduced. The questions are not necessarily displayed in the same order as they are show on the actual survey, but rather grouped when they are related. Each point from *a* to *d* is in the same order and represent a different page of questions in the online form.

a) Background information

What is your age?

Answers: *30 and below, 31-40, 41-50* or *51 and above*

What is your gender?

Answers: *Female* or *male*

How would you describe your work?

Answers: *Administrative support, technical* or *managerial/supervisory*

Those three pieces of information are necessary to create groups within the sample. Doing so, if behaviour changes depending on the age, the gender or the type of work, this can be identified.

Data use: data is sorted to show only answers from the desired profile type, which then can be analysed.

b) Presence information

In this category, the questions are clearly intended on identifying occupants' daily and weekly schedules as well as office localisation.

Which floor is your office on?

Answers: *Ground floor, 1, 2, 3, 4, 5, 6, 7, 8th floor, technical floor* and *no fixed office*

On which facade are the windows of your office located?

Answers checklist: *Front (Rue De Mot – De Motstraat), left-hand side (DM24 building), back, right-hand side (Rue du Cornet – Hoornstraat / Library)*

These first two questions give back where the occupant's office is located. With the localisation information, we aim at identifying whether the office orientation and level are important regarding heating/cooling needs or not.

Data use: very much like the background questions, data can be filtered to display answers from offices facing a certain directions, or from certain floors. On the other hand, these data may help to check that the sample is representative (all floors and orientations are represented).

Which kind of office do you work in?

Answers: *Individual office* or *shared office*

A distinction must be made between individual and shared offices and this question will enable us to differentiate groups within the sample.

Data use: this can be used to filter answers related to one or the other type of office.

Do you use FlexiTime to manage your schedule?

Answers: *Yes* or *no*

For all answer sheets where this response is *no*, the daily schedule given on each answer sheet should look alike and if not an average schedule can be drawn from it and considered as a standard schedule. If FlexiTime is used, deviation from standard schedules can be quantified.

Data use: filtering according to this answer before analysing schedules.

Which days of the week do you usually work?

Answers checklist: *Monday, Tuesday, Wednesday, Thursday, Friday, Saturday* and *Sunday*

At what time do you usually get to your office at the start of the day?

Answers: *6.00* to *11.00* with a 10' time step, *later than 11.00*

Usually, do you leave your office for your lunch break?

Answers: *Yes* or *no*

If so, at what time do you usually take your lunch break?

Answers: *earlier than 11.00, 11.00* to *14.30* with a 10' time step, *later than 14.30*

If so, how long does your lunch break last usually?

Answers: *less than 30', 30'* to *1h15'* with a 5' time step, *more than 1h15'*

At what time do you usually leave your office at the end of the day?

Answers: *earlier than 15.00, 15.00* to *22.00* with a 10' time step

Excluding lunch, for how long do you leave your office over a usual day?

Answers: *no answer, less than 10', 10', 20', 30', 40', 50', 1h, 1h30', 2h, 2h30', 3h, 3h30', more than 3h*

This is the foundation of the occupant's schedule: when does he/she work? With answers to those questions, we learn deviations from the theoretical work schedule (Mon-Fri, 9am-5pm).

Also, the main variation in energy consumption over a day comes with the lunch break. Therefore it is important to know whether occupants leave the room to have their lunch or not, at what time and when they are back. Extra significant breaks over the day can also modify the occupancy of the office. Later in the survey, it is also asked if the occupants turn off the lights and their computers as they leave the room (questions 19, 20, 25 and 26), so we can assume such a behaviour if they leave the room during lunch.

Data use: for each answer sheet, these times can be translated into binary values, like presented in the table in the example case that:

Occupant 1 leaves his office for lunch at 12.30 and takes 35' for his break;

Occupant 2 takes his lunch break out of his office at 12.10 and takes 1h05' to eat and rest.

Day	Time	Occupant 1	Occupant 2
Monday	00.00	0	0
Monday	00.05	0	0

Tuesday	13.00	0	0
Tuesday	13.05	1	0
Tuesday	13.10	1	0
Tuesday	13.15	1	1
Tuesday	13.20	1	1

On average, how many hours per week do you not attend work at your office?

Answers: *no answer, 0* to *37, I am never in my office*

How many free days do you take between April and October included?

Answers: *no answer, 0* to *60, more than 60*

These questions identify for how long over a week and by extrapolation over a year people are out of their office and then whether they are more present during winter (heating) period or during summer (cooling) period. This is of influence on yearly heating/cooling loads.

Data use: these results are a bit trickier to translate into occupancy. The easiest way is to multiply the occupancy value by a weekly factor $f_{week} = \frac{t_{work} - t_{away}}{t_{work}}$, where t_{work} is the weekly amount of time an occupant works, and t_{away} is the amount of time he/she spends away from the office.

c) Lighting

Where is your desk work space placed in the room?

Answers: *By the window, in the middle of the room, by the wall opposite to the window*

This question is asked in the hope of finding whether a relation exists between natural lighting and use of artificial lighting and sun blinds. A correlation with facade orientation may also appear.

Data use: compare use of lighting and window blinds (question 18 to 22), as well as cooling demand (Questions 28 and 30) according to different answers.

How many ceiling light bulbs/neon lamps are lit if the light is on?

Answers: *2, 4, 6, 8, more than 8*

Depending on the occupant, only half of the lights might be on if, for example, natural lighting is sufficient by the windows but artificial lighting necessary by the door of the office.

Data use: consider load as a fraction of the installed load. If only 2 out of 4 lights are on, lighting load can be described as being 0.5. Indeed, benchmarking always return the full installed loads and the figures gathered here need to compare to that.

In winter/summer, at your arrival in the morning, do you turn on the lights?

Answers: *Nearly always* or *nearly never*

When you leave at night, do you turn off the lights?

Answers: *Nearly always* or *nearly never*

Answers to these questions will differentiate passive from active lighting users. In connection with the occupant's schedule, a lighting schedule can be fitted with this information. A difference is made between winter and summer as it is expected that even a passive user will turn on the lights on a winter morning.

Data use: a table can be produced for lighting load.

If the outdoor lighting conditions change, do you react?

Answers: *Nearly always* or *nearly never*

If so, do you mainly...

Answers: *Switch on/off the light?* or *open/close the window blinds?*

Once again this tries to differentiate passive from active users, this time involving sun blinds.

If an occupant is active, does his/her activity require electrical energy consumption, by means of lighting (operating sun blinds is only a temporary smaller use of electricity).

Data use: in terms of figures, if a user switches on/off the lights, this corresponds to a change in the lighting load table. Lighting condition changes can be related to solar radiation given by the weather station.

d) Computer and appliances

What electrical appliances do you have in your office?

Answers: *Desktop computer, laptop/notebook, printer, none* or *other (specify)*

How many computers do you use at the same time?

Answers: *I don't use any, 1, 2, 3, 4, more than 4.*

This enables estimation of the installed power in that office.

Data use: the profile of the responder can be related to a certain installed appliances power that will correspond to running appliances.

Over night time, in what state is your...

When you leave for a break, in what state is your...

- Computer?

- Screen?

Answers: *Fully on, stand by* or *off*

Because the load changes depending on the mode in which an appliance is, answer to this question enables fitting to the occupant's daily schedule the appliance electrical load related.

Data use: an appliances schedule, copied on the model of the occupancy table can be derived. Hosni et al. (1999) characterizes appliances power consumption according to their type and state mode. A value from 0 to 1, where 1 represents installed power, is easily derived.

11.5. ZONES GEOMETRY

The following table includes the complete geometrical description of the zones and walls defined in the simulation model.

Wall	**Zone**	**Orientation**	**Heavy**	**Heavy**	**U_{avg}**	**Light**	**Glazing**	**Frame**

			opaque	**Opaque AU**		**opaque**		
		-	m²	W/K	W/m²-K	m²	m²	m²
1	1	NE	117.47	153.94	1.31	0.00	25.47	3.13
2	2	NE	23.49	30.79	1.31	0.00	5.09	0.63
3	2	SE	37.42	42.06	1.12	4.05	20.55	7.80
4	2	SW	25.68	16.69	0.65	0.00	37.20	3.06
5	3	SW	25.45	16.54	0.65	0.00	36.90	3.51
6	4	SW	17.12	11.13	0.65	0.00	24.80	2.04
7	5	SW	8.56	5.56	0.65	0.00	12.40	1.02
8	5	NW	37.42	42.06	1.12	4.05	20.55	7.80
9	5	NE	17.62	23.09	1.31	0.00	3.82	0.47
10	6	NE	504.00	594.36	1.18	81.00	411.00	156.00
11	7	NE	50.40	59.44	1.18	8.10	41.10	15.60
12	7	SE	287.36	324.36	1.13	32.40	164.40	62.40
13	7	SW	50.40	59.44	1.18	8.10	41.10	15.60
14	8	SW	504.00	594.36	1.18	81.00	411.00	156.00
15	9	SW	50.40	59.44	1.18	8.10	41.10	15.60
16	9	NW	287.36	324.36	1.13	32.40	164.40	62.40
17	9	NE	50.40	59.44	1.18	8.10	41.10	15.60
18	6	H	270.80	157.06	0.58	0.00	0.00	0.00
19	7	H	90.70	52.61	0.58	0.00	0.00	0.00
20	8	H	270.80	157.06	0.58	0.00	0.00	0.00
21	9	H	90.70	52.61	0.58	0.00	0.00	0.00
TOTAL			**2817.55**	**2836.39**	**1.01**	**267.30**	**1501.98**	**528.66**

CHAPTER 7 GENERAL CONCLUSION AND PERSPECTIVES

CHAPTER 7: GENERAL CONCLUSION AND PERSPECTIVES

This thesis has presented the development and the application of a simulation tool and the associated evidence-based calibration methodology dedicated to the analysis/diagnosis of the energy performance of existing buildings. The model and the methodology have been applied to a synthetic case and to a real building.

Building Energy Simulation and Energy Efficiency Services

Forward (predictive) building energy simulation models have been used for design and optimization of buildings for numerous years. More recently, the use of these models was extended to other stages of the building life cycle (Figure 1), such as energy services activities (including inspection/audit, evaluation of Energy Conservation Opportunities and on-going performance analysis).

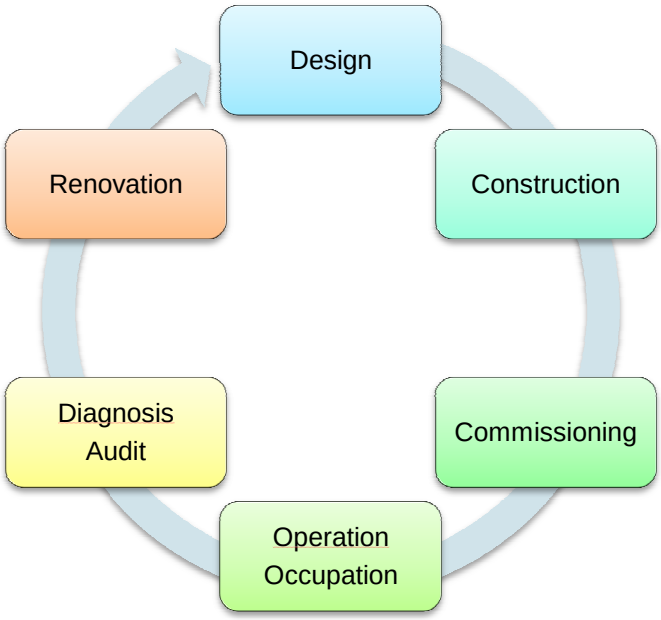

Figure 1: Building Life-Cycle

It is commonly admitted that using a building simulation model to assist in analyzing the energy use of an existing building requires the model to be able to closely represent its actual behavior. In the frame of energy services activities, the calibration of a simulation model to an existing situation is usually a highly underdetermined problem. Indeed, only very scarce and limited information are usually available about the building (e.g. as-built files) and its performance (e.g. monthly energy billing data).

Current commercial building energy simulation software's are not adapted to the study of existing situations. Most of these simulation packages have been developed to support the design of new buildings and include numerous details and aspects that cannot be investigated in practice. A simplified building energy simulation model has been designed and developed so as to fit with the requirements of whole-building energy use analysis (i.e. prediction of hourly heating and cooling needs and subsequent final energy consumptions) while minimizing the amount of parameters to adjust. When compared to reference detailed building simulation models (e.g. Trnsys, EnergyPlus…), the simplified model demonstrated an accuracy of less than 8% when predicting annual heating and cooling needs.

Model Calibration Methodology

Regarding the advantages and limitations of existing calibration methodologies and the requirements of an energy efficiency service process, it was decided to develop a new systematic evidence-based calibration methodology integrating sensitivity, uncertainty and measurements issues.

The basic principle of this new methodology is to give priority to the physical identification of the model's parameters (i.e. to the direct measurement) and relies on the definition of two types of hierarchy:

- A hierarchy of the model's parameters by order of influence built based on the results of a preliminary sensitivity analysis based on the Morris' sampling method and allowing (1) "factor fixing" (i.e. identification of non-influential parameters that could be set to their "best-guess" value) and (2) "parameters screening" (i.e. classification of influential parameters by order of importance).
- A hierarchy among the source of information exploited to identify the value of the parameters based on the reliability of the available data (e.g. direct measurements > observation > default value).

Following these main rules, the user is guided all along the energy use analysis process. The information provided by the preliminary sensitivity analysis is used to orient the data collection work (i.e. the inspection of the building) and the progressive adjustment of the parameters.

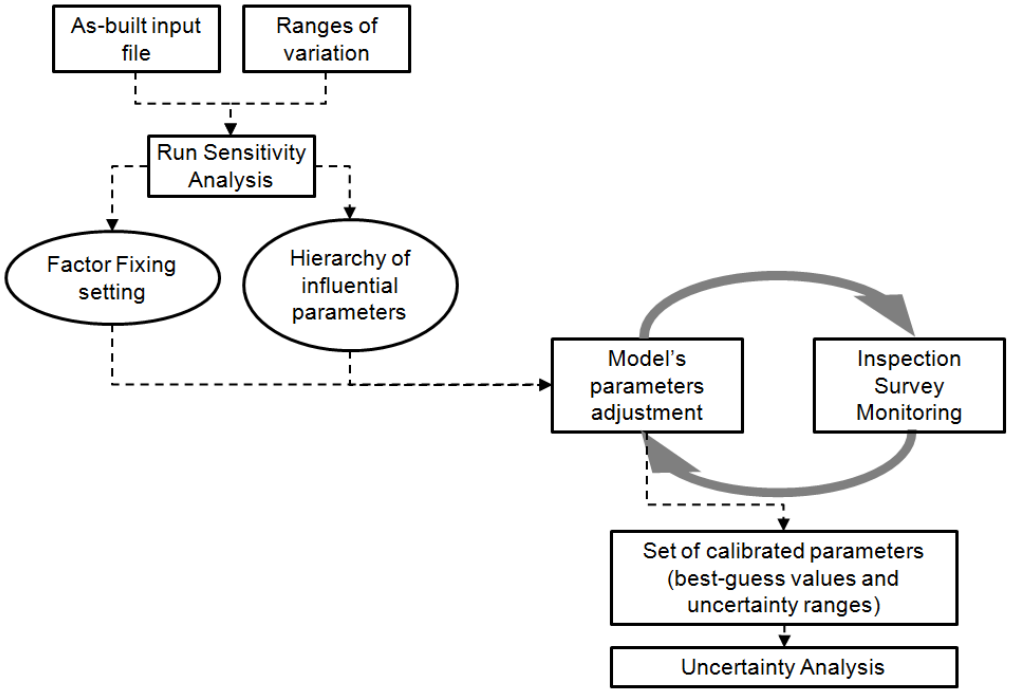

Figure 2: Main steps of the evidence-based calibration methodology

All along the calibration process, the values of the parameters are updated, as well as the related probability ranges (reflecting the confidence/uncertainty on the considered value of the parameter). These ranges of variation are used at the end of the calibration process to quantify the uncertainty on the final outputs of the calibrated model by means of the Latin Hypercube Monte Carlo sampling method.

At each step of the calibration process, it is proposed to characterize the quality of the calibrated model by means of:

- Classical statistical indexes (Mean Bias Error and Coefficient of Variation of the Root Mean Squared Error) computed on a monthly basis for gas/fuel, peak electricity and offpeak electricity consumptions and,
- Visual comparison of available recorded data (e.g. power measurements) and corresponding predicted values.

If available, recorded and predicted (quarter-)hourly power demand profiles should be compared to qualify the accuracy of the calibrated model.

Selection and application of a sensitivity analysis method

The (global) Morris sensitivity analysis method was used in the frame of this work. This "screening" method allows classifying model's parameters by order of influence and takes interactions and high-order effects into account. Comparing to other global methods, the Morris design is able to characterize both local and global effects by computing mean and standard deviation values of "elementary effects".

A first sensitivity analysis has been carried out on two typical cases defined to be representative of the Belgian building stock in order to proceed to an initial screening of the model's parameters. The main impacts on final energy consumption indexes were due to:

- Envelope characteristics;
- Air (ventilation and infiltration) renewal rate(s);
- Indoor heating, cooling and humidity setpoints;
- Internal gains densities and schedules;
- HVAC system components performance.

Behavioral issues (e.g. operating schedules of artificial lighting and appliances) were highlighted as influential parameters and should be investigated when analyzing a real building case.

On the contrary, some parameters were identified as weakly influential when analyzing global consumptions:

- Outdoor combined (convective-radiation) heat transfer coefficient;
- Internal gains convective-radiation split;
- Walls absorbance and emissivity.

Of course, these last parameters can have stronger impacts when analyzing comfort issues (e.g. operative temperature…etc).

The analysis of the variations of intermediate and final consumptions allowed identifying the following trends:

- Natural gas consumption is generally a good representation of the heating needs of the building;
- Total electricity consumption is a too global index to allow the clear distinction of the various influences and the identification of the variations of the cooling needs;
- The distinction between peak and off-peak electricity consumptions or winter and summer gas and electricity consumptions is useful to analyze the answer of the model to parameters changes;
- Highly influential parameters are also involved in high-order effects (i.e. curvature and interaction effects);

These observations confirm that the use of a fully automated method to solve the highly underdetermined calibration problem can be hazardous. Indeed, the numerous compensation and

interaction effects identified make difficult (if not impossible) the definition of a well-conditioned (optimization-based) calibration algorithm relying on the very little amount of available energy consumption data (monthly bills).

Development and use of a Virtual Test Bed

A Virtual Calibration Test Bed (VCTB) has been developed and consists in a detailed model (implemented in Trnsys) of a typical building equipped with a complete HVAC system. This model includes numerous influences usually neglected in building simulation (e.g. stochastic behavioral profiles for lighting and appliances use…). This fictitious building case has been used to generate synthetic energy use data (e.g. whole-building monthly energy bills and sub-hourly power demand profile).

It was noticed that recently developed stochastic behavioral profiles were useful to general realistic sub-hourly demand profiles but had no impact on globalized/averaged energy consumption data in comparison with standard “sharp” operating/occupancy/use profiles.

The proposed simplified building energy simulation model and the associated calibration methodology have been applied to this synthetic case as if it was a real building case. The use of a synthetic case allowed:

- Checking the robustness of the calibration method ,
- Studying the quality of the calibrated model at each stage of the adjustment process by comparing reference (from the VCTB) and predicted (from the simplified model) energy demands,
- Highlighting useful measurements that could be performed in practice,

Three data collection levels were investigated to represent a complete evidence-based calibration process, from as-built data collection (Level 1) to short-term/spot local monitoring data (Level 3) through visual observation and inspection (Level 2). Data collection, sensitivity, accuracy and uncertainty issues were discussed at each level:

- The initial as-built model (Level 1) gave a fair representation of the main trends of the building energy use but results were not reliable enough (too important uncertainty) to allow drawing conclusions on the energy end-use. Following the methodology developed earlier, a preliminary sensitivity analysis was conducted in order to proceed to “factor fixing” and to orient the data collection and the parameters adjustment processes during the next phases of the calibration.
- The Level 2 calibration, relying on data available during an inspection of the building (BEMS analysis…), resulted in a model giving an acceptable representation of the energy behavior of the building. Main seasonal and daily variations were represented but uncertainties remained too important to allow a proper quantification of the energy end-users.
- At the end of the monitoring campaign, the Level 3 calibration model was able to predict the building energy performance with a satisfying accuracy. Among others, local power measurements (at floor level) were highlighted as useful to help in characterizing actual internal gains (lighting and appliances) power demands and profiles/schedules.

It was interesting to study the evolution of the values of the statistical indexes (MBE and CV(RMSE)) computed on monthly and hourly values. A saturation effect was noticed when looking at the indexes computed based on 12 monthly values. As soon as the seasonal variations of the energy use were well represented by the model, finer adjustments did not lead to any significant improvement (i.e. decrease)

of these indexes. However, indexes computed on hourly values were more able to reflect the improvement of the models on shorter time scales (e.g. adjustment of the hourly profiles…).

This observation confirmed that, in the frame of a typical calibration process (where main available energy use data consist in monthly energy bills), additional and specific visual verifications are needed to evaluate the quality of the calibrated model (e.g. comparison of hourly global or local power demand profiles, analysis of the evolution of the predicted values of indoor temperature and humidity…).

Conducting preliminary sensitivity analysis was very useful to highlight influential parameters and orient the calibration process. It was interesting to notice that the progressive adjustment of the parameters (and the narrowing of the corresponding uncertainty/confidence ranges) did not lead to important modifications of the hierarchy between influential and non-influential parameters built at the beginning of the calibration process.

However, narrowing the uncertainty ranges led to significant decrease of the uncertainty on the outputs of the model. All along the calibration process, the improvement of the quality of the model was clearly reflected by the decrease of the uncertainty on the energy performance predicted by the calibrated model. Future research could focus on the setting of uncertainty range and could envisage other uncertainty analysis techniques (such as variance-based methods).

Further improvements of the test bed would consist in improving some of the stochastic profiles used in the present model and in adding physical effects such as ducts and pipes fouling, more realistic and detailed dynamic boiler and chiller models… A better representation of the air flows in the building (by means of a dynamic interzonal flow model) would also help in representing heat and mass transfers between zones in a more realistic manner.

The developed test bed could be used to investigate supplemental calibration issues:

- Definition and assessment of new goodness-of-fit (GOF) criteria (e.g. new limit maximal values of statistical indexes, statistical indexes computed on shorter time-scales, combined/weighted objectives functions…)
- Evaluation of other calibration levels (implying more specific and long-term measurements)
- Assessment of other calibration methods (totally or partially automated methods)
- Generation of synthetic pre- and post-retrofit data in order to check the ability of calibrated models to predict energy savings.

Application to a Case Study

The last part of the present work consisted in applying the proposed tool and methodology to real building case, located in Brussels. As already done for the synthetic case, the calibration process consisted in:

- Building the as-built input file (Level 1)
- Running a preliminary sensitivity analysis
- Proceeding to building inspection (and focusing on important issues identified by the sensitivity analysis, Level 2)
- Performing short-term specific monitoring (power, temperature, humidity and operating time metering) to allow a “physical identification” of the most important parameters
- Running an uncertainty analysis in order to characterize the accuracy/validity of the calibrated model

This case study allowed clearly identifying the potential interactions between the calibration work and the data collection process. The analysis of the results of the sensitivity analysis and of the

intermediate simulation results of the model allowed focusing on the most important issues when performing building/system inspections and measurements.

Both statistical criteria and visual verifications were used to analyze the accuracy of the calibrated model and point out the issues that should have been investigated in order to continue improving the model. However, this case study confirmed that it was possible to calibrate a hourly simulation model by means of relatively little amount of monitoring data. The use of a systematic evidence-based method allowed optimizing the efforts (i.e. minimizing the monitoring and modeling work while maximizing the quality of the model) and reaching an acceptable level of accuracy.

The calibrated model was used to disaggregate the final electricity use and identify the main hot and chilled water consumers. The calibrated model allowed identifying simple (direct) Energy Conservation Opportunities (i.e. modification of the parking heating system) and can be used to assess more complex options (walls insulation, schedules and/or setpoints adjustment…).

No evaluation of ECOs was done since no data was available to check the validity of such evaluation. In addition to such simulation work, additional measurements and on-field investigations could be done to characterize the use of solar shadings (and their impact on solar gains), indoor conditions during summer (indoor temperature setpoints), cooling system performance (chiller and cooling towers energy use)…

Discussion and perspectives

Both applications (real and synthetic cases) allowed highlighting the complexity and the limits of calibration as it is used today. Calibration remains a highly underdetermined problem and a compromise has to be found between data collection and modeling efforts and model's requirements (Figure 3).

At the end of these applications, it seems hard (if not impossible) to define a general calibration criteria able to warrant the quality of a calibrated model in every situation. This makes again less likely the appearance of a "perfect automated calibration method".

The influences and interactions occurring in office buildings are so complex that analysis of very global and aggregated energy use indexes (e.g. monthly energy bills) cannot be used to orient the calibration of a forward building energy simulation model involving a few tens of parameters (as it is done in non-evidence-based methods).

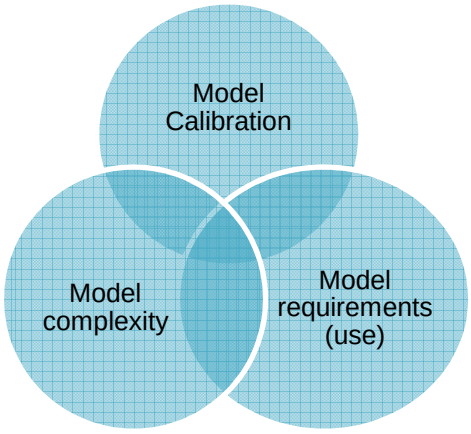

Figure 3: Compromise between modeling-calibration-requirements

At the end of this work, it is believed that (at least) partially manual methods remain more efficient and the best quality assurance.

The applied calibration methodology is far to be automated and still partially relies on user's skills since it remains important to stay critical when analyzing the model's outputs. However, the application of an evidence-based method ensures sticking to reality and avoids bad representation and hazardous adjustment of the parameters. Moreover, the intensive use of a sensitivity analysis method was of a great help to orient data collection (similarly to "experimental design") and parameters adjustment processes. Defining confidence/uncertainty ranges for each parameter, in addition to a "best-guess" value, also allowed quantifying the uncertainty on the final outputs of the model and helped the user in evaluating and criticizing the quality of the calibrated model.

Another advantage of the proposed method is its flexibility. The diversity of the buildings composing the non-residential building stock makes mandatory to keep the calibration method as flexible as possible:

- Inspection and monitoring needs could vary a lot from case to case, depending on the initial uncertainties on the building/system description;
- Various sources and types of data have to be collected (field observations, BEMS analysis, various types of loggers…) and treated to allow translation into parameters values;

The set up of an automated adjustment method could be envisaged to finalize the calibration work. Indeed, after having collected a maximal amount of data (taking into account time and money constrains) to allow "physical" identification of the most influential parameters, an optimization-based approach could be used to refine the values of the last (non-adjusted) influential parameters. Since the dimension of the problem should have been drastically reduced by following the evidence-based approach (e.g. at the end of the evidence-based approach only 3 or 4 influential parameters have not been identified by means of direct or indirect measurements), it is believed that a well-conditioned optimization problem could be built and solved. Such improvement should be envisaged in further works.

It has to be reminded that the accuracy of the model (compared to detailed commercial simulation software) is about a few percents when predicting annual heating and cooling demands. Moreover, it is important to keep in mind that the simulation model remains an abstraction of the reality and it is not realistic to try to develop a perfectly accurate model. In addition to uncertainties on monitoring and recorded (billing) data, the model's accuracy has also to be considered when proceeding to automated refinement of model's parameters. Continuing the adjustment of the model's parameters too far (i.e. to reach a 0% error) would actually consist in "modeling" the error induced by the use of a simulation model itself. Such final automated adjustment can be useful to investigate the potential sources of discrepancies between the reality and the model but should not be considered as evidence or proof of any "physical effect".

In the frame of building energy services, it is important to reach a good compromise between efforts, time and money spent in modeling and data collection work and model's requirements. If the model is dedicated to energy end-use analysis and to whole-building level on-going commissioning (i.e. comparison between recorded and reference computed weekly or monthly demands and consumptions), it seems rational to proceed to some spot and short-term monitoring in order to reach an acceptable level of accuracy (equivalent to Level 3 calibration defined earlier). The use of sensitivity analysis and the critical analysis of the simulation results should help the analyst to focus on the main monitoring issues.

If the model is dedicated to short-time step energy performance prediction (such as hourly or sub-hourly peak demands prediction), a more detailed model should be developed and a particular attention should be paid to secondary effects such as use of solar shadings, solar masks, variations of

the occupancy rate… Such model would require very complete information about building use, operation and occupancy. To this end, supplemental calibration levels (not envisaged in the present study) might be investigated and could consist in a continuous improvement of the model by means of continuous monitoring of lighting, appliances and HVAC components consumptions. More specific metering should be envisaged at this stage (such as water flow measurements) in order to check the performance of some HVAC components (chiller, boilers…) and to improve the knowledge about building use and operation profiles/schedules.

Today, at the early stages of an energy services process, it is rare to go further than the inspection stage (Level 2) when collecting data. As-built data are usually analyzed and, sometimes, completed by a few spot-measurements. Unfortunately, it has been demonstrated that even if the models based on such limited information provide interesting information and main trends of energy end-use, they are not accurate enough to allow proper quantification of the energy consumers and accurate evaluation of renovation options.

It is usually believed that simulation models able to represent the energy end-use are able to simulate ECOs with acceptable accuracy. Accuracy issues become even more important when energy savings are considered for energy contracting. It is also often envisaged to develop more specific simulation models (of a part of the installation only) to quantify the impact of specific ECOs (e.g. replacement of old pumps by VSD pumps). However, even if calibrated models are useful to assist energy use analysis of an actual situation, the validity of a calibrated model to evaluate ECOs is generally not demonstrated due to lack of postretrofit data. A potential application of a Virtual Calibration Test Bed, such as the one developed in the present work, would be to study the validity of more simplified models when evaluating ECOs at lower costs (i.e. without requiring actual pre-retrofit and post-retrofit data but by generating synthetic pre- and post-retrofit data for numerous ECOs). This issue is studied in the frame of the IEA-ECBCS Annex 55 project (Reliability of energy efficient building retrofitting – probably assessment of performance and cost). Other issues, such as the rebound effect, should also be taken into account when evaluating ECOs. For these reasons, authors generally recommend to use monitoring/measurements to accurately quantify energy savings.

More generally one can say that the fate of simulation-based energy use analysis and energy-use metering are linked. Building energy simulation model and their calibration will certainly become more popular and less hazardous as energy use metering will become more common, making easier the analysis and the modeling of building and HVAC system behavior.